Thesis for the Degree of Master of Philosophy

Towards The Development Of Polyproline Based Organocatalysts

by

Athina Fotopoulou

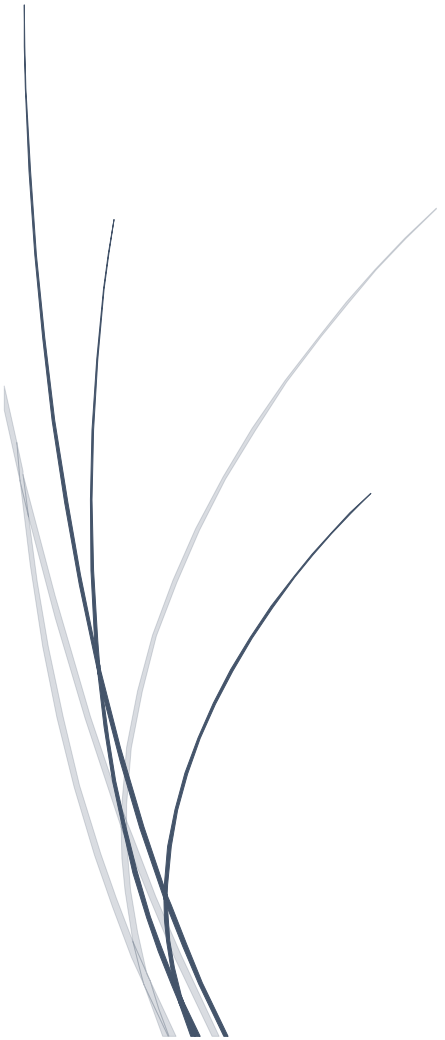

Division of Natural Sciences

University of Kent

May 2025

Abstract

Organocatalysis is a rapidly growing field and over the last decades it has attracted a lot of attention. Considering the importance of enantiomerically pure compounds in various fields, the development of new methods for the synthesis of such compounds is crucial. In this regard, peptides have been developed as enantioselective catalysts. Obtainment of both enantiomers or diastereomers is often important, which can be achieved through stereodivergent organocatalysis.

Specifically, polyproline peptides can be synthesized through an easily accessible amino acid, while introduction of functional groups capable of performing organocatalytic transformation, can be achieved with high position control. Depending on the environment, polyproline appears as two rigid and interconvertible chiral secondary structures (PolPro I and PolPro II). PolPro I is a right-handed helix with all the amide bonds in cis-conformation and parallel to the helix axis. On the other hand, PolPro II is a more extended, left-handed helix, with all the amide bonds in trans-conformation and perpendicular to the axis.

In this context, this study explored the synthesis of a series of polyproline peptides and the investigation of their activity in enantioselective and stereodivergent organocatalysis. After synthesizing the required monomers, three polyproline peptides (**PP 1**, **PP 2** and **PP 3**) were prepared through Solid Phase Peptide Synthesis, analysed via Circular Dichroism spectroscopy and tested as catalysts for the asymmetric aldol reaction between p-nitrobenzaldehyde and cyclohexanone. Various conditions were employed, including the use of different additives, temperatures and solvents, leading to moderately high to high yields for all three peptides. Although **PP 1** catalyzed the reaction with a high dr, the observed enantioselectivities were relatively low. **PP 2** and **PP 3** led to higher enantioselectivities than **PP 1**, suggesting that incorporation of a six-membered ring in the middle of a polyproline helix (**PP 2**) along with a functionalized proline unit (**PP 3**) can lead to more promising catalytic results. **PP 2** and **PP 3** exhibit their highest enantioselectivities in different solvents, suggesting that the solvent interacts with each polyproline in a different manner, influencing the catalysis.

Moreover, this thesis discussed the development of a series of different polyproline peptides and their use as catalysts for the acyl transfer reaction. After preparation of the necessary monomers, three polyproline peptides (**PP 4**, **PP 7** and **PP 8**) were synthesized through SPPS, analysed via CD spectroscopy and tested as catalysts for the KR of racemic 1-phenylethanol with Ac_2O, in the presence of Et_3N. Different reaction conditions were used, including the use of different equivalents of Et_3N and temperatures. **PP 4** catalyzed the reaction achieving the desirable conversion. Nevertheless, the observed ee values were relatively low. Between **PP 7** and **PP 8** the fastest catalyst was depending on the conditions applied, with all the examined cases exhibiting low

enantioselectivities. Nevertheless, the desired conversions were achieved, while exchanging L-proline for D-proline units along the peptide backbone appeared to influence their catalytic activity. Thus, these results can be employed to further research how structural changes along the peptide's units can affect the catalytic outcome.

Declaration

I declare that the work presented in this thesis is my own and was written in my own words. I certify that it was performed during my candidature for a research degree at the University of Kent.

A. Fotopoulou

Acknowledgments

First, I would like to thank my supervisor Dr Aniello Palma for providing me with guidance and support throughout my degree, and helping me to develop my skills and expand my knowledge. Secondly, I would like to thank the academics and staff of the School of Physical Sciences for their help and advice. I would particularly like to thank Dr Andrew Morrell, Dr Bianca Cavazzin, Dr Dean Johnson and Dr David Beal for helping me conduct HPLC, LCMS and GC-MS measurements in the School of Physical Sciences, as well as Kevin Howland for his guidance regarding the CD measurements in the School of Biosciences. Further thanks to all the past members of the Palma group and the members of my laboratory for helping me and providing a fun environment to work in. I would also like to thank the friends that I made during my time in Kent, for providing a supportive and delightful environment. Lastly, I would like to thank my family and friends for their support and encouragement over the course of my studies.

Table of Contents

Abstract i

Declaration iii

Acknowledgments iv

Table of Contents v

List of Abbreviations ix

List of Figures and Schemes xi

List of Tables xxiii

Chapter 1 1

Introduction 1

Context 3

1.1 Introduction 3

1.1.1 Chirality 3

1.1.2 Organocatalysis 3

1.1.2.1 Historical Overview 4

1.1.2.2 Stereodivergent Organocatalysis 8

1.1.2.2.1 Examples of Stereodivergent Catalysts 9

1.1.3 Peptides as Organocatalysts 13

1.1.3.1 Examples of Peptides as Catalysts 14

1.1.4 Polyproline 18

1.1.4.1 Main Characteristics 18

1.1.4.2 Crystal Structure 20

1.1.4.3 Detection 21

1.1.4.4 Mechanism 21

1.1.4.5 Factors That Influence the Polyproline Conformation 22

1.1.4.5.1 Solvent 22

1.1.4.5.2 Chain Length 23

1.1.4.5.3 Substituents 23

1.1.4.6 Applications 23

1.1.5 Aldol Asymmetric Reaction 24

1.1.6 Acyl Transfer Reaction 25

1.2 Project Aims 27

1.2.1 Application of Polyproline Peptides in the Aldol Asymmetric Reaction 28

1.2.2 Application of Polyproline Peptides in the Kinetic Resolution of a Racemic Alcohol 30

1.3 References 32

Chapter 2 39
Application of Polyproline Peptides in the Aldol Catalytic Reaction 39
2.1 Introduction 41
2.1.1 Synthetic Strategies of Peptides 41
2.1.1.1 Solid Phase Peptide Synthesis 42
2.1.1.1.1 Resin 42
2.1.1.1.2 Amino Acids 43
2.1.1.1.3 Coupling Agents 44
2.1.1.1.4 Solvents 47
2.1.1.1.5 Kaiser Test 47
2.1.1.1.6 Chloranil Test 48
2.1.1.1.7 Synthesis of Polyprolines Based on SPPS 48
2.2 Results and Discussion 49
2.2.1 Monomers 49
2.2.1.1 Synthesis of N-Fmoc-trans-4-Boc-amino-L-proline (A7) 50
2.2.1.2 Alternative Synthesis of N-Fmoc-trans-4-Boc-amino-L-proline (A7) 52
2.2.1.3 Synthesis of (S)-1-N-Boc-4-N-Fmoc-piperazine-2-carboxylic Acid (C2) 53
2.2.1.4 Synthesis of N-Fmoc-cis-4-phenyl- L-proline (D3) 54
2.2.1.5 Synthesis of 4-N-acetyl-piperazine-2-carboxylic acid (E2) 55
2.2.2 Peptides 56
2.2.2.1 Synthesis of Peptides 56
2.2.2.1.1 Solid Phase Peptide Synthesis 57
2.2.2.1.2 Synthesis of Peptides Manually 58
2.2.2.1.3 Synthesis of Peptides on the Peptide Synthesizer 60
2.2.2.2 Analysis and Purification of Peptides 61
2.2.2.3 CD Analysis 66
2.2.3 Application of PP 1, PP2 and PP 3 in the Aldol Asymmetric Reaction 68
2.3 Conclusions and Future Work 80
2.3.1 Conclusions 80
2.3.2 Future Outlook 82
2.4 References 84
2.5 Chemicals and Instrumentation 86
2.6 Experimental Information 87
2.6.1 Monomers 87
2.6.1.1 General Procedures 87
2.6.1.2 Synthesis of A7 88

2.6.1.3 Alternative Synthesis of A7 92
2.6.1.4 Synthesis of C2 94
2.6.1.5 Synthesis of D3 95
2.6.1.6 Synthesis of E2 96
2.6.2 Peptides 97
2.6.2.1 General Procedures 97
2.6.2.2 Synthesis of PP 1, PP 2 and PP 3 99
2.6.3 Aldol Asymmetric Reaction 99
2.6.3.1 General Procedures 99
2.6.3.2 Syntesis of 2-(hydroxyl-(p-nitrophenyl)methyl)cyclohexan-1-one 100
Chapter 3 105
Application of Polyproline Peptides in the Kinetic Resolution of a Racemic Alcohol 105
3.1 Introduction: Examples of Peptide Catalysts for Asymmetric Acyl Transfer Reactions 107
3.2 Results and Discussion 111
3.2.1 Target Peptide Group 5 111
3.2.1.1 Synthesis of N-Fmoc-trans-4-hydroxypyridine-L-proline (F3) 111
3.2.1.2 Synthesis of PP 4 Peptide 111
3.2.1.2.1 Analysis of PP 4 Peptide 112
3.2.1.2.2 CD Analysis of PP 4 Peptide 113
3.2.1.3 Application of PP 4 in the Kinetic Resolution of a Racemic Alcohol 113
3.2.2 Target Peptide Group 6 130
3.2.2.1 Monomers G2, G4, G6, G8 130
3.2.2.2 Synthetic Attempt of Target Peptide 6 131
3.2.2.2.1 Analysis of PP 5 Peptide 133
3.2.2.3 PP 6 Peptide 133
3.2.2.4 Synthesis of PP 7 and PP 8 Peptides 134
3.2.2.4.1 Analysis of PP 7, PP 8 and PP 9 Peptides 136
3.2.2.4.2 CD Analysis of PP 7, PP 8 and PP 9 Peptides 138
3.2.2.5 Application of PP 7 and PP 8 in the Kinetic Resolution of a Racemic Alcohol 140
3.3 Conclusions and Future Work 159
3.3.1 Conclusions 159
3.3.1.1 Target Peptide Group 5 159
3.3.1.2 Target Peptide Group 6 160
3.3.2 Future Outlook 161
3.4 References 161
3.5 Chemicals and Instrumentation 162

3.6 Experimental Information 163
3.6.1 General Procedures 163
3.6.2 PP 4 164
3.6.2.1 Synthesis of F3 164
3.6.2.2 Synthesis of PP 4 Peptide 166
3.6.2.3 KR of a Racemic Alcohol Using PP 4 166
3.6.3 PP 7 and PP 8 168
3.6.3.1 Synthesis of PP 7 Peptide 169
3.6.3.2 Synthesis of PP 8 Peptide 169
3.6.3.3 KR of a Racemic Alcohol Using PP 7, PP8 and PP9 170
Chapter 4 175
Conclusions 175
4.1 Application of Polyproline Peptides in the Aldol Asymmetric Reaction 177
4.2 Application of Polyproline Peptides in the Kinetic Resolution of a Racemic Alcohol 179
Appendix 1 183
Further Analysis: Chapter 2 183
AP1.1 Monomers 185
AP1.1.1 ^{1}H-NMR Spectra 185
AP1.1.2 ^{13}C-NMR Spectra 199
AP1.2 Peptides 212
AP1.2.1 ^{1}H-NMR Spectra 213
AP1.3 Aldol Catalytic Reaction 216
AP1.3.1 ^{1}H-NMR Spectra 216
AP1.3.2 ^{13}C-NMR Spectrum 253
AP1.3.3 Chiral HPLC 254
Appendix 2 261
Further Analysis: Chapter 3 261
AP2.1 Monomers 263
AP2.1.1 ^{1}H-NMR Spectra 263
AP2.1.2 ^{13}C-NMR Spectra 266
AP2.2 Peptides 269
AP2.2.1 ^{1}H-NMR Spectra 269
AP2.3 Kinetic resolution of a Racemic Alcohol 272
AP2.3.1 ^{1}H-NMR Spectra 272
AP2.3.2 ^{13}C-Spectra 356

List of Abbreviations

δ	Chemical Shift
Ac_2O	Acetic Anhydride
Aq	Aqueous
Boc	Tert-Butyloxycarbonyl
Boc_2O	Di-Tert-Butyl Dicarbonate
BOP	Benzotriazol-1-yloxy)tris(dimethylamino)phosphonium hexafluorophosphate
CBz	Benzyl Chloroformate
CD	Circular Dichroism
$CDCl_3$	Chloroform
DCC	N, N'-Dicyclohexylcarbodiimide
DCE	1,2-Dichloroethane
DCM	Dichloromethane
DIAD	Diisopropyl Azodicarboxylate
DIC	N, N'-Diisopropylcarbodiimide
DIPEA	N, N'-Diisopropylethylamine
DMAP	4-(Dimethylamino)pyridine
DMF	Dimethylformamide
DMSO	Dimethyl sulfoxide
DNA	Deoxyribose Nucleic Acid
dr	Diastereoisomeric Ratio
ee	Enantiomeric Excess
eq	Equivalents
er	Enantiomeric Ratio
ESI -MS	Electrospray Ionisation- Mass Spectrometry
EtOH	Ethanol
EtOAc	Ethyl Acetate
FA	Formic Acid
Fmoc	Fluorenylmethyloxycarbonyl
Fmoc-Cl	9-Fluorenylmethyloxycarbonyl Chloride
Fmoc-OSu	9-Fluorenylmethyl-Succinimidyl Carbonate
Fmoc-Pro-OH	Fmoc-Proline
FRET	Fluorescence Resonance Energy Transfer
FT-IR	Fourier Transform-Infrared
GC-MS	Gas Chromatography - Mass Spectrometry
h	Hours
HBTU	Hexafluorophosphate Benzotriazole Tetramethyl Uronium
HCl	Hydrochloric Acid
HOBt	1-Hydroxybenzotriazole Hydrate
HPLC	High Performance Liquid Chromatography
IMS-MS	Ion Mobility Spectrometry-Mass Spectrometry
J	Coupling Constant
KCN	Potassium Cyanide
KR	Kinetic Resolution
LC-MS	Liquid Chromatography-Mass Spectrometry
LUMO	Lowest Unoccupied Molecular Orbital
MBHA	Methylbenzyhydryl Amine

MeCN	Acetonitrile
$MgSO_4$	Magnesium Sulphate
Na_2CO_3	Sodium Carbonate
NCA	N-Carboxy-Anhydride
NH_4OAc	Ammonium Acetate
n-Hex	Hexane
NMI	N-Methylimidazole
NMP	N-Methylpyrrolidone
NMR	Nuclear Magnetic Resonance
PolPro	Polyproline
PPh_3	Triphenylphosphine
pTSA	p-Toluenesulfonic Acid
PyBOP	Benzotriazol-1-yl-oxytripyrrolidinophosphonium Hexafluorophosphate
RNA	Ribonucleic Acid
RP-HPLC	Reversed Phase-High Pressure Liquid Chromatography
RT	Room Temperature
Sec-alcohols	Secondary Alcohols
SPPS	Solid Phase Peptide Synthesis
TBTU	2-(1H-Benzotriazole-1-yl)-1,1,3,3-Tetramethylaminium Tetrafluoroborate
TEA	Triethylamine
TFA	Trifluoroacetic Acid
TFE	2,2,2-Trifluoroethanol
THF	Tetrahydrofuran
TLC	Thin Layer Chromatography
UV	Ultraviolet

List of Figures and Schemes

Figure 1: Enantiomers of DOPA (left) and Carvone (right). 3
Figure 2: General Structure of a Peptide.[24] 13
Figure 3: Illustration of the Peptide Bond and the Three Torsion Angles.[19] 13
Figure 4: Schematic Representation of the Transition States Corresponding to the Aldol Reaction Between Acetone and p-Nitrobenzaldehyde Catalyzed by the Tripeptide.[28] 16
Figure 5: Peptide That Has a Proline at Position m.[19] 19
Figure 6: Polyproline I (pink) and Polyproline II (blue) in Top (left) and Side (right) View. 19
Figure 7: Oligoprolines as Molecular Ruler and Scaffold.[32] 24
Figure 8: General Catalytic Cycle for the Asymmetric Acylation of Sec-Alcohols.[12,80,82] 27
Figure 9: Target Peptides 1-4. 29
Figure 10: Structures of Rink Amide Resin (up), Wang Resin (middle) and 2-Chlorotrityl Chloride Resin (bottom).[8] 43
Figure 11: Structures of a) DCC, b) DIC, c) BOP, d) PyBOP, e) HBTU and e) TBTU.[6] 45
Figure 12: Proline Tetramer Fmoc-$(Pro)_4$-NH_2.[18] 48
Figure 13: Azidoproline-Containing Oligoprolines.[19] 49
Figure 14: Structures of the Target Compounds. 49
Figure 15: Structures of Target Peptides. 56
Figure 16: Overview of the Solid-Phase Peptide Synthesis (SPPS) Cycle.[6,8] 58
Figure 17: LCMS Chromatograms of **PP 1** a) Before and b) After Purification (Determined Using UV Detection at 225 nm: >99 %, on a Kromasil 100-5-C18, 4.6 x 250 mm, 30 to 100 % B over 12 mins. A is 0.1 % formic acid/ H_2O and B is 0.1 % formic acid/MeOH). 61
Figure 18: LCMS Chromatogram of **PP 1** (Determined Using UV Detection at 225 nm: >99 %, on a Kromasil 100-5-C18, 4.6 x 250 mm, 30 to 100 % B over 12 mins. A is 0.1 % formic acid/ H_2O and B is 0.1 % formic acid/MeOH). 62
Figure 19: LCMS Chromatograms of **PP 1** a) Before and b) After Purification (Determined using UV Detection at 225 nm: >99 %, on a Kromasil 100-5-C18, 4.6 x 250 mm, ... 62
Figure 20: LCMS Chromatogram of **PP 1** (Determined by LCMS Using UV Detection at 225 nm: >99 %, on a Kromasil 100-5-C18, 4.6 x 250 mm, 20 to 100 % B over 16.5 mins. A is 0.1 % formic acid/ H_2O and B is 0.1 % formic acid/MeOH). 63
Figure 21: LCMS Chromatogram of **PP 1** (Determined by LCMS Using UV Detection at 225 nm: >99 %, on a Kromasil 100-5-C18, 4.6 x 250 mm, 20 to 100 % B over 14.5 mins. A is 0.1 % formic acid/ H_2O and B is 0.1 % formic acid/MeOH). 63
Figure 22: LCMS Chromatogram of **PP 2** (Determined by LCMS Using UV Detection at 225 nm: >99 %, on a Kromasil 100-5-C18, 4.6 x 250 mm, 30 to 100 % B over 12 mins. A is 0.1 % formic acid/H_2O and B is 0.1 % formic acid/MeOH). 63
Figure 23: LCMS Chromatograms of **PP 2** a) Before and b) After Purification (Determined by LCMS Using UV Detection at 225 nm: >99 %, on a Kromasil 100-5-C18, 4.6 x 250 mm, 40 to 100 % B over 17 mins. A is 0.1 % formic acid/H_2O and B is 0.1 % formic acid/MeOH). 64
Figure 24: LCMS Chromatograms of **PP 2** a) Before and b) After Purification (Determined by LCMS Using UV Detection at 225 nm: >99 %, on a Kromasil 100-5-C18, 4.6 x 250 mm, ... 64
Figure 25: LCMS Chromatogram of **PP 2** (Determined by LCMS Using UV Detection at 225 nm: >99 %, on a Kromasil 100-5-C18, 4.6 x 250 mm, 30 to 100 % B over 14.5 mins. A is 0.1 % formic acid/H_2O and B is 0.1 % formic acid/MeOH). 65

Figure 26: LCMS Chromatogram of **PP 3** (Determined by LCMS Using UV Detection at 225 nm: >99 %, on a Kromasil 100-5-C18, 4.6 x 250 mm, 10 to 100 % B over 12 mins. A is 0.1 % formic acid/H_2O and B is 0.1 % formic acid/MeOH). 65
Figure 27: LCMS Chromatogram of **PP 3** Before Purification (Determined by LCMS Using UV Detection at 225 nm: >99 %, on a Kromasil 100-5-C18, 4.6 x 250 mm, 60 to 100 % B over 16 mins. A is 0.1 % formic acid/H_2O and B is 0.1 % formic acid/MeOH). 65
Figure 28: HPLC Chromatogram of **PP 3** after Purification (Determined on an Agilent 1100 HPLC Using UV Detection at 225 nm: >99 %, on a Kromasil 100-5-C18, 4.6 x 250 mm, 40 to 100 % B over 14.5 mins. A is 0.1 % formic acid/H_2O and B is 0.1 % formic acid/MeOH). 66
Figure 29: CD Spectrum of **PP 1** in Aqueous Solution (blue) and in propanol (orange) at 20 °C and ≈ 100 µM. 67
Figure 30: CD Spectrum of **PP 2** in Aqueous Solution (blue) and in propanol (orange) at 20 °C and ≈ 100 µM. 68
Figure 31: CD Spectrum of **PP 3** in Aqueous Solution (blue) and in propanol (orange) at 20 °C and ≈ 100 µM. 68
Figure 32: Structures of Monomer **E3** and L-proline. 69
Figure 33: ^{1}H-NMR Spectrum of Aldol Reaction Using **PP 1** as a Potential Catalyst. 69
Figure 34 : The ^{1}H-NMR Spectrum of 2-(hydroxy(4-nitrophenyl)methyl)cyclohexanone Measured in $CDCl_3$ at 25 °C. 72
Figure 35: Chiral HPLC Analysis of Racemic 2-(hydroxyl-(p-nitrophenyl)methyl) cyclohexan-1- one Using **PP 1** in Anhydrous DMF (Table 5, Entry 16). 73
Figure 36: Chiral HPLC Analysis of Racemic 2-(hydroxyl-(p-nitrophenyl)methyl) cyclohexan-1- one Using **PP 1** and No Solvent (Table 5, Entry 17). 73
Figure 37: Chiral HPLC Analysis of Racemic 2-(hydroxyl-(p-nitrophenyl)methyl) cyclohexan-1- one Using **PP 1** in EtOH (Table 5, Entry 18). 74
Figure 38: Chiral HPLC Analysis of Racemic 2-(hydroxyl-(p-nitrophenyl)methyl) cyclohexan-1- one Using **PP 2** in DMF (Table 6, Entry 28). 75
Figure 39: Chiral HPLC Analysis of Racemic 2-(hydroxyl-(p-nitrophenyl)methyl) cyclohexan-1- one Using **PP 2** in propanol (Table 6, Entry 29). 75
Figure 40: Chiral HPLC Analysis of Racemic 2-(hydroxyl-(p-nitrophenyl)methyl) cyclohexan-1- one Using **PP 2** in MeOH (Table 6, Entry 30). 76
Figure 41: Chiral HPLC Analysis of Racemic 2-(hydroxyl-(p-nitrophenyl)methyl) cyclohexan-1- one Using **PP 3** in DMF (Table 7, Entry 31). 77
Figure 42: Chiral HPLC Analysis of Racemic 2-(hydroxyl-(p-nitrophenyl)methyl) cyclohexan-1- one Using **PP 3** in propanol (Table 7, Entry 32). 77
Figure 43: Chiral HPLC Analysis of Racemic 2-(hydroxyl-(p-nitrophenyl)methyl) cyclohexan-1- one Using **PP 3** in MeOH (Table 7, Entry 33). 77
Figure 44: Chiral HPLC Analysis of Racemic 2-(hydroxyl-(p-nitrophenyl)methyl) cyclohexan-1- one Using E**3** in DMF (Table 8, Entry 34). 78
Figure 45: Chiral HPLC Analysis of Racemic 2-(hydroxyl-(p-nitrophenyl)methyl) cyclohexan-1- one Using **E3** in propanol (Table 8, Entry 35). 78
Figure 46: Chiral HPLC Analysis of Racemic 2-(hydroxyl-(p-nitrophenyl)methyl) cyclohexan-1- one Using L-Proline in DMF (Table 9, Entry 36). 79
Figure 47: Chiral HPLC Analysis of Racemic 2-(hydroxyl-(p-nitrophenyl)methyl) cyclohexan-1- one Using L-Proline in propanol (Table 9, Entry 37). 79
Figure 48: Future Target Monomer. 83
Figure 49: Structure of DMAP.[5] 109
Figure 50: LCMS Chromatogram of **PP 4**. 113

Figure 51: CD Spectrum of **PP 4** in Aqueous Solution at 20 °C and ≈ 100 µM. 113
Figure 52: Structures of DMAP (left), Monomer **F2** (middle) and Monomer **F3** (right). 114
Figure 53: Chiral GC-MS Analysis of Reference Sample of 1-phenyl alcohol and the Produced Acetate. 114
Figure 54: ^{1}H-NMR Spectrum of 1-phenyl alcohol with Ac_2O Using DMAP as a Catalyst. 115
Figure 55: GC-MS Analysis of Reaction of 1-phenyl alcohol with Ac_2O Using **PP 4** at RT (Table 13, Entry 14). 117
Figure 56: GC-MS Analysis of Reaction of 1-phenyl alcohol with Ac_2O Using **PP 4** at RT (Table 13, Entry 16). 118
Figure 57: GC-MS Analysis of Reaction of 1-phenyl alcohol with Ac_2O Using **PP 4** at 0 °C (Table 14, Entry 19). 119
Figure 58: GC-MS Analysis of Reaction of 1-phenyl alcohol with Ac_2O Using **PP 4** at 0 °C (Table 14, Entry 20). 120
Figure 59: GC-MS Analysis of Reaction of 1-phenyl alcohol with Ac_2O Using **F2** at RT (Table 15, Entry 26). 122
Figure 60: GC-MS Analysis of Reaction of 1-phenyl alcohol with Ac_2O Using **F2** at RT (Table 15, Entry 29). 123
Figure 61: GC-MS Analysis of Reaction of 1-phenyl alcohol with Ac_2O Using **F2** at 0 °C (Table 16, Entry 30). 124
Figure 62: GC-MS Analysis of Reaction of 1-phenyl alcohol with Ac_2O Using **F2** at 0 °C (Table 16, Entry 31). 125
Figure 63: GC-MS Analysis of Reaction of 1-phenyl alcohol with Ac_2O Using **F3** at RT (Table 17, Entry 35). 126
Figure 64: GC-MS Analysis of Reaction of 1-phenyl alcohol with Ac_2O Using **F3** at RT (Table 17, Entry 38). 127
Figure 65: GC-MS Analysis of Reaction of 1-phenyl alcohol with Ac_2O Using **F3** at 0 °C (Table 18, Entry 39). 128
Figure 66: GC-MS Analysis of Reaction of 1-phenyl alcohol with Ac_2O Using **F3** at 0 °C (Table 18, Entry 40). 129
Figure 67: Structures of Target Monomers (**G2**, **G4**, **G6**, **G8**). 130
Figure 68: Structure of Peptide **PP 5**. 132
Figure 69: LCMS Chromatogram of **PP 5**. 133
Figure 70: Structure of Synthesized Peptide. 133
Figure 71: Structure of **PP 6**. 133
Figure 72: Structures of **PP 7**, **PP 8** and **J1**. 135
Figure 73: Structure of **PP 9**. 135
Figure 74: LCMS Chromatogram of **PP 9**. 136
Figure 75: HPLC Chromatogram of **PP 8** Before Purification. 137
Figure 76: HPLC Chromatogram of **PP 7** Before Purification. 137
Figure 77: CD Spectrum of **PP 7** in Aqueous Solution at 20 °C and ≈ 100 µM. 139
Figure 78: CD Spectrum of **PP 8** in Aqueous Solution at 20 °C and ≈ 100 µM. 139
Figure 79: CD Spectrum of **PP 9** in Aqueous Solution at 20 °C and ≈ 100 µM. 140
Figure 80: GC-MS Analysis of Reaction of 1-phenyl alcohol with Ac_2O Using **PP 7** at RT (Table 20, Entry 42). 142
Figure 81: GC-MS Analysis of Reaction of 1-phenyl alcohol with Ac_2O Using **PP 7** at RT (Table 20, Entry 44). 143
Figure 82: GC-MS Analysis of Reaction of 1-phenyl alcohol with Ac_2O Using **PP 7** at 0 °C (Table 21, Entry 45). 144

Figure 83: GC-MS Analysis of Reaction of 1-phenyl alcohol with Ac_2O Using **PP 7** at 0 °C (Table 21, Entry 48).....145
Figure 84: GC-MS Analysis of Reaction of 1-phenyl alcohol with Ac_2O Using **PP 8** at RT (Table 22, entry 49).....146
Figure 85: GC-MS Analysis of Reaction of 1-phenyl alcohol with Ac_2O Using **PP 8** at RT (Table 22, Entry 51).....147
Figure 86: GC-MS Analysis of Reaction of 1-phenyl alcohol with Ac_2O Using **PP 8** at 0 °C (Table 22, Entry 53).....149
Figure 87: GC-MS Analysis of Reaction of 1-phenyl alcohol with Ac_2O Using **PP 8** at 0 °C (Table 22, Entry 60).....150
Figure 88: GC-MS Analysis of Reaction of 1-phenyl alcohol with Ac_2O Using **PP 9** at RT (Table 23, Entry 64).....151
Figure 89: GC-MS Analysis of Reaction of 1-phenyl alcohol with Ac_2O Using **PP 9** at RT (Table 23, Entry 67).....152
Figure 90: GC-MS Analysis of Reaction of 1-phenyl alcohol with Ac_2O Using **PP 8** at 0 °C (Table 24, Entry 68).....153
Figure 91: GC-MS Analysis of Reaction of 1-phenyl alcohol with Ac_2O Using **PP 8** at 0 °C (Table 24, Entry 71).....154
Figure 92: GC-MS Analysis of Reaction of 1-phenyl alcohol with Ac_2O Using **J1** at RT (Table 25, Entry 77). 155
Figure 93: GC-MS Analysis of Reaction of 1-phenyl alcohol with Ac_2O Using **J1** at RT (Table 25, Entry 83). 156
Figure 94: GC-MS Analysis of Reaction of 1-phenyl alcohol with Ac_2O Using **J1** at 0 °C (Table 26, Entry 85). 157
Figure 95: GC-MS Analysis of Reaction of 1-phenyl alcohol with Ac_2O Using **J1** at 0 °C (Table 26, Entry 87). 158
Figure 96: ^{1}H-NMR Spectrum ($CDCl_3$, 400 MHz) of **A2.**.....185
Figure 97: ^{1}H-NMR Spectrum ($CDCl_3$, 400 MHz) of **A3.**.....186
Figure 98: ^{1}H-NMR Spectrum ($CDCl_3$, 400 MHz) of **A4.**.....187
Figure 99: ^{1}H-NMR Spectrum ($CDCl_3$, 400 MHz) of **A5.**.....188
Figure 100: ^{1}H-NMR Spectrum ($CDCl_3$, 400 MHz) of **A6.**.....189
Figure 101: ^{1}H-NMR Spectrum ($CDCl_3$, 400 MHz) of **A7.**.....190
Figure 102: ^{1}H-NMR Spectrum ($CDCl_3$, 400 MHz) of **B2.**.....191
Figure 103: ^{1}H-NMR Spectrum ($CDCl_3$, 400 MHz) of **B3.**.....192
Figure 104: ^{1}H-NMR Spectrum ($CDCl_3$, 400 MHz) of **C2.**.....193
Figure 105: ^{1}H-NMR Spectrum ($CDCl_3$, 400 MHz) of **D1.**.....194
Figure 106: ^{1}H-NMR Spectrum ($CDCl_3$, 400 MHz) of **D2.**.....195
Figure 107: ^{1}H-NMR Spectrum ($CDCl_3$, 400 MHz) of **D3.**.....196
Figure 108: ^{1}H-NMR Spectrum ($CDCl_3$, 400 MHz) of **E1.** 197
Figure 109: ^{1}H-NMR Spectrum ($CDCl_3$, 400 MHz) of **E2.** 198
Figure 110: ^{13}C-NMR Spectrum ($CDCl_3$, 100 MHz) of **A2**.....199
Figure 111: ^{13}C-NMR Spectrum ($CDCl_3$, 100 MHz) of **A3.** 200
Figure 112: ^{13}C-NMR Spectrum ($CDCl_3$, 100 MHz) of **A4.** 201
Figure 113: ^{13}C-NMR Spectrum ($CDCl_3$, 100 MHz) of **A5.**.....202
Figure 114: ^{13}C-NMR Spectrum ($CDCl_3$, 100 MHz) of **A6.**.....203
Figure 115: ^{13}C-NMR Spectrum (DMSO, 100 MHz) of **A7.** 204
Figure 116: ^{13}C-NMR Spectrum ($CDCl_3$, 100 MHz) of **B2.**.....205
Figure 117: ^{13}C-NMR Spectrum ($CDCl_3$, 100 MHz) of **B3.**.....206

Figure 118: ^{13}C-NMR Spectrum (DMSO, 100 MHz) of **C2.** 207
Figure 119: ^{13}C-NMR Spectrum ($CDCl_3$, 100 MHz) of **D1.** 208
Figure 120: ^{13}C-NMR Spectrum ($CDCl_3$, 100 MHz) of **D2.** 209
Figure 121: ^{13}C-NMR Spectrum ($CDCl_3$, 100 MHz) of **D3** 210
Figure 122: ^{13}C-NMR Spectrum ($CDCl_3$, 100 MHz) of **E1.** 211
Figure 123: ^{13}C-NMR Spectrum ($CDCl_3$, 100 MHz) of **E2.** 212
Figure 124: ^{1}H-NMR Spectrum ($CDCl_3$, 400 MHz) of **PP 1**. 213
Figure 125: ^{1}H-NMR Spectrum ($CDCl_3$, 400 MHz) of **PP 2**. 214
Figure 126: ^{1}H-NMR Spectrum ($CDCl_3$, 400 MHz) of **PP 3**. 215
Figure 127: ^{1}H-NMR Spectrum ($CDCl_3$, 400 MHz) of 2-(hydroxyl-(p-nitrophenyl)methyl)cyclohexan-1-one Using ammonium acetate. 216
Figure 128: ^{1}H-NMR Spectrum ($CDCl_3$, 400 MHz) of 2-(hydroxyl-(p-nitrophenyl)methyl)cyclohexan-1-one Using **PP 1** (Table 5, Entry 1). 217
Figure 129: ^{1}H-NMR Spectrum ($CDCl_3$, 400 MHz) of 2-(hydroxyl-(p-nitrophenyl)methyl)cyclohexan-1-one Using **PP 1** (Table 5, Entry 2). 218
Figure 130: ^{1}H-NMR Spectrum ($CDCl_3$, 400 MHz) of 2-(hydroxyl-(p-nitrophenyl)methyl)cyclohexan-1-one Using **PP 1** (Table 5, Entry 3). 219
Figure 131: ^{1}H-NMR Spectrum ($CDCl_3$, 400 MHz) of 2-(hydroxyl-(p-nitrophenyl)methyl)cyclohexan-1-one Using **PP 1** (Table 5, Entry 4). 220
Figure 132: ^{1}H-NMR Spectrum ($CDCl_3$, 400 MHz) of 2-(hydroxyl-(p-nitrophenyl)methyl)cyclohexan-1-one Using **PP 1** (Table 5, Entry 5). 221
Figure 133: ^{1}H-NMR Spectrum ($CDCl_3$, 400 MHz) of 2-(hydroxyl-(p-nitrophenyl)methyl)cyclohexan-1-one Using **PP 1** (Table 5, Entry 6). 222
Figure 134: ^{1}H-NMR Spectrum ($CDCl_3$, 400 MHz) of 2-(hydroxyl-(p-nitrophenyl)methyl)cyclohexan-1-one Using **PP 1** (Table 5, Entry 7). 223
Figure 135: ^{1}H-NMR Spectrum ($CDCl_3$, 400 MHz) of 2-(hydroxyl-(p-nitrophenyl)methyl)cyclohexan-1-one Using **PP 1** (Table 5, Entry 8). 224
Figure 136: ^{1}H-NMR Spectrum ($CDCl_3$, 400 MHz) of 2-(hydroxyl-(p-nitrophenyl)methyl)cyclohexan-1-one Using **PP 1** (Table 5, Entry 9). 225
Figure 137: ^{1}H-NMR Spectrum ($CDCl_3$, 400 MHz) of 2-(hydroxyl-(p-nitrophenyl)methyl)cyclohexan-1-one Using **PP 1** (Table 5, Entry 10). 226
Figure 138: ^{1}H-NMR Spectrum ($CDCl_3$, 400 MHz) of 2-(hydroxyl-(p-nitrophenyl)methyl)cyclohexan-1-one Using **PP 1** (Table 5, Entry 11). 227
Figure 139: ^{1}H-NMR Spectrum ($CDCl_3$, 400 MHz) of 2-(hydroxyl-(p-nitrophenyl)methyl)cyclohexan-1-one Using **PP 1** (Table 5, Entry 12). 228
Figure 140: ^{1}H-NMR Spectrum ($CDCl_3$, 400 MHz) of 2-(hydroxyl-(p-nitrophenyl)methyl)cyclohexan-1-one Using **PP 1** (Table 5, Entry 13). 229
Figure 141: ^{1}H-NMR Spectrum ($CDCl_3$, 400 MHz) of 2-(hydroxyl-(p-nitrophenyl)methyl)cyclohexan-1-one Using **PP 1** (Table 5, Entry 14). 230
Figure 142: ^{1}H-NMR Spectrum ($CDCl_3$, 400 MHz) of 2-(hydroxyl-(p-nitrophenyl)methyl)cyclohexan-1-one Using **PP 1** (Table 5, Entry 15). 231
Figure 143: ^{1}H-NMR Spectrum ($CDCl_3$, 400 MHz) of 2-(hydroxyl-(p-nitrophenyl)methyl)cyclohexan-1-one Using **PP 1** (Table 5, Entry 16). 232
Figure 144: ^{1}H-NMR Spectrum ($CDCl_3$, 400 MHz) of 2-(hydroxyl-(p-nitrophenyl)methyl)cyclohexan-1-one Using **PP 1** (Table 5, Entry 17). 233
Figure 145: ^{1}H-NMR Spectrum ($CDCl_3$, 400 MHz) of 2-(hydroxyl-(p-nitrophenyl)methyl)cyclohexan-1-one Using **PP 1** (Table 5, Entry 18). 234

Figure 146: ^{1}H-NMR Spectrum ($CDCl_3$, 400 MHz) of 2-(hydroxyl-(p-nitrophenyl)methyl)cyclohexan-1-one Using **PP 2** (Table 6, Entry 19). 235
Figure 147: ^{1}H-NMR Spectrum ($CDCl_3$, 400 MHz) of 2-(hydroxyl-(p-nitrophenyl)methyl)cyclohexan-1-one Using **PP 2** (Table 6, Entry 21). 236
Figure 148: ^{1}H-NMR Spectrum ($CDCl_3$, 400 MHz) of 2-(hydroxyl-(p-nitrophenyl)methyl)cyclohexan-1-one Using **PP 2** (Table 6, Entry 22). 237
Figure 149: ^{1}H-NMR Spectrum ($CDCl_3$, 400 MHz) of 2-(hydroxyl-(p-nitrophenyl)methyl)cyclohexan-1-one Using **PP 2** (Table 6, Entry 23). 238
Figure 150: ^{1}H-NMR Spectrum ($CDCl_3$, 400 MHz) of 2-(hydroxyl-(p-nitrophenyl)methyl)cyclohexan-1-one Using **PP 2** (Table 6, Entry 24). 239
Figure 151: ^{1}H-NMR Spectrum ($CDCl_3$, 400 MHz) of 2-(hydroxyl-(p-nitrophenyl)methyl)cyclohexan-1-one Using **PP 2** (Table 6, Entry 25). 240
Figure 152: ^{1}H-NMR Spectrum ($CDCl_3$, 400 MHz) of 2-(hydroxyl-(p-nitrophenyl)methyl)cyclohexan-1-one Using **PP 2** (Table 6, Entry 26). 241
Figure 153: ^{1}H-NMR Spectrum ($CDCl_3$, 400 MHz) of 2-(hydroxyl-(p-nitrophenyl)methyl)cyclohexan-1-one Using **PP 2** (Table 6, Entry 27). 242
Figure 154: ^{1}H-NMR Spectrum ($CDCl_3$, 400 MHz) of 2-(hydroxyl-(p-nitrophenyl)methyl)cyclohexan-1-one Using **PP 2** (Table 6, Entry 28). 243
Figure 155: ^{1}H-NMR Spectrum ($CDCl_3$, 400 MHz) of 2-(hydroxyl-(p-nitrophenyl)methyl)cyclohexan-1-one Using **PP 2** (Table 6, Entry 29). 244
Figure 156: ^{1}H-NMR Spectrum ($CDCl_3$, 400 MHz) of 2-(hydroxyl-(p-nitrophenyl)methyl)cyclohexan-1-one Using **PP 2** (Table 6, Entry 30). 245
Figure 157: ^{1}H-NMR Spectrum ($CDCl_3$, 400 MHz) of 2-(hydroxyl-(p-nitrophenyl)methyl)cyclohexan-1-one Using **PP 3** (Table 7, Entry 31). 246
Figure 158: ^{1}H-NMR Spectrum ($CDCl_3$, 400 MHz) of 2-(hydroxyl-(p-nitrophenyl)methyl)cyclohexan-1-one Using **PP 3** (Table 7, Entry 32). 247
Figure 159: ^{1}H-NMR Spectrum ($CDCl_3$, 400 MHz) of 2-(hydroxyl-(p-nitrophenyl)methyl)cyclohexan-1-one Using **PP 3** (Table 7, Entry 33). 248
Figure 160: ^{1}H-NMR Spectrum ($CDCl_3$, 400 MHz) of 2-(hydroxyl-(p-nitrophenyl)methyl)cyclohexan-1-one Using **E3** (Table 8, Entry 34). 249
Figure 161: ^{1}H-NMR Spectrum ($CDCl_3$, 400 MHz) of 2-(hydroxyl-(p-nitrophenyl)methyl)cyclohexan-1-one Using **E3** (Table 8, Entry 35). 250
Figure 162: ^{1}H-NMR Spectrum ($CDCl_3$, 400 MHz) of 2-(hydroxyl-(p-nitrophenyl)methyl)cyclohexan-1-one Using L-Proline (Table 9, Entry 36) 251
Figure 163: ^{1}H-NMR Spectrum ($CDCl_3$, 400 MHz) of 2-(hydroxyl-(p-nitrophenyl)methyl)cyclohexan-1-one Using L-Proline (Table 9, Entry 37) 252
Figure 164: ^{13}C-NMR Spectrum ($CDCl_3$, 100 MHz) of 2-(hydroxyl-(p-nitrophenyl)methyl)cyclohexan-1-one. 253
Figure 165: Chiral HPLC Analysis of Racemic 2-(hydroxyl-(p-nitrophenyl)methyl) cyclohexan-1- one (Chiralpak AD-H and a Mobile Phase n-hexane/i-PrPOH= 80/20 (v/v); 1 mL min-1; 254 nm; 25 ^{0}C). 254
Figure 166: Chiral HPLC Analysis of Racemic 2-(hydroxyl-(p-nitrophenyl)methyl) cyclohexan-1- one (Chiralpak AD-H and a Mobile Phase n-hexane/i-PrPOH= 80/20 (v/v); 1 mL min-1; 254 nm; 25 °C). 254
Figure 167: Chiral HPLC analysis of racemic 2-(hydroxyl-(p-nitrophenyl)methyl) cyclohexan-1- one (Chiralpak AD-H and a mobile phase n-hexane/i-PrPOH= 80/20 (v/v); 1 mL min-1; 254 nm; 25 ^{0}C). 255
Figure 168: Chiral HPLC Analysis of Racemic 2-(hydroxyl-(p-nitrophenyl)methyl) cyclohexan-1- one (Chiralpak AD-H and a Mobile Phase n-hexane/i-PrPOH= 80/20 (v/v); 1 mL min-1; 254 nm; 25 °C). 255
Figure 169: Chiral HPLC Analysis of Racemic 2-(hydroxyl-(p-nitrophenyl)methyl) cyclohexan-1- one (Chiralpak AD-H and a Mobile Phase n-hexane/i-PrPOH= 80/20 (v/v); 1 mL min-1; 254 nm; 25 °C). 256

Figure 170: Chiral HPLC Analysis of Racemic 2-(hydroxyl-(p-nitrophenyl)methyl) cyclohexan-1- one (Chiralpak AD-H and a Mobile Phase n-hexane/i-PrPOH= 80/20 (v/v); 1 mL min-1; 254 nm; 25 °C). 256
Figure 171: Chiral HPLC Analysis of Racemic 2-(hydroxyl-(p-nitrophenyl)methyl) cyclohexan-1- one (Chiralpak AD-H and a Mobile Phase n-hexane/i-PrPOH= 80/20 (v/v); 1 mL min-1; 254 nm; 25 °C). 257
Figure 172: Chiral HPLC Analysis of Racemic 2-(hydroxyl-(p-nitrophenyl)methyl) cyclohexan-1- one (Chiralpak AD-H and a Mobile Phase n-hexane/i-PrPOH= 80/20 (v/v); 1 mL min-1; 254 nm; 25 °C). 257
Figure 173: Chiral HPLC Analysis of Racemic 2-(hydroxyl-(p-nitrophenyl)methyl) cyclohexan-1- one (Chiralpak AD-H and a Mobile Phase n-hexane/i-PrPOH= 80/20 (v/v); 1 mL min-1; 254 nm; 25 °C). 258
Figure 174: Chiral HPLC Analysis of Racemic 2-(hydroxyl-(p-nitrophenyl)methyl) cyclohexan-1- one (Chiralpak AD-H and a Mobile Phase n-hexane/i-PrPOH= 80/20 (v/v); 1 mL min-1; 254 nm; 25 °C). 258
Figure 175: Chiral HPLC Analysis of Racemic 2-(hydroxyl-(p-nitrophenyl)methyl) cyclohexan-1- one (Chiralpak AD-H and a Mobile Phase n-hexane/i-PrPOH= 80/20 (v/v); 1 mL min-1; 254 nm; 25 °C). 259
Figure 176: Chiral HPLC Analysis of Racemic 2-(hydroxyl-(p-nitrophenyl)methyl) cyclohexan-1- one (Chiralpak AD-H and a Mobile Phase n-hexane/i-PrPOH= 80/20 (v/v); 1 mL min-1; 254 nm; 25 °C). 259
Figure 177: Chiral HPLC Analysis of Racemic 2-(hydroxyl-(p-nitrophenyl)methyl) cyclohexan-1- one (Chiralpak AD-H and a Mobile Phase n-hexane/i-PrPOH= 80/20 (v/v); 1 mL min-1; 254 nm; 25 °C). 260
Figure 178: Chiral HPLC Analysis of Racemic 2-(hydroxyl-(p-nitrophenyl)methyl) cyclohexan-1- one (Chiralpak AD-H and a Mobile Phase n-hexane/i-PrPOH= 80/20 (v/v); 1 mL min-1; 254 nm; 25 ^{0}C). 260
Figure 179: ^{1}H-NMR spectrum ($CDCl_3$, 400 MHz) of **F2**. 263
Figure 180: ^{1}H-NMR Spectrum (MeOD, 400 MHz) of **F3**. 264
Figure 181: ^{1}H-NMR Spectrum (DMSO, 40 MHz) of **G4**. 265
Figure 182: ^{13}C-NMR Spectrum ($CDCl_3$, 100 MHz) of **F2**. 266
Figure 183: ^{13}C-NMR Spectrum (MeOD, 100 MHz) of **F3**. 267
Figure 184: ^{13}C-NMR Spectrum ($CDCl_3$, 100 MHz) of **G4**. 268
Figure 185: ^{1}H-NMR spectrum ($CDCl_3$, 400 MHz) of **PP 4**. 269
Figure 186: ^{1}H-NMR Spectrum ($CDCl_3$, 400 MHz) of **PP 7**. 270
Figure 187: ^{1}H-NMR Spectrum ($CDCl_3$, 400 MHz) of **PP 8**. 271
Figure 188: ^{1}H-NMR Spectrum ($CDCl_3$, 400 MHz) of 1-phenyl alcohol with Ac_2O Using DMAP (Table 11, Entry 1). 272
Figure 189: ^{1}H-NMR Spectrum ($CDCl_3$, 400 MHz) from the Reaction of 1-phenyl alcohol with Ac_2O Using DMAP (Table 11, Entry 2). 273
Figure 190: ^{1}H-NMR Spectrum ($CDCl_3$, 400 MHz) from the Reaction of 1-phenyl alcohol with Ac_2O Using DMAP (Table 11, Entry 3). 274
Figure 191: ^{1}H-NMR Spectrum ($CDCl_3$, 400 MHz) from the Reaction of 1-phenyl alcohol with Ac_2O Using DMAP (Table 11, Entry 4). 275
Figure 192: ^{1}H-NMR Spectrum ($CDCl_3$, 400 MHz) from the Reaction of 1-phenyl alcohol with Ac_2O Using No Catalyst (Table 12, Entry 5) 276
Figure 193: ^{1}H-NMR Spectrum ($CDCl_3$, 400 MHz) from the Reaction of 1-phenyl alcohol with Ac_2O Using No Catalyst (Table 12, Entry 6) 277
Figure 194: ^{1}H-NMR Spectrum ($CDCl_3$, 400 MHz) from the Reaction of 1-phenyl alcohol with Ac_2O Using No Catalyst (Table 12, Entry 7) 278
Figure 195: ^{1}H-NMR Spectrum ($CDCl_3$, 400 MHz) from the Reaction of 1-phenyl alcohol with Ac_2O Using No Catalyst (Table 12, Entry 9) 279
Figure 196: ^{1}H-NMR Spectrum ($CDCl_3$, 400 MHz) from the Reaction of 1-phenyl alcohol with Ac_2O Using **PP 4** (Table 13, Entry 10). 280
Figure 197: ^{1}H-NMR Spectrum ($CDCl_3$, 400 MHz) from the Reaction of 1-phenyl alcohol with Ac_2O Using **PP 4** (Table 13, Entry 11). 281

Figure 198: ^{1}H-NMR Spectrum ($CDCl_3$, 400 MHz) from the Reaction of 1-phenyl alcohol with Ac_2O Using **PP 4** (Table 13, Entry 12). 282
Figure 199: ^{1}H-NMR Spectrum ($CDCl_3$, 400 MHz) from the Reaction of 1-phenyl alcohol with Ac_2O Using **PP 4** (Table 13, Entry 13). 283
Figure 200: ^{1}H-NMR Spectrum ($CDCl_3$, 400 MHz) from the Reaction of 1-phenyl alcohol with Ac_2O Using **PP 4** (Table 13, Entry 14). 284
Figure 201: ^{1}H-NMR Spectrum ($CDCl_3$, 400 MHz) from the Reaction of 1-phenyl alcohol with Ac_2O Using **PP 4** (Table 13, Entry 15). 285
Figure 202: ^{1}H-NMR Spectrum ($CDCl_3$, 400 MHz) from the Reaction of 1-phenyl alcohol with Ac_2O Using **PP 4** (Table 13, Entry 16). 286
Figure 203: ^{1}H-NMR Spectrum ($CDCl_3$, 400 MHz) from the Reaction of 1-phenyl alcohol with Ac_2O Using **PP 4** (Table 14, Entry 17). 287
Figure 204: ^{1}H-NMR Spectrum ($CDCl_3$, 400 MHz) from the Reaction of 1-phenyl alcohol with Ac_2O Using **PP 4** (Table 14, Entry 18). 288
Figure 205: ^{1}H-NMR Spectrum ($CDCl_3$, 400 MHz) from the Reaction of 1-phenyl alcohol with Ac_2O Using **PP 4** (Table 14, Entry 19). 289
Figure 206: ^{1}H-NMR Spectrum ($CDCl_3$, 400 MHz) from the Reaction of 1-phenyl alcohol with Ac_2O Using **PP 4** (Table 14, Entry 20). 290
Figure 207: ^{1}H-NMR Spectrum ($CDCl_3$, 400 MHz) from the Reaction of 1-phenyl alcohol with Ac_2O Using **F2** (Table 15, Entry 21). 291
Figure 208: ^{1}H-NMR Spectrum ($CDCl_3$, 400 MHz) from the Reaction of 1-phenyl alcohol with Ac_2O Using **F2** (Table 15, Entry 22). 292
Figure 209: ^{1}H-NMR Spectrum ($CDCl_3$, 400 MHz) from the Reaction of 1-phenyl alcohol with Ac_2O Using **F2** (Table 15, Entry 23). 293
Figure 210: ^{1}H-NMR Spectrum ($CDCl_3$, 400 MHz) from the Reaction of 1-phenyl alcohol with Ac_2O Using **F2** (Table 15, Entry 24). 294
Figure 211: ^{1}H-NMR Spectrum ($CDCl_3$, 400 MHz) from the Reaction of 1-phenyl alcohol with Ac_2O Using **F2** (Table 15, Entry 25). 295
Figure 212: ^{1}H-NMR Spectrum ($CDCl_3$, 400 MHz) from the Reaction of 1-phenyl alcohol with Ac_2O Using **F2** (Table 15, Entry 26). 296
Figure 213: ^{1}H-NMR Spectrum ($CDCl_3$, 400 MHz) from the Reaction of 1-phenyl alcohol with Ac_2O Using **F2** (Table 15, Entry 27). 297
Figure 214: ^{1}H-NMR Spectrum ($CDCl_3$, 400 MHz) from the Reaction of 1-phenyl alcohol with Ac_2O Using **F2** (Table 15, Entry 28). 298
Figure 215: ^{1}H-NMR Spectrum ($CDCl_3$, 400 MHz) from the Reaction of 1-phenyl alcohol with Ac_2O Using **F2** (Table 15, Entry 29). 299
Figure 216: ^{1}H-NMR Spectrum ($CDCl_3$, 400 MHz) from the Reaction of 1-phenyl alcohol with Ac_2O Using **F2** (Table 16, Entry 30). 300
Figure 217: ^{1}H-NMR Spectrum ($CDCl_3$, 400 MHz) from the Reaction of 1-phenyl alcohol with Ac_2O Using **F2** (Table 16, Entry 31). 301
Figure 218: ^{1}H-NMR Spectrum ($CDCl_3$, 400 MHz) from the Reaction of 1-phenyl alcohol with Ac_2O Using **F3** (Table 17, Entry 32). 302
Figure 219: ^{1}H-NMR Spectrum ($CDCl_3$, 400 MHz) from the Reaction of 1-phenyl alcohol with Ac_2O Using **F3** (Table 17, Entry 33). 303
Figure 220: ^{1}H-NMR Spectrum ($CDCl_3$, 400 MHz) from the Reaction of 1-phenyl alcohol with Ac_2O Using **F3** (Table 17, Entry 34). 304
Figure 221: ^{1}H-NMR Spectrum ($CDCl_3$, 400 MHz) from the Reaction of 1-phenyl alcohol with Ac_2O Using **F3** (Table 17, Entry 35). 305

Figure 222: ^{1}H-NMR Spectrum ($CDCl_3$, 400 MHz) from the Reaction of 1-phenyl alcohol with Ac_2O Using **F3** (Table 17, Entry 36). 306
Figure 223: ^{1}H-NMR Spectrum ($CDCl_3$, 400 MHz) from the Reaction of 1-phenyl alcohol with Ac_2O Using **F3** (Table 17, Entry 37). 307
Figure 224: ^{1}H-NMR Spectrum ($CDCl_3$, 400 MHz) from the Reaction of 1-phenyl alcohol with Ac_2O Using **F3** (Table 18, Entry 39). 308
Figure 225: ^{1}H-NMR Spectrum ($CDCl_3$, 400 MHz) from the Reaction of 1-phenyl alcohol with Ac_2O Using **F3** (Table 18, Entry 40). 309
Figure 226: ^{1}H-NMR Spectrum ($CDCl_3$, 400 MHz) from the Reaction of 1-phenyl alcohol with Ac_2O Using **PP 7** (Table 19, Entry 41). 310
Figure 227: ^{1}H-NMR Spectrum ($CDCl_3$, 400 MHz) from the Reaction of 1-phenyl alcohol with Ac_2O Using **PP 7** (Table 19, Entry 42). 311
Figure 228: ^{1}H-NMR Spectrum ($CDCl_3$, 400 MHz) from the Reaction of 1-phenyl alcohol with Ac_2O Using **PP 7** (Table 19, Entry 43). 312
Figure 229: ^{1}H-NMR Spectrum ($CDCl_3$, 400 MHz) from the Reaction of 1-phenyl alcohol with Ac_2O Using **PP 7** (Table 19, Entry 44). 313
Figure 230: ^{1}H-NMR Spectrum ($CDCl_3$, 400 MHz) from the Reaction of 1-phenyl alcohol with Ac_2O Using **PP 7** (Table 20, Entry 45). 314
Figure 231: ^{1}H-NMR Spectrum ($CDCl_3$, 400 MHz) from the Reaction of 1-phenyl alcohol with Ac_2O Using **PP 7** (Table 20, Entry 47). 315
Figure 232: ^{1}H-NMR Spectrum ($CDCl_3$, 400 MHz) from the Reaction of 1-phenyl alcohol with Ac_2O Using **PP 7** (Table 20, Entry 48). 316
Figure 233: ^{1}H-NMR Spectrum ($CDCl_3$, 400 MHz) from the Reaction of 1-phenyl alcohol with Ac_2O Using **PP 8** (Table 21, Entry 49). 317
Figure 234: ^{1}H-NMR Spectrum ($CDCl_3$, 400 MHz) from the Reaction of 1-phenyl alcohol with Ac_2O Using **PP 8** (Table 21, Entry 50). 318
Figure 235: ^{1}H-NMR Spectrum ($CDCl_3$, 400 MHz) from the Reaction of 1-phenyl alcohol with Ac_2O Using **PP 8** (Table 21, Entry 51). 319
Figure 236: ^{1}H-NMR Spectrum ($CDCl_3$, 400 MHz) from the Reaction of 1-phenyl alcohol with Ac_2O Using **PP 8** (Table 22, Entry 52). 320
Figure 237: ^{1}H-NMR Spectrum ($CDCl_3$, 400 MHz) from the Reaction of 1-phenyl alcohol with Ac_2O Using **PP 8** (Table 22, Entry 53). 321
Figure 238: ^{1}H-NMR Spectrum ($CDCl_3$, 400 MHz) from the Reaction of 1-phenyl alcohol with Ac_2O Using **PP 8** (Table 22, Entry 54). 322
Figure 239: ^{1}H-NMR Spectrum ($CDCl_3$, 400 MHz) from the Reaction of 1-phenyl alcohol with Ac_2O Using **PP 8** (Table 22, Entry 55). 323
Figure 240: ^{1}H-NMR Spectrum ($CDCl_3$, 400 MHz) from the Reaction of 1-phenyl alcohol with Ac_2O Using **PP 8** (Table 22, Entry 56). 324
Figure 241: ^{1}H-NMR Spectrum ($CDCl_3$, 400 MHz) from the Reaction of 1-phenyl alcohol with Ac_2O Using **PP 8** (Table 22, Entry 57). 325
Figure 242: ^{1}H-NMR Spectrum ($CDCl_3$, 400 MHz) from the Reaction of 1-phenyl alcohol with Ac_2O Using **PP 8** (Table 22, Entry 58). 326
Figure 243: ^{1}H-NMR Spectrum ($CDCl_3$, 400 MHz) from the Reaction of 1-phenyl alcohol with Ac_2O Using **PP 8** (Table 22, Entry 59). 327
Figure 244: ^{1}H-NMR Spectrum ($CDCl_3$, 400 MHz) from the Reaction of 1-phenyl alcohol with Ac_2O Using **PP 8** (Table 22, Entry 60). 328
Figure 245: ^{1}H-NMR Spectrum ($CDCl_3$, 400 MHz) from the Reaction of 1-phenyl alcohol with Ac_2O Using **PP 9** (Table 23, Entry 61). 329

Figure 246: ^{1}H-NMR Spectrum ($CDCl_3$, 400 MHz) from the Reaction of 1-phenyl alcohol with Ac_2O Using **PP 9** (Table 23, Entry 62).....330
Figure 247: ^{1}H-NMR Spectrum ($CDCl_3$, 400 MHz) from the Reaction of 1-phenyl alcohol with Ac_2O Using **PP 9** (Table 23, Entry 63).....331
Figure 248: ^{1}H-NMR Spectrum ($CDCl_3$, 400 MHz) from the Reaction of 1-phenyl alcohol with Ac_2O Using **PP 9** (Table 23, Entry 64).....332
Figure 249: ^{1}H-NMR Spectrum ($CDCl_3$, 400 MHz) from the Reaction of 1-phenyl alcohol with Ac_2O Using **PP 9** (Table 23, Entry 65).....333
Figure 250: ^{1}H-NMR Spectrum ($CDCl_3$, 400 MHz) from the Reaction of 1-phenyl alcohol with Ac_2O Using **PP 9** (Table 23, Entry 66).....334
Figure 251: ^{1}H-NMR Spectrum ($CDCl_3$, 400 MHz) from the Reaction of 1-phenyl alcohol with Ac_2O Using **PP 9** (Table 23, Entry 67).....335
Figure 252: ^{1}H-NMR Spectrum ($CDCl_3$, 400 MHz) from the Reaction of 1-phenyl alcohol with Ac_2O Using **PP 9** (Table 24, Entry 68).....336
Figure 253: ^{1}H-NMR Spectrum ($CDCl_3$, 400 MHz) from the Reaction of 1-phenyl alcohol with Ac_2O Using **PP 9** (Table 24, Entry 69).....337
Figure 254: ^{1}H-NMR Spectrum ($CDCl_3$, 400 MHz) from the Reaction of 1-phenyl alcohol with Ac_2O Using **PP 9** (Table 24, Entry 70).....338
Figure 255: ^{1}H-NMR Spectrum ($CDCl_3$, 400 MHz) from the Reaction of 1-phenyl alcohol with Ac_2O Using **PP 9** (Table 24, Entry 71).....339
Figure 256: ^{1}H-NMR Spectrum ($CDCl_3$, 400 MHz) from the Reaction of 1-phenyl alcohol with Ac_2O Using **J1** (Table 25, Entry 72).....340
Figure 257: ^{1}H-NMR Spectrum ($CDCl_3$, 400 MHz) from the Reaction of 1-phenyl alcohol with Ac_2O Using **J1** (Table 25, Entry 73).....341
Figure 258: ^{1}H-NMR Spectrum ($CDCl_3$, 400 MHz) from the Reaction of 1-phenyl alcohol with Ac_2O Using **J1** (Table 25, Entry 74).....342
Figure 259: ^{1}H-NMR Spectrum ($CDCl_3$, 400 MHz) from the Reaction of 1-phenyl alcohol with Ac_2O Using **J1** (Table 25, Entry 75).....343
Figure 260: ^{1}H-NMR Spectrum ($CDCl_3$, 400 MHz) from the Reaction of 1-phenyl alcohol with Ac_2O Using **J1** (Table 25, Entry 76).....344
Figure 261: ^{1}H-NMR Spectrum ($CDCl_3$, 400 MHz) from the Reaction of 1-phenyl alcohol with Ac_2O Using **J1** (Table 25, Entry 77).....345
Figure 262: ^{1}H-NMR Spectrum ($CDCl_3$, 400 MHz) from the Reaction of 1-phenyl alcohol with Ac_2O Using **J1** (Table 25, Entry 78).....346
Figure 263: ^{1}H-NMR Spectrum ($CDCl_3$, 400 MHz) from the Reaction of 1-phenyl alcohol with Ac_2O Using **J1** (Table 25, Entry 79).....347
Figure 264: ^{1}H-NMR Spectrum ($CDCl_3$, 400 MHz) from the Reaction of 1-phenyl alcohol with Ac_2O Using **J1** (Table 25, Entry 80).....348
Figure 265: ^{1}H-NMR Spectrum ($CDCl_3$, 400 MHz) from the Reaction of 1-phenyl alcohol with Ac_2O Using **J1** (Table 25, Entry 81).....349
Figure 266: ^{1}H-NMR Spectrum ($CDCl_3$, 400 MHz) from the Reaction of 1-phenyl alcohol with Ac_2O Using **J1** (Table 25, Entry 82).....350
Figure 267: ^{1}H-NMR Spectrum ($CDCl_3$, 400 MHz) from the Reaction of 1-phenyl alcohol with Ac_2O Using **J1** (Table 25, Entry 83).....351
Figure 268: ^{1}H-NMR Spectrum ($CDCl_3$, 400 MHz) from the Reaction of 1-phenyl alcohol with Ac_2O Using **J1** (Table 26, Entry 84).....352
Figure 269: ^{1}H-NMR Spectrum ($CDCl_3$, 400 MHz) from the Reaction of 1-phenyl alcohol with Ac_2O Using **J1** (Table 26, Entry 85).....353

Figure 270: ^{1}H-NMR Spectrum ($CDCl_3$, 400 MHz) from the Reaction of 1-phenyl alcohol with Ac_2O Using **J1** (Table 26, Entry 86).....354
Figure 271: ^{1}H-NMR Spectrum ($CDCl_3$, 400 MHz) from the Reaction of 1-phenyl alcohol with Ac_2O Using **J1** (Table 26, Entry 87).....355
Figure 272: ^{13}C-NMR Spectrum ($CDCl_3$, 100 MHz) of Reaction of 1-phenyl alcohol with Ac_2O.....356

Scheme 1: Rutter's mechanism for aldolase enzymes. 4
Scheme 2: The Hajos-Parrish-Eder-Sauer-Wiechert reaction mechanism.[8].....5
Scheme 3: Direct asymmetric aldol reaction catalyzed by proline.[7] 5
Scheme 4: The catalytic cycle of enamine activation.[7].....6
Scheme 5: The two stereochemical modes with enamine catalysis.[12].....7
Scheme 6: Organocatalyzed Diels-Alder reaction between cinnamaldehyde and cyclopentadiene.[10] .7
Scheme 7: The catalytic cycle of iminium activation.[12] 8
Scheme 8: Mannich reaction between isatin-imines and hydroxyacetone.[14].....9
Scheme 9: Possible transition state of Mannich reaction.[14].....10
Scheme 10: Catalytic Michael addition using a molecular motor.[15].....11
Scheme 11: Catalyst's structure depending on the step of the cycle, where: Step 1 (312 nm, 20 °C), Step 2 (70 °C), Step 3 (312 nm, -60 °C), Step 4 (-10 °C).[15].....12
Scheme 12: Aldol reaction catalyzed by peptide catalysts.[29] 15
Scheme 13: Aldol asymmetric reaction catalyzed by peptidic catalysts.[28].....16
Scheme 14: Aldol reaction catalyzed by diastereoselective peptide catalyst.[30] 17
Scheme 15: The possible products of an aldol reaction.[76] 25
Scheme 16: Types of catalyzed asymmetric acyl transfer process.[12,80] 26
Scheme 17: Aldol Reaction between p-nitrobenzaldehyde and cyclohexanone. 30
Scheme 18: Kinetic resolution of racemic alcohol 1-phenylethanol. 32
Scheme 19: Synthesis of proline NCA.[90] 41
Scheme 20: Diketopiperazine formation during the synthesis of peptides consisted of proline units.[98] 43
Scheme 21: Mechanism of DIC/HOBt coupling.[96].....46
Scheme 22: Epimerisation/racemisation mechanism through oxazolone intermediate.[100] 47
Scheme 23: Ninhydrin test.[102].....48
Scheme 24: Synthesis of N-Fmoc-trans-4-Boc-amino-L-proline (**A7**). 52
Scheme 25: Synthesis of N-Fmoc-trans-4-Boc-amino-L-proline (**B2**). 53
Scheme 26: Synthesis of (S)-1-N-Boc-4-N-Fmoc-piperazine-2-carboxylic acid (**C2**). 54
Scheme 27: Synthesis of N-Fmoc-trans-4-phenyl-L-proline (**C3**).....55
Scheme 28: 4-N-acetyl-piperazine-2-carboxylic acid (**E3**). 55
Scheme 29: Schematic representation for the solid-phase peptide synthesis (SPPS) using proline. ..58
Scheme 30: Aldol Reaction between p-nitrobenzaldehyde and cyclohexanone. 68
Scheme 31: Benzalcyclohexanone.....73
Scheme 32: Future reaction scheme for the synthesis of N-Fmoc-trans-4-Boc-amino-L-proline (**A7**). 83
Scheme 33: Reaction pathway for the synthesis of future monomer.....84
Scheme 34: KR of a sec-alcohol catalyzed by tetrapeptides.[126].....107
Scheme 35: KR of a sec-alcohol catalyzed by octapeptides.[83].....108
Scheme 36: KR of sec-alcohol catalyzed by a 4-PYY peptide.[129] 109
Scheme 37: Synthesis of N-Fmoc-trans-4-hydroxypyridine-L-proline (**F3**).....111
Scheme 38: KR of racemic alcohol 1-phenylethanol using **PP 4** as an organocatalyst.....114

Scheme 39: Synthetic attempts of monomers **G2**, **G4**, **G6**, **G8**. 131
Scheme 40: Synthetic attempt of **I2**. 134
Scheme 41: KR of racemic alcohol 1-phenylethanol using **PP 7** and **PP 8** as an organocatalyst..... 140

List of Tables

Table 1: Structures of Target Peptide Group 5-6.....31
Table 2: Preparation of the Kaiser Test Reagents. 48
Table 3: Coupling Reagents and Equivalents Used for the Synthesis of Each Peptide.....60
Table 4: Coupling Reagents and Equivalents Used for the Synthesis of Each Peptide.....61
Table 5: Optimization of Aldol Reaction Conditions Using **PP 1**.....71
Table 6: Optimization of Aldol Reaction Conditions Using **PP 2.**.....74
Table 7: Optimization of Aldol Reaction Conditions Using **PP 3.**.....76
Table 8: Optimization of Aldol Reaction Conditions Using **E3**.....78
Table 9: Optimization of Aldol Reaction Conditions Using **L-proline**. 79
Table 10: Structures of Target Peptide Groups 5 and 6. 110
Table 11: KR of Racemic 1-phenyl alcohol Using DMAP at RT.....115
Table 12: KR of Racemic 1-phenyl alcohol Using No Catalyst at RT. 116
Table 13: KR of Racemic 1-phenyl alcohol Using **PP 4** at RT.....116
Table 14: KR of Racemic 1-phenyl alcohol Using **PP 4** at 0 ℃. 119
Table 15: KR of Racemic 1-phenyl alcohol Using **F2** at RT. 121
Table 16: KR of Racemic 1-phenyl alcohol Using **F2** at 0 ℃.....124
Table 17: KR of Racemic 1-phenyl alcohol Using **F3** at RT. 126
Table 18: KR of Racemic 1-phenyl alcohol Using **F3** at 0 °C.....128
Table 19: KR of racemic 1-phenyl alcohol Using **PP 7** at RT.....141
Table 20: KR of Racemic 1-phenyl alcohol Using **PP 7** at 0 °C. 144
Table 21: KR of Racemic 1-phenyl alcohol Using **PP 8** at RT.....146
Table 22: KR of Racemic 1-phenyl alcohol Using **PP 8** at 0 °C. 148
Table 23: KR of Racemic 1-phenyl alcohol Using **PP 9** at RT.....151
Table 24: KR of Racemic 1-phenyl alcohol Using **PP 9** at 0 ℃. 153
Table 25: KR of Racemic 1-phenyl alcohol Using **J1** at RT. 155
Table 26: KR of Racemic 1-phenyl alcohol Using **J1** at 0 ℃. 157

Chapter 1

Introduction

Context

This study concerns the use of polyproline peptides as stereodivergent catalysts in organocatalysis, in the aldol reaction, and as enantioselective organocatalysts in the acyl transfer reaction. In this context, after introducing the importance of chirality, this chapter presents the field of organocatalysis, with a brief historical overview. Stereodivergent organocatalysis along with some examples of stereodivergent catalysts, is then analysed. The characteristics of peptides are then analysed and some examples of peptide catalysts are discussed. Lastly, this chapter analyses the characteristics of polyprolines as peptides.

1.1 Introduction

1.1.1 Chirality

Chirality is an important feature of the living world.[1] Most of the building blocks in nature are chiral, while they are mostly found in one stereoisomer.[1] For example, the natural amino acids which constitute the building blocks of proteins are usually found in the L-form.[1] Moreover, in the case of DNA and RNA, only the D-form of the monosaccharide sugars appear as minimum units.[1] Apart from that, many compounds that exhibit physiological activity are also chiral like drugs, pesticides and flavourings.[2] One enantiomer often shows desirable activity and the other presents an unfavourable one.[2] Some examples include the drug L-DOPA which is used for the treatment of Parkinson's disease, in contrast to its enantiomer which is inactive, as well as R-carvone which is a spearmint-smelling, while its enantiomer smells of caraway (Figure 1).[1] From these examples it is apparent that the selective synthesis of enantiomerically pure molecules is of outmost importance for many fields.[2,3] Enantioselective organocatalysis is a promising strategy in this regard.

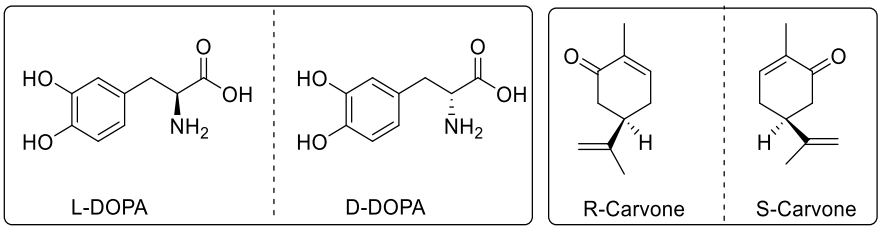

Figure 1: Enantiomers of DOPA (left) and Carvone (right).

1.1.2 Organocatalysis

Organocatalysis is defined as *"the acceleration of chemical reactions by employing a sub-stoichiometric quantity of a chiral organic compound that does not contain a metal atom"*.[4]

Characterized by operational simplicity, as well as availability and low toxicity of the catalyst, it is a very advantageous method for the synthesis of compounds with high enantiopurity.[5]

Despite being relatively new, it is a rapidly growing field over the last decades,[6] and is now widely accepted as one of the main branches of enantioselective synthesis,[7] at such a level that it is considered as a mode complementary to metal-catalyzed transformations.[5,7] Metal-based catalysts have many benefits, but the main drawbacks are that some organometallic systems are sensitive to air and moisture, while being toxic and expensive.[7] Nevertheless, most reactions in organocatalysis are tolerant to water and air, easy to perform, less expensive and usually have fewer toxicity issues.[5] Therefore, as the cost is lower and larger quantities can be used without toxicity issues,[7] organocatalysis is more advantageous than the conventional metal catalysis.[5]

In order to understand how organocatalysis was developed, it is important to have a brief historical overview of the field.

1.1.2.1 Historical Overview

Before 1997, only a few reports demonstrated the catalytic action of small organic compounds in asymmetric reactions. In 1964, a mechanism was proposed by Rutter for aldolase enzymes (Scheme 1), while in 1971 the Hajos-Parrish-Eder-Sauer-Wiechert reaction was discovered (Scheme 2).[5,7] Nevertheless, these publications focused on individual transformations, rather than establishing a general concept.[7] Therefore, the principles behind organocatalysis were not recognised.[7]

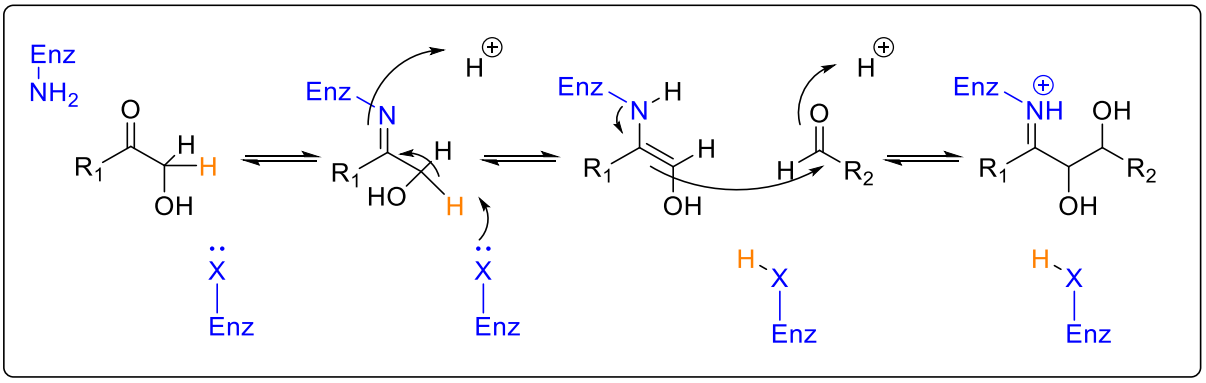

Scheme 1: Rutter's Mechanism for Aldolase Enzymes.

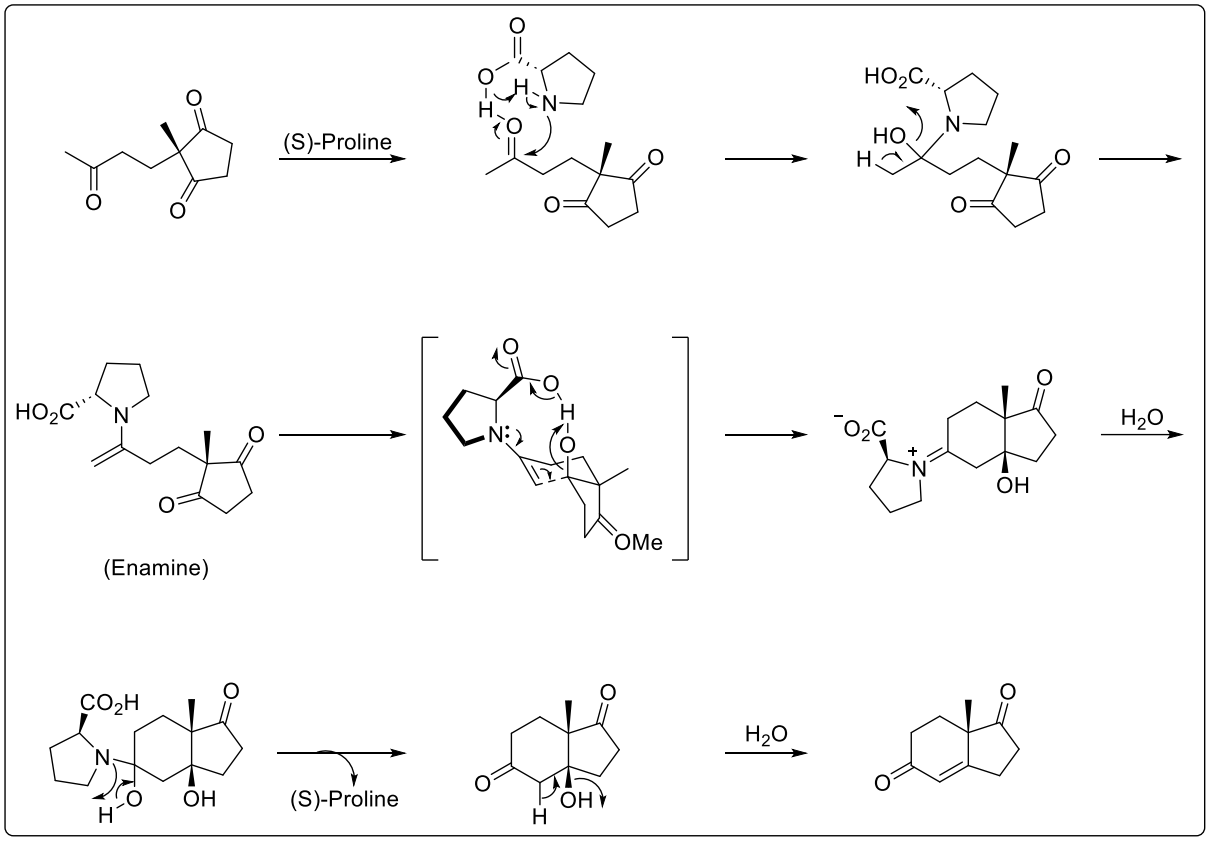

Scheme 2: The Hajos-Parrish-Eder-Sauer-Wiechert Reaction Mechanism.[8]

Organocatalysis emerged as a field after two publications in 2000, one by List, Lerner and Barbas and one by Ahrendt, Borths and MacMillan.[9,10] The former group showed that proline can be employed as a catalyst for the direct asymmetric aldol reaction between acetone and a range of aldehydes,[11] using the enamine mode in order to functionalize carbonyl-compounds at the α-carbon.[7] Using acetone and 4-nitrobenzaldehyde as starting materials, the product was obtained in 68 % yield and 76 % enantioselectivity (ee) (Scheme 3).[9] The importance of this work is that the underlying Hajos-Parrish reaction mechanism could be extended in other transformations.[11] Additionally, it was concluded that small molecules like proline were able to catalyze reactions in a similar manner as enzymes, through the enamine formation.[9]

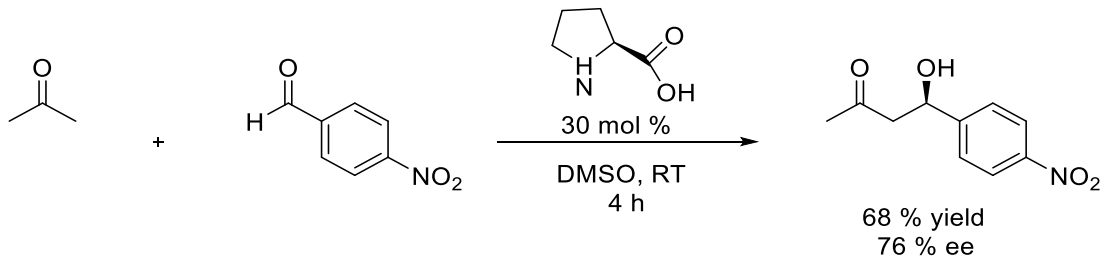

Scheme 3: Direct Asymmetric Aldol Reaction Catalyzed by Proline.[7]

In the enamine catalysis, the amine-containing catalyst interacts with the substrate, forming an enamine intermediate (Scheme 4).[7] At the same time, it interacts with an electrophile via hydrogen

bonding or electrostatic interaction.[7] Thus, it can also be described as a bifunctional type of catalysis.[7] Many enantioselective carbonyl α-functionalization processes have been developed through this type of activation.[7]

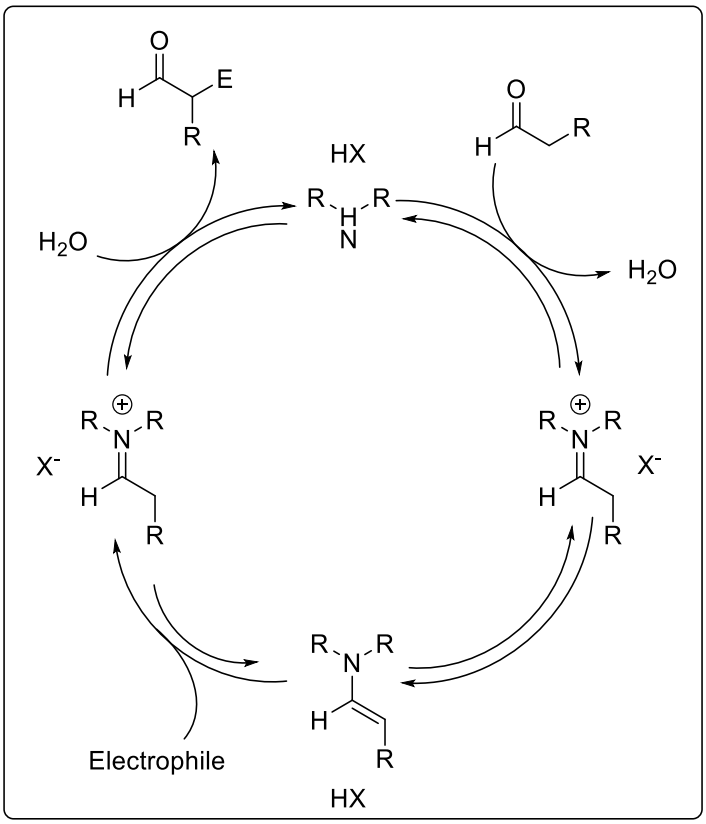

Scheme 4: The Catalytic Cycle of Enamine Activation.[7]

In enantioselective enamine catalysis, the enamine plays an important role, as it can direct the approach of the electrophile.[12] Enamine catalysts can be categorised as Type A and Type B catalysts (Scheme 5).[12] The former directs the approach of the electrophile through an internal acid/hydrogen bond donor, whereas the latter includes a bulky and non-acidic group which directs the enamine and blocks the approach of the electrophile from one side.[12] Simple amino acids like proline belong to Type A catalysts, and are usually employed for aldol and Mannich.[12]

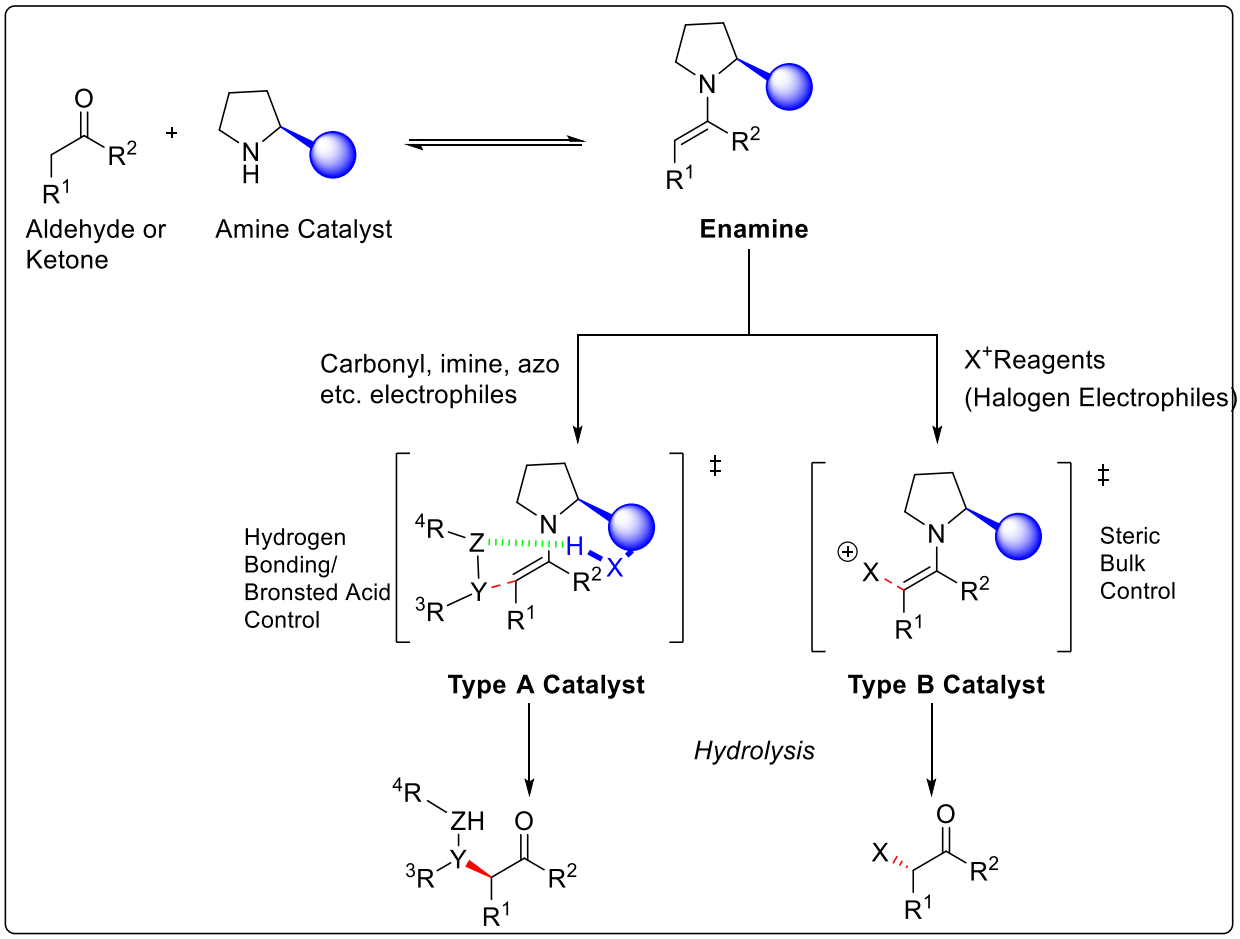

Scheme 5: The Two Stereochemical Modes with Enamine Catalysis.[12]

The second publication that altered the field of organocatalysis was by Ahrendt, Borths, and MacMillan and demonstrated the first highly enantioselective amine-catalyzed Diels-Alder reaction, through the iminium catalysis (Scheme 6).[10] Cyclopentadiene and cinnamaldehyde were the starting materials used, forming the product in 99 % yield, 1.3:1 exo: endo and 93 % ee.[10] This study showed how a general activation mode was employed for a number of reaction classes, while introducing the term organocatalysis to the literature.[10] Following these publications and due to the highlighted advantages of the method, the field of organocatalysis progressed rapidly.[7]

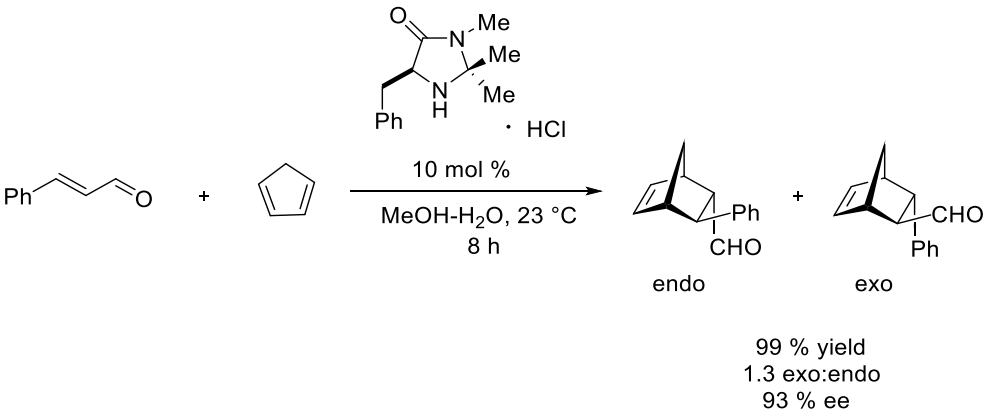

Scheme 6: Organocatalyzed Diels-Alder Reaction between Cinnamaldehyde and Cyclopentadiene.[10]

The iminium activation mode was the first mode that was ''*designed as a general strategy for asymmetric organic synthesis*''.[7] During this mode, condensation of chiral secondary amines with α, β-unsaturated aldehydes or ketones forms the iminium ion (Scheme 7).[5,6] The energy of the Lowest Unoccupied Molecular Orbital (LUMO) of the iminium ion is lowered, and as a result its electrophilicity is increased, and it can interact with nucleophiles.[5,6]

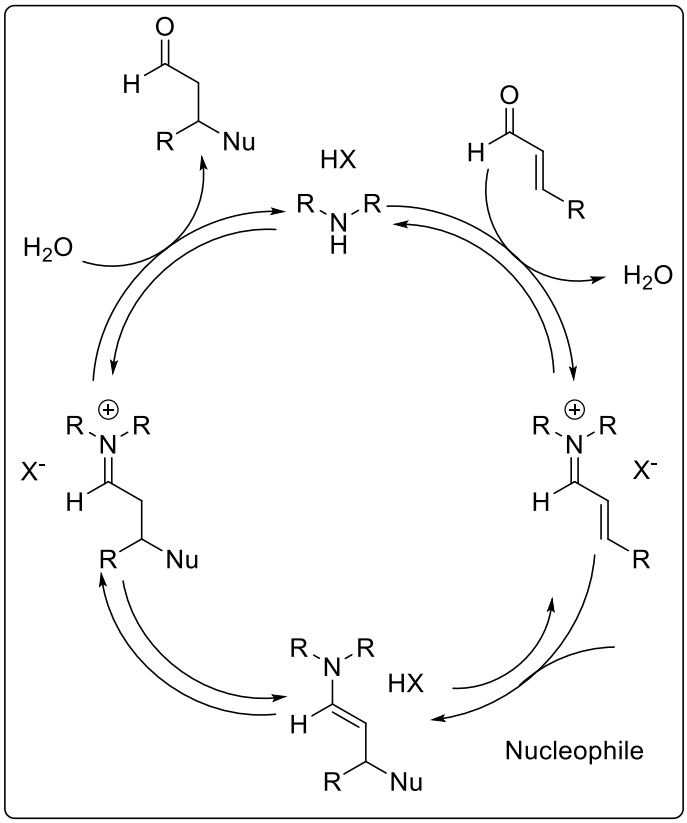

Scheme 7: The Catalytic Cycle of Iminium Activation.[12]

1.1.2.2 Stereodivergent Organocatalysis

Apart from enantioselective organocatalysis, another category is stereodivergent organocatalysis. Traditionally, in order to obtain each diastereomer or enantiomer of a product, separate reactions had to be performed.[3] Nevertheless, through stereodivergence, access to different stereoisomers from the same starting materials can be achieved.[3,13] Thus, it is a very important process in cases where obtainment of both diastereomeric or enantiomeric products is crucial, at the same time that it is characterized by efficiency and atom economy.[3]

Many stereodivergent reactions have been reported in the last 30 years, including metal-catalyzed and organocatalyzed processes.[3] The former usually includes structural changes of the ligand or the metal, while in the latter structural modifications of the organocatalysts are required.[2,3] Nevertheless, other factors apart from structural changes have also been shown to impact the stereo-control, like changes in the reaction conditions such as solvent, temperature, pressure, and

additives can also determine the stereodivergence.[2,3] In order to better understand how stereodivergent organocatalysis works and its different approaches, some examples of stereodivergent catalysts are discussed below.

1.1.2.2.1 Examples of Stereodivergent Catalysts

One such example is the solvent-dependent diastereodivergent synthesis. In this case, the solvent influences the stereochemical outcome and as a result, its selection is crucial.[14]

Guo *et al*. showed in 2012 that a chiral primary amino acid was able to act as a catalyst for an enantioselective diastereodivergent Mannich reaction.[14] Using isatin-imines and hydroxyacetone as stating materials, both the anti- and syn-oxindoles were formed in high yields (98 % and 88 % respectively) and enantioselectivities (99 % and 91 % respectively).[14] When diethyl ether was employed as a solvent, the anti-product was dominating, whereas when toluene was the solvent of choice, the syn-product was preferably formed (Scheme 8).[14]

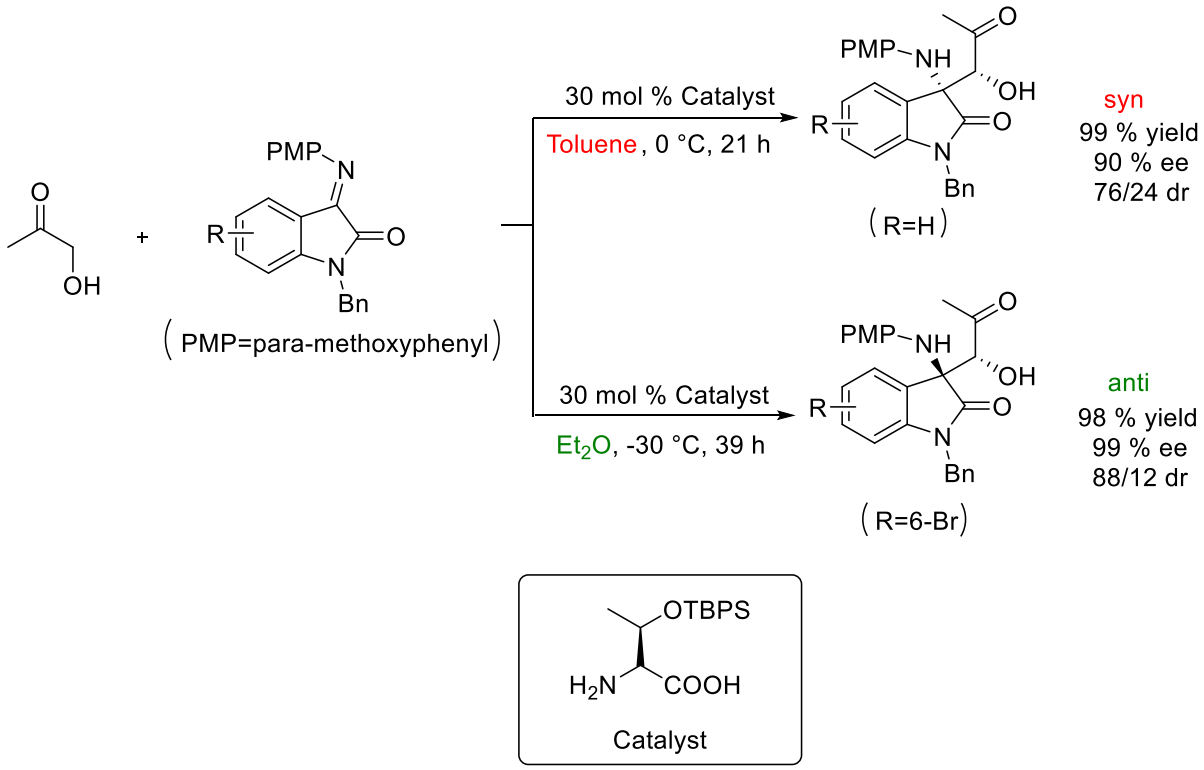

Scheme 8: Mannich Reaction between Isatin-imines and Hydroxyacetone.[14]

After investigating the underlying mechanistic pathways, it was revealed that there is a dynamic equilibrium between the E and Z isomers of the isatin imine (Scheme 9), while their ratio was dependant on the solvent.[14] The two isomers lead to two different transition states, **TSIII** and **TSIV**, which generate the anti-product and the syn-product respectively.[14]

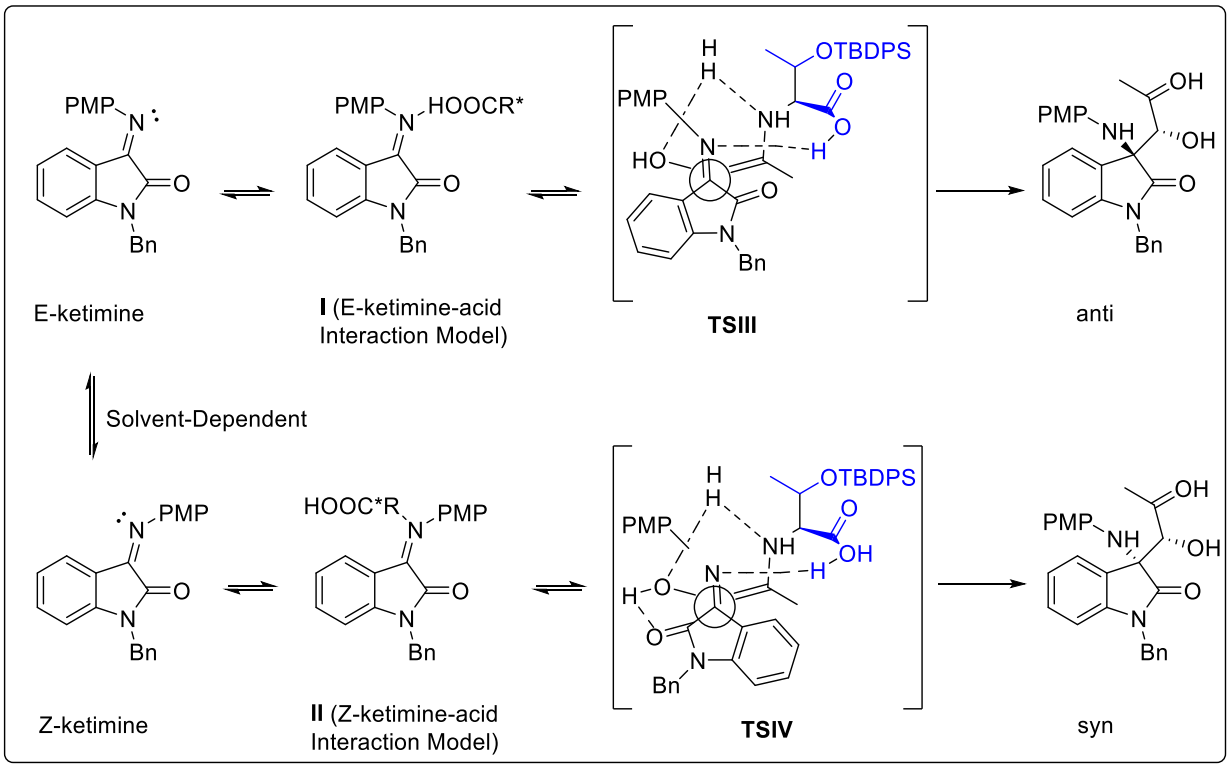

Scheme 9: Possible Transition State of Mannich Reaction.[14]

There are also other approaches for the switch of a chiral catalyst. One example is a molecular motor comprised of a ''*rotor*'' and a ''*stator*'' with an alkene moiety between them.[15] The structure of the catalyst is shown in Scheme 10 where A and B symbolize DMAP and thiourea respectively and therefore represent a bifunctional organocatalyst.[15] Through photochemical and thermal stimuli, a clockwise rotary cycle around the axle occurs, causing a stepwise switch on the position and configuration of A and B (steps one and two).[15] The two groups can be ''*remote*'' (stage I), in ''*close proximity*'' having an M helicity (stage II) or in ''*close proximity*'' with a P helicity (stage III).[15] Depending on the step of the cycle, the racemate (R, S), the one enantiomer or the other enantiomeric product is formed.[15] Through steps three and four the catalyst reaches the initial point.[15]

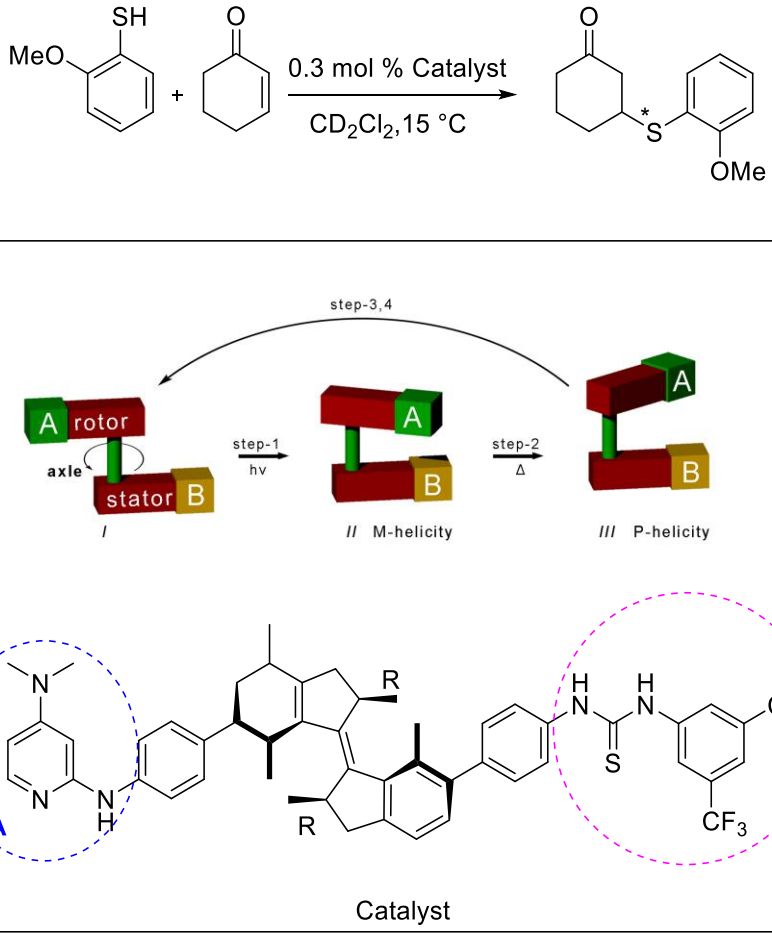

Scheme 10: Catalytic Michael Addition Using a Molecular Motor.[15]

More specifically, once the (P, P)-trans-**1** isomer of the catalyst was used in the Michael addition reaction, a racemic product (R, S) was formed in 7 % yield after 15 hours (Scheme 11). During the first step of the cycle, after photoisomerization, (P, P)-trans-**1** was converted to (M, M)-cis-**1**, which catalyzed the reaction faster, forming the (S)-enantiomeric product in 50 % yield and 75/25 enantiomeric ratio (er) (S/R). After a thermal helix inversion (step two), the isomer (P, P)-trans-**1** was converted to (P, P)-cis-**1**. Once used as catalyst for the asymmetric Michael addition, 83 % yield and inversion in the enantioselectivity were observed, with an er of 23/77 (S/R).

These results can be explained as the chirality of the stereogenic centers of the motor influences the helicity of the motor, and as a consequence, the orientation of the catalytic groups, leading to a different product configuration (R or S) of the catalytic reaction. The advantage of this system over other light-driven process is that through this catalytic molecular motor, control on the catalytic activity and stereoselectivity is achieved.[15]

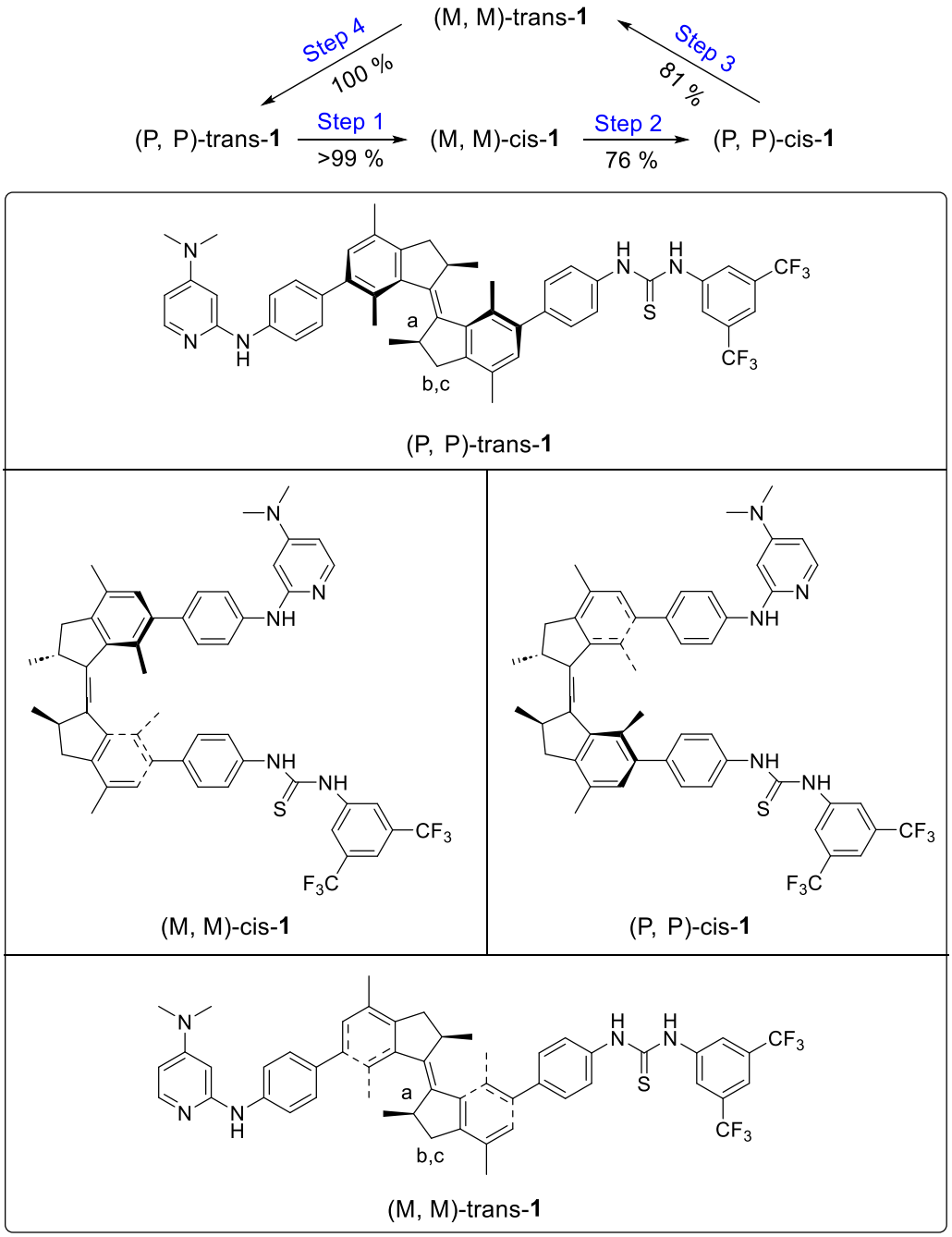

Scheme 11: Catalyst's Structure Depending on the Step of the Cycle, where: Step 1 (312 nm, 20 °C), Step 2 (70 °C), Step 3 (312 nm, -60 °C), Step 4 (-10 °C).[15]

In conclusion, the first example led to high yields and enantioselectivities, while a mechanistic explanation was also provided for this solvent-dependent behaviour. Regarding the second example, depending on the helicity of the motor, different configurations of the catalytic product are achieved, through a light-driven process. Therefore, from these examples it is apparent that there are different strategies in order to achieve stereodivergence.

Among various catalysts, peptides exhibit some unique properties making them very promising catalysts in enantioselective and stereodivergent organocatalysis. The reasons behind this are discussed in the following sections.

1.1.3 Peptides as Organocatalysts

Peptides are short chains comprised of amino acids residues (Figure 2).[16] The residues in a peptide are linked through peptide bonds between the carboxyl group of one amino acid and the amino group of another one.[16] Typically, peptides are distinguished from proteins by their shorter length, as they are typically built by less than 100 amino acids.[17] A peptide has a primary structure, which is the sequence of amino acids in the polypeptide chain, as well as a secondary structure which refers to *''the conformation of the peptide backbone and the three-dimensional arrangement of side chain groups''*.[16,18]

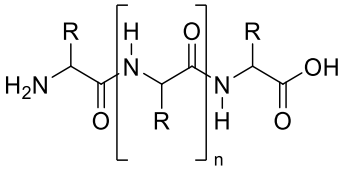

Figure 2: General Structure of a Peptide.[24]

A peptide has three main chain torsion angles: phi (ϕ), psi (ψ) and omega (ω) (Figure 3).[19] The first one is the angle between the alpha carbon and the nitrogen of the amine, while the second one is the angle between the alpha carbon and the carbon of the carbonyl group of the carboxylic acid group.[19] Lastly, omega refers to the angle of the peptide bond.[19] Omega is planar and can be either 0° or 180°, due to the partial double bond character of the peptide bond.[19] Nevertheless, phi and psi are able to rotate, leading to a three-dimensional structure.[19]

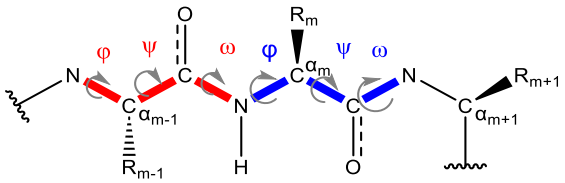

Figure 3: Illustration of the Peptide Bond and the Three Torsion Angles.[19]

Although they used to be considered unsuitable for catalysis, due to their unique advantages, short peptides have proved to be excellent asymmetric catalysts for various enantioselective organic transformations.[20,21] More specifically, they are characterized by structural simplicity, compared to the complexity of enzymes, as well as functional diversity.[20] As they can be comprised of a wide range of many amino acids, they offer the possibility of creating various combinations.[22] At the same time, functional groups can be incorporated in their side chains, leading to different interactions with substrates.[23] In addition, the synthesis of the opposite enantiomer can be easily achieved, which is usually not possible with natural enzymes, and the catalytic efficiency can easily be improved by alternating the amino acid sequence.[20] Moreover, small peptides comprised of less than ten amino acids, are easily prepared, while they are generally stable to air and moisture environments.[22–25]

Therefore, the development of smaller peptide catalysts is a promising field to explore as it will offer solutions to practical issues faced in organic synthesis,[26] while preserving the benefits of a small molecule catalyst.[27] Some examples of peptides that have been employed as organocatalysts are discussed below in order to obtain a better understanding of their action.

1.1.3.1 Examples of Peptides as Catalysts

In recent years, several peptide organocatalysts have been employed in asymmetric catalysis, leading to high yields and stereoselectivities.[28] Da and coworkers developed peptide-organocatalysts for the aldol asymmetric reaction between 4-nitrobenzaldehyde and acetone (an example of which is shown in Scheme 12).[29] The tetrapeptide contained a N-terminal primary amine group, which is also found in the active center of natural aldolases.[29] Moreover, they adopted a stable β-turn structure in methanol (MeOH), a common secondary structure observed in proteins.[29]

Based on the results, it is noteworthy that peptides with less than four units were characterized by significantly lower enantioselectivities, while the C-terminal carboxylic acid was found to have an important role in achieving high enantioselectivities.[29] Moreover, the enantioselectivity appeared to be solvent-dependent as the configuration of the aldol products was influenced by changing only the polarity of the solvent.[29] The R-product was obtained when strongly polar solvents like MeOH were employed, whereas the S-product was formed upon usage of apolar or weakly polar solvents like 1,2-dichloroethane (DCE).[29] More specifically, using 4-nitrobenzaldehyde and acetone as starting materials and MeOH as a solvent in the presence of benzoic acid, the product was obtained in 58 % yield and 95 % ee.[29] According to the results, the clear β-turn secondary structure in MeOH contributes to the conformation of the aldol product in this solvent and its high enantioselectivity, whereas the varied conformation observed in DCE contributes to the production of the S-product in low enantioselectivity.[29] It was speculated that different solvents have different influence on the secondary structure, leading to a different stereochemical outcome.[29]

Furthermore, the enantioselectivity of the reaction of the same aldehyde with hydroxyacetone was not influenced upon usage of different solvents.[29] Using acetonitrile (MeCN) as a solvent and (S)-BINOL as an additive, the product was obtained in 99 % yield, 87 % ee and 74/26 anti/syn ratio.[29] Among different additives, (S)-BINOL proved to be the optimal one.[29] In addition, both (S)- and (R)-BINOL led to the same configuration of aldol product.[29] It was thus suggested that BINOL acted as a co-catalyst, enhancing the catalytic activity of the peptide.[29]

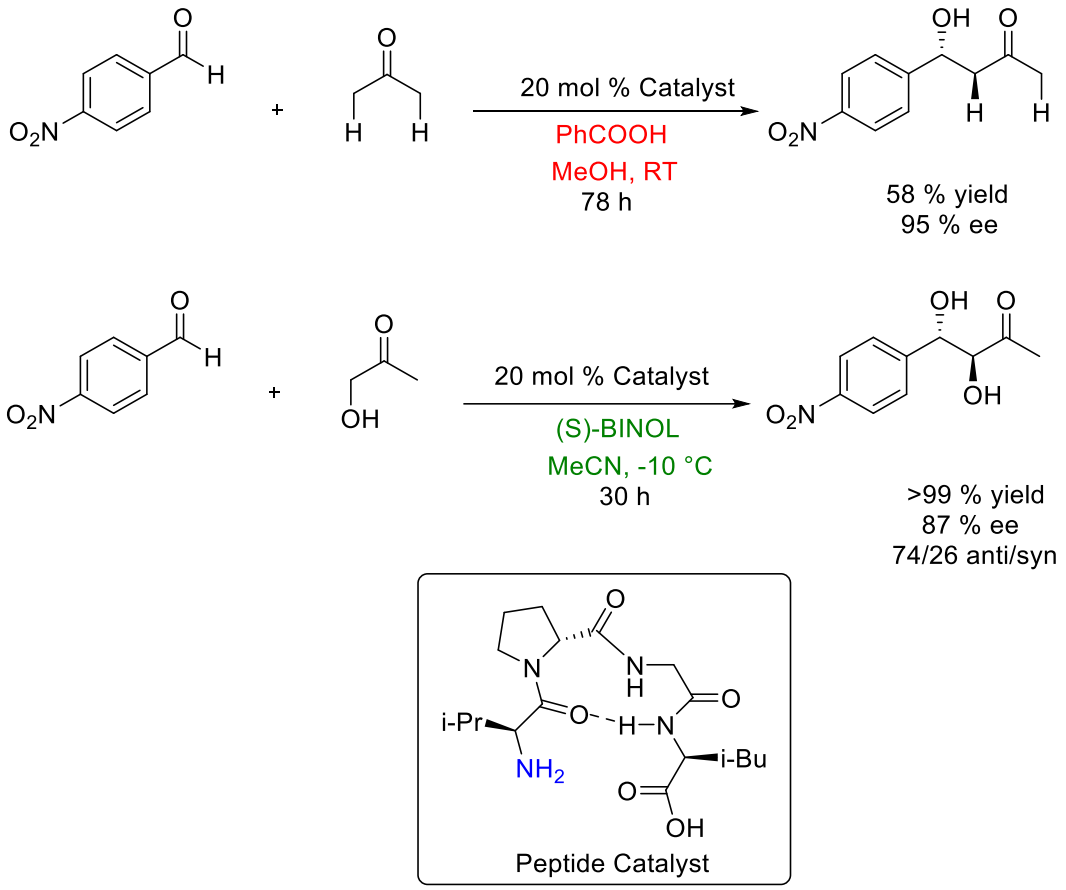

Scheme 12: Aldol Reaction Catalyzed by Peptide Catalysts.[29]

Illa, Ona *et al*. reported the synthesis of six novel tripeptides comprised of two L- or D-proline units and the β- or γ-enantiomer of cyclobutane in the middle (β-tripeptides or γ-tripeptide respectively).[28] The peptides were then tested as catalysts in the asymmetric aldol reaction between various aldehydes and acetone or cyclohexanone (Scheme 13).[28] According to the results, the γ-tripeptide led to higher yields and enantioselectivities than the β-tripeptide, possibly due to the high rigidity of the β-cyclobutane, which hinders some of the peptide catalysts to adopt the proper active conformation (yield up to 99 %, enantiomeric ratio (er) up to 93/7).[28] It is noteworthy that when catalysts **1**-**4** were employed in acetone, the S-product was the dominant one, whereas upon usage of ent-**3** and ent-**4** in anhydrous acetone, the major product was the R.[28] As a result, the configuration of the aldol products was controlled by the chirality of the proline units at the two ends of the tripeptide organocatalyst.[28]

Moreover, the selectivities of catalysts **1** and **2** proved to be similar in aqueous and non-aqueous solvents, whereas the selectivities of peptides **3** and **4** were higher upon usage of aqueous solvents.[28] A possible explanation for this observation is that ''water may compete with acetone to interact with the catalyst''.[28] For example, peptide **4** forms a more stable complex with water than

with acetone.[28] As a result, an increase in the concentration of water can lead to a decrease in the concentration of complex **4**-acetone, which consequently reduces the reaction rate.[28]

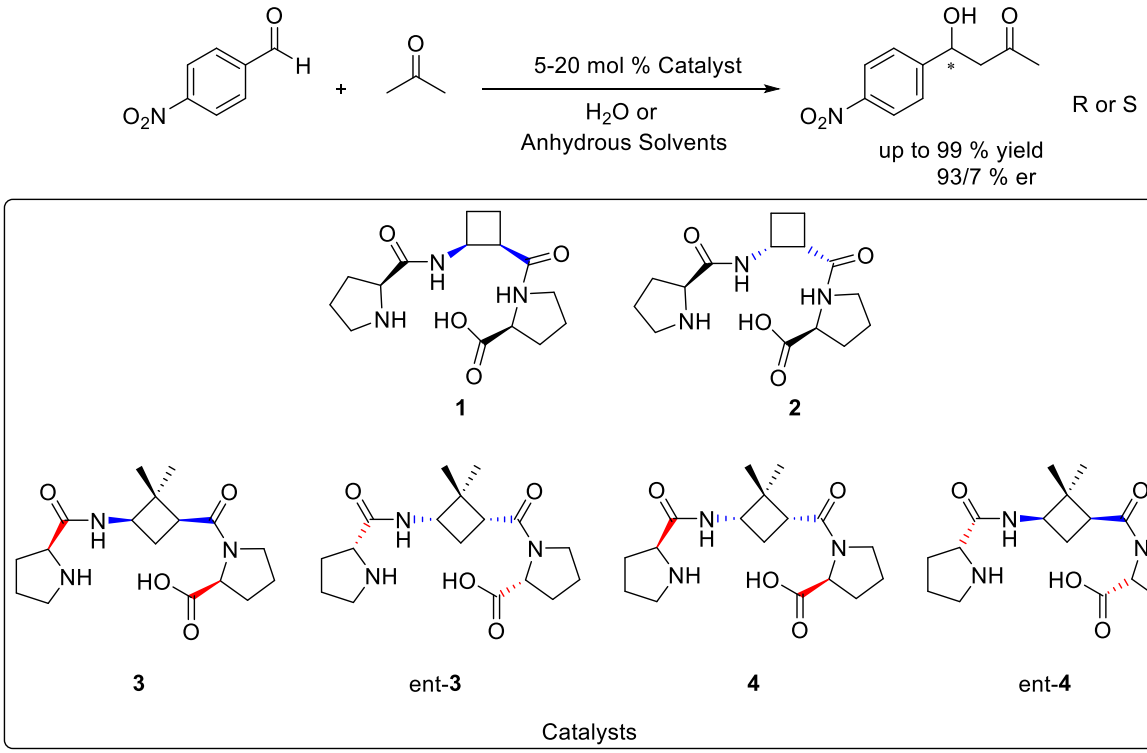

Scheme 13: Aldol Asymmetric Reaction Catalyzed by Peptidic Catalysts.[28]

Another factor that appeared to influence the enantioselectivity was the solvent.[28] Contrary to before, the R-product was the major one when catalysts **1**, **3** and **4** were used in water, while the S-product was dominant upon usage of ent-**3** and ent-**4**.[28] When **2** was employed as a catalyst for the aldol asymmetric reaction, a racemic product was obtained.[28] Through analysing the mechanism of the reaction, one can conclude that the transition state that determined the enantioselectivity is the one between the enamine and the aldehyde.[28] During the nucleophilic attack of the enamine to the carbonyl group of the aldehyde, there are two possible cases: if the attack occurs to the Re-face of the aldehyde, then the R enantiomer will be formed, whereas if the attack happens to the Si-face, the S-enantiomer will be produced (Figure 4).[28] Both experimental and theoretical data showed that the approach from the Re-face of the aldehyde is the favourable one.[28]

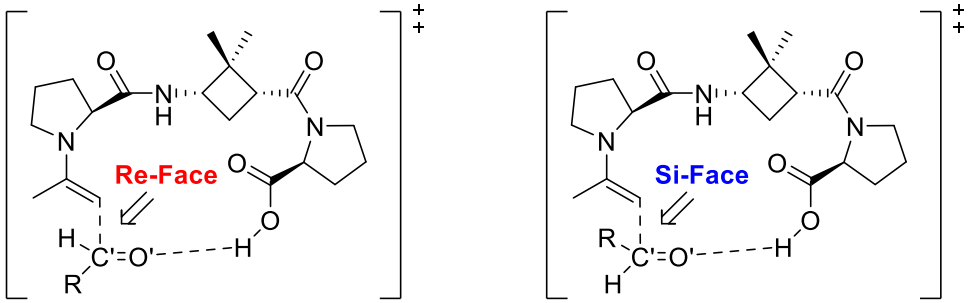

Figure 4: Schematic Representation of the Transition States Corresponding to the Aldol Reaction Between Acetone and p-Nitrobenzaldehyde Catalyzed by the Tripeptide.[28]

Another example of a peptide-based organocatalyst was developed by Messerer and Wennemers who prepared a peptide whose enantioselectivity was reversed in two different environments (Scheme 14).[30] More specifically, pure dimethyl sulfoxide (DMSO) or MeOH were the solvents of choice in one case, whereas a mixture of water with DMSO or MeOH was used in the other case.[30] Since the tripeptides had been already proved to catalyze the aldol reaction, and aiming to improve the peptide's solubility, a new peptide with a long N-alkyl amide chain was then prepared, instead of the previously used primary amide.[30] An analysis of the results highlighted that this peptide was as effective in the aldol reaction between cyclohexanone and 4-nitrobenzaldehyde, as the initial one.[30] As a result, the alkyl chain did not influence the enantioselectivity, while the anti-product was favoured.[30] Nevertheless, the solvent did influence the observed enantioselectivity.[30] In the presence of DMSO, the (R)-isomer was formed in high yield (98 %) and good enantioselectivity (55 % ee).[30] When water was added in DMSO, a switch was observed in the configuration of the product, as the (S) was the dominant isomer this time.[30] The enantioselectivity for the reaction in DMSO and 10 % water was 69 %. [30] Using CD spectroscopy, the peptide's conformation was analyzed.[30] According to the results, it was proved that upon solvent change, a conformational switch occurred from a β-turn to a conformation that has the opposite twist sense, leading to the reverse enantioselectivity.[30]

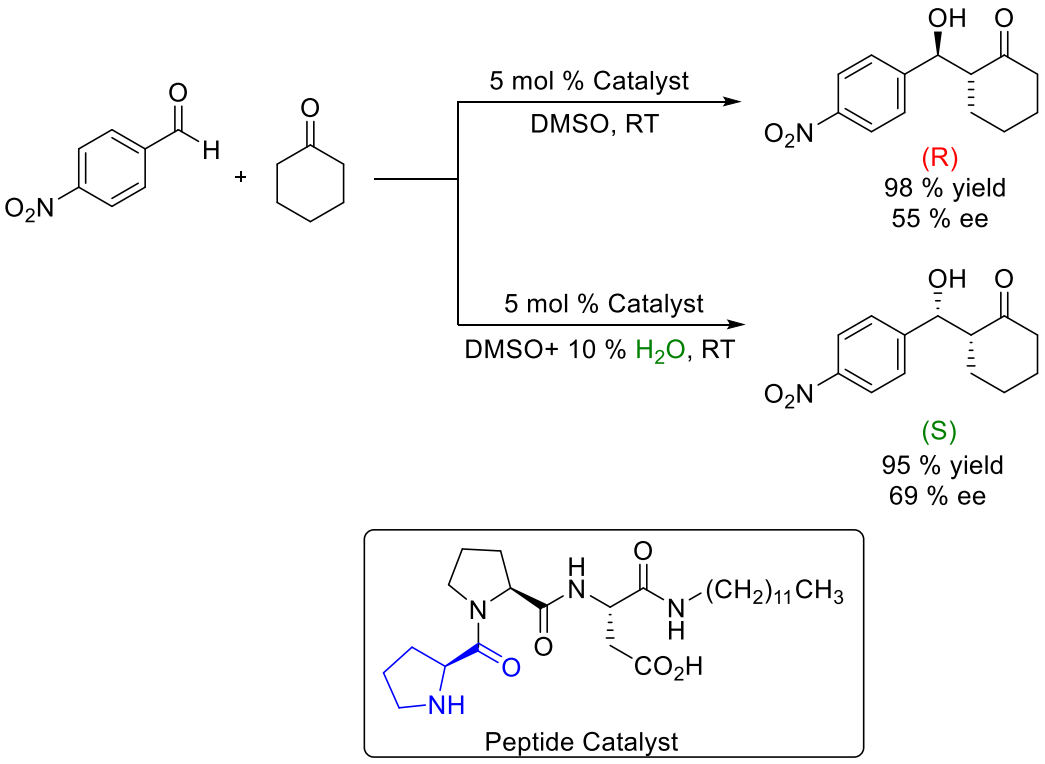

Scheme 14: Aldol Reaction Catalyzed by Diastereoselective Peptide Catalyst.[30]

In summary, some examples of peptide catalysts exhibiting interesting properties were discussed. In the first example, a small peptide adopting a secondary structure was employed as an organocatalyst. The peptide showed solvent-dependent behaviour, while the secondary structure

appeared to contribute to the observed enantioselectivity. Regarding the second example, small peptides comprised of proline units exhibited solvent dependent behaviour once employed as organocatalysts. The configuration of the product was determined by the chirality of the proline residues at the two ends of the peptide. In the third example, a peptide organocatalyst is described. According to the results, the alkyl chain did not influence the enantioselectivity, whereas change of the solvent led to conformational switch leading to a reverse of the enantioselectivity.

From these examples, we can conclude that due to their unique characteristics, small peptides are able to act as organocatalysts, while they can lead to high yields and enantioselectivities. Moreover, peptide catalysts that exhibit stereodivergence and more specifically solvent-dependent behaviour have been developed. Nevertheless, the rational design of effective peptidic organocatalysts remains a challenge. In this regard, it would be beneficial to investigate the catalytic activity of peptides in stereodivergent organocatalysis. Among various peptides, it was considered that polyprolines were the most promising ones for this purpose, as justified in the analysis below.

1.1.4 Polyproline

1.1.4.1 Main Characteristics

Polyprolines are secondary structures, that are mainly comprised of proline units.[31,32] L-Proline is a common amino acid in nature[52] which is characterized by some unique properties.[33,34] Firstly, its side-chain is covalently bonded to the peptide backbone tertiary nitrogen, forming a cyclic pyrrolidine ring.[35,36] Thus, proline is the only imino acid observed in proteins.[35,36] Another consequence of this cyclic imino nature of the side chain is that proline has only one hydrogen atom attached to its nitrogen. As a result, it is unable to donate protons, and can only serve as a proton acceptor.[33,35]

Moreover, as mentioned above (1.1.3), there are three torsion angles of a peptide: phi (ϕ), psi (ψ) and omega (ω).[19] For the 19 standard amino acids, the R-groups are much bulkier than the hydrogen and oxygen atom, and thus, due to steric hindrance, the cis-conformation (ω = 0°) is less favourable energetically.[19] Nevertheless, this is not the case for proline, which is the only naturally occurring amino acid where the side-chain is cyclized to the α-amino group (Figure 5).[19] Thus, it can adopt both the trans and the cis conformations, while the cis-trans amide isomerization is characterised by a lower barrier.[37] Therefore, in contrast to the other amino acids that appear in nature, the cis peptide bond for proline is energetically accessible, while polyproline occurs in two chiral helical conformations, Polyproline I (PolPro I) and Polyproline II (PolPro II) (Figure 6).

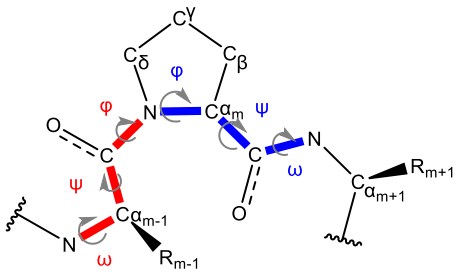

Figure 5: Peptide That Has a Proline at Position m.[19]

PolPro I is a right-handed helix with all the amide bonds in cis-conformation, a helical pitch of 5.6 Å per turn and an axial translation of 1.90 Å. 3.3 residues appear per turn, and the backbone dihedral angles (ϕ, ψ, ω) are (-75°, +160°, 0°) respectively, resulting in a compact structure, with all the amide bonds parallel to the helix axis. On the other hand, the other conformer of polyproline is a left-handed helix, with a trans-conformation of the amide bonds, and dihedral angles of (-75°, +145°, 180 °) respectively. 3.0 proline residues are present per turn, while the helical pitch of 9.4 Å leads to an almost perfect C_3 symmetry, making PolPro II resemble to a triangular prism.[36,38] The axial translation is 3.20 and all amide bonds are perpendicular to the axis. As a result, in contrast to PolPro I, the all-trans amide bonds of PolPro II's structure and the fact that it has a bigger translation per residue, lead to a more extended rod-like structure.[36,38]

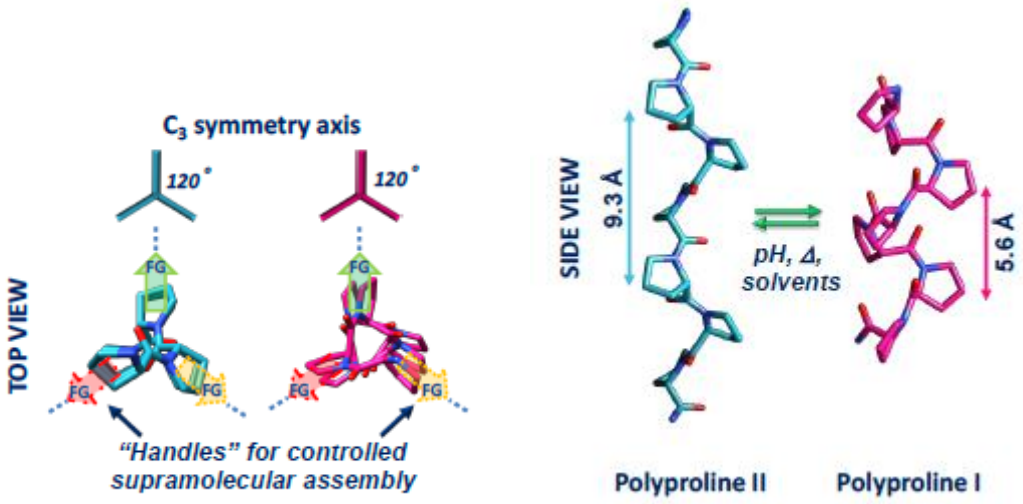

Figure 6: Polyproline I (pink) and Polyproline II (blue) in Top (left) and Side (right) View.

The transition between the helices depends on various parameters, like the solvent[39] and the peptide chain length,[39,40] while the two conformers have distinctly different applications as well.[32] PolPro II is found frequently in proteins,[41,42] and is more widely used in practical applications.[32] More specifically, it has many structural and functional roles.[33] For example, apart from being crucial for the structure of collagen,[32] it has an important role in protein–protein[31,33,38,43,44] or protein–nucleic acid interactions[31,38] and molecular recognition processes.[31,38,43] These interactions are involved in different pathologies, structural applications and drug carriers, rendering the research about PolPro

II even more crucial.[58] The reason for PolPro II's important role in protein structure and interactions lies in its structural properties.[58] As mentioned above, polyproline helices don't support intramolecular[61,62,64,68,72] or intermolecular hydrogen bonds[55] that stabilize other regular structures like α- helices and β-structure.[55] Thus, side-chains and backbone carbonyl and amide groups of the helix are exposed to solvent and available to participate in protein–protein interactions or interactions with solvent molecules.[66] The extended, open conformation and the lack of regular hydrogen bond[35,36,45,38,41] render PolPro II ideal for many molecular interactions.[55]

Although it used to be confused with other conformations, [66,43] PolPro II is now considered a distinct structural class.[55,58] It is the fourth most abundant regular secondary structure in proteins, while its occurrence is comparable to the one of 310 helices.[55,58] It is worth mentioning that although proline has higher propensity in the PolPro II helix,[55,56,62,43,46] other residues can also adopt this structure.[58, 44,46,47] Although they are called polyprolines, it has been proved that polypeptides containing other monomeric units apart from proline[58] or no proline residues at all [44,46,47] are able to adopt the PolPro II conformation. As a result, PolPro II refers to a structural class, rather than a peptide comprised solely of proline units.[58]

1.1.4.2 Crystal Structure

In 1955, Cowan and McGavin obtained the first structure of poly-L-proline, by means of X-Ray diffraction.[48] According to their results, the structure exists in a helical configuration, with three residues per turn and a residue repeat of 3.12 Å.[48] All the amide bonds are in trans conformation, while the helix is left-handed.[48] Hydrogen bonding appeared to be impossible, and it was suggested that poly-L-proline and collagen have very similar configurations.[48] In 1956, poly-L-proline was found to exist in two distinct forms. The first one (PolPro I) has a specific optical rotation of $[a]_D^{25}$=+40° in water, while the latter (PolPro II) has an optical rotation of [a_D^{25}]=-540°. After several days in water, PolPro I was observed to mutarotate to PolPro II.[49] Moreover, the X-Ray powder diffraction pattern of PolPro I appeared to be different from the one of PolPro II, and thus, it was concluded that the two isomers have different fundamental molecular configurations.[49]

Following that, in 1958 it was found that PolPro II has the same configuration in solid state and in water,[49] while reverse mutarotation from PolPro II to PolPro I was also observed in alcoholic media. In 1963, the structure of PolPro I was obtained, and it was proved that when in solution, it is right-handed with the peptide bonds in cis configuration.[50]

The crystal structure of PolPro II was obtained in 2014, providing valuable information about the parameters that define its unique secondary structure and had remained unknown.[51] It was found

that an hexaproline had an almost ideal C3-symmetry, with each proline contributing 3.0 Å, and the amides in the PolPro II helix interacting with each other.[51]

1.1.4.3 Detection

Circular Dichroism (CD) is one of the most useful methods for the characterisation of polyproline.[39] The CD spectrum of the structure in aqueous solution and TFE were obtained in 1963 and 1966 respectively. PolPro I is characterized by a CD spectrum with a medium intensity negative band at 198-200nm, a strong positive band at 214-215nm, and a weak negative band at 231-232nm, while the CD spectrum of PolPro II is comprised of a strong negative band at 202-206nm and a weak positive band at 225-229nm.[40,41,39]

Apart from CD, Nuclear Magnetic Resonance (NMR) spectroscopy has also been proved to be a valuable technique for the detection of these helices.[39] Torchia and Bovey demonstrated in 1970 that the isomerisation of PolPro I to PolPro II in D_2O can be monitored via NMR 200 MHz spectroscopy, by observing the resonances corresponding to the α-trans and α-cis protons.[53]

Ion Mobility Spectrometry-Mass spectrometry (IMS-MS) is another valuable method for the detection of polyproline peptides. More specifically, this method has been an important tool for studies concerning the mechanism of the transition between the two conformers.[54,55]

1.1.4.4 Mechanism

Despite the fact that early studies demonstrated that polyproline appears in two different conformations,[56] little information was known about the transition between these two structures. According to experimental results, the transition from PolPro I to PolPro II was believed to be characterized by one intermediate.[57] In 1960, it was concluded that this transition involves cis-trans isomerizations at the α-carbon-carbonyl carbon bond rather than the peptide bonds.[58] In 1970, based on ^{1}H-NMR, it was reported that during this transition, both cis and trans bonds were randomly found along the chain.[53] Nevertheless, theoretical studies that were conducted later on, showed that various stable isomers of polyproline are present during this transition.[59,60] This conclusion was in agreement with the experimental results by Doose *et al*., which had proved that polyprolines are characterized by ''*structural heterogeneity*''.[61]

Following that, Clemmer *et al*., examined polyprolines comprised of 13 proline units by means of IMS-MS, in order to give an insight into the intermediates of the transition from PolPro I to PolPro I.[55] According to this work, it was proved that apart from the two major conformers, six conformers also appeared as subpopulations of polyproline.[55] Moreover, it was demonstrated that the first steps

of the mechanism involve a flip from cis to trans of proline, and as a result, the transition occurs via sequential cis-trans isomerizations.[55]

The mechanism of the transition from PolPro II to PolPro I has also been investigated. According to Moradi *et al*., a zipper like mechanism starting from either the centre of the peptide or the aminated end is the most probable for this transformation.[60] Although this was in agreement with previous results which demonstrated that the mechanism begins at the N-terminal end,[62] other scientists supported the initialisation of the pathway from the C-terminal end.[53,63]

1.1.4.5 Factors That Influence the Polyproline Conformation

Various factors can influence the transition between PolPro I and PolPro II, with the polymer's length, the temperature, as well as the type and position of functional groups along the peptide chain being some of them.

1.1.4.5.1 Solvent

The solvent is considered to be one of the main factors that controls the stability of the PolPro II helix,[45,64,65,66] while polyproline is a paradigm of how the interaction of the peptide with the solvent can affect their structure as well as their function.[67,68]

Considering the all-cis conformation of the amide bonds, as well as the fact that it is a tight helix, the units of PolPro I are more hindered than the ones of PolPro II, with the carbonyl oxygen parallel to the helical axis and hidden by the proline units.[69] As a result, the importance of intrachain interactions outweighs possible favourable interactions of the peptide backbone with the solvent, and the configuration of each individual unit is highly influenced by the one of its neighbours.[69] As a result, PolPro I excludes the solvent from the peptide backbone and is favoured in non-polar solvents.[59,67] On the contrary, the PolPro II helix is more extended, and it dominates in polar solvents, which interact with the carbonyl groups of the peptide, stabilizing the helix.[54,59,67]

The influence of the solvent to the polyproline helices, has been demonstrated by means of NMR spectroscopy,[70] as well as CD spectroscopy. According to the study of the CD spectra of oligoprolines comprised of four, six and 13 units, it was proved that PolPro II is dominating in water and in TFE, whereas PolPro I is formed in MeOH and in propanol.[39] It is notable that the propensity forming PolPro I was more favourable in propanol than in MeOH, while this was the first spectroscopic evidence proving that PolPro I is favoured in pure aliphatic alcohol.[39] IMS experiments have also been conducted in this regard, showing that the right-handed helix is preferred in non-polar solvents, like propanol, and the left-handed one in polar solvents, like water.[54]

1.1.4.5.2 Chain Length

The chain length of the oligomer is another factor that influences the propensity for the formation of PolPro I or PolPro II, as well as their stability. NMR experiments have proved that at least four monomeric units are required in order for PolPro II to be formed in D_2O.[40] Kakinoki *et al*. demonstrated that polyprolines comprised of 13 and six units presented a conformational transition from PolPro II to PolPro I upon solvent change (water to propanol), according to CD. However, the same did not occur for a tetrameric polyproline. Moreover, it was proved that decreasing the number of units leads to a decrease on the stability of the PolPro II helix, while longer chains increase the stability of PolPro I.[39]

1.1.4.5.3 Substituents

Apart from the use of different solvents, functionalisation of polyprolines can also have a considerable impact on the polyproline helices. More specifically, the steric effects on the helical geometry can direct the formation of one conformer over the other.[66,71] Experimental results have shown that short and bulky side chains disfavour the formation of PolPro II, as they obstruct the interaction between the solvent and the peptide backbone, while the absence of functional groups favours that conformation.[65]

1.1.4.6 Applications

In 1967, Stryer and Haugland used polyprolines (1-12 units) as spacers to separate an energy donor and acceptor, based on Fluorescence Resonance Energy Transfer (FRET) experiments.[72] This was the first time that polyprolines were used as ''*molecular rulers*''.[73] Ever since they have attracted a lot of attention as ''*molecular rulers*'' or ''*scaffolds*'' (Figure 7).[73] Having rigid and well-defined structures, polyprolines are characterized by easy functionalization, solubility in aqueous and organic solvents and ability to define distance on a molecular level.[32] Due to these features, they have many applications, for instance they can be used for energy transfer, distance measurements, hierarchical supramolecular assemblies and size-controlled formation of metal nanoparticles.[73]

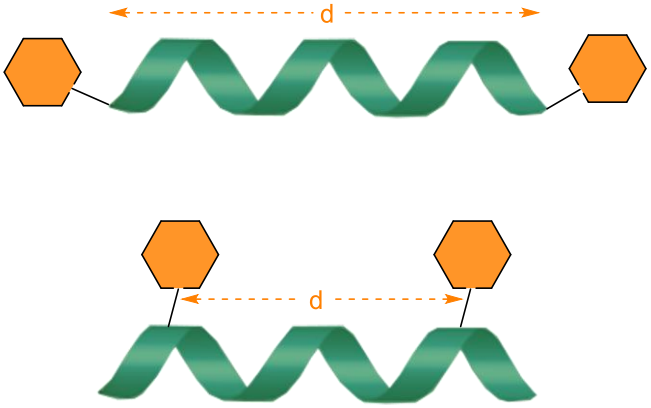

Figure 7: Oligoprolines as Molecular Ruler and Scaffold.[32]

Among the various applications of polyprolines, in this project we chose to employ polyproline peptides as organocatalysts. More specifically, one set of polyprolines were designed to be tested as catalysts in the aldol asymmetric reaction, while another group of polyproline peptides were prepared to be used as catalysts in the acyl transfer reaction. The main characteristics of these reactions as well as the reasoning behind choosing them are analysed below.

1.1.5 Aldol Asymmetric Reaction

The aldol reaction, one of the most studied reactions in the field,[74] is one of the most common reactions for the formation of carbon-carbon bonds.[75] An important aspect of the aldol reaction is that a new stereogenic center is formed, and hence, there is a potential asymmetric induction leading to the formation of optically enriched products.[74] Optically active β-hydroxy carbonyl compounds have many applications, at the same time that this moiety appears in various biologically active compounds like carbohydrates, antibodies and alkaloids.[74] As a result, the asymmetric aldol reaction is a very useful and important reaction for the synthesis of optically enriched compounds.[74]

An aldol reaction can lead to the formation of one or two stereogenic centers (Y=H or Y≠H respectively).[76] In case that the carbonyl compound is α-substituted, four possible stereoisomers (**1a**, **1b**, **2a**, **2b**) are formed (Scheme 15).[76] Products **1a** and **1b**, as well as **2a** and **2b** are enantiomers, whereas **1a**, **1b** and **2a**, **2b** are a pair of diastereomers.[76] Moreover, **1a** and **1b** have syn-configuration, whereas **2a** and **2b** are defined as anti.[76] When the carbonyl compound is α-unsubstituted (Y=H), then two possible products are formed (**3a**, **3b**) which are enantiomers.

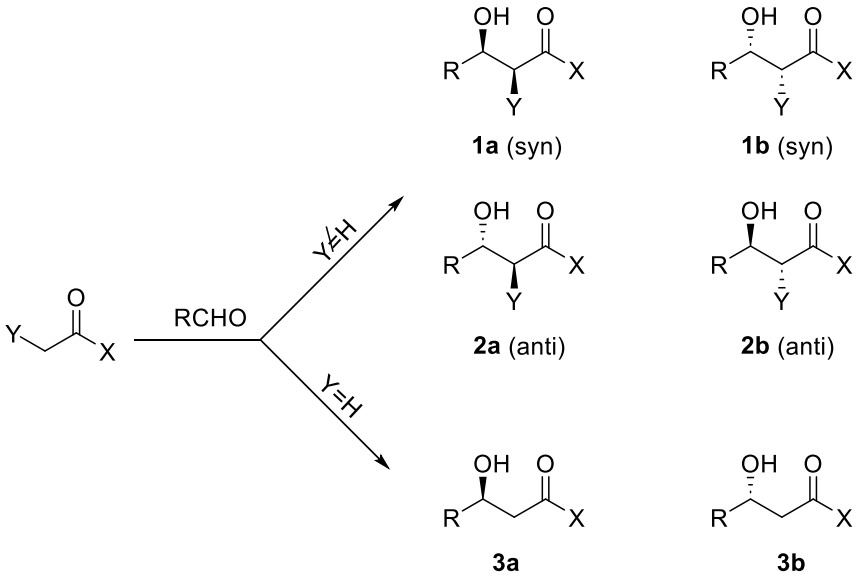

Scheme 15: The Possible Products of an Aldol Reaction.[76]

1.1.6 Acyl Transfer Reaction

In terms of the approach to follow in order to obtain an enantioenriched compound, apart from enantioselective synthesis and the chiral pool, another way is through kinetic resolution (KR).[77] KR is ''*the process when two enantiomers of a racemate are transformed to products at different rates*''.[78] More specifically, through the use of a chiral agent, one enantiomer of a racemate reacts faster than the other.[79] When the KR is efficient, one of the enantiomers is converted to the desired product, whereas the other one is recovered.[78] As a result, the maximum theoretical yield of enantiomerically pure product is 50 %.[12,80]

Among enantioselective organocatalytic transformations, one of the most effective and frequently used are the acyl transfer reactions.[81] If one of the components is racemic, then the process constitutes a kinetic resolution.[12,80] Acyl transfer reactions are classified in two categories, Type I and Type II (Scheme 16),[12] in the former, a ''*racemic or achiral/meso nucleophile reacts diastereo-selectively with an enantiomerically highly enriched acyl donor*'', while in the latter, ''*an enantiomerically highly enriched nucleophile reacts diastereo-selectively with a racemic or achiral/meso acyl donor*''.[80]

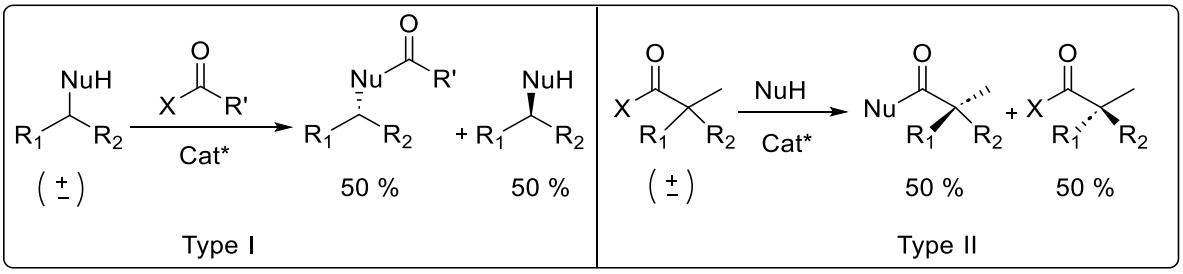

Scheme 16: Types of Catalyzed Asymmetric Acyl Transfer Process.[12,80]

Acyl transfer reactions are the most widely used in KR.[81] The main reasons behind this fact are that the required reagents are inexpensive, the racemic substrates are readily available, and the reactions can be easily performed.[1,77,81] Among various substrates, secondary alcohols (sec-alcohols) are the most studied substrates for nucleophilic organocatalytic acylative KR.[12,80] Racemic alcohols are usually readily available and inexpensive.[1] At the same time, alcohols are valuable intermediates in asymmetric synthesis as well as many types of industries.[1] Moreover, they are found in nature, and they can be converted to various other types of compounds.[1] For examples many bioactive compounds or adrenergic drugs are based on the structure of an alcohol. Therefore, obtaining enantiopure sec-alcohols is very important.[78] Nevertheless, despite the advances, the preparation of molecules that can catalyze the acylation of alcohols with high enantioselectivities is still a challenge.[78]

The mechanism for acyl transfer in the KR of sec-alcohols, based on both experimental and computational data,[82] is considered to be a three-step process (Figure 8).[12] The first step is a nucleophilic attack on an achiral acyl donor, leading to a reactive chiral acyl salt.[80] During the second step, an appropriate substrate performs a nucleophilic attack on the salt. The nucleophilicity of the hydroxyl unit is increased by the acetate anion, which acts as a Brønsted base in this case. [12] As a racemic mixture of the substrate is used, the attack can be performed by either enantiomer of the mixture, forming two transition states.[12] In order for a resolution to be observed, these transition states should have different energies.[12] It is noteworthy that this step is the rate-determining one.[80] At the final step, the acylated product is then formed, while the catalyst is regenerated via the use of stoichiometric amount of base.[82]

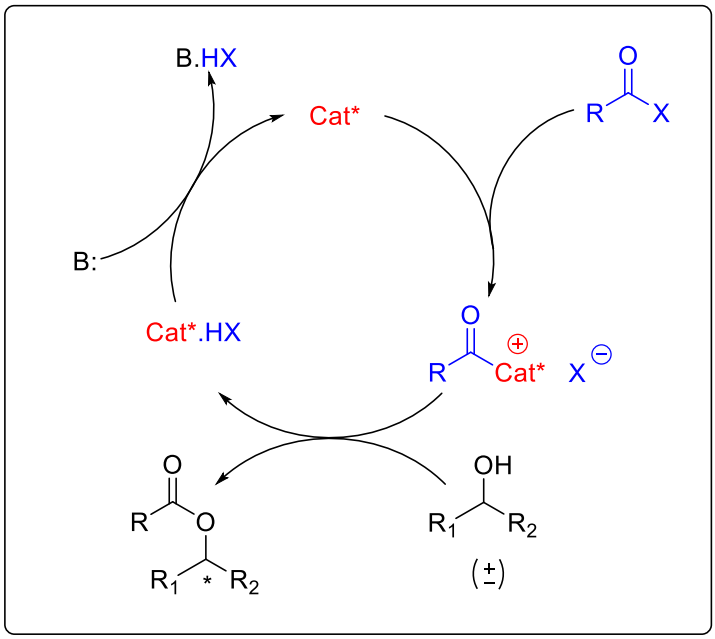

Figure 8: General Catalytic Cycle for the Asymmetric Acylation of Sec-Alcohols.[12,80,82]

Up until recently the only synthetically useful catalytic asymmetric acyl transfer was employed by hydrolytic enzymes.[12,80] More specifically, lipases and esterases led to high levels of stereoselectivity for the acylative KR of a plethora of sec-alcohols.[80] Despite that, enzymes are characterized by high cost, long reaction times and rigid operating parameters, while they are usually available only in one enantiomeric form.[81] These limitations have increased the interest for the development of small chiral catalysts that can serve as catalysts in acyl transfer prosesses.[80] In contrast to enzymes that typically have highly complex structures, high levels of enantioselectivities can be provided by simple structures, like proline or diketopiperazines.[83] Thus, short non-natural peptide-based catalysts are very promising for enantioselective transformations.[84] In the past decades, low molecular weight peptide catalysts have been developed as alternatives to enzymes.[85]

1.2 Project Aims

As analyzed above, organocatalysis has attracted a lot of attention over the past decades, emerging as a powerful strategy that is now considered complementary to metallic catalysis (Section 1.1.2). Through enantioselective organocatalysis small functionalized molecules can be prepared with high enantiopurity. Considering that two enantiomers can have different properties or exhibit different physiological activity, the development of methods that allow the synthesis of enantiomerically pure molecules from readily available starting materials is crucial. Although new catalysts have already been developed, there is still a need for novel compounds that can act as enantioselective organocatalysts offering increased reactivity and selectivity.

In many cases obtainment of both enantiomeric products is important. In order for this to be achieved through conventional methods, two separate reactions would have to be performed. Nevertheless, through stereodivergent organocatalysis both enantiomers or diastereomers can be obtained via small changes in the structure of the catalyst or the reaction conditions of the asymmetric transformation.

Among other compounds that could serve as stereodivergent organocatalysts, polyprolines offer many advantages. Polyprolines can be synthesized through an easily accessible amino acid, while introduction of functional groups capable of performing organocatalytic transformation can be achieved with high position control. Depending on the applied conditions, polyproline occurs into two rigid and interconvertible chiral secondary structures (PolPro I and PolPro II). Therefore, it is valuable to investigate whether polyprolines could act as an organocatalyst, and whether PolPro I and PolPro II could lead to the obtainment of different stereoisomers. In this regard, this project aims to explore the synthesis of functionalized polyproline scaffolds and the investigation of their action as organocatalysts.

The first objective of this research is the preparation of a series polyproline peptides, which will then be tested as catalysts for the aldol asymmetric reaction. It is worth mentioning that different solvents are to be used for each peptide, in order to demonstrate whether this will lead to a conformational change between PolPro I and PolPro II. If that is the case, once the polyproline will be employed as a catalyst, the effect of each conformation on the enantioselectivity of the aldol reaction can also be investigated.

A second phase of this research is focusing on the design of another set of polyproline peptides, which will be employed as catalysts for the acyl transfer reaction. Considering that this is a KR experiment, only one solvent will be used for the peptides in this part.

1.2.1 Application of Polyproline Peptides in the Aldol Asymmetric Reaction

Four polyproline peptides are designed in order to be tested as catalysts for the aldol asymmetric reaction (Figure 9).

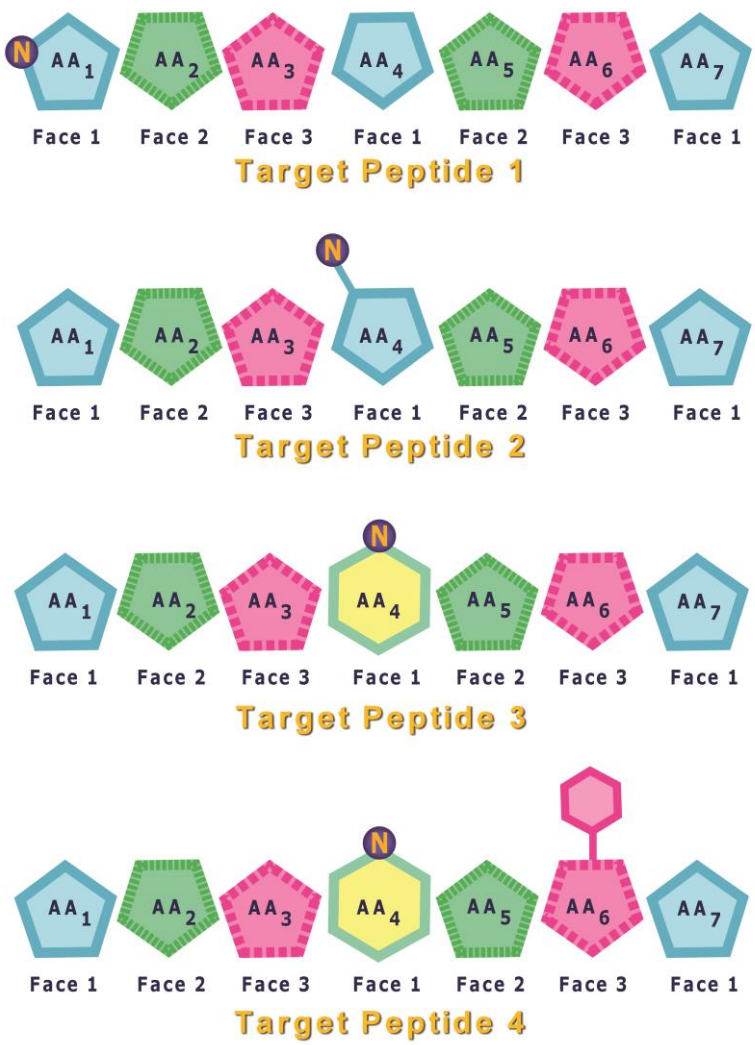

Figure 9: Target Peptides 1-4.

The rationale behind the synthesis of these peptides is to investigate the catalytic activity of a series of different polyprolines. The catalytic site is not the same for all the peptides. More specifically, for the first target peptide (Figure 9-Target Peptide 1) the catalytic site is the amine of the proline ring at the C-terminus, in order to determine whether a polyproline helix comprised only of un-functionalized proline units could act as an effective catalyst. For Target Peptide 2, the effect of a chiral primary amine that is pendant from the helix is investigated. Regarding Target Peptide 3, the catalytic site is the amine of the piperazine ring. In this way, the influence of a six-membered ring and a secondary amine on the catalytic activity is tested. This piperazine ring in particular is rigid, with a 1,2-diamine functionality, while it has been proved to act as an efficient organocatalyst.[86] The next polyproline (Figure 9-Target Peptide 4) is designed in order to investigate the effect of the phenol group, that is introduced on the polyproline helix, on the stereoselectivity of the catalyst.

Following the synthesis and characterisation of the polyproline peptides, our efforts will be directed towards the study of their activity as organocatalysts. Among various organocatalytic

transformations, the aldol asymmetric reaction is a powerful strategy for the construction of carbon-carbon bonds in an enantioselective manner. Considering the applications of the aldol products, the optically active β-hydroxy carbonyl compounds as well as their presence in biologically active molecules, their synthesis has been essential.[74] Many compounds that catalyze the aldol asymmetric reaction including enzymes, catalytic antibodies or small molecules have been documented over the past few years.[2] Nevertheless, there are still some challenges, mainly regarding the catalyst loading and the catalytic efficiency.[29,30] As a result, the development of novel molecules to overcome these limitations is crucial.[30] In this regard, the synthesized polyproline peptides will be tested as catalysts on the aldol reaction of 4-nitrobenzaldehyde with cyclohexanone (Scheme 17).

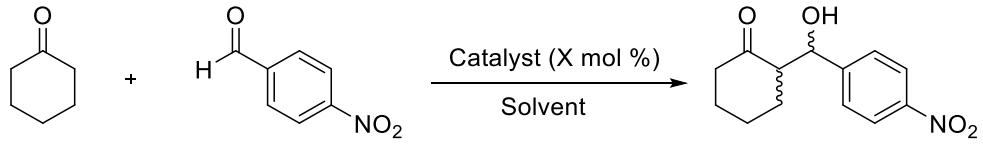

Scheme 17: Aldol Reaction Between p-nitrobenzaldehyde and cyclohexanone.

1.2.2 Application of Polyproline Peptides in the Kinetic Resolution of a Racemic Alcohol

The second objective of this project focuses on synthesizing another set of polyproline peptides in order to be tested as catalysts for the acyl transfer reaction (Table 1). For the first peptide the catalytic activity is deriving from the nitrogen atom on the functionalized proline residue (Table 1-Target Peptide Group 5). Considering the importance of 4-dimethylaminopyridine (DMAP) as a catalyst for the acyl transfer reactions,[82,87] the design of this peptide is based on the fact that the functional group at the C-4 position of the proline residue in the middle of the helix resembles the structure of DMAP.

Regarding the next four target peptides, the catalytic activity is expected to originate from the six membered-ring in the middle of the helix, while the chirality is a result of the polyproline helices' chirality (Table 1-Target Peptide Group 6). The rationale behind the design of these peptides is having a structure that resembles the one of DMAP, this time positioned within the helix. In this way, the catalytic efficiency can be investigated when the catalytic site is positioned within the helix. This series of four peptides is designed so that their catalytic activity can be compared depending on the position of the nitrogen on the six-membered ring.

Table 1: Structures of Target Peptide Group 5-6.

Target Peptide Group 5	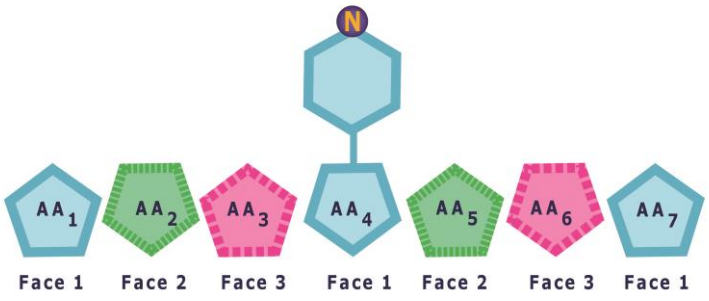
Target Peptide Group 6	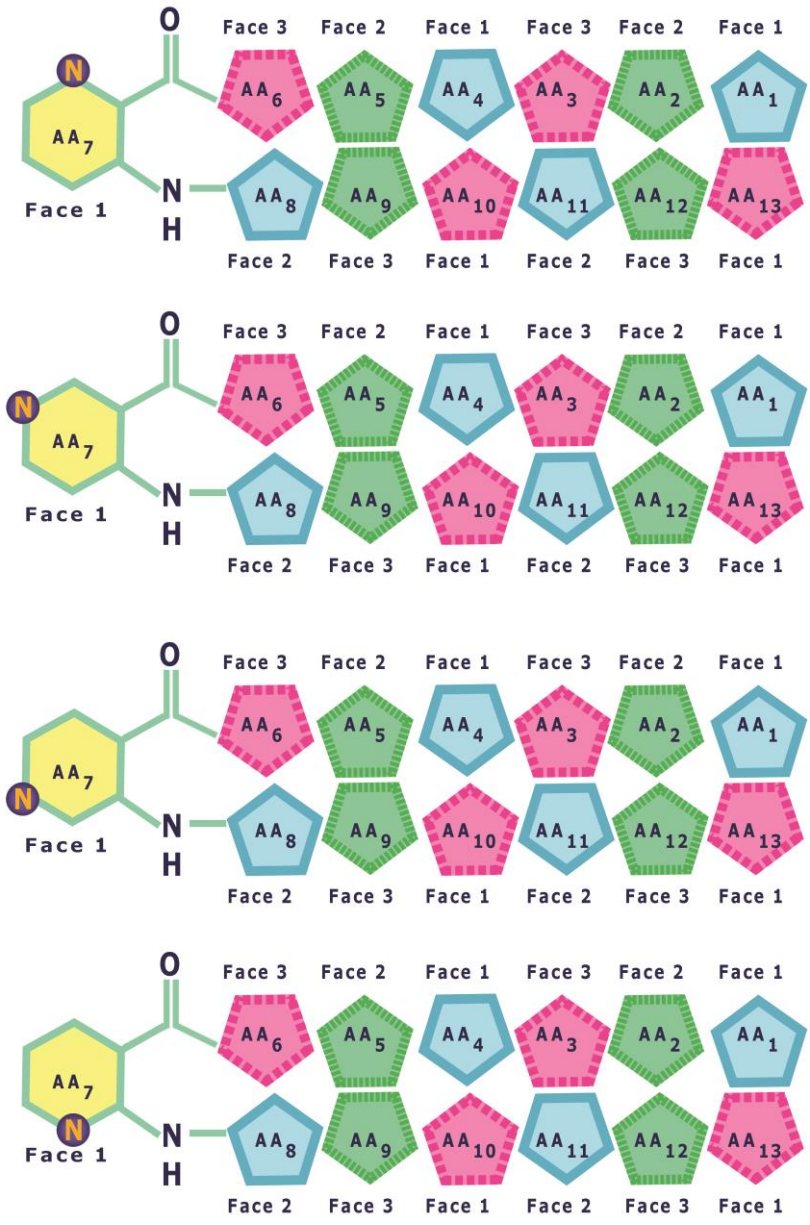

Following the synthesis and characterisation of these four peptides, our aim is to employ the synthesized polyprolines as catalysts in enantioselective organocatalysis. After exploring the aldol reaction during the first part of this project, our efforts will be directed towards the investigation of

the acyl transfer organocatalytic transformation. Acyl transfer reactions are among the most common enantioselective organocatalytic transformations (Section 1.1.1.5).[81] For a long time, enzymes were the only examples of catalysts for the asymmetric acyl transfer. Nevertheless, as their use has many disadvantages (Section 1.1.1.5), developing small chiral molecules able to catalyze this type of reaction has attracted a lot of attention.[80] Peptide-based catalysts in particular have been established as very promising alternatives to enzymes, mainly due to their high structural diversity and ability to form multiple non-covalent interactions simultaneously.[85] Despite the development of many novel catalysts, there are still many challenges, mainly regarding the preparation of easily accessible chiral catalysts, as well as the reactivity and selectivity of the reaction.[80] As a result, the preparation of novel chiral catalysts is an important goal for this field. In this context, the polyproline peptides will be tested as catalysts in the acyl transfer reaction of a racemic alcohol between 1-phenyl alcohol and acetic anhydride (Ac_2O) (Scheme 18).

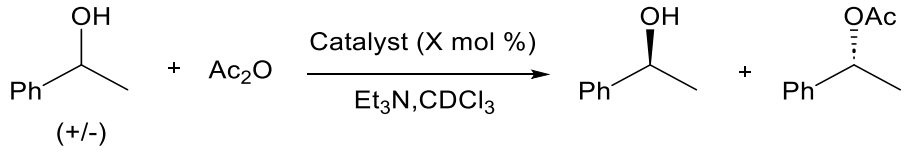

Scheme 18: KR of Racemic Alcohol 1-Phenylethanol.

1.3 References

1. Mesas Sánchez, L. Organocatalytic acylation for the kinetic resolution of secondary aryl alcohols: Synthetic applications and mechanistic studies. (Acta Universitatis Upsaliensis, 2014).
2. Escorihuela, J., Burguete, M. I. & Luis, S. V. New advances in dual stereocontrol for asymmetric reactions. *Chem. Soc. Rev.* **42**, 5595–5617 (2013).
3. Beletskaya, I. P., Nájera, C. & Yus, M. Stereodivergent catalysis. *Chem. Rev.* **118**, 5080–5200 (2018).
4. Agirre, M., Arrieta, A., Arrastia, I. & Cossío, F. P. Organocatalysts derived from unnatural α-amino acids: Scope and applications. *Chem. Asian. J.* **14**, 44–66 (2019).
5. Gaunt, M. J., Johansson, C. C. C., McNally, A. & Vo, N. T. Enantioselective organocatalysis. *Drug Discov. Today* **12**, 8–27 (2007).
6. Zou, Y. & Bach, T. Iminium and enamine catalysis in enantioselective photochemical reactions. *Chem. Soc. Rev.* **47**, 278–290 (2018).
7. MacMillan, D. W. C. The advent and development of organocatalysis. *Nature* **455**, 304–308 (2008).
8. Wang, Z. Hajos-Parrish-Eder-Sauer-Wiechert reaction. in *Comprehensive Organic Name Reactions and Reagents* 1305–1309 (2009).
9. List, B., Lerner, R. A. & Barbas, C. F. Proline-catalyzed direct asymmetric aldol reactions. *J. Am.*

Chem. Soc. **122**, 2395–2396 (2000).

10. Ahrendt, K. A., Borths, C. J. & MacMillan, D. W. C. New strategies for organic catalysis: The first highly enantioselective organocatalytic Diels- Alder reaction. *J. Am. Chem. Soc.* **122**, 4243–4244 (2000).

11. Sigman, M. S. & Jacobsen, E. N. Schiff base catalysts for the asymmetric Strecker reaction identified and optimized from parallel synthetic libraries. *J. Am. Chem. Soc.* **120**, 4901–4902 (1998).

12. List, D. B. *Asymmetric Organocatalysis*. *Topics in Current Chemistry* vol. 291 (Springer, 2010).

13. Krautwald, S. & Carreira, E. M. Stereodivergence in asymmetric catalysis. *J. Am. Chem. Soc.* **139**, 5627–5639 (2017).

14. Kumari, A., Jain, A. & Rana, N. K. A review on solvent-controlled stereodivergent catalysis. *Tetrahedron* **150**, (2024).

15. Wang, J. & Feringa, B. L. Dynamic control of chiral space in a catalytic asymmetric reaction using a molecular motor. *Science* **331**, 1429–1423 (2011).

16. Sewald, N. & Jakubke, H. D. Fundamental chemical and structural principles. in *Peptides: Chemistry and Biology* (Wiley-VCH, 2008).

17. Bodanszky, M. *Peptide Chemistry. A Practical Approach*. (Springer-Verlag, 1988).

18. Wilson, C. J. *et al.* Biomolecular assemblies: Moving from observation to predictive design. *Chem. Rev.* **118**, 11519–11574 (2018).

19. Gurung, D. *et al.* Proline isomerization: From the chemistry and biology to therapeutic opportunities. *Biology* **12**, 1–40 (2023).

20. Tsogoeva, S. Short peptides and peptide-like enzyme mimics-efficient organic catalysts in asymmetric synthesis. *Lett. Org. Chem.* **2**, 208–213 (2005).

21. Tsogoeva, S. B., Jagtap, S. B. & Ardemasova, Z. A. 4-trans-Amino-proline based di- and tetrapeptides as organic catalysts for asymmetric C-C bond formation reactions. *Tetrahedron Asymmetry* **17**, 989–992 (2006).

22. Wennemers, H. Asymmetric catalysis with peptides. *Chem. Commun.* **47**, 12036–12041 (2011).

23. Rajikumar, T. Development of new peptide organocatalyst for asymmetric reactions. (Muroran Institute of Technology, 2022).

24. Revell, J. D. & Wennemers, H. Peptidic catalysts developed by combinatorial screening methods. *Curr. Opin. Chem. Biol.* **11**, 269–278 (2007).

25. Berkessel, A. The discovery of catalytically active peptides through combinatorial chemistry. *Curr. Opin. Chem. Biol.* **7**, 409–419 (2003).

26. Kofoed, J., Nielsen, J. & Reymond, J. L. Discovery of new peptide-based catalysts for the direct asymmetric aldol reaction. *Bioorganic Med. Chem. Lett.* **13**, 2445–2447 (2003).

27. Jarvo, E. R. & Miller, S. J. Amino acids and peptides as asymmetric organocatalysts. *Tetrahedron* **58**, 2481–2495 (2002).

28. Illa, O. *et al.* Stereoselectivity of proline/cyclobutane amino acid-containing peptide organocatalysts for asymmetric aldol additions: A rationale. *J. Org. Chem.* **83**, 350–363

(2018).

29. Wu, F. C. *et al.* N-Primary-amine-terminal β-turn tetrapeptides as organocatalysts for highly enantioselective aldol reaction. *J. Org. Chem.* **74**, 4812–4818 (2009).

30. Metrano, A. J. *et al.* Asymmetric catalysis mediated by synthetic peptides, version 2.0: Expansion of scope and mechanisms. *Chem. Rev.* **120**, 11479–11615 (2020).

31. Adzhubei, A. A., Sternberg, M. J. E. & Makarov, A. A. Polyproline-II helix in proteins: Structure and function. *J. Mol. Biol.* **425**, 2100–2132 (2013).

32. Dobitz, S., Aronoff, M. R. & Wennemers, H. Oligoprolines as molecular entities for controlling distance in biological and material sciences. *Acc. Chem. Res.* **50**, 2420–2428 (2017).

33. Morgan, A. A. & Rubenstein, E. Proline: The distribution, frequency, positioning, and common functional roles of proline and polyproline sequences in the human proteome. *PLoS One* **8**, 1–9 (2013).

34. Zarrinpar, A., Bhattacharyya, R. P. & Lim, W. A. The structure and function of proline recognition domains. *Sci. STKE* **2003**, 1–10 (2003).

35. Deber, C. M., Brodsky, B. & Rath, A. Proline residues in proteins. *eLS* 1–9 (2010).

36. Rath, A., Davidson, A. R. & Deber, C. M. The structure of 'unstructured' regions in peptides and proteins: Role of the polyproline II helix in protein folding and recognition. *Biopolymers* **80**, 179–185 (2005).

37. Gkikas, M., Iatrou, H., Thomaidis, N. S., Alexandridis, P. & Hadjichristidis, N. Well-defined homopolypeptides, copolypeptides, and hybrids of poly(L-proline). *Biomacromolecules* **12**, 2396–2406 (2011).

38. Narwani, T. J. *et al.* Recent advances on polyproline II. *Amino Acids* **49**, 705–713 (2017).

39. Kakinoki, S., Hirano, Y. & Oka, M. On the stability of polyproline-I and II structures of proline oligopeptides. *Polym. Bull.* **53**, 109–115 (2005).

40. Rothe, M. & Rott, H. NMR spectroscopic detection of cis and trans peptide bonds in unprotected oligo-L-prolines. *Angew. Chemie Int. Ed. English* **15**, 770–771 (1976).

41. Kumar, P. & Bansal, M. Structural and functional analyses of PolyProline-II helices in globular proteins. *J. Struct. Biol.* **196**, 414–425 (2016).

42. Kümin, M., Sonntag, L. S. & Wennemers, H. Azidoproline containing helices: Stabilization of the polyproline II structure by a functionalizable group. *J. Am. Chem. Soc.* **129**, 466–467 (2007).

43. Bochicchio, B. & Tamburro, A. M. Polyproline II structure in proteins: Identification by chiroptical spectroscopies, stability, and functions. *Chirality* **14**, 782–792 (2002).

44. Mansiaux, Y., Joseph, A. P., Gelly, J. C. & de Brevern, A. G. Assignment of PolyProline II conformation and analysis of sequence-structure relationship. *PLoS One* **6**, 1–15 (2011).

45. Adzhubei, A. A. & Sternberg, M. J. E. Left-handed polyproline II helices commonly occur in globular proteins. *J. Mol. Biol.* **229**, 472–493 (1993).

46. Stapley, B. J. & Creamer, T. P. A survey of left-handed polyproline II helices. *Protein Sci.* **8**, 587–595 (1999).

47. Chellgren, B. W. & Creamer, T. P. Short sequences of non-proline residues can adopt the

polyproline II helical conformation. *Biochemistry* **43**, 5864–5869 (2004).

48. Cowan, B. P. M. & Mcgavin, S. Structure of poly-L-proline. *Nature* **176**, 501–503 (1955).

49. Harrington, W. F. & Sela, M. Studies on the structure of poly-L-proline in solution. *Biochim. Biophys. Acta* **27**, 24–41 (1958).

50. Traub, W. & Shmueli, U. Structure of poly-L-proline I. *Nature* **198**, 1165–1166 (1963).

51. Wilhelm, P., Lewandowski, B., Trapp, N. & Wennemers, H. A crystal structure of an oligoproline PPII-Helix, at last. *J. Am. Chem. Soc.* **136**, 15829–15832 (2014).

52. Mandal, D., Nasrolahi Shirazi, A. & Parang, K. Self-assembly of peptides to nanostructures. *Org. Biomol. Chem.* **12**, 3544–3561 (2014).

53. Torchia, D. A. & Bovey, F. A. A nuclear magnetic resonance study of poly (L-proline) in aqueous and aqueous salt solutions. *Macromolecules* **4**, 246–251 (1971).

54. Shi, L. *et al.* Ion mobility-mass spectrometry reveals the energetics of intermediates that guide polyproline folding. *J. Am. Soc. Mass Spectrom.* **27**, 22–30 (2015).

55. Shi, L. *et al.* Characterizing intermediates along the transition from polyproline I to polyproline II using ion mobility spectrometry-mass spectrometry. *J. Am. Chem. Soc.* **136**, 12702–12711 (2014).

56. Cowan, P. M., McGavin, S. & North, A. C. T. The polypeptide chain configuration of collagen. *Nature* **176**, 1062–1064 (1955).

57. Dukor, R. K. & Keiderling, T. A. Mutarotation studies of poly-L-proline using FTIR, electronic and vibrational circular dichroism. *Biospectroscopy* **2**, 83–100 (1996).

58. Steinberg, I. Z., Harrington, W. F., Berger, A., Sela, M. & Katchalski, E. The configurational changes of poly-L-proline in solution. *J. Am. Chem. Soc.* **82**, 5263–5279 (1960).

59. Moradi, M., Babin, V., Roland, C., Darden, T. A. & Sagui, C. Conformations and free energy landscapes of polyproline peptides. *Proc. Natl. Acad. Sci.* **106**, 20746–20751 (2009).

60. Moradi, M. *et al.* A classical molecular dynamics investigation of the free energy and structure of short polyproline conformers. *J. Chem. Phys.* **133**, 1–18 (2010).

61. Doose, S., Neuweiler, H., Barsch, H. & Sauer, M. Probing polyproline structure and dynamics by photoinduced electron transfer provides evidence for deviations from a regular polyproline type II helix. *Proc. Natl. Acad. Sci.* **104**, 17400–17405 (2007).

62. Lin, L. N. & Brandts, J. F. Kinetic mechanism for conformational transitions between poly-L-prolines I and II: A study utilizing the cis-trans specificity of a proline-specific protease. *Biochemistry* **19**, 3055–3059 (1980).

63. Kang, Y. K., Jhon, J. S. & Park, H. S. Conformational preferences of proline oligopeptides. *J. Phys. Chem. B* **110**, 17645–17655 (2006).

64. Creamer, T. P. & Campbell, M. N. Determinants of the polyproline II helix from modeling studies. *Adv. Protein Chem.* **62**, 263–282 (2002).

65. Kelly, M. A. *et al.* Host- guest study of left-handed polyproline II helix formation. *Biochemistry* **40**, 14376–14383 (2001).

66. Rucker, A. L. & Creamer, T. P. Polyproline II helical structure in protein unfolded states: lysine peptides revisited. *Protein Sci.* **11**, 980–985 (2002).

67. Shi, L., Holliday, A. E., Khanal, N., Russell, D. H. & Clemmer, D. E. Configurationally-coupled protonation of polyproline-7. *J. Am. Chem. Soc.* **137**, 8680–8683 (2015).

68. El-Baba, T. J., Fuller, D. R., Hales, D. A., Russell, D. H. & Clemmer, D. E. Solvent mediation of peptide conformations: Polyproline structures in water, methanol, ethanol, and 1-propanol as determined by ion mobility spectrometry-mass spectrometry. *J. Am. Soc. Mass Spectrom.* **30**, 77–84 (2018).

69. Schimmerl, P. & Flory, J. Conformational energy and configurational statistics of poly-L-proline. *Proc. Natl. Acad. Sci.* **58**, 52–59 (1967).

70. Deber, C. M., Bovey, F. A., Carver, J. P. & Biout, E. R. Nuclear magnetic resonance evidence for cis-Peptide bonds in proline oligomers. *J. Am. Chem. Soc.* **92**, 6191–6198 (1970).

71. Beausoleil, E. & Lubell, W. D. An examination of the steric effects of 5-tert-butylproline on the conformation of polyproline and the cooperative nature of type II to type I helical interconversion. *Biopolymers* **53**, 249–256 (2000).

72. Stryer Lubert, H. R. P. Energy transfer: A spectroscopic ruler. *Proc. Natl. Acad. Sci.* **58**, 719–726 (1967).

73. Garbuio, L. *et al.* Shape persistence of polyproline II helical oligoprolines. *Chem. - A Eur. J.* **21**, 10747–10753 (2015).

74. Bhanushali, M. & Zhao, C.-G. Developing novel organocatalyzed aldol reactions for the enantioselective synthesis of biologically active molecules. *Synthesis* **12**, 1815–1830 (2011).

75. Palomo, C., Oiarbide, M. & García, J. M. Current progress in the asymmetric aldol addition reaction. *Chem. Soc. Rev.* **33**, 65–75 (2004).

76. Braun, M. & Sacha, H. Recent advances in stereoselective aldol reactions of ester and thioester enolates. *J. Prakt. Chem.* **335**, 653–668 (1993).

77. Keith, J. M., Larrow, J. F. & Jacobsen, E. N. Practical considerations in kinetic resolution reactions. *Adv. Synth. Catal.* **343**, 5–26 (2001).

78. Pellissier, H. Catalytic non-enzymatic kinetic resolution. *Adv. Synth. Catal.* **353**, 1613–1666 (2011).

79. Krasnov, V. P., Gruzdev, D. A. & Levit, G. L. Nonenzymatic acylative kinetic resolution of racemic amines and related compounds. *Eur. J. Org. Chem.* **2012**, 1471–1493 (2012).

80. Spivey, A. C. & McDaid, P. Asymmetric acyl transfer reactions. in *Enantioselective Organocatalysis: Reactions and Experimental Procedures* 287–329 (2007).

81. Müller, C. E. & Schreiner, P. R. Organocatalytic enantioselective acyl transfer onto racemic as well as meso alcohols, amines, and thiols. *Angew. Chemie Int. Ed.* **50**, 6012–6042 (2011).

82. Mandai, H. *et al.* Enantioselective acyl transfer catalysis by a combination of common catalytic motifs and electrostatic interactions. *Nat. Commun.* **7**, 1–11 (2016).

83. Jarvo, E. R., Vasbinder, M. M. & Miller, S. J. Asymmetric acylation reactions catalyzed by conformationally biased octapeptides. *Tetrahedron* **56**, 9773–9779 (2000).

84. Müller, C. E. *et al.* Lipophilic oligopeptides for chemo- and enantioselective acyl transfer reactions onto alcohols. *J. Org. Chem.* **78**, 8465–8484 (2013).

85. Procházková, E. *et al.* Uncovering key structural features of an enantioselective peptide-catalyzed acylation utilizing advanced NMR techniques. *Angew. Chem. Int. Ed.* **55**, 15754–

15759 (2016).

86. Barros, M. T. & Phillips, A. M. F. Chiral piperazines as efficient catalysts for the asymmetric michael addition of aldehydes to nitroalkenes. *European J. Org. Chem.* **2007**, 178–185 (2007).

87. Fu, G. C. Enantioselective nucleophilic catalysis with 'planar-chiral' heterocycles. *Acc. Chem. Res.* **33**, 412–420 (2000).

Chapter 2

Application of Polyproline Peptides in the Aldol Catalytic Reaction

2.1 Introduction

2.1.1 Synthetic Strategies of Peptides

The first low molecular weight polyproline comprised exclusively by proline residues was synthesized in 1954, through polymerization, starting from L-proline.[1] Polymerization of the corresponding amino acid N-carboxy-anhydride (NCA) is a common way to synthesize peptides.[2–4] Nevertheless, in the case of proline, the NCA formation is characterized by poor synthetic yields due to the cyclic secondary amine and the associated conformational restrictions.[3] As a result, although proline NCAs have been successfully synthesized (Scheme 19),[2,4] their extensive use has been limited.[3]

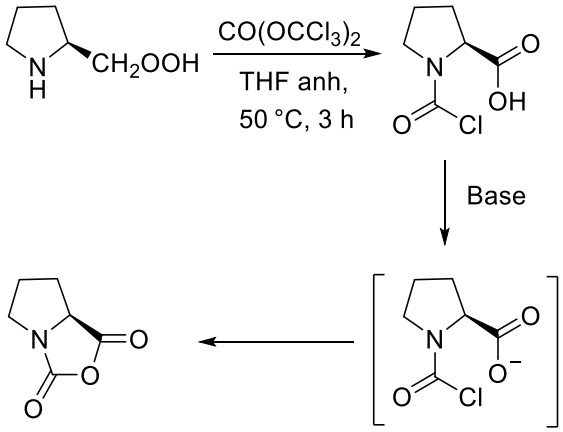

Scheme 19: Synthesis of Proline NCA.[2]

Another method that has proved to be an efficient for the successful preparation of polyproline helices is solid phase peptide synthesis (SPPS).[5,6] Aiming to overcome the difficulties associated with the synthesis of polypeptides, Merrifield developed the solid phase peptide synthesis in 1963.[7,8] Through an automated process, more complex peptides could be prepared, while the demanding purification steps were simplified.[6,8] As a result, the synthesis of peptides changed drastically, and offered new opportunities for research in biochemistry, medicinal chemistry and many other fields.[8]

In SPPS, after the attachment of the first amino acid to an insoluble solid support by a covalent bond, the peptide chain is assembled by addition of the succeeding amino acids one at a time in a stepwise manner.[6,7] Once the desired sequence is synthesized, the peptide is removed from the solid support.[6,7]

This approach has many advantages compared to conventional synthetic methods.[6,7,9] Firstly, all the steps can be carried in the same vessel, and as a result, the synthesis can be performed without the usual losses associated with transferring of the material.[6,7] Furthermore, as the growing insoluble peptide is attached to a solid support, excess reagents and by-products can be separated simply by washings and filtration.[7] This is very important, considering that in conventional synthetic reactions an effective purification procedure is required, which usually cannot be performed mechanically.[7] In addition, SPPS is comprised of a relatively simple series of reactions, which are repeated in a

stepwise manner until the desired peptide chain is assembled.[7,9] Thus, the required time for the peptide synthesis is less, while the procedure is simplified.[7] Lastly, it is a relatively inexpensive method, while various non-natural amino acids can be used.[5]

2.1.1.1 Solid Phase Peptide Synthesis

In order to perform a successful SPPS, it is crucial to select the appropriate resin, coupling agents and solvents, as well as use the most suitable protecting group for the amino acid employed and the tests that will allow to identify the completion of specific steps.[8] These principles are discussed in sections 2.1.1.1.1-2.1.1.1.6.

2.1.1.1.1 Resin

Many types of resins can be used in the SPPS.[8] In the case of linked resins, a linker is used as the link between the compound and the resin support.[8] According to the type of linker that is chosen, different reaction conditions are applied.[8] Some resins form a C-terminal amide bond, like the rink amide resin, whereas some others like the Merrifield, the Wang and the 2-chlorotrityl resins, give a C-terminal carboxylic acid once cleaved (Figure 10).[8] Both are connected to the polystyrene matrix via an ether linkage, and they are cleaved under strongly acidic conditions like the use of trifluoroacetic acid (TFA).[5,8] These resins are supplied with the amine protected by an Fmoc group, as this ensures stability on storage.[5,8] As a result, before the start of the peptide synthesis, the Fmoc group needs to be removed.[8]

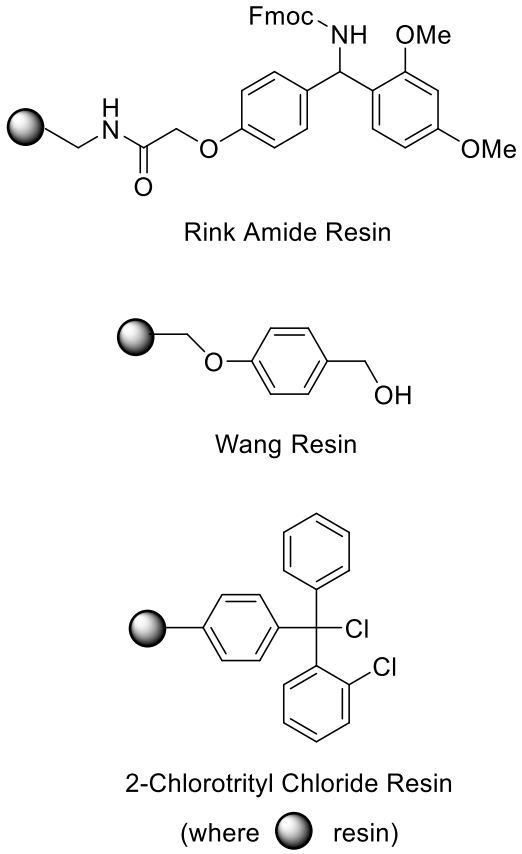

Figure 10: Structures of Rink Amide Resin (up), Wang Resin (middle) and 2-Chlorotrityl Chloride Resin (bottom).[8]

It is notable that the Wang resin is unsuitable for the preparation of peptides using proline or its derivatives.[10] After addition of an amino acid, during the deprotection process, a free amino dipeptide ester is generated which often cyclises forming the free cyclic dipeptide (Scheme 20).[10] As a result, apart from the rink amide resin, 2-chlorotrytil resin is also recommended in these cases.[10] This is extremely acid labile and as it is sterically hindered, it hinders the formation of diketopiperazines.[8]

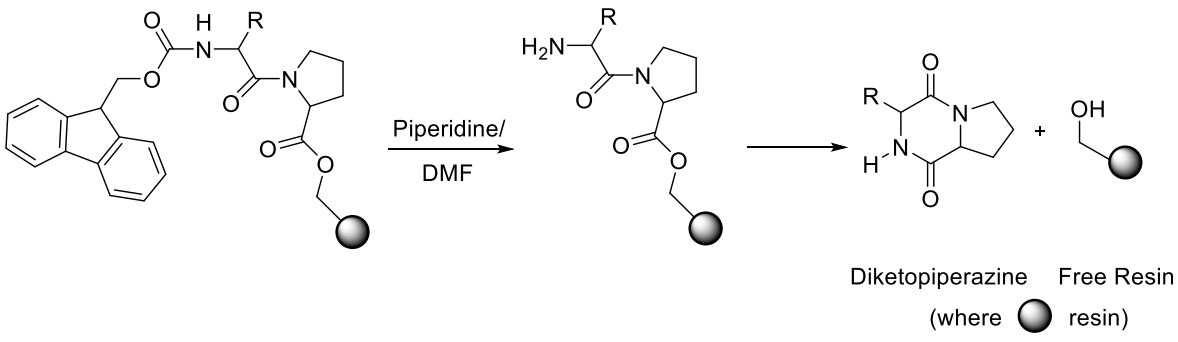

Scheme 20: Diketopiperazine Formation During the Synthesis of Peptides Consisted of Proline Units.[10]

2.1.1.1.2 Amino Acids

In order to prevent polymerisation of the amino acid, it is important that amino acids are protected.[8] Side-chain functional groups of amino acids should be masked with permanent protecting groups

that are stable in the conditions used during the peptide synthesis, while the α-amino group is protected by temporary protecting group which can be easily removed under mild conditions.[6,8] Ideally, an ''*orthogonal*'' protection is desired, meaning the side chain and N-α protecting groups can be removed under different conditions.[8]

SPPS using Fmoc-protected amino acids is the chosen synthetic approach for the majority of peptides, with the Boc SPPS now only being used for specific applications.[11] When Boc is used as the protecting group, it temporarily protects the N-α-nitrogen groups of the amino acids, while benzyl groups are employed as permanent protecting groups.[8] Considering they are both acid labile, Boc and benzyl don't provide an orthogonal protection.[8] Moreover, the deprotection by-product is volatile.[11] In contrast, Fmoc SPPS provides an ''*orthogonal combination of temporary and permanent protecting groups removable under exceptionally mild conditions*''.[11] More specifically, in Fmoc SPPS only small amounts of TFA are needed, and any adducts can be easily washed away.[8,11] As a result, it can be easily automated, and difficulties that were encountered during the Boc SPPS can be overcome.[11]

2.1.1.1.3 Coupling Agents

Among the most commonly used coupling reagents are (Figure 11):

- Carbodiimides: Dicyclohexylcarbodiimide (DCC) and diisopropylcarbodiimide (DIC) are the most frequently coupling agents used.[8] As DCC is almost insoluble in the majority of organic solvents, it is mostly used in solution phase reactions.[8] On the contrary, DIC is appropriate for reactions on resin, as its by-product is more soluble.[8]
- Phosphonium-based reagents: Benzotriazol-1-yloxy)tris(dimethylamino)phosphonium hexafluorophosphate (BOP) was one of the first agents developed.[8] (Benzotriazol-1-yloxy)tripyrrolidinophosphonium hexafluorophosphate (PyBOP) is as efficient, while it is characterized by fast coupling reactions.[8]
- Aminium-Based reagents: two frequently used coupling reagents are O-(Benzotriazol-1-yl)-N,N,N',N'-tetramethyluronium hexafluorophosphate (HBTU) and O-(Benzotriazol-1-yl)-N,N,N',N'-tetramethyluronium tetrafluoroborate (TBTU).[8]

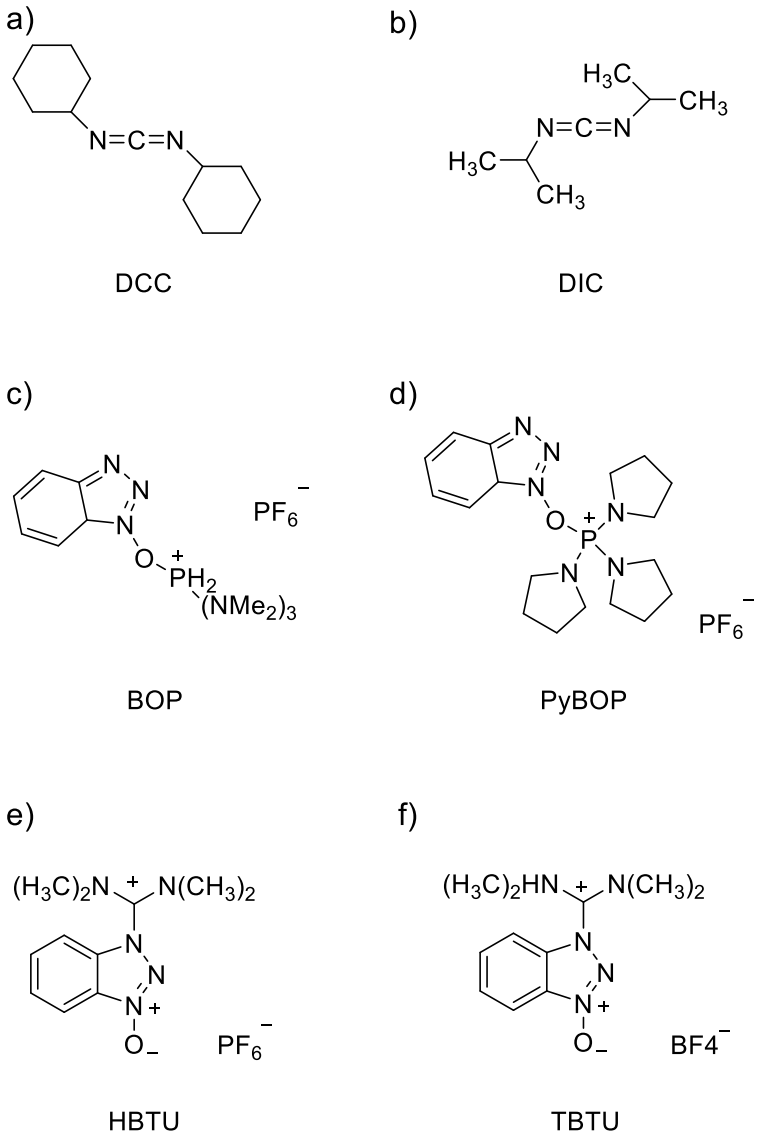

Figure 11: Structures of a) DCC, b) DIC, c) BOP, d) PyBOP, e) HBTU and e) TBTU.[6]

After addition of the coupling reagents, the N-protected amino acid is converted into the corresponding reactive activated ester.[8] A tertiary amine, usually diisopropylethylamine (DIPEA), is necessary to form the carboxylate of the N-protected amino acid, which reacts with the coupling reagents.[8] Once the solution is added to the resin, the free amines on the end of the peptide chain react with the activated ester, forming a new amide bond (Scheme 21).[5,8]

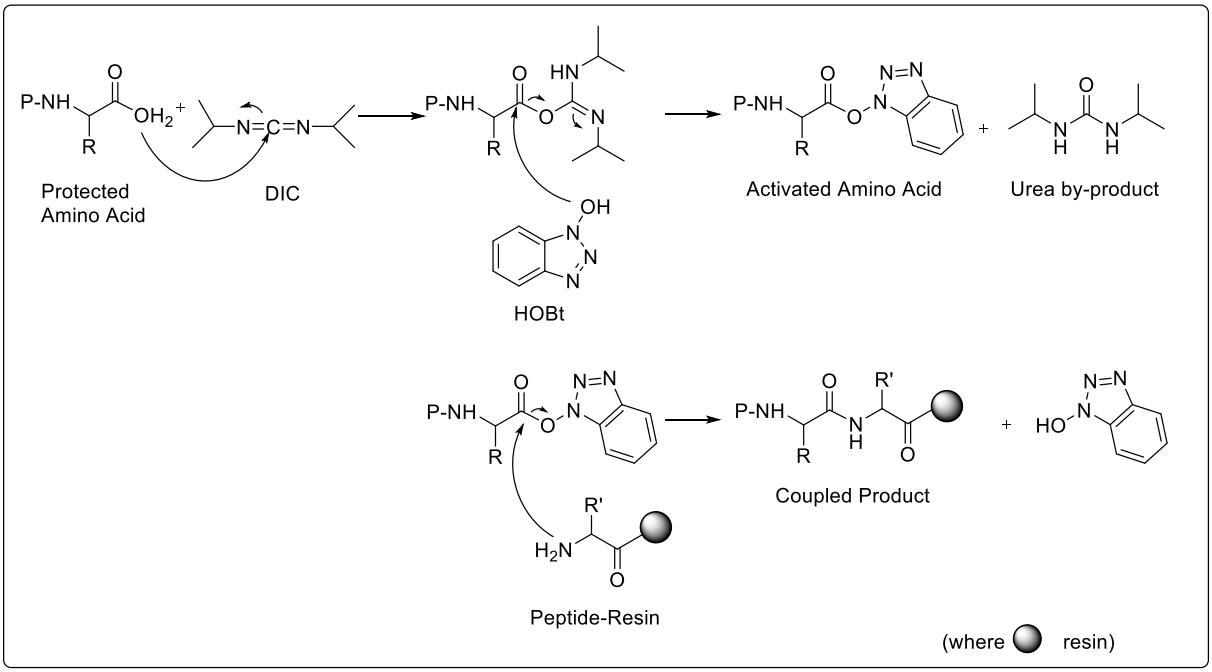

Scheme 21: Mechanism of DIC/HOBt Coupling.[8]

It is noteworthy that 1-Hydroxybenzotriazole (HOBt) is a coupling additive and its role is important as it reduces the degree of racemization that can be created after the activation of the protected amino acid.[8]

There are two mechanisms of epimerisation in peptide synthesis (Scheme 22).[12] During path B, strong activation of the carboxylate group of the amino acid leads to the oxazolone intermediate.[12] After Nα attack from the same amino acid, the epimerisation product is formed.[12] In the second mechanism, path A, epimerisation occurs through direct Hα abstraction by a base, and therefore this path is observed more in amino acids with highly acidic alpha protons.[12] Following this step, re-protonation of the anionic amino acid leads to the formation of the epimerisation products.[12]

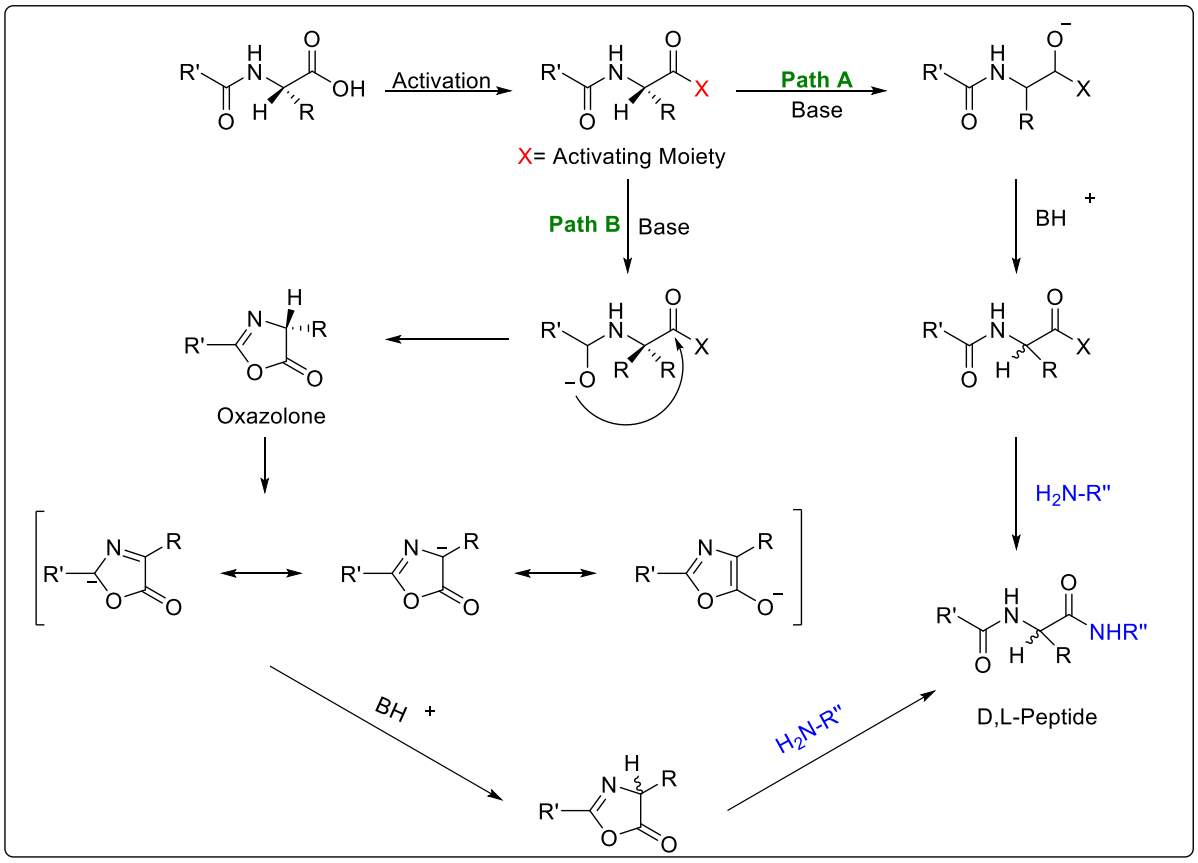

Scheme 22: Epimerisation/Racemisation Mechanism Through Oxazolone Intermediate.[12]

Epimerisation of an amino acid can influence the conformation of the peptide, leading to molecules with different biological activities.[12] Moreover, epimerisation renders the purification process more difficult, as the epimerised products have similar physical characteristics.[12] In order to avoid that, HOBt is used as a coupling additive.[12] As shown in Scheme 21, HOBt converts the unstable intermediates into stable active esters, reducing epimerisation.[12]

2.1.1.1.4 Solvents

The most commonly used solvents, proved to be efficient for the coupling steps during the peptide synthesis, are dimethylformamide (DMF) and N-methylpyrrolidone (NMP), among which DMF is more widely used.[8]

2.1.1.1.5 Kaiser Test

The Kaiser test (also known as ninhydrin test) is used in order to detect the presence of primary amines.[8] The test is based on the reaction of ninhydrin with primary amines, which produces an intense blue colour, known as Ruhemann's purple (Scheme 23).[13] When this colour appears, unreacted N-terminal amines are present, indicating unsuccessful coupling (positive result).[8] Secondary amines, such as N-terminal proline, produce a less intense red-brown colour.[8]

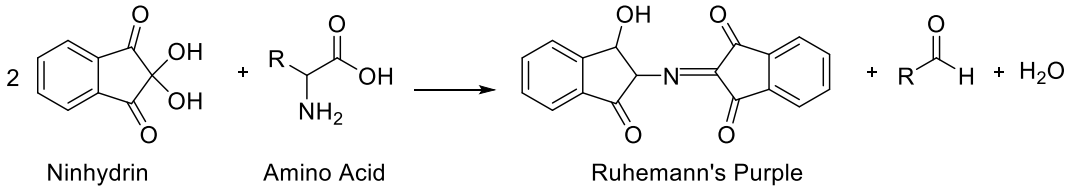

Scheme 23: Ninhydrin Test.[14]

In order to prepare the solutions used during the Kaiser test ninhydrin, phenol, potassium cyanide (KCN) and pyridine are needed (Table 2).[8] It is noteworthy that excess heating can result in a false positive result, as it can lead to loss of the Fmoc protecting group through reaction with pyridine, that is one of the reagents used.[8]

Table 2: Preparation of the Kaiser Test Reagents.

Reagents	Preparation
Reagent A	KCN (16.5 mg) was dissolved in deionised water (25 mL).
	This solution (1.0 mL) was diluted in pyridine (49 mL).
Reagent B	Ninhydrin (1.0 g) was dissolved in 1-butanol (20 mL).
Reagent C	Phenol (40 g) was dissolved in 20 mL of 1-butanol (20 mL).

2.1.1.1.6 Chloranil Test

Since the Kaiser test cannot be used for the detection of secondary amines, an alternative test is recommended for these cases.[8] The solution used is consisted by p-chloranil (1 g) and DMF (49 mL).[8] Presence of blue/purple colour indicates a positive result, showing an unsuccessful coupling.[8]

2.1.1.1.7 Synthesis of Polyprolines Based on SPPS

Based on this technique, polyprolines comprised of four, six and 13 units have been synthesized.[15] Garbuio, Luca, *et al*. designed oligoprolines with five, eight, 11, 14, and 17 residues.[16] Wennemers and co-workers synthesized an oligoproline with six residues, obtaining the first crystal structure of the PolPro II helix (detailed in Chapter 1).[17] In the Palma group, polyproline helices, as short as four residues were prepared, adopting a PolPro II conformation. (Figure 12).[18]

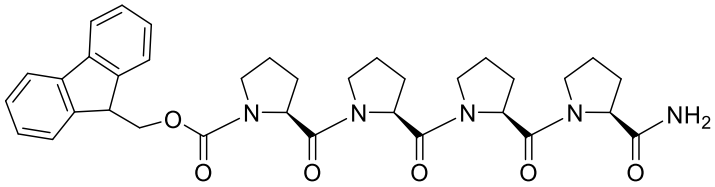

Figure 12: Proline Tetramer Fmoc-$(Pro)_4$-NH_2.[18]

Lastly, Erdmann and Wennemers have also synthesized azidoproline containing oligoprolines of various lengths through SPPS (Figure 13).[19]

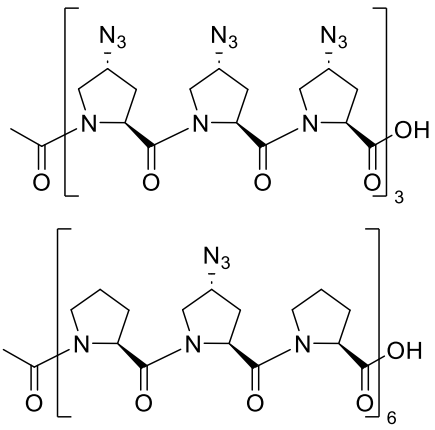

Figure 13: Azidoproline-Containing Oligoprolines.[19]

Therefore, SPPS is a technique that has been successfully employed for the preparation of various peptides by other research groups and is characterized by numerous benefits as described above. As a result, it was considered to be a suitable method for the synthesis of the designed polyprolines peptides.

2.2 Results and Discussion

As described in more detail in section 1.2, the first objective of this project was the use of polyproline peptides in organocatalysis.

2.2.1 Monomers

In order to synthesize the target peptides, the first step was the preparation of the corresponding monomers: N-Fmoc-trans-4-Boc-amino-L-proline (**A7**), (S)-1-N-Boc-4-N-Fmoc-piperazine-2-carboxylic acid (**C2**), N-Fmoc-cis-4-phenoxy-L-proline (**D3**), and 4-N-acetyl-piperazine-2-carboxylic acid (**E2**) (Figure 14).

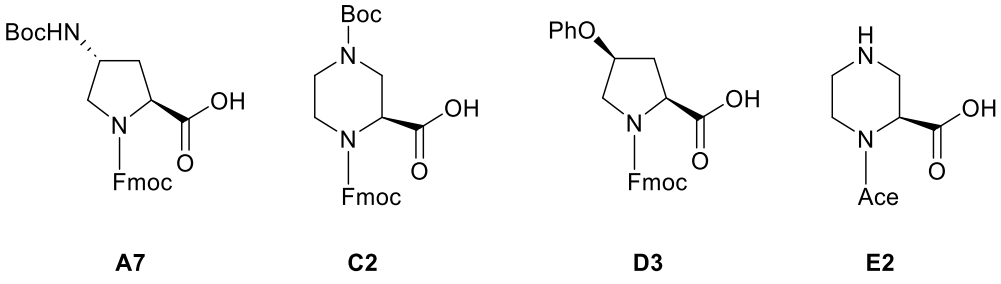

Figure 14: Structures of the Target Compounds.

Prior to the peptide synthesis, any free groups of the monomeric units need to be protected. Once the synthesis is completed the protecting groups can be removed, generating the peptide's main chain with the functionalized amino acid. As a result, **A7**, **C2** and **D3** will be prepared using

protecting groups suitable for their direct introduction into the peptides. More specifically, the carboxylic acid functionality and Fmoc protecting group are chosen as they are a requirement for the type of peptide synthesis that will be performed. Monomer **E2** doesn't have an Fmoc protecting group as it was synthesised in order to compare its catalytic activity with the one of monomer **C2**, and therefore, it will not be incorporated into a peptide.

The structures of the individual compounds were characterised by NMR, Liquid Chromatography-Mass Spectrometry (LCMS), and Fourier Transform-Infrared Spectroscopy (FT-IR). Column chromatography and recrystallization were used for the majority of steps as purification methods, while inert atmosphere was necessary for many of the reactions that were conducted.

2.2.1.1 Synthesis of N-Fmoc-trans-4-Boc-amino-L-proline (A7)

The first target compound was **A7** (Figure 14), where a chiral amino group is introduced at the C-4 position of the pyrrolidine ring. As mentioned in Section 1.2.1, the rationale behind its design was that once incorporated into a polyproline peptide, the effect of a primary amine that is pendant from the helix could be investigated. Since both the pyrrolidine ring and the carboxylic group are necessary for an effective asymmetric induction, it was considered crucial to maintain the proline backbone and introduce a chiral group at the C-4 position.[20] In this way, steric hindrance was induced from one side of the pyrrolidine ring. It is worth mentioning that 4-hydroxyproline have been employed as catalysts for the aldol reaction, while 4-trans-amino-proline peptides have been proven efficient catalysts for the aldol reaction.[20] More specifically, it has been shown that 4-trans-amino-proline di- and tetra-peptides can catalyze the reaction at lower loadings with good yields and enantioselectivities.[20] Therefore, the synthesis of a peptide where the catalytic site would be the amino group at the C-4 position of the proline monomeric unit, could be very promising.[20]

For the synthesis of the first building block (**A7**), a multi-step pathway was followed (Scheme 24). Firstly, the commercially available trans-4-hydroxyproline (**A1**) was protected as a benzyl ester. The carboxylic group was masked in order to avoid unwanted side reactions, while permitting chromatographic purification. This was achieved by treatment with benzyl alcohol (BnOH) and p-toluenesulfonic acid (pTSA), while water was removed using a Dean Stark apparatus.[21] It is noteworthy that instead of benzene that was reported in the literature,[21] toluene was the solvent of choice, while the desired compound was obtained in 95 % yield. A Boc protection reaction followed, using di-tert-butyl decarbonate (Boc_2O), sodium carbonate (Na_2CO_3) and water.[22] THF was used instead of 1,4-dioxane, and the crude material was purified with column chromatography, to afford the N-Boc-trans-4-hydroxy-L-proline benzyl ester (**A3**) as a yellow oil.

After that, an Appel reaction was performed for the introduction of the bromide group at the C-4 position, with inversion of the stereochemistry. This was achieved by addition of carbon tetrabromide (CBr_4), triphenylphosphine (PPh_3) and DCM under inert atmosphere,[23] while column chromatography was used as the purification method. The next step involved the conversion of the bromide into the azide ester, with sodium azide (NaN_3) in DMF. The presence of the azide group was confirmed through FT-IR analysis, as it has a clear and characteristic N=N stretching frequency at ~2100 cm^{-1}. N-Boc-trans-4-azido-L-proline benzyl ester (**A5**) was used for the next reaction without further purification.

It is notable that NaN_3 is highly toxic,[24] and thus it should be handled with caution. More specifically, the risk lies in the ability of NaN_3 to react with some metals, strong acids and some chlorinated solvents, forming explosive azides.[24] As a result, during the synthesis of the azide compound, the use of elevated temperature, metal spatulas and rotary evaporator was avoided, as these can lead to explosion.[24] Moreover, the pH of the generated waste was monitored and ensured to be basic, as NaN_3 reacts with acids to form hydrazoic acid (HN_3), which is highly toxic, explosive and more readily inhaled.[24]

After the synthesis of **A5**, removal of the Boc protecting group was achieved[25] through treatment with TFA and DCM. Introduction of the Fmoc protecting group followed, using Na_2CO_3 and water. It is noteworthy that N-9-Fluorenylmethoxycarbonyl chloride (Fmoc-Cl) and THF were used instead of N-(9-Fluorenylmethoxycarbonyloxy)succinimide (Fmoc-OSu) and 1,4-dioxane, leading to 70 % yield.[23] Finally, a hydrogenation reaction in order to remove the benzyl group,[23] and protection of the free amine with a Boc group were performed in one step, leading to the final product **A7**. The hydrogenation was achieved using palladium on carbon (Pd/C), conducting the reaction under a hydrogen (H_2) atmosphere overnight. After its completion, the precipitate was filtered off using a Celite filter. The presence of the Boc protecting group was confirmed via ^{1}H-NMR analysis, as it showed the added 9 tert-butyl (tBu) protons. Recrystallisation from DCM/Et_2O was firstly attempted, but as the product was still relatively impure, purification by column chromatography gave **A7** in high purity.

Nevertheless, the last reaction was characterized by low yield. One possible explanation for this observation is the formation of side products. At the same time, combination of Boc_2O and Pd/C could lead to a less effective Boc protection. As a result, the obtained yield could be improved by conducting the hydrogenation and Boc protection reaction as two separate reactions.

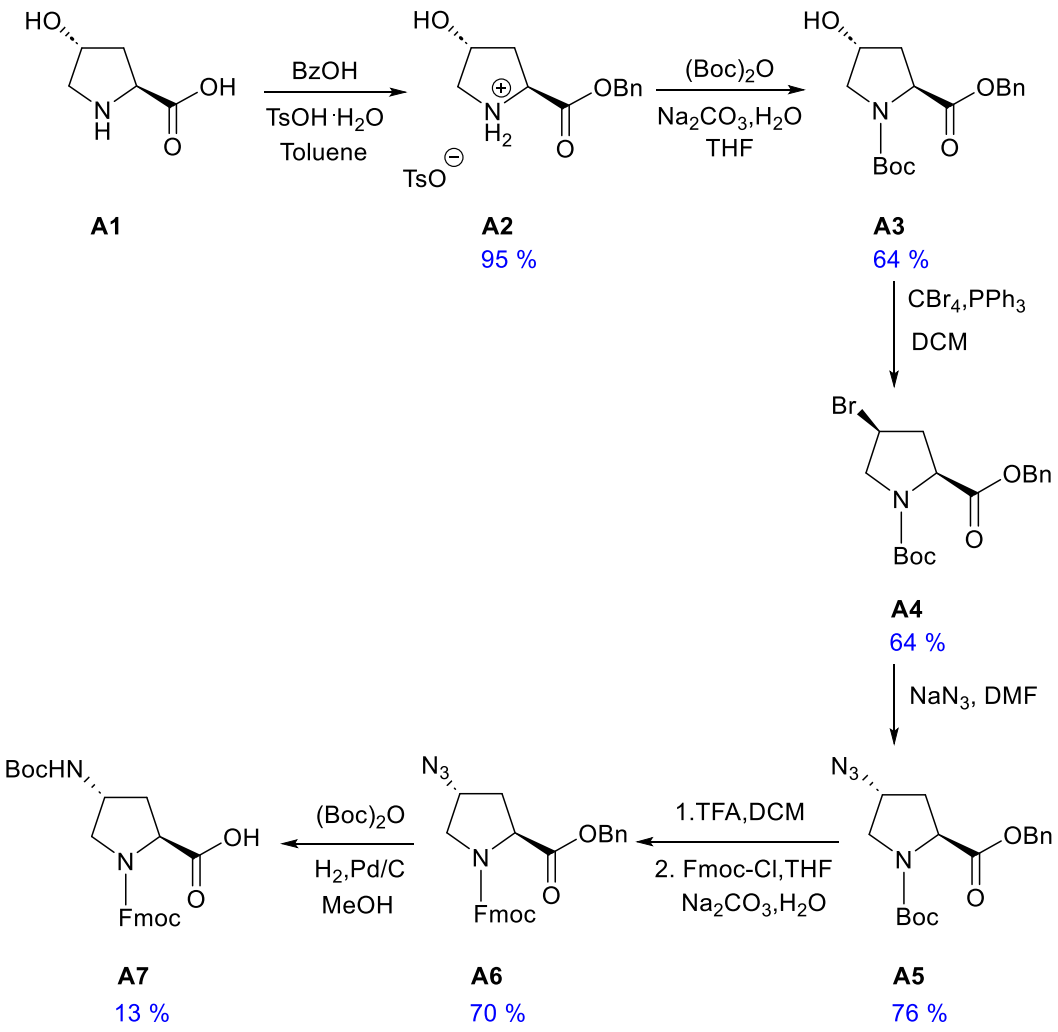

Scheme 24: Synthesis of N-Fmoc-trans-4-Boc-amino-L-proline (**A7**).

2.2.1.2 Alternative Synthesis of N-Fmoc-trans-4-Boc-amino-L-proline (A7)

In order to optimize product formation, an alternative pathway was investigated for the synthesis of **A7** (Scheme 25). Using a different starting material (**B1**), a saponification reaction along with introduction of the benzyl group, was followed by a mesylation reaction (Scheme 25). After that, the four last steps were similar with the ones in Scheme 24, with the difference that the hydrogenation and Boc protection reaction were conducted as two different reactions this time.

More specifically, starting from the commercially available N-Boc-cis-4-hydroxy-L-proline methyl ester (**B1**), the first step was a saponification reaction, along with introduction of the benzyl group. This was performed using sodium hydroxide (NaOH) and THF,[26] followed by addition of benzyl bromide (BnBr), DMF and triethylamine (Et_3N),[27] leading to obtainment of **B2** in 45 % yield. The next step involved activation of the hydroxyl group with methanesulfonyl chloride (MsCl) using Et_3N and DCM under inert atmosphere (89 % yield).[23] The four last steps performed in Scheme 25 were then repeated, leading to the obtainment of **A7**. The hydrogenation and Boc protection reaction were

conducted as two different reactions this time, while 2.5 equivalents of Boc_2O were used. It is notable that although the yield of the last reaction was increased as shown in Scheme 25 compared to Scheme 24, its value was still low. A probable cause of not achieving the expected yield is the purification method that was applied. Due to the obtained results, the pathway for the synthesis of **A7** needs to be further improved, and thus, this monomer was not used for the preparation of any peptide.

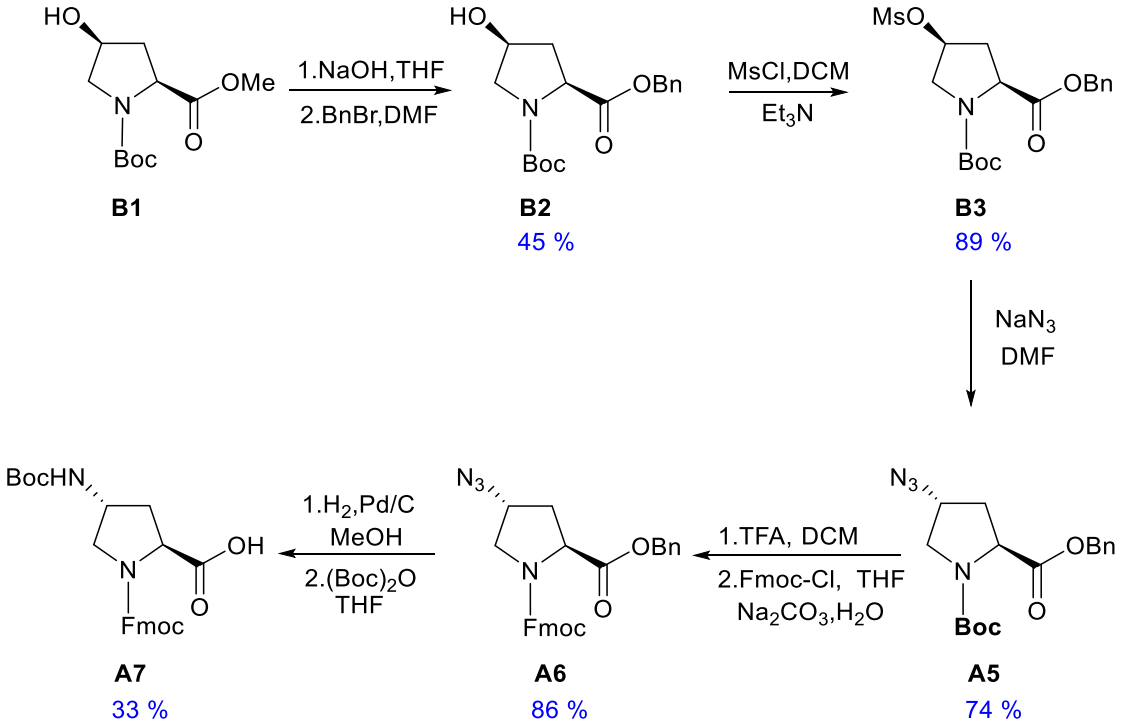

Scheme 25: Synthesis of N-Fmoc-trans-4-Boc-amino-L-proline (**B2**).

2.2.1.3 Synthesis of (S)-1-N-Boc-4-N-Fmoc-piperazine-2-carboxylic Acid (C2)

This monomer was designed so that once the corresponding peptide would be prepared, the effect of a secondary amine that is part of a six-membered ring within the polyproline helix, can be investigated. Piperazine in particular, has been characterized by interesting properties as an organocatalyst.[28] It is a rigid structure, with a diamine functionality within a cyclic framework.[29] Examples of catalysts comprised of piperazine have proved to be efficient organocatalysts,[30] with high catalytic activity in asymmetric transformations.[28] Thus, piperazine chemistry can be very useful in the design of new catalysts.[30] In this respect, the target monomer **C2** was designed using piperazine-2-carboxylic acid as the main unit.

In order for the monomer to be used in peptide synthesis, it was necessary to protect the amino groups. More specifically, in order to obtain **C2** (Figure 14), an Fmoc protection reaction of the commercially available (2R)-1-(Tert butoxycarbonyl)piperazine-2-carboxylic acid (**C1**) was performed

(Scheme 26) using Fmoc-Cl and THF, while Na_2CO_3 was employed as a base.[23] After 24 h, the reaction was completed according to TLC analysis. The product was isolated after aqueous workup and extraction with DCM. Recrystallization from Et_2O/n-Hex afforded the target monomer as a white crystalline solid in 63 % yield.

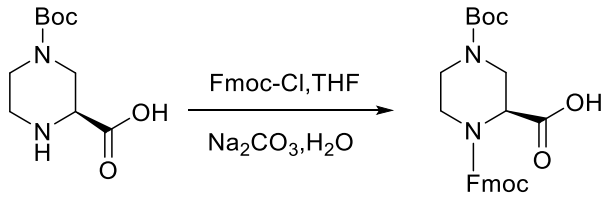

C1 **C2**
63 %

Scheme 26: Synthesis of (S)-1-N-Boc-4-N-Fmoc-piperazine-2-carboxylic acid (**C2**).

2.2.1.4 Synthesis of N-Fmoc-cis-4-phenyl- L-proline (D3)

Regarding the third target monomer **D3** (Figure 14), the C-4 position was functionalized by a phenyl group using proline as a basis. In this way, once incorporated into a peptide comprised of un-functionalized proline residues and one **C2** catalytic unit, the effect of the phenyl group on the catalytic outcome could be investigated.

The synthesis of **D3** was achieved using N-Boc-trans-4-hydroxy-L-proline benzyl ester (**A3**) as a starting material, through a synthetic approach shown in Scheme 27. First, a Mitsunobu reaction was performed, for the introduction of the phenyl group at the C-4 position, with inversion of the stereochemistry. PPh_3, THF and diisopropyl azodicarboxylate (DIAD) were used,[31] while the crude material was purified by column chromatography. Following that, removal of the Boc group, introduction of the Fmoc group, and a hydrogenation reaction using the usual conditions, yielded **D3** as the final product.

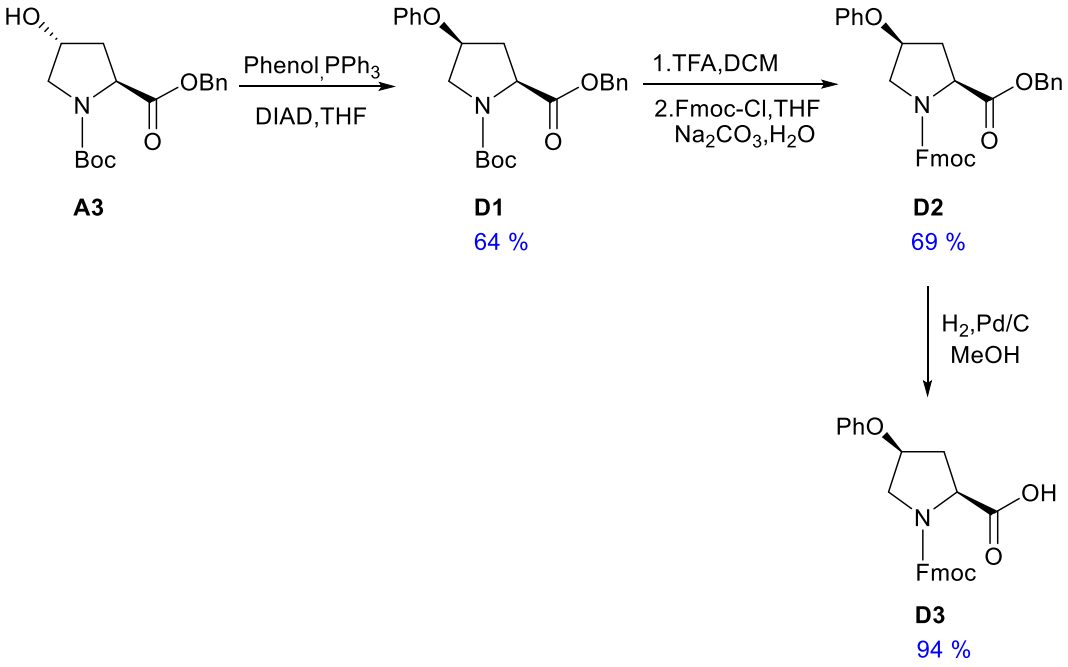

Scheme 27: Synthesis of N-Fmoc-trans-4-phenyl-L-proline (**C3**).

2.2.1.5 Synthesis of 4-N-acetyl-piperazine-2-carboxylic acid (E2)

Similarly to **D3**, **E2** was based on a piperazine-2-carboxylic acid (Figure 14). As it wasn't used for the peptide synthesis, the Fmoc protecting group was not necessary. Therefore, only acetylation of the free amine was performed.

In Scheme 28 the synthetic sequence to assemble **E2** is shown.[32] For the acetylation of the amine, using Ac_2O and aqueous NaOH solution, the reaction was completed after stirring at room temperature overnight.[33] After addition of concentrated HCl until pH reached ~ 2-3, and extraction with DCM, **E1** was obtained. Following that, removal of the Boc protecting group with the usual conditions and purification through Biotage, led to the desired product (**E2**) in 80 % yield.

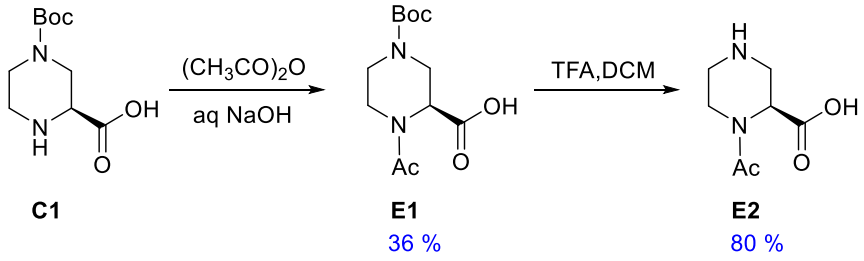

Scheme 28: 4-N-acetyl-piperazine-2-carboxylic acid (**E3**).

2.2.2 Peptides

2.2.2.1 Synthesis of Peptides

The next step involved the synthesis of a series of peptides comprised of proline monomers and functionalized monomeric units (Figure 15). Since **A7** was not employed for the preparation of the corresponding peptide (Figure 9-Target Peptide 2), three polyprolines were synthesized: **PP 1**, **PP 2** and **PP 3** corresponding to Figure 9-Target Peptides 1, 3 and 4 respectively. **PP 1** is comprised of seven un-functionalized proline units. **PP 2** has six un-functionalized proline units and a **C2** at the fourth position of the peptide chain. **PP 3** is identical to **PP 2**, with the difference of having a **D3** as a sixth monomeric unit. It is notable that **PP 2** and **PP 3** have capped ends in order for these sites not to influence the catalytic activity, which is not the case for **PP 1** as the amine of the proline ring at the C-terminus is the catalytic site of the peptide.

As mentioned in section 1.1.4.1, ~ 3 residues appear per turn on the polyproline helix, while a PolPro II to PolPro I conformational transition can occur from a minimum of six residues long peptide (section 1.1.4.5.1). Hence, we designed **PP 1**- **PP 3** to be comprised of seven residues in total. As a result, in case of showing a conformational transition, these peptides could be employed in stereodivergent organocatalysis.

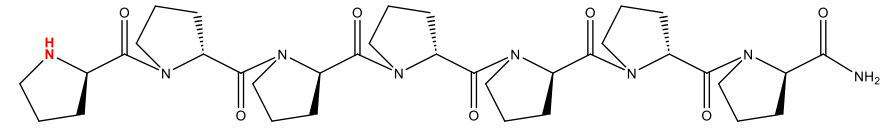

PP 1

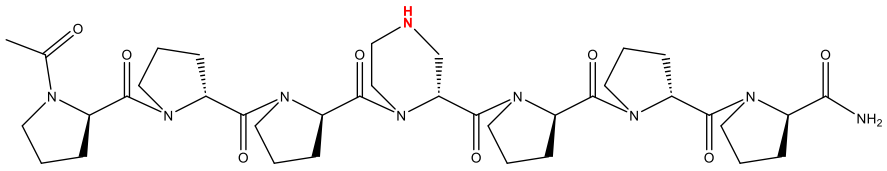

PP 2

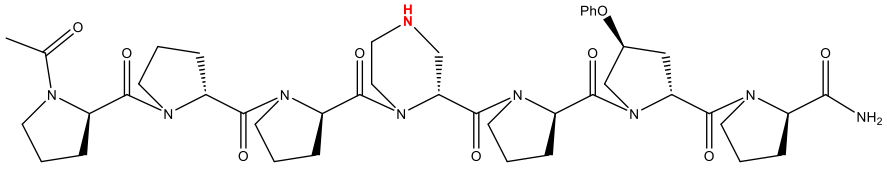

PP 3

Figure 15: Structures of Target Peptides.

2.2.2.1.1 Solid Phase Peptide Synthesis

Steps: It is noteworthy that the desired peptide sequence is assembled from the C-terminus to the N-terminus (C -> N).[6] The steps that need to be followed during this technique are the following (Figure 16):

- Before starting the synthesis, the resin support needs to be well swollen in DCM.[6,8] It is notable that DCM is the solvent of choice for this step as it reduces aggregation.[5]
- After washing with DMF (x 4), deprotection of the Fmoc group at the N-terminus follows using 20 % piperidine in DMF.[6,8]
- Subsequently to washing with DMF (x 4), the first Fmoc protected amino acid is attached onto the resin via its carboxyl group. More specifically, the protected amino acid is mixed with the coupling reagents, while smooth agitation of the beads is recommended in order to improve the coupling yield.

  After washing with DMF (x 4), a solution of DMF with 50 eq of Ac_2O and 50 eq of DIPEA is then added, in order to cap any free remaining primary amine and render them unreactive for the couplings that will follow. After the capping procedure, the resin and the peptide vessel should be washed thoroughly with DMF (x 4), as the step that follows is usually Fmoc deprotection and any free acetic acid will react with the deprotected amines.[5] The outcome of this procedure is checked via the Kaiser test which identifies the presence of unreacted primary amines.[6,8]
- Washing, deprotection of the Fmoc group, and addition of the second amino acid follows. Since the target peptides are comprised mainly of proline units, the chloranil test is used, in order to detect the presence of any secondary amines.[6,8]
- These two steps of Fmoc deprotection and amino acid coupling complete one cycle. The cycle is repeated until the desirable peptide chain length is obtained.[6,8]

  After each coupling the resin is filtered and washed with DMF (x 4) in order to remove any excess of reactants and side products.[6,8]
- Once the peptide has been synthesized it is cleaved from the resin using 95 % TFA in DCM.[6,8] The resin is washed with the cleavage cocktail (x 2) and the filtrate is concentrated under reduced pressure. Upon addition of cold Et_2O the filtrate is precipitating and then centrifuged. After decanting the solution, the solid is washed with cold Et_2O (x 3) in order to isolate the peptide.

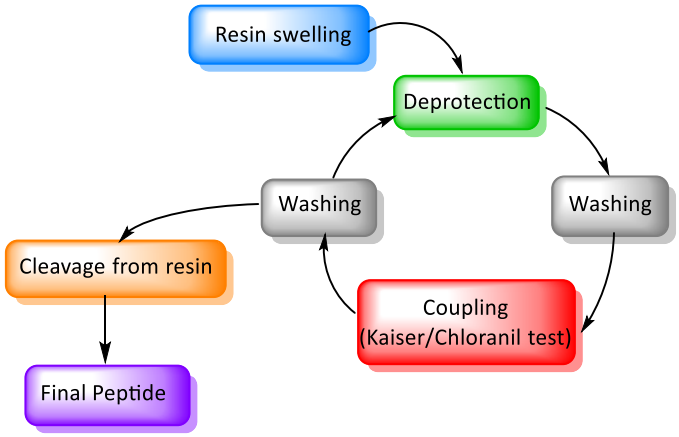

Figure 16: Overview of the Solid-Phase Peptide Synthesis (SPPS) Cycle.[6,8]

All polyproline peptides were synthesized using SPPS. The synthesis of the polyproline peptides in this chapter was performed using two different ways, through manual SPPS which was carried out first, and automated SPPS. In both cases, Fmoc-based SPPS and rink amide resin were used (Scheme 29). This type of resin is compatible with Fmoc chemistry and final cleavage using TFA.[6]

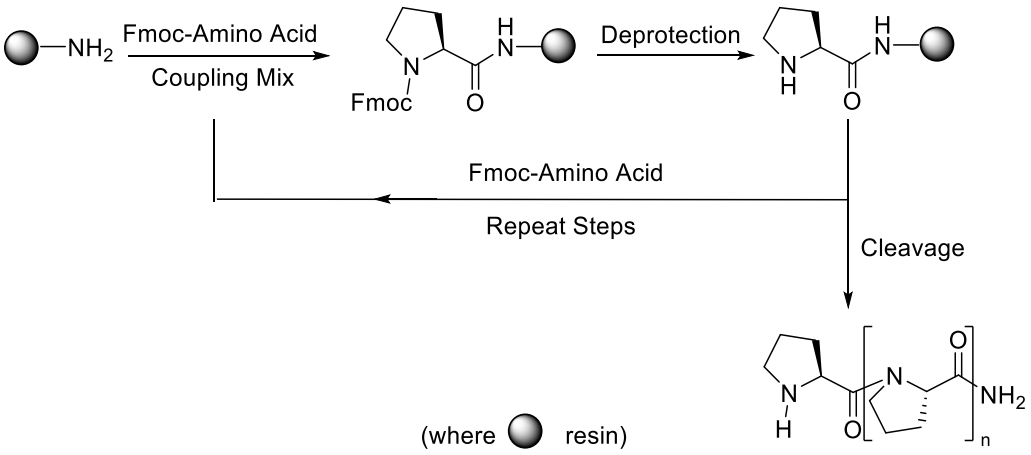

Scheme 29: Schematic Representation for the Solid-Phase Peptide Synthesis (SPPS) Using proline.

2.2.2.1.2 Synthesis of Peptides Manually

The rink amide MBHA resin was swelled in DCM (4 mL) for one hour, under smooth agitation. After washing with DMF (x 4), deprotection of the Fmoc group followed. In order to achieve this, a solution of 20 % piperidine in DMF (4 mL) was added to the resin and agitated for 40 min. It is notable that adding the solution of 20 % piperidine in DMF (4 mL) to the resin, agitating for 20 min and repeating this process one more time proved to be more effective. The first Fmoc protected amino acid (Fmoc-amino acid) was then linked onto the resin. For this purpose, the amino acid was mixed with the coupling reagents in DMF and after sonicating for one minute, this solution was added to the resin beads. The period of two hours was chosen as the optimal time for the coupling reaction in order to reduce the possibility of partially incomplete coupling. A solution of 10 % Ac_20

and 2.5 % DIPEA in DMF (4 mL) was then added in order to cap all the unreacted amines on the surface of the resin.[8] The outcome of this procedure was checked via the Kaiser test.[8]

The Fmoc group was again deprotected and the coupling of the second amino acid followed, using the chloranil test in order to monitor whether a successful outcome would occur.[8] The coupling reagents for **PP 1** and **PP 2** were two equivalents of PyBOP, two equivalents of HOBt, and four equivalents of DIPEA (Table 3 a, c). Nevertheless, the coupling procedure had to be repeated two or even three times. This was not ideal, as it required more time, but also more quantity of amino acids which were often precious, especially in the case of using the functionalized monomers. In order to overcome this, different equivalents of PyBOP, HOBt and DIPEA were used. During the synthesis of **PP 2**, the equivalents of PyBOP were doubled (Table 3 c). Although this improved the coupling procedure, the use of three equivalents of PyBOP, three equivalents of HOBt and six equivalents of DIPEA proved to be the optimum ratio. As a result, this ratio was then used for the synthesis of **PP 1**, **PP 2** and **PP 3** (Table 3 b, d, f). It is noteworthy that a different set of reagents was also used during the manual synthesis of **PP 2** (Table 3 e). By using ten equivalents of Oxima Pure and ten equivalents of diisopropylcarbodiimide (DIC) in DMF, this polyproline was successfully synthesized, without repeating any coupling step.

After removal of the protecting group on the amino acid that was introduced, the coupling and deprotection steps were repeated until the desired peptide sequence was assembled.[8] Before the final step, the capping procedure was repeated using the same conditions as the ones mentioned above. This wasn't applied for **PP 1**, as the amine of the last proline unit needs to be free in order to act as a catalytic site.

Cleavage with a solution of 95 % TFA in DCM (4 mL) followed. After 90 min of smooth agitation, the resin was washed with the same solution (x 2). The obtained solution was collected and evaporated and the peptide precipitated with cold Et_2O. It is noted that for all the peptides that were synthesized, the cleavage procedure had to be repeated twice in order for the product to precipitate upon addition of cold Et_2O.

Table 3: Coupling Reagents and Equivalents Used for the Synthesis of Each Peptide.

	PEPTIDE	COUPLING REAGENTS	EQUIVALENTS
a	**PP 1**	Fmoc-amino acid /PyBOP/HOBt/DIPEA	2/2/2/4
b		Fmoc-amino acid/PyBOP/HOBt/DIPEA	2/3/3/6
c	**PP 2**	Fmoc-amino acid/PyBOP/HOBt/DIPEA	2/2/2/4 (Couplings 1-4)
			2/4/2/4 (Couplings 5-7)
d		Fmoc-amino acid/PyBOP/HOBt/DIPEA	2/3/3/6
e		Fmoc-amino acid/Oxima/DIC	2/10/10
f	**PP 3**	Fmoc-amino acid/PyBOP/HOBt/DIPEA	2/3/3/6

2.2.2.1.3 Synthesis of Peptides on the Peptide Synthesizer

The synthesis of all the peptides was also performed using a Liberty™ microwave peptide synthesiser (CEM), and rink amide MBHA resin on a 0.1 mmol scale.

The resin was swollen in DCM and was then placed on the apparatus, with the rest of the reagents. Single deprotection of the Fmoc group, followed by couplings interspaced with washings were performed. Two equivalents of the Fmoc-amino acid, five equivalents of HOBt, one equivalent of PyBOP and five equivalents of DIPEA were used in the beginning as coupling reagents for the synthesis of **PP 1** and **PP 2** (Table 4 a, c). Nevertheless, using three equivalents of Oxima Pure and six equivalents of DIC proved to be more efficient (Table 4 b). After trying different concentrations of the two coupling reagents, the use of three equivalents of Oxima Pure and six equivalents of DIC were the optimum ones (Table 4 b, d and f) yielding **PP 1** and **PP 2** in 64 % and 66 % yield respectively. Lastly, it was proved that addition of 0.5 equivalent of DIPEA in Oxima Pure, led to a better outcome (Table 4 e), affording **PP 3** in 66 % Due to the high temperatures used and their acidic nature, activators like Oxima Pure can prematurely remove acid sensitive groups.[34] By using small amounts of base, acid sensitive linkages can be stabilized, while it doesn't interfere with the activation process.[34]

Once the desired peptide chain was created, the capping procedure was performed. As mentioned above this was applied only for **PP 2** and **PP 3**. The resin was then removed from the apparatus, and cleavage was performed using the same conditions as in the manual SPPS (as described in section 2.2.2.1.2). As mentioned above, the cleavage procedure had to be repeated twice in most cases in order to obtain a sufficient amount of peptide. After this process, precipitation of the peptide upon addition of cold Et_2O followed.

Table 4: Coupling Reagents and Equivalents Used for the Synthesis of Each Peptide.

	PEPTIDE	COUPLING REAGENTS	EQUIVALENTS
a	**PP 1**	Fmoc-amino acid/PyBOP/HOBt/DIPEA	2/5/1/5
b		Fmoc-amino acid/Oxima/DIC	2/3/6
c	**PP 2**	Fmoc-amino acid/PyBOP/HOBt/DIPEA	2/1/5/5
d		Fmoc-amino acid/Oxima/ DIC	3/3/6
e		Fmoc-amino acid/Oxima /DIC/DIPEA	3/3/6/0.3
f	**PP 3**	Fmoc-amino acid/Oxima/DIC	3/3/6

2.2.2.2 Analysis and Purification of Peptides

All peptides were analysed via LCMS, while crude products were purified through Preparative High-Performance Liquid Chromatography (RP-HPLC) when needed.

Concerning **PP 1**, after the first manual synthesis, the LCMS analysis revealed the formation of a mixture of polyprolines, comprised of six, seven and eight proline units (Figure 17 a). The peak corresponding to six monomeric units was possibly due to unsuccessful coupling, whereas the one with eight residues could originate from longer coupling times or repeating coupling steps. After purification via preparative RP-HPLC, the target peptide was successfully isolated, as shown in Figure 17 b.

a)

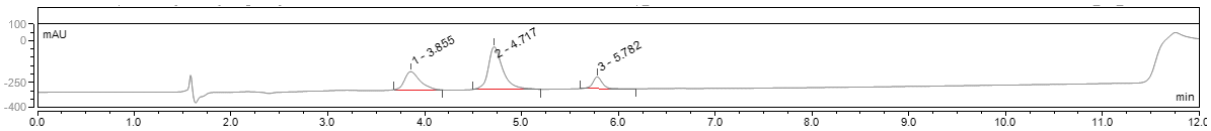

b)

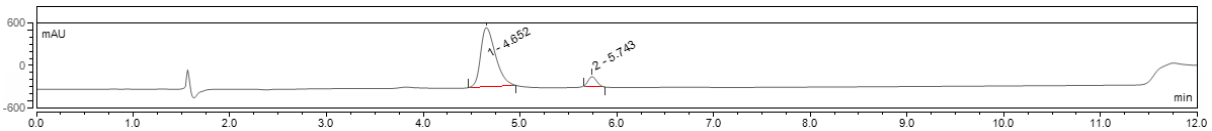

Figure 17: LCMS Chromatograms of **PP 1** a) Before and b) After Purification (Determined Using UV Detection at 225 nm: >99 %, on a Kromasil 100-5-C18, 4.6 x 250 mm, 30 to 100 % B over 12 mins. A is 0.1 % formic acid/ H_2O and B is 0.1 % formic acid/MeOH).

Another attempt resulted in four peaks at the LCMS chromatogram of the product peptide. These correspond to polyprolines with three, five, six and seven residues (Figure 18). In this case, optimising the synthetic procedure was decided to be more efficient than a purification method. As

mentioned above, the generation of undesirable, shorter chain peptides is an indication that the corresponding coupling steps were not fully completed, leaving some amines unreacted. Thus, changes on the coupling procedure were considered essential in order to avoid additional purification steps.

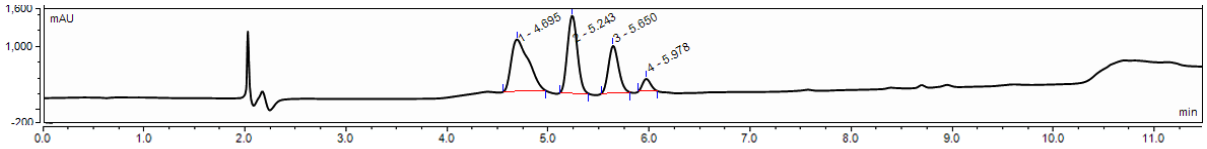

Figure 18: LCMS Chromatogram of **PP 1** (Determined Using UV Detection at 225 nm: >99 %, on a Kromasil 100-5-C18, 4.6 x 250 mm, 30 to 100 % B over 12 mins. A is 0.1 % formic acid/ H_2O and B is 0.1 % formic acid/MeOH).

After increasing the equivalents of HOBt, PyBOP and DIPEA from two, two and four to three, three and six respectively, the obtained product showed a significantly improved LCMS profile (Figure 19 a). The major peak represents a heptamer polyproline, while some minor impurities can also be observed. Preparative RP-HPLC was used as a purification method, resulting in the desired peptide in a high degree of purity (Figure 19 b).

a)

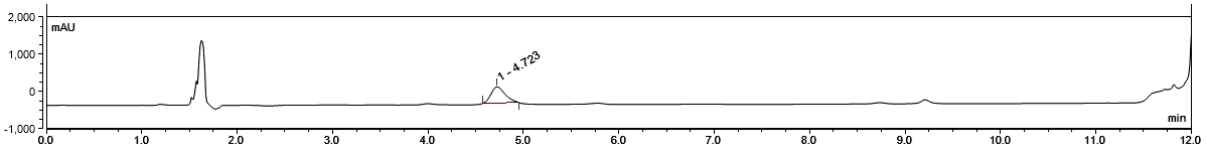

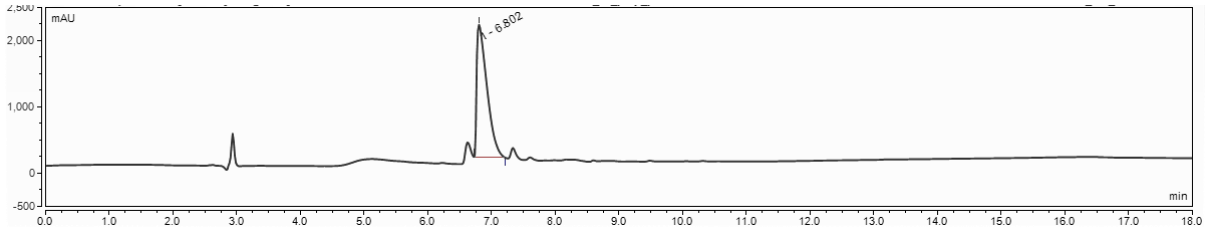

Figure 19: LCMS Chromatograms of **PP 1** a) Before and b) After Purification (Determined using UV Detection at 225 nm: >99 %, on a Kromasil 100-5-C18, 4.6 x 250 mm,
a) 30 100 % B over 12 mins. A is 0.1 % formic acid/ H_2O and B is 0.1 % formic acid/MeOH).
b) 30 100 % B over 18 mins. A is 0.1 % formic acid/ H_2O and B is 0.1 % formic acid/MeOH).

b)

Once the synthesis of **PP 1** was performed on the peptide synthesizer, the LCMS confirmed the mass of the target peptide (Figure 20).

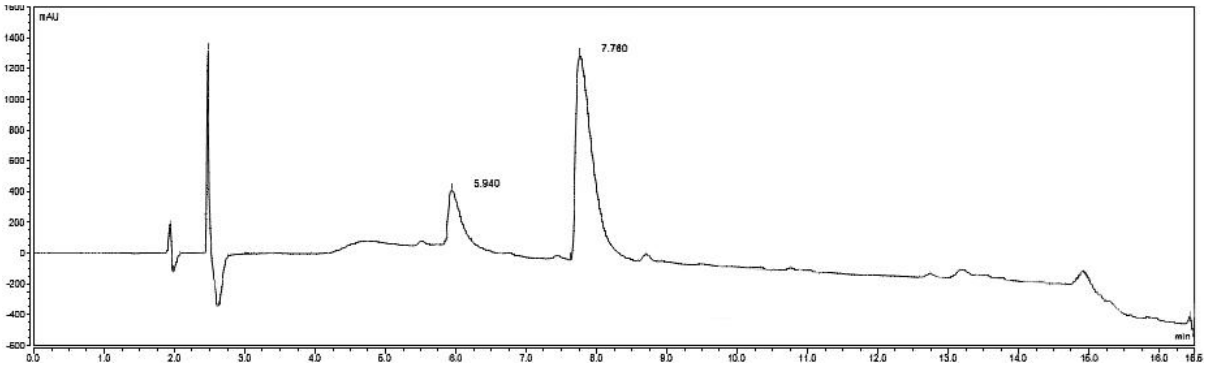

Figure 20: LCMS Chromatogram of **PP 1** (Determined by LCMS Using UV Detection at 225 nm: >99 %, on a Kromasil 100-5-C18, 4.6 x 250 mm, 20 to 100 % B over 16.5 mins. A is 0.1 % formic acid/ H_2O and B is 0.1 % formic acid/MeOH).

Lastly, Figure 21 shows the LCMS chromatogram of **PP 1** after applying the optimised conditions on the peptide synthesizer. The crude sample displays a strong peak at retention time 6.76 min which is the target peptide. It is noteworthy that this peptide was used further without any purification.

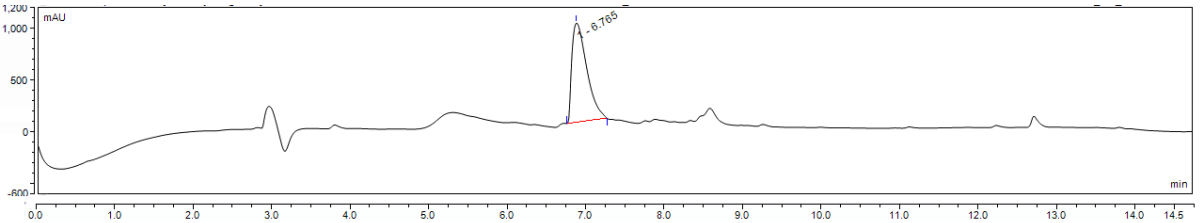

Figure 21: LCMS Chromatogram of **PP 1** (Determined by LCMS Using UV Detection at 225 nm: >99 %, on a Kromasil 100-5-C18, 4.6 x 250 mm, 20 to 100 % B over 14.5 mins. A is 0.1 % formic acid/ H_2O and B is 0.1 % formic acid/MeOH).

In regards to **PP 2**, after the first manual synthesis, the LCMS chromatogram of the crude sample revealed the presence of three products (Figure 22). These are corresponding to the target peptide, but also a polyproline with one and two more proline units respectively. Similarly, to the case of **PP 1**, the formation of the undesirable peptides was possibly due to longer coupling time or repeating coupling steps.

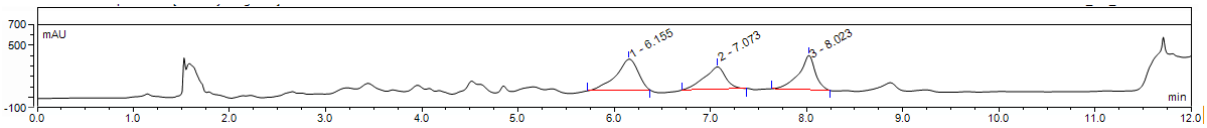

Figure 22: LCMS Chromatogram of **PP 2** (Determined by LCMS Using UV Detection at 225 nm: >99 %, on a Kromasil 100-5-C18, 4.6 x 250 mm, 30 to 100 % B over 12 mins. A is 0.1 % formic acid/H_2O and B is 0.1 % formic acid/MeOH).

In order to improve the synthesis, the equivalents of coupling reagents were increased. This led to the obtainment of a product with higher purity, with one major peak at the LCMS chromatogram

(Figure 23 a). The crude material was purified through preparative RP-HPLC, and the target peptide was isolated successfully as indicated by LCMS (Figure 23 b).

a)

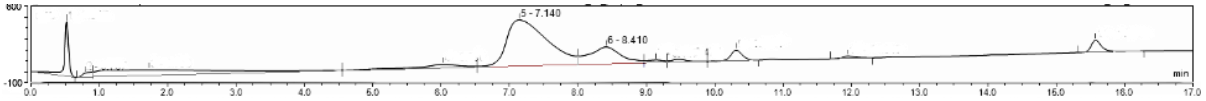

b)

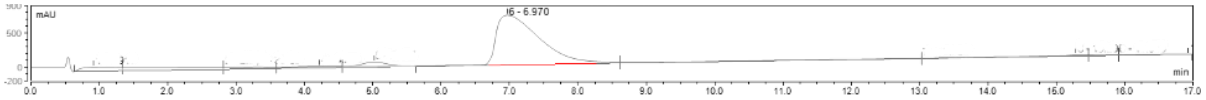

Figure 23: LCMS Chromatograms of **PP 2** a) Before and b) After Purification (Determined by LCMS Using UV Detection at 225 nm: >99 %, on a Kromasil 100-5-C18, 4.6 x 250 mm, 40 to 100 % B over 17 mins. A is 0.1 % formic acid/H_2O and B is 0.1 % formic acid/MeOH).

The synthesis was also performed using the peptide synthesizer, with the LCMS confirming the mass of the desired peptide as the major peak (Figure 24 a). One notable observation is that a minor shoulder peak was also present and thus, preparative RP-HPLC was performed leading to the desired peptide with a high degree of purity (Figure 24 b).

a)

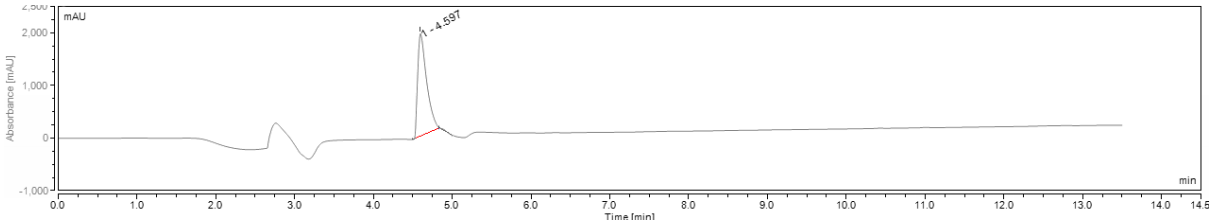

b)

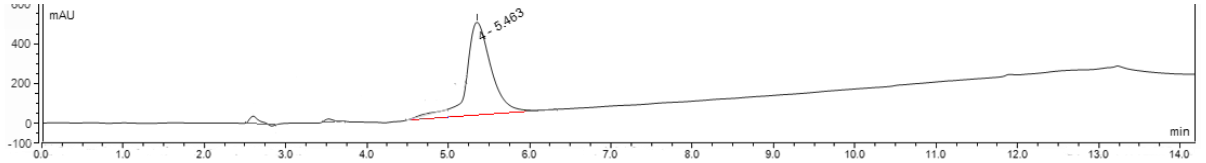

Figure 24: LCMS Chromatograms of **PP 2** a) Before and b) After Purification (Determined by LCMS Using UV Detection at 225 nm: >99 %, on a Kromasil 100-5-C18, 4.6 x 250 mm,
a) 60 to 100 % B over 14.5 mins. A is 0.1 % formic acid/H_2O and B is 0.1 % formic acid/MeOH.
b) 50 to 100 % B over 14.5 mins. A is 0.1 % formic acid/H_2O and B is 0.1 % formic acid/MeOH).

Lastly, aiming to further optimise the synthesis, DIPEA was added in the coupling reagents. The LCMS analysis for this attempt shows that the target polyproline was synthesized successfully, without any purification step being necessary (Figure 25).

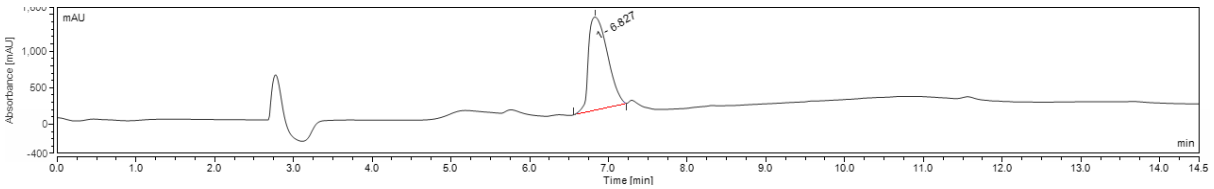

Figure 25: LCMS Chromatogram of **PP 2** (Determined by LCMS Using UV Detection at 225 nm: >99 %, on a Kromasil 100-5-C18, 4.6 x 250 mm, 30 to 100 % B over 14.5 mins. A is 0.1 % formic acid/H_2O and B is 0.1 % formic acid/MeOH).

For the synthesis of **PP 3**, two synthetic attempts were performed. The first one was performed manually, with three equivalents of HOBt, three equivalents of PyBOP and six equivalents of DIPEA being used. As shown in Figure 26, the LCMS chromatogram of the crude material displays one major peak, which corresponds to the target peptide, in addition to showing a minor impurity peak.

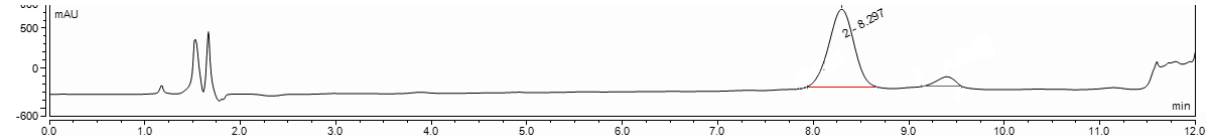

Figure 26: LCMS Chromatogram of **PP 3** (Determined by LCMS Using UV Detection at 225 nm: >99 %, on a Kromasil 100-5-C18, 4.6 x 250 mm, 10 to 100 % B over 12 mins. A is 0.1 % formic acid/H_2O and B is 0.1 % formic acid/MeOH).

PP 3 was also synthesized on the peptide synthesizer leading to an improved outcome. The LCMS analysis revealed the presence of a single strong peak which represents the desired polyproline (Figure 27).

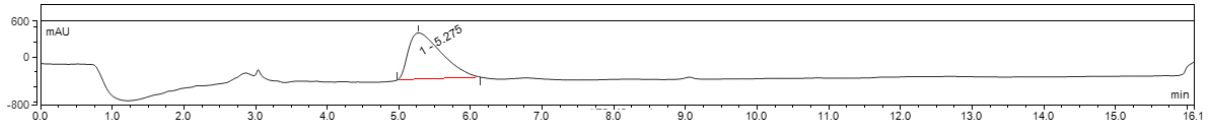

Figure 27: LCMS Chromatogram of **PP 3** Before Purification (Determined by LCMS Using UV Detection at 225 nm: >99 %, on a Kromasil 100-5-C18, 4.6 x 250 mm, 60 to 100 % B over 16 mins. A is 0.1 % formic acid/H_2O and B is 0.1 % formic acid/MeOH).

Preparative RP-HPLC was performed, leading to the desired peptide with a high degree of purity (Figure 28).

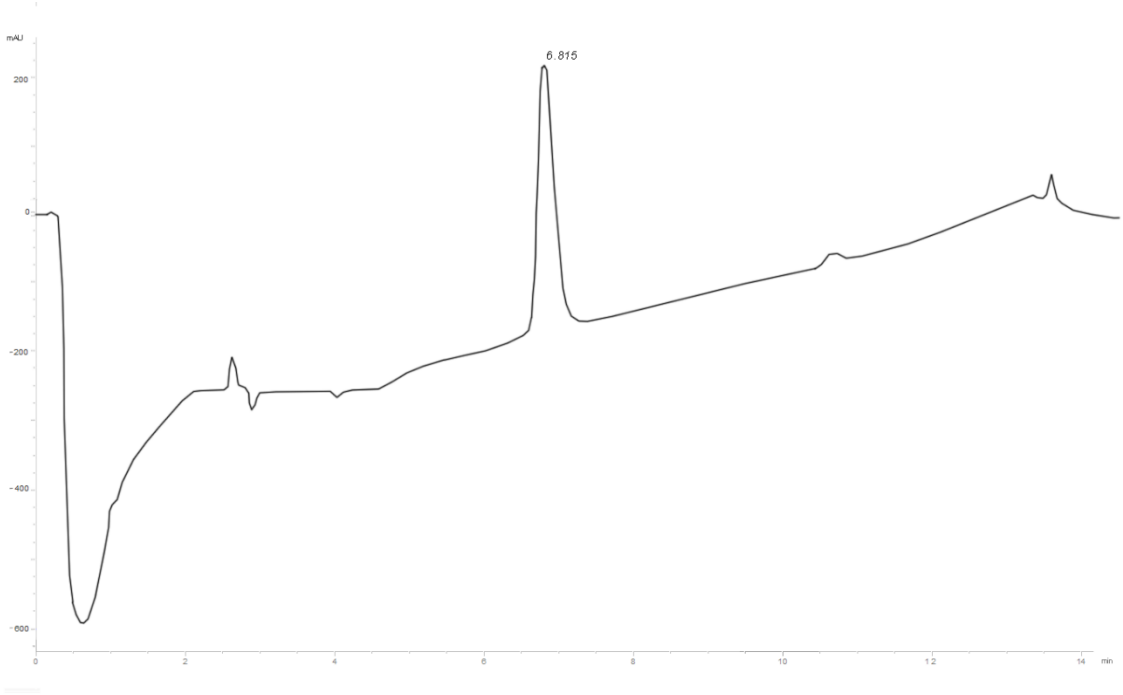

Figure 28: HPLC Chromatogram of **PP 3** after Purification (Determined on an Agilent 1100 HPLC Using UV Detection at 225 nm: >99 %, on a Kromasil 100-5-C18, 4.6 x 250 mm, 40 to 100 % B over 14.5 mins. A is 0.1 % formic acid/H_2O and B is 0.1 % formic acid/MeOH).

2.2.2.3 CD Analysis

CD spectroscopy is a very valuable technique for the conformational analysis of polyprolines, which can be used in order for the two helices to be distinguished, as further detailed in Chapter 1.[15]

After their synthesis, **PP 1**, **PP 2** and **PP 3** were analysed through CD spectroscopy in two different solvents. Two samples were prepared for each peptide, one in water and one in propanol. As mentioned in Chapter 1 (1.3), in this way the effect of the solvent on the conformation of each peptide could be investigated. The samples were left to equilibrate for seven days at 20 °C before the measurements were taken.

The CD spectrum of **PP 1** in water showed a strong negative band at 205 nm and a weak positive band at 225 nm (Figure 29-blue). The same peptide in propanol, exhibited a broad negative band at 200 nm, a positive band at 215 nm and a broad negative band at 235 nm (Figure 29-orange). For **PP 2**, the CD spectrum in water was characterised by a broad negative band at 205 nm (Figure 30-blue), while the spectrum in propanol showed a broad negative band at 205 (Figure 30-orange). The CD spectrum of **PP 3** in water presented a broad negative band at 208 nm (Figure 31-blue). The spectrum for the same peptide in propanol was characterized by a broad negative band at 205 nm, and a weak positive band at 225 nm (Figure 31-orange).

From these data, one can observe that the conformation of **PP 1** in water was indicative of a PolPro II conformation, while the one in propanol was consistent with the CD profile reported for PPI. As a result, there was a conformational switch. Regarding **PP 2**, it presented a negative band in both solvents, while a positive band appeared only in propanol. The same occured for **PP 3**, as there was no significant shift in intensities which could suggest that a conformational change was occurring. Therefore, these peptides appeared to adopt a similar conformation in the two solvents which is characteristic of a PolPro II helix.

As a result, we can observe that only **PP 1** showed a conformational switch depending on the solvent applied, while the rest peptides adopted a PolPro II conformation. According to these results, the helicity from a polyproline comprised of seven un-functionalized units can lead to a conformational switch, whereas once chiral functionalized units are introduced within the helix, this length is not sufficient in order for a conformational transition to occur. **PP 1** can therefore be examined as a catalyst in stereodivergent organocatalysis, while **PP 2** and **PP 3** will be tested as enantioselective organocatalysts.

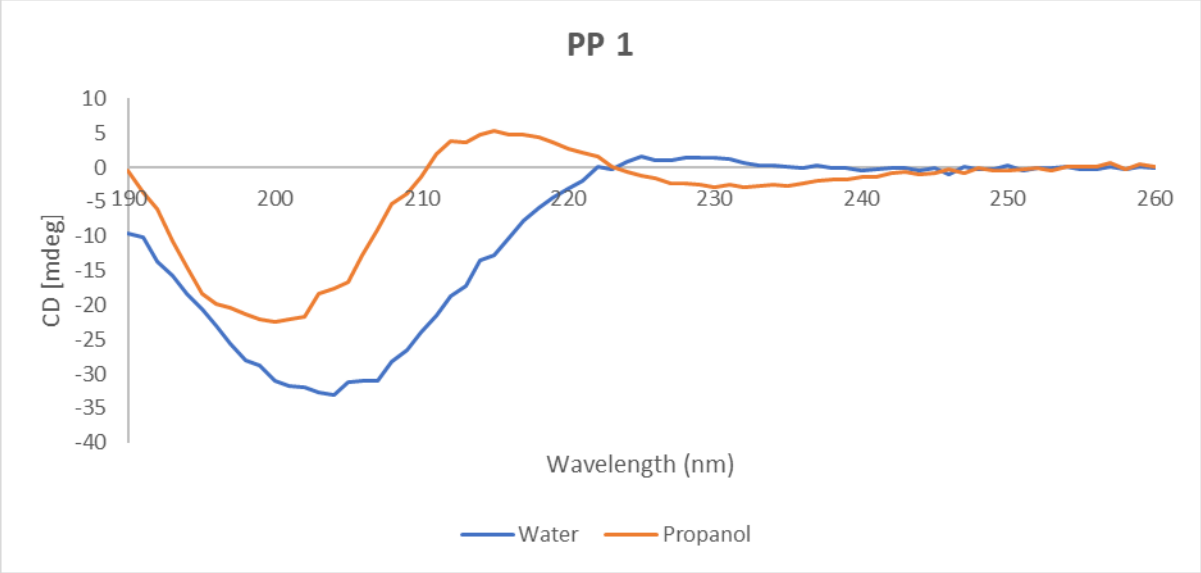

Figure 29: CD Spectrum of **PP 1** in Aqueous Solution (blue) and in propanol (orange) at 20 °C and ≈ 100 µM.

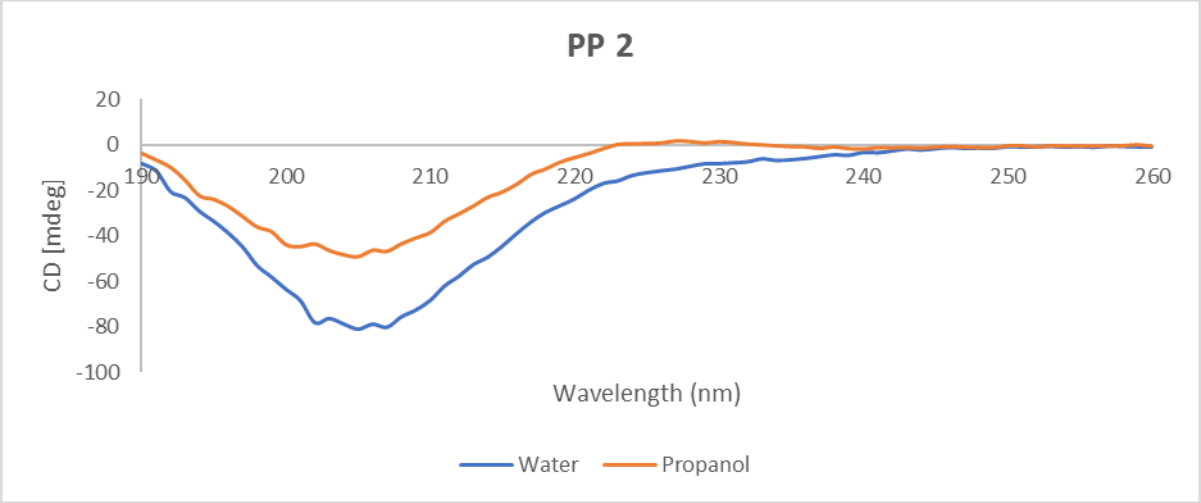

Figure 30: CD Spectrum of **PP 2** in Aqueous Solution (blue) and in propanol (orange) at 20 °C and ≈ 100 μM.

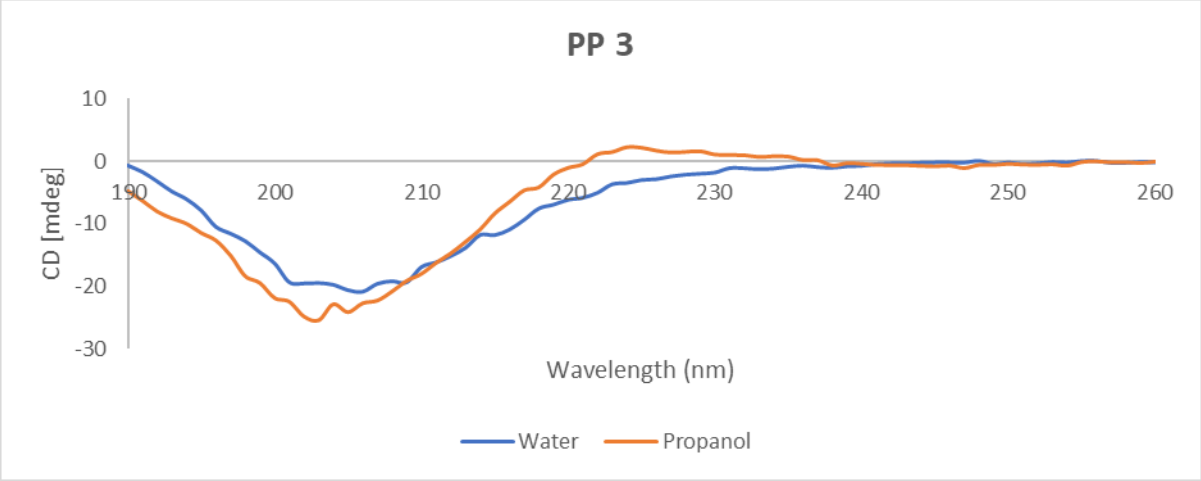

Figure 31: CD Spectrum of **PP 3** in Aqueous Solution (blue) and in propanol (orange) at 20 °C and ≈ 100 μM.

2.2.3 Application of PP 1, PP2 and PP 3 in the Aldol Asymmetric Reaction

Following the preparation of the polyproline peptides, our efforts were directed towards the study of their catalytic ability on the aldol reaction. Highly electrophilic acceptors like 4-nitrobenzaldehyde and simple donor such as cyclohexanone are often used,[35] and thus, they were employed here as benchmark substrates (Scheme 30).

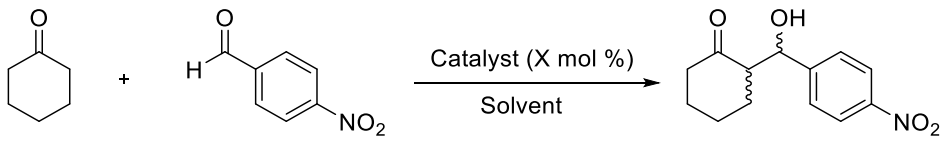

Scheme 30: Aldol Reaction Between p-nitrobenzaldehyde and cyclohexanone.

The same reaction was also performed in the presence of a non-chiral catalyst, instead of polyproline. More specifically, ammonium acetate (NH_4OAc) was used so that its action could be

compared to the one of the target compounds. Apart from that, the activity of monomer **E3** was also investigated in order to compare it with the one of **PP 2** and **PP 3** (Figure 32). Lastly, **L-proline** was tested as a catalyst for the aldol reaction, as it was used as a reference.

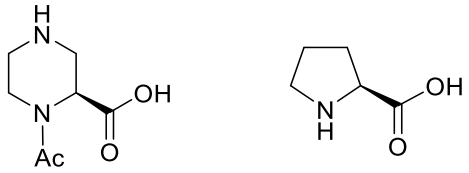

E3 L-proline

Figure 32: Structures of Monomer **E3** and L-proline.

All the reactions were monitored through TLC. After that, they were analysed via ^{1}H-NMR in order to determine the dr (anti/syn). As demomnstrated by Deng *et al*., the syn-configuration of the desired aldol product shows a peak around 5.49 ppm, while the peaks corresponding to the anti-product appear around 4.92 ppm.[36] Based on that, the syn and anti-products of the aldol reaction under the influence of **PP 1**-**PP 3** were idenitified. Figure 33 shows a typical ^{1}H-NMR spectrum of an aldol reaction between 4-nitrobenzaldehyde and cyclohexanone, using **PP 1** as a potential catalyst. As indicated by the spectrum, the syn-product is characterized by a signal around 5.49 ppm, while the peaks corresponding to the anti-product appears around 4.92 ppm (Figure 33).

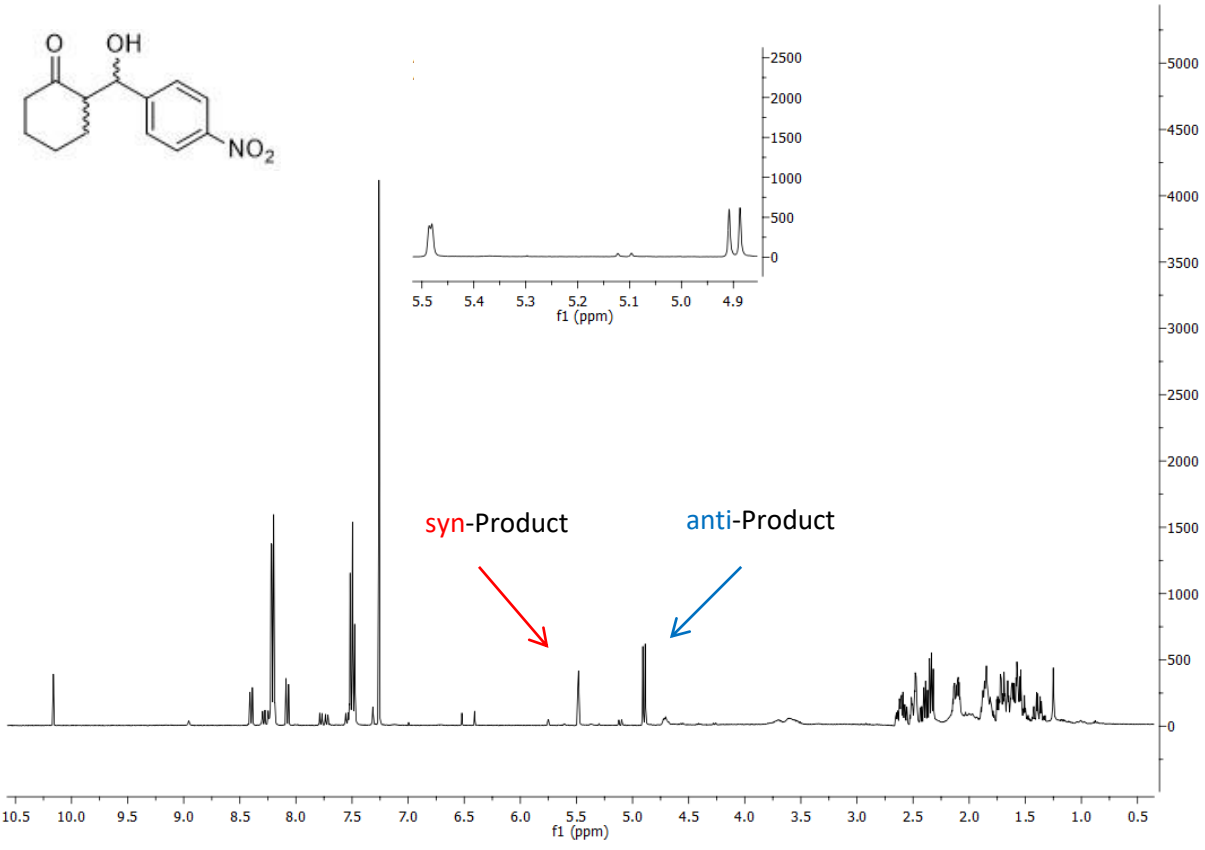

Figure 33: ^{1}H-NMR Spectrum of Aldol Reaction Using **PP 1** as a Potential Catalyst.

The optimum aldol products for each case were then selected. After concentrating under reduced pressure, each sample was dissolved in n-hexane-isopropanol, centrifuged, and filtered through a 0.2 µm PTFE syringe filter. Analysis via HPLC with a chiral stationary phase (Chiralpak AD-H and a mobile phase n-hexane/i-PrPOH= 80/20 (v/v); 1 mL min-1; 254 nm; 25 °C) followed. According to Messerer and Wennemers, the four stereoisomers of the product are defined as **1** (2*R*,1'*R*)), **2** (2*S*,1'*S*), **3** (2*S*,1'*R*), **4** (2*R*,1'*S*) Further details about the chiral-HPLC are illustrated in Appendix 1. Based on that, the enantiomeric excess (ee) values for the product, 2-(Hydroxyl-(p-nitrophenyl)methyl)cyclohexan-1-one, of each reaction were determined.

Our study was initiated by testing NH_4OAc as a catalyst for the aldol reaction. According to the obtained NMR spectrum, the catalyst led to no selectivity (Appendix 1). The next step was the investigation of the activity of **PP 1**. In order to find the optimum reaction conditions, different solvents, temperatures and additives were investigated, which are summarised in Table 5.

Using 10 % loading of **PP 1**, the reaction was firstly performed in 2,2,2-Trifluoroethanol (TFE). TFE was chosen as a solvent for these experiments for many reasons. Firstly, it is known that the PolPro II helix is found in aqueous solvents or TFE, whereas the PolPro I one is dominating in less polar solvents like MeOH or propanol. In addition, TFE has higher acidity than ethanol (EtOH) (pKa 12.5 and 16.0 respectively), while its three fluorine atoms render it less nucleophilic. Due to these two properties, TFE has showed enhanced reactivity. Moreover, regarding peptide chemistry, it can solubilise various polar molecules, the same time that it is relatively volatile in comparison to other solvents like DMF or DMSO, which makes its removal easier.

Table 5: Optimization of Aldol Reaction Conditions Using **PP 1**.

Entry	Solvent	T (°C)	Additive (%)	Yield[b] (%)	dr (anti/syn)[b]	ee % (anti)[c]	ee % (syn)[c]
1	TFE	RT	None	70	71/29	-	-
2	TFE	40	None	73	68/32	-	-
3	TFE	RT	TFA 15 %	4.5	56/44	-	-
4	TFE	40	TFA 15 %	12	63/38	-	-
5	TFE	40	TFA 10 %	16	50/50	-	-
6	TFE	40	TFA 5 %	4	63/38	-	-
7	TFE	40	AcOH 15 %	20	63/38	-	-
8	TFE	40	AcOH 10 %	15	61/39	-	-
9	TFE	40	AcOH 5 %	9.5	58/42	-	-
10	H_2O	RT	TFA 15 %	7	64/36	-	-
11	H_2O	40	TFA 15 %	88	56/44	-	-
12	DMF	RT	TFA 15 %	81	61/39	-	-
13	DMF	40	TFA 15 %	87	57/43	-	-
14	EtOH	RT	TFA 15 %	79	63/37	-	-
15	EtOH	40	TFA 15 %	97	49/51	-	-
16	DMF	40	None	80	63/38	14	13
17	None	40	None	72	69/31	4	8
18	EtOH	40	None	85	59/41	9	1

[a] Unless otherwise specified, aldol reactions were carried out with 4-nitrobenzaldehyde (0.2 mmol), cyclohexanone (0.8 mmol) in the specified solvent (1.0 mL); the time for full conversion was monitored by TLC. The dash "-" indicates that no ee % was recorded. [b] Determined by ^{1}H-NMR analysis of the crude products. [c] Determined by HPLC analysis with Chiralpak AD-H column.

According to the ^{1}H-NMR results, when TFE was used, the aldol products were formed in 70 % and 73 % yields at RT and 40 °C respectively. In order to find the optimum conditions, the reaction was then investigated in the presence of additives, as it has been demonstrated that this can improve the activity of organocatalysts. More specifically, it has been shown that the protonated L-prolinethioamide can catalyze the aldol addition with better yield than its base derivative.[37] Addition of TFA had also a positive effect when N'-benzyl-N'-L-prolyl-L-proline hydrazide was employed as a catalyst for the aldol reaction.[37]

Based on these results, the catalytic activity of **PP 1** in the aldol reaction was tested upon addition of additives. Firstly, it was conducted in the presence of 0.15 equivalents of TFA as an additive at room temperature and 40 °C. It is notable that the achieved yields were significantly lower (up to 12 %). Nevertheless, higher yields were observed at 40 °C. The influence of additives on the catalytic

activity was then examined in different quantities. More specifically, 0.05 and 0.10 equivalents of TFA were used. Apart from that, AcOH was also tested as an additive (0.05, 0.10 and 0.15 equivalents). Overall, the conversions varied from 4 % to 16 %, and as a result they were significantly lower compared to the reaction without any additives.

In all the reactions where TFE was employed as a medium, additional peaks are observed at the aliphatic region of the ^{1}H-NMR spectrum (Figure 34). The additional peaks indicate the formation of side products, like self-aldol products of cyclohexanone. In order to achieve an optimised result, different solvents were examined, while the concentration was also increased.

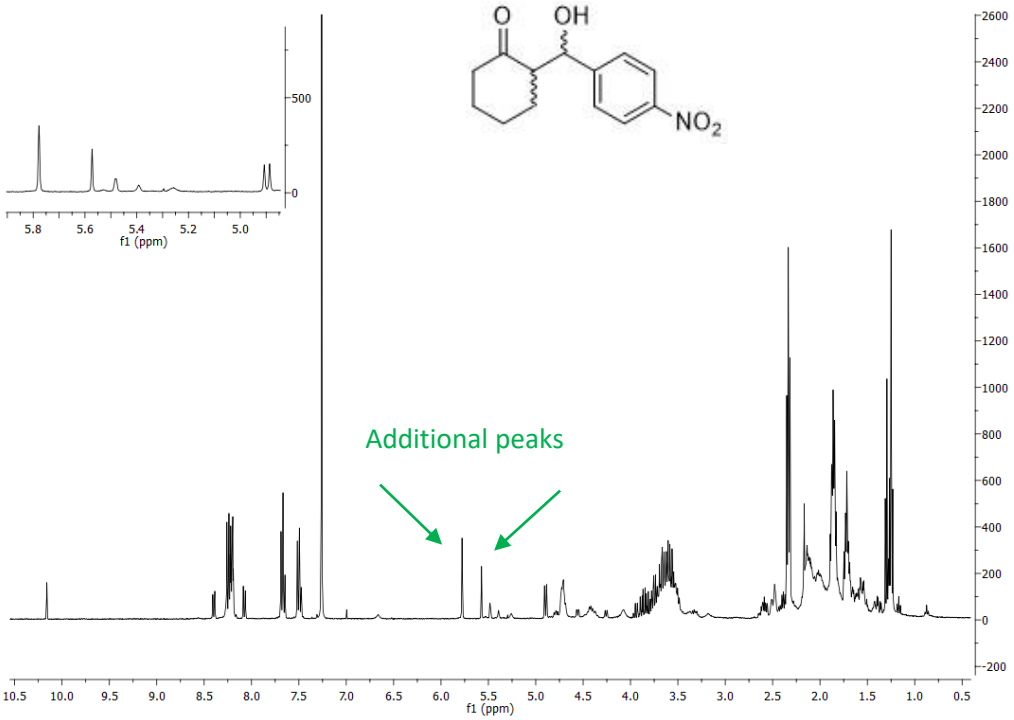

Figure 34 : The ^{1}H-NMR Spectrum of 2-(hydroxy(4-nitrophenyl)methyl)cyclohexanone Measured in $CDCl_3$ at 25 °C.

Using H_2O, anhydrous DMF and EtOH as solvents, and 0.15 equivalents of TFA, the reaction was performed at room temperature and 40 °C respectively. The products for all these reactions were obtained in higher yields when the reactions proceeded at 40 °C. Concerning DMF and EtOH, those were the highest observed at the time (87 % and 97 % respectively). Nevertheless, the additional undesirable peaks were still present on the ^{1}H-NMR spectra when these solvents were employed. This finding suggests that a side product, benzalcyclohexanone, was created upon usage of acidic additives in those solvents (Scheme 31). Since the presence of side-products could affect the accurate determination of ee, our efforts focused on optimising the reaction conditions in order to obtain the desired product in sufficient purity.

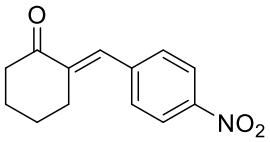

Scheme 31: Benzalcyclohexanone.

After the above-mentioned results, the next step involved performing the reaction in different solvents, without using any additives. The reaction was performed in anhydrous DMF and EtOH, as well as without any solvent, at 40 °C. According to the results, these conditions led to the best combination of yield (up to 85 %) and dr (anti/syn).

As the obtained NMR was not characterized by the additional undesirable peaks in the aliphatic region, these products were analysed via chiral-HPLC, in order to determine their enantioselectivities.[38] Based on the chiral-HPLC results, when DMF, no solvent and EtOH were used, the obtained ee for the anti-product were 14 %, 4 % and 9 % respectively, while the ee for the syn-product were 13 %, 8 % and 1 % respectively. Thus, both values observed for each solvent were very low for **PP 1**, with the one in DMF being slightly higher both for the syn- and the anti-products. Figures 35, 36 and 37 show the chiral-HPLC graphs obtained when **PP 1** was used as a tested catalyst, in DMF, no solvent and EtOH respectively.

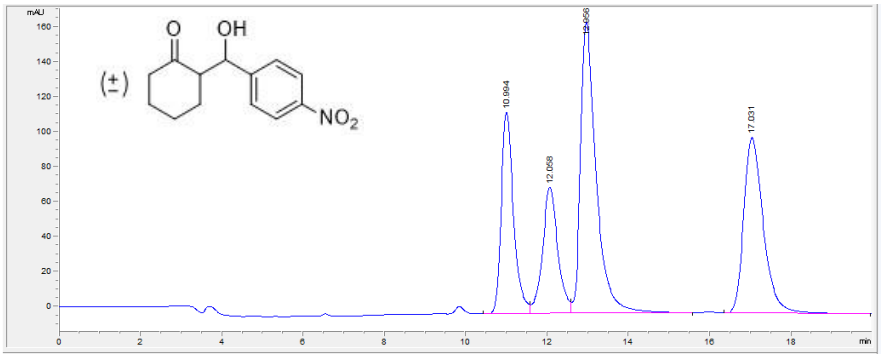

Figure 35: Chiral HPLC Analysis of Racemic 2-(hydroxyl-(p-nitrophenyl)methyl) cyclohexan-1- one Using **PP 1** in Anhydrous DMF (Table 5, Entry 16).

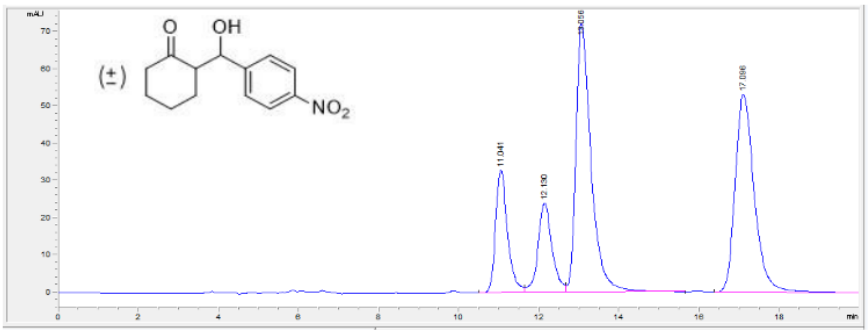

Figure 36: Chiral HPLC Analysis of Racemic 2-(hydroxyl-(p-nitrophenyl)methyl) cyclohexan-1- one Using **PP 1** and No Solvent (Table 5, Entry 17).

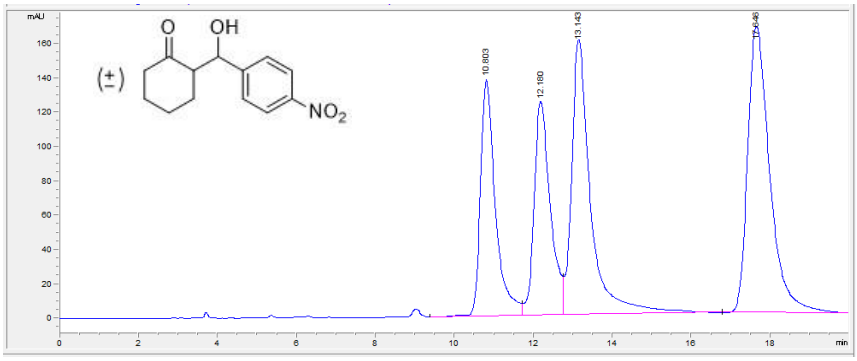

Figure 37: Chiral HPLC Analysis of Racemic 2-(hydroxyl-(p-nitrophenyl)methyl) cyclohexan-1- one Using **PP 1** in EtOH (Table 5, Entry 18).

The second polyproline peptide that was tested on the aldol reaction was **PP 2**, in 10 % loading. Taking into consideration the preliminary results from **PP 1**, a concentration of 1.3 M was set as a starting point. H_2O and anhydrous DMF were firstly examined as solvents, using TFA (0.15 equivalents) as an additive at room temperature and at 40 °C (Table 6).

Table 6: Optimization of Aldol Reaction Conditions Using **PP 2.**

Entry	Solvent	T (°C)	Additive (%)	Yield[b] (%)	dr (anti/syn)[b]	ee % (anti)[c]	ee % (syn)[c]
19	H_2O	RT	TFA 15 %	12	60/40	-	-
20	H_2O	40	TFA 15 %	11	50/50	-	-
21	H_2O	40	TFA 10 %	3	50/50	-	-
22	DMF	RT	TFA 15 %	13	54/46	-	-
23	DMF	40	TFA 15 %	9.5	53/47	-	-
24	DMF	40	TFA 10 %	14	54/46	-	-
25	EtOH	40	TFA 15 %	94	47/53	-	-
26	$CHCl_3$	40	TFA 10 %	14	57/43	-	-
27	MeOH	40	TFA 15 %	64	22/78	-	-
28	DMF	40	None	93	54/46	5	24
29	Propanol	40	None	83	60/40	4	32
30	MeOH	40	None	100	50/50	2	8

[a] Unless otherwise specified, aldol reactions were carried out with 4-nitrobenzaldehyde (0.2 mmol), cyclohexanone (0.8 mmol) in the specified solvent (1.0 mL); the time for full conversion was monitored by TLC. The dash "-" indicates that no ee % was recorded. [b] Determined by ^{1}H-NMR analysis of the crude products. [c] Determined by HPLC analysis with Chiralpak AD-H column.

The reaction was also performed with 0.10 equivalents of TFA using H_2O, anhydrous DMF and $CHCl_3$ at 40 °C. Based on the ^{1}H-NMR results, all these reactions led to a very low yield (3-14 %). As a result, a set of different solvents were then tested. The aldol reaction in MeOH and EtOH at 40 °C with 0.15 equivalents of TFA afforded the products in a yield of 64 % yield, and 94 % respectively.

Regarding the reaction in MeOH, based on the ^{1}H-NMR spectrum, the dr (anti/syn) of the crude product was 22/78. Considering that impurities of the crude product could affect the determination of the ee, a purification step was conducted before the analysis via chiral-HPLC. After purification using a chromatographic tank, the isolated products exhibited a yield of 97 %, and 47/53 of dr (anti/syn). From these results we can observe that the dr drastically changed, at the same time that the yield remained the same. A possible explanation for this finding is epimerization of the product on silica gel. After analysis via chiral-HPLC, the enantioselectivities for the anti- and the syn-product were very low, and almost the same, 4 % and 5 % respectively.

After these preliminary results, the reaction was investigated in anhydrous DMF, propanol and MeOH at 40 °C in the absence of any additives. The expected aldol addition products were obtained in good yields under these conditions. More specifically, the achieved yields were 93 %, 83 % and 100 %. Since the reaction conditions had been optimised, the products were analysed via chiral-HPLC (Figures 38, 39 and 40). The observed ee for the anti-product in anhydrous DMF, propanol and MeOH were 5 %, 4 % and 2 %, and the ee for the syn-product were 24 %, 32 % and 8 % respectively. As a result, no enantioselectivity was observed for the anti-product, whereas the values for the syn-product in DMF and propanol were very low but the highest observed for **PP 2** and **PP 1**.

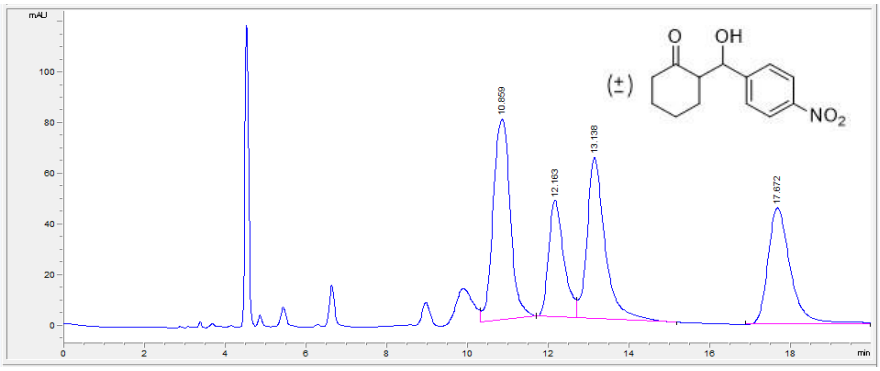

Figure 38: Chiral HPLC Analysis of Racemic 2-(hydroxyl-(p-nitrophenyl)methyl) cyclohexan-1- one Using **PP 2** in DMF (Table 6, Entry 28).

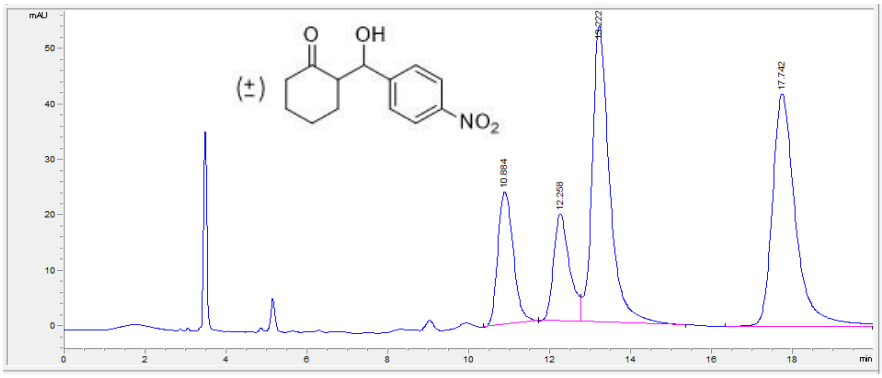

Figure 39: Chiral HPLC Analysis of Racemic 2-(hydroxyl-(p-nitrophenyl)methyl) cyclohexan-1- one Using **PP 2** in propanol (Table 6, Entry 29).

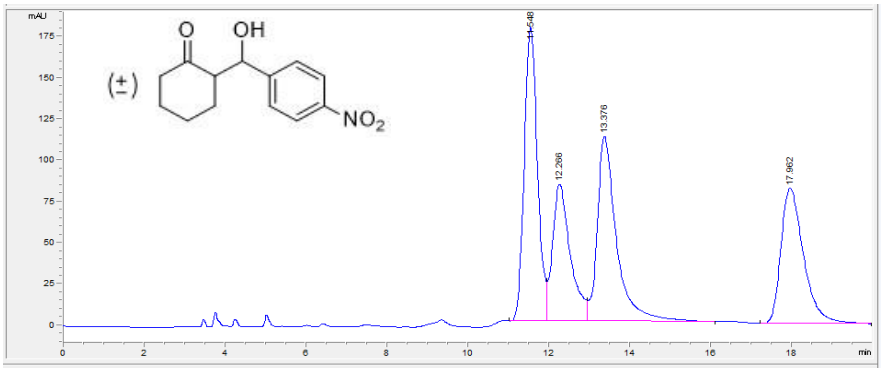

Figure 40: Chiral HPLC Analysis of Racemic 2-(hydroxyl-(p-nitrophenyl)methyl) cyclohexan-1- one Using **PP 2** in MeOH (Table 6, Entry 30).

Since the conditions had already been optimised when **PP 3** was tested as a catalyst, the aldol reaction was performed in anhydrous DMF at 40 °C, in the absence of any additives (Table 7).

Table 7: Optimization of Aldol Reaction Conditions Using **PP 3.**

Entry	Solvent	T (°C)	Additive (%)	Yield[b] (%)	dr (anti/syn)[b]	ee % (anti)[c]	ee % (syn)[c]
31	DMF	40	None	78	65/35	2	37
32	Propanol	40	None	75	67/33	4	12
33	MeOH	40	None	84	60/40	4	10

[a] Unless otherwise specified, aldol reactions were carried out with 4-nitrobenzaldehyde (0.2 mmol), cyclohexanone (0.8 mmol) in the specified solvent (1.0 mL); the time for full conversion was monitored by TLC. The dash "-" indicates that no ee % was recorded. [b] Determined by ^{1}H-NMR analysis of the crude products. [c] Determined by HPLC analysis with Chiralpak AD-H column.

According to the ^{1}H-NMR results, the product was formed in 78 % yield. After that, propanol was tested as solvent, using again 40 °C and no additive. The observed yield this time was again moderate (75 %). Lastly, the reaction was conducted in MeOH under the same conditions, with the yield being 84 %. All three products were then analysed through the chiral-HPLC in order to determine the enantioselectivity. The observed ee for the anti-enantiomer were very low for all three solvents (2-4 %). The values were relatively increased for the syn-enantiomer as the ee (syn) recorded in anhydrous DMF, propanol and MeOH was 37 %, 12% and 10 % respectively (Figures 41, 42 and 43). As a result, the ee (syn-product) in anhydrous DMF was the highest achieved by that time. Nevertheless, incorporation of the phenol group into the **PP 2** helix had no significant improvement on the yields or the catalytic activity of the peptide on the aldol asymmetric reaction.

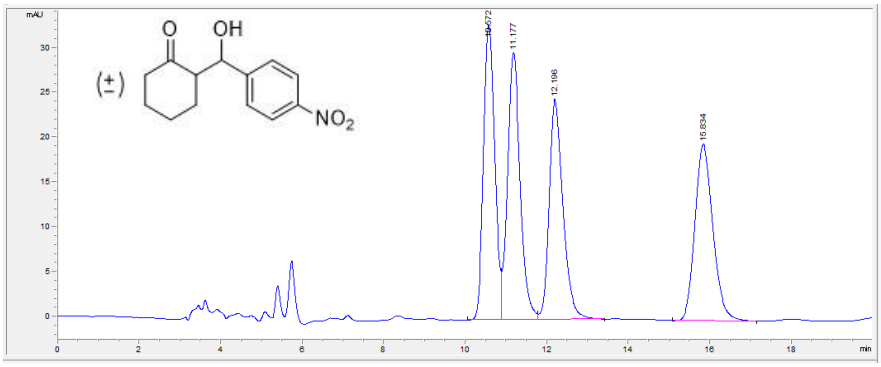

Figure 41: Chiral HPLC Analysis of Racemic 2-(hydroxyl-(p-nitrophenyl)methyl) cyclohexan-1- one Using **PP 3** in DMF (Table 7, Entry 31).

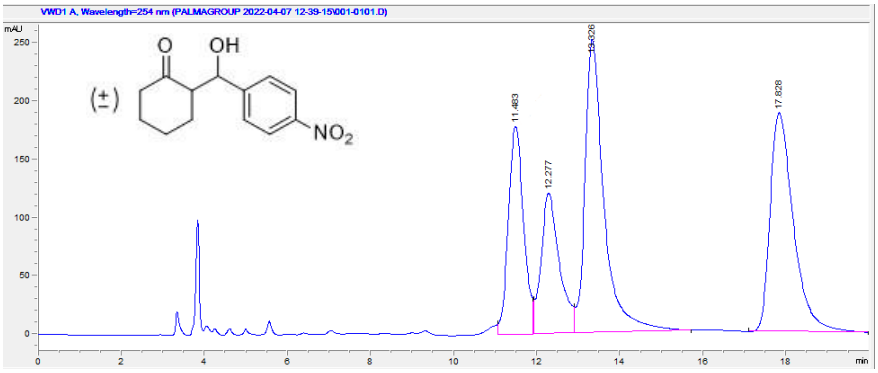

Figure 42: Chiral HPLC Analysis of Racemic 2-(hydroxyl-(p-nitrophenyl)methyl) cyclohexan-1- one Using **PP 3** in propanol (Table 7, Entry 32).

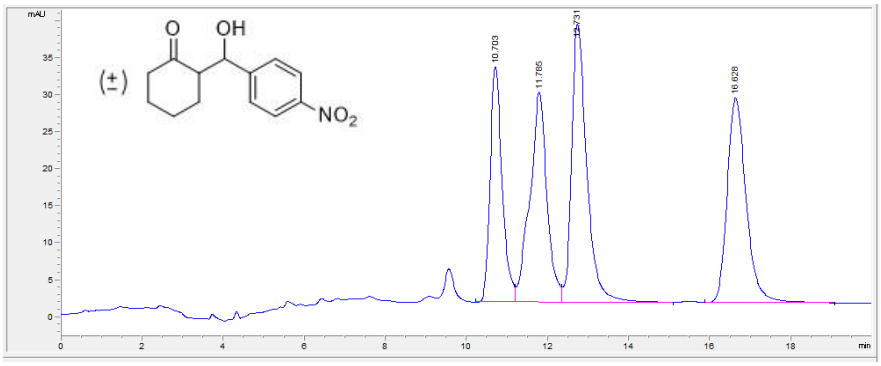

Figure 43: Chiral HPLC Analysis of Racemic 2-(hydroxyl-(p-nitrophenyl)methyl) cyclohexan-1- one Using **PP 3** in MeOH (Table 7, Entry 33).

Apart from the polyproline peptides, monomer **E3** was also investigated, as aforementioned. Using anhydrous DMF at 40 °C in the absence of any additives, the obtained yield was 47 % (Table 8).

Table 8: Optimization of Aldol Reaction Conditions Using **E3**.

Entry	Solvent	T (°C)	Additive (%)	Yield[b] (%)	dr (anti/syn)[b]	ee % (anti)[c]	ee % (syn)[c]
34	DMF	40	None	47	45/55	2	2
35	Propanol	40	None	34	54/46	6	5

[a] Unless otherwise specified, aldol reactions were carried out with 4-nitrobenzaldehyde (0.2 mmol), cyclohexanone (0.8 mmol) in the specified solvent (1.0 mL); the time for full conversion was monitored by TLC. The dash "-" indicates that no ee % was recorded. [b] Determined by ^{1}H-NMR analysis of the crude products. [c] Determined by HPLC analysis with Chiralpak AD-H column.

The same reaction conditions were applied, with the difference of propanol instead of anhydrous DMF, leading to a lower yield of 34 %. After analysis through chiral-HPLC (Figures 44 and 45), when anhydrous DMF was employed both the syn- and the anti-product were obtained in 2 % ee, while the use of propanol led to observed ee of 6 % and 5 % for the anti and syn-enantiomer respectively.

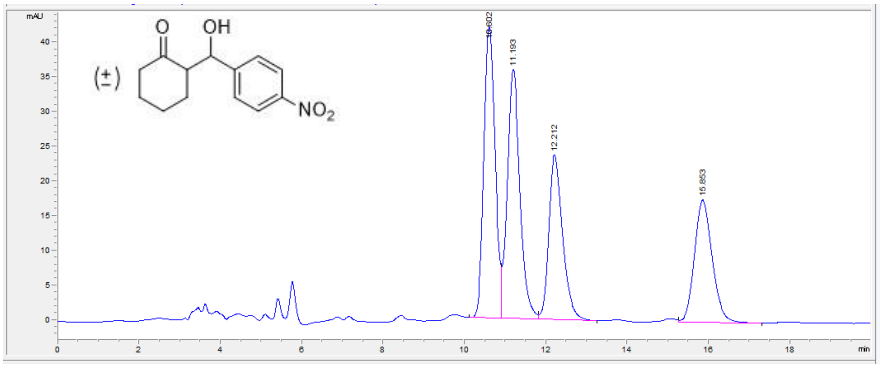

Figure 44: Chiral HPLC Analysis of Racemic 2-(hydroxyl-(p-nitrophenyl)methyl) cyclohexan-1- one Using E**3** in DMF (Table 8, Entry 34).

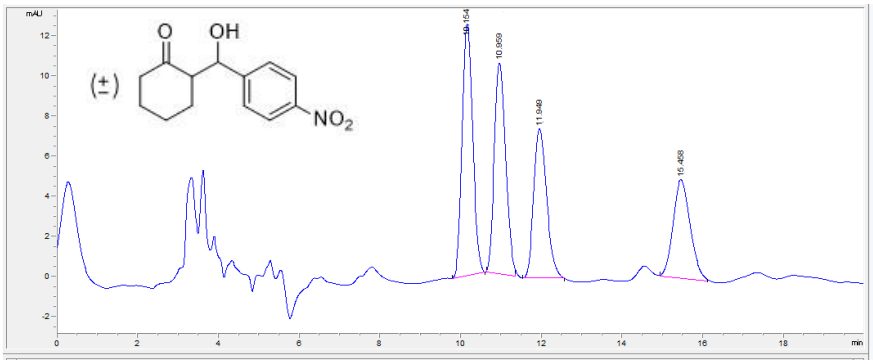

Figure 45: Chiral HPLC Analysis of Racemic 2-(hydroxyl-(p-nitrophenyl)methyl) cyclohexan-1- one Using **E3** in propanol (Table 8, Entry 35).

Lastly, **L-proline** was used as a catalyst for the aldol reaction in anhydrous DMF and propanol at 40 °C (Table 9). Since the peptides and **E3** have been purified through preparative RP-HPLC and biotage respectively, where 0.05 equivalents of formic acid (FA) were applied, the same amount of additive was used in the case of L-proline.

Table 9: Optimization of Aldol Reaction Conditions Using **L-proline**.

Entry	Solvent	T (°C)	Additive (%)	Yield[b] (%)	dr (anti/syn)[b]	ee % (anti)[c]	ee % (syn)[c]
36	DMF	40	FA 5 %	86	42/58	7	12
37	Propanol	40	FA 5 %	86	42/58	38	39

[a] Unless otherwise specified, aldol reactions were carried out with 4-nitrobenzaldehyde (0.2 mmol), cyclohexanone (0.8 mmol) in the specified solvent (1.0 mL); the time for full conversion was monitored by TLC. The dash "-" indicates that no ee % was recorded. [b] Determined by ^{1}H-NMR analysis of the crude products. [c] Determined by HPLC analysis with Chiralpak AD-H column.

The reaction afforded the products at the same yield (86 %) and dr (anti/syn) (42/58). After analysis through chiral-HPLC (Figures 46 and 47), the enantioselectivities in DMF were relatively low (up to 12 %), while the values in the case of propanol reached 38 % and 39 % for the anti and syn-enantiomers respectively.

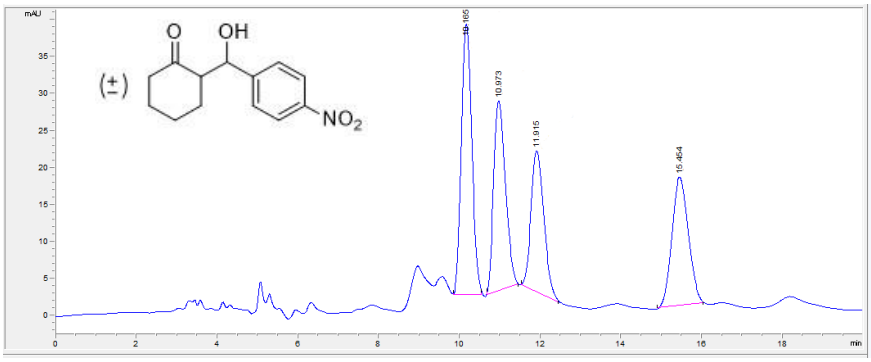

Figure 46: Chiral HPLC Analysis of Racemic 2-(hydroxyl-(p-nitrophenyl)methyl) cyclohexan-1- one Using L-Proline in DMF (Table 9, Entry 36).

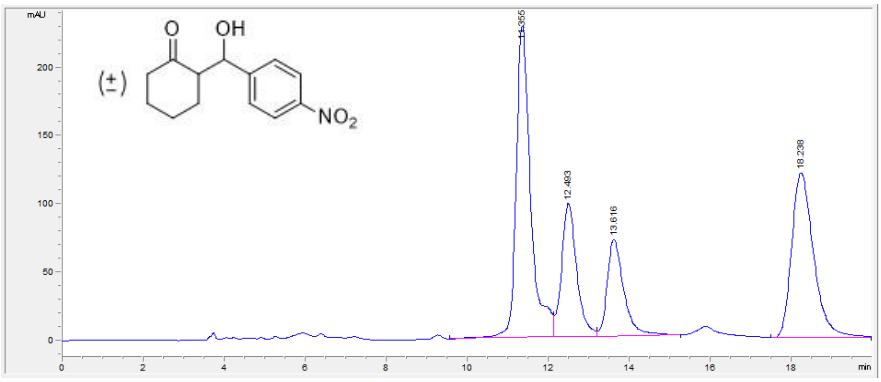

Figure 47: Chiral HPLC Analysis of Racemic 2-(hydroxyl-(p-nitrophenyl)methyl) cyclohexan-1- one Using L-Proline in propanol (Table 9, Entry 37).

2.3 Conclusions and Future Work

2.3.1 Conclusions

This chapter described the synthesis and characterisation of functionalized proline and piperazine units. After being incorporated into peptides, they were tested as potential catalysts in enantioselective organocatalysis.

To summarize, in order to obtain **A7**, a multi-step reaction pathway was performed starting from trans-4-hydroxyproline. A benzylation reaction and a Boc protection were followed by an Appel reaction. After that, introduction of the azide group on the C-4 position, removal of the Boc protection group and introduction of the Fmoc protection group were conducted. Lastly, a Boc protection reaction along with a hydrogenation reaction in one step led to the final product. All the steps were characterized by good to high yields, except from the last step where the yield was low.

In order to obtain the final product in a higher yield, an alternative reaction pathway was designed. This time starting from N-Boc-cis-4-hydroxy-L-proline methyl ester, the first step was a saponification reaction which was followed by a mesylation reaction and introduction of the azide group. The next steps were identical to the ones performed in the initial pathway, apart from the fact that the hydrogenation reaction and Boc protection reaction of the last step were now conducted as two different steps. In this way, we were able to investigate whether this would lead to a better yield. The results showed that although the yield of the last reaction was improved, it was still relatively low. One possible explanation for this is the purification method that was used, and thus, a future outlook could be the use of a different purification method of **A7**.

Regarding the second target compound (**C2**), it was synthesized successfully through an Fmoc protection. In order to obtain **D3**, a multi-step reaction pathway was used. More specifically, a Mitsunobu reaction, followed by a Boc deprotection reaction, an Fmoc protection reaction and a hydrogenation reaction led to the final product. The steps were characterized by moderately high to high yields. Lastly, **E2** was also synthesized through an acetylation reaction, followed by a Boc deprotection reaction.

After that, four target polyproline peptides were synthesized using Fmoc-based SPPS and rink amide resin, both manually and by using a peptide synthesizer. During the manual synthesis, HOBt, PyBOP and DIPEA in DMF were used as coupling reagents. In order to optimise the synthesis, the equivalents of the coupling reagents were increased, leading to a more efficient procedure. When the peptide synthesizer was used, Oxima Pure and DIC in DMF proved to be more effective as coupling reagents. It is notable that addition of DIPEA to the coupling mix led to purer peptides. In this way, the peptides could be synthesized in an automated way, in a significantly more time

efficient manner. All the desired peptides were synthesized successfully, as indicated by LCMS analysis, while preparative RP-HPLC was performed as a purification method when needed.

From the CD analysis we were able to obtain useful information for the conformation of the peptides. Two solvents were used for this process, water and propanol, in order to determine whether the synthesized polyprolines could show a switch from a PolPro II to a PolPro I conformation. **PP 1** showed a shift from PolPro II in water to PolPro I in propanol. **PP 2** and **PP 3** presented a relatively similar CD spectrum in both solvents, which was characteristic of the PolPro II helix. As a result, only **PP 1** could be used as stereodivergent organocatalysts, whereas **PP 2** and **PP 3** could be examined as enantioselective organocatalys.

Following that, the catalytic activity of the synthesized peptides was investigated on the aldol asymmetric reaction. Using p-nitrobenzaldehyde and cyclohexanone, 10 % loading of each peptide was used, in various conditions. More specifically, for **PP 1**, TFE was used at 40 °C and room temperature, while the use of additives (TFA and AcOH) 40 °C was also investigated. After that, H_2O, DMF and EtOH were also employed both at 40 °C and room temperature, using TFA as an additive (0.15 equivalents). Although the use of additives has proved to have a positive effect on the enantioselectivity and the yield of catalytic reactions, in all the cases where additives were employed, undesirable peaks were observed on the NMR spectra, indicating the presence of a by-product. Thus, DMF, no solvent and EtOH were used at 40 °C without the use of any additive, which led to the optimum results for **PP 1**.

Regarding **PP 2** various conditions were also tested. H_2O and DMF were initially used at room temperature and 40 °C, as well as EtOH and $CHCl_3$ at 40 °C, all in the presence of TFA. All these cases led to very low reaction yields, except from EtOH which led to a yield of 94 % but a dr of 47/53. Therefore, another solvent was employed, MeOH, at 40 °C in the presence of TFA, which led to a yield of 64 % and a dr of 22/78. Nevertheless, after purification via a chromatographic tank, the dr was 47/53. This observation could be explained through the self-disproportionation of enantiomers (section 2.2.3). The best combination of yield and dr values for **PP 2** were when DMF, propanol and MeOH were employed at 40 °C without the use of any additive, which matches the optimum conditions for **PP 1**.

Since **PP 3** was designed in order to compare its catalytic activity with the one of **PP 2, PP 3** was also tested in DMF, propanol and EtOH at 40 °C without the use of any additive. Finally, **E3** and L-proline were employed in order for their catalytic activity to be compared with the one of the corresponding peptides. As a result, they were only tested in the optimum conditions.

By applying the optimum conditions, moderately high to high yields were observed, which are higher than the yield of the corresponding monomer **E3**, and similar to the yield of L-proline. Regarding **PP**

1, it led to a high dr, with the highest value observed when no solvent was employed (69/31). Nevertheless, it exhibited relatively low values of ee in all the examined cases (1-14 %). The best dr and the ee for **PP 2** were in propanol, with the values being 60/40 and 32 % respectively. For **PP 3**, the highest combination of dr and ee were observed once DMF was employed as a solvent (65/35 and 37 % respectively). Regarding **E3**, both the dr and the ee were lower compared to all the three synthesized polyprolines. L-proline led to relatively lower value of dr (42/58), while when the highest ee was observed in propanol (39 %).

In conclusion, considering the results of **PP 1**, a heptameric un-functionalized polyproline helix is able to switch from a PolPro II to a PolPro I conformation upon solvent exchange, while it can catalyze the aldol reaction with yields and high dr. Nevertheless, the chirality of the helix is not enough to lead to good values of ee. **PP 2** and **PP 3** were only able to adopt a PolPro II conformation, at the same time that they catalyzed the aldol reaction with high yields, good dr and moderate values of ee. Thus, incorporation of a six-membered ring in the polyproline helix in the case of **PP 2**, along with a functionalized proline residue in the case of **PP 3** led to better ee than **PP 1**. It is notable that the introduction of the phenol group on **PP 3** could not lead to a difference in enantioselectivity. Nevertheless, the two polyprolines exhibited the highest ee in different solvents (propanol for **PP 2** and DMF for **PP 3**), suggesting a different interaction of each helix with the solvent, which influences the enantioselectivity and as a result, the catalytic outcome. Lastly, although no stereodivergence was observed and the ee values were relatively low, we can observe that high yields were achieved, with good values of dr. Therefore, these results can act as a starting point for further research.

2.3.2 Future Outlook

Regarding the synthesis of **A7**, another purification method like preparative RP-HPLC could be used for the last step of the pathway, in order to optimise the yield. Another reaction pathway could also be attempted in order to investigate whether this would lead to a higher overall yield (Scheme 32). Following that, the preparation of the corresponding peptide, using **A7**, and the investigation of its catalytic activity would be possible.

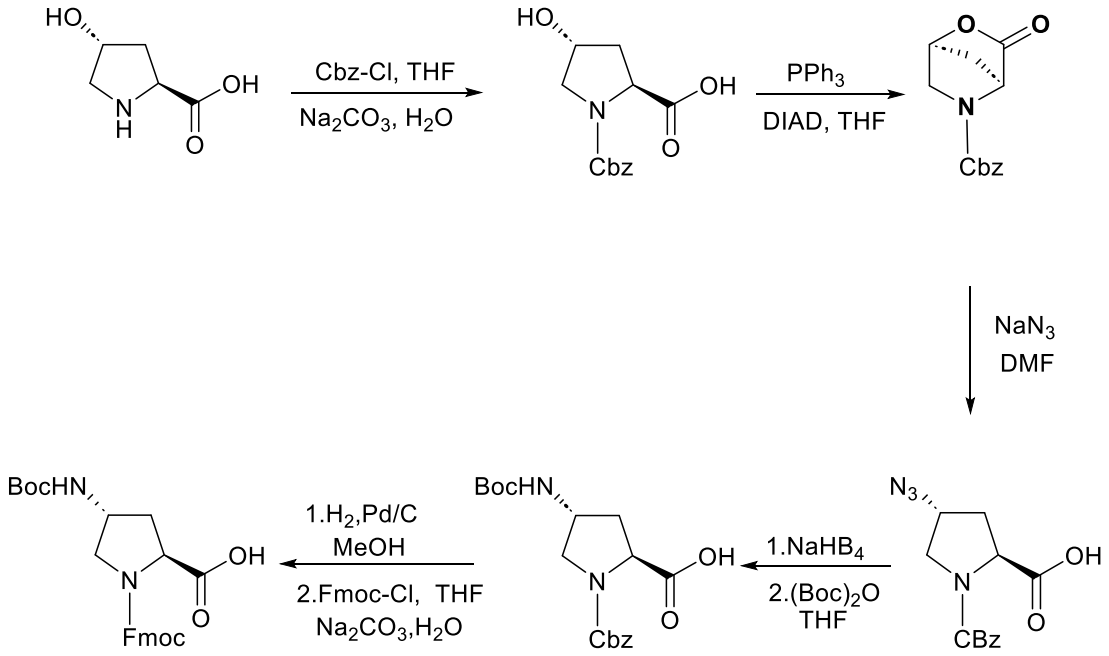

Scheme 32: Future Reaction Scheme for the Synthesis of N-Fmoc-trans-4-Boc-amino-L-proline (**A7**).

A future direction regarding the peptides could be to synthesize **PP 2** and **PP 3** in longer chain length so that the transition between PolPro II and PolPro I could be achieved. In this way, the polyprolines could be tested as stereodivergent organocatalysts.

From the results obtained when **PP 1** was employed as a catalyst, we can observe that incorporation of a five-membered pyrrolidine ring within a polyproline helix did not lead to high enantioselectivity. Considering that a more nucleophilic nitrogen atom leads to a most reactive enamine or iminium ion,[39] the synthesis of a peptide comprised of proline units and a pyrrolidine ring with two nitrogen atoms could be a promising organocatalyst. The designed functionalized proline analogue (Figure 48) has already been synthesized, it can be synthesized using SPPS and can be easily functionalized.[40] A possible synthetic pathway for the preparation of this monomer is shown in Scheme 33. Once synthesized, it could then be tested as an organocatalyst.

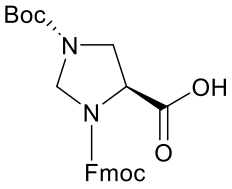

Figure 48: Future Target Monomer.

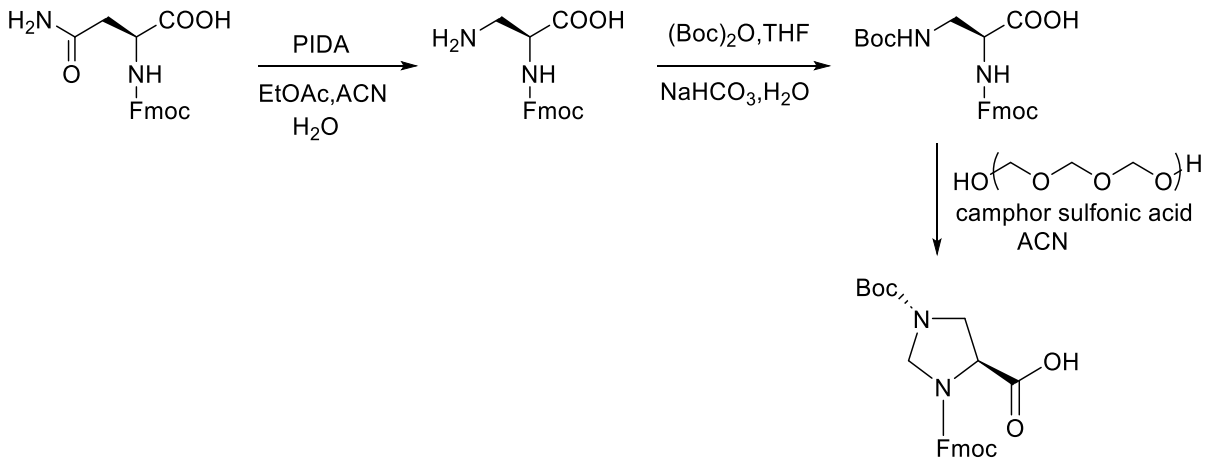

Scheme 33: Reaction Pathway for the Synthesis of Future Monomer.

2.4 References

1. Berger, A., Kurtz, J. & Katchalski, E. Poly-L-proline. *J. Am. Chem. Soc.* **76**, 5552–5554 (1954).
2. Gulín, O. P., Rabanal, F. & Giralt, E. Efficient preparation of proline N-carboxyanhydride using polymer-supported bases. *Org. Lett.* **8**, 5385–5388 (2006).
3. Deming, T. J. & Curtin, S. A. Chain initiation efficiency in cobalt- and nickel-mediated polypeptide synthesis. *J. Am. Chem. Soc.* **122**, 5710–5717 (2000).
4. Iizuka, Y., Uchida, C., Wakamatsu, K. & Oya, M. Synthesis and properties of high molecular weight polypeptides containing proline. **66**, 1269–1272 (1993).
5. Pashuck T. Synthesis of self-assembling peptide-based hydrogels for regenerative medicine using solid-phase peptide synthesis. in *Biomaterials for Tissue Engineering* 177–192 (Humana Press, 2018).
6. Amblard, M., Fehrentz, J. A., Martinez, J. & Subra, G. Methods and protocols of modern solid phase peptide synthesis. *Mol. Biotechnol.* **33**, 239–254 (2006).
7. Merrifield, R. B. Solid phase peptide synthesis. I. The synthesis of a tetrapeptide. *J. Am. Chem. Soc.* **85**, 2149–2154 (1963).
8. Aapptec. Practical synthesis guide to solid phase peptide chemistry. 1–76 (2011).
9. Datta, N. & Kontomichalou, P. Automated peptide synthesis. *Nat. Publ. Gr.* **207**, 522–523 (1965).
10. Stewart, A. S. J. Method of peptide synthesis of peptides containing a proline residue or hydroxyproline residue at or adjacent to the C-terminal end of the peptide. U.S. 7,645,858 B2 (2010).
11. Behrendt, R., White, P. & Offer, J. Advances in Fmoc solid-phase peptide synthesis. *J. Pept. Sci.* **22**, 4–27 (2016).
12. Duengo, S., Muhajir, M. I., Hidayat, A. T., Musa, W. J. A. & Maharani, R. Epimerisation in Peptide Synthesis. *Molecules* **28**, 1–39 (2023).
13. Sarin, V. K., Kent, S. B. H., Tam, J. P. & Merrifield, R. B. Quantitative monitoring of solid-phase peptide synthesis by the ninhydrin reaction. *Anal. Biochem.* **117**, 147–157 (1981).

14. Sandlers, Y. Amino acids profiling for the diagnosis of metabolic disorders. in *Clinical Biochemistry - Fundamentals of Medical and Laboratory Science* 1–21 (IntechOpen, 2019).

15. Kakinoki, S., Hirano, Y. & Oka, M. On the stability of polyproline-I and II structures of proline oligopeptides. *Polym. Bull.* **53**, 109–115 (2005).

16. Garbuio, L. *et al.* Shape persistence of polyproline II helical oligoprolines. *Chem. - A Eur. J.* **21**, 10747–10753 (2015).

17. Wilhelm, P., Lewandowski, B., Trapp, N. & Wennemers, H. A crystal structure of an oligoproline PPII-Helix, at last. *J. Am. Chem. Soc.* **136**, 15829–15832 (2014).

18. Brightwell, D. F. *et al.* A reversibly porous supramolecular peptide framework. *Chem. Eur. J.* **28**, (2022).

19. Erdmann, R. S. & Wennemers, H. Functionalizable collagen model peptides. *J. Am. Chem. Soc.* **132**, 13957–13959 (2010).

20. Remuzon, P. Trans-4-hydroxy-L-proline, a useful and versatile chiral starting block. *Tetrahedron* **52**, 13803–13835 (1996).

21. Agarkov, A., Greenfield, S. J., Ohishi, T., Collibee, S. E. & Gilbertson, S. R. Catalysis with phosphine-containing amino acids in various 'turn' motifs. *J. Org. Chem.* **69**, 8077–8085 (2004).

22. Kitamoto, T., Ozawa, T., Abe, M., Marubayashi, S. & Yamazaki, T. Incorporation of fluoroprolines to proctolin: Study on the effect of a fluorine atom toward peptidic conformation. *J. Fluor. Chem.* **129**, 286–293 (2008).

23. Pícha, J., Buděšínský, M., Macháčková, K., Collinsová, M. & Jiráček, J. Optimized syntheses of Fmoc azido amino acids for the preparation of azidopeptides. *J. Pept. Sci.* **23**, 202–214 (2017).

24. Keicher, T. & Löbbecke, S. Lab-scale synthesis of azido compounds: Safety measures and analysis. in *Organic Azides: Syntheses and Applications* (ed. Banert, S. B. and K.) 1–27 (2009).

25. Zanardi, F. *et al.* Discovery of subnanomolar arginine-glycine-aspartate-based αvβ3/αvβ5 integrin binders embedding 4-aminoproline residues. *J. Med. Chem.* **51**, 1771–1782 (2008).

26. Hodges, J. A. & Raines, R. T. Stereoelectronic and steric effects in the collagen triple helix: Toward a code for strand association. *J. Am. Chem. Soc.* **127**, 15923–15932 (2005).

27. Shi, J. *et al.* Discovery of potent and orally bioavailable dihydropyrazole GPR40 agonists. *J. Med. Chem.* **61**, 681–694 (2018).

28. Gupta, N. *et al.* Ordered short channel mesoporous silica modified with 1,3,5-triazine-piperazine as a versatile recyclable basic catalyst for cross-aldol, Knoevenagel and conjugate addition reactions with isatins. *RSC Adv.* **5**, 17843–17850 (2015).

29. Barros, M. T. & Phillips, A. M. F. Chiral piperazines as efficient catalysts for the asymmetric michael addition of aldehydes to nitroalkenes. *European J. Org. Chem.* **2007**, 178–185 (2007).

30. Shanmuganathan, S., Greiner, L. & De María, P. D. Silica-immobilized piperazine: A sustainable organocatalyst for aldol and Knoevenagel reactions. *Tetrahedron Lett.* **51**, 6670–6672 (2010).

31. Pabbaraja, S. *et al.* Synthesis and biological evaluation of 12-, 13-, 14-membered macrolides and open chain 2,6-trans-disubstituted dihydropyran analogues for aspergillides. *Tetrahedron Lett.* **59**, 2570–2576 (2018).

32. Kim, J. *et al.* Low-dielectric-constant polyimide aerogel composite films with low water uptake. *Polym. J.* **48**, 829–834 (2016).

33. Du, D. *et al.* Bio- and medicinally compatible α-amino-acid modification via merging photoredox and N-heterocyclic carbene catalysis. *Org. Lett.* **22**, 6370–6375 (2020).

34. Singh, S. CarboMAX - Enhanced peptide coupling at elevated temperatures. *AP Note* **0124**, 1–5 (2018).

35. Metrano, A. J. *et al.* Asymmetric catalysis mediated by synthetic peptides, version 2.0: Expansion of scope and mechanisms. *Chem. Rev.* **120**, 11479–11615 (2020).

36. Deng, J., Zhao, B. & Deng, J. Optically active helical polyacetylene bearing ferrocenyl amino-acid derivative in pendants. Preparation and application as chiral organocatalyst for asymmetric aldol reaction. *Ind. Eng. Chem. Res.* **55**, 7328–7337 (2016).

37. Gryko, D., Zimnicka, M. & Lipiński, R. Brønsted acids as additives for the direct asymmetric aldol reaction catalyzed by L-prolinethioamides. Direct evidence for enamine-iminium catalysis. *J. Org. Chem.* **72**, 964–970 (2007).

38. Messerer, M. & Wennemers, H. Reversing the enantioselectivity of a peptide catalyst by changing the solvent. *Synlett* **4**, 499–502 (2011).

39. Doyle, L. S. NH-Isoxazolidines as Organocatalysts. (National University of Ireland, Maynooth, 2009).

40. Aronoff, M. R., Egli, J., Menichelli, M. & Wennemers, H. γ-Azaproline confers pH responsiveness and functionalizability on collagen triple helices. *Angew. Chemie* **131**, 3175–3178 (2019).

2.5 Chemicals and Instrumentation

Commercially available reagents obtained from Acros Organics, Amersham, Alfa Aesar, Sigma Aldrich, Fisher Scientific and FluoroChem, were used without further purification unless otherwise stated. All air-and moisture-insensitive reactions were carried out under ambient atmosphere, and monitored by thin layer chromatography (TLC). Analytical TLC was performed using FluoroChem pre-coated silica gel 60 F254 aluminium plates, that were subjected to UV light or visualised using a vanillin stain, by subsequent heating. All air-and moisture-sensitive reactions were carried out using oven-dried glassware employing standard Schlenk techniques under an atmosphere of N_2. Flash column chromatography was performed on Acros Organics ultrapure 60 silica gel with a particle size 60-200 μm. ^{1}H and ^{13}C NMR spectra were obtained on a Bruker AVII MHz spectrometer. Chemical shifts were reported in parts per million (ppm) from low to high field, using TMS as a reference. Coupling constants (J) are reported in Hertz (Hz). Standard abbreviations indicating multiplicity were used as follows: s = singlet, d = doublet, t = triplet, q = quartet, m = multiplet. In the case of some complex multiplets with contributions from more than one signal absolute assignment was not possible.

FT-IR spectra were recorded on a Shimadzu IR Affinity-1S spectrophotometer, with peaks being reported in wavenumbers (cm^{-1}).

Low resolution mass spectrometry was carried out by the mass spectrometry services at the University of Kent. The data were collected on a Thermo MSQ Plus LCMS system, using a Kromasil C18 HPLC column (250 mm x 4.6 mm x 5 mm). Stereochemical purity was determined by Chiral Stationary Phase HPLC on an Agilent 1100 series Instrument, with a Chiralpak AD-H column, flow rate of 1.00 mL min^{-1}, detection at 254 nm, n-hexane-isopropanol isocratic eluents.

CD spectra were obtained on a J-715 (Jasco) spectrophotometer using a quartz cell was used with a 1 mm path length. CD spectra were recorded using a spectral bandwidth of 190-260 nm, at 20 °C. Each CD spectrum was formed of four accumulations, prior to subtracting the background signal. CD data are given as mean residual molar ellipticities (deg cm^2 $dmol^{-1}$). Peptide samples were prepared at approximately 100 μM, and were incubated for at least seven days.

2.6 Experimental Information

2.6.1 Monomers

2.6.1.1 General Procedures

Boc Protection-General Procedure

Na_2CO_3 and H_2O were added to a solution of the proline derivative in THF. After cooling to 0 °C with an ice bath, Boc_2O was added in one portion. The reaction mixture was stirred at 0 °C for 1 h, and then at room temperature overnight. The solvent was then removed in *vacuo* and the residue was diluted with H_2O. Concentrated HCl was added to this solution, until pH ~ 1 was reached, and the reaction mixture was extracted with DCM (x 3). Combined organic layers were washed with H_2O and brine, dried over $MgSO_4$, filtered, and concentrated in *vacuo*.

Azide Reaction-General Procedure

In a N_2-purged round bottom flask, the proline derivative and NaN_3 were suspended in anhydrous DMF. The mixture was stirred under N_2 atmosphere at 55 °C for 20 h. A glass shield was used as a precaution, due to the explosive nature of the azide group. After allowing to cool to room temperature, the solvent was removed under compressed air. The reaction mixture was then extracted with EtOAc (x 3), and combined organic layers were washed with H_2O and brine, dried over $MgSO_4$, filtered, and concentrated in *vacuo*.

Boc Deprotection-General Procedure

The proline derivative was dissolved in DCM, and the whole was cooled to 0 °C.TFA was added, and the reaction mixture was stirred at room temperature for 2 h. After that, volatile materials were removed.

Fmoc Protection-General Procedure

The starting material was dissolved in H_2O with Na_2CO_3. After cooling to 0 °C with an ice bath, Fmoc-Cl in THF was added dropwise during a period of 15 minutes under vigorous stirring. Stirring was continued at 0 °C for 1 h, and then at room temperature overnight. The reaction mixture was cooled again with an ice bath, and concentrated HCl was added dropwise until pH ∼ 0–1 was reached. Thereafter, H_2O was added, and extraction with DCM (x 3) followed. Combined organic layers were washed with H_2O and brine, dried over $MgSO_4$, filtered and concentrated in *vacuo*.

Hydrogenation-General Procedure

Pd/C was placed in a three-neck round bottom flask, sealed with two septa and attached to a Schlenk line apparatus. After carefully evacuating the flask and re-filling with N_2 (x 3), EtOAc was added onto the Pd/C, followed by the same volume of MeOH. The proline was then dissolved in the minimum volume of MeOH and added into the reaction vessel, which was evacuated and re-filled with N_2 again (x 3). A H_2 balloon was then added, and the reaction was left under stirring at room temperature overnight. The H_2 balloon was removed and the reaction solution was filtered through a Celite filter to remove any residual Pd/C. The filtrate was washed with MeOH and concentrated in *vacuo*.

2.6.1.2 Synthesis of A7

Synthesis of A2

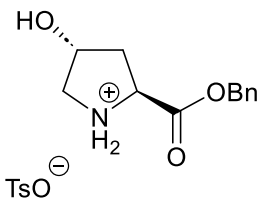

A1 (10 g, 76.30 mmol, 1 eq) was dissolved in toluene (60 mL), and BnOH (60 mL) followed by pTSA (14.79 g, 77.50 mmol, 1 eq) were added. The reaction mixture was heated under reflux at 125 °C for 20 h, and H_2O was removed using a Dean Stark apparatus. The mixture was then cooled to room

temperature, and the product crystallized upon addition of Et_2O (800 mL). The solid was collected by filtration, washed with Et_2O (250 mL) and dried in *vacuo* to afford the desired product as a white crystalline solid (28.4 g, 95 %). **^{1}H-NMR** (400 MHz, $CDCl_3$) δ 7.76 – 7.04 (m, 5H), 5.09 (dd, J = 35.7, 12.1 Hz, 1H), 4.67 (dd, J = 55.6, 45.3 Hz, 1H), 3.83 – 3.39 (m, 1H), 2.44 (dd, J = 13.7, 7.9 Hz, 1H), 2.31 (s, 1H), 2.08 – 1.98 (m, 1H), 1.24 (dt, J = 13.1, 7.1 Hz, 1H). **^{13}C-NMR** (100 MHz, $CDCl_3$) δ 169.09, 141.03, 140.68, 134.43, 129.02, 128.69 (d, J = 4.8 Hz), 128.40, 125.95, 77.28 (d, J = 11.4 Hz), 77.02, 76.70, 69.88, 68.32, 58.48, 37.78, 21.34. **IR** (KBr) v: 3385, 2929, 2773, 1747, 1242, 1201, 1152, 1123, 1034, 1027, 1002, 824, 742, 681, 562 cm^{-1}. **ESI-MS** (m/z): $[M + H]^+$ for $C_{12}H_{16}NO_3^+$ 222.3.

Synthesis of A3

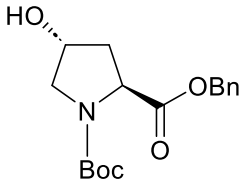

Following the Boc protection-general procedure, Na_2CO_3 (2.96 g, 27.96 mmol, 1.1 eq), and H_2O (20 mL) were added to a solution of **A2** (10 g, 25.42 mmol, 1 eq) in THF (50 mL). After cooling to 0 °C, Boc_2O (6.10 g, 27.96 mmol, 1.1 eq) was added in one portion. The crude residue was purified by flash chromatography on silica gel (n-Hex/EtOAc 6:4), to afford the desired product as a yellow oil (5.2 g, 64 %). **^{1}H-NMR** (400 MHz, $CDCl_3$) δ 7.34 (d, J = 4.6 Hz, 5H), 5.29 – 5.05 (m, 2H), 4.46 (dt, J = 16.1, 7.8 Hz, 2H), 3.56 (ddd, J = 55.9, 27.9, 7.8 Hz, 2H), 2.10 – 2.00 (m, 2H), 1.39 (d, J = 44.8 Hz, 9H). **^{13}C-NMR** (100MHz, $CDCl_3$) δ 207.17, 172.94, 172.64, 153.97, 135.73, 135.46, 128.79 – 127.90 (m), 80.32 (d, J = 16.3 Hz), 77.31 (d, J = 11.6 Hz), 77.05, 76.74, 70.18, 69.46, 66.80, 60.44, 58.01, 57.67, 54.69, 39.17, 38.44, 30.97, 28.30 (d, J = 19.9 Hz), 21.08, 14.21. **IR** (KBr) v: 3427, 2920, 2850, 1749, 1667, 1398, 1366, 1261, 1153, 1124, 1087, 978, 735, 697 cm^{-1}. **ESI-MS** (m/z): $[M + H]^+$ for $C_{17}H_{23}NO_5$ 322.4.

Synthesis of A4

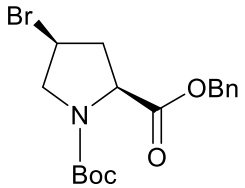

A solution of **A3** (1 g, 3.11 mmol, 1 eq) in anhydrous DCM (30 mL) was cooled to 0 °C. CBr_4 (2.58 g, 7.77 mmol, 2.5 eq), followed by PPh_3 (2.04 g, 7.77 mmol, 2.5 eq) were then added. The reaction

mixture was stirred at 0 °C for 1 h, and then at room temperature overnight under a N_2 atmosphere. Extraction with DCM (3 x 150 mL) followed, and combined organic phases were dried over $MgSO_4$, filtered and concentrated in *vacuo*. The crude residue was purified by flash chromatography on silica gel (n-Hex/EtOAc 85:15), yielding the pure product as a pale-yellow oil (0.76 g, 64 %). **^{1}H-NMR** (400 MHz, $CDCl_3$) δ 7.39 – 7.29 (m, 5H), 5.32 – 5.07 (m, 2H), 4.50 – 3.98 (m, 3H), 3.77 – 3.57 (m, 1H), 2.89 – 2.37 (m, 2H), 2.18 – 2.03 (m, 1H), 1.49 – 1.31 (m, 9H). **^{13}C-NMR** (100 MHz, $CDCl_3$) δ 151.59, 128.80 – 128.33 (m), 128.22, 80.70, 77.37, 77.05, 76.73, 67.13, 58.38, 58.03, 55.67, 55.27, 42.30, 41.42, 40.97, 40.00, 28.34, 28.13, 14.21. **IR** (KBr) ν: 2972, 2935, 2874, 1720, 1686, 1400, 1366, 1149, 1109, 999, 754, 702, 525 cm^{-1}. **ESI-MS** (m/z): $[M + H]^+$ for $C_{17}H_{22}BrNO_4$ 384.2.

Synthesis of A5

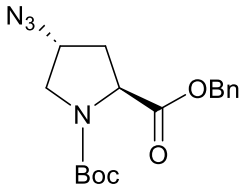

As by the azide reaction-general procedure, **A4** (0.51 g, 1.34 mmol, 1 eq) and NaN_3 (0.43 g, 6.7 mmol, 5 eq) were suspended in anhydrous DMF (19 mL). After extraction with EtOAc (3 x 100 mL), the product was obtained as a yellow oil (0.35 g, 76 %). **^{1}H-NMR** (400 MHz, $CDCl_3$) δ 7.39 – 7.30 (m, 5H), 5.29 – 5.07 (m, 2H), 4.43 (dt, J = 15.0, 7.0 Hz, 1H), 4.20 – 4.12 (m, 1H), 3.70 (dt, J = 10.4, 5.2 Hz, 1H), 3.53 (ddd, J = 50.4, 11.5, 2.9 Hz, 1H), 2.39 – 2.26 (m, 1H), 2.16 (dt, J = 11.6, 5.3 Hz, 1H), 1.48 – 1.32 (m, 10H). **^{13}C-NMR** (100 MHz, $CDCl_3$) δ 128.64 (d, J = 11.1 Hz), 128.30 (d, J = 30.3 Hz), 80.74, 77.34, 77.03, 76.71, 67.04, 58.68, 57.86, 57.58, 51.26, 36.32, 28.26 (d, J = 19.8 Hz). **IR** (KBr) ν: 2976, 2932, 2100, 1745, 1697, 1393, 1366, 1258, 1177, 1153, 1124, 747, 698 cm^{-1}. **ESI-MS** (m/z): $[M + Na]^+$ for $C_{17}H_{22}N_4O_4$ 369.4.

Synthesis of A6

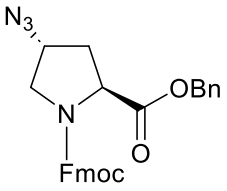

Using the Boc deprotection-general procedure, TFA (0.67 mL, 13 mmol, 10 eq) was added to a solution of **A5** (0.35 g, 1.30 mmol, 1 eq) in DCM (3 mL). Based on the Fmoc protection protocol, the yellow oil was dissolved in H_2O (2.8 mL) and Na_2CO_3 (0.23 g, 2.73 mmol, 2.1 eq). Fmoc-Cl (0.35 g,

1.36 mmol, 1.05 eq) in THF (4.8 mL) was then added. Concentrated HCl was added dropwise until pH ~ 0-1 was reached. After addition of H_2O (100 mL), the reaction mixture was extracted with DCM (3 x 80 mL), yielding the desired product as a yellow oil (0.43 g, 70 %). **^{1}H-NMR** (400 MHz, $CDCl_3$) δ 7.81 – 7.28 (m, 13H), 5.31 – 5.00 (m, 2H), 4.57 – 4.39 (m, 2H), 4.34 – 3.97 (m, 4H), 3.82 – 3.54 (m, 4H), 2.44 – 2.32 (m, 1H), 2.25 – 2.15 (m, 1H), 1.88 – 1.82 (m, 2H), 1.48 (s, 1H), 1.25 (s, 1H). **^{13}C-NMR** (100 MHz, $CDCl_3$) δ 171.69, 144.34, 141.55, 141.32, 128.73 – 128.10 (m), 127.68 (d, J = 13.3 Hz), 127.10, 125.00 (d, J = 13.9 Hz), 124.71, 120.23 – 119.63 (m), 77.29 (d, J = 11.6 Hz), 77.03, 76.71, 67.99, 67.79, 67.22 (d, J = 8.2 Hz), 65.21, 59.31, 58.56, 58.04 – 57.85 (m), 57.61, 51.88, 51.36, 50.38, 47.12, 36.47, 35.27, 27.83, 25.63. **IR** (KBr) ν: 2975, 2930, 2879, 1746, 1702, 1592, 1588, 1396, 1364, 1354, 1273, 1206, 1160, 1129, 1072, 992, 816, 768, 724, 543 cm^{-1}. **ESI-MS** (m/z): $[M + Na]^+$ for $C_{27}H_{24}N_4O_4$ 491.5.

Synthesis of A7

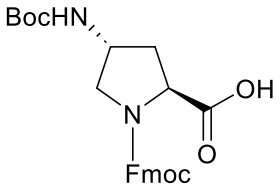

Following the hydrogenation-general procedure, Pd/C 10 % (100 mg) was placed in a three-neck round bottom flask, and EtOAc (3 mL) followed by MeOH (3 mL) were added. **A6** (0.40 g, 0.85 mmol, 1 eq) and Boc_2O were dissolved in MeOH (3.5 mL), and added into the reaction vessel. The reaction was left under stirring at room temperature overnight, under a hydrogen atmosphere. After that, the resulting precipitate was filtered off by vacuum filtration using a Celite filter, and was washed with MeOH. Recrystallization from DCM/Et_2O followed. The residue was then purified by flash chromatography on silica gel (DCM/MeOH 7:3), to give the final product as a colourless oil (0.05 g, 13 %). **^{1}H-NMR** (400 MHz, DMSO) δ 7.95 – 7.24 (m, 8H), 4.55 – 3.70 (m, 4H), 3.17 – 2.83 (m, 1H), 2.14 (dddd, J = 23.9, 21.3, 17.7, 8.6 Hz, 2H), 1.49 – 1.32 (m, 9H). **^{13}C-NMR** (100 MHz, DMSO) δ 141.15, 128.18, 127.46 (dd, J = 22.3, 14.8 Hz), 125.69, 124.64, 120.38 (d, J = 9.3 Hz), 40.62, 40.41, 40.20, 39.90 (d, J = 18.2 Hz), 39.79, 39.59, 39.47 (d, J = 21.0 Hz), 28.66, 28.39. **IR** (KBr) ν: FT-IR 2974, 2929, 1686, 1448, 1415, 1367, 1250, 1160, 1129, 911, 759, 732, 648, 620, 540 cm^{-1}. **ESI-MS** (m/z): $[M + Na]^+$ for $C_{25}H_{28}N_2O_6$ 475.2.

2.6.1.3 Alternative Synthesis of A7

Synthesis of B2

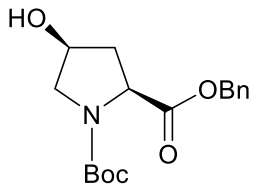

B1 (1 g, 4.08 mmol, 1 eq) was dissolved in THF (16.44 mL). After cooling to 0 °C, NaOH (7.01 mL) was added, and the whole was stirred at room temperature overnight. The reaction mixture was concentrated under reduced pressure and acidified with concentrated HCl. Extraction with EtOAc (3 x 150 mL) followed, and combined organic layers were dried over $MgSO_4$, filtered and concentrated in *vacuo*. The crude residue was dissolved in DMF (5.23 mL). BnBr (0.49 mL, 4.16 mmol, 1 eq), followed by Et_3N (0.76 mL, 5.47 mmol, 1.34 eq) were added, and the reaction mixture was stirred at room temperature for 72 h. It was then concentrated under reduced pressure and extracted with EtOAc (3 x 150 mL). Combined organic layers were washed with brine (3 x 150 mL), dried over $MgSO_4$, filtered and concentrated in *vacuo*. The crude material was purified by flash chromatography on silica gel (n-Hex/EtOAc 1:1) to afford the desired product as a colourless oil (0.60 g, 45 %). **^{1}H-NMR** (400 MHz, $CDCl_3$) δ 7.34 (d, J = 11.8 Hz, 5H), 5.30 (d, J = 12.4 Hz, 1H), 5.12 (d, J = 12.4 Hz, 1H), 4.39 (dt, J = 41.4, 11.8 Hz, 3H), 3.56 (ddt, J = 32.5, 21.4, 14.5 Hz, 3H), 2.38 – 2.22 (m, 2H), 2.14 – 1.99 (m, 2H), 1.42 (dd, J = 37.9, 23.4 Hz, 13H).

Synthesis of B3

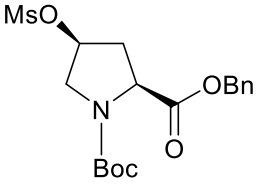

B3 (0.60 g, 1.87 mmol, 1 eq) was dissolved in anhydrous DCM (5 mL), and Et_3N (0.27 mL, 1.98 mmol, 1.06 eq) was added. The reaction mixture was cooled to 0 °C, and MsCl (0.29 mL, 3.73 mmol, 2 eq) was added dropwise under N_2 atmosphere. Stirring was continued for 30 minutes at 0 °C, and then for 3 hours at room temperature. The solvent was removed under reduced pressure, and concentrated HCl was added to eliminate the excess of base. Extraction with EtOAc (3 x 100 mL) followed, and combined organic layers were washed with brine (3 x 100 mL), dried over $MgSO_4$, filtered and concentrated in *vacuo*, to afford the final product as a pale-orange oil (0.64 g, 89 %). **^{1}H-NMR** (400 MHz, $CDCl_3$) δ 7.36 – 7.24 (m, 5H), 5.27 – 5.04 (m, 2H), 4.46 – 4.22 (m, 6H), 3.69 – 3.33 (m,

7H), 2.47 – 1.93 (m, 5H), 1.42 (t, J = 9.0 Hz, 11H). **^{13}C-NMR** (100 MHz, $CDCl_3$) δ 128.66, 77.28 (d, J = 11.5 Hz), 77.02, 76.71, 67.53, 58.06, 28.26 (d, J = 14.8 Hz). **IR** (KBr) v: 2971, 2936, 1697, 1685, 1399, 1364, 1157, 1127, 1083, 954, 899, 751, 697, 524 cm^{-1}. **ESI-MS** (m/z): $[M + H]^+$ for $C_{18}H_{25}NO_7S$ 400.0.

Synthesis of A5

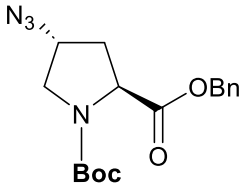

As by the azide reaction-general procedure, **B3** (0.60 g, 1.67 mmol, 1 equiv) and NaN_3 (0.54 g, 8.35 mmol, 5 equiv) were suspended in anhydrous DMF (20 mL). After extraction with EtOAc (3 x 100 mL), the product was obtained as a yellow oil (0.42 g, 74 %). **^{1}H-NMR** (400 MHz, $CDCl_3$) δ 7.32 (t, J = 4.0 Hz, 5H), 5.21 – 4.99 (m, 2H), 4.46 – 4.25 (m, 1H), 4.17 – 4.02 (m, 1H), 3.68 – 3.39 (m, 2H), 2.34 – 2.21 (m, 1H), 2.11 (ddd, J = 24.4, 15.1, 9.2 Hz, 1H), 1.47 – 1.27 (m, 10H).

Synthesis of A6

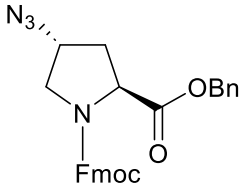

Using the Boc deprotection-general procedure, TFA (0.94 mL, 12.3 mmol, 10 eq) was added to a solution of **A5** (0.42 g, 1.23 mmol, 1 eq) in DCM (6 mL). Based on the Fmoc protection protocol, the yellow oil was dissolved in H_2O (6.6 mL) and Na_2CO_3 (0.22 g, 5.33 mmol, 2.1 eq). Fmoc-Cl (0.33 g, 2.67 mmol, 1.05 eq) in THF (11.4 mL) was then added. Concentrated HCl was added dropwise until pH ~ 0-1 was reached. After addition of H_2O (100 mL), the reaction mixture was extracted with DCM (3 x 100 mL), yielding the desired product as a yellow oil (0.50 g, 86 %). **^{1}H-NMR** (400 MHz, $CDCl_3$) δ 7.80 – 7.26 (m, 13H), 5.14 (ddt, J = 17.7, 15.3, 12.2 Hz, 1H), 4.58 – 3.97 (m, 5H), 3.83 – 3.55 (m, 2H), 2.44 – 2.15 (m, 1H).

Synthesis of A7

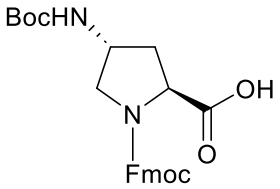

As by the hydrogenation protocol, Pd/C 10 % (100 mg) was placed in a three-neck round bottom flask, and EtOAc (3 mL) followed by MeOH (3 mL) were added. **A6** (1.06 g, 2.26 mmol, 1 eq) and Boc_2O were dissolved in MeOH (3.5 mL), and added into the reaction vessel. The reaction was left under stirring at room temperature overnight, under a hydrogen atmosphere. After that, the resulting precipitate was filtered off by vacuum filtration using a Celite filter, and was washed with MeOH to give the product as a pale-yellow oil (0.40 g, 50 %). Following the Boc protection-general procedure, Na_2CO_3 (0.13 g, 1.24 mmol, 1.1 eq) and H_2O (20 mL) were added to a solution of the yellow oil (0.40 g, 1.13 mmol, 1 eq) in THF (20 mL). After cooling to 0 °C, Boc_2O (0.62 g, 2.82 mmol, 2.5 eq) was added in one portion. After recrystallization from DCM/ n-Hex, the desired product was obtained as a colourless oil (0.17 g, 33 %). **^{1}H-NMR** (400 MHz, $CDCl_3$) δ 7.79 – 7.28 (m, 8H), 4.55 – 3.54 (m, 6H), 3.40 – 2.72 (m, 4H), 2.30 (dd, J = 11.0, 4.7 Hz, 1H), 2.00 (d, J = 0.5 Hz, 1H), 1.64 – 1.36 (m, 7H).

2.6.1.4 Synthesis of C2

Synthesis of C2

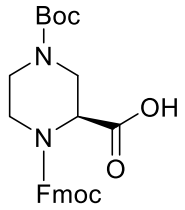

C2 was prepared according to the Fmoc protection-general procedure. (2R)-1-(Tert-butoxycarbonyl)piperazine-2-carboxylic acid (**C1**) (0.8 g, 3.47 mmol, 1 eq) was dissolved in H_2O (3.5 mL) and Na_2CO_3 (0.61 g, 7.29 mmol, 2.1 eq). Fmoc-Cl (0.90 g, 3.47 mmol, 1.0 eq) in THF (7 mL) was then added. Concentrated HCl was added dropwise until pH ~ 0-1 was reached. After addition of H_2O (100 mL), the reaction mixture was extracted with DCM (3 x 100 mL). After recrystallization from Et_2O/n-Hex, the desired product was obtained as a white solid (1.0 g, 63 %). **^{1}H-NMR** (400 MHz, $CDCl_3$) δ 7.74 – 6.97 (m, 8H), 4.75 – 3.61 (m, 7H), 3.30 – 2.64 (m, 2H), 1.83 – 1.65 (m, 1H), 1.32 (d, J = 3.8 Hz, 9H). **^{13}C-NMR** (100 MHz, DMSO) δ 171.76, 155.62, 144.12, 141.20, 128.21, 127.66, 125.63 (d, J = 9.1 Hz), 120.64, 79.77, 67.65, 54.07, 47.00, 41.26, 40.97, 40.63, 40.33 (d, J = 18.8 Hz), 40.21, 40.00, 39.79, 39.58, 39.37, 28.35. **IR** (KBr) v: 2955, 1753, 1682, 1647, 1468, 1438,1357, 1224, 1183, 1169, 1121,1079, 893, 775, 761, 735, 695, 442, 422, 412 cm^{-1}. **ESI-MS** (m/z): $[M + Na]^+$ for $C_{25}H_{28}N_2O_6$ 475.2.

2.6.1.5 Synthesis of D3

Synthesis of D1

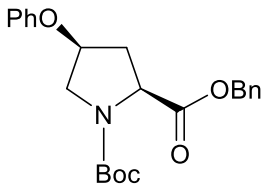

A3 (1.66 g, 5.16 mmol, 1 eq) was dissolved in THF (20 mL). PPh_3 (1.49 g, 5.68 mmol, 1.1 eq), followed by DIAD (1.09 mL, 5.68 mmol, 1.1 eq) were added at 0 °C. After stirring for 15 minutes, Ph-OH (0.49 g, 5.26 mmol, 1 eq) was added under inert atmosphere, and the resulting reaction mixture was stirred further for another 5 hours. The reaction mixture was diluted with cold H_2O and extracted with EtOAc (3 x 150 mL). Combined organic layers were washed with brine (3 x 150 mL), dried over $MgSO_4$, filtered, and concentrated in *vacuo* to give the crude product. Purification by flash chromatography on silica gel (n-Hex/EtOAc 8:2) afforded the desired product as a yellow oil (1.32 g, 64 %). **^{1}H-NMR** (400 MHz, $CDCl_3$) δ 7.34 – 6.63 (m, 10H), 5.11 (ddd, J = 46.3, 26.3, 12.4 Hz, 2H), 4.88 – 4.80 (m, 1H), 4.48 (ddd, J = 11.6, 8.6, 5.5 Hz, 1H), 3.83 – 3.57 (m, 2H), 2.53 – 2.30 (m, 2H), 1.37 (d, J = 42.6 Hz, 9H). **^{13}C-NMR** (100 MHz, $CDCl_3$) δ 171.79, 171.44, 156.63, 154.23, 153.82, 135.69 (d, J = 11.9 Hz), 129.60, 128.41 (dd, J = 16.8, 9.3 Hz), 128.08, 121.35 (d, J = 3.6 Hz), 115.56 (d, J = 6.8 Hz), 80.26, 77.31 (d, J = 11.7 Hz), 77.05, 76.73, 75.40, 74.41, 66.87 (d, J = 5.5 Hz), 60.42, 58.00, 57.67, 52.14, 51.77, 40.86, 36.35, 35.41, 28.31 (d, J = 19.5 Hz), 23.86, 21.08, 20.81, 17.51, 17.31, 14.67, 14.22. **IR** (KBr) v: 2974, 1756, 1698, 1497,1398,1367,1238,1159,1119,1079,1072,966, 890 750,674 cm^{-1}. **ESI-MS** (m/z): $[M + H]^+$ for $C_{23}H_{27}NO_5$ 320.6.

Synthesis of D2

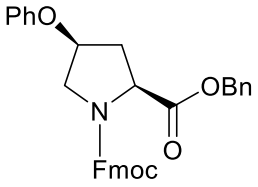

Following the Boc deprotection-general procedure, TFA (1.93 mL, 13 mmol, 10 eq) was added to a solution of **D1** (1.0 g, 2.52 mmol, 1 eq) in DCM (10 mL). Based on the Fmoc protection protocol, the yellow oil was dissolved in H_2O (3.5 mL) and Na_2CO_3 (0.44 g, 5.29 mmol, 2.1 eq). Fmoc-Cl (1.63 g, 6.3 mmol, 2.5 eq) in THF (7 mL) was then added. Concentrated HCl was added dropwise until pH ~ 0-1 was reached. After addition of H_2O (100 mL), the reaction mixture was extracted with DCM (3 x 150 mL), yielding the desired product was obtained as a yellow oil (0.89 g, 69 %). **^{1}H-NMR** (400 MHz,

$CDCl_3$) δ 7.82 – 6.69 (m, 18H), 5.27 – 4.88 (m, 3H), 4.72 – 4.48 (m, 1H), 4.45 – 4.23 (m, 2H), 3.90 – 3.78 (m, 2H), 2.49 (dddd, J = 24.2, 13.9, 11.7, 9.3 Hz, 2H). **^{13}C-NMR** (100 MHz, $CDCl_3$) δ 171.15, 170.94, 156.46, 154.50, 144.20, 143.72, 141.30 (d, J = 11.3 Hz), 135.52 (d, J = 14.5 Hz), 129.66 (d, J = 5.8 Hz), 128.51 (d, J = 3.9 Hz), 128.36 – 127.98 (m), 127.68 (d, J = 4.7 Hz), 127.06 (d, J = 3.7 Hz), 125.16 (d, J = 21.0 Hz), 124.98, 121.57 (d, J = 8.2 Hz), 119.94, 115.73 (d, J = 8.2 Hz), 77.35, 77.04, 76.72, 75.39, 74.36, 67.63 (d, J = 14.3 Hz), 67.09, 58.57 – 58.13 (m), 58.02 (d, J = 21.3 Hz), 52.40, 51.98, 47.19 (d, J = 6.3 Hz), 36.52, 35.37. **IR** (KBr) v: 2950, 1754, 1702, 1450,1419, 1340, 1232, 1211, 1187, 1166, 1115, 1082,1069, 967, 753, 737, 692 cm^{-1}. **ESI-MS** (m/z): $[M + H]^+$ for $C_{33}H_{29}NO_5$ 519.5.

Synthesis of D3

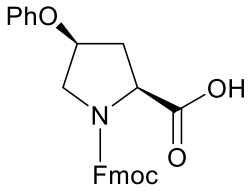

As by the hydrogenation-general procedure, Pd/C 5 % (0.185 mg) was placed in a three-neck round bottom flask, and EtOAc (3 mL) followed by MeOH (3 mL) were added. **D2** (0.8 g, 1.54 mmol, 1 eq) was dissolved in MeOH (3.5 mL), and added into the reaction vessel. The reaction was left under stirring at room temperature overnight, under a hydrogen atmosphere. The resulting precipitate was filtered off by vacuum filtration using a Celite filter, and was washed with MeOH. After recrystallization from Et_2O/n-Hex, the desired product was obtained as a white solid (0.62 g, 94%). **^{1}H-NMR** (400 MHz, $CDCl_3$) δ 7.78 – 6.72 (m, 13H), 4.94 (s, 1H), 4.66 – 4.15 (m, 4H), 3.75 (s, 2H), 2.80 – 2.31 (m, 2H). **^{13}C-NMR** (100 MHz, $CDCl_3$) δ 129.68, 127.78, 127.13, 124.95, 121.85 – 121.63 (m), 120.01, 115.86, 77.34, 77.02, 76.70, 47.19. **IR** (KBr) v: 2954, 1753, 1680, 1647, 1451, 1424, 1349, 1314, 1227, 1199, 1109, 1020, 958, 833, 768, 735, 725, 597, 542, 427 cm^{-1}. **ESI-MS** (m/z): $[M + Na]^+$ calc $C_{26}H_{23}NO_5$ 452.47.

2.6.1.6 Synthesis of E2

Synthesis of E1

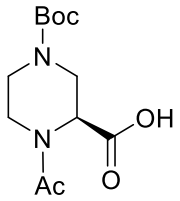

To a solution of the commercially available **C1** (0.5 g, 2.17 mmol, 1 eq) in aqueous NaOH 30% (6 mL) solution, Ac_2O (0.6 mL, 6.51 mmol, 3eq) was added slowly at 0 °C. The reaction mixture was stirred at room temperature. It was then acidified by addition of HCl, until the pH reached ~ 2-3. Extraction with DCM (3 x 100 mL) followed, and combined organic layers were washed with brine (3 x 100 mL), dried over $MgSO_4$, filtered and concentrated in *vacuo*. The crude was purified by flash chromatography on silica gel (n-Hex/EtOAc 6:4), to afford the desired product as a pale-yellow (0.21 g, 36 %). **^{1}H-NMR** (400 MHz, $CDCl_3$) δ 5.18 (d, J = 3.1 Hz, 1H), 4.62 (t, J = 16.6 Hz, 1H), 4.46 – 3.81 (m, 2H), 3.71 – 3.44 (m, 2H), 3.17 – 2.74 (m, 2H), 2.21 – 2.03 (m, 3H), 1.45 (d, J = 5.2 Hz, 9H). **^{13}C-NMR** (100 MHz, $CDCl_3$) δ 176.89, 171.56, 80.86, 77.34, 77.03, 76.71, 51.85, 43.36, 28.22, 21.40, 20.70. **IR** (KBr) v: 2976, 2926, 1697,1686, 1617, 1608, 1422, 1368, 1226, 1158, 1128, 1028, 961, 860, 611, 544 cm^{-1}. **ESI-MS** (m/z): $[M + Na]^+$ for $C_{12}H_{20}N_2O_5$ 295.4.

Synthesis of E2

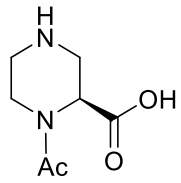

Following the Boc deprotection-general procedure, TFA (0.07 mL, 0,.92 mmol, 10 eq) was added to a solution of **E1** (0.025 g, 0.092 mmol, 1 eq) in DCM (0.32 mL). The product was obtained as a pale-yellow oil (13 mg, 80 %). **^{1}H-NMR** (400 MHz, MeOD) δ 4.15 – 3.88 (m, 1H), 3.65 – 3.33 (m, 2H), 3.28 – 2.85 (m, 2H), 2.23 – 2.13 (m, 3H), 1.32 – 1.18 (m, 3H). **^{13}C-NMR** (100 MHz, $CDCl_3$) δ 77.39, 77.07, 76.75, 49.38 (d, J = 19.9 Hz), 49.07, 48.86. **ESI-MS** (m/z): $[M + H]^+$ for $C_7H_{12}N_2O_3$ 173.0.

2.6.2 Peptides

2.6.2.1 General Procedures

Manual SPPS-General Protocol

Standard Fmoc SPPS procedures were performed using Rink amide MBHA resin. The reactions were carried out using a 25 mL peptide synthesis vessel. The resin (300 mg, 0.24 mmol, 1 eq) was swollen in DCM (5 mL) for 1 h. It was then washed with DMF (3 x 3 mL) and DMF/Piperidine (20 %) (3 mL) was added. After agitating for 40 mins, the resin was again washed with DMF (3 x 3 mL).

A solution of Fmoc-Pro-OH (2 eq), HOBt (2 eq), PyBOP (4 eq) and DIPEA (4 eq) in DMF (2 mL) were sonicated for 3 mins and then added to the resin, and the whole was agitated for 2h. It was again

washed with DMF (3x 3 mL). Ac_2O, DIPEA, and DMF (10:2.5:100) (3 mL) were added as the capping mixture. After agitating for 1 h, the resin was again washed with DMF (3x 3 mL).

The Kaiser test followed, by adding 2-3 drops of reagent A, B and C to a glass vial containing a few resin beads. 2-3 drops of the same reagents were also added to an empty glass vial, as a reference sample. Both vials were heated at 110 °C for 5 mins, and their colour was compared.

The Fmoc deprotection and coupling step were repeated in order to add the second amino acid.

After that, the chloranil test was carried out, by dissolving p-chloranil (1 g) in DMF (49 mL). 2-3 drops of this solution were added to a glass vial containing a few resin beads. 2-3 drops of the same reagents were also added to an empty glass vial, as a reference sample. After 5 mins at room temperature, the colour of the two vials was compared.

These steps were then repeated until the desired sequence was synthesized. After the addition of last amino acid, DMF/Piperidine (20 %) (3 mL) was added. Following washing with DMF (3 x 3 mL), the capping step was repeated. The resin was then washed with DMF (3 x 3 mL), and the chloranil test was carried out to confirm successful capping. The resin was washed with DCM (3 x 3 mL), and then transferred to a round-bottom flask before the peptide was cleaved from the resin using TFA (95 % in DCM) (3 x 3 mL). After spinning for 2 h, the whole was transferred to a peptide synthesis vessel, and the resin was washed with the cleavage cocktail (2 x 1 mL). The solution was then collected in a round bottom flask, and TFA was removed under reduced pressure. The product precipitated upon addition of cold Et_2O, and was centrifuged. The solution was decanted, and the solid was repeatedly washed with cold Et_2O and dried under vacuum.

SPPS on the peptide synthesizer-General Protocol

Standard Fmoc SPPS procedures were again performed using Rink amide MBHA resin on a 0.1 mmol scale, using a Liberty™ microwave peptide synthesiser (CEM). The resin (300 mg, 0.24 mmol, 1 eq) was swollen in DCM (5 mL) for 1 h, using a 25 mL peptide synthesis vessel. It was then washed with DMF (3 x 3 mL) and place on the peptide synthesis apparatus. Following the same steps as on the manual peptide synthesis, repeated steps of single deprotections, and couplings interspaced with washings were then performed.

Deprotection: 20 % piperidine in DMF for 5 min with 30 W microwave irradiation at 90 °C. Coupling: Fmoc-protected amino acid, DIC, Oxyma Pure and DMF for 5 min at 90 °C with 30 W microwave irradiation. Washings: DMF. Once the desired sequence has been synthesized, the peptide is transferred to a round bottom flask, and the cleavage procedure is performed similarly as in the manual peptide synthesis.

2.6.2.2 Synthesis of PP 1, PP 2 and PP 3

Synthesis of PP 1

PP 1 was synthesized using both SPPS protocols. Purification by preparative RP-HPLC, yielded a white solid as the final product (80 mg, 64 %). **^{1}H-NMR** (400 MHz, $CDCl_3$) δ 8.20 (s, 1H), 6.62 – 6.56 (m, 1H), 5.30 (s, 1H), 5.15 (s, 1H), 4.71 – 4.58 (m, 4H), 4.42 (dd, J = 58.1, 7.8 Hz, 3H), 4.19 (d, J = 8.6 Hz, 1H), 3.75 – 3.39 (m, 13H), 3.32 – 3.14 (m, 3H), 2.51 (s, 1H), 2.36 – 1.44 (m, 49H), 1.18 (s, 7H), 0.90 – 0.78 (m, 3H). **ESI-MS** (m/z): $[M + H]^+$ calc for $C_{35}H_{22}N8O_7$ 696.4; found, 697.2.

Synthesis of PP 2

PP 2 was synthesized using both SPPS protocol. For the fourth coupling, the previously synthesized **C2** monomer was used. Purification by preparative RP-HPLC, yielded a white solid as the final product (90 mg, 66 %). **^{1}H-NMR** (400 MHz, $CDCl_3$) δ 7.64 (s, 1H), 7.16 (s, 1H), 5.50 (d, J = 40.0 Hz, 2H), 4.78 (s, 2H), 4.69 – 4.48 (m, 6H), 4.40 (d, J = 26.4 Hz, 1H), 4.32 (dd, J = 15.2, 7.2 Hz, 2H), 4.01 (d, J = 12.9 Hz, 2H), 3.77 (dd, J = 29.3, 9.3 Hz, 9H), 3.65 – 3.18 (m, 28H), 2.34 – 1.67 (m, 49H). **ESI-MS** (m/z): $[M + H]^+$ calc for $C_{37}H_{55}N_9O_8$ 753.4; found, 754.4.

Synthesis of PP 3

PP 3 was synthesized using both SPPS protocol. For the fourth and sixth couplings, the previously synthesized **C2** and **D3** monomers were used. Purification by preparative RP-HPLC, yielded a white solid as the final product (100 mg, 64 %). **^{1}H-NMR** (400 MHz, $CDCl_3$) δ 7.66 – 7.44 (m, 1H), 7.26 – 7.21 (m, 1H), 6.83 (ddd, *J* = 83.1, 36.4, 29.5 Hz, 3H), 5.12 (s, 1H), 4.96 (d, *J* = 6.5 Hz, 1H), 4.81 (dd, *J* = 8.4, 4.3 Hz, 1H), 4.67 – 4.52 (m, 2H), 4.22 – 4.10 (m, 1H), 3.83 – 3.64 (m, 3H), 3.54 (d, *J* = 12.5 Hz, 4H), 3.43 (d, *J* = 9.2 Hz, 2H), 2.19 – 2.04 (m, 5H), 1.97 – 1.46 (m, 17H). **ESI-MS** (m/z): $[M + H]^+$ calc for $C_{43}H_{59}N_9O_9$ 845.4; found, 846.4.

2.6.3 Aldol Asymmetric Reaction

2.6.3.1 General Procedures

Aldol Reaction of 4-nitrobenzaldehyde and cyclohexanone-General Protocol

The catalyst candidate with 10% loading was dissolved in the expected solvent, and the whole was stirred for 1 hour. Cyclohexanone (30 µL, 0.33 mmol, 5 eq) followed by 4-nitrobenzaldehyde (10 mg, 0.07 mmol, 1 eq) were then added. The reaction was monitored by TLC until completion.

2.6.3.2 Syntesis of 2-(hydroxyl-(p-nitrophenyl)methyl)cyclohexan-1-one

In the HPLC analysis below, the numbering (1-4) refers to the peaks of each Chromatogram based on elution order.

Synthesis of 2-(hydroxyl-(p-nitrophenyl)methyl)cyclohexan-1-one using PP 1 in DMF (Table 5, Entry 16)

2-(hydroxyl-(p-nitrophenyl)methyl)cyclohexan-1-one was synthesized using the aldol reaction general protocol, and was obtained as a colourless solid. **^{1}H-NMR** (400 MHz, $CDCl_3$) δ 8.27 – 8.13 (m, 2H), 7.51 – 7.43 (m, 2H), 5.45 (d, J = 2.2 Hz, 0.5H), 4.87 (d, J = 8.3 Hz, 0.5H), 3.75 – 3.36 (m, 1H), 2.64 – 2.35 (m, 2H), 2.14 – 2.00 (m, 1H), 1.65 – 1.17 (m, 5H).**^{13}C-NMR** (100 MHz, $CDCl_3$) δ (214.43, 148.34, 127.89, 126.62, 123.53, 74.04, 70.14, 57.00, 42.66, 30.77, 27.75, 24.74. **HPLC:** Chiralpak AD-H; n-hexane/i-PrOH = 80/20 (v/v); 1.00 mL min^{-1}; 254 nm; 25 °C; **1** (11.0 min, 20%, (2R, 1'R)); **2** (12.1 min, 20%, (2S, 1'S)); **3** (13.1 min, 20%, (2S, 1'R)); **4** (17.0 min, 20%, (2R, 1'S)).

Syntesis of 2-(hydroxyl-(p-nitrophenyl)methyl)cyclohexan-1-one using PP 1 without adding any solvent (Table 5, Entry 17)

2-(hydroxyl-(p-nitrophenyl)methyl)cyclohexan-1-one was synthesized using the aldol reaction general protocol, and was obtained as a colourless solid. **HPLC:** Chiralpak AD-H; n-hexane/i-PrOH = 80/20 (v/v); 1.00 mL min^{-1}; 254 nm; 25 °C; **1** (11.0 min, 20%, (2R, 1'R)); **2** (12.1 min, 20%, (2S, 1'S)); **3** (13.1 min, 20%, (2S, 1'R)); **4** (17.1 min, 20%, (2R, 1'S)).

Syntesis of 2-(hydroxyl-(p-nitrophenyl)methyl)cyclohexan-1-one using PP 1 in EtOH (Table 5, Entry 18)

2-(hydroxyl-(p-nitrophenyl)methyl)cyclohexan-1-one was synthesized using the aldol reaction general protocol, and was obtained as a colourless solid. **HPLC:** Chiralpak AD-H; n-hexane/i-PrOH = 80/20 (v/v); 1.00 mL min^{-1}; 254 nm; 25 °C; **1** (10.9 min, 20%, (2R, 1'R)); **2** (12.2 min, 20%, (2S, 1'S)); **3** (13.1 min, 20%, (2S, 1'R)); **4** (17.7 min, 20%, (2R, 1'S)).

Syntesis of 2-(hydroxyl-(p-nitrophenyl)methyl)cyclohexan-1-one using PP 2 in DMF (Table 6, Entry 28)

2-(hydroxyl-(p-nitrophenyl)methyl)cyclohexan-1-one was synthesized using the aldol reaction general protocol, and was obtained as a colourless solid. **HPLC:** Chiralpak AD-H; n-hexane/i-PrOH =

80/20 (v/v); 1.00 mL min^{-1}; 254 nm; 25 °C; **1** (10.9 min, 20%, (2R, 1'R)); **2** (12.2 min, 20%, (2S, 1'S)); **3** (13.1 min, 20%, (2S, 1'R)); **4** (17.7 min, 20%, (2R, 1'S)).

Syntesis of 2-(hydroxyl-(p-nitrophenyl)methyl)cyclohexan-1-one using PP 2 in propanol (Table 6, Entry 29)

2-(hydroxyl-(p-nitrophenyl)methyl)cyclohexan-1-one was synthesized using the aldol reaction general protocol, and was obtained as a colourless solid. **HPLC:** Chiralpak AD-H; n-hexane/i-PrOH = 80/20 (v/v); 1.00 mL min^{-1}; 254 nm; 25 °C; **1** (10.9 min, 20%, (2R, 1'R)); **2** (12.3 min, 20%, (2S, 1'S)); **3** (13.2 min, 20%, (2S, 1'R)); **4** (17.7 min, 20%, (2R, 1'S)).

Syntesis of 2-(hydroxyl-(p-nitrophenyl)methyl)cyclohexan-1-one using PP 2 in MeOH (Table 6, Entry 30)

2-(hydroxyl-(p-nitrophenyl)methyl)cyclohexan-1-one was synthesized using the aldol reaction general protocol, and was obtained as a colourless solid. **HPLC:** Chiralpak AD-H; n-hexane/i-PrOH = 80/20 (v/v); 1.00 mL min^{-1}; 254 nm; 25 °C; **1** (11.6 min, 20%, (2R, 1'R)); **2** (12.3 min, 20%, (2S, 1'S)); **3** (13.4 min, 20%, (2S, 1'R)); **4** (18.0 min, 20%, (2R, 1'S)).

Syntesis of 2-(hydroxyl-(p-nitrophenyl)methyl)cyclohexan-1-one Using PP 3 in DMF (Table 7, Entry 31)

2-(hydroxyl-(p-nitrophenyl)methyl)cyclohexan-1-one was synthesized using the aldol reaction general protocol, and was obtained as a colourless solid. **HPLC:** Chiralpak AD-H; n-hexane/i-PrOH = 80/20 (v/v); 1.00 mL min^{-1}; 254 nm; 25 °C; **1** (10.6 min, 20%, (2R, 1'R)); **2** (11.2 min, 20%, (2S, 1'S)); **3** (12.2 min, 20%, (2S, 1'R)); **4** (15.8 min, 20%, (2R, 1'S)).

Syntesis of 2-(hydroxyl-(p-nitrophenyl)methyl)cyclohexan-1-one Using PP 3 in propanol (Table 7, Entry 32)

2-(hydroxyl-(p-nitrophenyl)methyl)cyclohexan-1-one was synthesized using the aldol reaction general protocol, and was obtained as a colourless solid. **HPLC:** Chiralpak AD-H; n-hexane/i-PrOH = 80/20 (v/v); 1.00 mL min^{-1}; 254 nm; 25 °C; **1** (11.5 min, 20%, (2R, 1'R)); **2** (12.3 min, 20%, (2S, 1'S)); **3** (13.3 min, 20%, (2S, 1'R)); **4** (17.8 min, 20%, (2R, 1'S)).

Syntesis of 2-(hydroxyl-(p-nitrophenyl)methyl)cyclohexan-1-one Using PP 3 in MeOH (Table 7, Entry 33)

2-(hydroxyl-(p-nitrophenyl)methyl)cyclohexan-1-one was synthesized using the aldol reaction general protocol, and was obtained as a colourless solid. **HPLC:** Chiralpak AD-H; n-hexane/i-PrOH = 80/20 (v/v); 1.00 mL min^{-1}; 254 nm; 25 °C; **1** (10.7 min, 20%, (2R, 1'R)); **2** (11.8 min, 20%, (2S, 1'S)); **3** (12.7 min, 20%, (2S, 1'R)); **4** (16.6 min, 20%, (2R, 1'S)).

Syntesis of 2-(hydroxyl-(p-nitrophenyl)methyl)cyclohexan-1-one Using E3 in DMF (Table 8, Entry 34)

2-(hydroxyl-(p-nitrophenyl)methyl)cyclohexan-1-one was synthesized using the aldol reaction general protocol, and was obtained as a colourless solid. **HPLC:** Chiralpak AD-H; n-hexane/i-PrOH = 80/20 (v/v); 1.00 mL min^{-1}; 254 nm; 25 °C; **1** (10.6 min, 20%, (2R, 1'R)); **2** (11.2 min, 20%, (2S, 1'S)); **3** (12.2 min, 20%, (2S, 1'R)); **4** (15.9 min, 20%, (2R, 1'S)).

Syntesis of 2-(hydroxyl-(p-nitrophenyl)methyl)cyclohexan-1-one Using E3 in propanol (Table 8, Entry 35)

2-(hydroxyl-(p-nitrophenyl)methyl)cyclohexan-1-one was synthesized using the aldol reaction general protocol, and was obtained as a colourless solid. **HPLC:** Chiralpak AD-H; n-hexane/i-PrOH = 80/20 (v/v); 1.00 mL min^{-1}; 254 nm; 25 °C; **1** (10.2 min, 20%, (2R, 1'R)); **2** (11.1 min, 20%, (2S, 1'S)); **3** (11.9 min, 20%, (2S, 1'R)); **4** (15.5 min, 20%, (2R, 1'S)).

Syntesis of 2-(hydroxyl-(p-nitrophenyl)methyl)cyclohexan-1-one Using L-Proline in DMF (Table 9, Entry 36)

2-(hydroxyl-(p-nitrophenyl)methyl)cyclohexan-1-one was synthesized using the aldol reaction general protocol, and was obtained as a colourless solid. **HPLC:** Chiralpak AD-H; n-hexane/i-PrOH = 80/20 (v/v); 1.00 mL min^{-1}; 254 nm; 25 °C; **1** (10.2 min, 20%, (2R, 1'R)); **2** (11.0 min, 20%, (2S, 1'S)); **3** (11.9 min, 20%, (2S, 1'R)); **4** (15.5 min, 20%, (2R, 1'S)).

Syntesis of 2-(hydroxyl-(p-nitrophenyl)methyl)cyclohexan-1-one Using L-Proline in propanol (Table 9, Entry 37)

2-(hydroxyl-(p-nitrophenyl)methyl)cyclohexan-1-one was synthesized using the aldol reaction general protocol, and was obtained as a colourless solid. **HPLC:** Chiralpak AD-H; n-hexane/i-PrOH = 80/20 (v/v); 1.00 mL min^{-1}; 254 nm; 25 °C; **1** (11.4 min, 20%, (2R, 1'R)); **2** (12.5 min, 20%, (2S, 1'S)); **3** (13.6 min, 20%, (2S, 1'R)); **4** (18.2 min, 20%, (2R, 1'S)).

Chapter 3

Application of Polyproline Peptides in the Kinetic Resolution of a Racemic Alcohol

3.1 Introduction: Examples of Peptide Catalysts for Asymmetric Acyl Transfer Reactions

Short peptides that have well-defined secondary structures have already proved to serve as catalysts in the KR of alcohols.[1,2] Copeland, Jarvo and Miller synthesized a series of short peptides with a well-defined conformation, which were tested as catalysts in KR experiments.[3] The tetrapeptides have a catalytically active alkylimidazole substructure and enantiomeric proline units in the (i+1) position (Scheme 34).[3] The acylation reaction was performed in toluene using 2-5 mol % of catalyst at 25 °C.[3] According to this study, peptides with D-proline in the (i+1) position preferentially acylated the (S,S)-product, with the highest conversion and ee being 71 % and 89 % respectively.[3] It is notable that when D-proline was exchanged with L-proline, the opposite enantiomeric product (R,R) was obtained. The highest conversion and ee achieved in this case were 61 % and 99 % respectively.[3] Thus, the stereochemical configuration of one residue, located at the (i+1) position of the catalyst, was able to dictate the stereochemical outcome of a KR.[3]

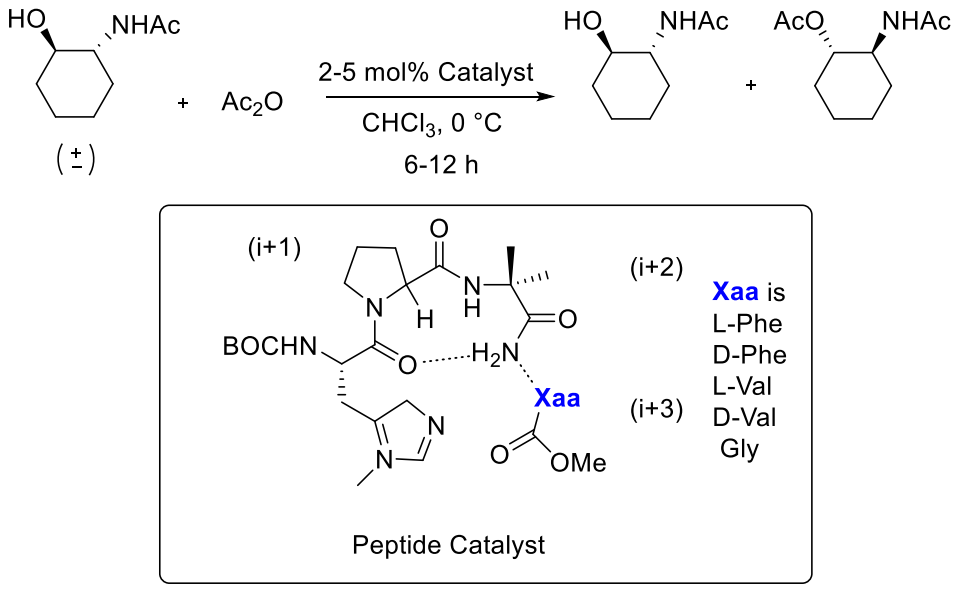

Scheme 34: KR of a Sec-Alcohol Catalyzed by Tetrapeptides.[3]

In 2000, Jarvo, Vasbinder and Miller developed short peptides containing imidazole functional groups, that can act as effective catalysts for the acylation asymmetric reaction (Scheme 35).[1] A series of peptides were synthesized using SPPS, and employed as catalysts: catalyst **2**, without any secondary structure; peptide **3** which adopts a β-turn; and peptide **4** with a β-hairpin conformation.[1] It is noteworthy that peptide **4** was developed after replacing the IA unit of peptide **3** for π-methylhistidine (Pmh), as well as exchanging the L-Pro unit for D-Pro.[1] Moreover, peptide **5** was comprised of eight units, while **6** was identical to **5** apart from swapping the D-Pro in the (i+3) position with an L-Pro.[1] After employing these catalysts in the KR of racemic substrates, **2** proved to be ineffective as a catalyst, while **4** showed better enantioselectivity than **3**.[1] **5** showed the highest enantioselectivity among them, which got decreased dramatically when peptide **6** was used.[1] As

indicated in the previous example, a change on one stereogenic centre, from D-Pro to L-Pro, led to a significant change in the enantioselectivity.[1]

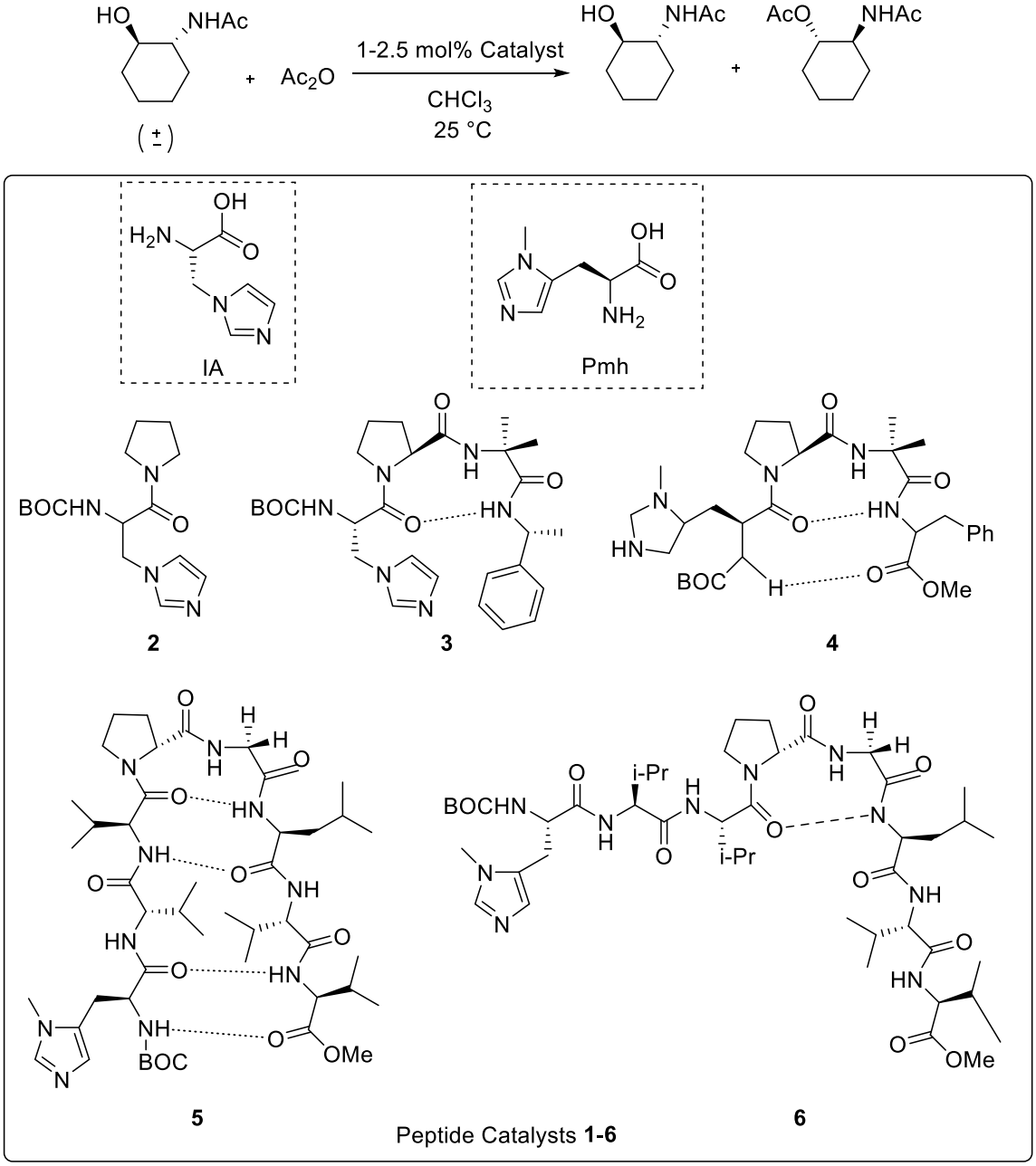

Scheme 35: KR of a Sec-Alcohol Catalyzed by Octapeptides.[1]

Another example of catalysts worth mentioning are catalysts that are derivatives of DMAP. DMAP (Figure 49) has been recognized as a classic acyl transfer catalyst.[4] It is a mild and inexpensive nucleophilic catalyst that is commercially available with low cost, at the same time that it has many applications.[5] After its discovery as a catalyst for the acyl transfer reactions, many DMAP-derivatives that are able to catalyze the same kind of reaction have been developed.[5,6] Nevertheless, only a few peptide auxiliaries in conjunction with DMAP have been used in the KR of sec-alcohols [7–9] This might be due to the challenging process of designing an interaction between the peptide and DMAP that

will lead to an appropriate chiral environment around the acylation centre.[7] Despite that, employing such a catalyst would offer many benefits, mainly associated with the advantages of using DMAP.[7]

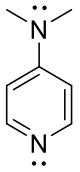

Figure 49: Structure of DMAP.[5]

In this context, Cozett, Rudy E. *et al*. designed a series of peptides containing 4-pyrrolidinopyridine (PPY) with C-3 carboxamides as side chains.[7] These were then tested as catalysts in the KR of sec-alcohols (an example of which is shown in Scheme 36).[7] It is noteworthy that a tryptophan was introduced in the peptide chain in order to promote π-stacking interactions between the peptide side chain and the pyridinium ring of the intermediate (Scheme 36).[7] Through this study, the potential of DMAP-based peptide catalysts is demonstrated.[7]

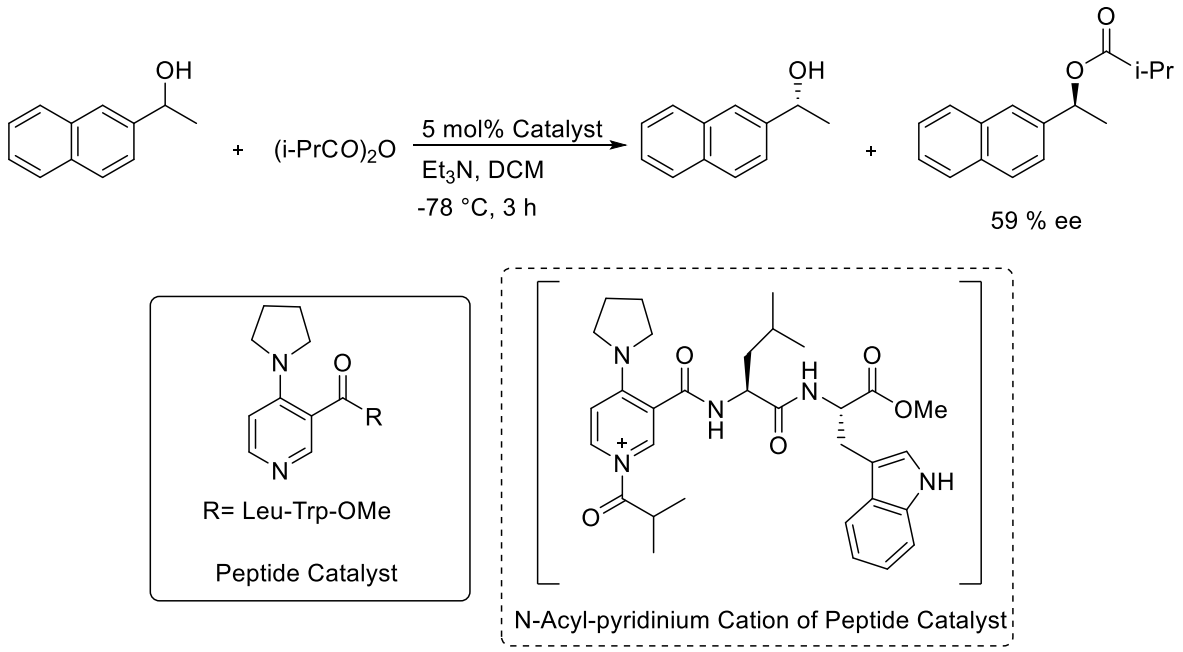

Scheme 36: KR of Sec-Alcohol Catalyzed by a 4-PYY Peptide.[7]

In conclusion, the asymmetric acyl transfer reaction has received a lot of attention recently.[10] Although enzymes lead to excellent efficiencies when employed in these reactions, they are also characterized by some limitations.[3] Peptides offer a valuable alternative as catalysts, while peptide-based catalysts have already been prepared and showed interesting properties in the KR of acyl transfer reactions.[10] Nevertheless, considering the limited applications of KR compared to the other types of resolution (like the classical and chromatographic resolution), some parameters could be further improved. For example, the use of inexpensive racemates, as well as the development of highly selective and available peptide asymmetric catalysts employed at low loading still remains challenging. Thus, there is a need for further studies on the preparation of peptide and their use as

catalysts. In this context, this chapter describes the synthesis and characterisation of polyproline peptides that are subsequentially tested as catalysts in the enantioselective acyl transfer reaction (section 1.2.2) (Table 10).

Table 10: Structures of Target Peptide Groups 5 and 6.

Target Peptide Group 5	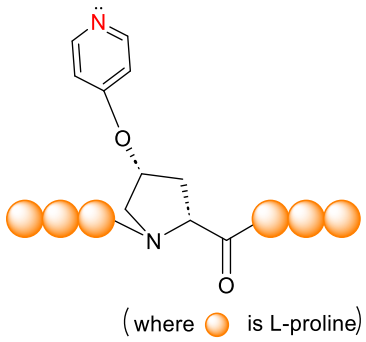
Target Peptide Group 6	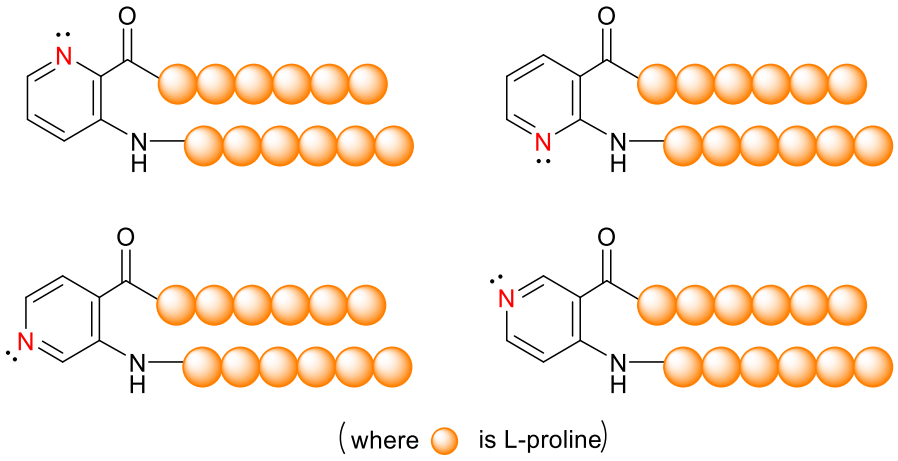

3.2 Results and Discussion

3.2.1 Target Peptide Group 5

As described in more detail in section 1.2.2, the second objective of this project focuses on the preparation of another polyproline peptide (Table 10-Target Peptide Group 5) to be tested as a catalyst for the acyl transfer reaction.

3.2.1.1 Synthesis of N-Fmoc-trans-4-hydroxypyridine-L-proline (F3)

In order to prepare the first target peptide, the first step was the synthesis of the corresponding functionalized proline monomer. The synthesis of the N-Fmoc-trans-4-hydroxypyridine-L-proline (**F3**) was achieved via a multi-step synthetic pathway (Scheme 37). Starting from the N-Boc-trans-4-hydroxy-L-proline methyl ester (**B1**), 4-hydroxy pyridine, PPh_3 and a catalytic amount of DIAD in THF were used,[11] with inversion of the stereochemistry at the C-4 position. The product (**F2**) was purified through column chromatography, and was obtained in 83 % yield. The next step involved hydrolysis of the ester by treatment with Lithium Hydroxide (LiOH) and a mixed solvent system of MeOH and THF.[12] After that, removal of the Boc protecting group and introduction of the Fmoc group were performed. The crude material was purified through column chromatography to yield the final product in 70 % yield (**F3**).

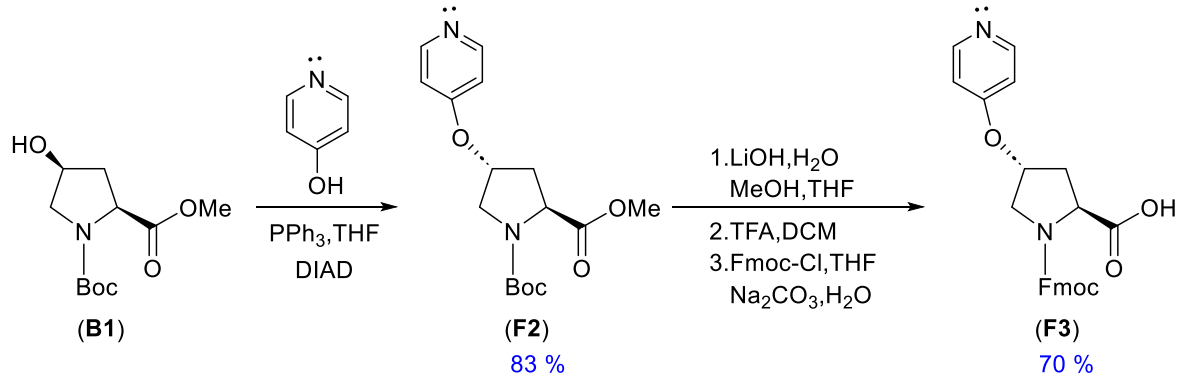

Scheme 37: Synthesis of N-Fmoc-trans-4-hydroxypyridine-L-proline (**F3**).

3.2.1.2 Synthesis of PP 4 Peptide

The first target peptide (**PP 4**), as shown in Table 10-Target Peptide Group 5, is comprised of six un-functionalized proline units and one functionalized proline residue (**F3**) in the middle of the helix. The rationale behind the design of this peptide has already been discussed in section 1.2.2.

In this part of the project, the target peptides are aimed to be used as catalysts in enantioselective acyl transfer reactions. Considering the examples discussed in section 3.1, in order for the peptides to be effective catalysts it is important to adopt a secondary structure. Since the heptamers **PP 1**-**PP**

3 were able to adopt a stable PolPro II conformation, it was decided for **PP 4** to be comprised of seven units in total.

For the synthesis of the **PP 4** peptide, the SPPS technique was used, the principles of which have been described in section 2.1.1.1. Since the procedure had already been optimised, the synthesis was performed on the peptide synthesizer applying the optimum conditions, using again rink amide MBHA resin on a 0.1 mmol scale.

The resin was swollen in DCM and was then placed on the apparatus, with the rest of the reagents. Single deprotection of the Fmoc group, followed by couplings interspaced with washings was performed. The coupling reagents used were three equivalents of the Fmoc-amino acid, three equivalents of Oxima Pure, six equivalents of DIC and 0.5 equivalents of DIPEA.

Once the desired peptide chain was created, the resin was removed from the apparatus, and the capping procedure was performed manually, using a solution of 10 % Ac_2O and 2.5 % DIPEA in DMF (4 mL). Following that, cleavage was performed, using 95 % TFA in DCM (4 mL). After 90 min of smooth agitation, the resin was washed with the same solution twice. The obtained solution was collected and evaporated, and the peptide precipitated with cold Et_2O. Similarly to **PP 1**-**PP 3**, the cleavage procedure had to be repeated twice in order for the product to precipitate upon addition of cold Et_2O. After centrifugation, the solution was decanted and the solid was washed with cold Et_2O three time. This procedure was repeated three times in order to isolate the peptide.

After that, a ^{19}F-NMR was performed and the peptide was exposed to an ion exchange resin.[13] Although there is no fluorine in the peptide, ^{19}F-NMR was performed in order to confirm that all the impurities had been removed. More specifically, a peptide vessel was equipped with a Purolite A400 resin in between of glass wool, rinsed successively with deionised H_2O (5 x 50 mL), 4 % NaOH in deionised H_2O (300 mL), deionised H_2O (5 x 50 mL) and MeOH (5 x 50 mL) and dried. The peptide was dissolved in MeOH (5 mL), added to the dried vessel equipped with the ion exchange resin and smoothly agitated for 2 days. Following that, the obtained liquid was collected, washed with MeOH (x 3) and dried. A ^{19}F-NMR was undertaken again, and compared with the one before the ion resin treatment. The desired peptide was obtained with a yield of 67 %.

3.2.1.2.1 Analysis of PP 4 Peptide

Following its synthesis, **PP 4** was analysed via LCMS. According to the results, the peptide was successfully synthesized, with one major peak observed at 3.22 min (Figure 50). For this reason, **PP 4** was used in the next step without further purification.

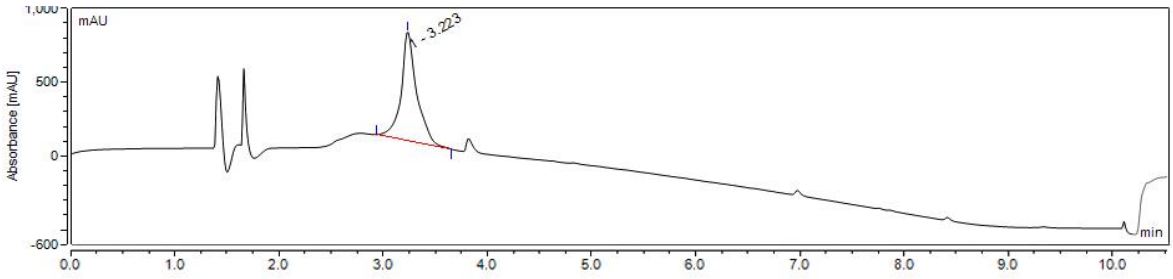

Figure 50: LCMS Chromatogram of **PP 4**.

3.2.1.2.2 CD Analysis of PP 4 Peptide

After its successful synthesis and the LCMS analysis, **PP 4** was analysed through CD spectroscopy. More specifically, water was used as a solvent, while the sample was left to equilibrate for seven days at 20 °C before the measurement was taken. The obtained spectrum presented a strong negative band at 205 nm and a weak positive band at 225 nm (Figure 51). Based on these data, once it is placed in water, **PP 4** adopts a PolPro II conformation.

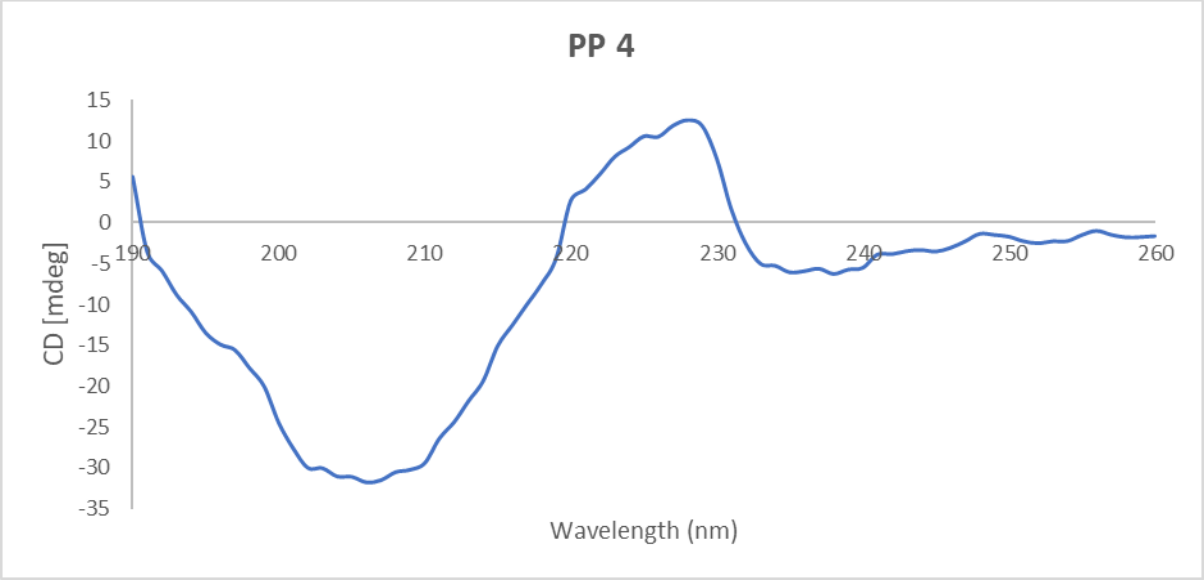

Figure 51: CD Spectrum of **PP 4** in Aqueous Solution at 20 °C and ≈ 100 μM.

3.2.1.3 Application of PP 4 in the Kinetic Resolution of a Racemic Alcohol

The next step involved investigating the catalytic properties of **PP 4** in the KR of a sec-alcohol. The synthesized peptide was employed for the reaction between 1-phenyl alcohol and Ac_2O in the presence of Et_3N, while $CDCl_3$ was the solvent of choice (Scheme 38). These conditions have been employed efficiently for a range of aryl alkyl sec-alcohols with DMAP as a catalyst.[5]

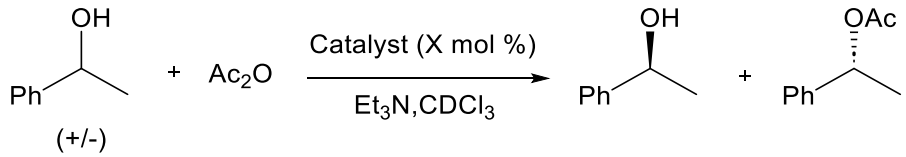

Scheme 38: KR of Racemic Alcohol 1-phenylethanol Using **PP 4** as an Organocatalyst.

Apart from the desired peptide, DMAP was also used as a catalyst in order to act as a refence, while the reaction was also run using no catalyst. Moreover, the catalytic activity of monomers **F2** and **F3** were examined and compared with the one of **PP 4** (Figure 52).

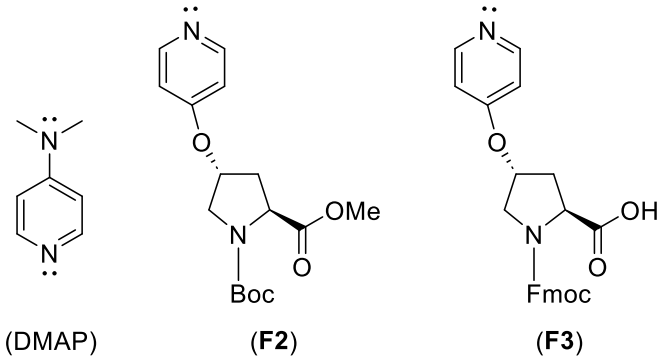

Figure 52: Structures of DMAP (left), Monomer **F2** (middle) and Monomer **F3** (right).

All the reactions performed where monitored by ^{1}H-NMR. The products obtained from the optimum conditions for each case were then analysed through Gas Chromatography - Mass Spectrometry (GC-MS) with a chiral stationary phase. Based on that, the enantiomeric excess (ee) values for the alcohol and the acetate product of each reaction were determined. Figure 53 shows a reference sample of 1-phenyl alcohol and the produced acetate, after a GC-MS analysis. According to the analysis, the elution order is as follows: S-acetate (10.854 min), R-alcohol (11.015 min), R-acetate (11.151 min), S-alcohol (11.287 min).

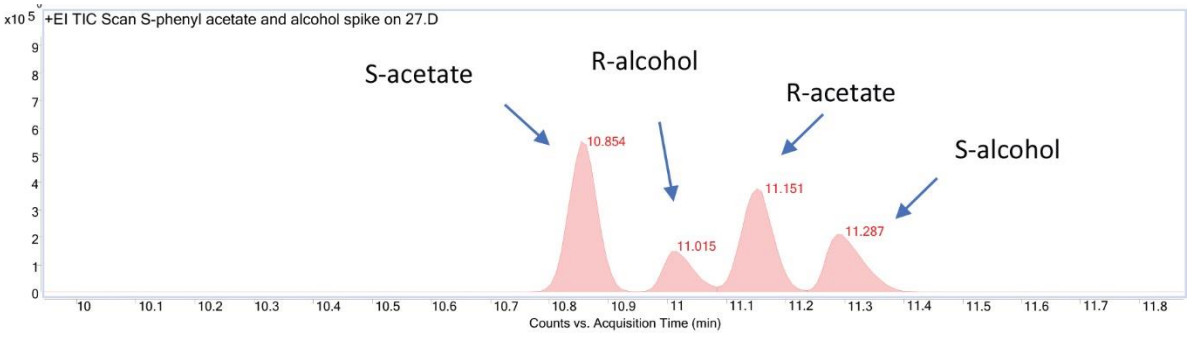

Figure 53: Chiral GC-MS Analysis of Reference Sample of 1-phenyl alcohol and the Produced Acetate.

The experiments were initiated using DMAP (2 %) as a catalyst, 0.75 equivalents of Ac_2O and 1.6 equivalents of Et_3N in $CDCl_3$ (800 µL) at room temperature as a starting point (Table 11, entries 1 and 2 respectively). While monitoring this reaction, it was observed that the conditions needed to be

altered in order to have full conversion, which was achieved once quantity of Ac_2O was added (additional 0.75 equivalents). The reaction was performed from the beginning using the increased amount of Ac_2O (1.5 equivalents) and a 5 % loading of DMAP, and was complete within 24 hours according to ^{1}H-NMR (Table 11, Entry 4).

Table 11: KR of Racemic 1-phenyl alcohol Using DMAP at RT.

Entry	Catalyst (mol %)	Ac_2O (eq)	Et_3N (eq)	Time[b]	Yield[c] (%)	$ee_{alcohol}$ %[d]	$ee_{acetate}$ %[d]
1	2 %	0.75	1.6	19 h	81	-	-
2	2 %	0.75	1.6	36 h	81	-	-
3	2 %	0.75	1.6	60 h	100	-	-
4	5 %	1.5	1.6	24 h	100	-	-

[a] Reaction conditions: rac-alcohol (0.16 mmol), Ac_2O (0.75 or 1.5 eq), Et_3N (0.75 or 1.6 mmol) in 800 µL of $CDCl_3$ at RT. [b] Where h indicates hours and d indicates days. [c] Determined by ^{1}H-NMR analysis of the crude products. [d] Determined by chiral GC-MS analysis.

Figure 54 shows a typical ^{1}H-NMR spectrum of an acyl transfer reaction between 1-phenyl alcohol and Ac_2O, under the influence of DMAP. From the ratio of the integrals, it can be observed that the peaks corresponding to the produced acetate appear around 4.80 ppm, while the ones for the alcohol appear around 5.81 ppm.

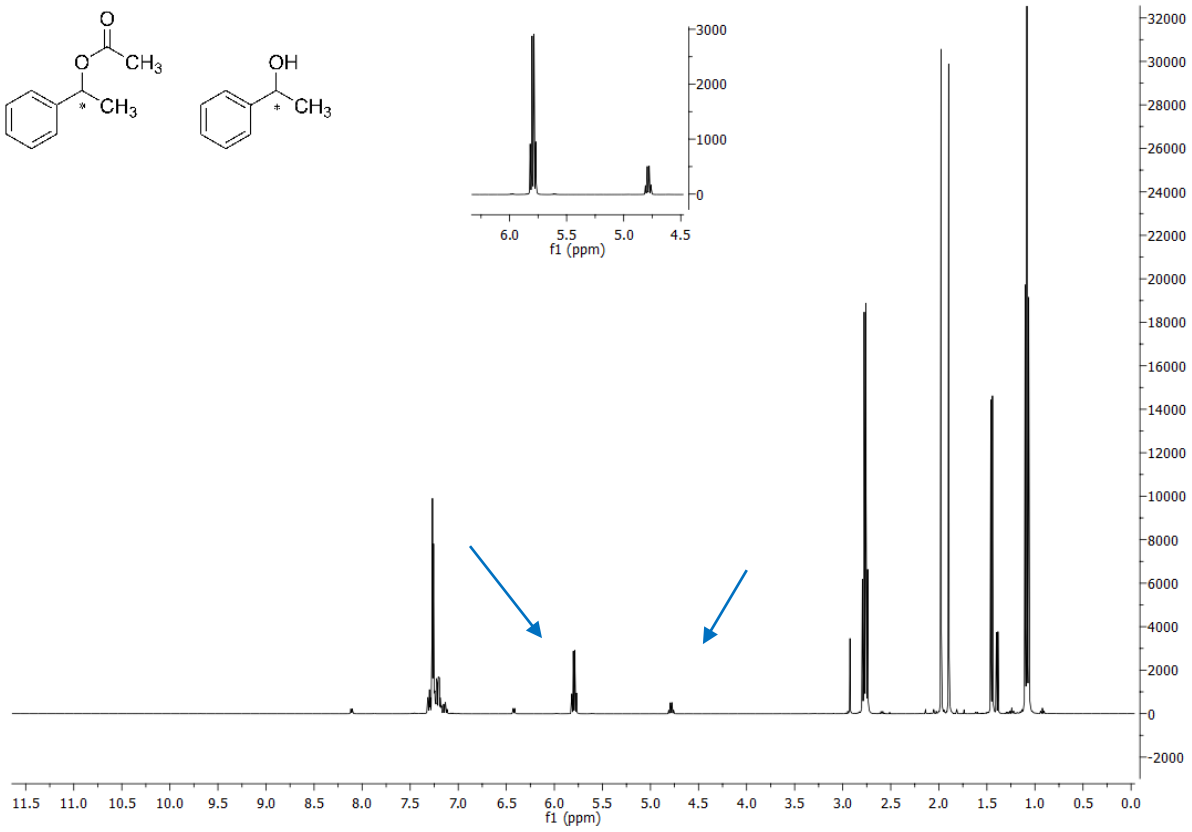

Figure 54: ^{1}H-NMR Spectrum of 1-phenyl alcohol with Ac_2O Using DMAP as a Catalyst.

A blank experiment was also run under the same conditions, with the yield reaching 47 % in 4 days (Table 12, Entry 9).

Table 12: KR of Racemic 1-phenyl alcohol Using No Catalyst at RT.

Entry	Catalyst (mol %)	Ac_2O (eq)	Et_3N (eq)	Time[b]	Yield[c] (%)	$ee_{alcohol}$ %[d]	$ee_{acetate}$ %[d]
5	-	1.5	1.6	20 h	27	-	-
6	-	1.5	1.6	24h	30	-	-
7	-	1.5	1.6	48 h	31	-	-
8	-	1.5	1.6	3 d	44	-	-
9	-	1.5	1.6	4 d	47	-	-

[a] Reaction conditions: rac-alcohol (0.16 mmol), Ac_2O (0.75 or 1.5 eq), Et_3N (0.75 or 1.6 mmol) in 800 µL of $CDCl_3$ at RT. [b] Where h indicates hours and d indicates days. [c] Determined by ^{1}H-NMR analysis of the crude products. [d] Determined by chiral GC-MS analysis.

After that, **PP 4** was employed in 5 % loading, using 1.5 equivalents of Ac_2O and 1.6 equivalents of Et_3N, leading to a 50 % conversion in 25 hours (Table 13, Entry 14). An aliquot of the reaction mixture was then analyzed through chiral GC-MS analysis.

Table 13: KR of Racemic 1-phenyl alcohol Using **PP 4** at RT.

Entry	Catalyst (mol %)	Ac_2O (eq)	Et_3N (eq)	Time[b]	Yield[c] (%)	$ee_{alcohol}$ %[d]	$ee_{acetate}$ %[d]
10	5 %	1.5	1.6	16.30 h	42	-	-
11	5 %	1.5	1.6	17.30 h	44	-	-
12	5 %	1.5	1.6	19.30 h	46	-	-
13	5 %	1.5	1.6	20 h	48	-	-
14	5 %	1.5	1.6	25 h	50	4	0
15	5 %	1.5	0.75	39 h	44	-	-
16	5 %	1.5	0.75	48 h	50	7	2

[a] Reaction conditions: rac-alcohol (0.16 mmol), Ac_2O (0.75 or 1.5 eq), Et_3N (0.75 or 1.6 mmol) in 800 µL of $CDCl_3$ at RT. [b] Where h indicates hours and d indicates days. [c] Determined by ^{1}H-NMR analysis of the crude products. [d] Determined by chiral GC-MS analysis.

The obtained ee values after the GC-MS analysis were 4 % for the alcohol and 0 % for the acetate (Figure 55). Thus, the reaction was also run using a decreased amount of Et_3N (0.75 equivalents) in order to investigate whether that could have an effect on the reaction outcome. Once this reaction was performed, the yield was 50 % in 48 hours. This time, the ee was 7 % and 2 % for the alcohol and the acetate respectively according to the GC-MS analysis (Figure 56).

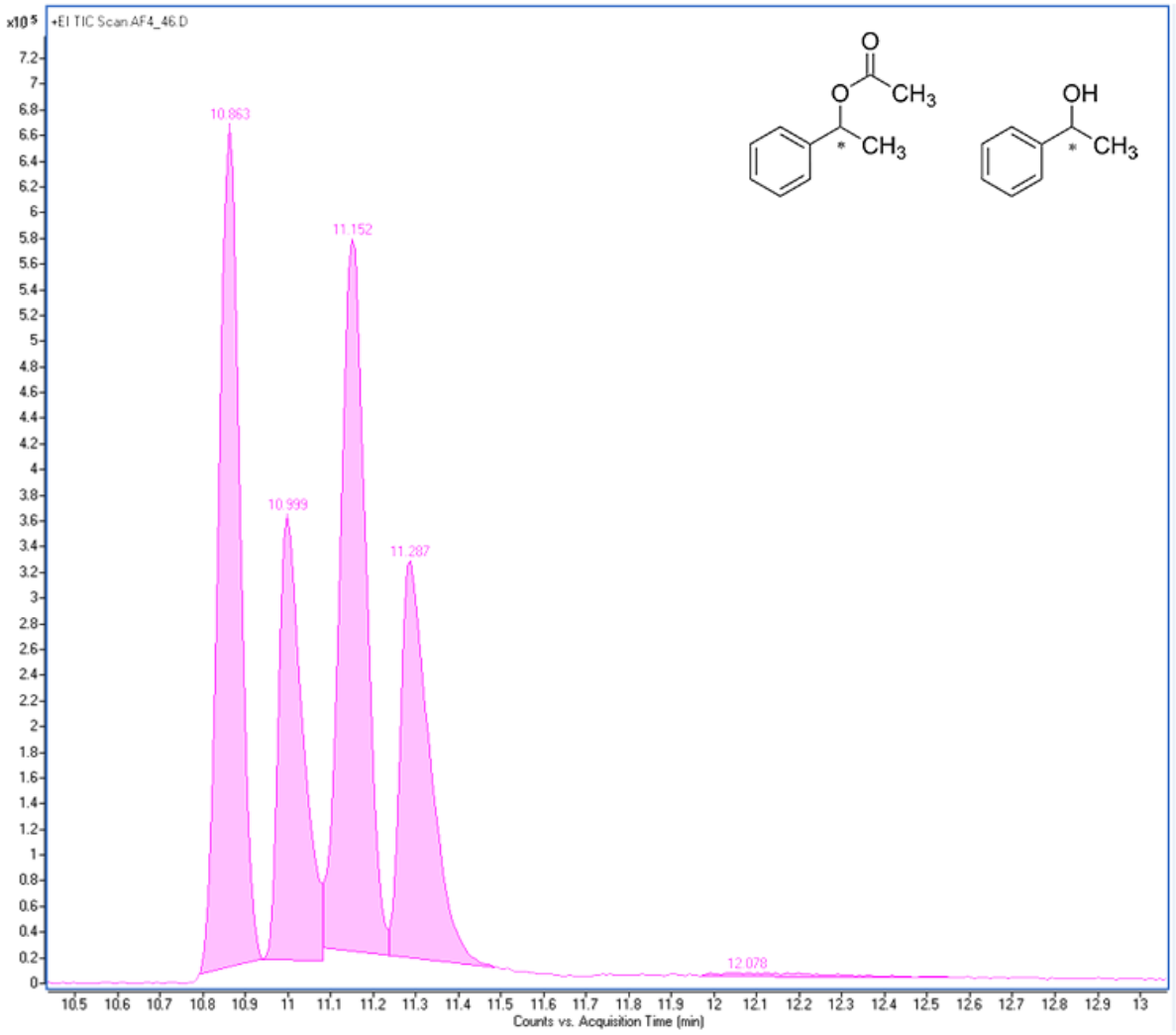

Figure 55: GC-MS Analysis of Reaction of 1-phenyl alcohol with Ac_2O Using **PP 4** at RT (Table 13, Entry 14).

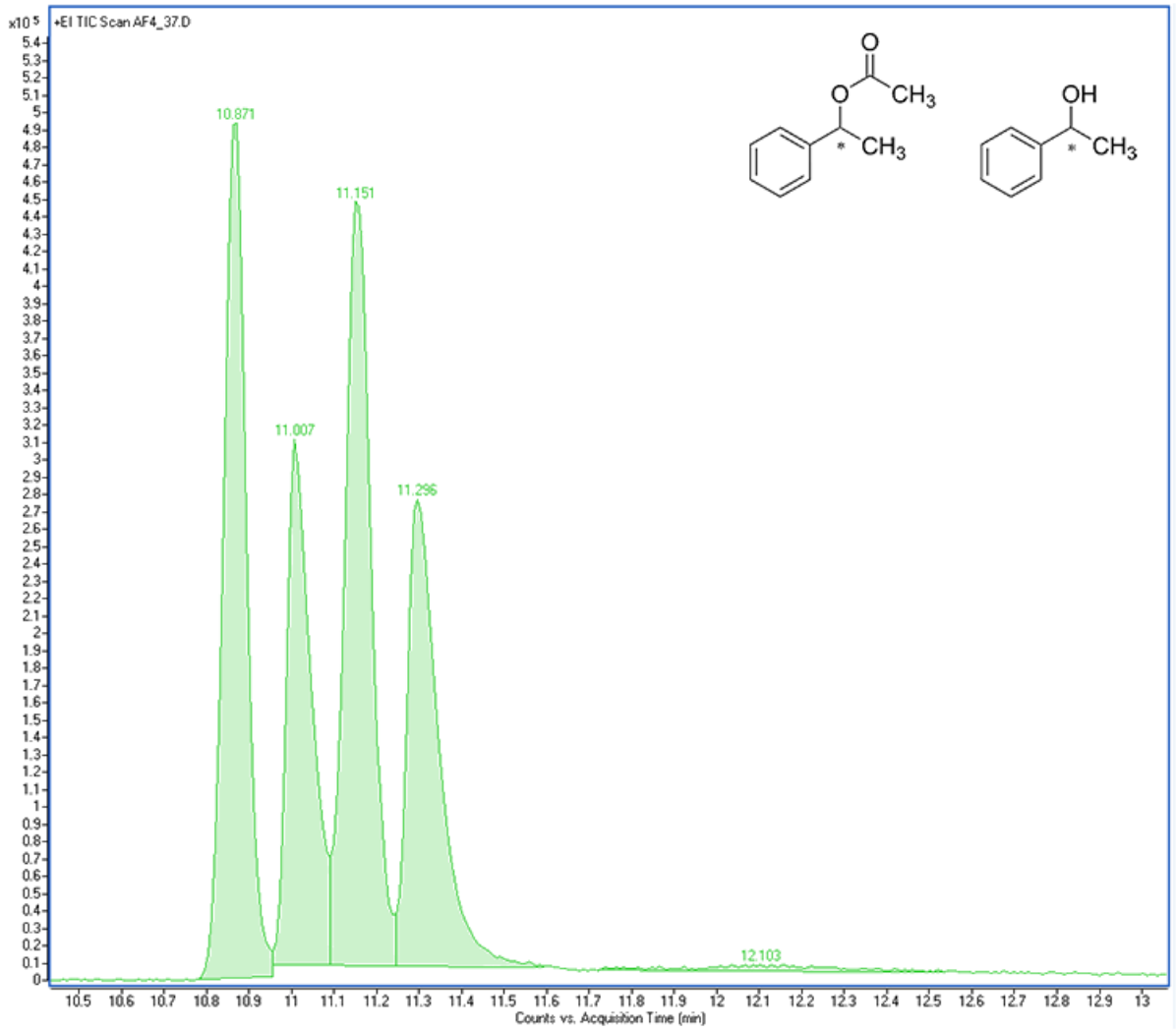

Figure 56: GC-MS Analysis of Reaction of 1-phenyl alcohol with Ac_2O Using **PP 4** at RT (Table 13, Entry 16).

In order to improve this, 5 % of catalyst and 1.5 equivalents of Ac_2O were employed, but the reaction was performed at 0 °C instead of room temperature (Table 14). More specifically, when 1.6 equivalents of Et_3N were added, 43 % of conversion was achieved in 40 hours at 0 °C (Table 14, Entry 19), while upon addition of 0.75 equivalents of Et_3N, 4 days were necessary for the conversion to reach 51 % (Table 14, Entry 20). The products from both the reactions were analysed through chiral GC-MS, and the ee value was 2 % both for the alcohol and the acetate at both equivalents of Et_3N (Figures 57 and 58).

Table 14: KR of Racemic 1-phenyl alcohol Using **PP 4** at 0 ℃.

Entry	Catalyst (mol %)	Ac_2O (eq)	Et_3N (eq)	Time[b]	Yield[c] (%)	$ee_{alcohol}$ %[d]	$ee_{acetate}$ %[d]
17	5 %	1.5	1.6	20 h	19	-	-
18	5 %	1.5	1.6	24 h	23	-	-
19	5 %	1.5	1.6	40 h	43	0	0
20	5 %	1.5	0.75	4 d	51	1	1

[a] Reaction conditions: rac-alcohol (0.16 mmol), Ac_2O (0.75 or 1.5 eq), Et_3N (0.75 or 1.6 mmol) in 800 µL of $CDCl_3$ at RT. [b] Where h indicates hours and d indicates days. [c] Determined by ^{1}H-NMR analysis of the crude products. [d] Determined by chiral GC-MS analysis.

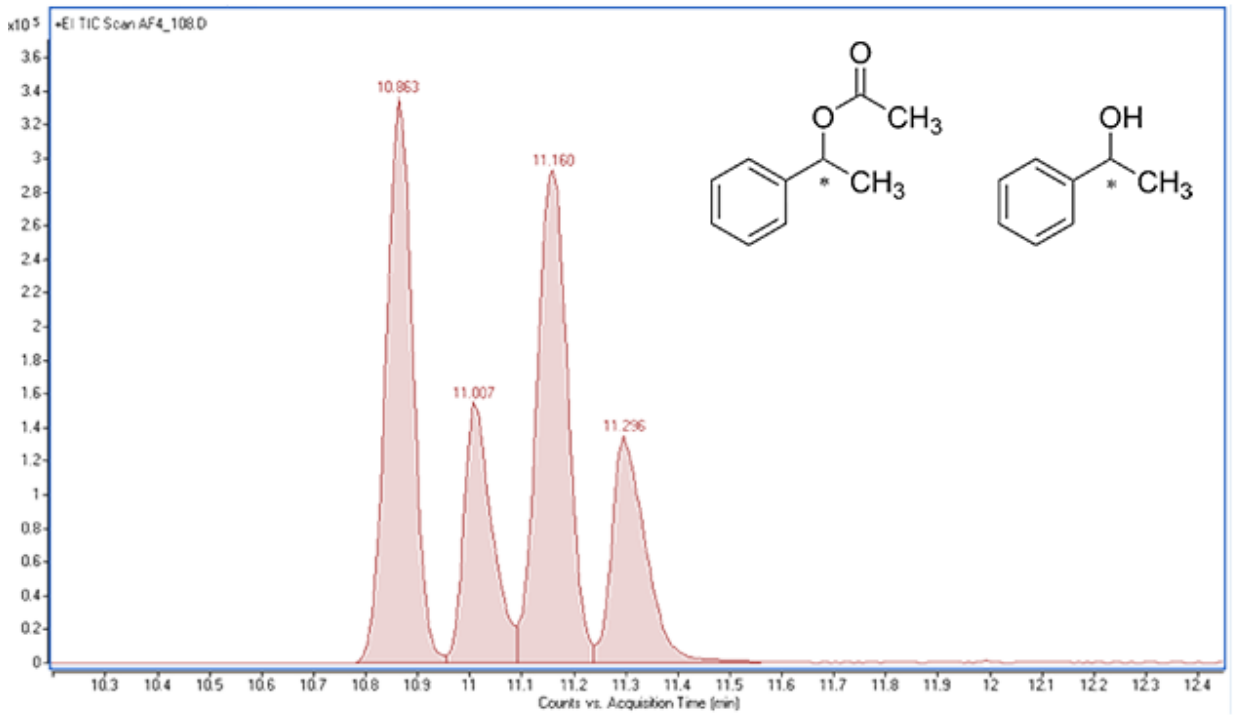

Figure 57: GC-MS Analysis of Reaction of 1-phenyl alcohol with Ac_2O Using **PP 4** at 0 °C (Table 14, Entry 19).

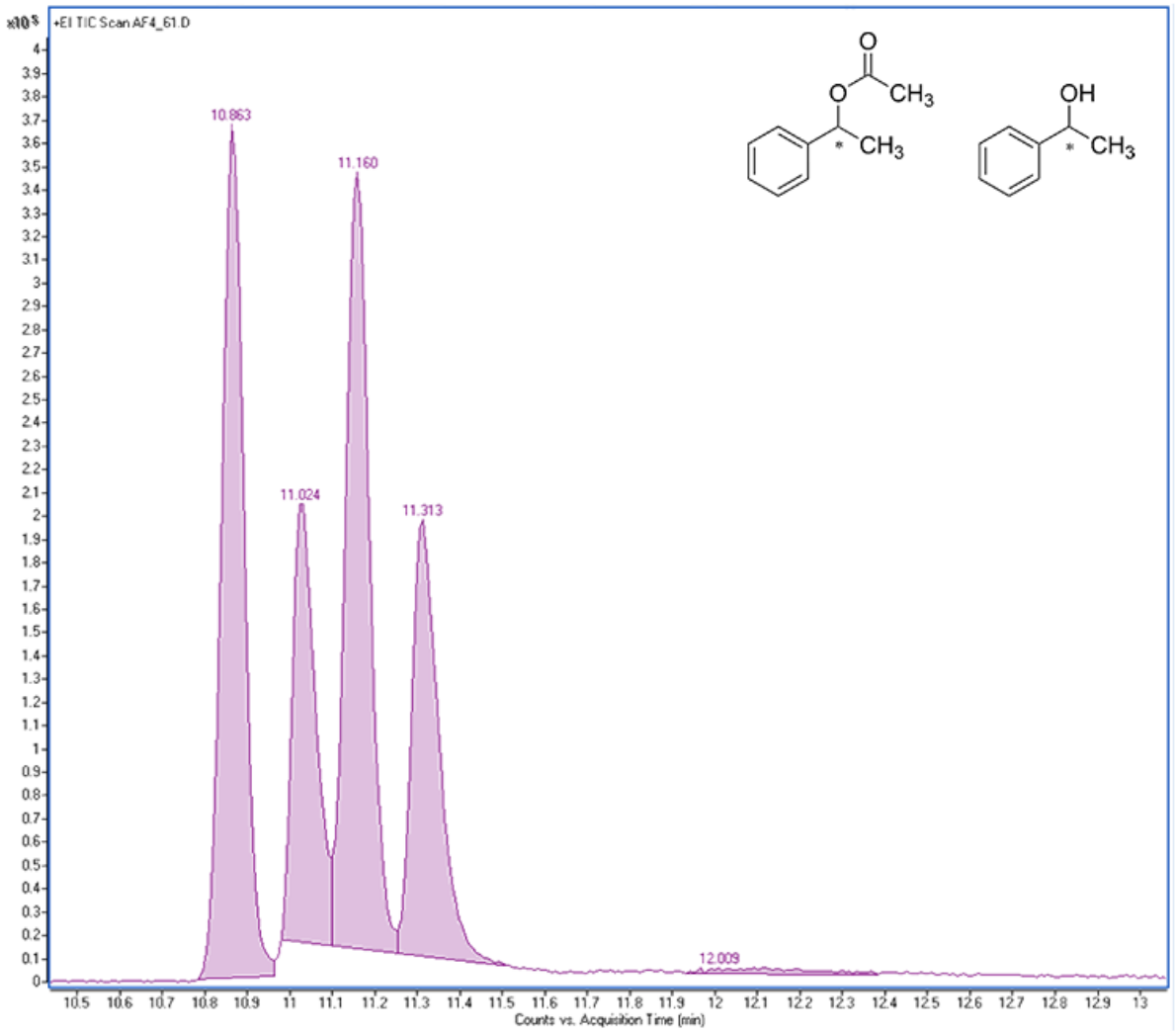

Figure 58: GC-MS Analysis of Reaction of 1-phenyl alcohol with Ac_2O Using **PP 4** at 0 °C (Table 14, Entry 20).

Concerning the intermediate **F2**, the reaction was initially performed using 1.6 equivalents of Et_3N at room temperature, reaching 50 % conversion in 28 hours (Table 15, Entry 26). Once the crude product was run through the chiral GC-MS, the ee was 8 % for the alcohol and 2 % for the acetate (Figure 59). The same reaction was also performed using 0.75 equivalents of Et_3N, and after 4 days (51 % yield), the recorded ee values were 2 % both for the alcohol and the acetate (Table 15, Entry 29) (Figure 60).

Table 15: KR of Racemic 1-phenyl alcohol Using **F2** at RT.

Entry	Catalyst (mol %)	Ac_2O (eq)	Et_3N (eq)	Time[b]	Yield[c] (%)	$ee_{alcohol}$ %[d]	$ee_{acetate}$ %[d]
21	5 %	1.5	1.6	16.3 h	40	-	-
22	5 %	1.5	1.6	17.3 h	42	-	-
23	5 %	1.5	1.6	20 h	45	-	-
24	5 %	1.5	1.6	23 h	47	-	-
25	5 %	1.5	1.6	25 h	48	-	-
26	5 %	1.5	1.6	28 h	50	8	2
27	5 %	1.5	0.75	20 h	40	-	-
28	5 %	1.5	0.75	24 h	47	-	-
29	5 %	1.5	0.75	4 d	51	2	2

[a] Reaction conditions: rac-alcohol (0.16 mmol), Ac_2O (0.75 or 1.5 eq), Et_3N (0.75 or 1.6 mmol) in 800 µL of $CDCl_3$ at RT. [b] Where h indicates hours and d indicates days. [c] Determined by ^{1}H-NMR analysis of the crude products. [d] Determined by chiral GC-MS analysis.

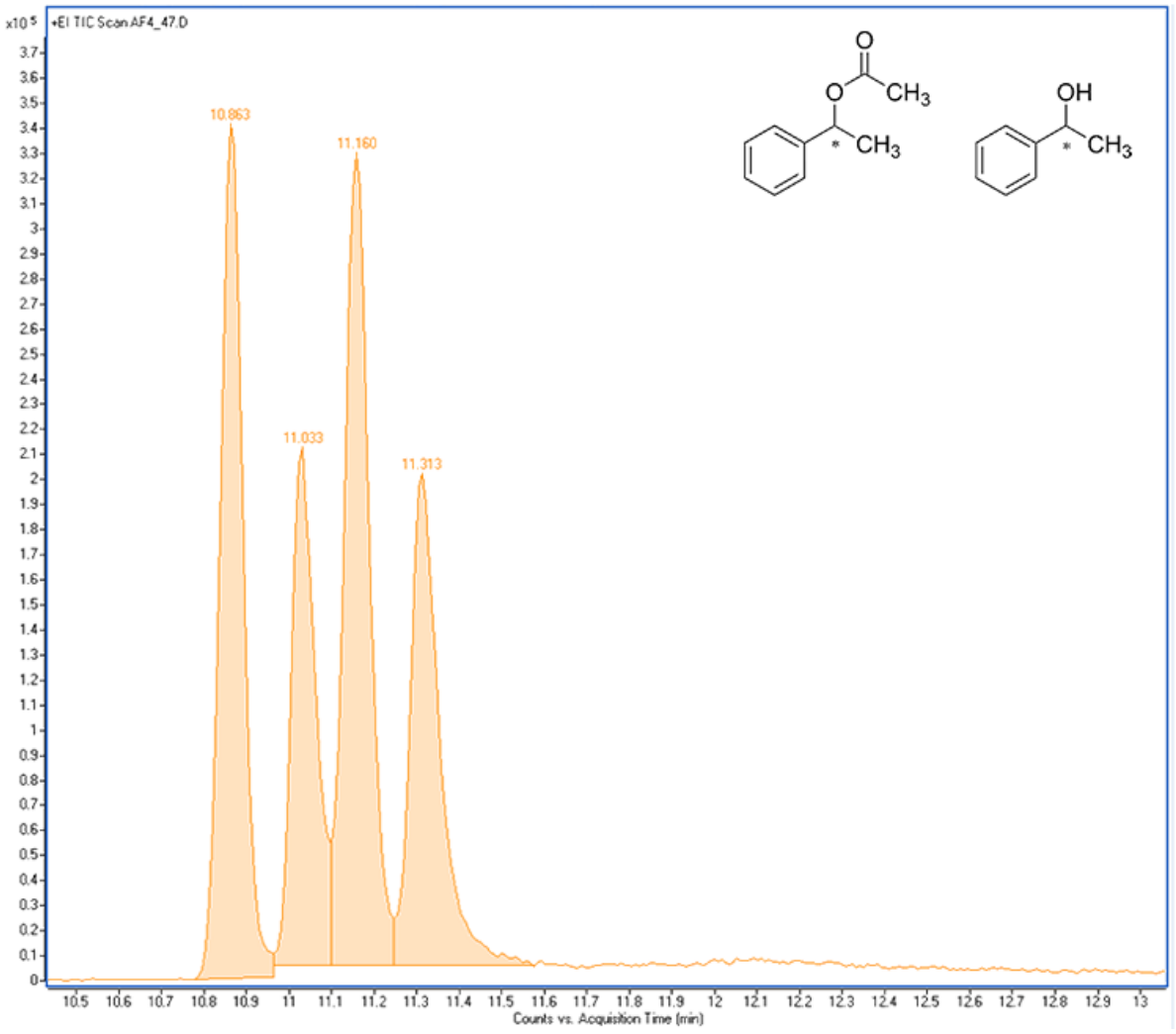

Figure 59: GC-MS Analysis of Reaction of 1-phenyl alcohol with Ac_2O Using **F2** at RT (Table 15, Entry 26).

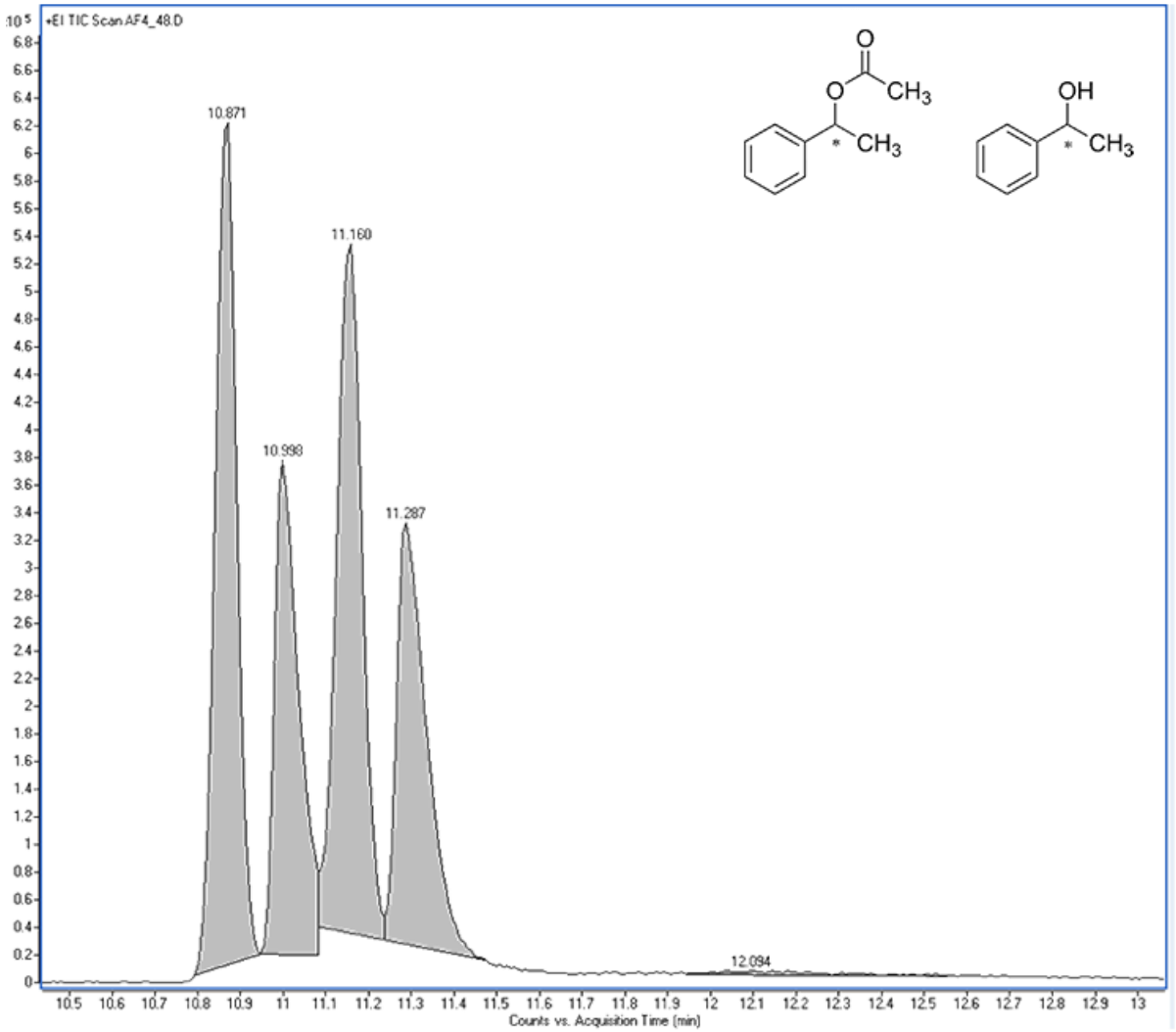

Figure 60: GC-MS Analysis of Reaction of 1-phenyl alcohol with Ac_2O Using **F2** at RT (Table 15, Entry 29).

Similarly to **PP 4**, monomer **F2** was tested as a catalyst at 0 °C using 0.75 and 1.6 equivalents of Et_3N respectively (Table 16, entries 30 and 31 respectively). The ee for both the alcohol and the acetate was 2 % in the former, and 2 % in the latter (Figures 61 and 62).

Table 16: KR of Racemic 1-phenyl alcohol Using **F2** at 0 ℃.

Entry	Catalyst (mol %)	Ac_2O (eq)	Et_3N (eq)	Time[b]	Yield[c] (%)	$ee_{alcohol}$ %[d]	$ee_{acetate}$ %[d]
30	5 %	1.5	1.6	40 h	32	2	2
31	5 %	1.5	0.75	4 d	48	2	2

[a] Reaction conditions: rac-alcohol (0.16 mmol), Ac_2O (0.75 or 1.5 eq), Et_3N (0.75 or 1.6 mmol) in 800 µL of $CDCl_3$ at RT. [b] Where h indicates hours and d indicates days. [c] Determined by ^{1}H-NMR analysis of the crude products. [d] Determined by chiral GC-MS analysis.

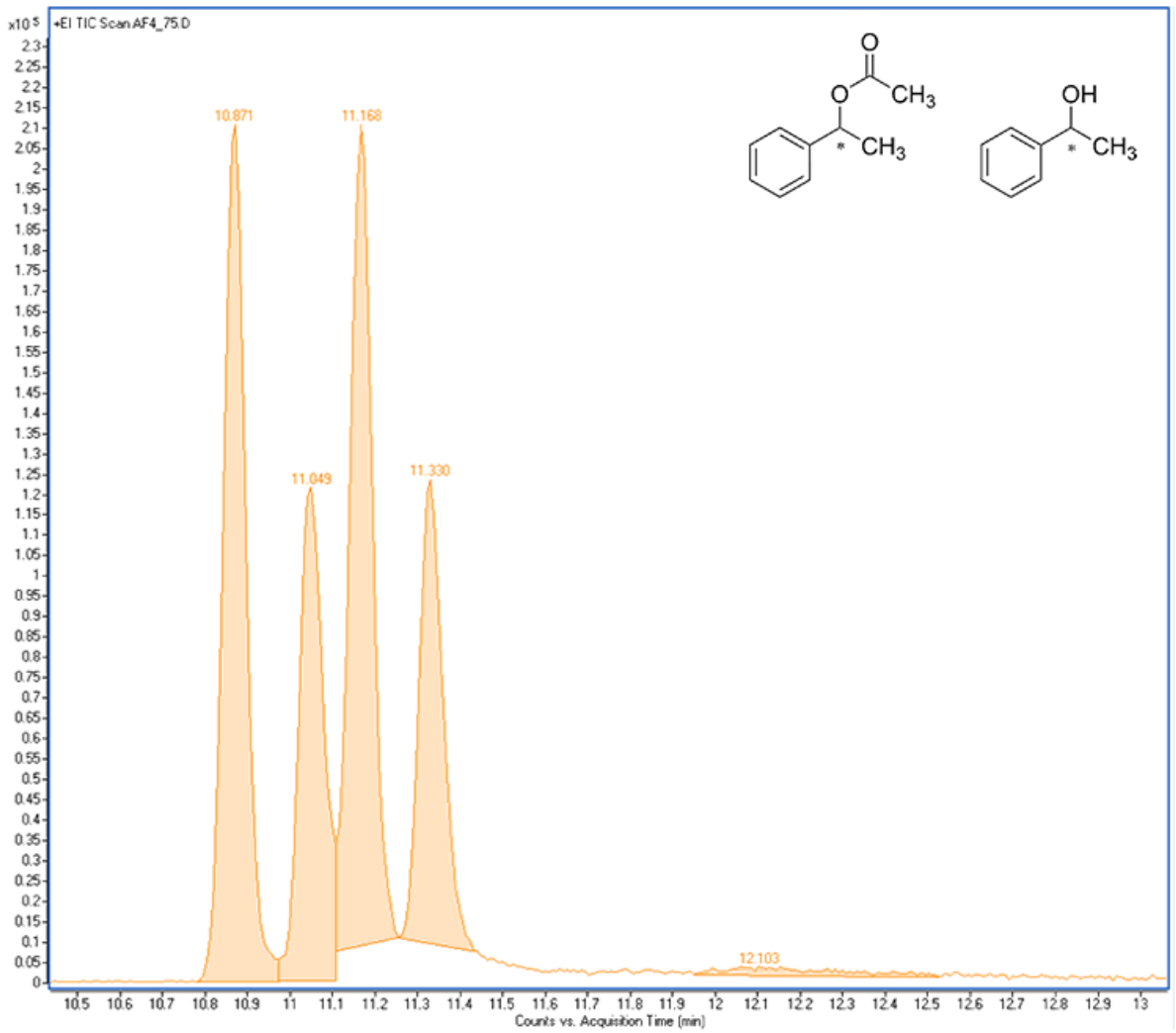

Figure 61: GC-MS Analysis of Reaction of 1-phenyl alcohol with Ac_2O Using **F2** at 0 °C (Table 16, Entry 30).

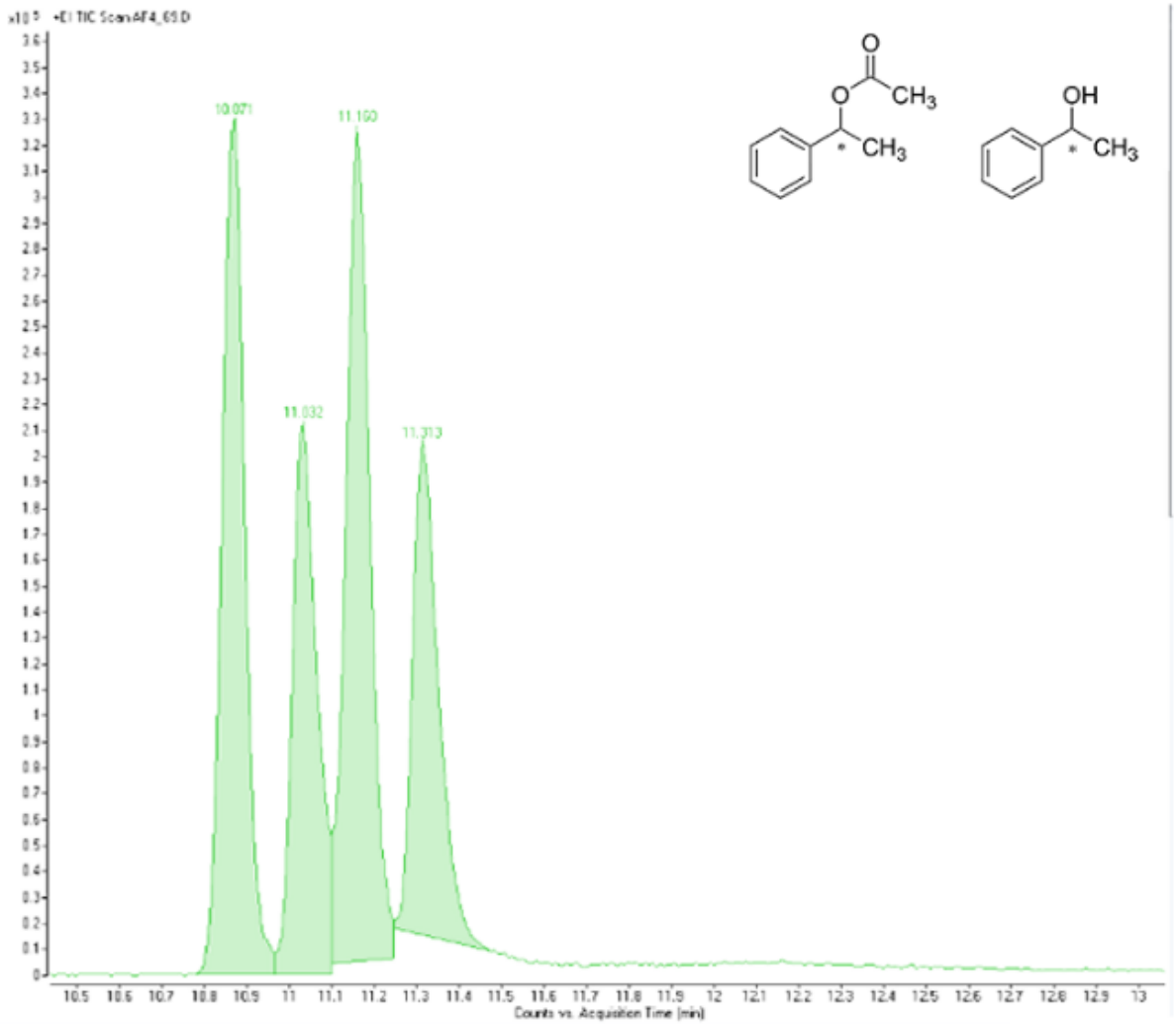

Figure 62: GC-MS Analysis of Reaction of 1-phenyl alcohol with Ac_2O Using **F2** at 0 °C (Table 16, Entry 31).

Lastly, **F3** was employed as a catalyst following the same conditions. Once 1.6 equivalents of Et_3N were used at room temperature, 50 % conversion was achieved at 24 hours (Table 17, Entry 35), whereas upon addition of 0.75 equivalents of Et_3N the same conversion was achieved in 72 hours (Table 17, Entry 38). After analysis through the chiral GC-MS, 2 % ee was recorded both for the alcohol and the acetate when double eq of Et_3N were used, while 6 % and 1 % ee were obtained for the alcohol and the acetate respectively when 0.75 equivalents of Et_3N were added (Figures 63 and 64).

Table 17: KR of Racemic 1-phenyl alcohol Using **F3** at RT.

Entry	Catalyst (mol %)	Ac_2O (eq)	Et_3N (eq)	Time[b]	Yield[c] (%)	$ee_{alcohol}$ %[d]	$ee_{acetate}$ %[d]
32	5 %	1.5	1.6	1.30 h	19	-	-
33	5 %	1.5	1.6	3.5 h	21	-	-
34	5 %	1.5	1.6	19 h	46	-	-
35	5 %	1.5	1.6	24 h	50	2	2
36	5 %	1.5	0.75	20 h	26	-	-
37	5 %	1.5	0.75	24 h	29	-	-
38	5 %	1.5	0.75	72 h	50	6	1

[a] Reaction conditions: rac-alcohol (0.16 mmol), Ac_2O (0.75 or 1.5 eq), Et_3N (0.75 or 1.6 mmol) in 800 µL of $CDCl_3$ at RT [b] Where h indicates hours and d indicates days. [c] Determined by ^{1}H-NMR analysis of the crude products. [d] Determined by chiral GC-MS analysis.

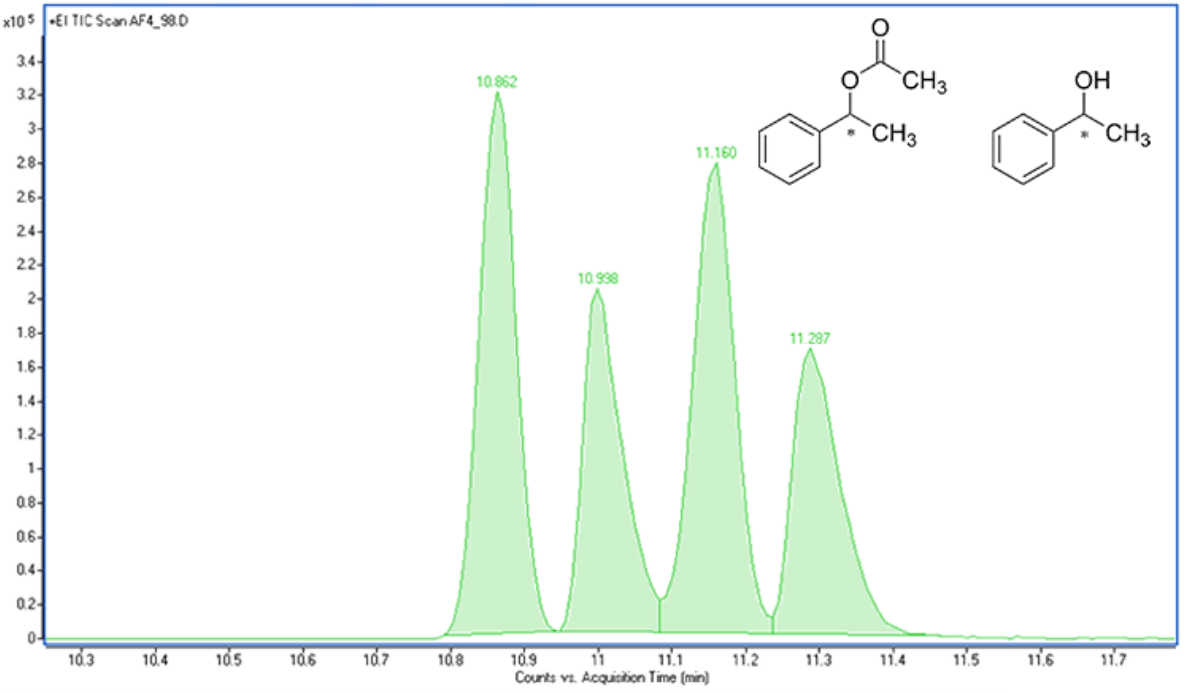

Figure 63: GC-MS Analysis of Reaction of 1-phenyl alcohol with Ac_2O Using **F3** at RT (Table 17, Entry 35).

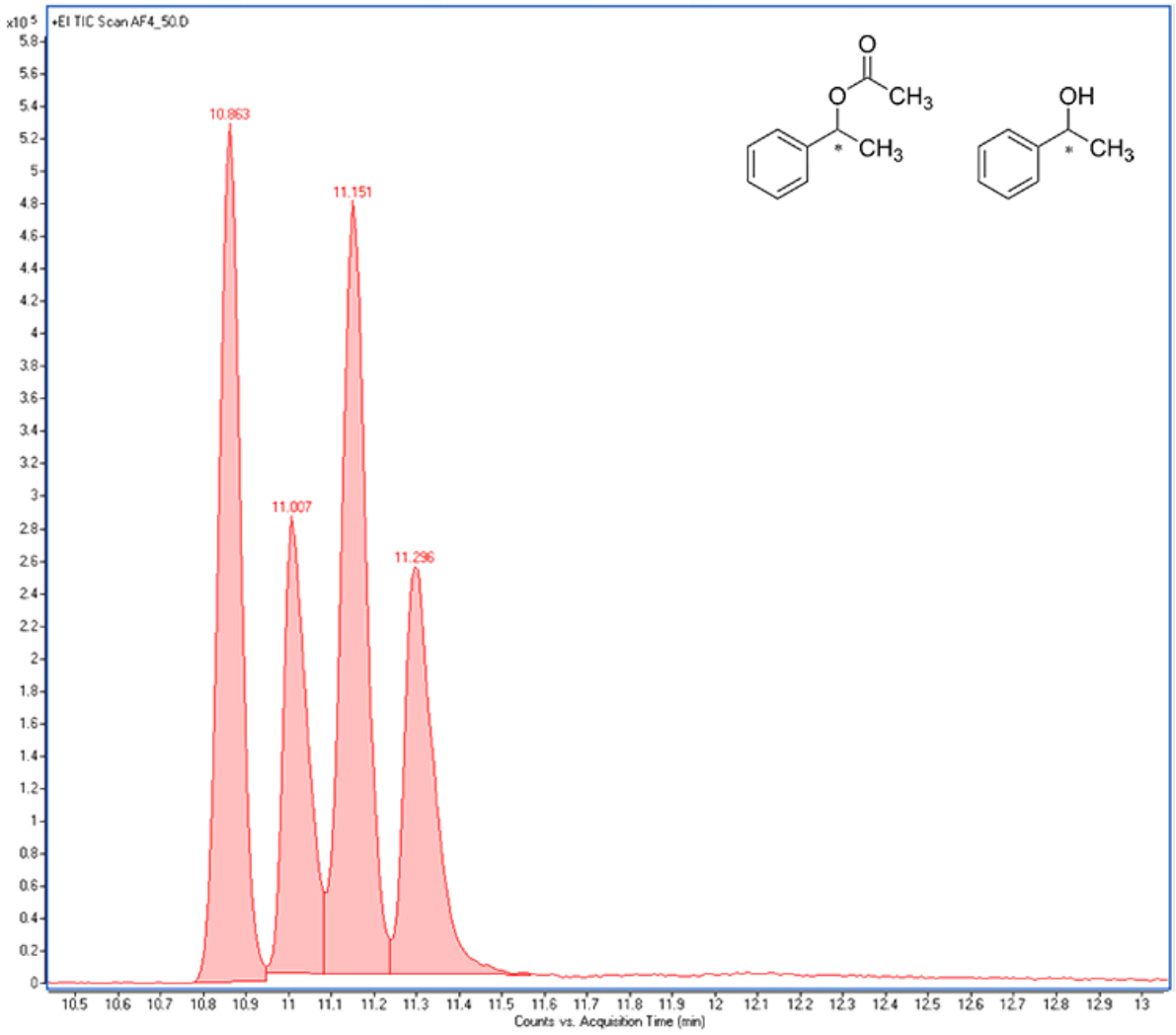

Figure 64: GC-MS Analysis of Reaction of 1-phenyl alcohol with Ac_2O Using **F3** at RT (Table 17, Entry 38).

When the reaction was performed using 1.6 and 0.75 equivalents of Et_3N in 0 °C, 50 % conversion was achieved in 40 hours and 4 days respectively (Table 18, entries 39 and 40 respectively), while the observed values for the ee were 1 % (Figures 65 and 66).

Table 18: KR of Racemic 1-phenyl alcohol Using **F3** at 0 °C.

Entry	Catalyst (mol %)	Ac_2O (eq)	Et_3N (eq)	Time[b]	Yield[c] (%)	$ee_{alcohol}$ %[d]	$ee_{acetate}$ %[d]
39	5 %	1.5	1.6	40 h	49	1	1
40	5 %	1.5	0.75	4 d	48	1	1

[a] Reaction conditions: rac-alcohol (0.16 mmol), Ac_2O (0.75 or 1.5 eq), Et_3N (0.75 or 1.6 mmol) in 800 µL of $CDCl_3$ at RT. [b] Where h indicates hours and d indicates days. [c] Determined by ^{1}H-NMR analysis of the crude products. [d] Determined by chiral GC-MS analysis.

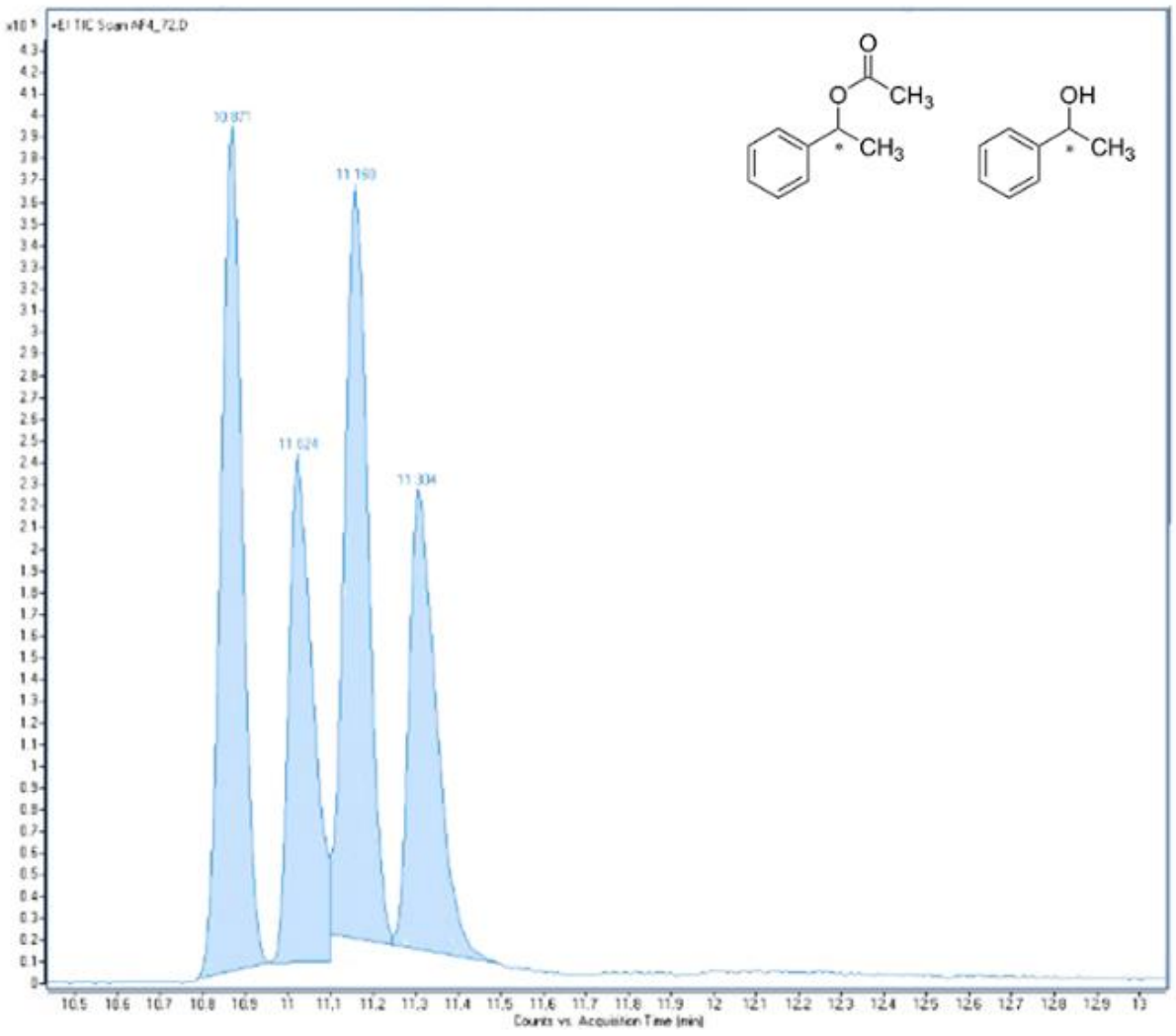

Figure 65: GC-MS Analysis of Reaction of 1-phenyl alcohol with Ac_2O Using **F3** at 0 °C (Table 18, Entry 39).

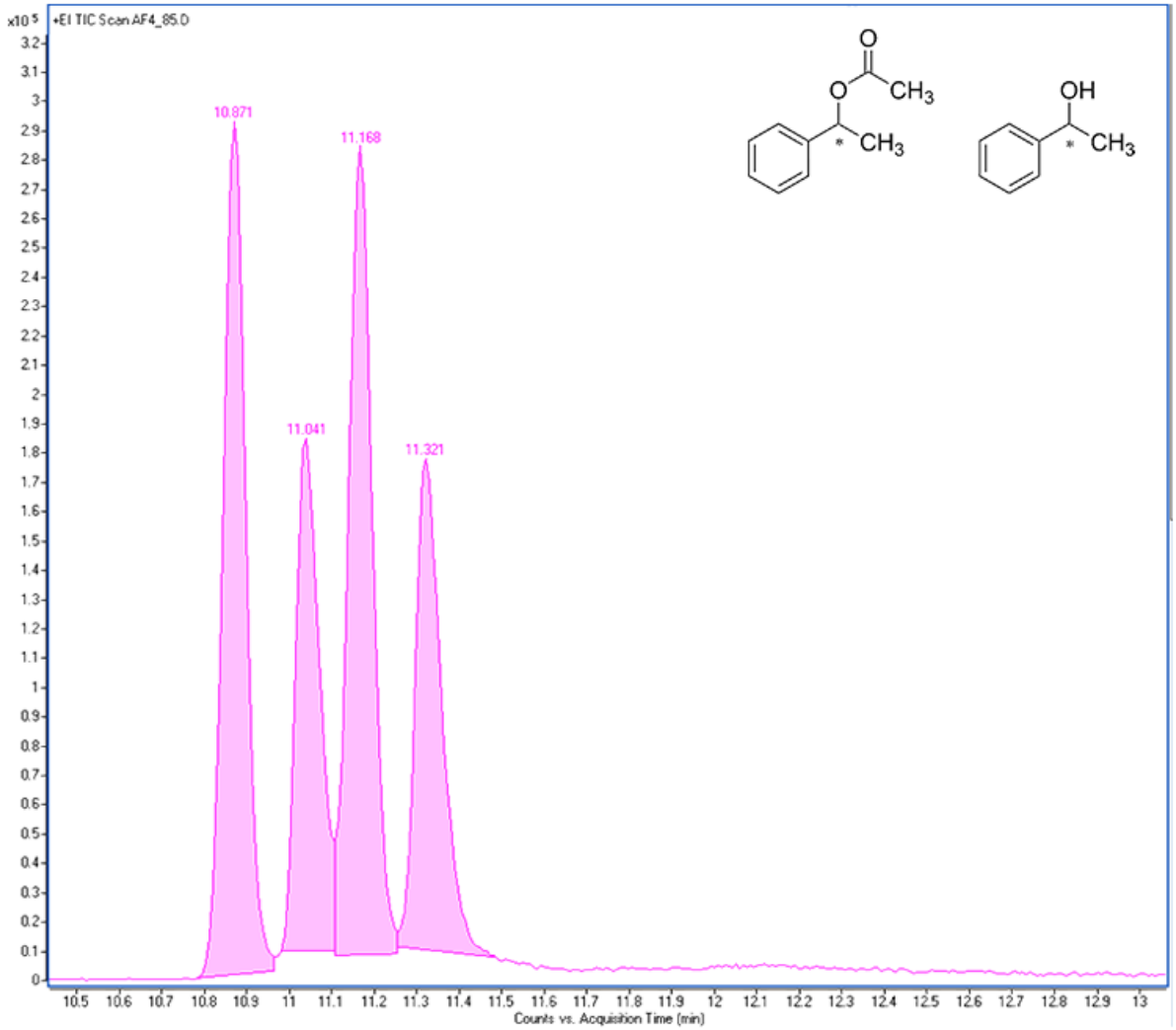

Figure 66: GC-MS Analysis of Reaction of 1-phenyl alcohol with Ac_2O Using **F3** at 0 °C (Table 18, Entry 40).

Overall, **PP 4**, **F2** and **F3** all catalyzed the reaction at approximately the same time when 1.6 equivalents of Et_3N were used at room temperature, while the same amount of time was also needed for all three catalysts when 1.6 eq and 0.75 equivalents of Et_3N were employed at 0 °C. It is notable that once 0.75 equivalents of Et_3N were used at room temperature, **PP 4** led to the fastest conversion, and as a result this is the more efficient catalyst for these conditions. One can observe that when **PP 4** was employed as a catalyst, the enantiomeric excess of the acetate was rather low in all the examined cases. Regarding **F2** and **F3**, there is no differentiation on the ee of the acetate.

3.2.2 Target Peptide Group 6

3.2.2.1 Monomers G2, G4, G6, G8

Before the preparation of the four target peptides (Table 10-Target Peptide Group 6), the four corresponding monomers had to be properly functionalized first. Considering that the polyproline peptides are synthesized using Fmoc-based SPPS, incorporation of the Fmoc group to the monomeric units was necessary. As a result, a series of Fmoc protection reactions was performed to the corresponding amino-functionalized nicotinic and picolinic acids monomers. More specifically, the four target monomeric units were: 3-Fmoc amino picolinic acid (**G2**), 2-Fmoc amino nicotinic acid (**G4**), 3-Fmoc amino iso-nicotinic acid (**G6**), 4-Fmoc amino nicotinic acid (**G8**) (Figure 67).

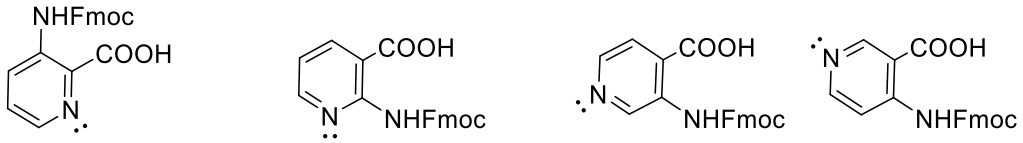

(**G2**) (**G4**) (**G6**) (**G8**)

Figure 67: Structures of Target Monomers (**G2**, **G4**, **G6**, **G8**).

The first experiments involved an Fmoc protection reaction using Fmoc-Cl, THF and aqueous solution of LiOH (Scheme 39).[14] This reaction was conducted on 3-amino picolinic acid (**G1**) and 2-amino nicotinic acid (**G3**), as well as the 3-amino iso-nicotinic acid (**G5**), and 4-amino nicotinic acid (**G7**). From these reactions, only the one starting from **G3** proved to be successful, yielding the desired monomer. This suggests that the nucleophilicity of the amine has a strong influence on the outcome of the reaction. A future direction could be to investigate other reaction conditions in order to further research the reasoning behind these results.

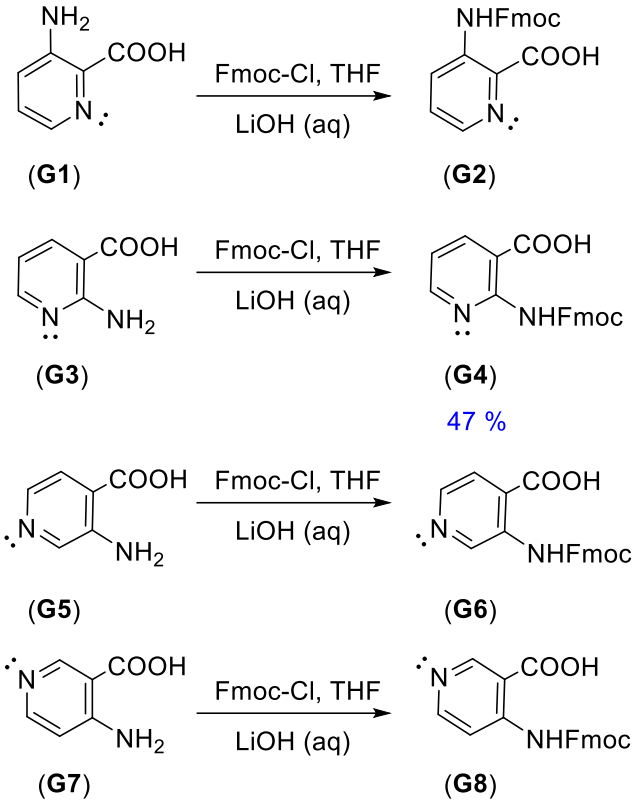

Scheme 39: Synthetic Attempts of Monomers **G2**, **G4**, **G6**, **G8**.

3.2.2.2 Synthetic Attempt of Target Peptide 6

Since only **G4** was obtained, the synthesis of one peptide (**PP 5**) was attempted (Figure 68). This peptide is comprised of 12 un-functionalized proline residues and one **G4** unit in the middle of the helix. Considering the catalytic results obtained from **PP 4**, designing a peptide with longer chain length could be one of the parameters leading to better catalytic results. As mentioned in section 1.1.4.1, ~ 3 residues appear per turn on the polyproline helix, at the same time that each of **PP 1**-**PP 3** which were comprised of seven units in total, were able to adopt a stable polyproline conformation. Since a polyproline peptide comprised of 13 residues has already been synthesized and proved to adopt a stable PolPro II conformation in water,[15] it was decided to prepare a peptide with 13 units. The rationale behind the design of this peptide was the investigation of the catalytic efficiency when the catalytic site is positioned within the helix.

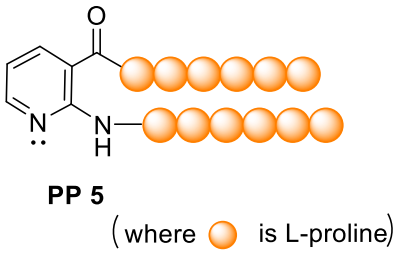

PP 5

(where ● is L-proline)

Figure 68: Structure of Peptide **PP 5**.

Similarly to **PP 4**, the synthesis of **PP 5** was achieved through the SPPS protocol. Using the peptide synthesizer, the already optimised conditions were applied. Three equivalents of the Fmoc-amino acid, three equivalents of Oxima Pure, six equivalents of DIC and 0.5 equivalents of DIPEA were used as coupling reagents. Once the desired peptide chain was created, the resin was then removed from the apparatus. Following that, cleavage was performed using 95 % TFA in DCM (4 mL). After 90 min of smooth agitation, the resin was washed with the same solution (x 2). The obtained solution was collected and evaporated, and the peptide precipitated with cold Et_2O After centrifugation, the solution was decanted and the solid was washed with cold Et_2O three times. This procedure was repeated (x 3) in order to isolate the peptide.

3.2.2.2.1 Analysis of PP 5 Peptide

PP 5 was then analysed via LCMS. According to the LCMS analysis, the profile did not correspond to **PP 5** (Figure 69). Instead, it corresponded to a peptide comprised of six proline residues and one **G4** unit (Figure 70). This suggests that the peptide chain could not be elongated, and as a result the synthesis of **PP 5** was not successful. Although the SPPS procedure had already been optimised, issues with the coupling efficiency can be observed during the synthesis of long chain peptides having non-natural amino acids. One possible way to overcome this issue is to change the conditions applied. The efficiency of the coupling procedure can be increased via the use of strong coupling reagents or additives which improve the chain elongation. Considering that the conditions used during SPPS had already been optimised, the modification of the peptide backbone was considered a more effective strategy.

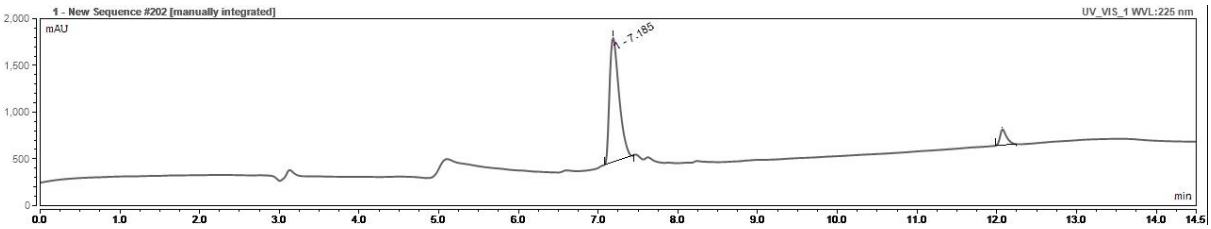

Figure 69: LCMS Chromatogram of **PP 5**.

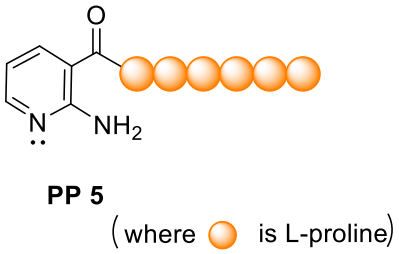

Figure 70: Structure of Synthesized Peptide.

3.2.2.3 PP 6 Peptide

In this regard, another peptide (**PP 6**) comprised of the same number of proline residues and 2-amino nicotinic acid (**G9**) was designed, with a slightly different geometry (Figure 71).

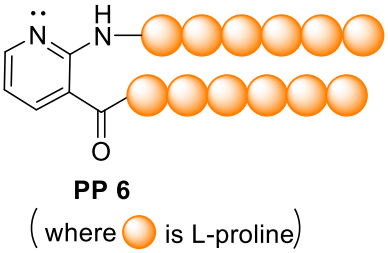

Figure 71: Structure of **PP 6**.

More specifically, in order for this peptide to be synthesized, a dimer (**I2**) between Fmoc-L-proline and monomer **G9** was required before using SPPS for the incorporation of the remaining proline units (Scheme 40).

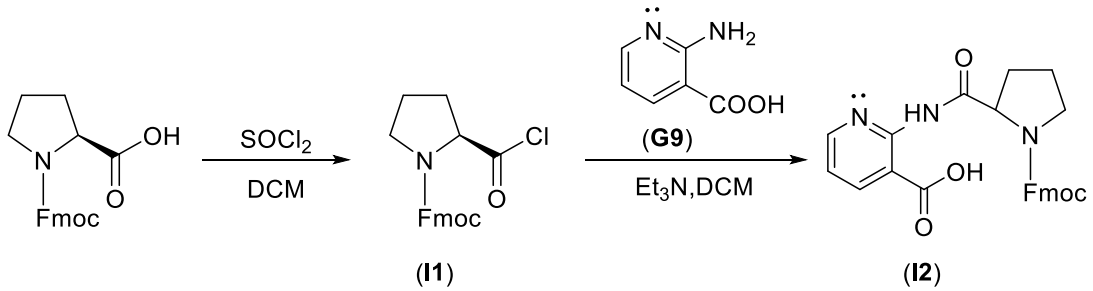

Scheme 40: Synthetic Attempt of **I2**.

Concerning the synthesis of **I2**, the first reaction involved using thionyl chloride ($SOCl_2$) in DCM, in order to convert the carboxylic acid group into an acid chloride, a reaction that was successful according to ^{1}H-NMR. The next step involved addition of **G9** in the presence of Et_3N and DCM as a solvent, at room temperature. This reaction did not lead to a successful outcome, and thus, the designed peptide could not be synthesized. This reaction should be further investigated, but it was not possible due to time limitations. For example, the second step of the reaction could be performed using DCC and DCM as a solvent at room temperature, as these conditions have proved to be successful for the synthesis of similar structures.

3.2.2.4 Synthesis of PP 7 and PP 8 Peptides

Following the above, a set of two different peptides was designed (**PP 7** and **PP 8**), comprised of eight proline residues and the commercially available 6-(methoxycarbonyl) picolinic acid monomeric unit (**J1**) in the middle (Figure 72). **PP 7** is comprised of eight L-proline residues and a **J1** unit in the middle of the helix, while in **PP 8** the last four L-proline units were exchanged with D-proline residues. These peptides were chosen in order to investigate whether the difference in the stereogenic centre of proline could affect the enantioselectivity of the acyl transfer reaction, a phenomenon that has already been demonstrated for other peptides (section 3.1).

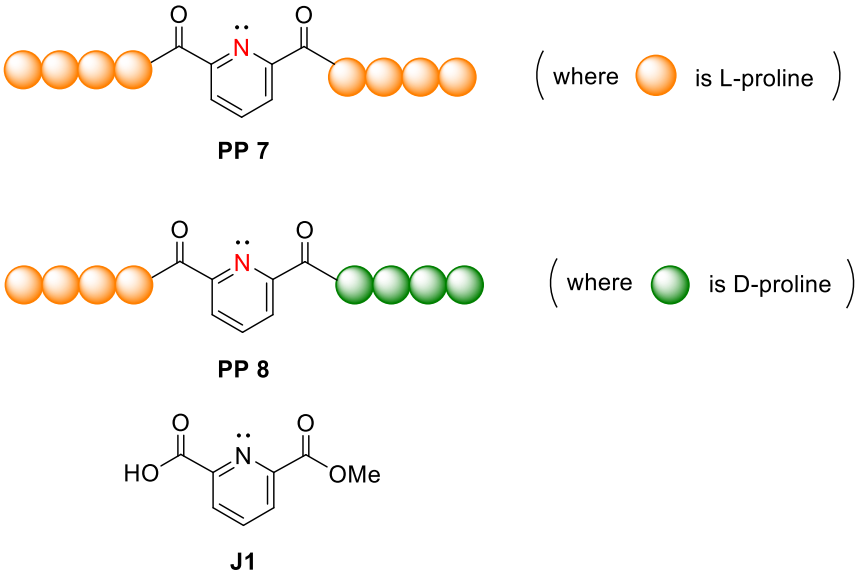

Figure 72: Structures of **PP 7**, **PP 8** and **J1**.

Based on the SPPS technique, the synthesis was performed on the peptide synthesized using the conditions that had already been optimised. In order for each peptide to be prepared, two separate synthetic cycles needed to be followed on the peptide synthesizer. During the first one a peptide consisted of four prolines and one **J1** unit was synthesized (**PP 9**) (Figure 73).

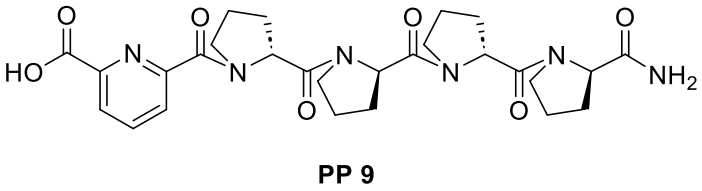

Figure 73: Structure of **PP 9**.

Three equivalents of the Fmoc-amino acid, three equivalents of Oxima Pure, six equivalents of DIC and 0.5 equivalents of DIPEA were used as coupling reagents. Once the desired peptide chain was created, the resin was then removed from the apparatus, and the capping procedure was performed manually, using a solution of 10 % Ac_2O and 2.5 % DIPEA in DMF (4 mL). Following that, cleavage was performed, using 95 % TFA in DCM (4 mL). After 90 min of smooth agitation, the resin was washed with the same solution twice. The obtained solution was collected and evaporated, and the peptide precipitated with Et_2O. Similarly to the cases of **PP 1**-**PP 3**, the cleavage procedure had to be repeated twice, in order for the product to precipitate upon addition of cold Et_2O. After centrifugation, the solution was decanted and the solid was washed with cold Et_2O three times. This procedure was repeated three times in order to isolate the peptide.

After that, a ^{19}F-NMR was recorded, and the peptide was exposed to an ion exchange resin. More specifically, a peptide vessel was equipped with a Purolite A400 resin in between of glass wool, rinsed successively with deionised H_2O (5 x 50 mL), 4 % NaOH in deionised H_2O (300 mL), deionised

H_2O (5 x 50 mL) and MeOH (5 x 50 mL) and dried. The peptide was dissolved in MeOH (5 mL), added to the dried vessel equipped with the ion exchange resin and smoothly agitated for two days. Following that, the obtained liquid was collected, washed with MeOH three times and dried. A ^{19}F-NMR was recorded again, and compared with the one before the ion resin treatment.

Once this procedure was complete, the second cycle begun. The preparation of the desired peptides was achieved using four prolines, either in the L-form for the synthesis of **PP 7** or in the D-form for **PP 8**, and the newly synthesized **PP 9** on the peptide synthesizer. The exact same conditions as described above were used. When the desired peptide chain was created, the resin was then removed from the apparatus, and the capping procedure was performed manually, using a solution of 10 % Ac_2O and 2.5 % DIPEA in DMF (4 mL). Following that, cleavage was performed, using 95 % TFA in DCM (4 mL). After 90 min of smooth agitation, the resin was washed with the same solution two times. The obtained solution was collected and evaporated, and the peptide precipitated with cold Et_2O. After centrifugation, the solution was decanted and the solid was washed with cold Et_2O three times. This procedure was repeated three times in order to isolate the peptide. Peptides **PP 7** and **PP 8** were obtained in 65 % and 62 % yield respectively.

3.2.2.4.1 Analysis of PP 7, PP 8 and PP 9 Peptides

Before completing the preparation of **PP 7** and **PP 8** peptides, **PP 9** was analysed through LCMS, in order to identify whether a successful synthesis had occurred. According to the results (Figure 74) one main peak was presented, which corresponded to the desired peptide. Due to the lack of impurities, **PP 9** was used in the next steps without further purification.

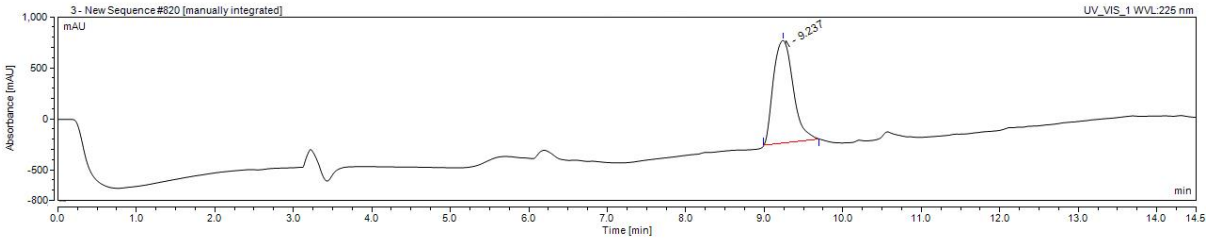

Figure 74: LCMS Chromatogram of **PP 9**.

After completing the synthesis of **PP 7** and **PP 8**, their analysis via LCMS followed, confirming the presence of the desired peptides. It is notable that the HPLC chromatogram of **PP 7** (Figure 75) presented one main peak at 7.60 min, and one smaller peak at 7.27 min. On the contrary, the chromatogram of **PP 8** (Figure 76) showed one main peak at 7.20 min and one small peak just after that 7.55 min.

In order to separate the two peaks, **PP 8** was purified through preparative RP-HPLC. Once the purified material was obtained, the HPLC analysis showed that the isolated main peak still consisted of two peaks that differentiated in height. Moreover, analysis of the two peaks through LCMS confirmed they had the same mass. As a result, the two peaks represent two rotamers of the peptide between D-proline and L-proline.

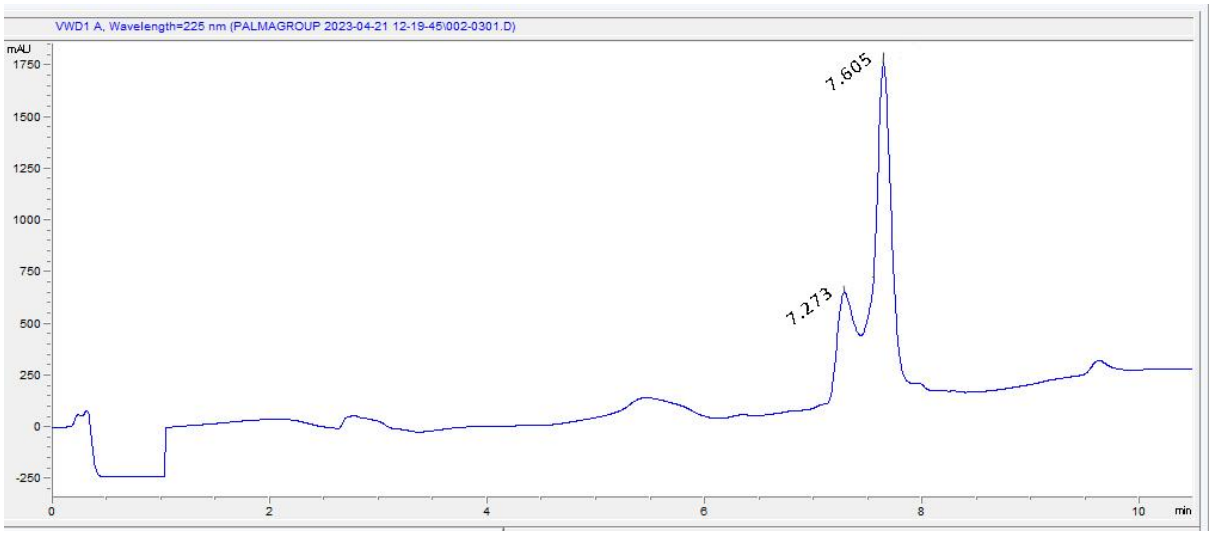

Figure 76: HPLC Chromatogram of **PP 7** Before Purification.

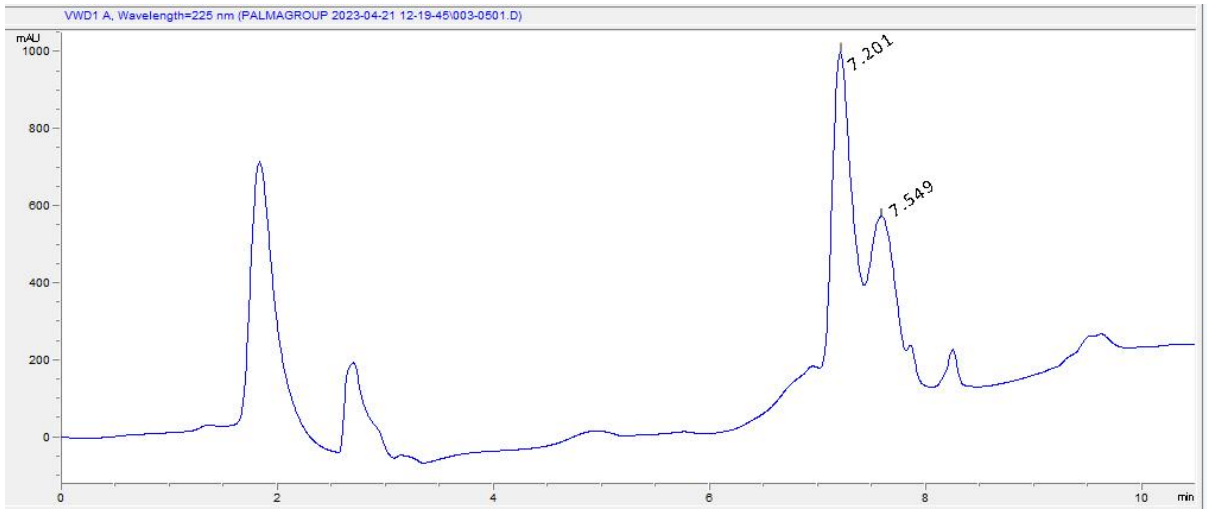

Figure 75: HPLC Chromatogram of **PP 8** Before Purification.

3.2.2.4.2 CD Analysis of PP 7, PP 8 and PP 9 Peptides

Using CD spectroscopy, **PP 7** and **PP 8** were analysed in water and samples that were left to equilibrate for seven days at 20 °C before the measurement was taken. The obtained spectrum for **PP 7** presented a strong negative band at 205 nm and a weak positive band at 225 nm (Figure 77). Based on the data regarding **PP 8**, the spectrum showed a strong negative band around 205 nm and a strong positive band at 225 nm (Figure 78). Lastly, **PP 9** was also analysed through CD spectroscopy. The obtained spectrum presented a strong negative band at 205 nm and a weak positive band at 225 nm (Figure 79). As a result, once placed in water, all three peptides have a conformation that is representative of a PolPro II conformation.

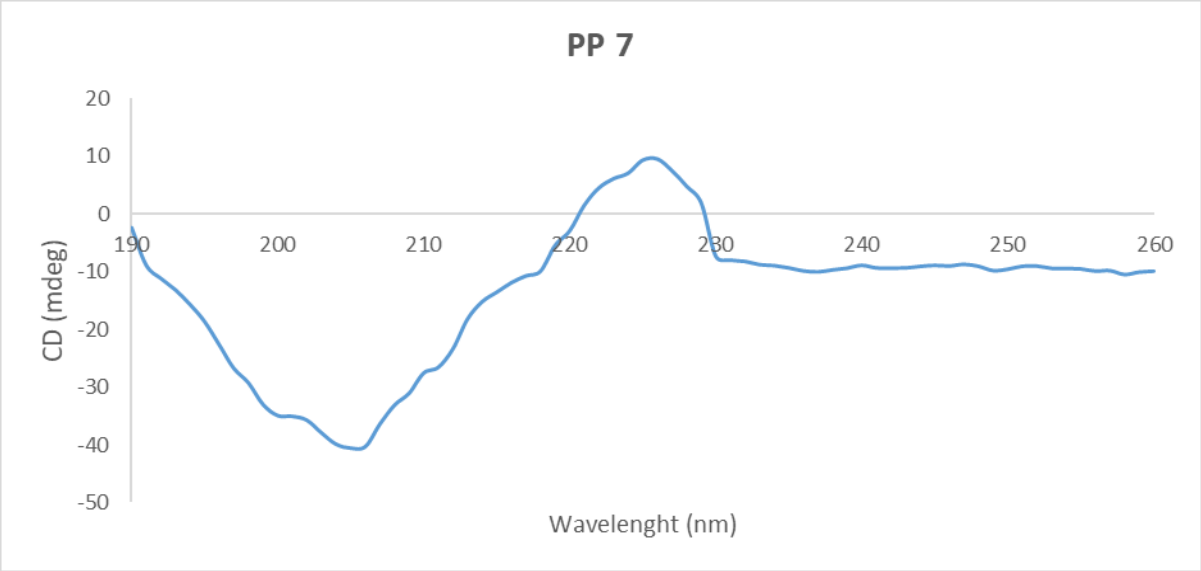

Figure 77: CD Spectrum of **PP 7** in Aqueous Solution at 20 °C and ≈ 100 µM.

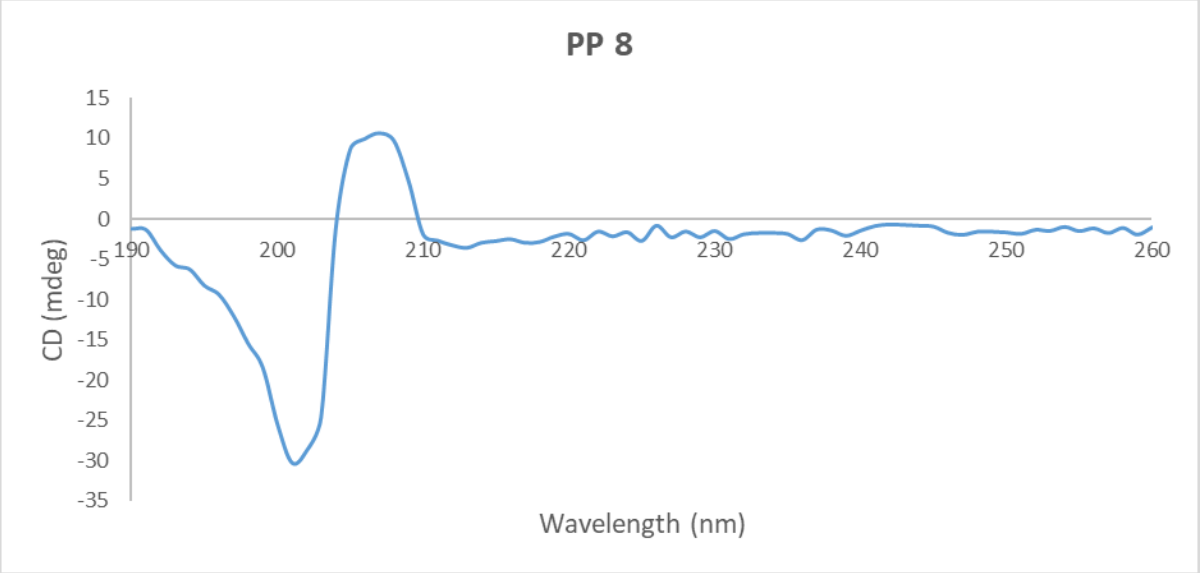

Figure 78: CD Spectrum of **PP 8** in Aqueous Solution at 20 °C and ≈ 100 µM.

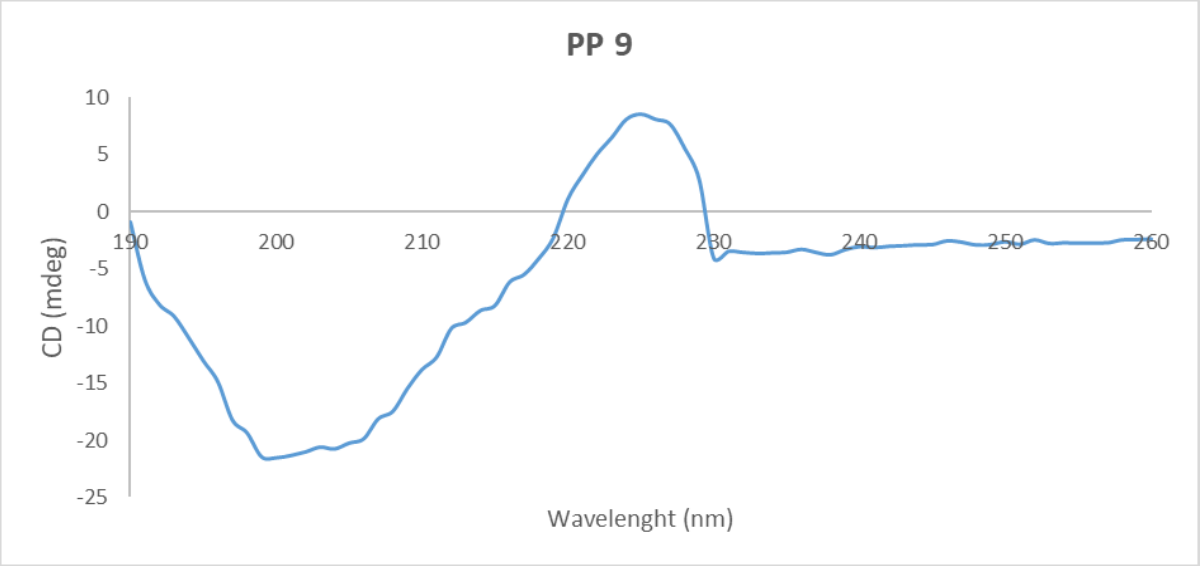

Figure 79: CD Spectrum of **PP 9** in Aqueous Solution at 20 °C and ≈ 100 μM.

3.2.2.5 Application of PP 7 and PP 8 in the Kinetic Resolution of a Racemic Alcohol

After their successful synthesis, analysis and characterisation, **PP 7** and **PP 8** were tested as catalysts for the KR of racemic alcohol 1-phenylethanol (Scheme 41). More specifically, the reaction involved Ac_2O and Et_3N as reagents, while $CDCl_3$ was again the solvent of choice.

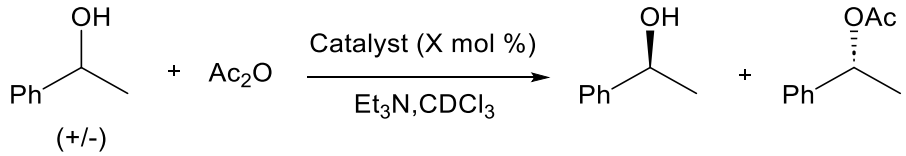

Scheme 41: KR of Racemic alcohol 1-phenylethanol Using **PP 7** and **PP 8** as an Organocatalyst.

Apart from the desired peptides, the catalytic activity of **PP 9** and monomer **J1**, which were employed during the synthesis of the target peptides, were also examined and compared with the one of **PP 7** and **PP 8**.

Similarly to **PP 4**, all the reactions performed where monitored through ^{1}H-NMR, while the products obtained from the optimum conditions for each case were then analysed through GC-MS with a chiral stationary phase. Based on this, the enantiomeric excess (ee) values for the alcohol and the acetate product of each reaction were determined.

PP 7 and **PP 8** were firstly tested in 5 % loading. As the reaction conditions had already been optimised, 1.5 equivalents of Ac_2O were used. Nevertheless, the effect of Et_3N was investigated in this part of the project as well, and thus, every potential catalyst was tested upon addition of 0.75 and 1.6 equivalents of Et_3N respectively.

Starting with **PP 7**, the conversion reached 47 % in 43 h when 1.6 equivalents of Et_3N were used (Table 19, Entry 42). A reaction aliquot was then run through chiral GC-MS analysis. Based on the results, the enantiomeric excess for the alcohol was bigger than the one of acetate (5 % and 1 % respectively) (Figure 80). 42 hours were necessary for 42 % conversion to occur, upon addition of 0.75 equivalents of Et_3N (Table 19, Entry 44). According to the GC-MS analysis, the enantioselectivities for the alcohol and the acetate were 6 % and 3 % (Figure 81).

Table 19: KR of racemic 1-phenyl alcohol Using **PP 7** at RT.

Entry	Catalyst (mol %)	Ac_2O (eq)	Et_3N (eq)	Time[b]	Yield[c] (%)	$ee_{alcohol}$ %[d]	$ee_{acetate}$ %[d]
41	5 %	1.5	1.6	18 h	46	-	-
42	5 %	1.5	1.6	43 h	47	5	1
43	5 %	1.5	0.75	18 h	33	-	-
44	5 %	1.5	0.75	42 h	42	6	3

[a] Reaction conditions: rac-alcohol (0.16 mmol), Ac_2O (0.75 or 1.5 eq), Et_3N (0.75 or 1.6 mmol) in 800 µL of $CDCl_3$ at RT. [b] Where h indicates hours and d indicates days. [c] Determined by ^{1}H-NMR analysis of the crude products. [d] Determined by chiral GC-MS analysis.

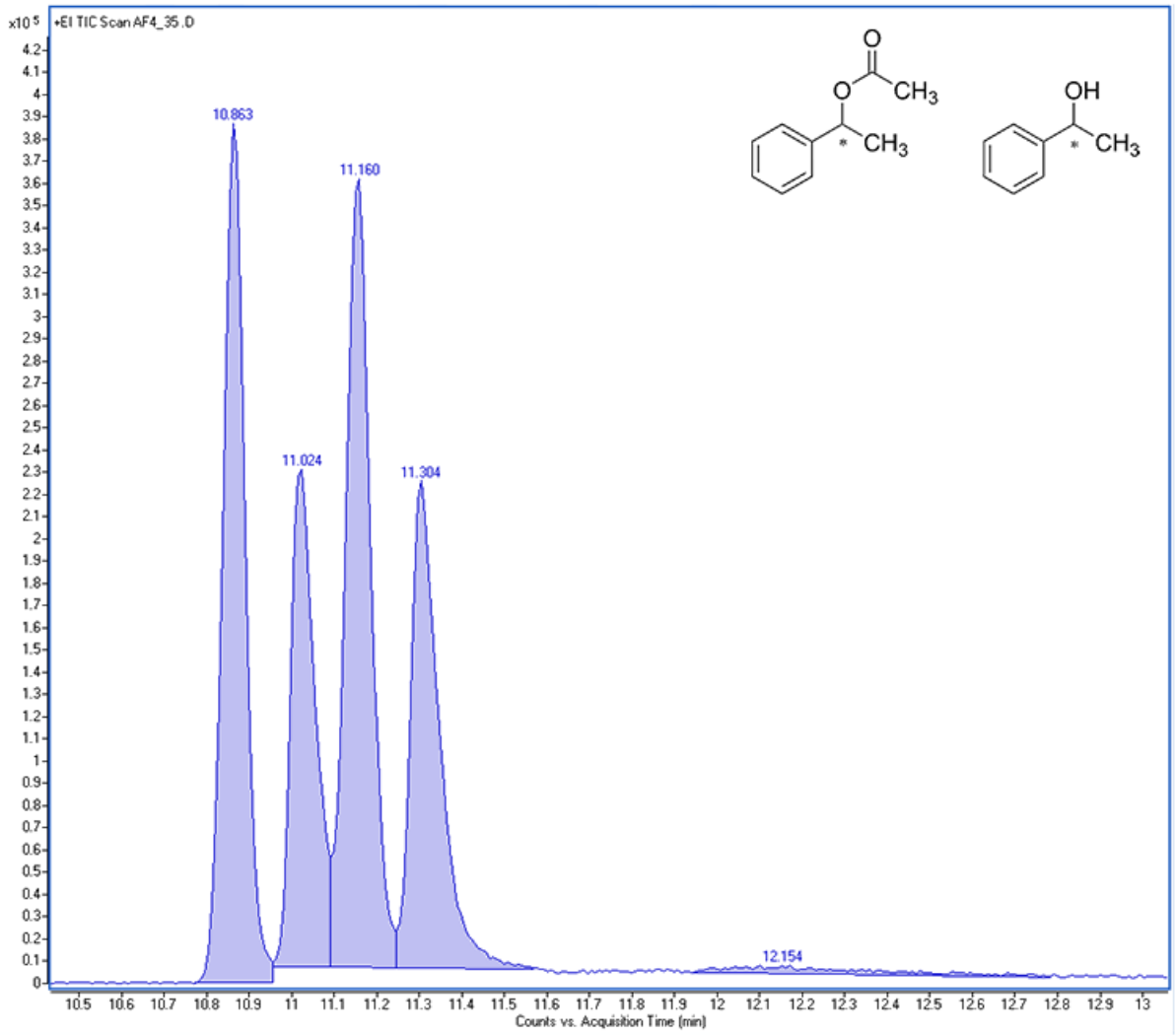

Figure 80: GC-MS Analysis of Reaction of 1-phenyl alcohol with Ac_2O Using **PP 7** at RT (Table 20, Entry 42).

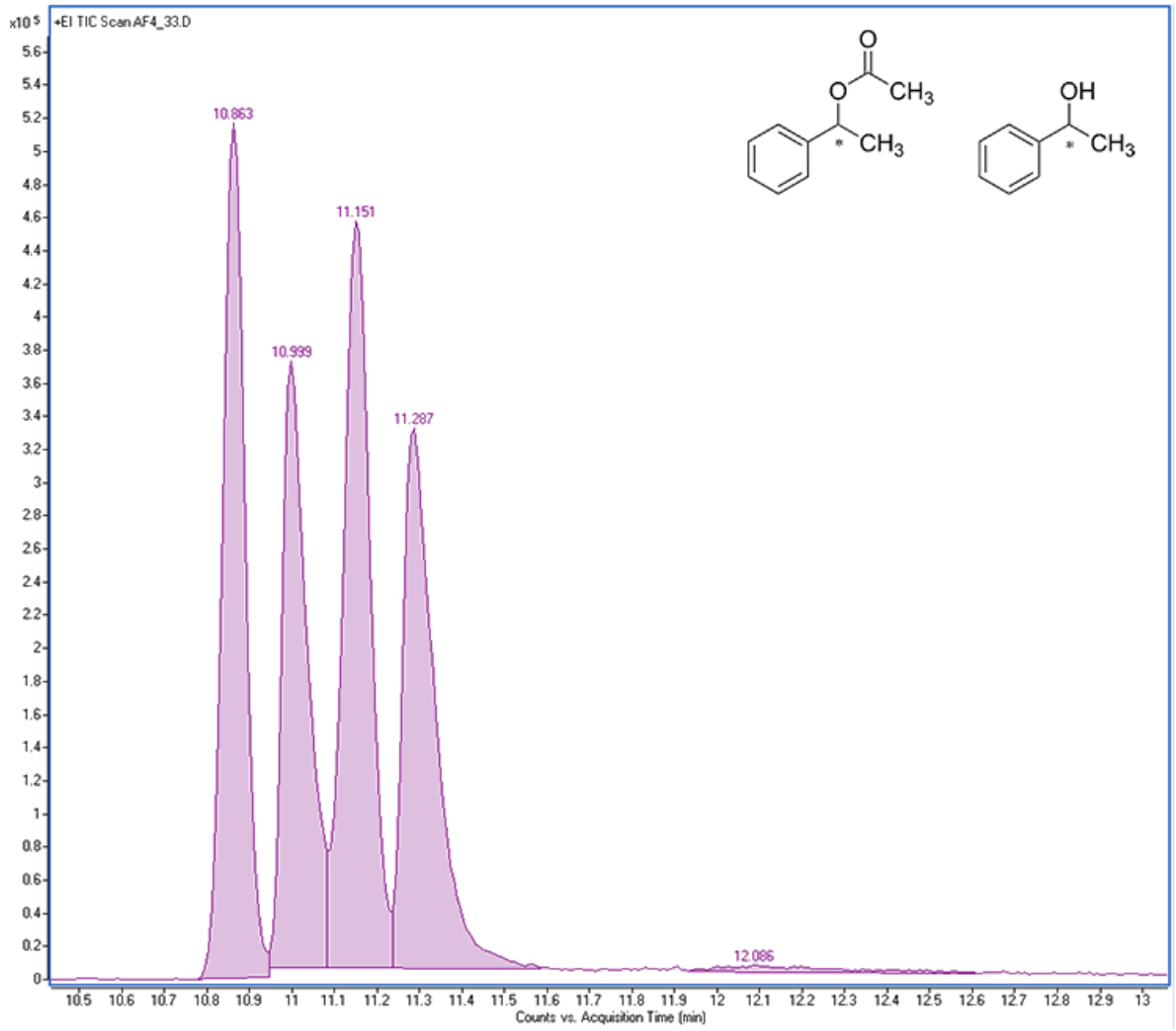

Figure 81: GC-MS Analysis of Reaction of 1-phenyl alcohol with Ac_2O Using **PP 7** at RT (Table 20, Entry 44).

Aiming to improve the low enantioselectivities obtained, the same experiment was also performed at 0 °C. Using 5 % loading again, the conversion reached 50 % in 4 days when 1.6 equivalents of Et_3N were used (Table 20, Entry 45). The ee proved to be very low and identical for the alcohol and the acetate (2 %) (Figure 82). 7 days were necessary for the same conversion once of 0.75 equivalents of Et_3N were added (Table 20, Entry 48) (Figure 83).

Table 20: KR of Racemic 1-phenyl alcohol Using **PP 7** at 0 °C.

Entry	Catalyst (mol %)	Ac_2O (eq)	Et_3N (eq)	Time[b]	Yield[c] (%)	$ee_{alcohol}$ %[d]	$ee_{acetate}$ %[d]
45	5 %	1.5	1.6	4 d	50	2	2
46	5 %	1.5	0.75	20 h	25	-	-
47	5 %	1.5	0.75	6 d	44	-	-
48	5 %	1.5	0.75	7 d	49	0	0

[a] Reaction conditions: rac-alcohol (0.16 mmol), Ac_2O (0.75 or 1.5 eq), Et_3N (0.75 or 1.6 mmol) in 800 µL of $CDCl_3$ at RT. [b] Where h indicates hours and d indicates days. [c] Determined by ^{1}H-NMR analysis of the crude products. [d] Determined by chiral GC-MS analysis.

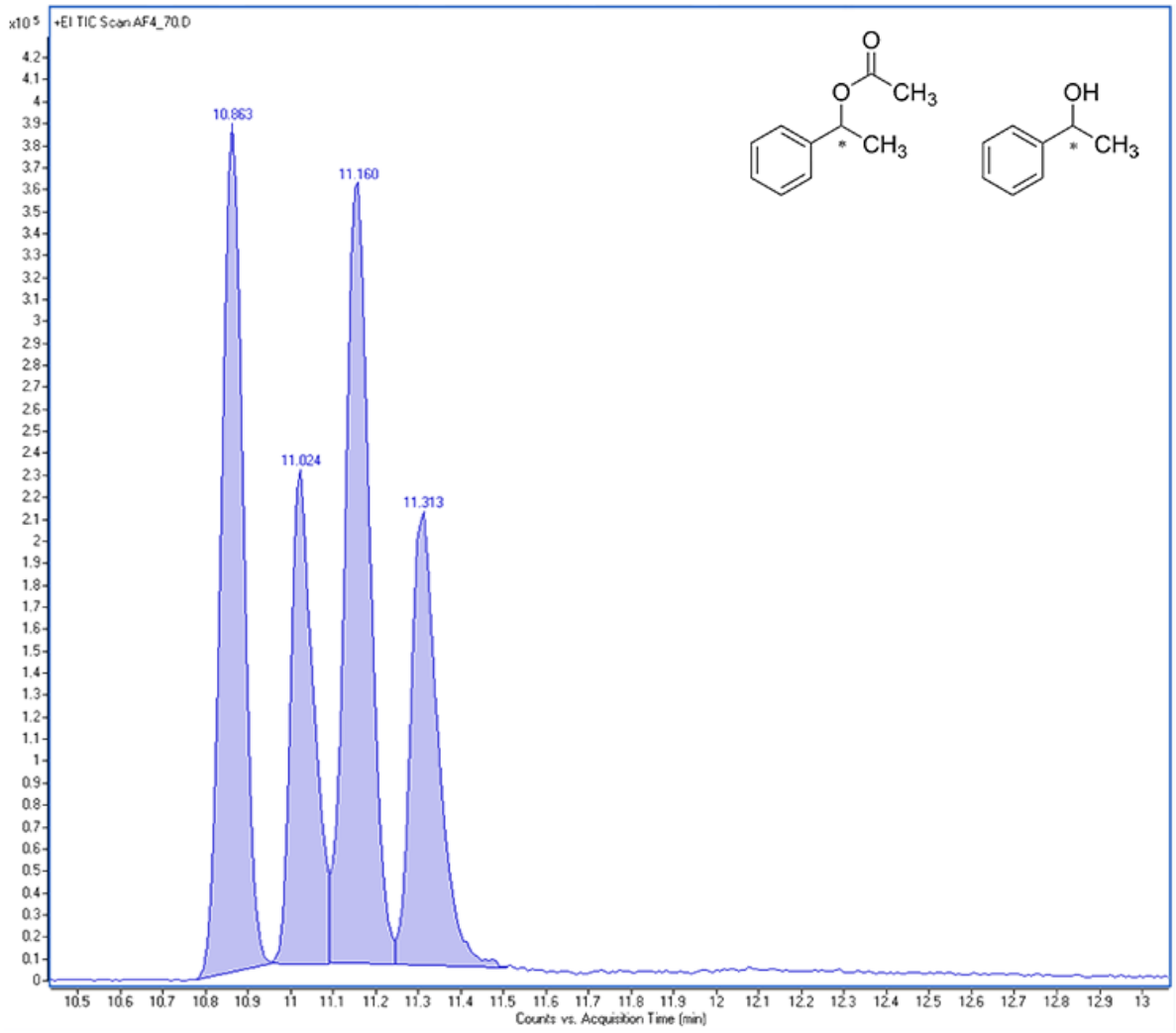

Figure 82: GC-MS Analysis of Reaction of 1-phenyl alcohol with Ac_2O Using **PP 7** at 0 °C (Table 21, Entry 45).

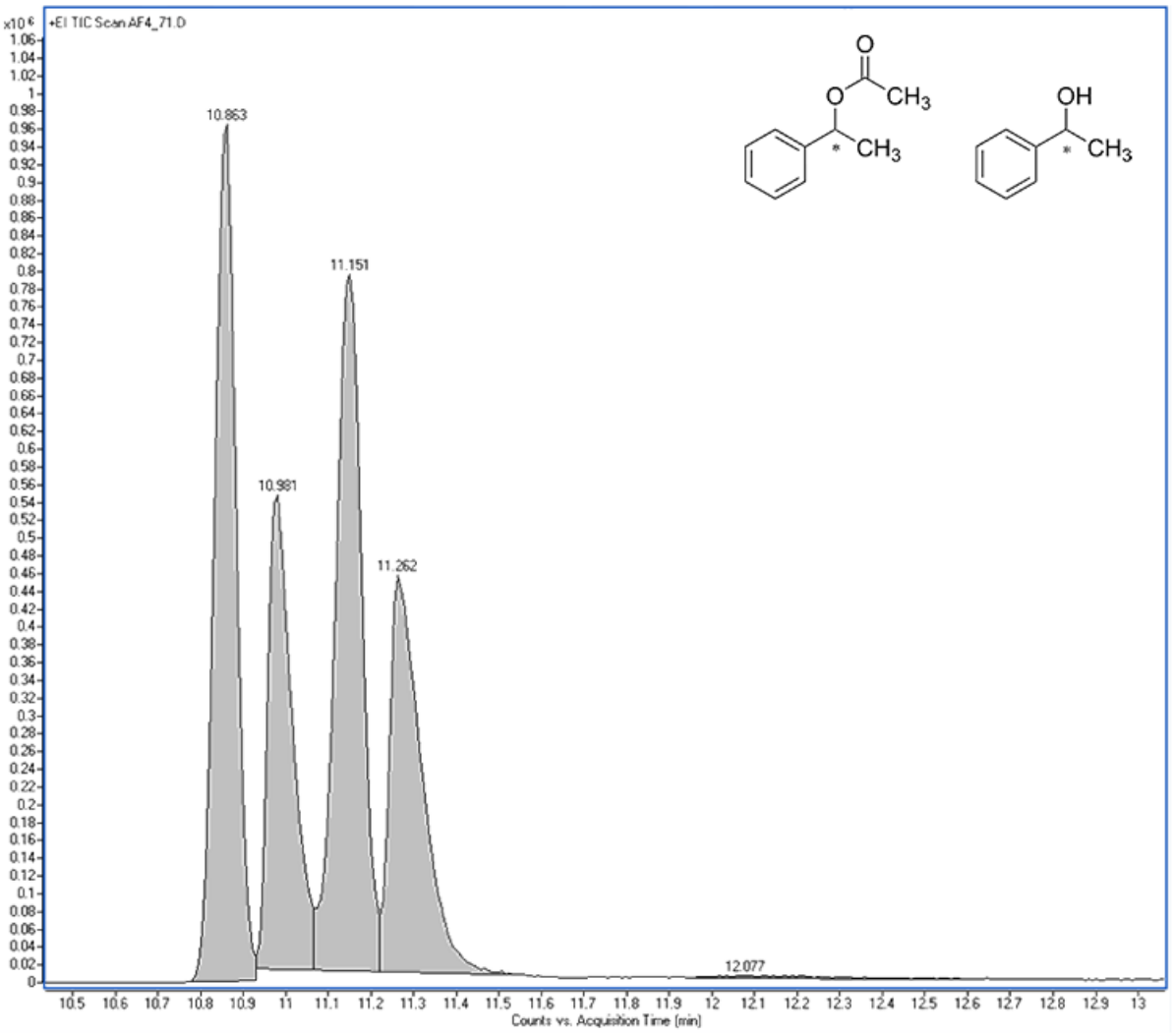

Figure 83: GC-MS Analysis of Reaction of 1-phenyl alcohol with Ac_2O Using **PP 7** at 0 °C (Table 21, Entry 48).

Regarding **PP 8**, 43 % conversion was achieved in 19 hours when 1.5 equivalents of Et_3N were applied (Table 21, Entry 49), whereas the same conversion was reached in 42 h in the case of 0.75 equivalents of Et_3N (Table 21, Entry 51). After GC-MS analysis, the ee for the acetate remained the same in both cases (2 %) (Figure 84), whereas the value for alcohol was increased from 3 % to 8 % when the equivalents of Et_3N were decreased in half (Figure 85).

Table 21: KR of Racemic 1-phenyl alcohol Using **PP 8** at RT.

Entry	Catalyst (mol %)	Ac_2O (eq)	Et_3N (eq)	Time[b]	Yield[c] (%)	$ee_{alcohol}$ %[d]	$ee_{acetate}$ %[d]
49	5 %	1.5	1.6	19 h	43	3	2
50	5 %	1.5	0.75	18 h	38	-	-
51	5 %	1.5	0.75	42 h	49	8	2

[a] Reaction conditions: rac-alcohol (0.16 mmol), Ac_2O (0.75 or 1.5 eq), Et_3N (0.75 or 1.6 mmol) in 800 µL of $CDCl_3$ at RT. [b] Where h indicates hours and d indicates days. [c] Determined by ^{1}H-NMR analysis of the crude products. [d] Determined by chiral GC-MS analysis.

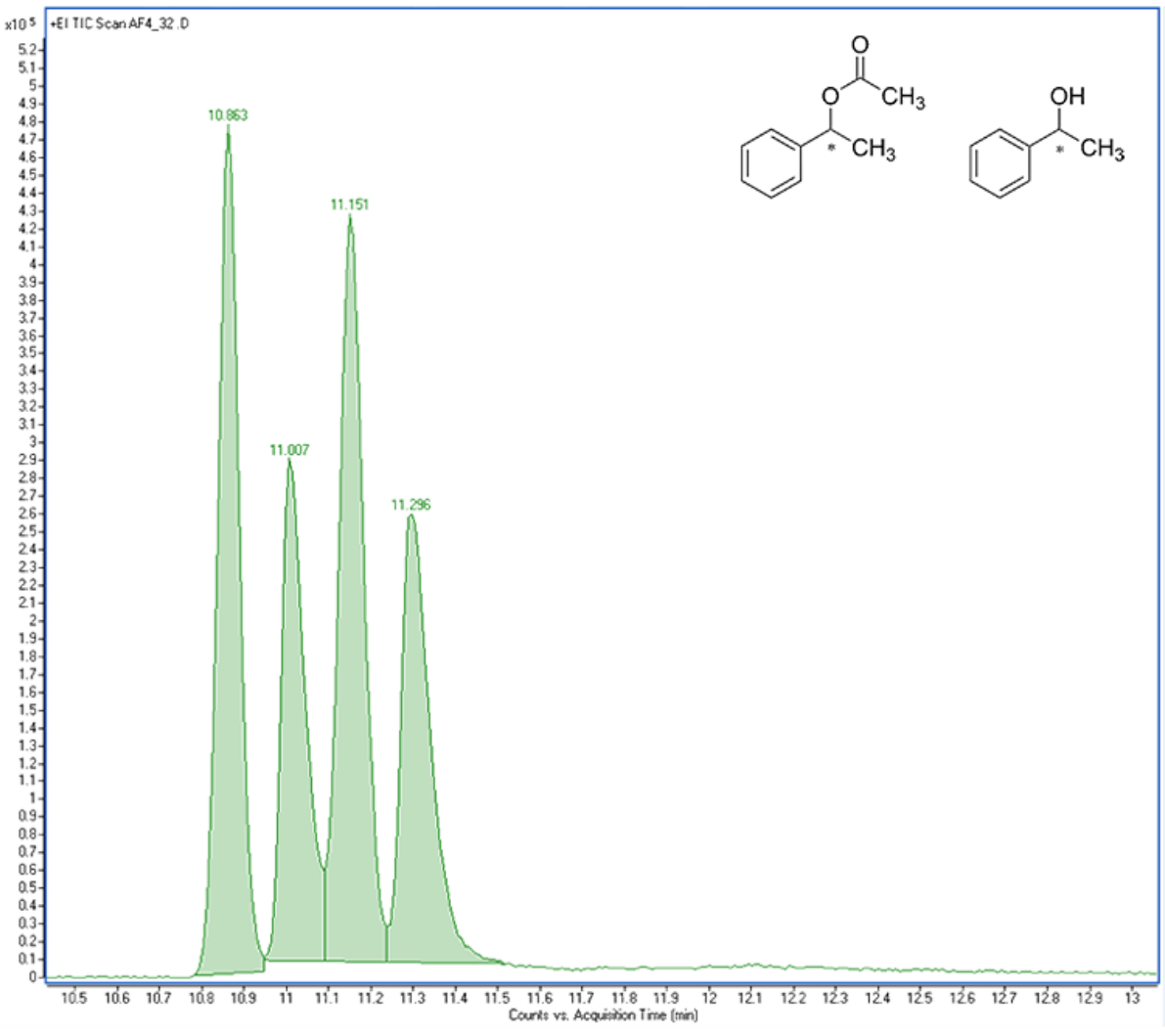

Figure 84: GC-MS Analysis of Reaction of 1-phenyl alcohol with Ac_2O Using **PP 8** at RT (Table 22, entry 49).

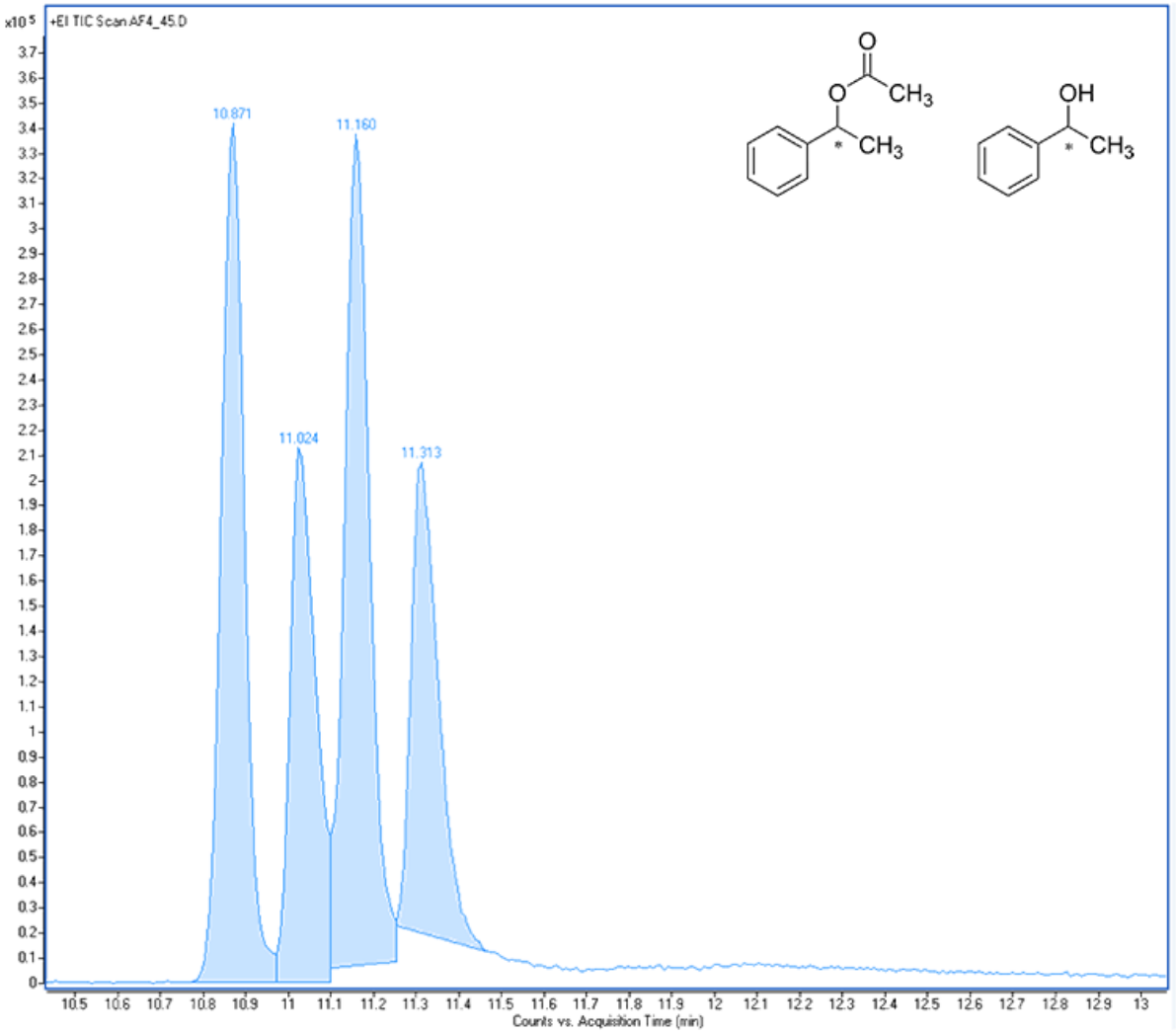

Figure 85: GC-MS Analysis of Reaction of 1-phenyl alcohol with Ac_2O Using **PP 8** at RT (Table 22, Entry 51).

Once **PP 8** was employed as an organocatalyst at 0 ℃, 6 days were required for 47 % yield once 1.6 equivalents of Et_3N were added (Table 22, Entry 53), whereas 24 days were necessary for the same conversion to occur when 0.75 equivalents of Et_3N were used (Table 22, Entry 60). After GC analysis, the observed ee 1 % for both the alcohol and the acetate (Figures 86), with slightly higher values (3 %) in the case of using 0.75 equivalents of Et_3N (Figure 87).

Table 22: KR of Racemic 1-phenyl alcohol Using **PP 8** at 0 °C.

Entry	Catalyst (mol %)	Ac_2O (eq)	Et_3N (eq)	Time[b]	Yield[c] (%)	$ee_{alcohol}$ %[d]	$ee_{acetate}$ %[d]
52	5 %	1.5	1.6	4 d	33	-	-
53	5 %	1.5	1.6	6 d	47	1	1
54	5 %	1.5	0.75	4 d	15	-	-
55	5 %	1.5	0.75	6 d	26	-	-
56	5 %	1.5	0.75	8 d	29	-	-
57	5 %	1.5	0.75	12 d	35	-	-
58	5 %	1.5	0.75	18 d	41	-	-
59	5 %	1.5	0.75	19 d	43	-	-
60	5 %	1.5	0.75	24 d	48	3	3

[a] Reaction conditions: rac-alcohol (0.16 mmol), Ac_2O (0.75 or 1.5 eq), Et_3N (0.75 or 1.6 mmol) in 800 µL of $CDCl_3$ at RT. [b] Where h indicates hours and d indicates days. [c] Determined by ^{1}H-NMR analysis of the crude products. [d] Determined by chiral GC-MS analysis.

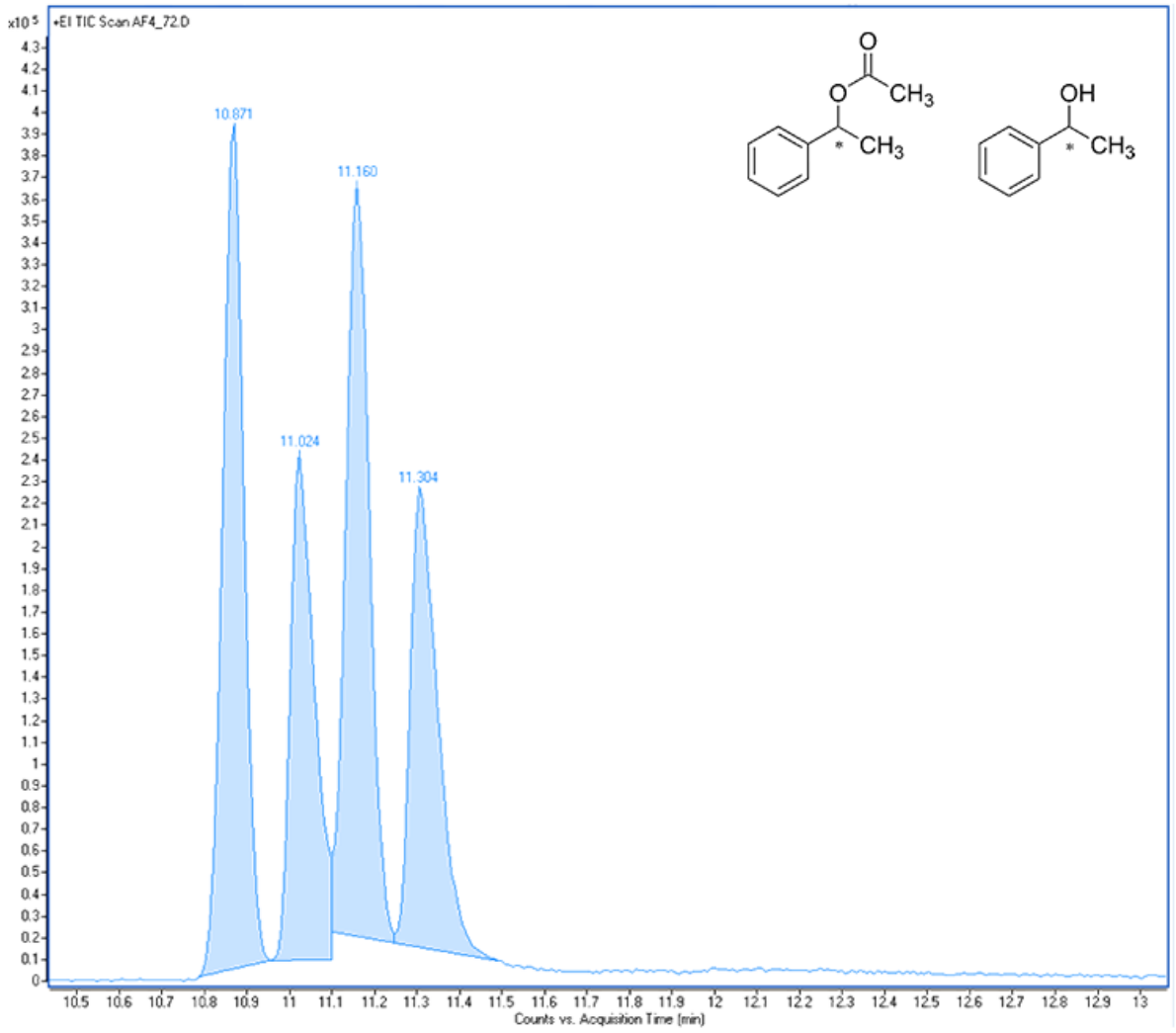

Figure 86: GC-MS Analysis of Reaction of 1-phenyl alcohol with Ac_2O Using **PP 8** at 0 °C (Table 22, Entry 53).

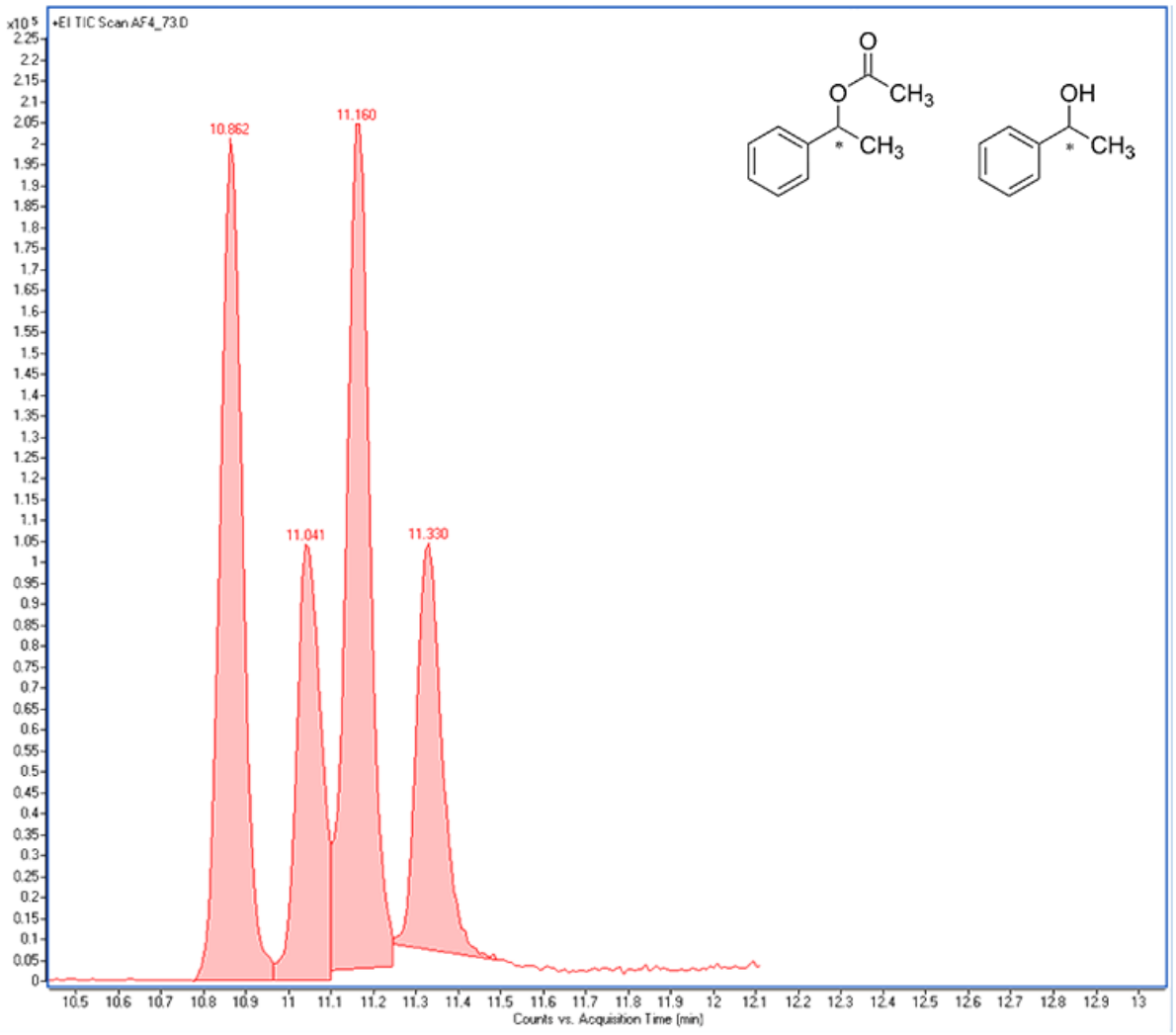

Figure 87: GC-MS Analysis of Reaction of 1-phenyl alcohol with Ac_2O Using **PP 8** at 0 °C (Table 22, Entry 60).

According to the ^{1}H-NMR results, **PP 9** required more time in order to reach 50 % yield. More specifically, 50 hours and 71 hours where needed upon addition of 1.6 and 0.75 equivalents of Et_3N respectively (Table 23, entries 64 and 67 respectively). The ee of the acetate remained again the same in both cases (1 %), whereas there was a slight increase for the ee of the alcohol (Figures 88 and 89).

Table 23: KR of Racemic 1-phenyl alcohol Using **PP 9** at RT.

Entry	Catalyst (mol %)	Ac_2O (eq)	Et_3N (eq)	Time[b]	Yield[c] (%)	$ee_{alcohol}$ %[d]	$ee_{acetate}$ %[d]
61	5 %	1.5	1.6	24 h	27	-	-
62	5 %	1.5	1.6	40 h	39	-	-
63	5 %	1.5	1.6	48 h	48	-	-
64	5 %	1.5	1.6	50 h	50	3	1
65	5 %	1.5	0.75	23 h	22	-	-
66	5 %	1.5	0.75	48 h	42	-	-
67	5 %	1.5	0.75	71 h	51	5	1

[a] Reaction conditions: rac-alcohol (0.16 mmol), Ac_2O (0.75 or 1.5 eq), Et_3N (0.75 or 1.6 mmol) in 800 μL of $CDCl_3$ at RT. [b] Where h indicates hours and d indicates days. [c] Determined by ^{1}H-NMR analysis of the crude products. [d] Determined by chiral GC-MS analysis.

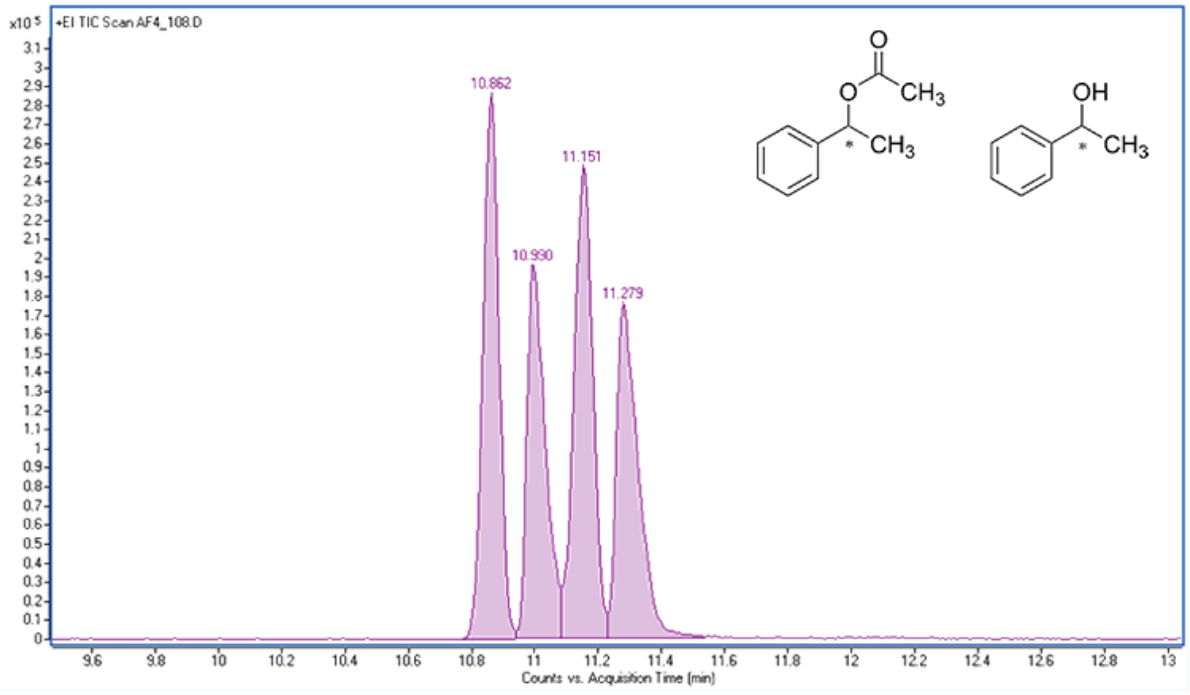

Figure 88: GC-MS Analysis of Reaction of 1-phenyl alcohol with Ac_2O Using **PP 9** at RT (Table 23, Entry 64).

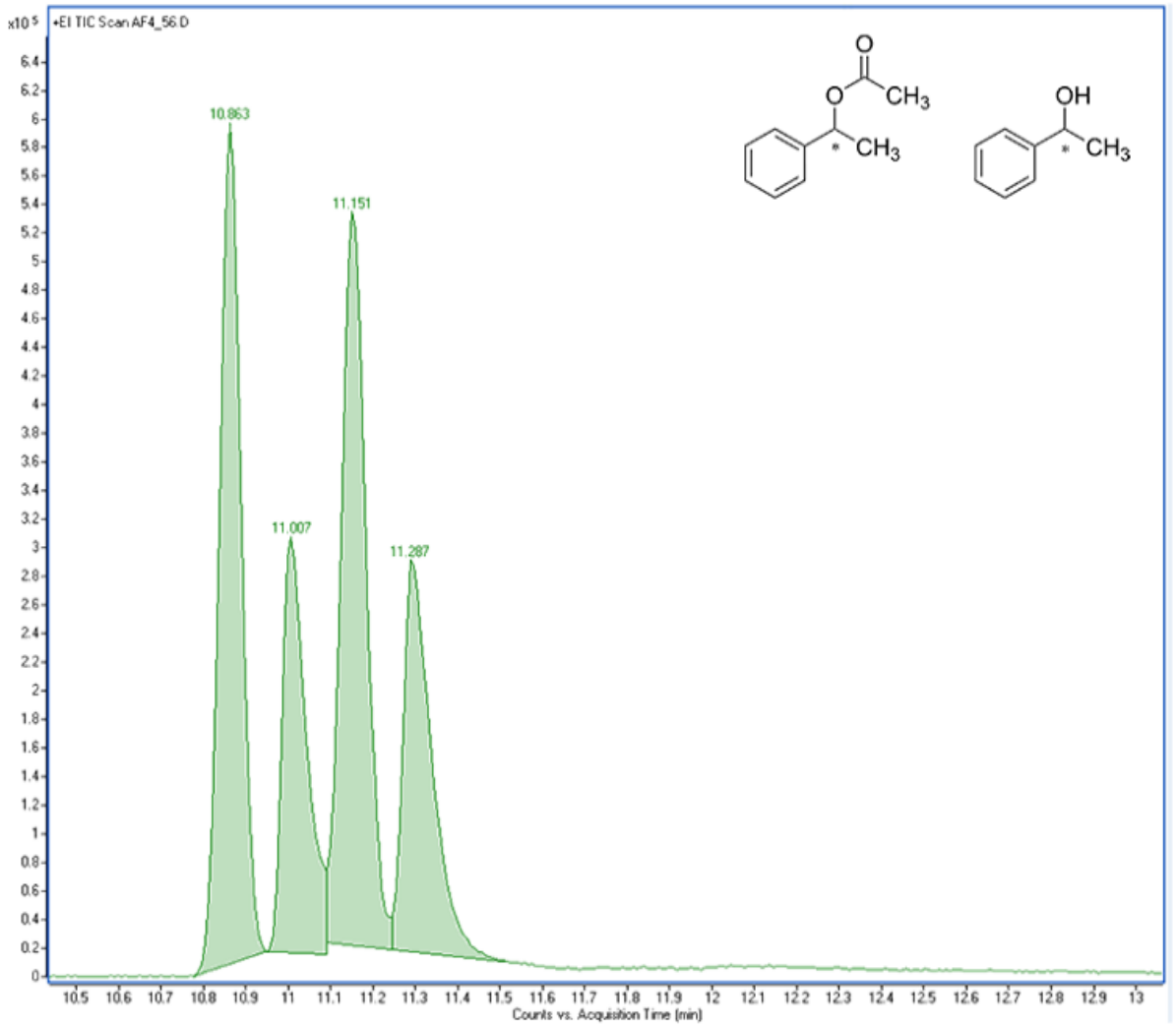

Figure 89: GC-MS Analysis of Reaction of 1-phenyl alcohol with Ac_2O Using **PP 9** at RT (Table 23, Entry 67).

PP 9 required 3 days in order to reach 50 % conversion when 1.6 equivalents of Et_3N were used at 0 °C (Table 24, Entry 68), while the double number of days was needed when half amount of Et_3N was added (Table 24, Entry 71). According the GC-MS analysis, all the ee values were identical to each other (1 %) (Figures 90 and 91).

Table 24: KR of Racemic 1-phenyl alcohol Using **PP 9** at 0 ℃.

Entry	Catalyst (mol %)	Ac_2O (eq)	Et_3N (eq)	Time[b]	Yield[c] (%)	$ee_{alcohol}$ %[d]	$ee_{acetate}$ %[d]
68	5 %	1.5	1.6	3 d	48	1	1
69	5 %	1.5	0.75	20 h	13	-	-
70	5 %	1.5	0.75	24 h	17	-	-
71	5 %	1.5	0.75	6 d	50	1	1

[a] Reaction conditions: rac-alcohol (0.16 mmol), Ac_2O (0.75 or 1.5 eq), Et_3N (0.75 or 1.6 mmol) in 800 µL of $CDCl_3$ at RT. [b] Where h indicates hours and d indicates days. [c] Determined by ^{1}H-NMR analysis of the crude products. [d] Determined by chiral GC-MS analysis.

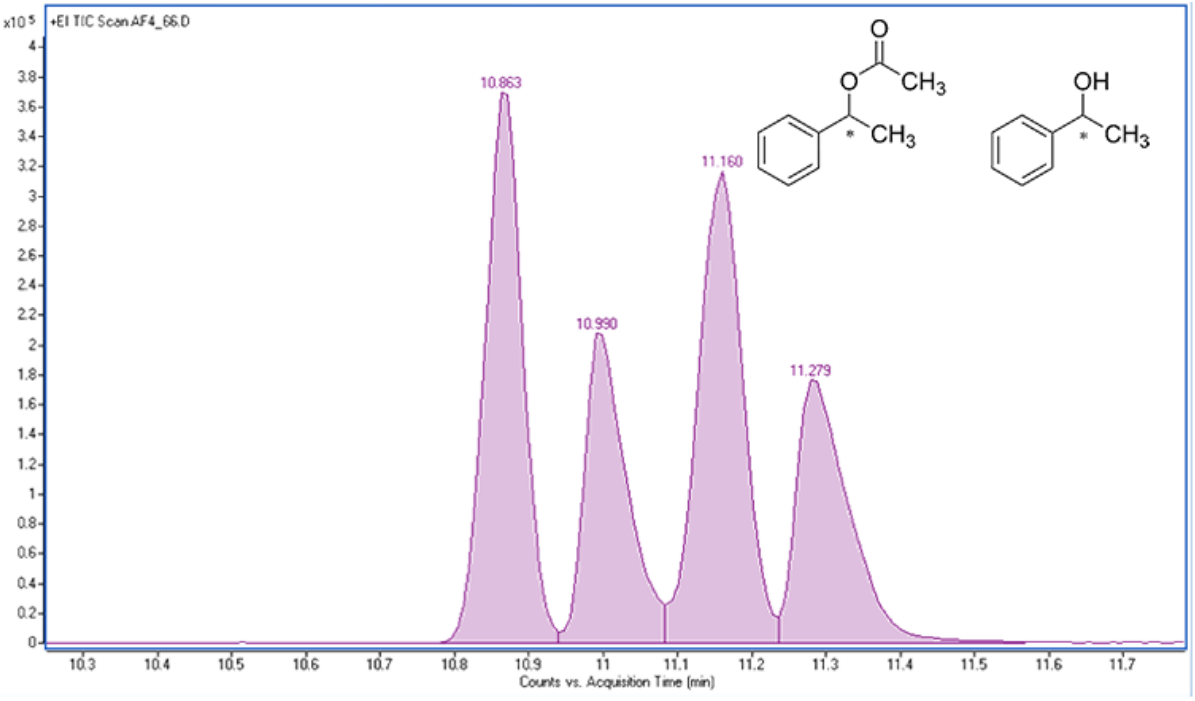

Figure 90: GC-MS Analysis of Reaction of 1-phenyl alcohol with Ac_2O Using **PP 8** at 0 °C (Table 24, Entry 68).

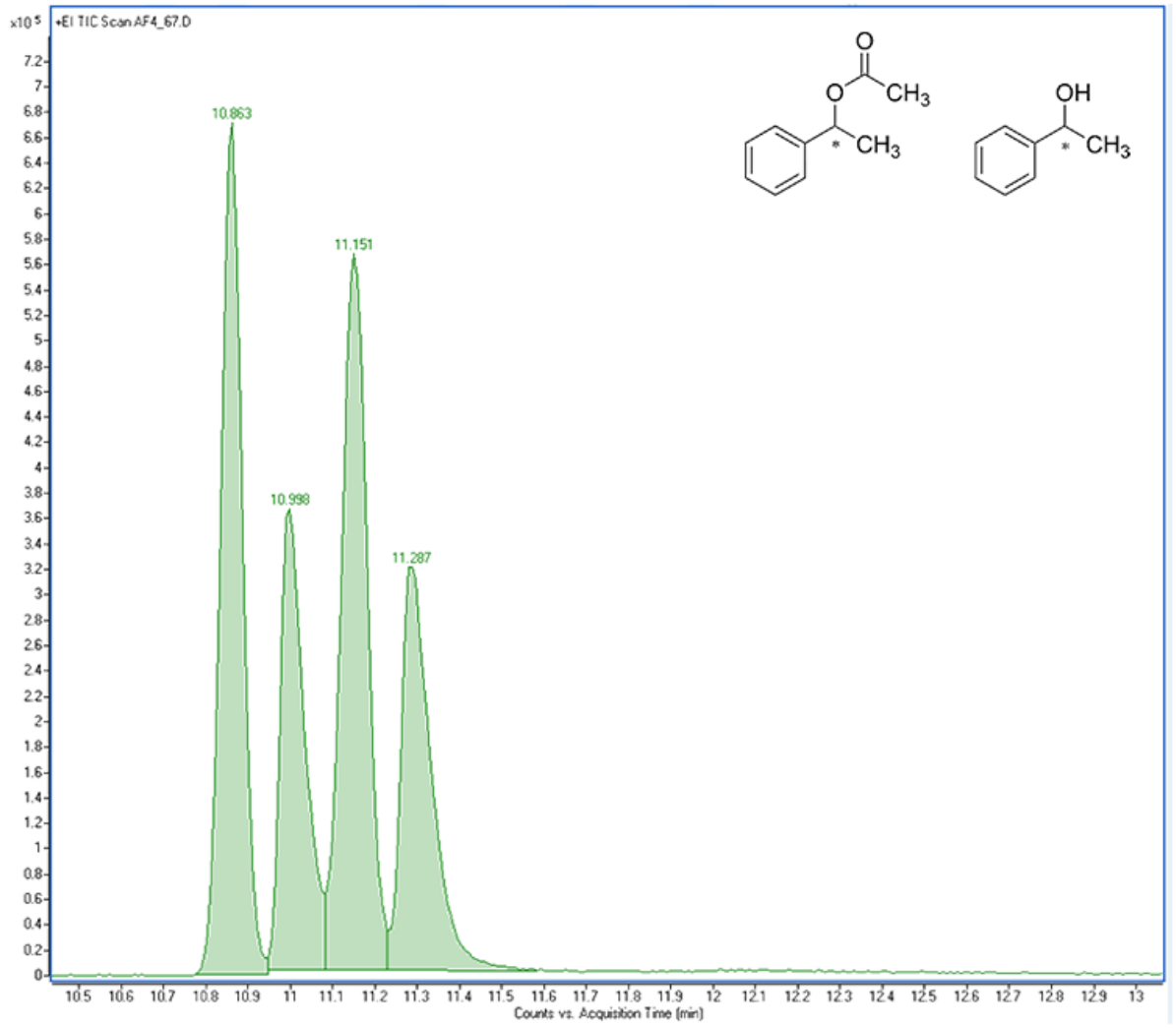

Figure 91: GC-MS Analysis of Reaction of 1-phenyl alcohol with Ac_2O Using **PP 8** at 0 °C (Table 24, Entry 71).

Lastly, concerning the monomer **J1**, 60 hours were required for a 49 % conversion of the alcohol once 1.6 equivalents were used (Table 25, Entry 77), whereas the same conversion was achieved in 7 days in the case of 0.75 equivalents of Et_3N (Table 25, Entry 83). The recorded ee after GC-MS analysis were varying from 0-3 % (Figures 92 and 93).

Table 25: KR of Racemic 1-phenyl alcohol Using **J1** at RT.

Entry	Catalyst (mol %)	Ac_2O (eq)	Et_3N (eq)	Time[b]	Yield[c] (%)	$ee_{alcohol}$ %[d]	$ee_{acetate}$ %[d]
72	5 %	1.5	1.6	16.3 h	20	-	-
73	5 %	1.5	1.6	17.3 h	21	-	-
74	5 %	1.5	1.6	23 h	25	-	-
75	5 %	1.5	1.6	24 h	26	-	-
76	5 %	1.5	1.6	48 h	43	-	-
77	5 %	1.5	1.6	60 h	49	3	0
78	5 %	1.5	0.75	23 h	12	-	-
79	5 %	1.5	0.75	48 h	26	-	-
80	5 %	1.5	0.75	71 h	33	-	-
81	5 %	1.5	0.75	4 d	38	-	-
82	5 %	1.5	0.75	6 d	45	-	-
83	5 %	1.5	0.75	7 d	48	0	1

[a] Reaction conditions: rac-alcohol (0.16 mmol), Ac_2O (0.75 or 1.5 eq), Et_3N (0.75 or 1.6 mmol) in 800 µL of $CDCl_3$ at RT. [b] Where h indicates hours and d indicates days. [c] Determined by ^{1}H-NMR analysis of the crude products. [d] Determined by chiral GC-MS analysis.

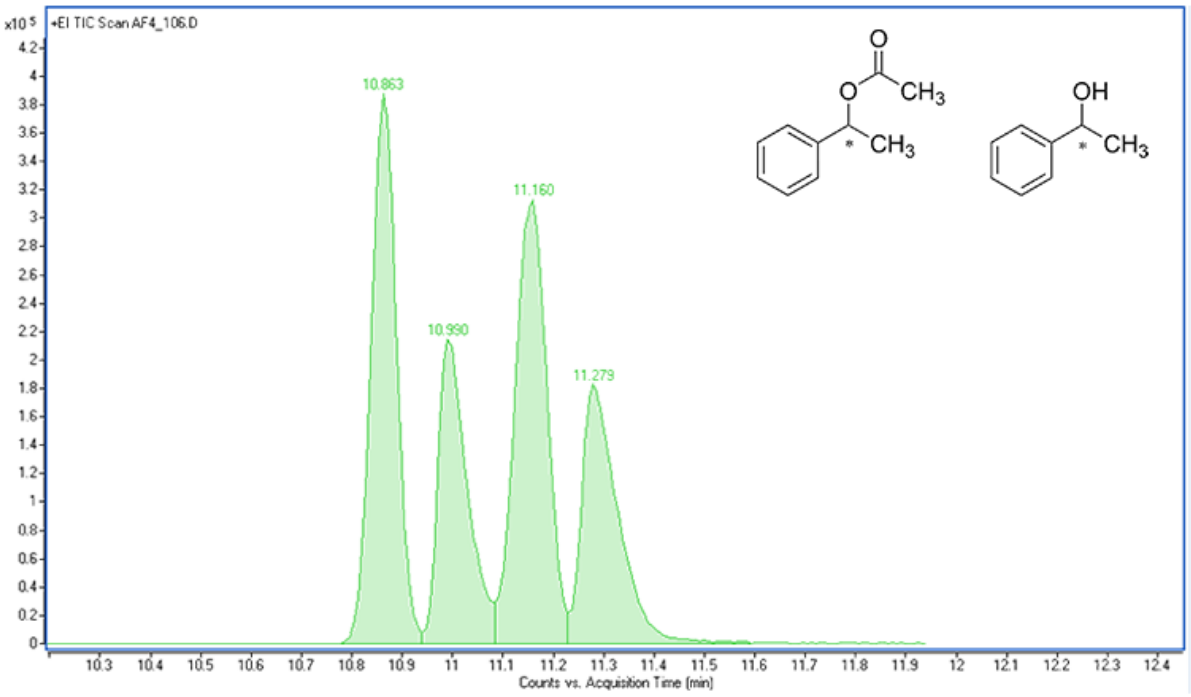

Figure 92: GC-MS Analysis of Reaction of 1-phenyl alcohol with Ac_2O Using **J1** at RT (Table 25, Entry 77).

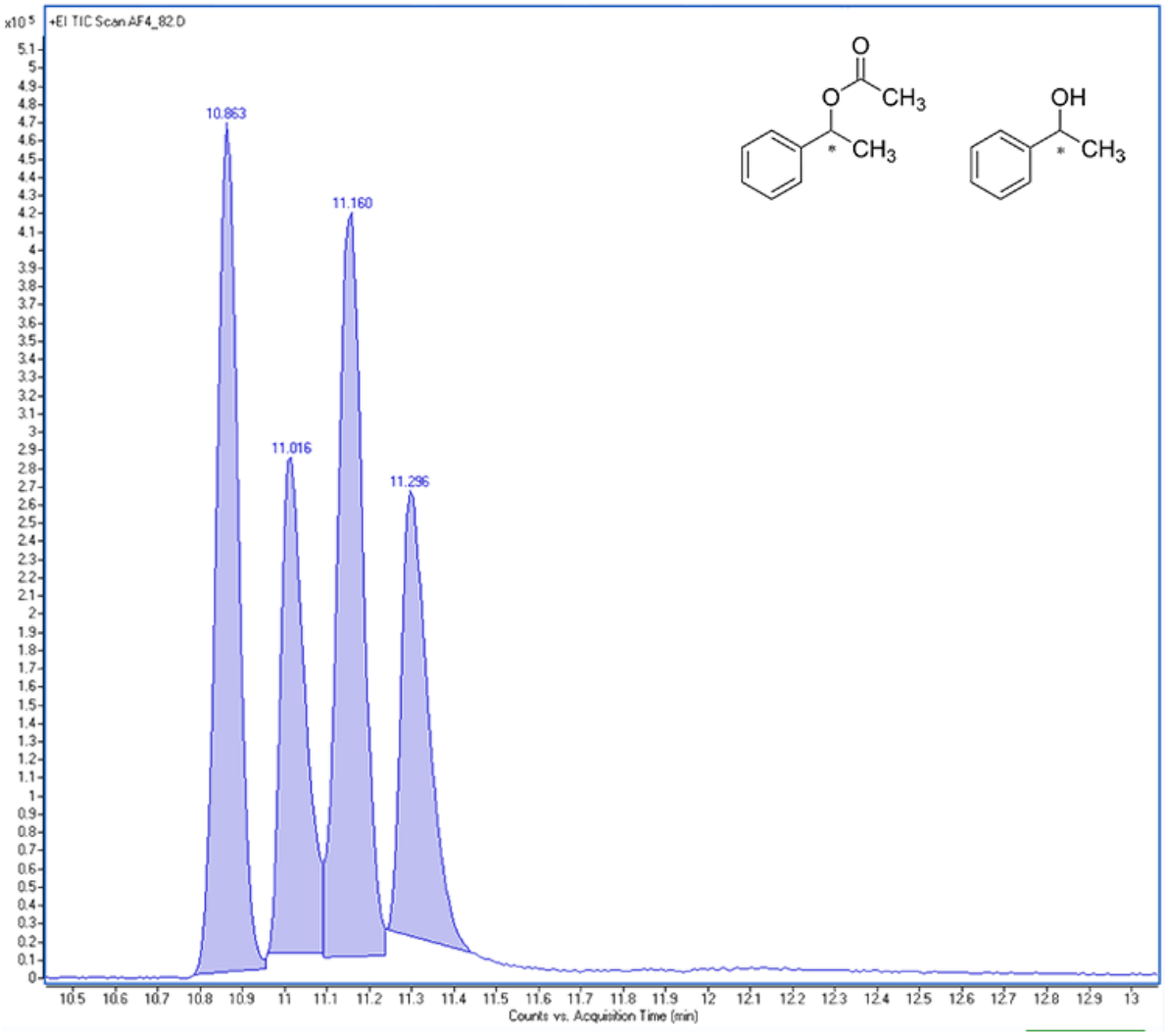

Figure 93: GC-MS Analysis of Reaction of 1-phenyl alcohol with Ac_2O Using **J1** at RT (Table 25, Entry 83).

The same reaction was also performed at 0 °C. 48 % conversion was achieved in 4 days once 1.6 equivalents of Et_3N were used (Table 26, Entry 85), while 6 days were necessary for the same yield when 0.75 equivalents of Et_3N were used (Table 26, Entry 87). The obtained ee were almost identical, varying from 1-2 % (Figures 94 and 95).

Table 26: KR of Racemic 1-phenyl alcohol Using **J1** at 0 ℃.

Entry	Catalyst (mol %)	Ac_2O (eq)	Et_3N (eq)	Time[b]	Yield[c] (%)	$ee_{alcohol}$ %[d]	$ee_{acetate}$ %[d]
84	5 %	1.5	1.6	3 d	39	-	-
85	5 %	1.5	1.6	4 d	48	1	1
86	5 %	1.5	0.75	4 d	34	-	-
87	5 %	1.5	0.75	6 d	48	2	2

[a] Reaction conditions: rac-alcohol (0.16 mmol), Ac_2O (0.75 or 1.5 eq), Et_3N (0.75 or 1.6 mmol) in 800 µL of $CDCl_3$ at RT. [b] Where h indicates hours and d indicates days. [c] Determined by ^{1}H-NMR analysis of the crude products. [d] Determined by chiral GC-MS analysis.

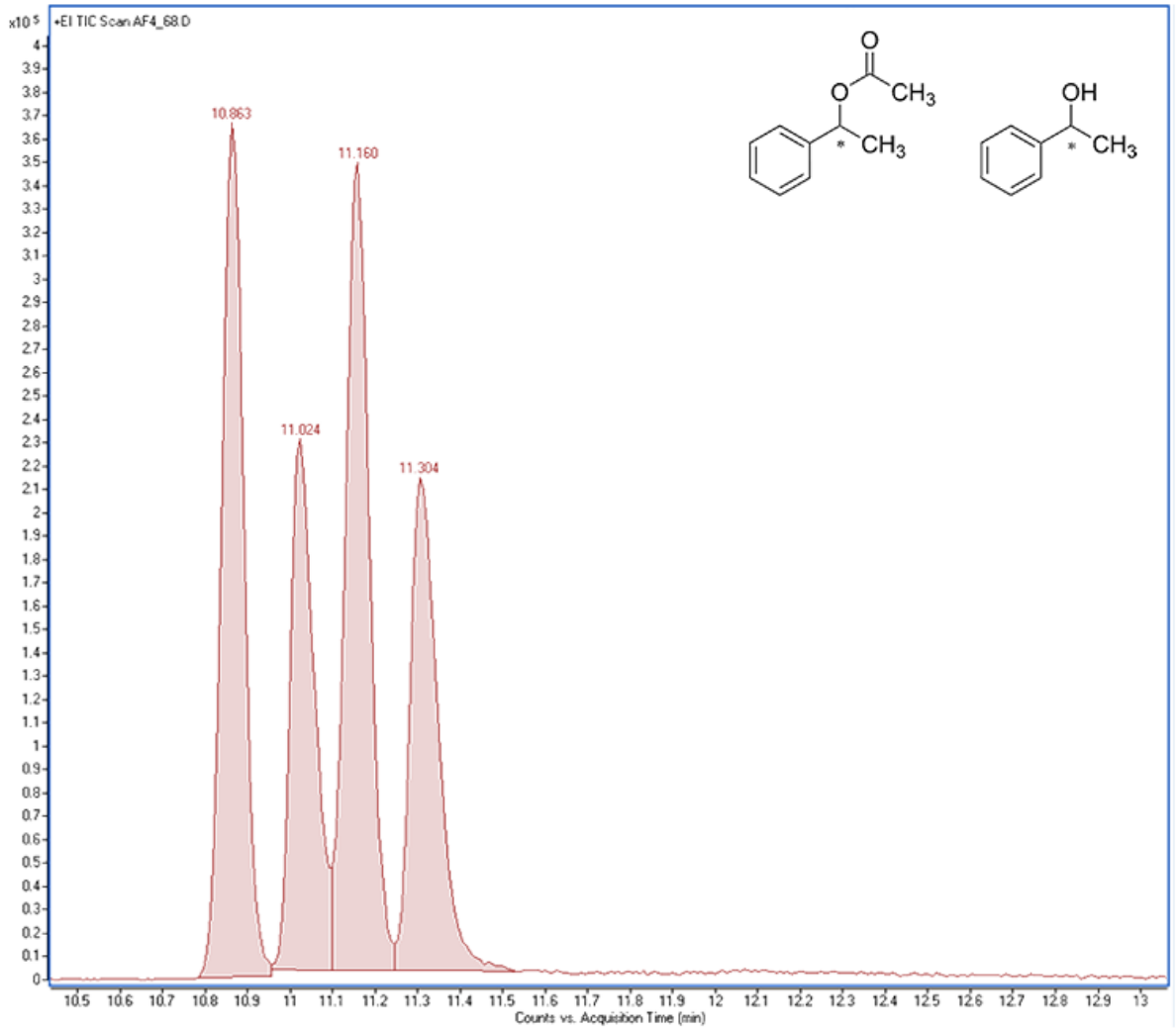

Figure 94: GC-MS Analysis of Reaction of 1-phenyl alcohol with Ac_2O Using **J1** at 0 °C (Table 26, Entry 85).

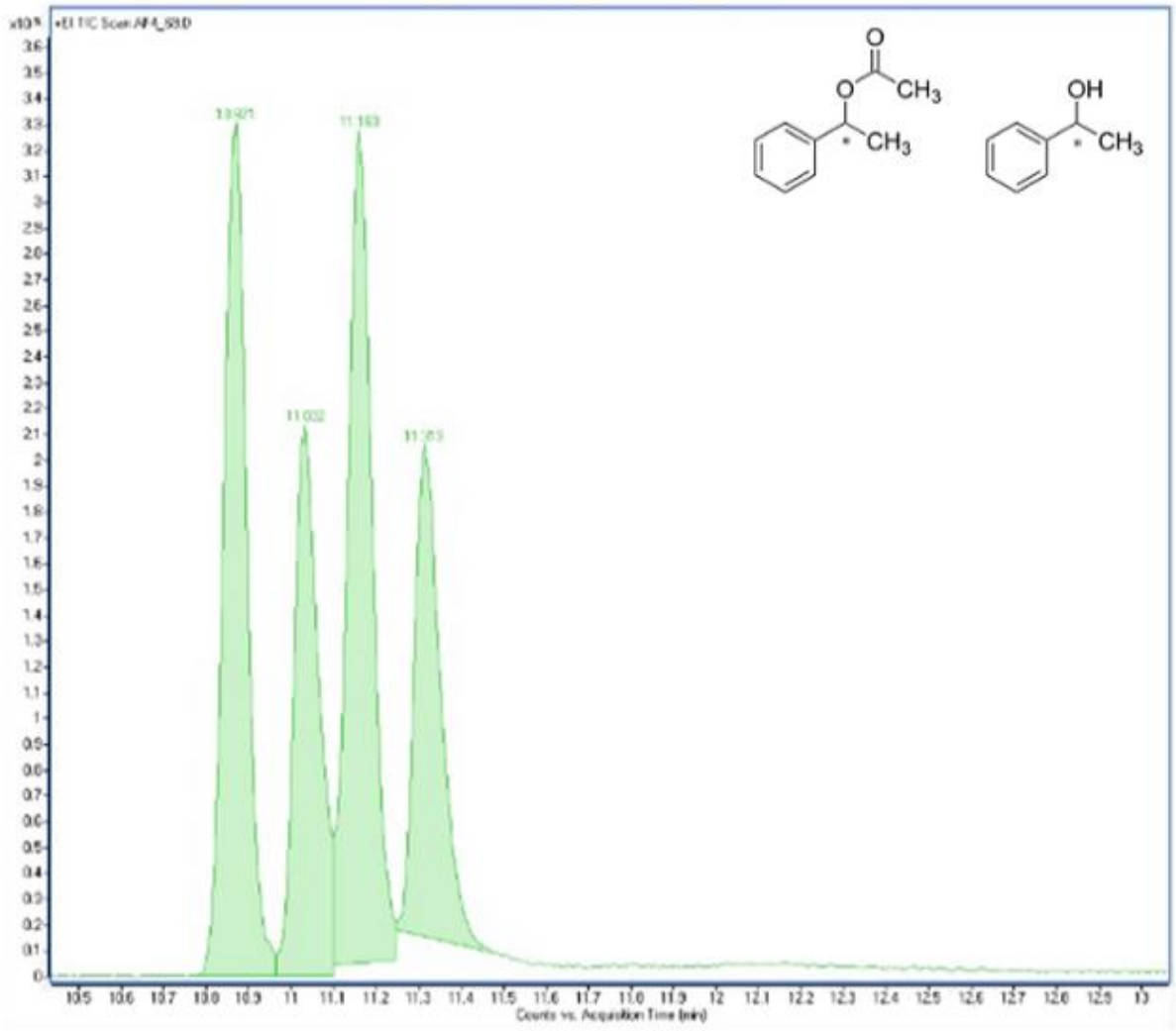

Figure 95: GC-MS Analysis of Reaction of 1-phenyl alcohol with Ac_2O Using **J1** at 0 °C (Table 26, Entry 87).

Overall, we can observe that once 1.6 equivalents of Et_3N were employed at RT, **PP 8** catalyzed the acyl transfer reaction in significantly lower time than **PP 7**. This suggests that the change in the proline monomeric units influenced the catalytic activity of the peptide. Under the same conditions, **PP 7** catalyzed the reaction faster than **J1** and slightly faster than **PP 9**. When 0.75 equivalents of Et_3N were used at RT, **PP 7** and **PP 8** required approximately the same time to catalyze the reaction, which was faster than **PP 9** and remarkably faster than **J1.** These results prove that the quantity of Et_3N plays an important role in the catalytic reaction, while both peptides were more efficient catalysts than the corresponding monomer. It is noteworthy that when 0.75 equivalents of Et_3N were used at 0 °C, **PP 7** catalyzed the reaction much faster than **PP 8**, but in similar times as **PP 9** and **J1**.

Regarding the ee, both **PP 7** and **PP 8** showed very low values for acetate in all the conditions examined. Both polyprolines exhibited the highest ee the alcohol when 0.75 equivalents of Et_3N were used at RT, which were higher than the corresponding values of **J1**. Moreover, the ee values of the alcohol were higher at RT than at 0 °C. Although no enantioselectivity was observed, the desired conversions were achieved and an investigation of different reaction conditions was performed.

3.3 Conclusions and Future Work

3.3.1 Conclusions

A series of polyproline peptides were designed, in order to be tested as catalysts for the asymmetric acyl transfer reaction. The synthesis of the corresponding monomers, the preparation and characterisation of the peptides, and their use as catalyst was described. The conclusions for Target Peptide Group 5 and 6 are discussed below.

3.3.1.1 Target Peptide Group 5

Regarding the first target peptide, the synthesis of the corresponding monomer **F3** was required before its preparation. Starting from **B1,** a multi-step reaction pathway was followed. Firstly, a Mitsunobu reaction was performed. After that, hydrolysis of the ester, a Boc deprotection reaction and an Fmoc protection reaction led to the final product.

After that, **PP 4** comprised of six proline units and one **F3** residue was synthesized according to the Fmoc-based SPPS protocol, on a peptide synthesizer. Oxima Pure, DIC and DIPEA were used as coupling reagents, while the peptide was also treated with an ion exchange resin, after cleavage from the resin and precipitation upon cold Et_2O. Based on the LCMS chromatogram, the peptide was synthesized successfully, and did not need any further purification. Lastly, a CD analysis was

performed in water, revealing that the conformation of **PP 4** in that solvent is indicative of a PolPro II conformation.

The catalytic activity of the peptide was then investigated on the reaction of racemic 1-phenylethanol with Ac_2O in the presence of Et_3N, using $CDCl_3$ as a solvent. The catalytic capacity of monomers **F2** and **F3** were also tested in order to be compared with the one of the peptide **PP 4**. DMAP was firstly employed as a reference catalyst. Using 5 % loading of **PP 4** and 1.5 equivalents of Ac_2O, various conditions were investigated. More specifically, different quantities of Et_3N were used (1.6 and 0.75 equivalents), while the reaction was conducted both at room temperature and at 0 °C. Regarding the time, **PP 4**, **F2** and **F3** exhibited comparable times for 50 % conversion, except for the case when 1.6 equivalents of Et_3N were used at room temperature, where **PP 4** led to the fastest conversion. As a result, among the tested polyprolines, **PP 4** was the best catalyst for these conditions. This result indicates that an **F3** monomeric unit in the middle of the helix of a heptamer peptide is able to act as an efficient catalyst, while the equivalents of Et_3N influence the catalytic reaction. As far as the ee are concerned, the values for the ee of the acetate were very low in all the examined cases. Therefore, a polyproline with an **F3** unit incorporated in the middle of the helix (**PP 4**) is able to catalyze the KR between of racemic 1-phenylethanol with Ac_2O. Nevertheless, the structure of **PP 4** was not sufficient in order for it to act as an enantioselective organocatalyst.

3.3.1.2 Target Peptide Group 6

The synthesis of a series of monomers (**G2**, **G4**, **G6**, **G8**) was attempted, in order to synthesize peptide **PP 5**. In order to achieve this, an Fmoc protection reaction was performed using Fmoc-Cl and LiOH in THF. From the four target monomers, only **G4** was prepared successfully. **PP 5** was prepared using the **G4** monomer. Applying the SPPS proticik on a peptide synthesizer, Oxima Pure, DIC and DIPEA were used as coupling reagents. Nevertheless, analysis through LCMS revealed that the obtained peptide was not the desired one.

An alternative peptide was then designed (**PP 6**), the preparation of which required the synthesis of a dimer. In this way, the dimer could be used during the peptide synthesis, possibly avoiding the synthetic challenge that was faced during the preparation of **PP 5**. The synthesis of the dimer included a reaction between Fmoc-proline and $SOCl_2$ in DCM leading to **I1**, followed by a reaction between **I1** with **G9**. Although **I1** was obtained, its reaction with **G9** was not successful, and would need further investigation.

As a result, another approach was followed. Two set of peptides were designed, **PP 7**, consisted of eight units of L-proline and one **J1** unit in the middle, and **PP 8** which was comprised of four units L-proline, one **J1** residue and four units of D-proline. Using the optimum conditions on the peptide

synthesizer, the preparation of these peptides was achieved via SPPS, employing Oxima Pure, DIC and DIPEA as coupling reagents. According to LCMS analysis, their synthesis was successful, while after CD analysis, both peptides presented a conformation indicative of a PolPro II in water.

Following that, **PP 7** and **PP 8** were tested as organocatalysts in the KR of racemic 1-phenylethanol with Ac_2O in the presence of Et_3N, using $CDCl_3$ as a solvent. The catalytic capacities of **PP 9** and **J1** were also tested, in order to be compared with the ones of peptides **PP 7** and **PP 8**. The reaction was performed similarly to **PP 4**, using different equivalents of Et_3N (1.6 and 0.75), at room temperature and at 0 °C. Regarding the time of the catalytic reaction, when 1.6 equivalents of Et_3N were used at room temperature, **PP 8** catalyzed the reaction remarkably faster than **PP 7**, while both needed less time than **J1** and **PP 9**. Once 0.75 equivalents of Et_3N were used at room temperature, **PP 7** and **PP 8** catalyzed the reaction at approximately the same time, which was faster than **PP 9** and significantly faster than **J1**. Lastly, after employing 0.75 equivalents of Et_3N at 0 °C, **PP 7** catalyzed the reaction much faster than **PP 8**, and in similar times as **PP 9** and **J1**. From these results we can conclude that **PP 7** and **PP 8** led to the fastest conversions at room temperature, with the change in the proline monomeric units influencing the activity of the peptides. As far as the ee values are concerned, **PP 7** and **PP 8** exhibited very low ee for the acetate in all the conditions examined. Thus, although no ee was observed, the reaction conditions were optimised and the desired conversions were obtained.

3.3.2 Future Outlook

Regarding the monomers, a future direction is to further investigate the reaction for the preparation of **G2**, **G4**, **G6** and **G8**. Different reaction conditions could be employed for this purpose, like the use of Fmoc-Cl and Na_2CO_3 in water at room temperature. Moreover, it would also be beneficial to further research the reaction between **I1** and **G9**. For example, the reaction could be performed using DCC and DCM at room temperature in order to investigate whether this would lead to a successful outcome.

Considering that all three peptides showed very low selectivity, a future direction could be expanding the reaction scope. For example, different substrates could be employed, or reaction conditions different from the ones that were tested in this project.

3.4 References

1. Jarvo, E. R., Vasbinder, M. M. & Miller, S. J. Asymmetric acylation reactions catalyzed by conformationally biased octapeptides. *Tetrahedron* **56**, 9773–9779 (2000).
2. Miller, S. J., Copeland, G. T., Papaioannou, N., Horstmann, T. E. & Ruel, E. M. Kinetic resolution of alcohols catalyzed by tripeptides containing the N-alkylimidazole substructure. *J. Am. Chem. Soc.* **120**, 1629–1630 (1998).

3. Copeland, G. T., Jarvo, E. R. & Miller, S. J. Minimal acylase-like peptides. Conformational control of absolute stereospecificity. *J. Org. Chem.* **63**, 6784–6785 (1998).
4. Xie, M. S. *et al.* Rational design of 2-substituted DMAP-N-oxides as acyl transfer catalysts: Dynamic kinetic resolution of azlactones. *J. Am. Chem. Soc.* **142**, 19226–19238 (2020).
5. List, D. B. *Asymmetric Organocatalysis*. *Topics in Current Chemistry* vol. 291 (Springer, 2010).
6. Zhang, S. peng, Fu, X. kai & Fu, S. dong. Rationally designed 4-phenoxy substituted prolinamide phenols organocatalyst for the direct aldol reaction in water. *Tetrahedron Lett.* **50**, 1173–1176 (2009).
7. Cozett, R. E., Venter, G. A., Gokada, M. R. & Hunter, R. Catalytic enantioselective acyl transfer: The case for 4-PPY with a C-3 carboxamide peptide auxiliary based on synthesis and modelling studies. *Org. Biomol. Chem.* **14**, 10914–10925 (2016).
8. Schedel, H. *et al.* Asymmetric desymmetrization of meso-diols by C2-symmetric chiral 4-pyrrolidinopyridines. *Beilstein J. Org. Chem.* **8**, 1778–1787 (2012).
9. Tabanella, S., Valancogne, I. & Jackson, R. F. W. Preparation of enantiomerically pure pyridyl amino acids from serine. *Org. Biomol. Chem.* **1**, 4254–4261 (2003).
10. Spivey, A. C. & McDaid, P. Asymmetric acyl transfer reactions. in *Enantioselective Organocatalysis: Reactions and Experimental Procedures* 287–329 (2007).
11. Pabbaraja, S. *et al.* Synthesis and biological evaluation of 12-, 13-, 14-membered macrolides and open chain 2,6-trans-disubstituted dihydropyran analogues for aspergillides. *Tetrahedron Lett.* **59**, 2570–2576 (2018).
12. Fuwa, H., Ishigai, K., Goto, T., Suzuki, A. & Sasaki, M. Synthetic studies on gambieric acids, potent antifungal polycyclic ether natural products: Reassignment of the absolute configuration of the nonacyclic polyether core by NMR analysis of model compounds. *J. Org. Chem.* **74**, 4024–4040 (2009).
13. Carvajal, J. S. R., Quinteros, D. & Romero, M. R. Application of ion exchange resins in protein seperation and purification. in *Ion Exchange Resins: Biomedical and Environmental Applications* 1–23 (Materials Research Forum LLC, 2023).
14. Garland, K. *et al.* Optimization of globomycin analogs as novel gram-negative antibiotics. *Bioorganic Med. Chem. Lett.* **30**, 127419 (2020).
15. Kakinoki, S., Hirano, Y. & Oka, M. On the stability of polyproline-I and II structures of proline oligopeptides. *Polym. Bull.* **53**, 109–115 (2005).

3.5 Chemicals and Instrumentation

Commercially available reagents obtained from Acros Organics, Sigma Aldrich, Fisher Scientific and FluoroChem, were used without further purification unless otherwise stated. All air-and moisture-insensitive reactions were carried out under ambient atmosphere, and monitored by thin layer chromatography (TLC). Analytical TLC was performed using FluoroChem pre-coated silica gel 60 F254 aluminium plates, that were subjected to UV light or visualised using a vanillin stain, by subsequent heating. All air-and moisture-sensitive reactions were carried out using oven-dried glassware employing standard Schlenk techniques under an atmosphere of N_2. Flash column chromatography was performed on Acros Organics ultrapure 60 silica gel with a particle size 60-200 μm. ^{1}H, ^{13}C and ^{19}F NMR spectra were obtained on a Bruker AVII MHz spectrometer. Chemical shifts

were reported in parts per million (ppm) from low to high field, using TMS as a reference. Coupling constants (J) are reported in Hertz (Hz). Standard abbreviations indicating multiplicity were used as follows: s = singlet, d = doublet, t = triplet, q = quartet, m = multiplet. In the case of some complex multiplets with contributions from more than one signal absolute assignment was not possible. FT-IR spectra were recorded on a Shimadzu IR Affinity-1S spectrophotometer, with peaks being reported in wavenumbers (cm^{-1}). Low resolution mass spectrometry was carried out by the mass spectrometry services at the University of Kent. The data were collected on a Thermo MSQ Plus LCMS system, using a Kromasil C18 HPLC column (250 mm x 4.6 mm x 5 mm).

3.6 Experimental Information

3.6.1 General Procedures

Boc Deprotection-General Procedure

The proline derivative was dissolved in DCM, and the whole was cooled to 0 °C.TFA was added, and the reaction mixture was stirred at room temperature for 2 hours. After that, volatile materials were removed.

Fmoc Protection Using Fmoc-Cl, LiOH (aq) and THF-General Procedure

Fmoc-Cl was added to the starting material, followed by H_20: EtOH (3:1). The whole was stirred at 60 °C overnight. It was then acidified using HCl (1 M) until pH reached ~ 4-5, and extracted with EtOAc (3 x 50 mL). Combined organic layers were dried over $MgSO_4$, filtered and concentrated in *vacuo*.

Solid Phase Peptide Synthesis on the Peptide Synthesizer-General Protocol

Standard Fmoc SPPS procedures were again performed using Rink amide MBHA resin on a 0.1 mmol scale, using a Liberty™ microwave peptide synthesiser (CEM). The resin (300 mg, 0.24 mmol, 1 eq) was swollen in DCM (5 mL) for 1 h, using a 25 mL peptide synthesis vessel. It was then washed with DMF (3 x 3 mL) and place on the peptide synthesis apparatus. Following the same steps as on the manual peptide synthesis (described in Chapter 3), repeated steps of single deprotections, and couplings interspaced with washings were then performed.

Deprotection: 20 % piperidine in DMF for 5 min with 30 W microwave irradiation at 90 °C. Coupling: Fmoc-protected amino acid, DIC, Oxyma Pure, DIPEA and DMF for 5 min at 90 °C with 30 W microwave irradiation. Washings: DMF. Once the desired sequence has been synthesized, the peptide transferred to a round bottom flask, and the cleavage procedure is performed similarly as in the manual peptide synthesis.

The resin was washed with DMF (3 x 3 mL), followed by DCM (3 x 3 mL). A solution of 10 % Ac_2O and 2.5 % DIPEA in DMF was added as the capping solution (3 mL). After spinning for 1 h, the resin was washed with MeOH (3 x 3 mL), and then transferred to a round-bottom flask before the peptide was cleaved from the resin using TFA (95 % in DCM) (3 x 3 mL). After spinning for 2h, the whole was transferred to a peptide synthesis vessel, and the resin was washed with the cleavage cocktail (2 x 1 mL). The solution was then collected in a round bottom flask, and TFA was removed under reduced pressure. The product precipitated upon addition of cold Et_2O, and was centrifuged. The solution was decanted, and the solid was repeatedly washed with cold Et_2O and dried under vacuum to afford the desired peptide.

KR of a Racemic Alcohol-General Protocol

Et_3N (160 µL, 1.12 mmol) was added to a solution of (±)-1-phenylethanol (20 µL, 0.16 mmol) in $CDCl_3$ (700 µL). The catalyst candidate (2-5 mol %) was dissolved in $CDCl_3$ (100 µL) and added to this solution. After cooling the whole to 0 °C, acetic anhydride (110 µL, 1.6 mmol) was added. The reaction was left under stirring. When ^{1}H-NMR showed an adequate conversion, the reaction was stopped. The conversion was analysed through ^{1}H-NMR and the enantiomeric excess was analysed by chiral GC-MS.

3.6.2 PP 4

3.6.2.1 Synthesis of F3

Synthesis of F2

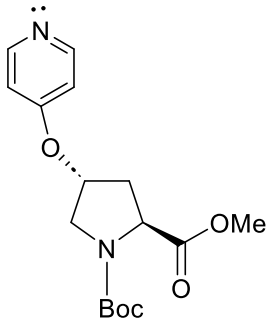

F1 (0.11 g, 0.46 mmol, 1 eq) was dissolved in THF (15 mL). 4-hydroxy pyridine (0.05 g, 0.55 mmol, 1.2 eq) was added under inert atmosphere. Triphenylphospine (0.18 g, 0.69 mmol, 1.5 eq), followed by diisopropyl azodicarboxylate (0.14 mL, 0.69 mmol, 1.5 eq) were then added at 0 °C. Stirring was continued for 30 minutes at 0 °C, and then at room temperature overnight. After that, the reaction mixture was concentrated, and the residue was treated with EtOAc (100 mL) and then Hexane (100 mL), and the excess of 4-hydroxy pyridine was filtered off as a yellow solid. The filtrate was

concentrated under *vacuo* to accelerate crystallization of triphenylphosphine oxide, and filtered off. The filtrate was evaporated and then purified by flash chromatography on silica gel (n-Hex/EtOAc 6/4), which afforded product as a yellow oil (0.12 mg, 83 %). **^{1}H-NMR** (400 MHz, $CDCl_3$) δ 8.39 (d, J = 4.7 Hz, 1H), 7.68 – 7.34 (m, 1H), 6.71 (t, J = 6.0 Hz, 2H), 4.98 – 4.85 (m, 1H), 4.50 – 4.30 (m, 1H), 3.83 – 3.50 (m, 5H), 2.59 – 1.85 (m, 2H), 1.39 (dd, J = 21.4, 10.8 Hz, 9H). **^{13}C-NMR** (100 MHz, $CDCl_3$) δ 172.92 (d, J = 17.8 Hz), 172.80, 162.99, 154.09, 153.45, 151.12 (d, J = 4.2 Hz), 132.93, 131.93 (t, J = 6.7 Hz), 128.44 (d, J = 12.1 Hz), 111.02, 110.77, 80.52, 80.32, 77.49 (d, J = 12.0 Hz), 77.23, 76.91, 75.25, 74.61 (d, J = 19.4 Hz), 57.76, 57.43, 52.19 (d, J = 16.5 Hz), 51.74 (d, J = 15.6 Hz), 51.61, 36.24, 35.31, 29.56, 28.17 (d, J = 11.3 Hz), 21.58, 14.07 (d, J = 8.0 Hz). **IR** (KBr) ν: 2974, 2936, 2880, 1748, 1697, 1394, 1365, 1356, 1273, 1207, 1158, 1130, 815, 767, 722, 546 cm^{-1}. **ESI-MS** (m/z): $[M + H]^+$ calc for $C_{16}H_{22}N_2O_5$ 322.1.

Synthesis of F3

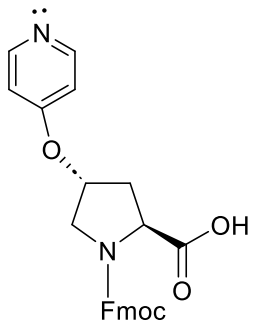

F2 (0.43 g, 1.34 mmol, 1 eq) was dissolved in THF (1.2 mL) and MeOH (0.6 mL). LiOH (0.12 g, 2.83 mmol, 2 eq) in H_2O (0.5 mL) was added, and the whole was stirred for 2 h. The reaction mixture was then concentrated under reduced pressure. Following the Boc deprotection-general procedure, anhydrous TFA (1.3 mL, 7.65 mmol, 15 eq) was added of the crude in DCM (6 mL). Based on the Fmoc protection protocol, the N-Boc-trans-4-hydroxypyridine-L-proline methyl ester (**F2**) (0.12 g, 0.40 mmol, 1 eq) was dissolved in H_2O (0.42 mL) and sodium carbonate (0.05 g, 0.60 mmol, 1.5 eq). Fmoc-Cl (0.15 g, 0.60 mmol, 1.5 eq) in THF (0.84 mL) was then added. Extraction with Et_2O (3 x 100 mL) followed. Combined aqueous layer was acidified with concentrated HCl until pH 1-2 was reached, and then extracted with DCM (3 x 100 mL). Combined organic layers were dried over $MgSO_4$, filtered and concentrated in *vacuo*. The crude residue was purified through flash chromatography on silica gel (DCM/MeOH 9/1) to afford the final product as a white solid (0.12 g, 70 %). **^{1}H-NMR** (400 MHz, MeOD) δ 8.46 – 6.90 (m, 12H), 5.17 – 5.01 (m, 1H), 4.26 (dddt, J = 25.2, 12.2, 9.1, 7.1 Hz, 4H), 3.85 – 3.75 (m, 1H), 3.71 – 3.50 (m, 1H), 3.32 – 3.21 (m, 1H), 2.55 – 2.16 (m, 1H). **^{13}C-NMR** (100 MHz, MeOD) δ 127.39, 119.48, 111.49 – 110.64 (m), 50.11 – 49.31 (m), 48.25, 47.93 (d, J =

20.6 Hz), 47.72 – 47.11 (m), 46.98. **IR** (KBr) ν: 3358, 1636, 1592, 1509, 1387, 1295, 1201, 1055, 1002, 826 cm^{-1}. **ESI-MS** (m/z): $[M + H]^+$ calc for $C_{25}H_{22}N_2O_5$ 430.1.

3.6.2.2 Synthesis of PP 4 Peptide

PP 4 was synthesized using the SPPS on the peptide synthesizer protocol. The peptide was obtained as a white solid (100 mg, 67 %). **^{1}H-NMR** (400 MHz, $CDCl_3$) δ 2.47 – 2.09 (m, 181H), 2.06 – 1.89 (m, 114H). **ESI-MS** (m/z): $[M + H]^+$ calc for $C_{47}H_{57}N_9O_9$ 832.4.

3.6.2.3 KR of a Racemic Alcohol Using PP 4

Reaction of 1-Phenyl Alcohol with Ac_2O Using PP 4 at RT (Table 13, Entry 14)

The product was synthesized using the KR of racemic 1-phenylethanol general protocol. **^{1}H-NMR** (400 MHz, $CDCl_3$) δ 10.56 (s, 2H), 7.42 – 7.05 (m, 10H), 5.81 (q, *J* = 6.6 Hz, 1H), 4.80 (q, *J* = 6.5 Hz, 1H), 2.15 (s, 12H), 2.01 – 1.98 (m, 3H), 1.89 (s, 5H), 1.44 (dd, *J* = 23.9, 6.6 Hz, 6H). **^{13}C-NMR** (100 MHz, $CDCl_3$) δ 170.36, 145.88, 141.69, 129.02 – 124.52, 77.10, 72.33, 70.39, 45.64, 45.64, 30.62 – 28.89, 25.20, 21.78 (d, *J* = 85.6 Hz), 8.64. **GC-MS:** Retention times (min): S-acetate 10.86, R-alcohol 11.00, R-acetate 11.15, S-alcohol 11.29.

Reaction of 1-Phenyl Alcohol with Ac_2O Using PP 4 at RT (Table 13, Entry 16)

The product was synthesized using the KR of racemic 1-phenylethanol general protocol. **^{1}H-NMR** (400 MHz, $CDCl_3$) δ 10.74 (s, 2H), 7.48 – 6.93 (m, 11H), 5.79 – 5.70 (m, 1H), 4.78 – 4.67 (m, 1H), 2.07 (dd, *J* = 6.7, 2.7 Hz, 7H), 1.93 (dd, *J* = 6.3, 2.4 Hz, 3H), 1.85 – 1.80 (m, 5H), 1.44 – 1.31 (m, 7H). **GC-MS:** Retention times (min): S-acetate 10.87, R-alcohol 11.01, R-acetate 11.15, S-alcohol 11.30.

Reaction of 1-Phenyl Alcohol with Ac_2O Using PP 4 at 0 °C (Table 14, Entry 19)

The product was synthesized using the KR of racemic 1-phenylethanol general protocol. **^{1}H-NMR** (400 MHz, $CDCl_3$) δ 10.58 (s, 2H), 7.42 – 6.99 (m, 9H), 5.79 (q, *J* = 6.6 Hz, 0.7H), 4.77 (q, *J* = 6.5 Hz, 1H), 2.11 (d, *J* = 7.2 Hz, 7H), 1.99 – 1.95 (m, 2H), 1.86 (d, *J* = 7.2 Hz, 4H), 1.47 – 1.35 (m, 6H). **GC-MS:** Retention times (min): S-acetate 10.86, R-alcohol 11.01, R-acetate 11.16, S-alcohol 11.30.

Reaction of 1-Phenyl Alcohol with Ac_2O Using PP 4 at 0 °C (Table 14, Entry 20)

The product was synthesized using the KR of racemic 1-phenylethanol general protocol. **^{1}H-NMR** (400 MHz, $CDCl_3$) δ 10.73 (s, 2H), 7.42 – 7.06 (m, 9H), 5.81 (q, *J* = 6.6 Hz, 0.7H), 4.81 (q, *J* = 6.5 Hz,

1H), 2.14 (d, *J* = 3.9 Hz, 7H), 2.03 – 1.97 (m, 2H), 1.90 (s, 4H), 1.44 (dd, *J* = 22.7, 6.5 Hz, 6H). **GC-MS:** Retention times (min): S-acetate 10.86, R-alcohol 11.02, R-acetate 11.16, S-alcohol 11.31.

Reaction of 1-Phenyl Alcohol with Ac_2O Using F2 at RT (Table 15, Entry 26)

The product was synthesized using the KR of racemic 1-phenylethanol general protocol. **^{1}H-NMR** (400 MHz, $CDCl_3$) δ 8.36 (s, 1H), 7.48 – 7.05 (m, 10H), 5.81 (q, *J* = 6.6 Hz, 1H), 4.83 (q, *J* = 6.3 Hz, 1H), 2.02 – 1.97 (m, 3H), 1.94 (d, *J* = 0.9 Hz, 2H), 1.49 – 1.32 (m, 9H). **GC-MS:** Retention times (min): S-acetate 10.87, R-alcohol 11.00, R-acetate 11.16, S-alcohol 11.28.

Reaction of 1-Phenyl Alcohol with Ac_2O Using F2 at RT (Table 15, Entry 29)

The product was synthesized using the KR of racemic 1-phenylethanol general protocol. **^{1}H-NMR** (400 MHz, $CDCl_3$) δ 9.88 – 9.46 (m, 1H), 7.48 – 7.10 (m, 10H), 5.83 (q, *J* = 6.6 Hz, 1H), 4.83 (q, *J* = 6.5 Hz, 1H), 2.20 – 2.12 (m, 10H), 2.03 – 1.99 (m, 3H), 1.93 (s, 4H), 1.45 (dt, *J* = 11.5, 5.8 Hz, 6H). **GC-MS:** Retention times (min): S-acetate 10.87, R-alcohol 11.00, R-acetate 11.16, S-alcohol 11.29.

Reaction of 1-Phenyl Alcohol with Ac_2O Using F2 at 0 °C (Table 16, Entry 30)

The product was synthesized using the KR of racemic 1-phenylethanol general protocol. **^{1}H-NMR** (400 MHz, $CDCl_3$) δ 11.83 (s, 3H), 7.46 – 7.08 (m, 11H), 5.83 (q, *J* = 6.6 Hz, 1H), 4.82 (q, *J* = 6.5 Hz, 1H), 2.17 (s, 11H), 2.01 (d, *J* = 6.0 Hz,4H), 1.92 (s, 7H), 1.45 (dt, *J* = 10.7, 5.4 Hz, 7H). **GC-MS:** Retention times (min): S-acetate 10.87, R-alcohol 11.05, R-acetate 11.17, S-alcohol 11.33.

Reaction of 1-Phenyl Alcohol with Ac_2O Using F2 at 0 °C (Table 16, Entry 31)

The product was synthesized using the KR of racemic 1-phenylethanol general protocol. **^{1}H-NMR** (400 MHz, $CDCl_3$) δ 10.22 (s, 2H), 7.42 – 7.06 (m, 12H), 5.80 (dd, *J* = 13.1, 6.5 Hz, 1H), 4.80 (dd, *J* = 12.9, 6.4 Hz, 1H), 2.17 – 2.12 (m, 14H), 2.00 (dd, *J* = 5.3, 3.7 Hz, 4H), 1.93 – 1.87 (m, 5H), 1.44 (ddd, *J* = 13.5, 8.9, 4.0 Hz, 7H). **GC-MS:** Retention times (min): S-acetate 10.87, R-alcohol 11.03, R-acetate 11.16, S-alcohol 11.31.

Reaction of 1-Phenyl Alcohol with Ac_2O Using F3 at RT (Table 17, Entry 35)

The product was synthesized using the KR of racemic 1-phenylethanol general protocol. **^{1}H-NMR** (400 MHz, $CDCl_3$) δ 10.73 (s, 2H), 7.37 – 7.01 (m, 11H), 5.77 (q, *J* = 6.6 Hz, 1H), 4.76 (q, *J* = 6.5 Hz, 1H), 2.16 – 2.07 (m, 18H), 1.95 (d, *J* = 7.6 Hz, 3H), 1.85 (d, *J* = 3.1 Hz, 5H), 1.40 (dd, *J* = 25.1, 6.5 Hz, 7H). **GC-MS:** Retention times (min): S-acetate 10.86, R-alcohol 11.00, R-acetate 11.16, S-alcohol 11.29.

Reaction of 1-Phenyl Alcohol with Ac_2O Using F3 at RT (Table 17, Entry 38)

The product was synthesized using the KR of racemic 1-phenylethanol general protocol. **^{1}H-NMR** (400 MHz, $CDCl_3$) δ 10.91 (s, 3H), 7.28 (s, 13H), 5.81 (s, 1H), 4.81 (s, 1H), 1.99 (s, 3H), 1.92 (s, 4H), 1.47 (s, 10H). **GC-MS:** Retention times (min): S-acetate 10.86, R-alcohol 11.01, R-acetate 11.15, S-alcohol 11.30.

Reaction of 1-Phenyl Alcohol with Ac_2O Using F3 at 0 °C (Table 18, Entry 39)

The product was synthesized using the KR of racemic 1-phenylethanol general protocol. **^{1}H-NMR** (400 MHz, $CDCl_3$) δ 10.74 (s, 2H), 7.41 – 7.04 (m, 10H), 5.82 (q, *J* = 6.6 Hz, 1H), 4.81 (q, *J* = 6.5 Hz, 1H), 2.15 (d, *J* = 3.9 Hz, 12H), 2.00 (d, *J* = 3.5 Hz, 3H), 1.92 – 1.89 (m, 5H), 1.45 (dd, *J* = 23.2, 6.5 Hz, 6H). **GC-MS:** Retention times (min): S-acetate 10.87, R-alcohol 11.02, R-acetate 11.16, S-alcohol 11.30.

Reaction of 1-Phenyl Alcohol with Ac_2O Using F3 at 0 °C (Table 18, Entry 40)

The product was synthesized using the KR of racemic 1-phenylethanol general protocol. **^{1}H-NMR** (400 MHz, $CDCl_3$) δ 10.52 – 9.61 (m, 2H), 7.42 – 7.10 (m, 10H), 5.84 (q, *J* = 6.6 Hz, 0.9H), 4.85 (q, *J* = 6.5 Hz, 1H), 2.21 – 2.15 (m, 15H), 2.03 (d, *J* = 3.6 Hz, 3H), 1.94 (s, 5H), 1.48 (dd, *J* = 21.1, 6.5 Hz, 6H). **GC-MS:** Retention times (min): S-acetate 10.87, R-alcohol 11.04, R-acetate 11.17, S-alcohol 11.32.

3.6.3 PP 7 and PP 8

Synthesis of G4

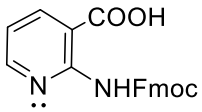

THF (8 mL) was added to a solution of the starting material (0.5 g, 3.62 mmol, 1 eq) in aqueous 1N LiOH (6 mL). Fmoc-Cl (1.41 g, 5.43 mmol, 1.5 mmol) in THF (2 mL), followed by a solution of aqueous 1N LiOH (9 mL) were added slowly to this solution under vigorous stirring in ice-bath. After 1h at 0 °C, the reaction was left under stirring at room temperature overnight. The pH was adjusted to ∼ 12 by adding NaOH (1M), and the reaction mixture was extracted with Et_2O (x 3). Aqueous layers were combined and acidified upon addition of HCl. Once the pH reached∼ 1-2, they were then extracted with DCM (x 3). Combined organic layers were dried over MgSO4, filtered, and concentrated under *vacuo*, to afford the desired product (0.61 g, 47 %). **^{1}H-NMR** (400 MHz, DMSO) δ 10.59 (s, 1H), 8.52 (dd, *J* = 4.8, 1.9 Hz, 1H), 8.22 (dd, *J* = 7.7, 1.9 Hz, 1H), 7.91 (d, *J* = 7.5 Hz, 2H), 7.75 (d, *J* = 7.4 Hz, 2H), 7.47 – 7.20 (m, 5H), 4.43 – 4.36 (m, 2H), 4.36 – 4.29 (m, 1H). **^{13}C-NMR** (100 MHz, DMSO) δ 168.38, 152.78, 151.97, 151.25,

144.11, 141.21, 140.22, 127.92, 125.73, 120.65, 119.58, 116.69, 66.82, 46.88. **IR** (KBr) v: 3854, 3734, 3649, 3566, 2369, 1734, 1699, 1638, 1508, 1227, 1061, 758, 689, 532 cm^{-1}. **ESI-MS** (m/z): $[M + H]^+$ calc for $C_{21}H_{16}N_2O_4$ 361.11.

Synthetic Attempts of G2, G4, G6, G8

The synthesis of compounds **G2**, **G4**, **G6**, **G8** was attempted using the Fmoc-Cl, LiOH (aq) and THF protocol.

Synthetic Attempt of I2

The starting material (1 g, 2.96 mmol, 1 eq) was dissolved in DCM, and $SOCl_2$ (2.15 mL, 29.6 mmol, 10 eq) was add slowly. The whole was refluxed at 85 °C. After 2h, a few drops of DMF were added, and the reaction mixture was left under stirring for 1.30 h. It was then concentrated in *vacuo,* before moving to the next step.

G11 (0.28 g, 2 mmol, 1 eq) was dissolved in DCM (15 mL) and stirred for 2 h. After that, a solution of **I1** (2.96 mmol, 1.05 g, 1.5 eq) in DCM (15 mL) was added, followed by Et_3N (0.73 mL, 6 mmol, 3 eq) at 0 °C. solution brought to room temperature, and stirred overnight. The whole was allowed to warm up to room temperature and stirred at room temperature overnight.

3.6.3.1 Synthesis of PP 7 Peptide

PP 7 was synthesized using the SPPS on the peptide synthesizer protocol. The peptide was obtained as a white solid (110 mg, 65 %). **^{1}H-NMR** (400 MHz, $CDCl_3$) δ 8.31 – 7.69 (m, 3H), 6.80 – 6.56 (m, 1H), 5.56 – 5.07 (m, 2H), 4.90 – 4.17 (m, 5H), 3.70 (dddd, *J* = 34.1, 27.3, 26.7, 18.5 Hz, 12H), 2.57 (d, *J* = 6.0 Hz, 1H), 2.39 – 1.63 (m, 29H), 1.40 – 1.18 (m, 1H), 0.87 (s, 1H). **ESI-MS** (m/z): $[M + H]^+$ calc for $C_{47}H_{63}N_{11}O_{10}$ 942.5.

3.6.3.2 Synthesis of PP 8 Peptide

PP 8 was synthesized using the SPPS on the peptide synthesizer protocol. The peptide was obtained as a white solid (105 mg, 62 %). **^{1}H-NMR** (400 MHz, $CDCl_3$) δ 8.33 – 7.76 (m, 3H), 6.70 (d, J = 34.1 Hz, 1H), 5.24 (s, 1H), 4.95 – 4.17 (m, 6H), 4.04 – 3.25 (m, 12H), 2.40 – 1.78 (m, 22H), 1.29 (d, J = 31.1 Hz, 2H). **ESI-MS** (m/z): $[M + H]^+$ calc for $C_{47}H_{63}N_{11}O_{10}$ 942.5.

3.6.3.3 KR of a Racemic Alcohol Using PP 7, PP8 and PP9

Reaction of 1-Phenyl Alcohol with Ac_2O Using PP 7 at RT (Table 19, Entry 42)

The product was synthesized using the KR of racemic 1-phenylethanol general protocol. **^{1}H-NMR** (400 MHz, $CDCl_3$) δ 10.55 (s, 1H), 7.35 – 7.10 (m, 10H), 5.79 (q, *J* = 6.6 Hz, 0.9H), 4.82 – 4.73 (m, 1H), 2.15 – 2.11 (m, 12H), 1.97 (d, *J* = 3.5 Hz, 3H), 1.87 (s, 4H), 1.42 (dd, *J* = 24.2, 6.5 Hz, 6H). **GC-MS:** Retention times (min): S-acetate 10.86, R-alcohol 11.02, R-acetate 11.16, S-alcohol 11.30.

Reaction of 1-Phenyl Alcohol with Ac_2O Using PP 7 at RT (Table 19, Entry 44)

The product was synthesized using the KR of racemic 1-phenylethanol general protocol. **^{1}H-NMR** (400 MHz, $CDCl_3$) δ 9.18 (s, 1H), 7.38 – 7.14 (m, 9H), 5.84 (q, *J* = 6.6 Hz, 0.7H), 4.83 (q, *J* = 6.5 Hz, 1H), 2.16 (d, *J* = 3.8 Hz, 7H), 2.01 (d, *J* = 7.6 Hz, 2H), 1.93 (s, 3H), 1.47 (dd, *J* = 23.5, 6.5 Hz, 5H). **GC:** Retention times (min): S-acetate 10.86, R-alcohol 11.00, R-acetate 11.15, S-alcohol 11.29.

Reaction of 1-Phenyl Alcohol with Ac_2O Using PP 7 at 0 °C (Table 20, Entry 45)

The product was synthesized using the KR of racemic 1-phenylethanol general protocol. **^{1}H-NMR** (400 MHz, $CDCl_3$) δ 11.41 (s, 2H), 7.37 – 7.09 (m, 10H), 5.80 (q, *J* = 6.6 Hz, 1H), 4.79 (q, *J* = 6.5 Hz, 1H), 2.16 – 2.12 (m, 23H), 1.99 (s, 3H), 1.89 (s, 6H), 1.46 (d, *J* = 6.6 Hz, 3H), 1.40 (d, *J* = 6.5 Hz, 3H). **GC-MS:** Retention times (min): S-acetate 10.86, R-alcohol 11.02, R-acetate 11.16, S-alcohol 11.31.

Reaction of 1-Phenyl Alcohol with Ac_2O Using PP 7 at 0 °C (Table 20, Entry 48)

The product was synthesized using the KR of racemic 1-phenylethanol general protocol. **^{1}H-NMR** (400 MHz, $CDCl_3$) δ 10.13 (s, 2H), 7.42 – 7.01 (m, 10H), 5.82 (q, *J* = 6.6 Hz, 1H), 4.82 (q, *J* = 6.5 Hz, 1H), 2.01 (d, *J* = 1.6 Hz, 3H), 1.93 (s, 5H), 1.45 (ddd, *J* = 24.6, 6.6, 1.4 Hz, 6H). **GC-MS:** Retention times (min): S-acetate 10.86, R-alcohol 10.98, R-acetate 11.15, S-alcohol 11.26.

Reaction of 1-Phenyl Alcohol with Ac_2O Using PP 8 at RT (Table 21, Entry 49)

The product was synthesized using the KR of racemic 1-phenylethanol general protocol. **^{1}H-NMR** (400 MHz, $CDCl_3$) δ 10.21 (s, 2H), 7.38 – 7.06 (m, 10H), 5.78 (q, *J* = 6.6 Hz, 0.7H), 4.77 (q, *J* = 6.5 Hz, 1H), 2.12 (s, 15H), 1.97 (s, 2H), 1.86 (s, 4H), 1.41 (dd, *J* = 25.8, 6.5 Hz, 6H). **GC-MS:** Retention times (min): S-acetate 10.86, R-alcohol 11.01, R-acetate 11.15, S-alcohol 11.30.

Reaction of 1-Phenyl Alcohol with Ac_2O Using PP 8 at RT (Table 21, Entry 51)

The product was synthesized using the KR of racemic 1-phenylethanol general protocol. **^{1}H-NMR** (400 MHz, $CDCl_3$) δ 9.92 (s, 2H), 7.36 – 7.13 (m, 10H), 5.86 – 5.78 (m, 1H), 4.86 – 4.78 (m, 1H), 2.18 – 2.13 (m, 11H), 2.01 (dd, *J* = 4.4, 3.0 Hz, 3H), 1.93 (s, 5H), 1.45 (ddd, *J* = 11.8, 6.4, 4.9 Hz, 6H). **GC-MS:** Retention times (min): S-acetate 10.87, R-alcohol 11.02, R-acetate 11.16, S-alcohol 11.31.

Reaction of 1-Phenyl Alcohol with Ac_2O Using PP 8 at 0 °C (Table 22, Entry 53)

The product was synthesized using the KR of racemic 1-phenylethanol general protocol. **^{1}H-NMR** (400 MHz, $CDCl_3$) δ 11.90 (s, 4H), 7.32 – 7.00 (m, 10H), 5.75 (q, *J* = 6.6 Hz, 1H), 4.74 (q, *J* = 6.5 Hz, 1H), 2.11 – 2.07 (m, 11H), 1.94 (s, 3H), 1.85 (s, 10H), 1.43 – 1.31 (m, 7H). **GC-MS:** Retention times (min): S-acetate 10.87, R-alcohol 11.02, R-acetate 11.16, S-alcohol 11.30.

Reaction of 1-Phenyl Alcohol with Ac_2O Using PP 8 at 0 °C (Table 22, Entry 60)

The product was synthesized using the KR of racemic 1-phenylethanol general protocol. **^{1}H-NMR** (400 MHz, $CDCl_3$) δ 11.30 (s, 7H), 7.41 – 7.16 (m, 10H), 5.85 (q, *J* = 6.3 Hz, 1H), 4.92 – 4.73 (m, 1H), 2.22 – 2.17 (m, 2H), 2.05 (dd, *J* = 2.1, 1.5 Hz, 3H), 2.01 (d, *J* = 0.8 Hz, 19H), 1.48 (ddd, *J* = 7.3, 6.2, 1.8 Hz, 6H). **GC-MS:** Retention times (min): S-acetate 10.86, R-alcohol 11.04, R-acetate 11.16, S-alcohol 11.33.

Reaction of 1-Phenyl Alcohol with Ac_2O Using PP 9 at RT (Table 23, Entry 64)

The product was synthesized using the KR of racemic 1-phenylethanol general protocol. **^{1}H-NMR** (400 MHz, $CDCl_3$) δ 7.41 – 6.98 (m, 9H), 5.81 (q, *J* = 6.6 Hz, 1H), 4.83 (q, *J* = 6.4 Hz, 1H), 2.15 (s, 1H), 2.00 (s, 2H), 1.92 (s, 1H), 1.45 (dd, *J* = 13.8, 6.5 Hz, 5H). **GC-MS:** Retention times (min): S-acetate 10.86, R-alcohol 11.00, R-acetate 11.15, S-alcohol 11.28.

Reaction of 1-Phenyl Alcohol with Ac_2O Using PP 9 at RT (Table 23, Entry 67)

The product was synthesized using the KR of racemic 1-phenylethanol general protocol. **^{1}H-NMR** (400 MHz, $CDCl_3$) δ 9.72 – 9.32 (m, 2H), 7.39 – 7.13 (m, 10H), 5.83 (q, *J* = 6.6 Hz, 1H), 4.83 (q, *J* = 6.5 Hz, 1H), 2.18 – 2.11 (m, 11H), 2.01 (d, *J* = 3.6 Hz, 3H), 1.93 (s, 4H), 1.46 (dd, *J* = 23.1, 6.5 Hz, 7H). **GC-MS:** Retention times (min): S-acetate 10.86, R-alcohol 11.01, R-acetate 11.15, S-alcohol 11.29.

Reaction of 1-Phenyl Alcohol with Ac_2O Using PP 9 at 0 °C (Table 24, Entry 68)

The product was synthesized using the KR of racemic 1-phenylethanol general protocol. **^{1}H-NMR** (400 MHz, $CDCl_3$) δ 8.64 (s, 1H), 7.31 – 7.12 (m, 10H), 5.79 (q, *J* = 6.6 Hz, 0.9H), 4.78 (q, *J* = 6.5 Hz, 1H), 2.13 – 2.10 (m, 8H), 1.97 (d, *J* = 3.7 Hz, 3H), 1.89 (s, 4H), 1.42 (dd, *J* = 21.8, 6.5 Hz, 6H). **GC-MS:** Retention times (min): S-acetate 10.86, R-alcohol 11.00, R-acetate 11.16, S-alcohol 11.28.

Reaction of 1-Phenyl Alcohol with Ac_2O Using PP 9 at 0 °C (Table 24, Entry 71)

The product was synthesized using the KR of racemic 1-phenylethanol general protocol. **^{1}H-NMR** (400 MHz, $CDCl_3$) δ 10.41 (s, 4H), 7.70 – 6.93 (m, 13H), 5.97 – 5.74 (m, 1H), 4.81 (d, *J* = 6.2 Hz, 1H), 3.12 – 2.94 (m, 7H), 2.22 – 1.88 (m, 22H), 1.43 (dd, *J* = 23.4, 6.5 Hz, 7H). **GC-MS:** Retention times (min): S-acetate 10.86, R-alcohol 11.00, R-acetate 11.15, S-alcohol 11.29.

Reaction of 1-Phenyl Alcohol with Ac_2O Using J1 at RT (Table 25, Entry 77)

The product was synthesized using the KR of racemic 1-phenylethanol general protocol. **^{1}H-NMR** (400 MHz, $CDCl_3$) δ 7.35 – 7.10 (m, 17H), 6.13 (q, *J* = 6.6 Hz, 1H), 5.80 (q, *J* = 6.6 Hz, 1H), 1.98 (s, 6H), 1.66 (d, *J* = 6.6 Hz, 3H), 1.43 (dt, *J* = 11.7, 5.9 Hz, 8H). **GC-MS:** Retention times (min): S-acetate 10.86, R-alcohol 11.00, R-acetate 11.16, S-alcohol 11.28.

Reaction of 1-Phenyl Alcohol with Ac_2O Using J1 at RT (Table 25, Entry 83)

The product was synthesized using the KR of racemic 1-phenylethanol general protocol. **^{1}H-NMR** (400 MHz, $CDCl_3$) δ 9.40 (s, 2H), 7.41 – 7.10 (m, 11H), 5.82 (q, *J* = 6.6 Hz, 1H), 4.81 (q, *J* = 6.5 Hz, 1H), 2.13 (s, 3H), 2.00 (s, 3H), 1.94 (s, 5H), 1.53 – 1.37 (m, 7H). **GC-MS:** Retention times (min): S-acetate 10.86, R-alcohol 11.02, R-acetate 11.16, S-alcohol 11.30.

Reaction of 1-Phenyl Alcohol with Ac_2O Using J1 at 0 °C (Table 26, Entry 85)

The product was synthesized using the KR of racemic 1-phenylethanol general protocol. **^{1}H-NMR** (400 MHz, $CDCl_3$) δ 11.11 (s, 2H), 7.37 – 7.10 (m, 10H), 5.81 (q, *J* = 6.6 Hz, 0.9H), 4.81 (q, *J* = 6.5 Hz, 1H), 2.00 (s, 3H), 1.89 (d, *J* = 3.2 Hz, 6H), 1.44 (dd, *J* = 23.0, 6.5 Hz, 6H). **GC-MS:** Retention times (min): S-acetate 10.86, R-alcohol 11.02, R-acetate 11.16, S-alcohol 11.30.

Reaction of 1-Phenyl Alcohol with Ac_2O Using J1 at 0 °C (Table 26, Entry 87)

The product was synthesized using the KR of racemic 1-phenylethanol general protocol. **^{1}H-NMR** (400 MHz, $CDCl_3$) δ 10.21 (s, 1H), 7.37 – 7.13 (m, 10H), 5.82 (q, *J* = 6.6 Hz, 0.9H), 4.82 (q, *J* = 6.5 Hz, 1H), 2.00 (d, *J* = 7.0 Hz, 3H), 1.93 – 1.90 (m, 5H), 1.45 (dd, *J* = 22.3, 6.5 Hz, 6H). **GC-MS:** Retention times (min): S-acetate 10.87, R-alcohol 11.03, R-acetate 11.16, S-alcohol 11.31.

Chapter 4

Conclusions

Organocatalysis is a relatively new field that is characterized by many advantages and is now considered complementary to metallic catalysis. Through enantioselective organocatalysis the synthesis of enantiomerically pure molecules can be achieved. Considering the importance of chiral compounds, this is of outmost importance for many fields. Apart from achieving enantioselectivity, in many cases it is important to obtain both enantiomeric or diastereomeric products. This can be achieved through stereodivergennt organocatalysis, by making minor changes in the structure of the catalyst or the reaction conditions.

Specifically, peptides, due to their unique characteristics, are able to catalyze asymmetric transformations leading to high yields and enantioselectivities, at the same time that they can exhibit stereodivergence. Among various peptides, polyprolines have many advantageous properties. They can be prepared via an easily accessible amino acid, at the same time introduction of functional groups capable of performing organocatalytic transformations can be achieved with high position control. Moreover, polyproline shows a conformational switch between two rigid chiral secondary structures (PolPro I and PolPro II), depending on the conditions used. For this reason, the focus of this research has been the study of polyprolines and identifying whether they could act as organocatalysts.

In this context, this project included the preparation of polyproline peptides and the investigation of their use as organocatalysts.

4.1 Application of Polyproline Peptides in the Aldol Asymmetric Reaction

The first objective of the project was the synthesis of four polyprolines to be used as catalysts in the aldol asymmetric reaction.

In order to do this, the first step towards this direction was the preparation of the monomers that were required for the synthesis of the corresponding peptides. Three compounds (**A7**, **C2** and **D3**) were prepared for this purpose, while monomer **E2** was also synthesized in order to compare its catalytic activity with the one of the corresponding peptide. Regarding **A7**, although two different reaction pathways were employed, due to the low yield of the last reaction, the synthesis required further optimisation and the monomer was not employed for the preparation of the corresponding peptide. **C2** was obtained through an Fmoc protection, **D3** was synthesized successfully through a multi-step reaction pathway and **E2** was obtain after an acetylation reaction and Boc protection reaction.

After that, the synthesis of three polyproline peptides (**PP 1**, **PP 2** and **PP 3**) was performed via SPPS both manually as well as using a peptide synthesizer. Two different sets of coupling reagents were employed in both cases. The peptides were analysed through LCMS, at the same time that

Preparative RP-HPLC was used as a purification method when needed. Moreover, the three peptides were analysed through CD spectroscopy where **PP 1** presented a switch from PolPro II in water to PolPro I in propanol, while **PP 2** and **PP 3** showed a spectrum indicative of the PolPro II conformation in both solvents. As a result, **PP 2** and **PP 3** could not be employed as stereodivergent organocatalysts and were tested as enantioselective organocatalysts.

The catalytic activity of the polyproline peptides was then investigated on the asymmetric aldol reaction between p-nitrobenzaldehyde and cyclohexanone. Various conditions were employed, including different temperature, additives and solvents. Specifically, for **PP 1,** a by-product was observed when TFE was used as a catalyst at room temperature and 40 °C in the presence of different equivalents of TFA or AcOH. To rectify this, different solvents were tested, with optimum results obtained when DMF, no solvent or EtOH was used at 40 °C, in the absence of any additives. In regards of **PP 2**, among various solvents that were employed in the presence of TFA, MeOH led to a dr of 22/78. Nevertheless, after purification via a chromatographic tank, the final dr was 47/53. This observation could be explained through the self-disproportionation of enantiomers. Following that, DMF, propanol and MeOH were employed as solvents at 40 °C in the absence of any additives, leading to the highest combination of yields and dr for **PP 2**. Concerning **PP 3**, as it was designed in order for its activity to be compared to the one of **PP 2**, it was employed as a catalyst using the optimum conditions applied for **PP 2.** Lastly, **E3** and L-proline were also tested as catalysts in DMF and propanol at 40 °C in the absence of any additives, in order to compare their activity with the one of the peptides. The products from the aldol reaction were then analysed through chiral-HPLC.

Overall, we can observe that moderately high to high yields were achieved for all three polyproline peptides. **PP 1** exhibited a switch from PolPro II to PolPro I upon solvent exchange, while it led to the highest dr, but relatively low ee. These results suggest that a heptameric un-functionalized polyproline helix is able to catalyze the aldol asymmetric reaction, but is not sufficient in order for high ee to be achieved. **PP 2** and **PP 3** were characterized by higher ee values. Nevertheless, they did not show a conformational switch, while **PP 3** did not lead to a reverse on the enantioselectivity of **PP 2** as it was originally expected. This suggests that seven units were not sufficient for a conformational switch to occur, at the same time that introduction of the phenol group on **PP 3** could not lead to a reverse on the enantioselectivity. It is notable that the optimum solvent was different for each polyproline. Therefore, each helix interacts with the solvent in a different manner, influencing the catalytic outcome.

As a future direction, a different purification method or another reaction pathway could be explored for the synthesis of **A7**. In this way the preparation of the corresponding peptide could be achieved in order to investigate its catalytic activity. Regarding the peptides, **PP 2** and **PP 3** could be

synthesized in longer peptide chains and research whether that would lead a conformational switch, and thus, better organocatalytic results. Aiming to increase the reactivity of the enamine, a future step could be the preparation of a peptide comprised of proline units and a pyrrolidine ring with two nitrogen atoms (as described under Conclusions and future work in Chapter 2), in order to investigate its catalytic activity on the aldol reaction.

By completing this study, there is now an established protocol for the synthesis of un-functionalized and functionalized polyproline peptides, at the same time their conformation in two different solvents has been documented. Moreover, their use in the aldol asymmetric reaction has been investigated in various conditions, leading to high yields. Although no stereodivergence was observed and the enantioselectivities were relatively low, these results can act as a starting point for further research towards the development of novel peptide-based organocatalysts.

4.2 Application of Polyproline Peptides in the Kinetic Resolution of a Racemic Alcohol

The second objective of this project was the preparation of another set of polyprolines to be employed as catalysts for the acyl transfer of a racemic alcohol.

The first step toward this goal was the synthesis of peptide **PP 4**. In order to achieve that, the preparation of the corresponding monomer (**F3**) was required. **F3** was synthesized successfully through a multi-step reaction pathway. After that, **PP 4** was synthesized using the SPPS method on a peptide synthesizer, using the optimum conditions, without the need of purification.

PP 4 was then employed as catalyst for the KR of racemic 1-phenylethanol. Monomers **F2** and **F3** were also tested in order to compare their catalytic activity with the one of the peptide. Different conditions were tested, including different equivalents of Et_3N (1.6 and 0.75) and different temperatures (room temperature and 0 °C). The outcome of this process was that **PP 4** led to the fastest conversion when 1.6 equivalents of Et_3N were employed at room temperature. Thus, **PP4** is the most efficient catalyst under these conditions. Nevertheless, in all the other conditions the conversion times were comparable between **PP 4**, **F2** and **F3**, at the same time that in all the examined cases the ee values were low. These results suggest that the designed polyproline can lead to the desired conversion faster than the corresponding monomers only under specific circumstances, while it is not sufficient for any enantioselectivity to be achieved.

The next step involved the preparation of the peptides of Target Peptide Group 6. For this purpose, the preparation of a series of monomers was designed. Nevertheless, only the synthesis of **G4** proved to be successful, suggesting the strong influence of the nucleophilicity of the amine on the outcome of the reaction. By employing **G4** as a monomer, **PP 5** was synthesized via the SPPS method on a peptide synthesizer. According to LCMS analysis, the synthesized peptide was not the desired

one, raising concerns regarding the coupling efficiency. To overcome this, a slightly different polyproline was designed (**PP 6**), which required the preparation of a dimer (**I2**). Since **I2** was not obtained, different reaction conditions could be used in the future in order to achieve its synthesis. For example, DCC and DCM could be employed at room temperature. In order to overcome this and due to time limitations, a third approach was followed. **PP 7** and **PP 8** were synthesized successfully through the SPPS method on a peptide synthesizer and were used further without purification.

PP 7 and **PP 8** were then employed as catalysts for the KR of racemic alcohol 1-phenylethanol. The monomer **J1** as well as peptide **PP 9** were also tested as catalysts so that their activity could be compared to the ones of the peptides. Similarly to **PP 4,** different equivalents of Et_3N (1.6 and 0.75) and different temperatures (room temperature and 0 °C). were also employed. **PP 8** catalyzed the reaction significantly faster than **PP 7** when 1.6 equivalents of Et_3N were used at room temperature, and faster than **J1** and **PP 9**. **PP 7** and **PP 8** catalyzed the reaction at approximately the same time when 0.75 equivalents of Et_3N were used at room temperature, which was faster than **PP 9** and significantly faster than **J1**. Nevertheless, once 0.75 equivalents of Et_3N were employed at 0 °C, **PP 7** catalyzed the reaction faster than **PP 8**. As a result, we can observe that the best catalyst is changing depending on the conditions used, suggesting that the change of the proline units on the peptide backbone of **PP 7** and **PP 8** influences the catalytic activity. Regarding the ee, the examined polyprolines exhibited very low values.

As a future direction, the reaction conditions for the obtainment of monomers **G2**, **G4**, **G6** and **G8** could be further investigated. For example, Fmoc-Cl and Na_2CO_3 in water could be also used at room temperature. In this way, the corresponding peptides employing these monomers (Table 1-Target Peptide Group 6) could then be prepared. The reaction between **I1** and **G9** could also be further researched. Employing DCC and DCM at room temperature could be one possible way for the successful synthesis of **I2**. Once this will be achieved, peptide **PP 6** could be synthesized and tested as a catalyst in the KR of a racemic sec-alcohol. Regarding the peptides tested as catalysts and since no selectivity was observed, a future direction could include the synthesis of a macrocycle structure to be tested as a catalyst. Considering that a macrocycle has already been synthesized and characterized in the Palma group, a novel macrocycle could be developed. The effect that this macrocycle would have in an acyl transfer reaction could then be investigated.

By completing this research, a series of polyproline peptides was synthesized, their conformation was characterized, and their use in the KR of sec-alcohols was investigated. Although no enantioselectivity was observed, the desired conversions were obtained. Moreover, these results can be employed in order to further investigate how exchanging L-proline with D-proline units in the peptide backbone could affect the catalytic outcome. Lastly, by optimising the conditions for the

obtainment of monomers **G2**, **G4**, **G6** and **G8**, the rest peptides of Target peptide group 6 could be synthesized and employed as catalysts for the KR of a sec-alcohol.

Appendix 1

Further Analysis: Chapter 2

AP1.1 Monomers

AP1.1.1 ^{1}H-NMR Spectra

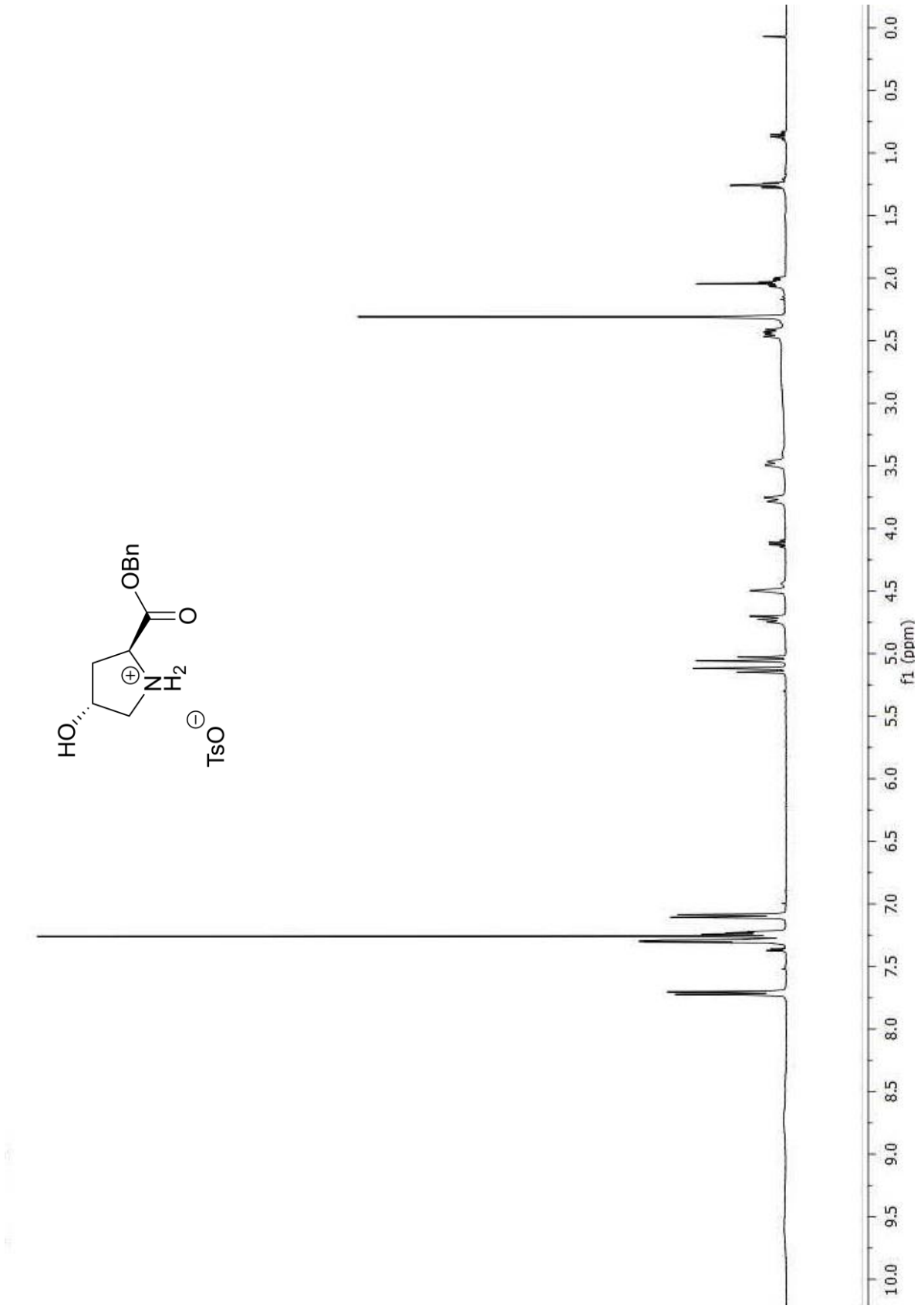

Figure 96: ^{1}H-NMR Spectrum ($CDCl_3$, 400 MHz) of **A2.**

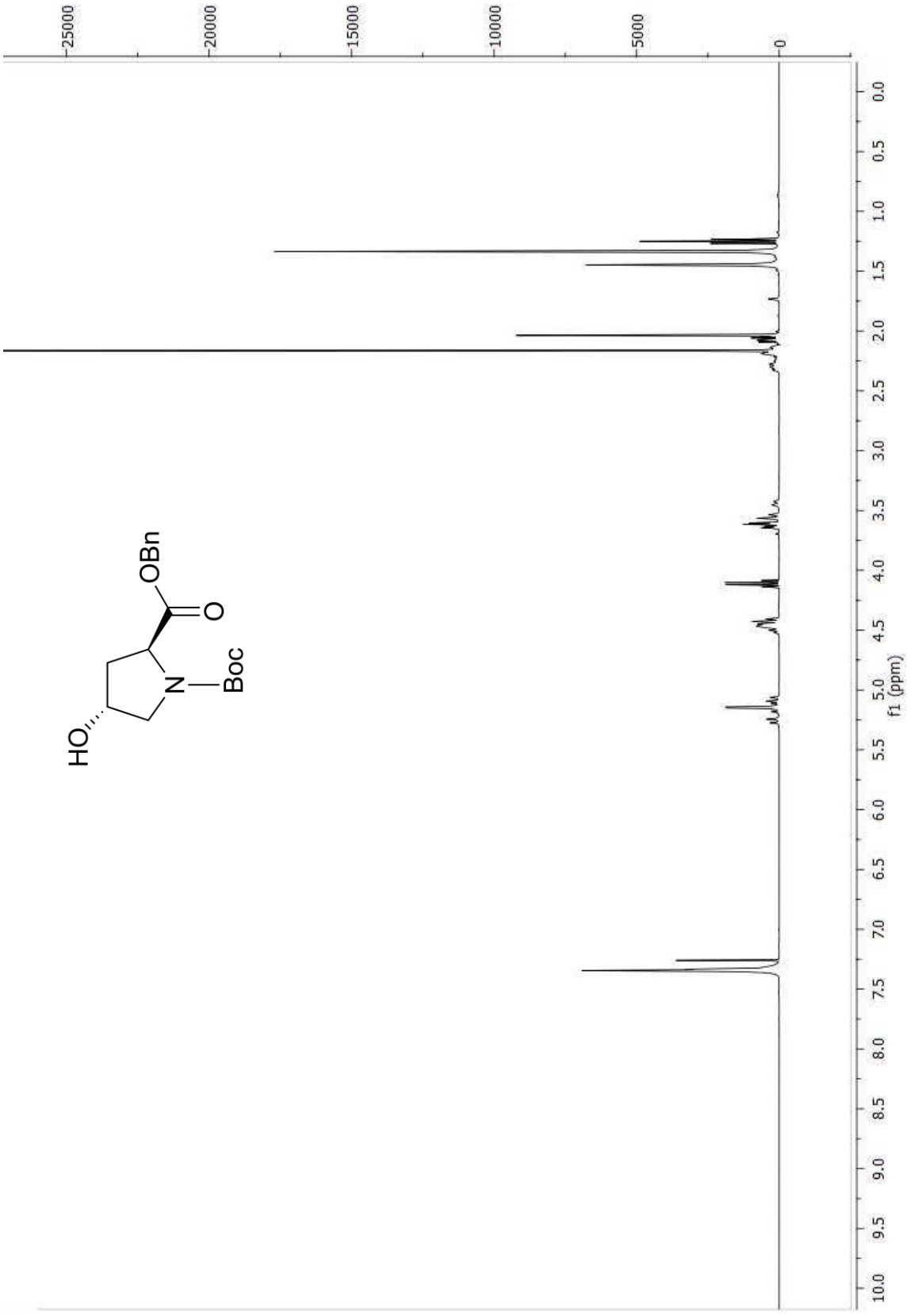

Figure 97: ^{1}H-NMR Spectrum ($CDCl_3$, 400 MHz) of **A3.**

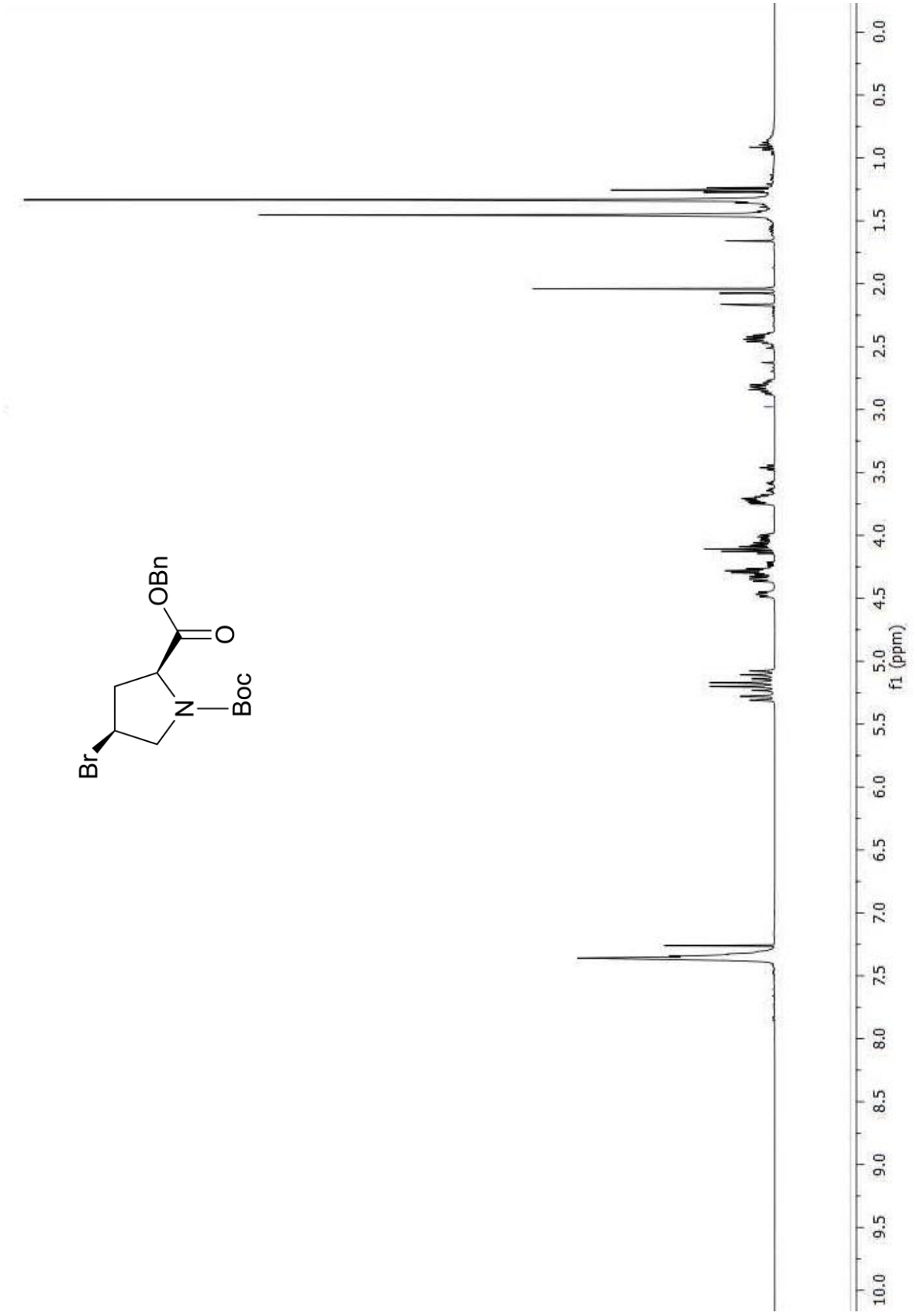

Figure 98: ^{1}H-NMR Spectrum ($CDCl_3$, 400 MHz) of **A4.**

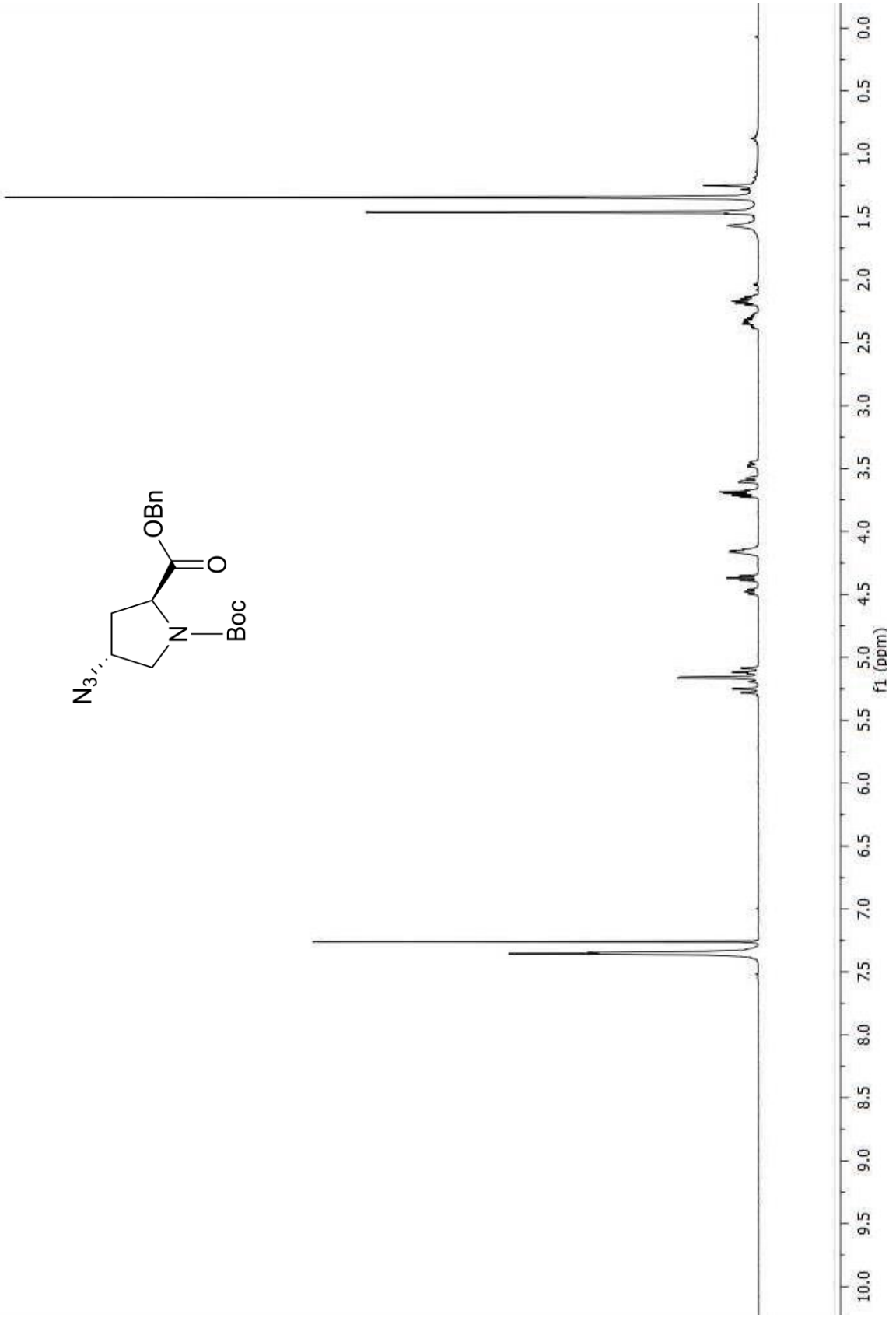

Figure 99: ^{1}H-NMR Spectrum ($CDCl_3$, 400 MHz) of **A5.**

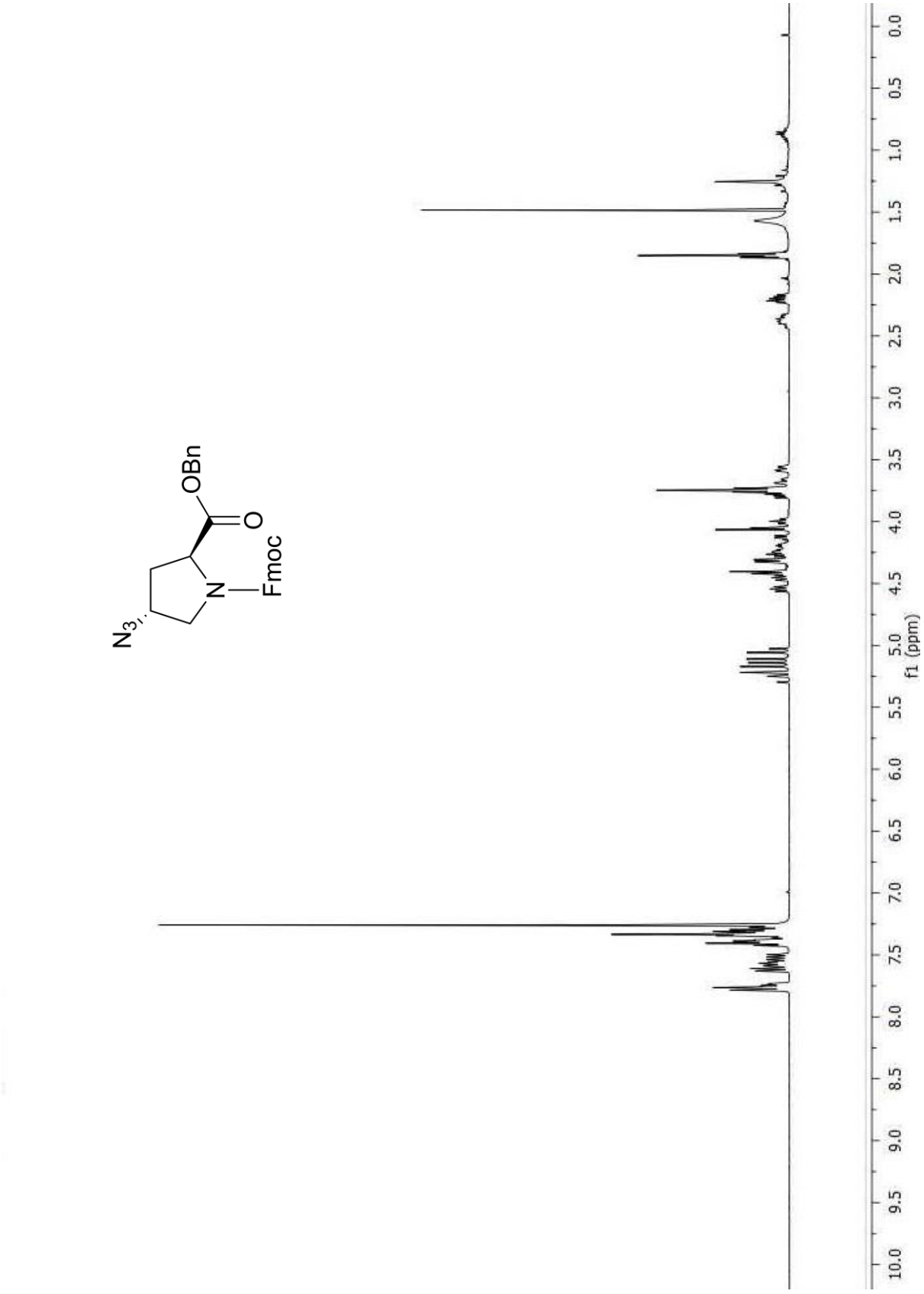

Figure 100: ^{1}H-NMR Spectrum ($CDCl_3$, 400 MHz) of **A6.**

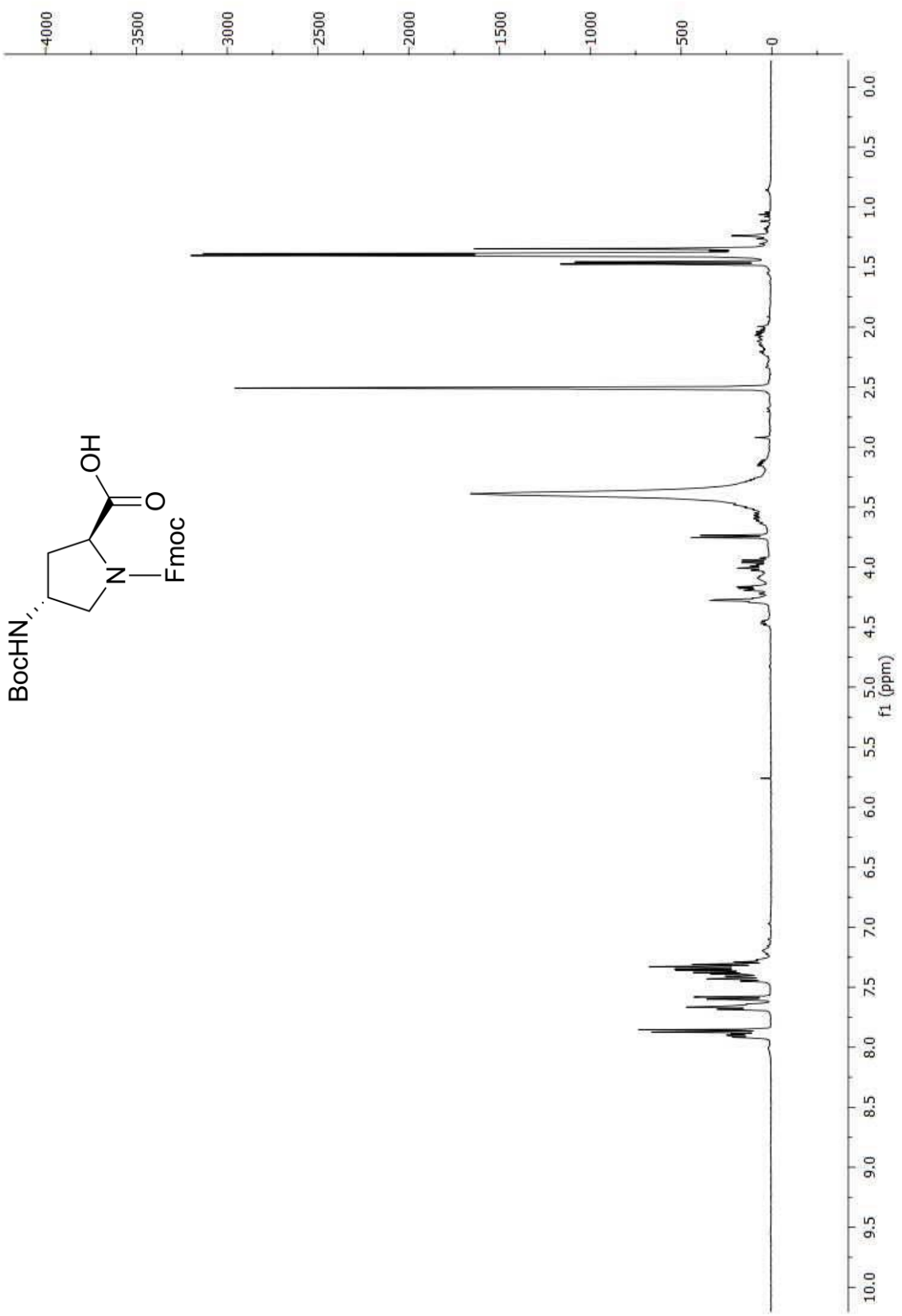

Figure 101: ^{1}H-NMR Spectrum ($CDCl_3$, 400 MHz) of **A7.**

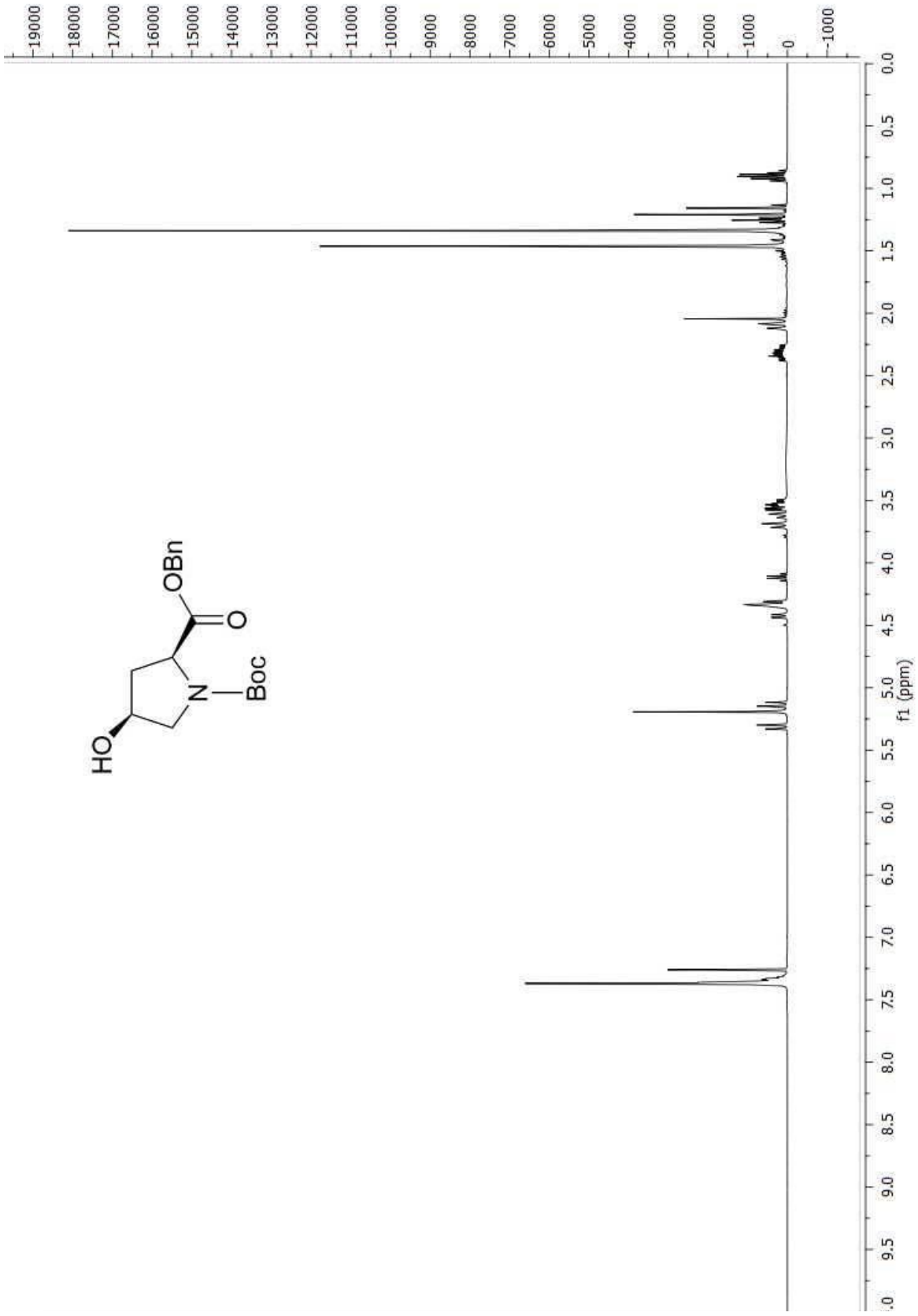

Figure 102: ^{1}H-NMR Spectrum ($CDCl_3$, 400 MHz) of **B2.**

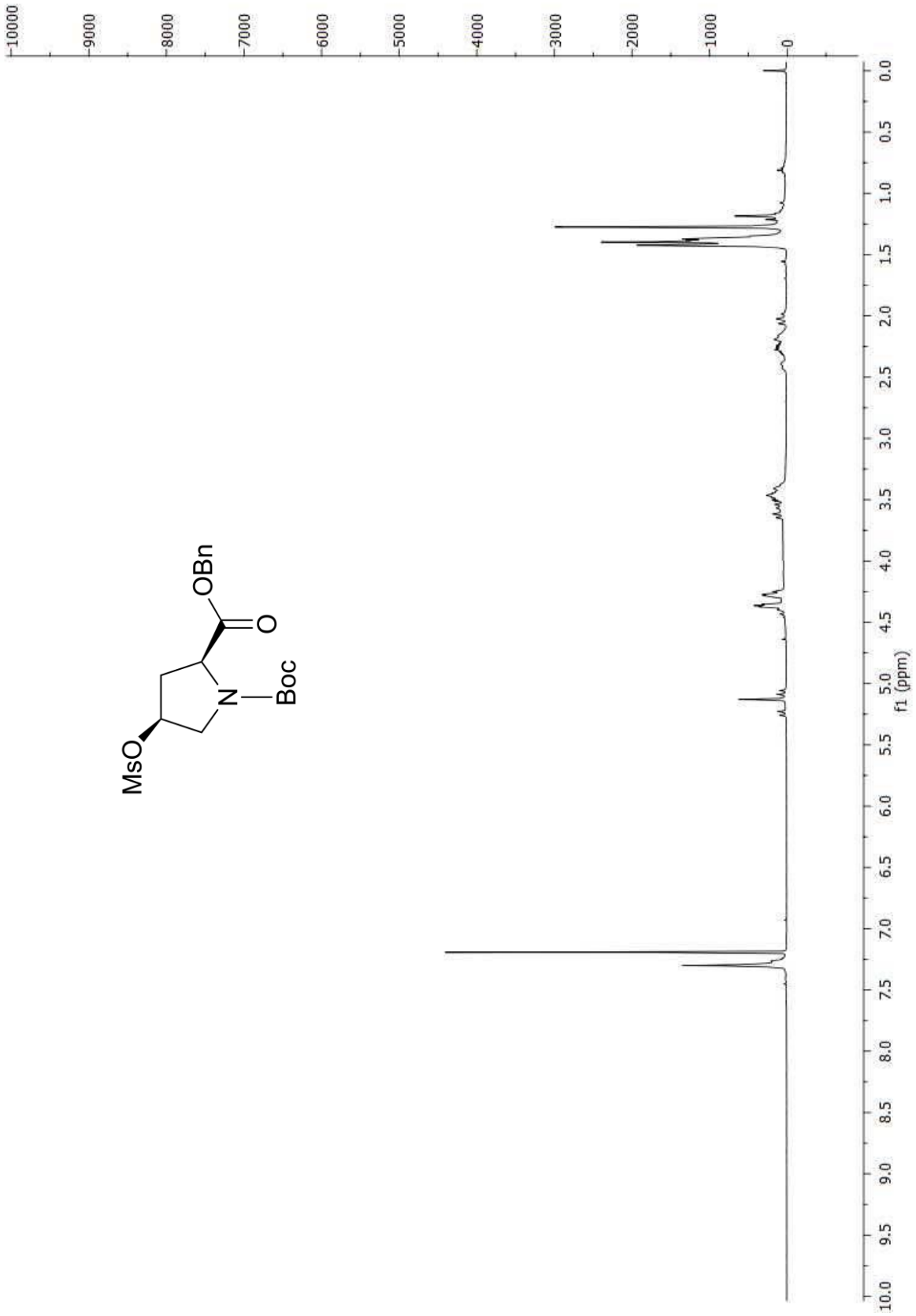

Figure 103: ^{1}H-NMR Spectrum ($CDCl_3$, 400 MHz) of **B3.**

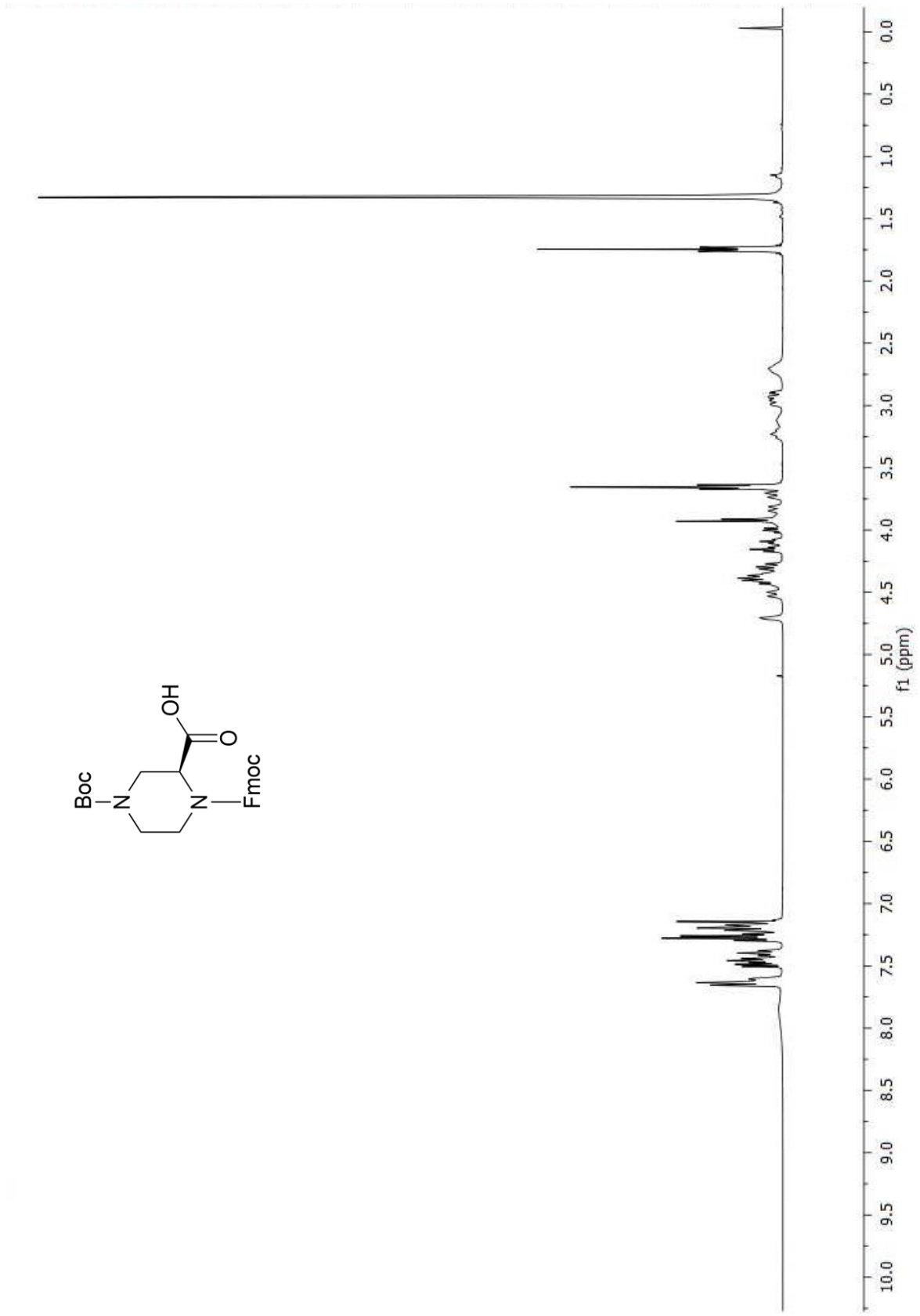

Figure 104: ^{1}H-NMR Spectrum ($CDCl_3$, 400 MHz) of **C2.**

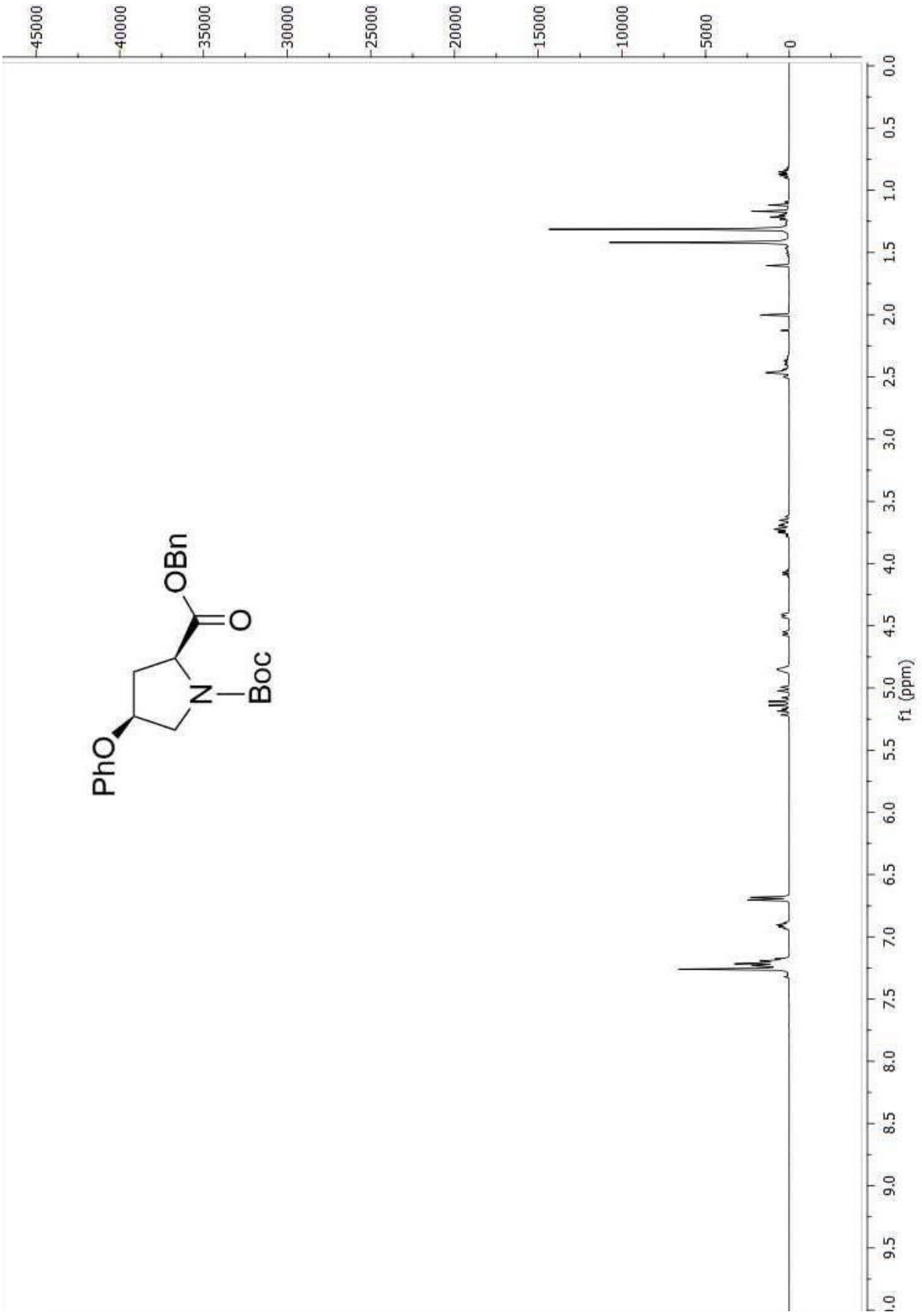

Figure 105: ^{1}H-NMR Spectrum ($CDCl_3$, 400 MHz) of **D1.**

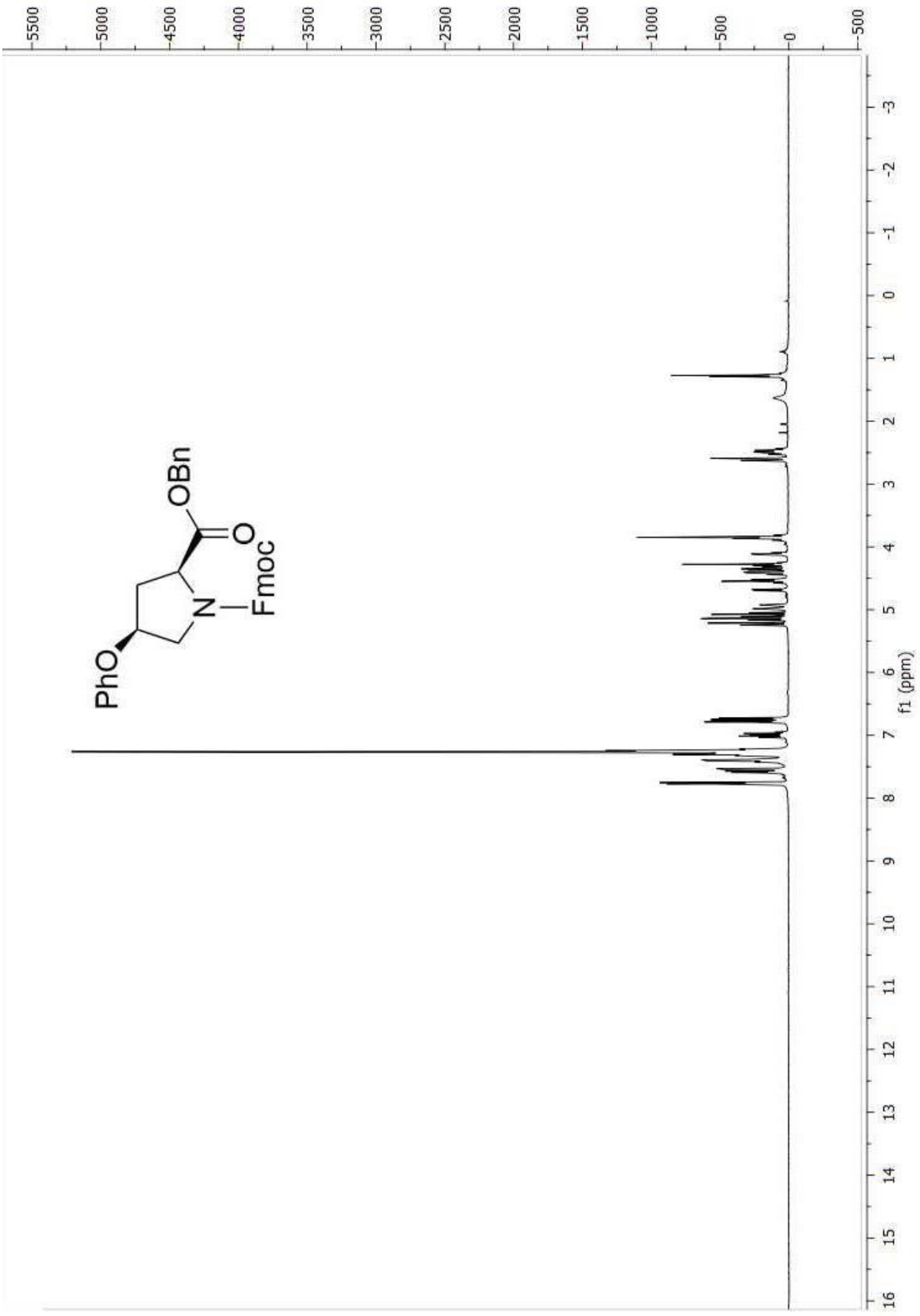

Figure 106: ^{1}H-NMR Spectrum ($CDCl_3$, 400 MHz) of **D2.**

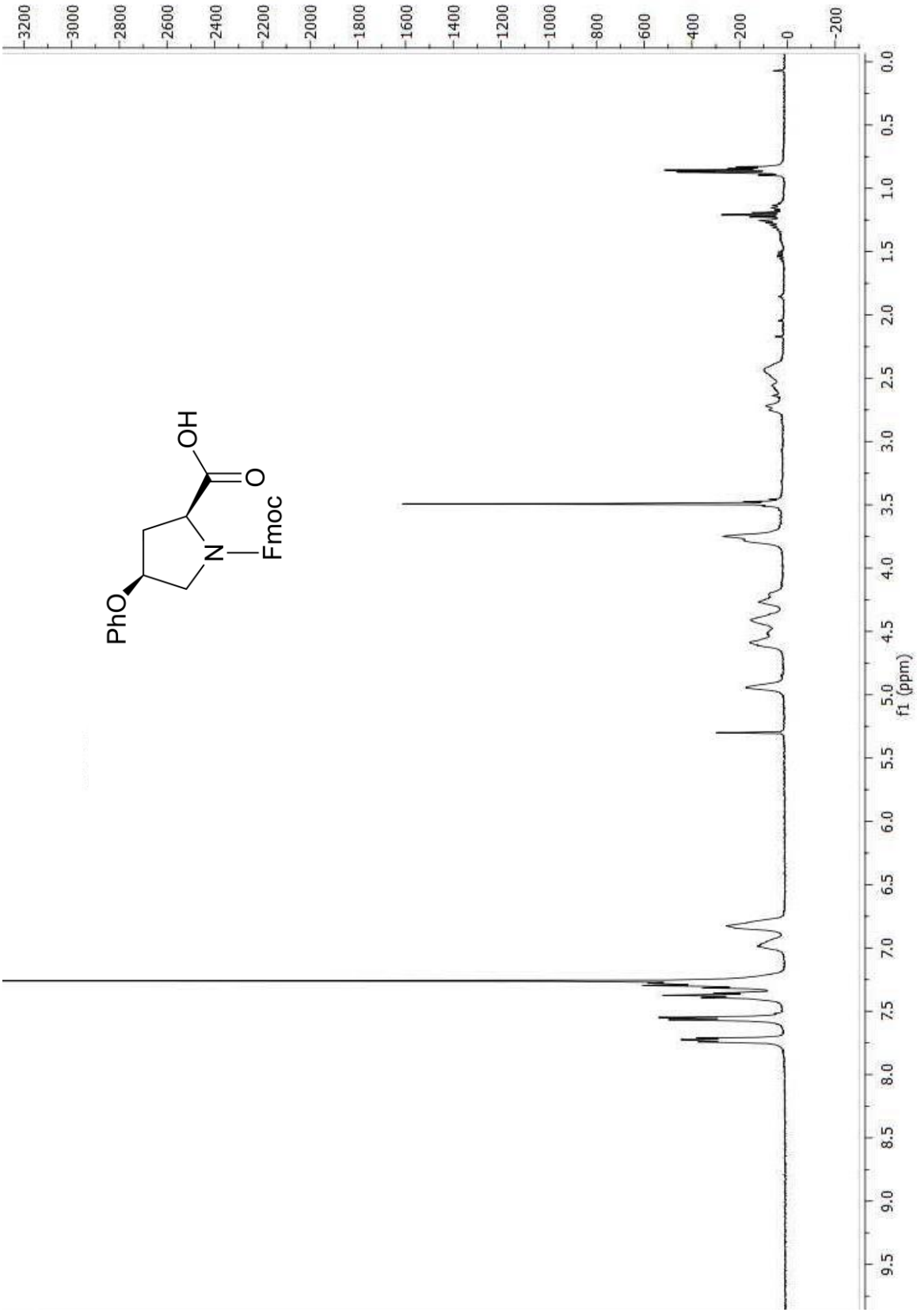

Figure 107: ^{1}H-NMR Spectrum ($CDCl_3$, 400 MHz) of **D3.**

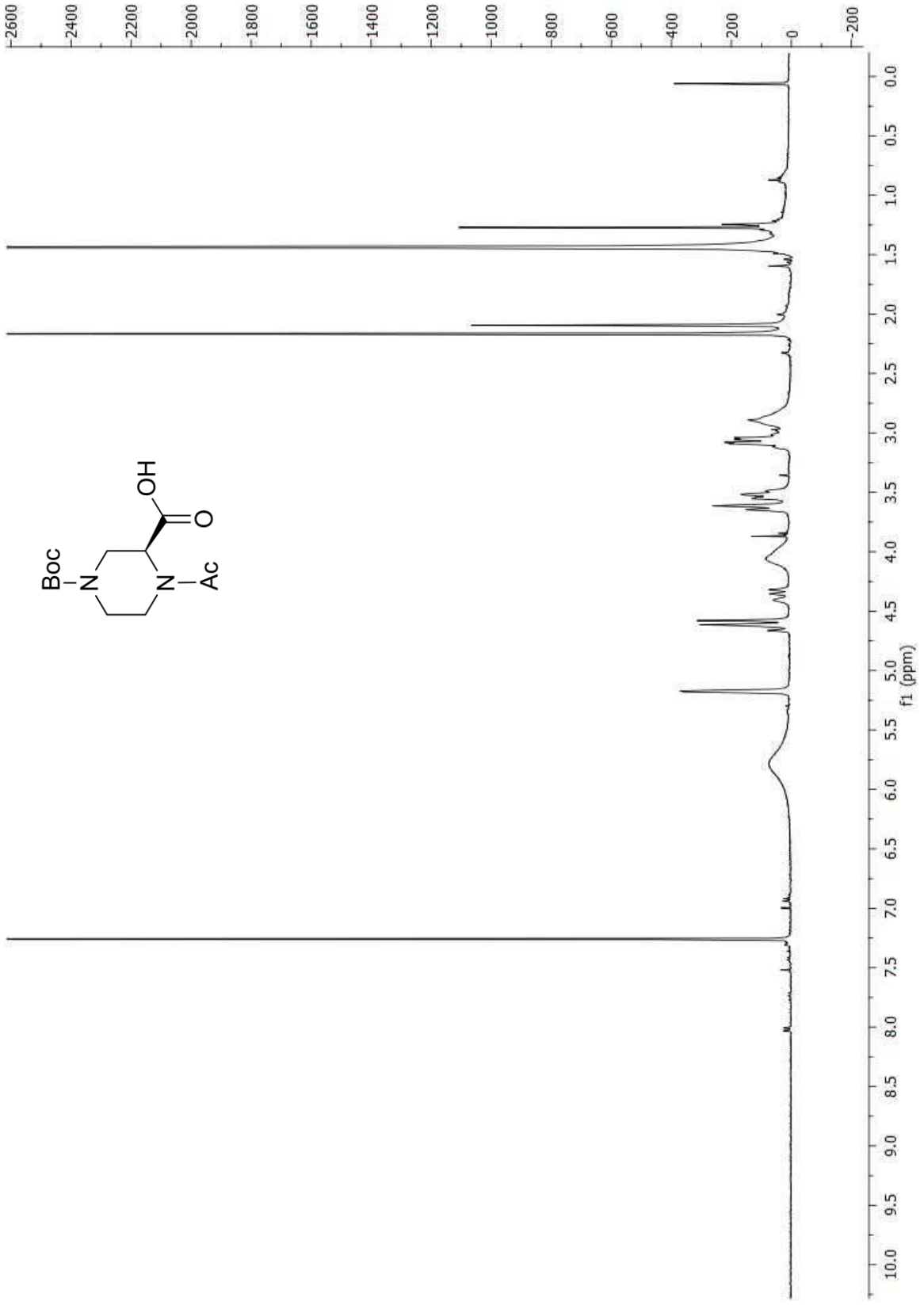

Figure 108: ^{1}H-NMR Spectrum ($CDCl_3$, 400 MHz) of **E1.**

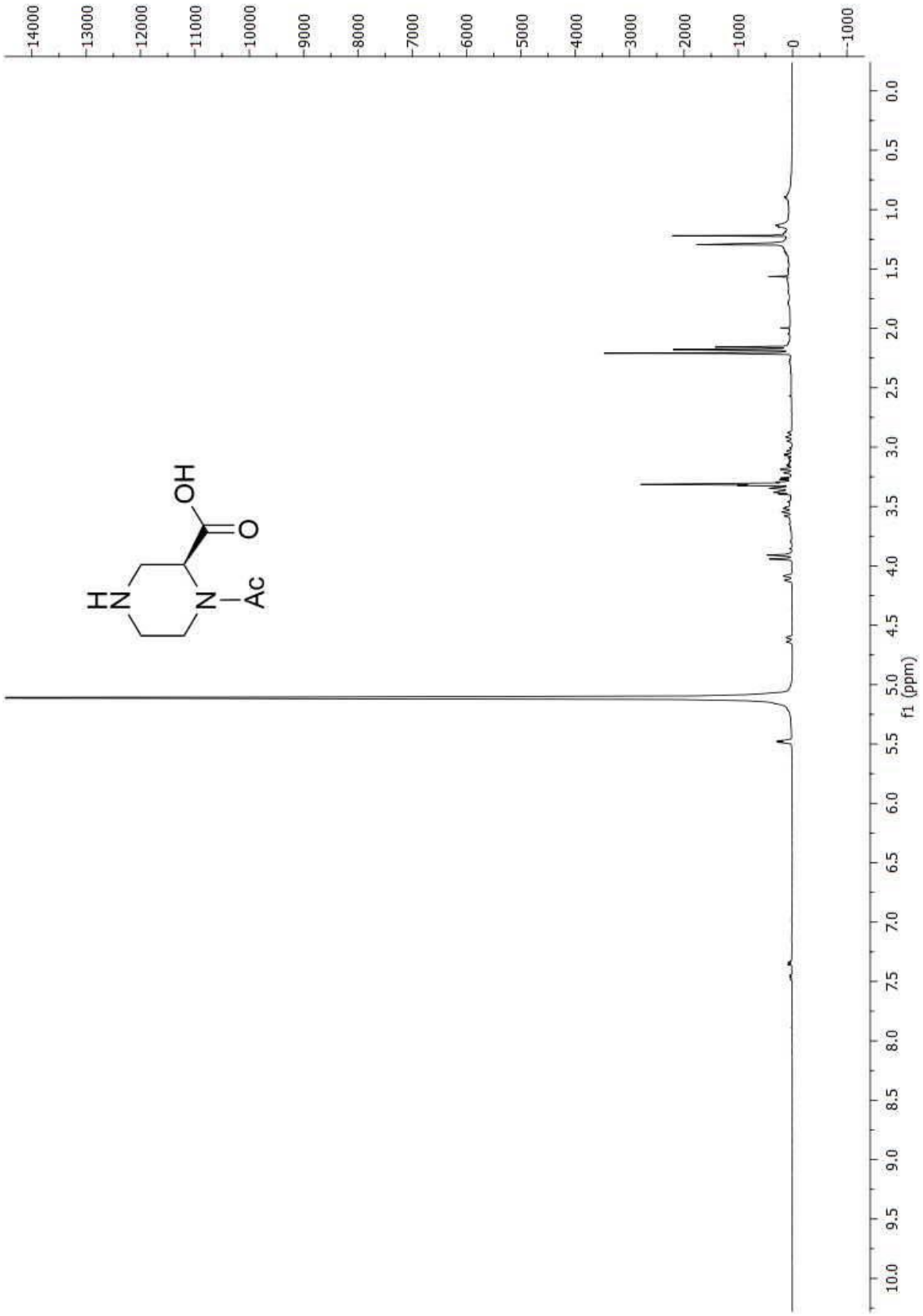

Figure 109: ^{1}H-NMR Spectrum ($CDCl_3$, 400 MHz) of **E2.**

AP1.1.2 ^{13}C-NMR Spectra

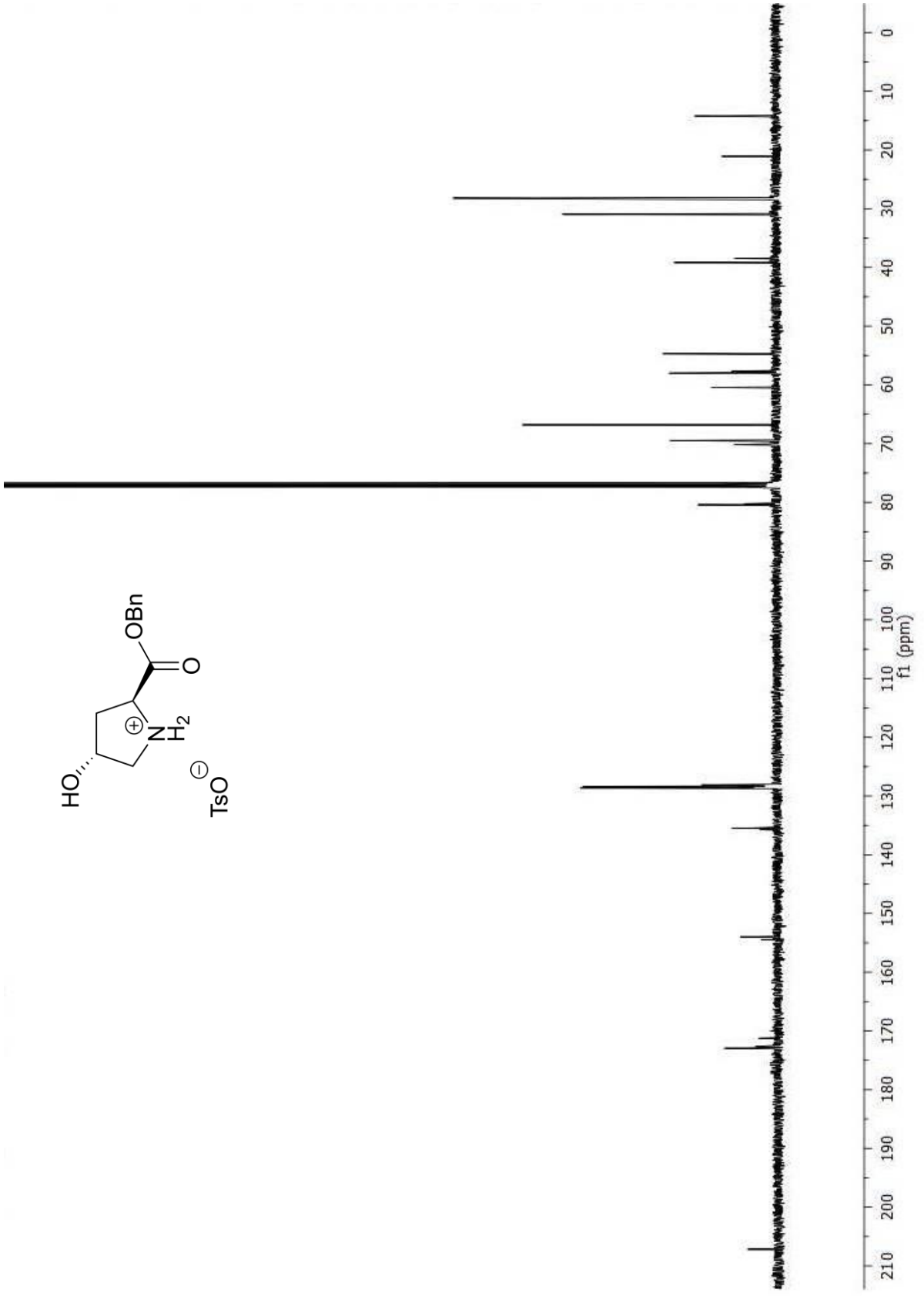

Figure 110: ^{13}C-NMR Spectrum ($CDCl_3$, 100 MHz) of **A2**.

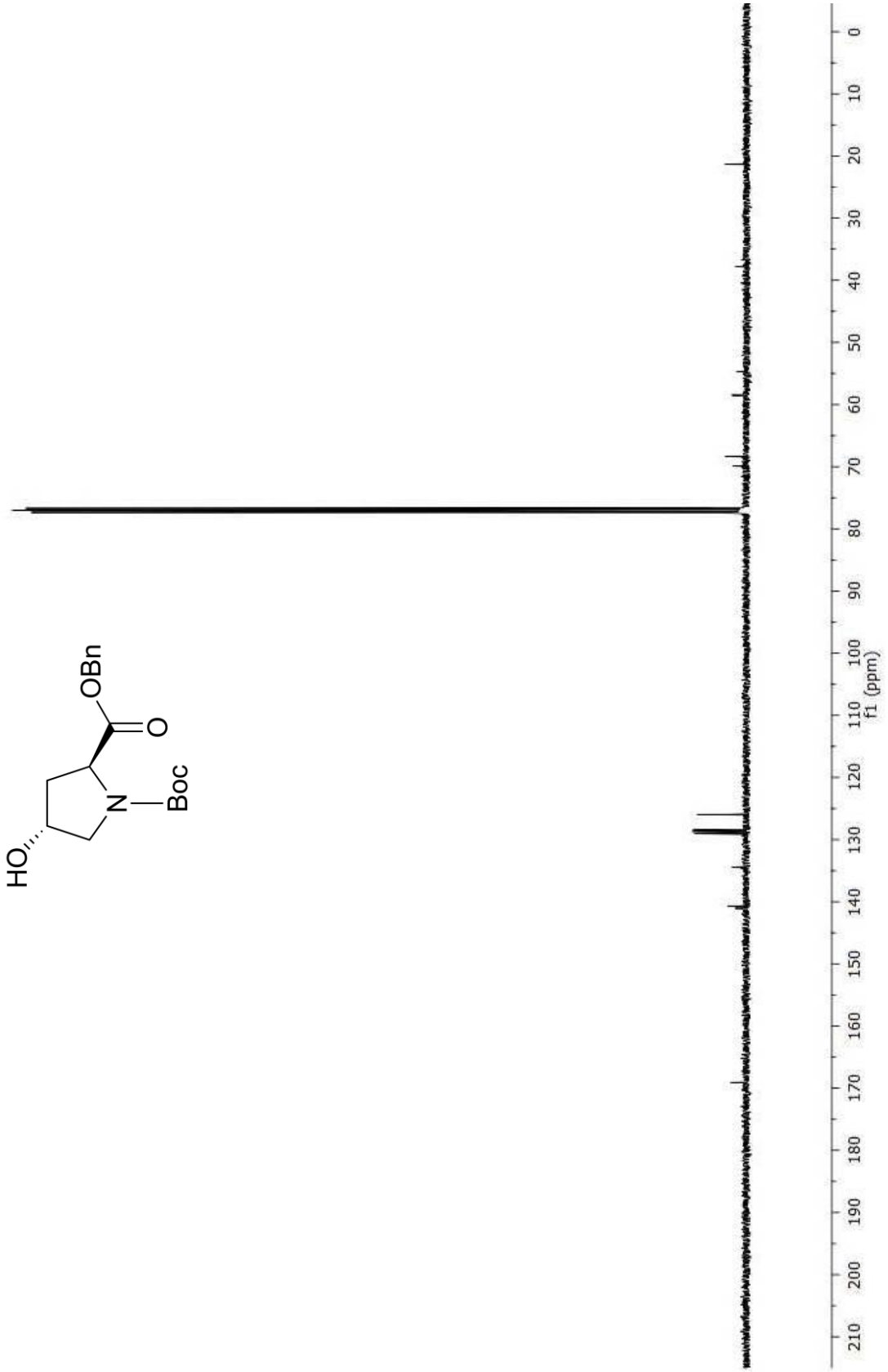

Figure 111: ^{13}C-NMR Spectrum ($CDCl_3$, 100 MHz) of **A3.**

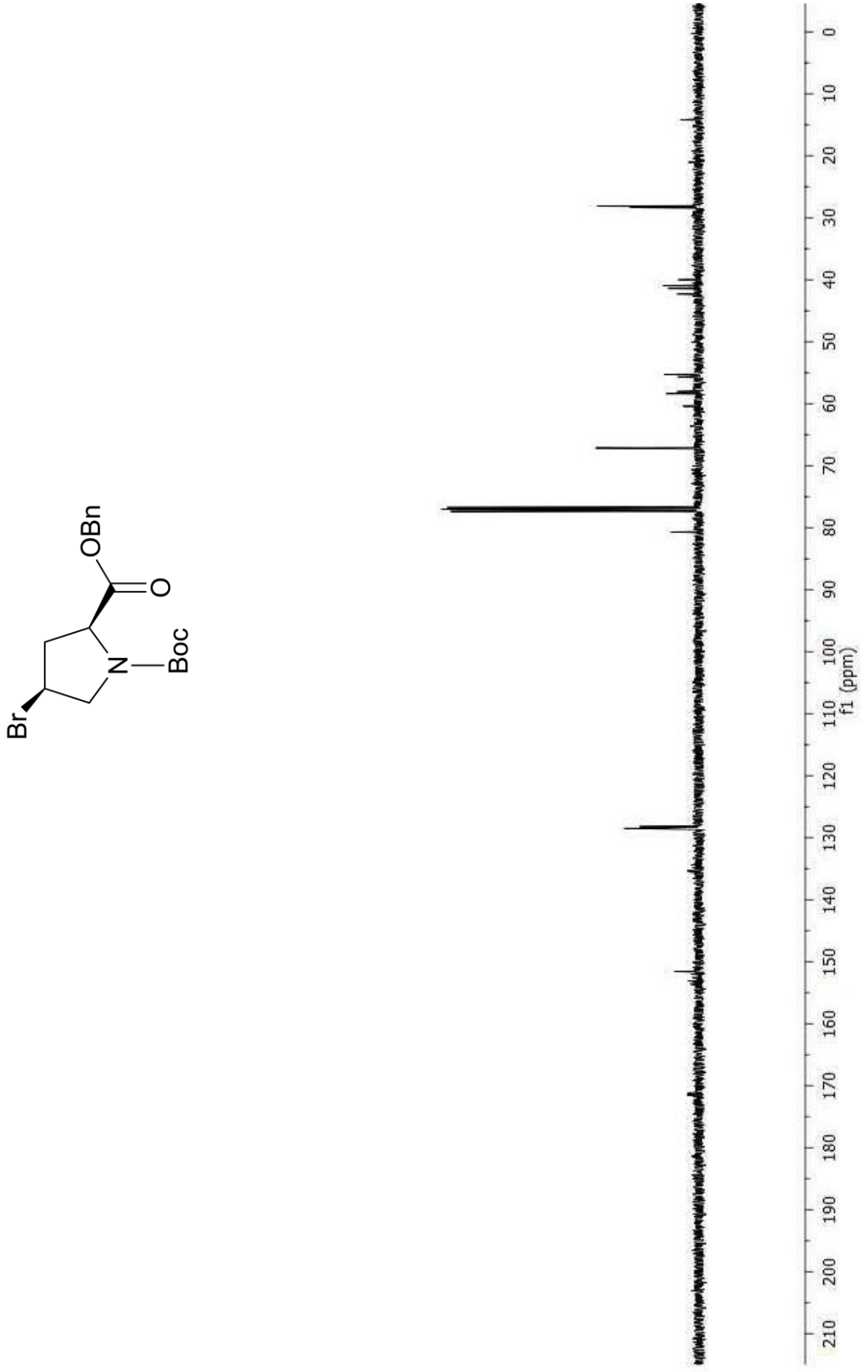

Figure 112: ^{13}C-NMR Spectrum ($CDCl_3$, 100 MHz) of **A4.**

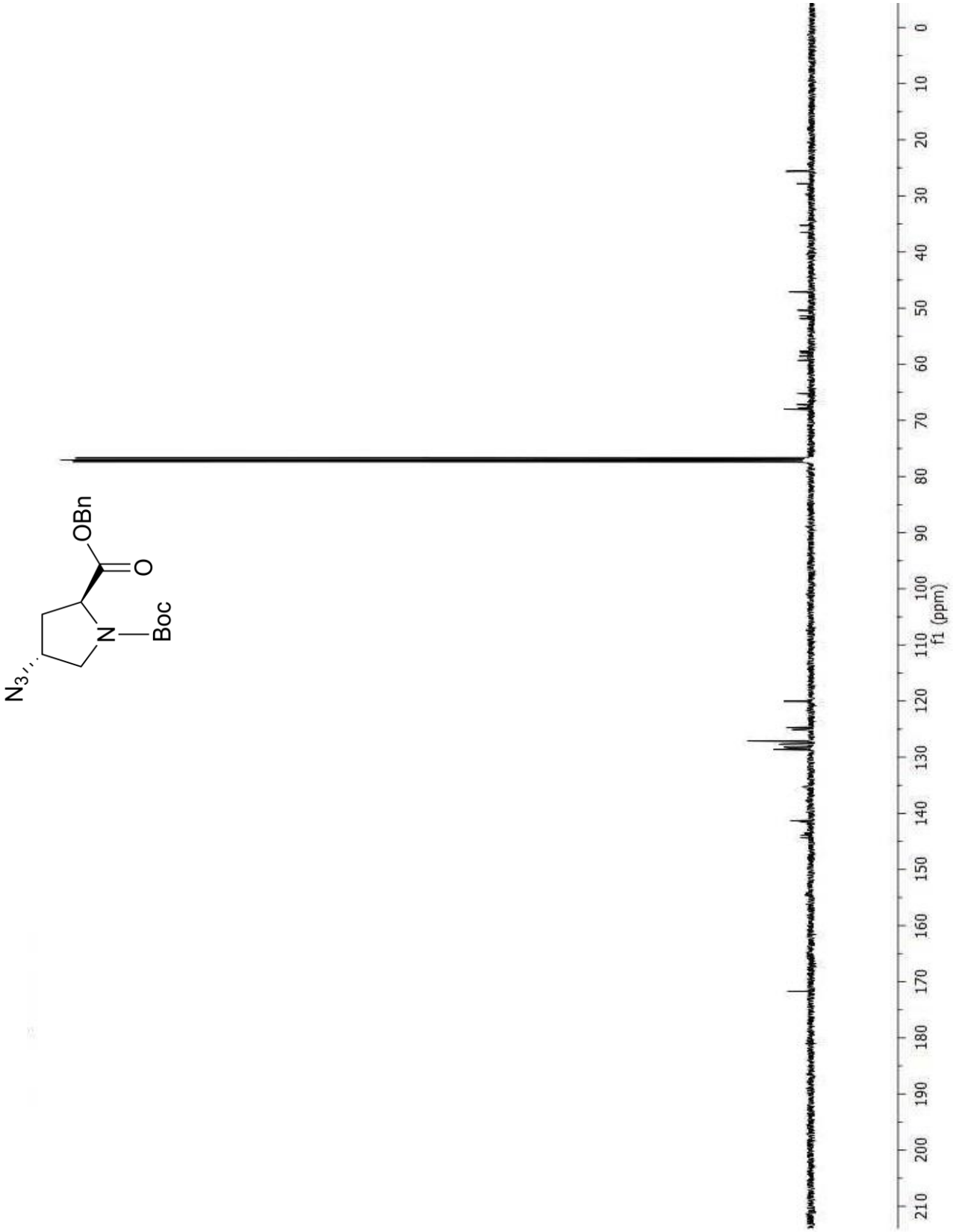

Figure 113: ^{13}C-NMR Spectrum ($CDCl_3$, 100 MHz) of **A5.**

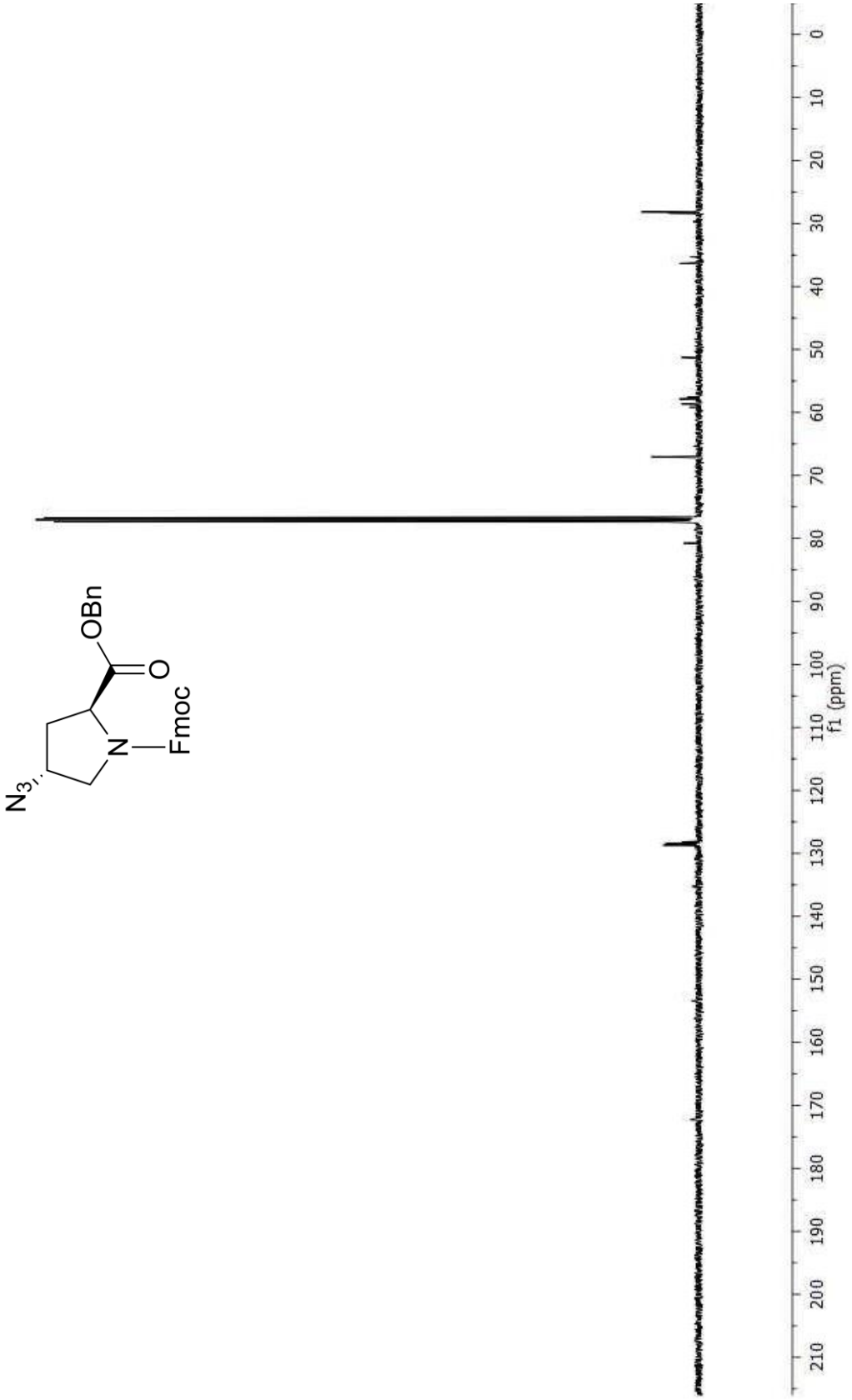

Figure 114: ^{13}C-NMR Spectrum ($CDCl_3$, 100 MHz) of **A6.**

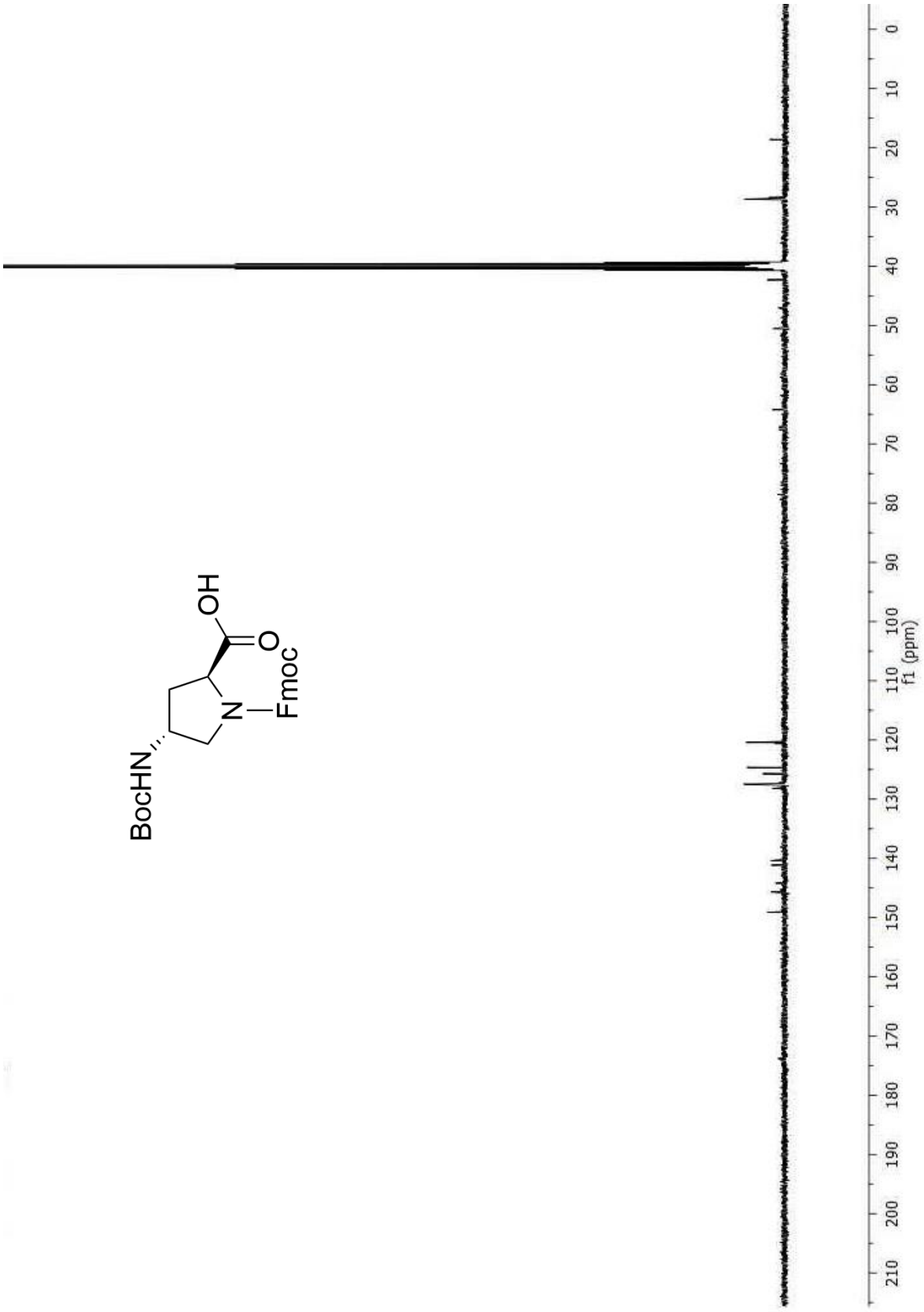

Figure 115: ^{13}C-NMR Spectrum (DMSO, 100 MHz) of **A7.**

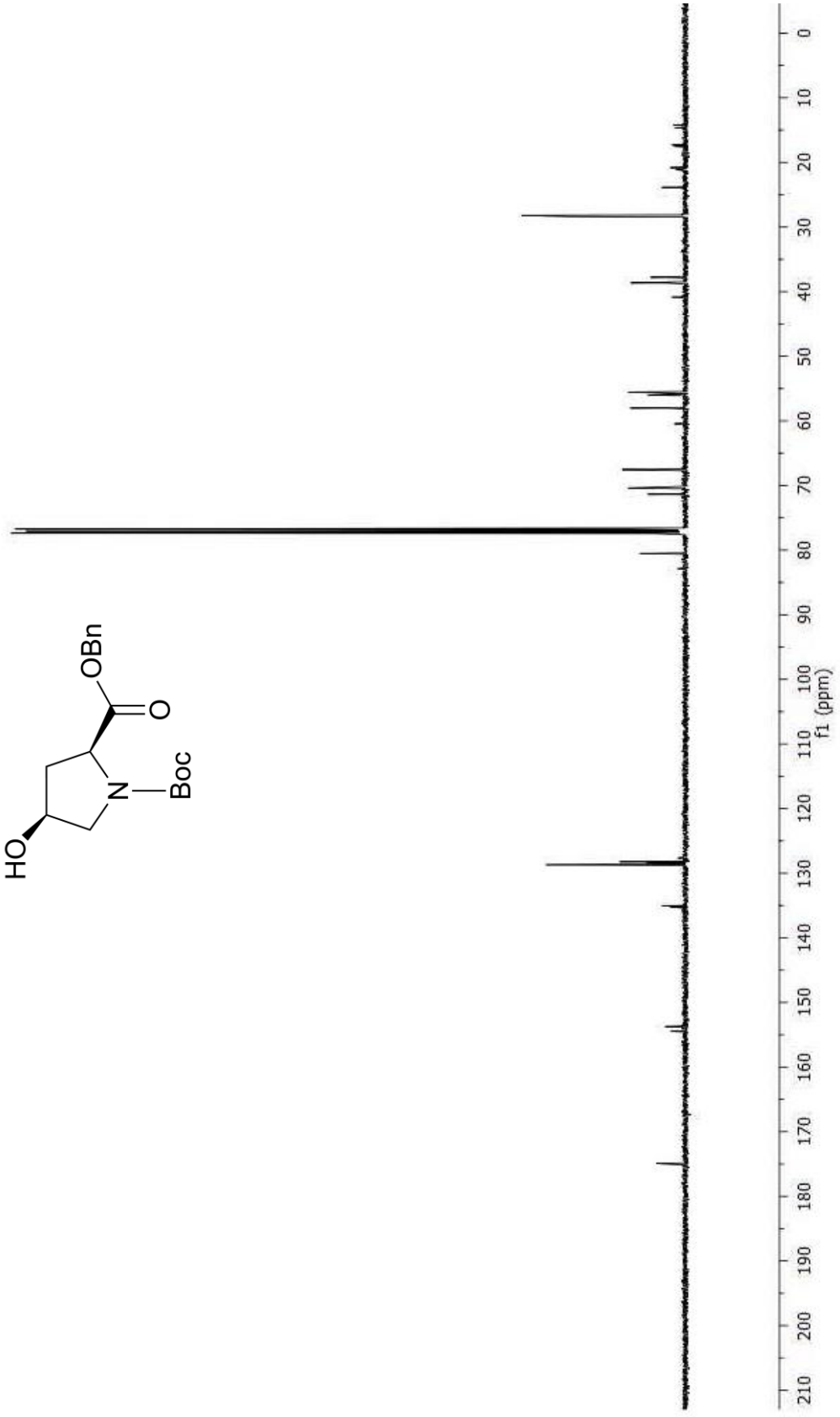

Figure 116: ^{13}C-NMR Spectrum ($CDCl_3$, 100 MHz) of **B2.**

Figure 117: ^{13}C-NMR Spectrum ($CDCl_3$, 100 MHz) of **B3.**

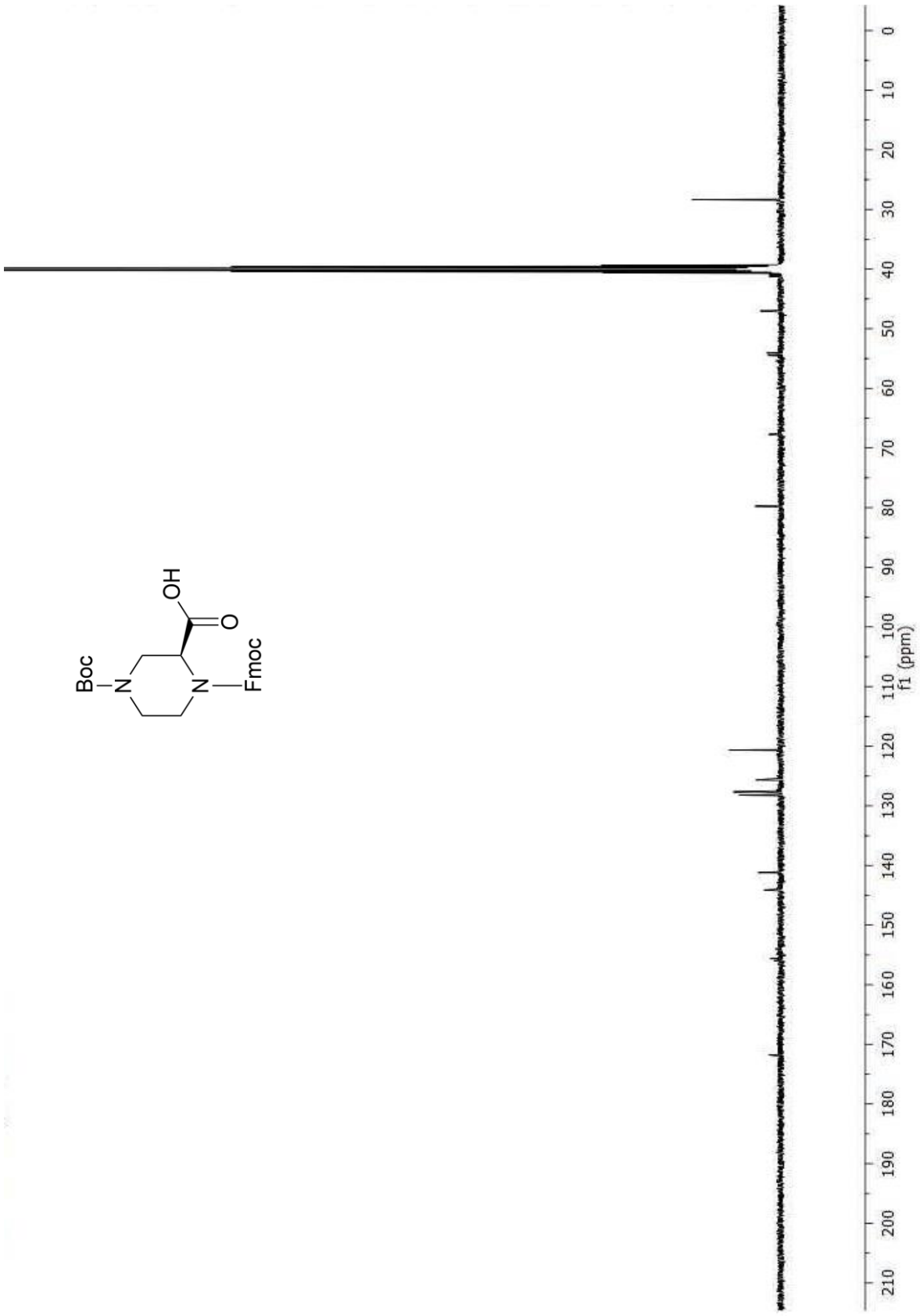

Figure 118: ^{13}C-NMR Spectrum (DMSO, 100 MHz) of **C2.**

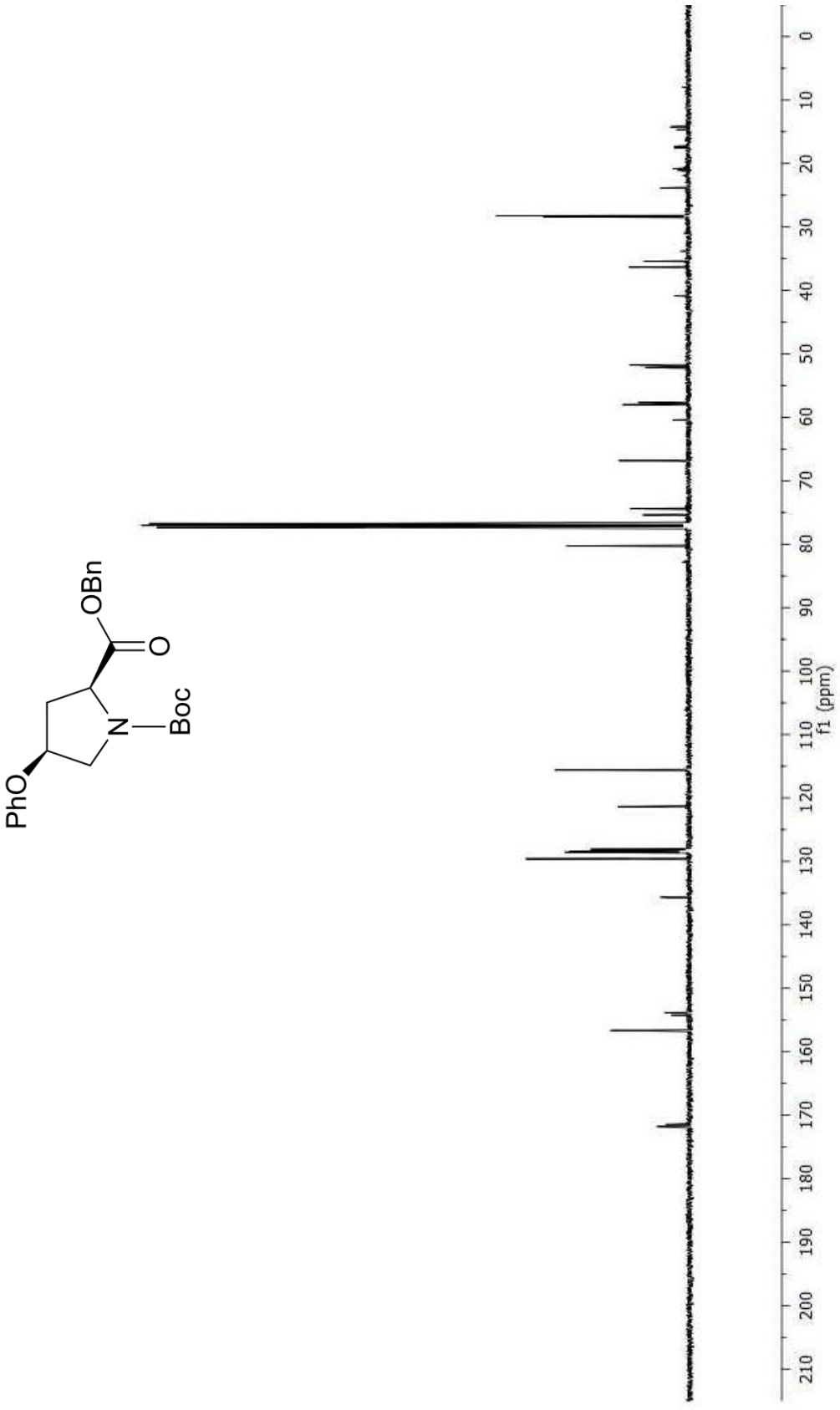

Figure 119: ^{13}C-NMR Spectrum ($CDCl_3$, 100 MHz) of **D1.**

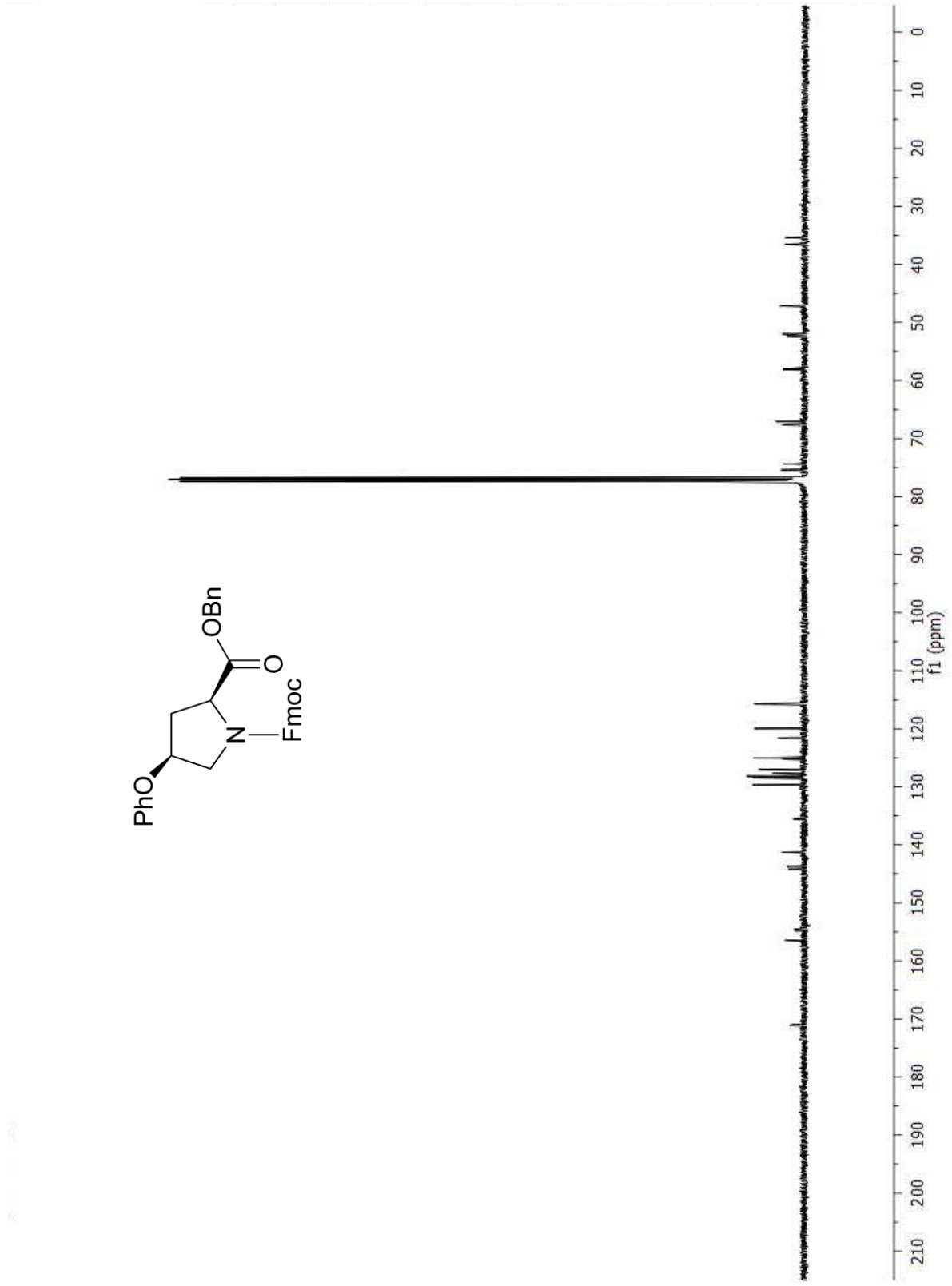

Figure 120: ^{13}C-NMR Spectrum ($CDCl_3$, 100 MHz) of **D2.**

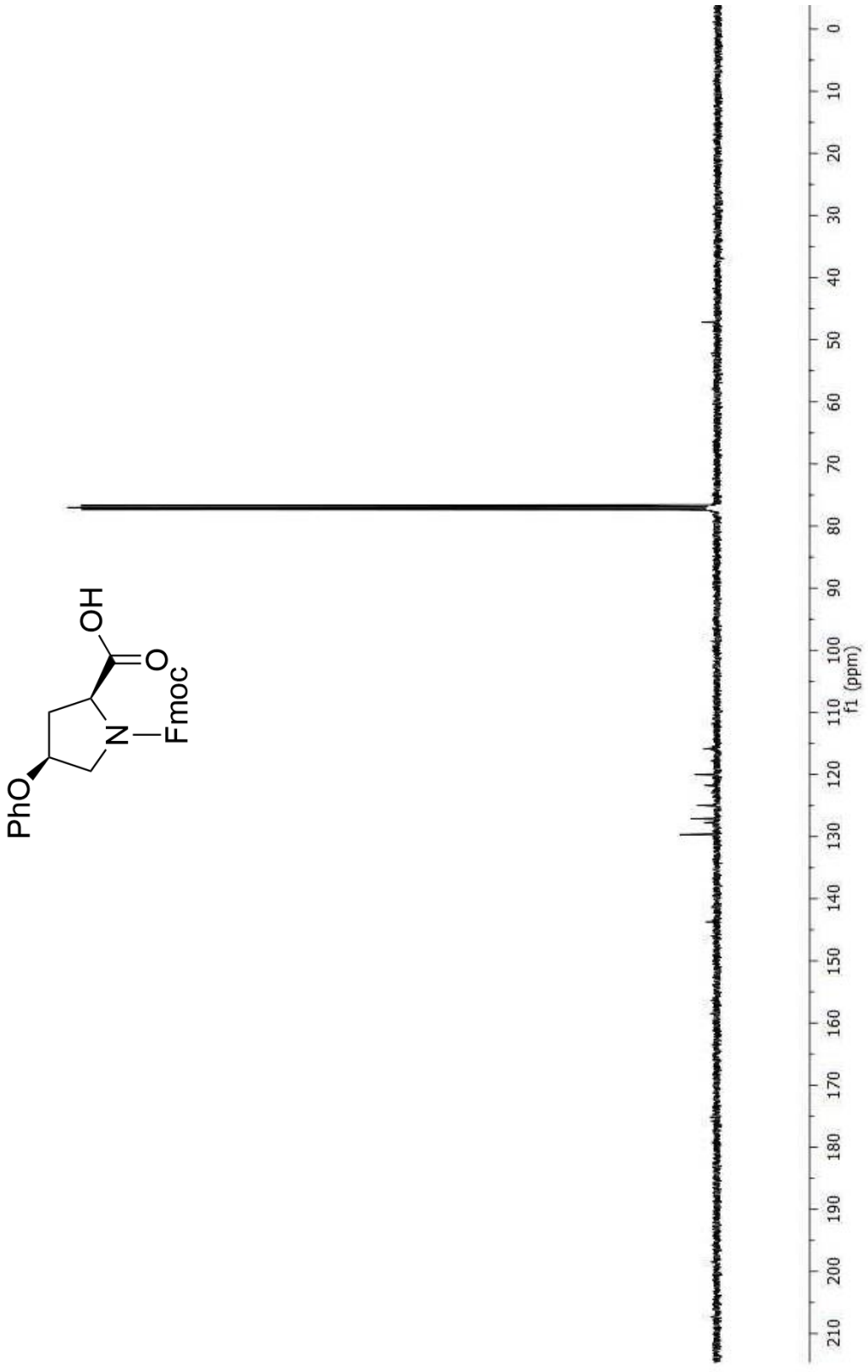

Figure 121: ^{13}C-NMR Spectrum ($CDCl_3$, 100 MHz) of **D3**

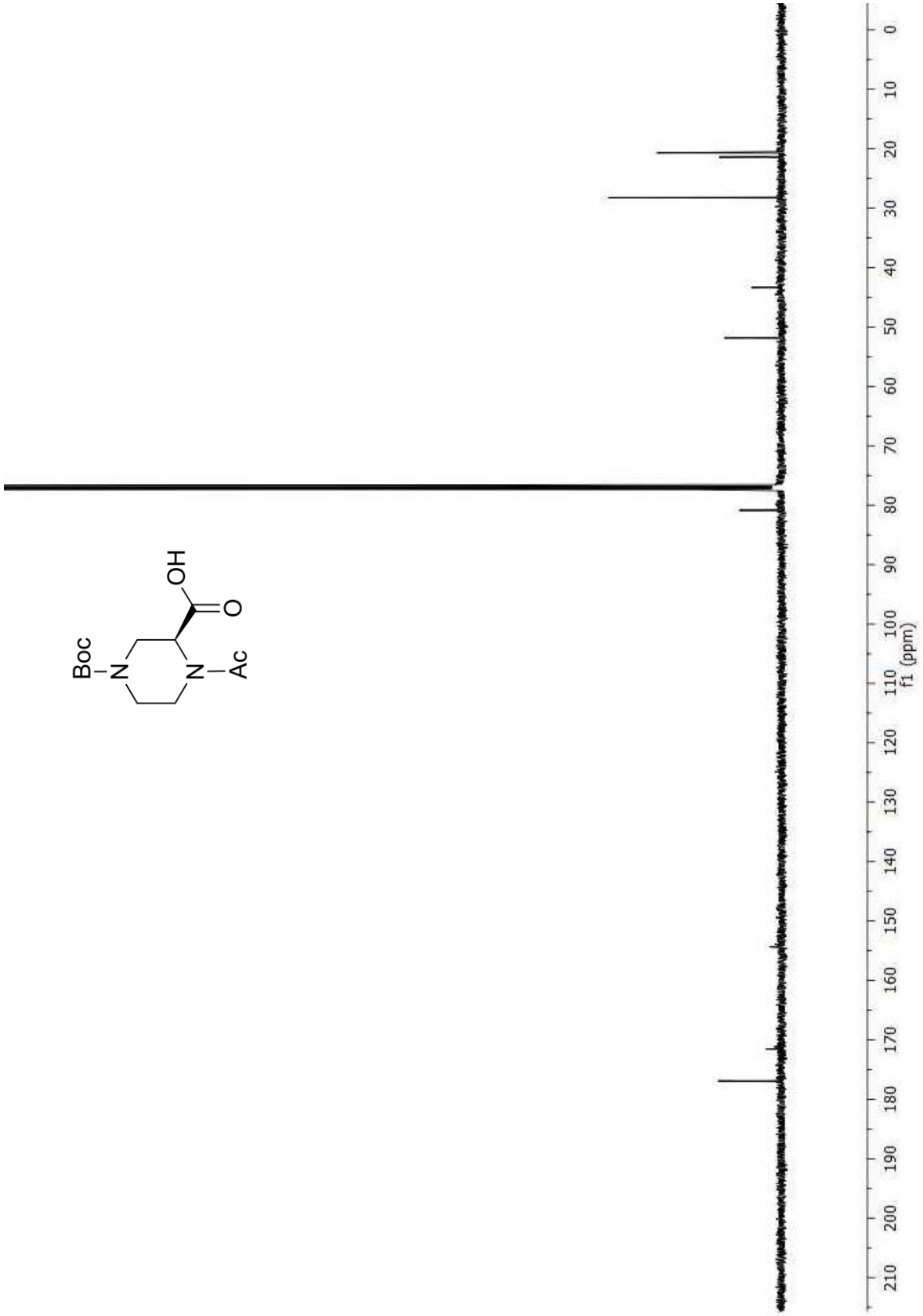

Figure 122: ^{13}C-NMR Spectrum ($CDCl_3$, 100 MHz) of **E1.**

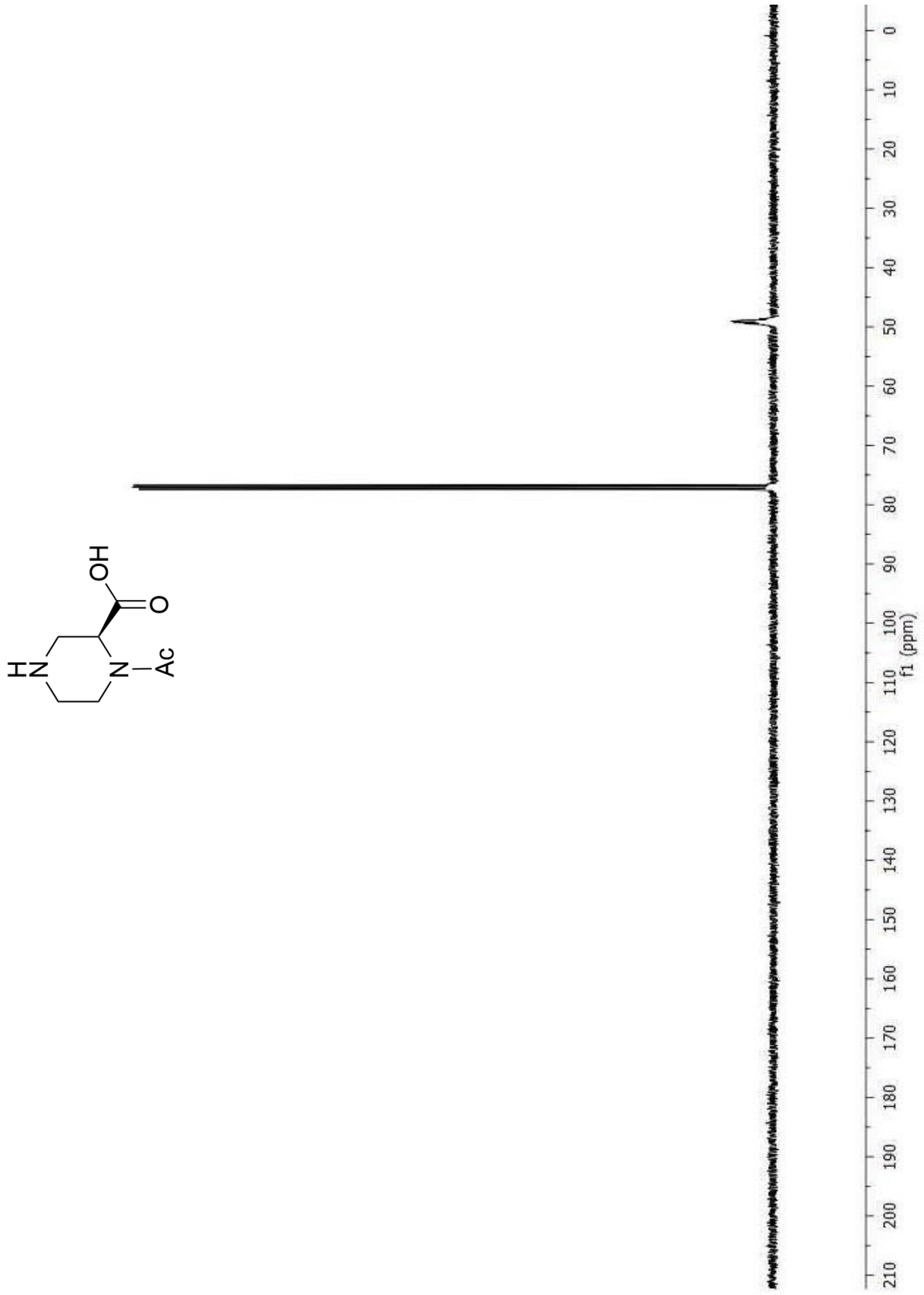

Figure 123: ^{13}C-NMR Spectrum ($CDCl_3$, 100 MHz) of **E2.**

AP1.2 Peptides

AP1.2.1 ^{1}H-NMR Spectra

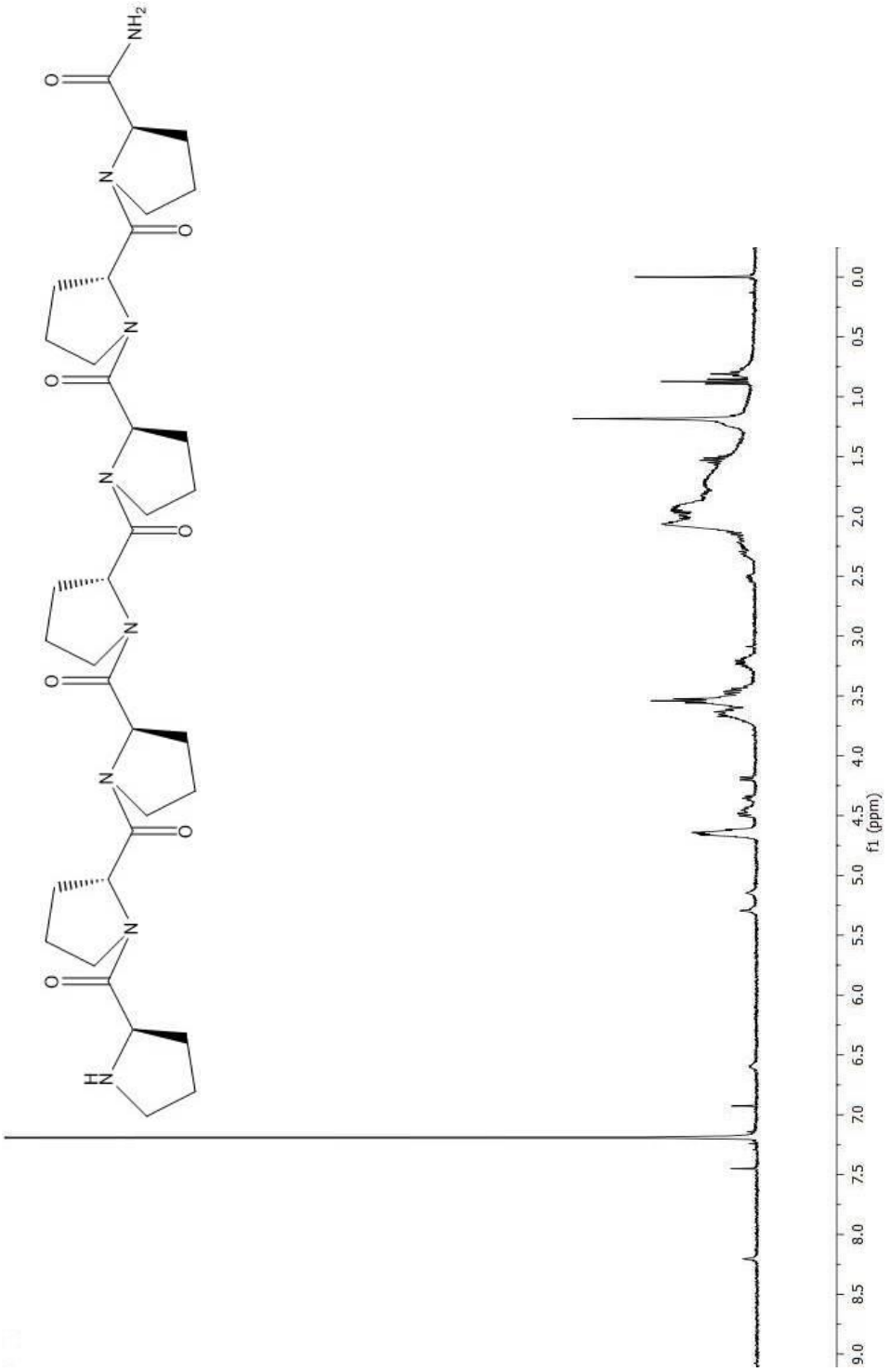

Figure 124: ^{1}H-NMR Spectrum ($CDCl_3$, 400 MHz) of **PP 1**.

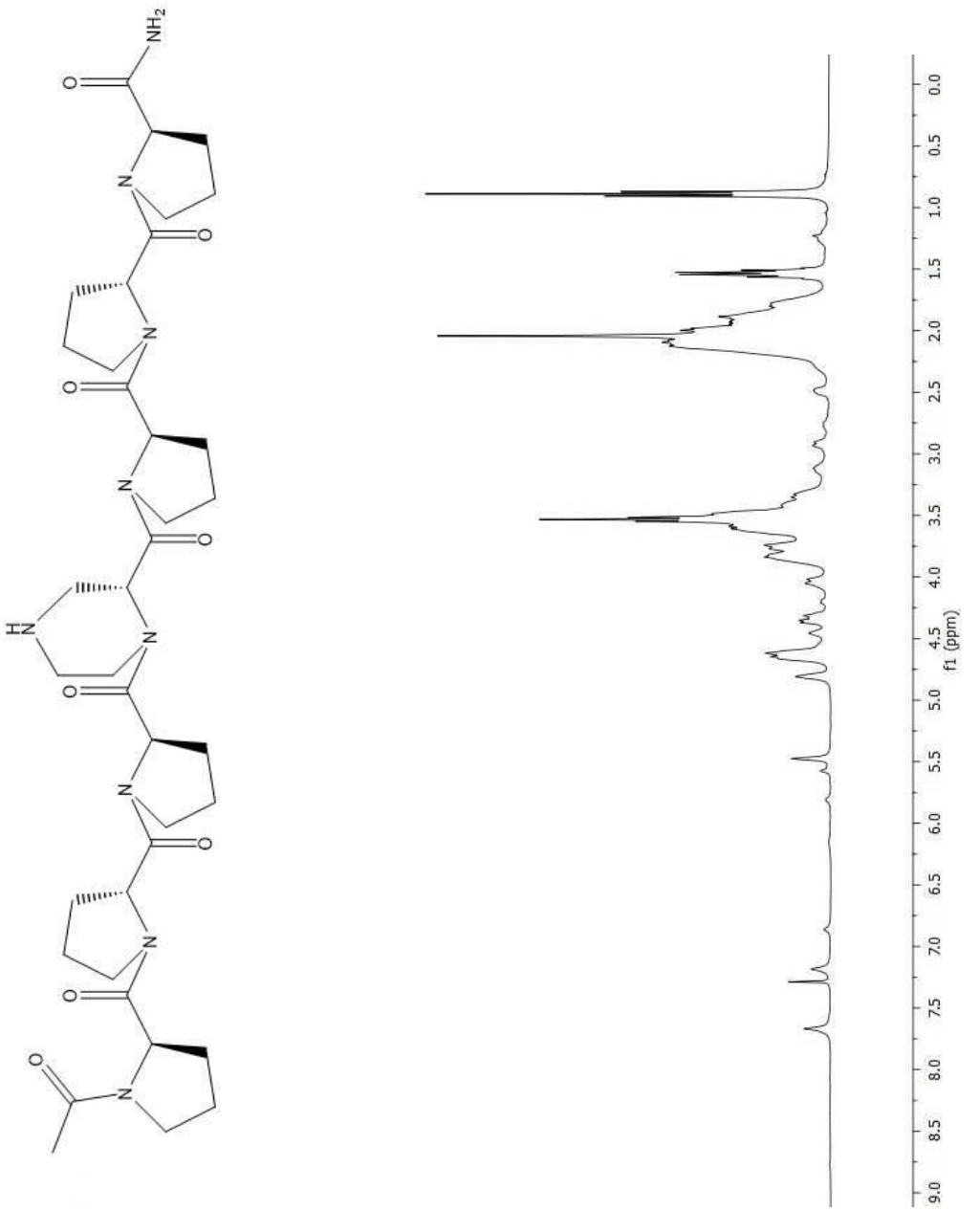

Figure 125: ^{1}H-NMR Spectrum ($CDCl_3$, 400 MHz) of **PP 2**.

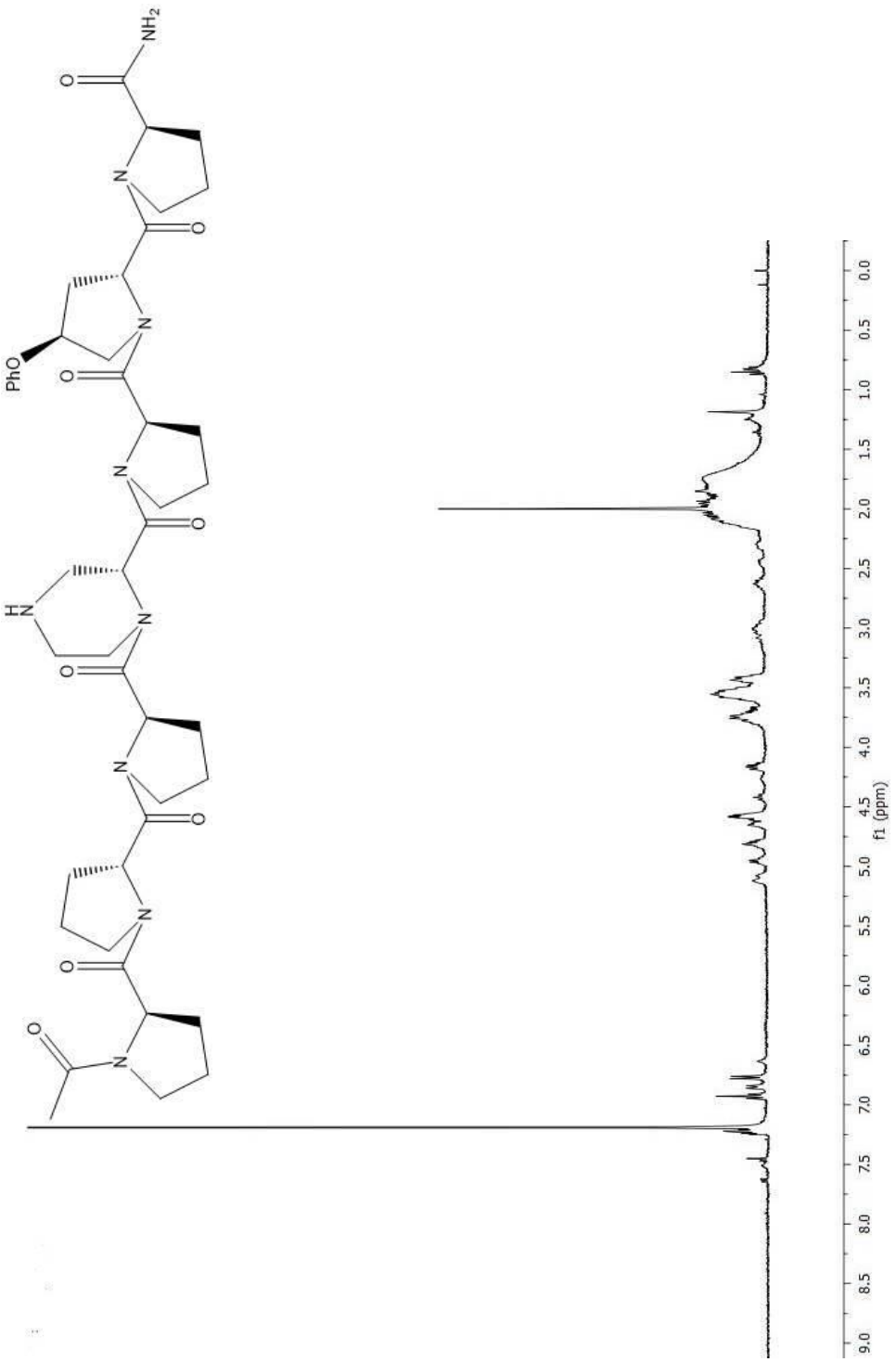

Figure 126: ^{1}H-NMR Spectrum ($CDCl_3$, 400 MHz) of **PP 3**.

AP1.3 Aldol Catalytic Reaction

AP1.3.1 ^{1}H-NMR Spectra

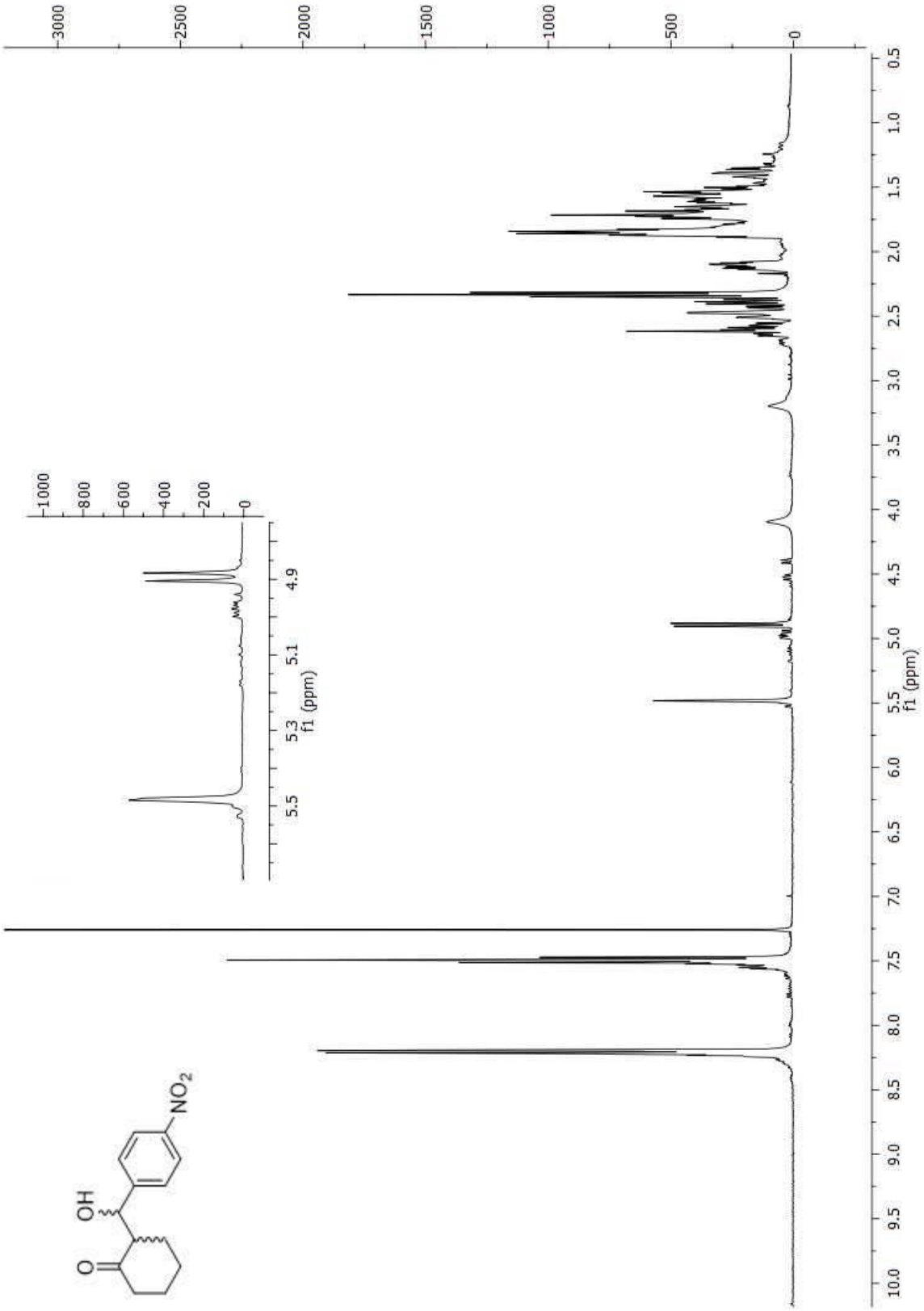

Figure 127: ^{1}H-NMR Spectrum ($CDCl_3$, 400 MHz) of 2-(hydroxyl-(p-nitrophenyl)methyl)cyclohexan-1-one Using ammonium acetate.

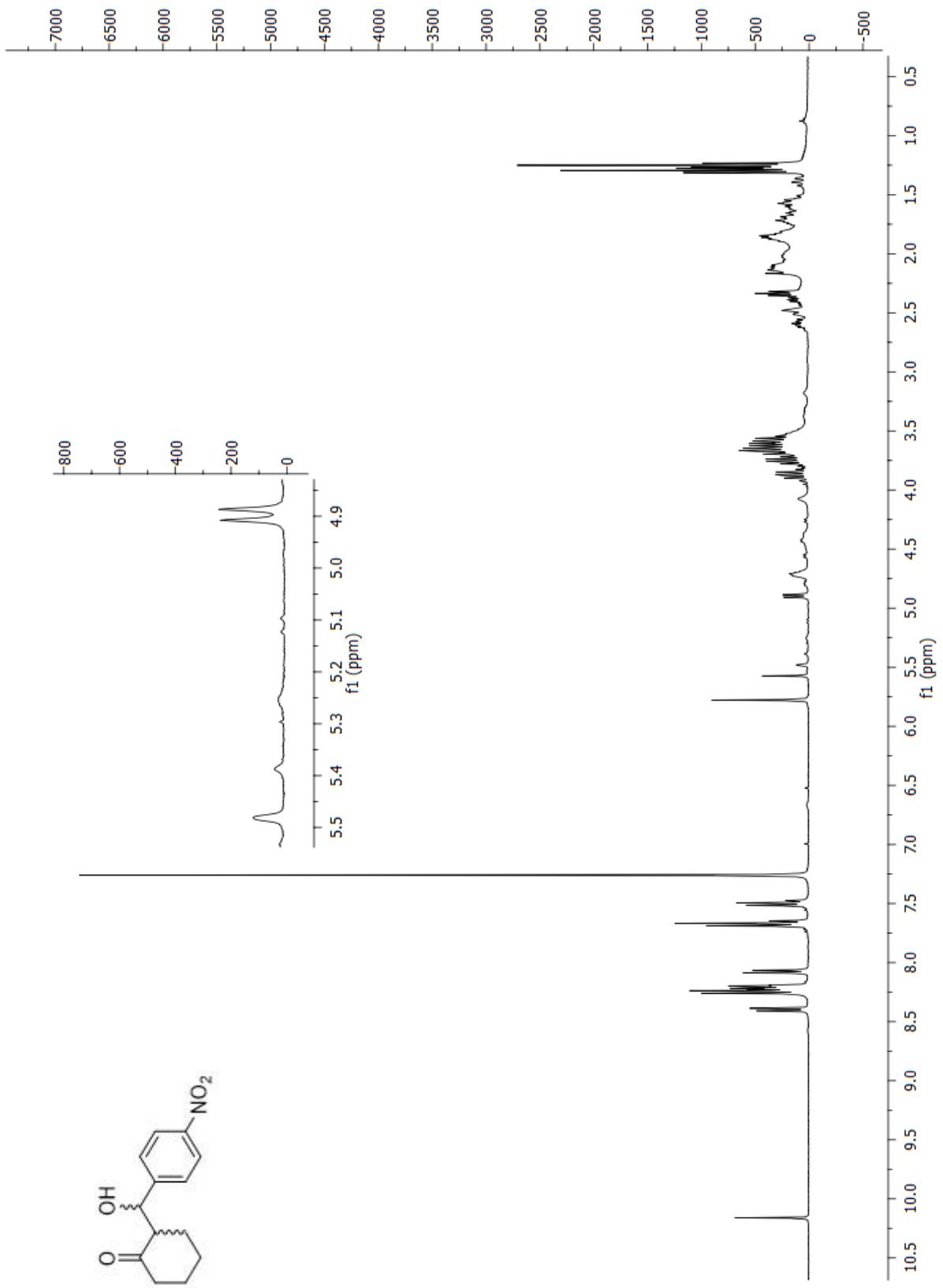

Figure 128: ^{1}H-NMR Spectrum ($CDCl_3$, 400 MHz) of 2-(hydroxyl-(p-nitrophenyl)methyl)cyclohexan-1-one Using **PP 1** (Table 5, Entry 1).

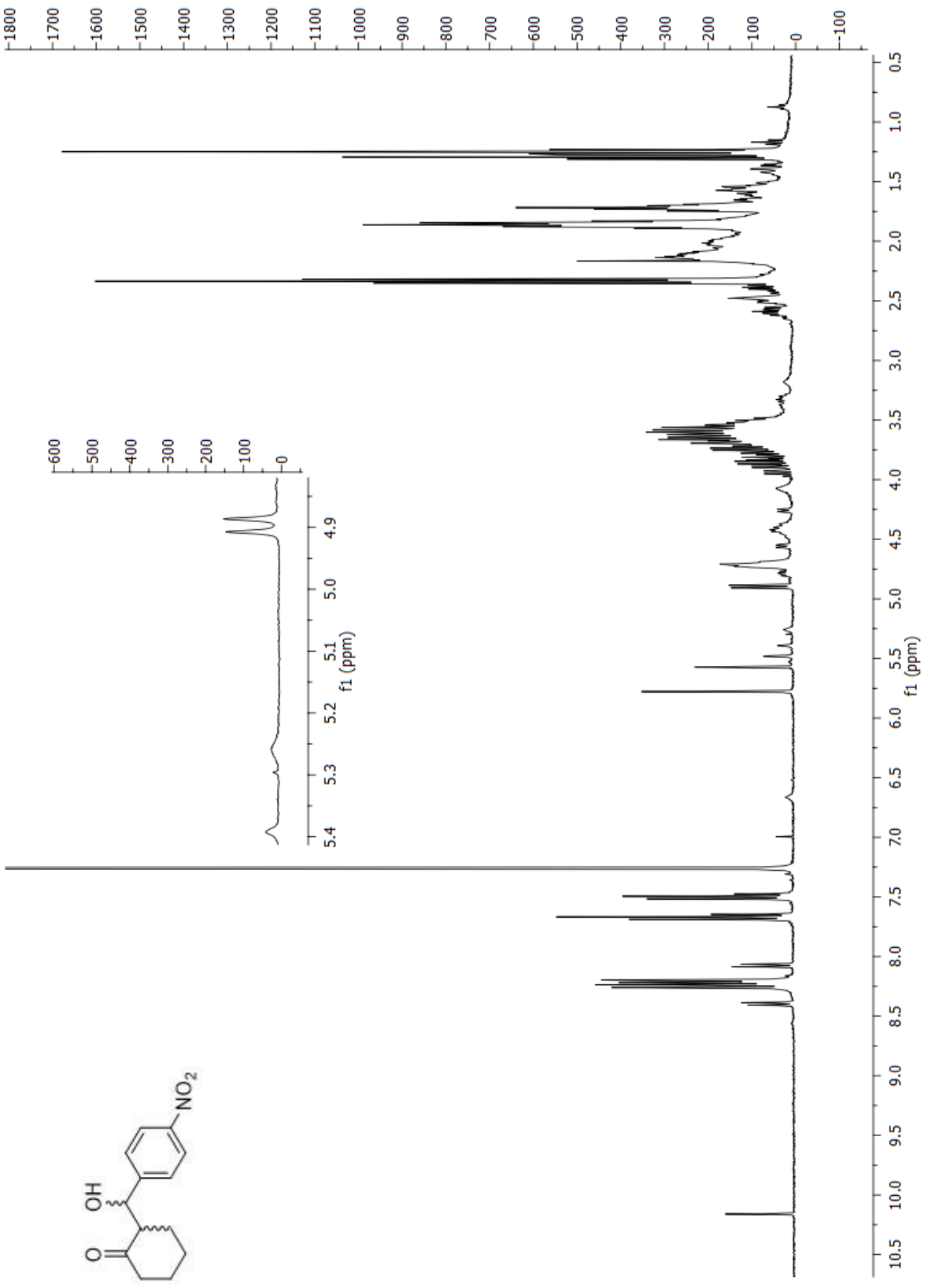

Figure 129: ^{1}H-NMR Spectrum ($CDCl_3$, 400 MHz) of 2-(hydroxyl-(p-nitrophenyl)methyl)cyclohexan-1-one Using **PP 1** (Table 5, Entry 2).

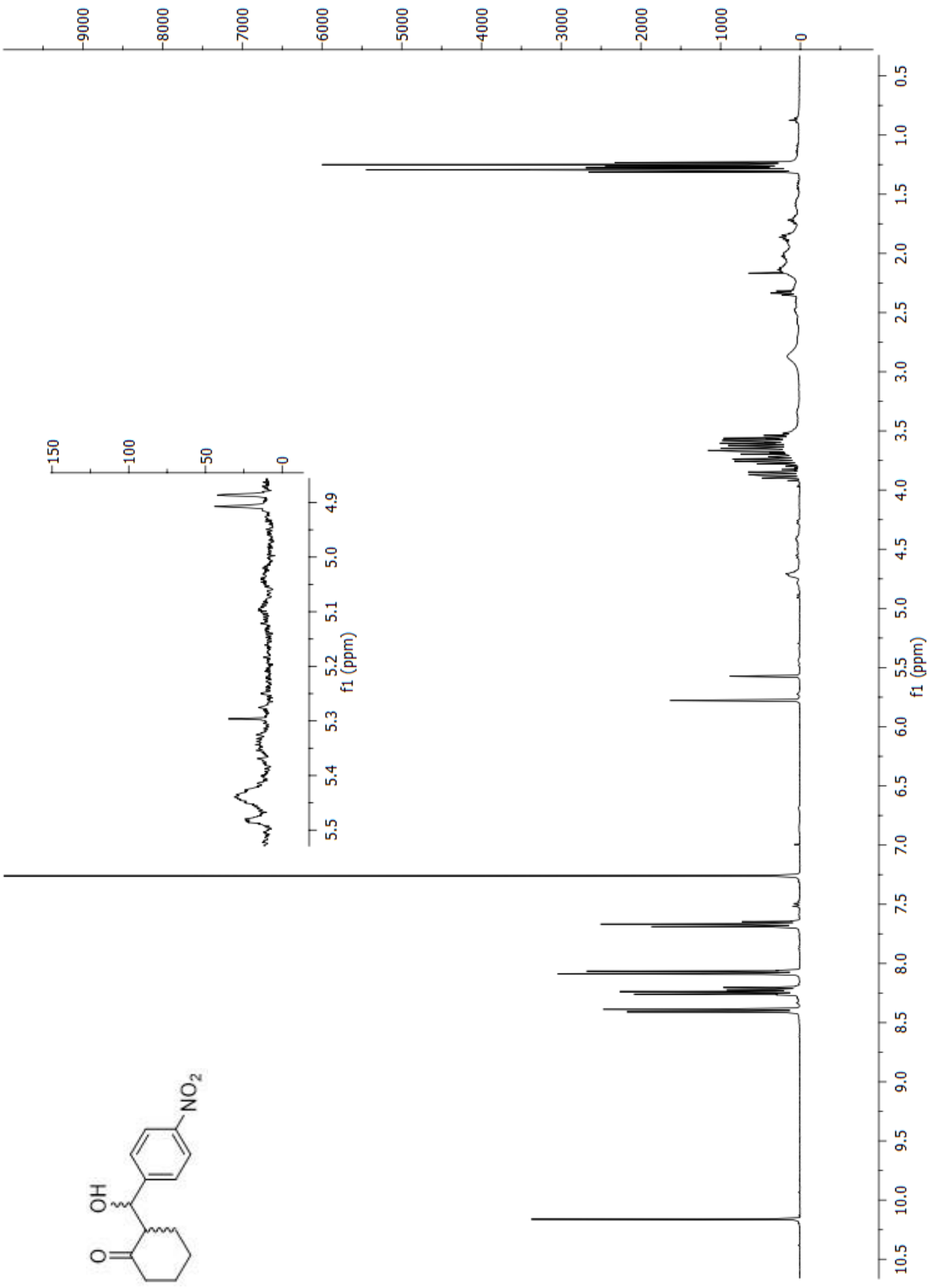

Figure 130: ^{1}H-NMR Spectrum ($CDCl_3$, 400 MHz) of 2-(hydroxyl-(p-nitrophenyl)methyl)cyclohexan-1-one Using **PP 1** (Table 5, Entry 3).

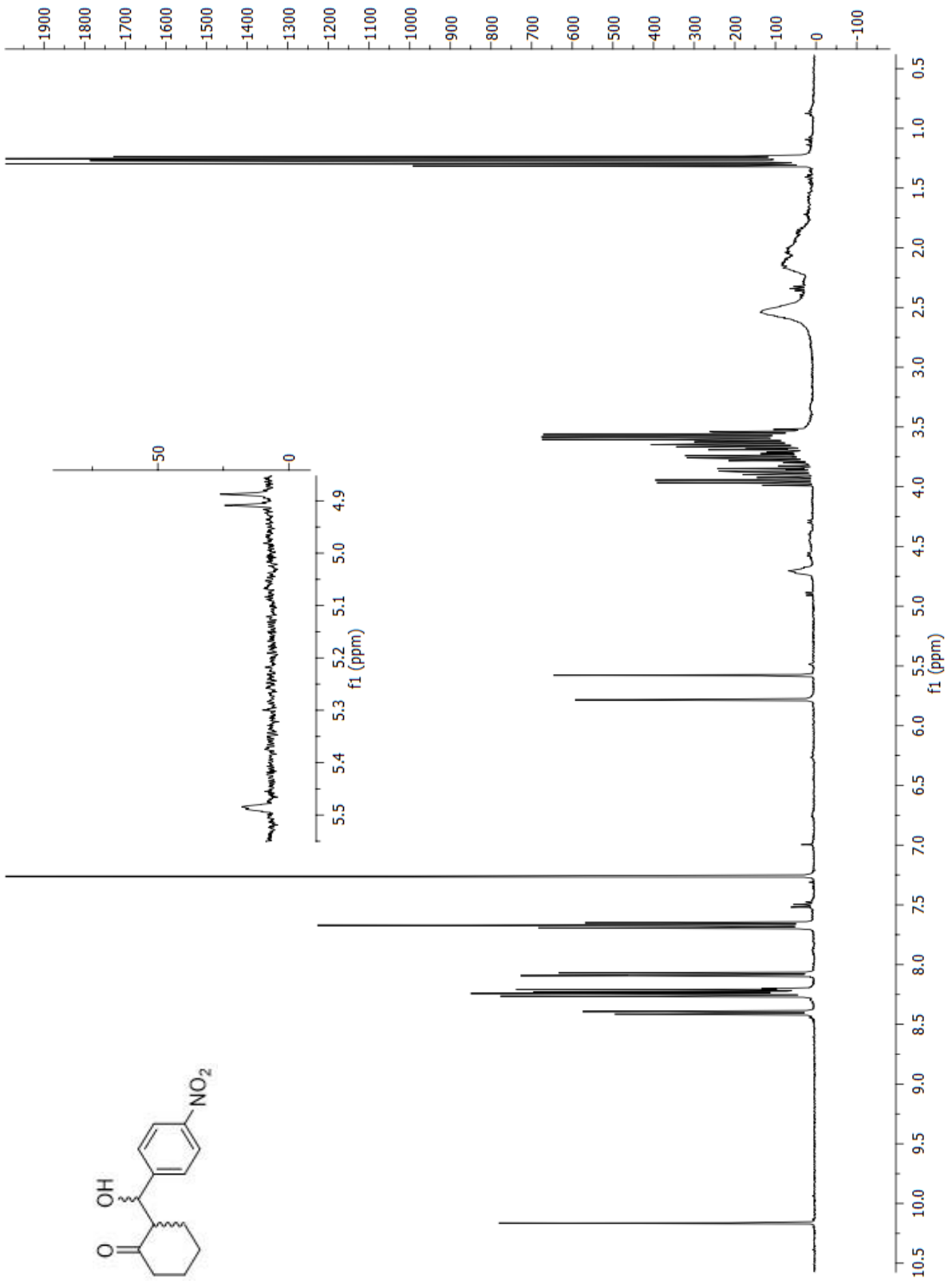

Figure 131: ^{1}H-NMR Spectrum ($CDCl_3$, 400 MHz) of 2-(hydroxyl-(p-nitrophenyl)methyl)cyclohexan-1-one Using **PP 1** (Table 5, Entry 4).

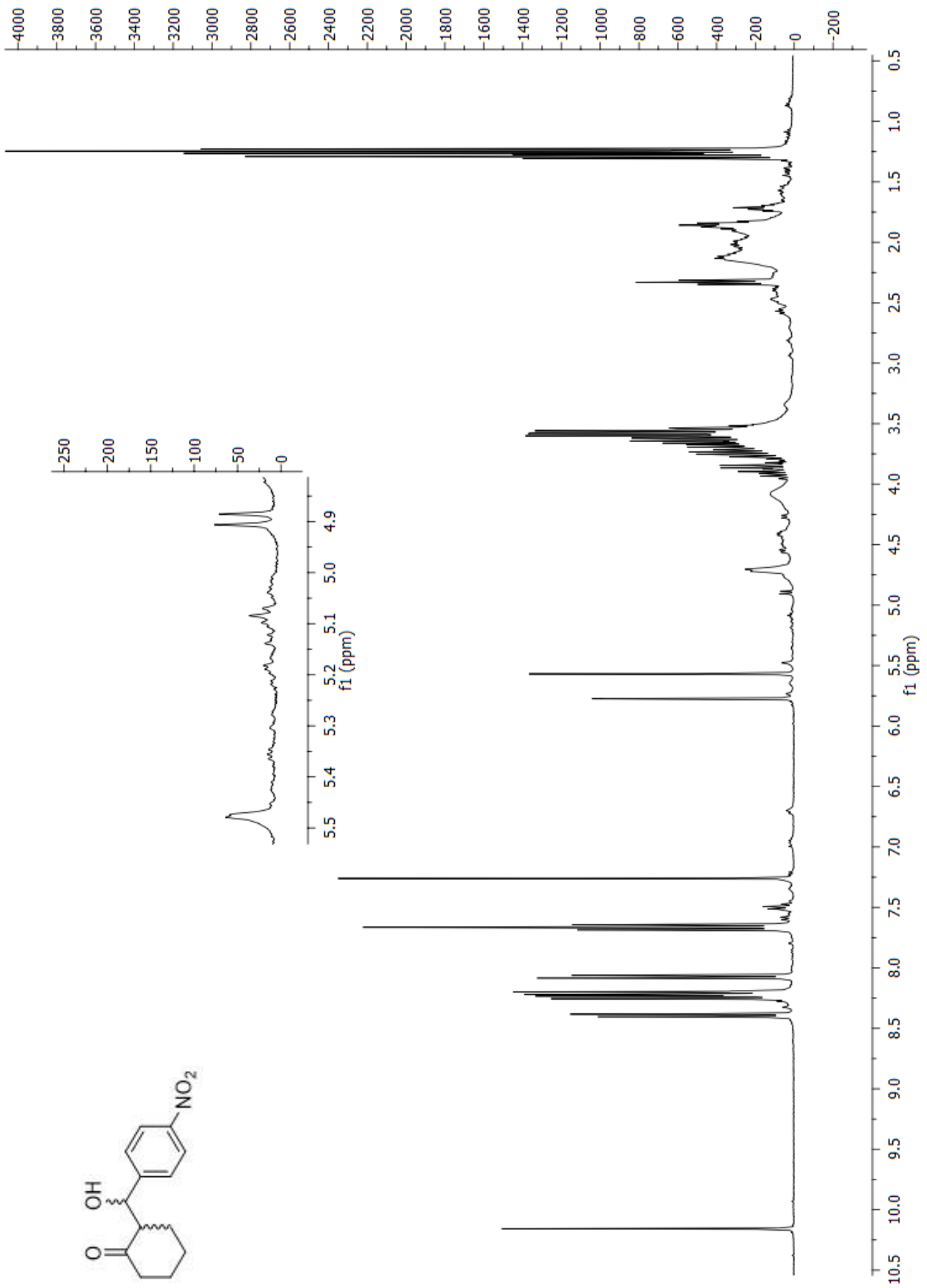

Figure 132: ^{1}H-NMR Spectrum ($CDCl_3$, 400 MHz) of 2-(hydroxyl-(p-nitrophenyl)methyl)cyclohexan-1-one Using **PP 1** (Table 5, Entry 5).

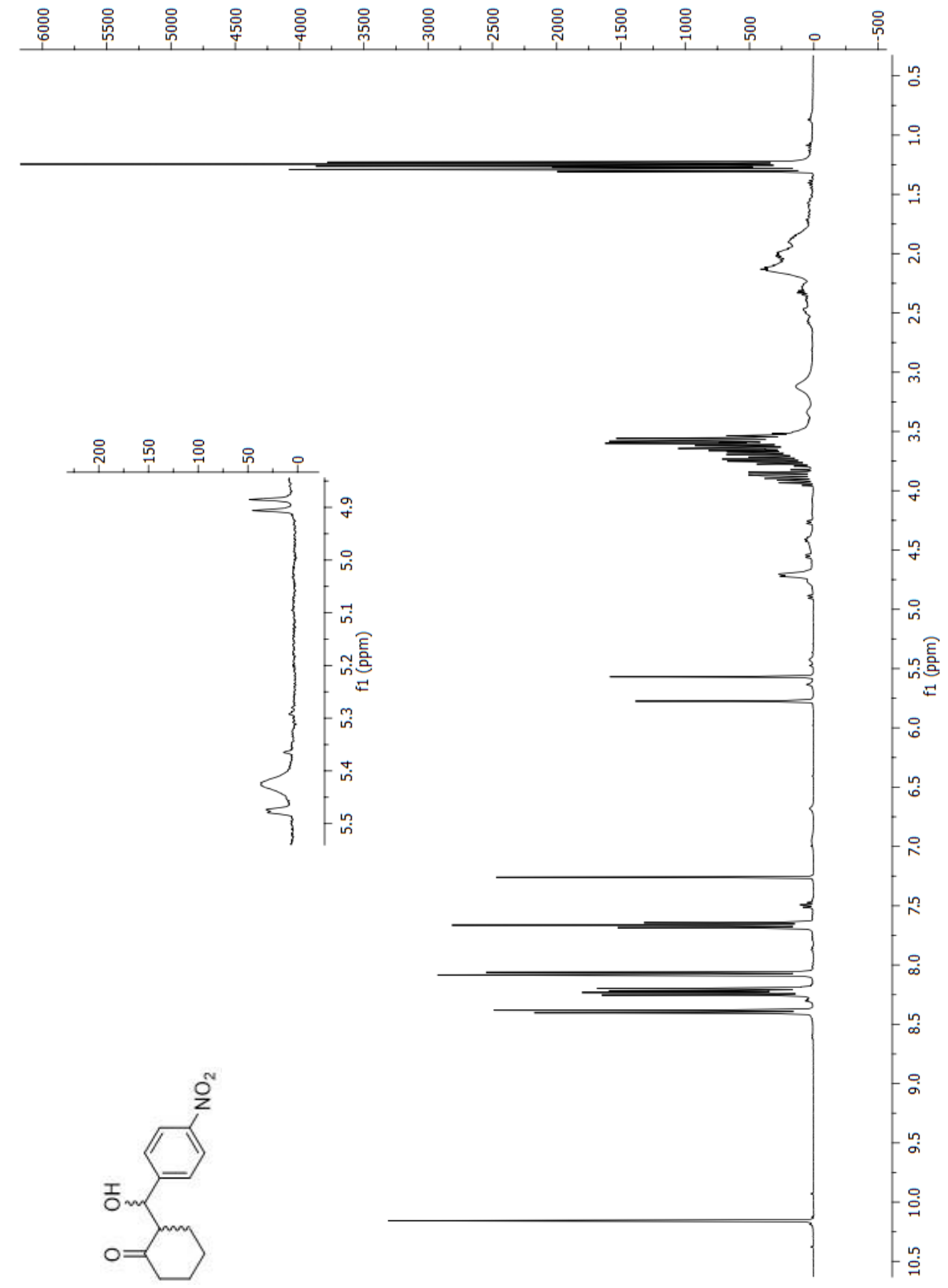

Figure 133: ^{1}H-NMR Spectrum ($CDCl_3$, 400 MHz) of 2-(hydroxyl-(p-nitrophenyl)methyl)cyclohexan-1-one Using **PP 1** (Table 5, Entry 6).

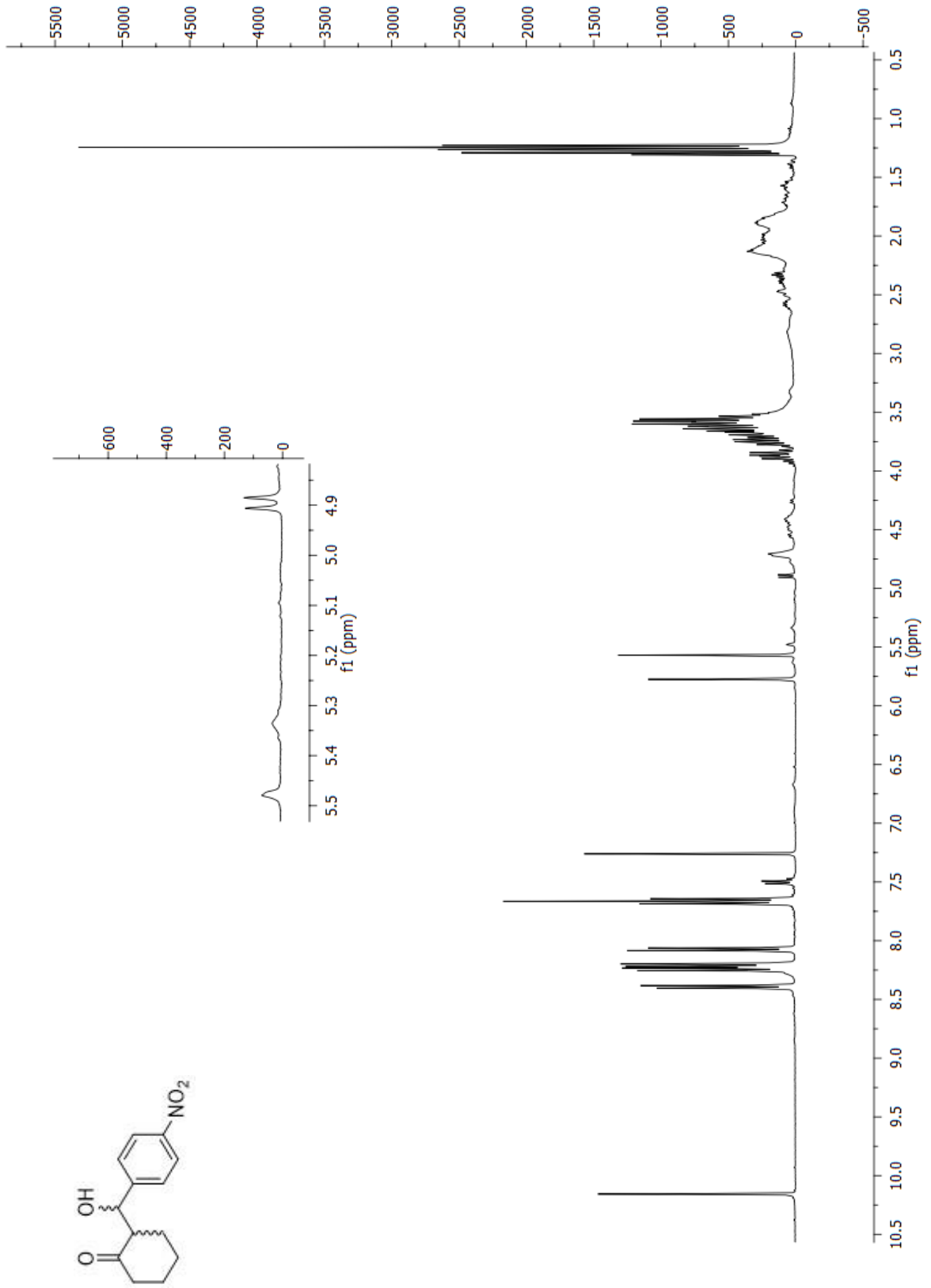

Figure 134: ^{1}H-NMR Spectrum ($CDCl_3$, 400 MHz) of 2-(hydroxyl-(p-nitrophenyl)methyl)cyclohexan-1-one Using **PP 1** (Table 5, Entry 7).

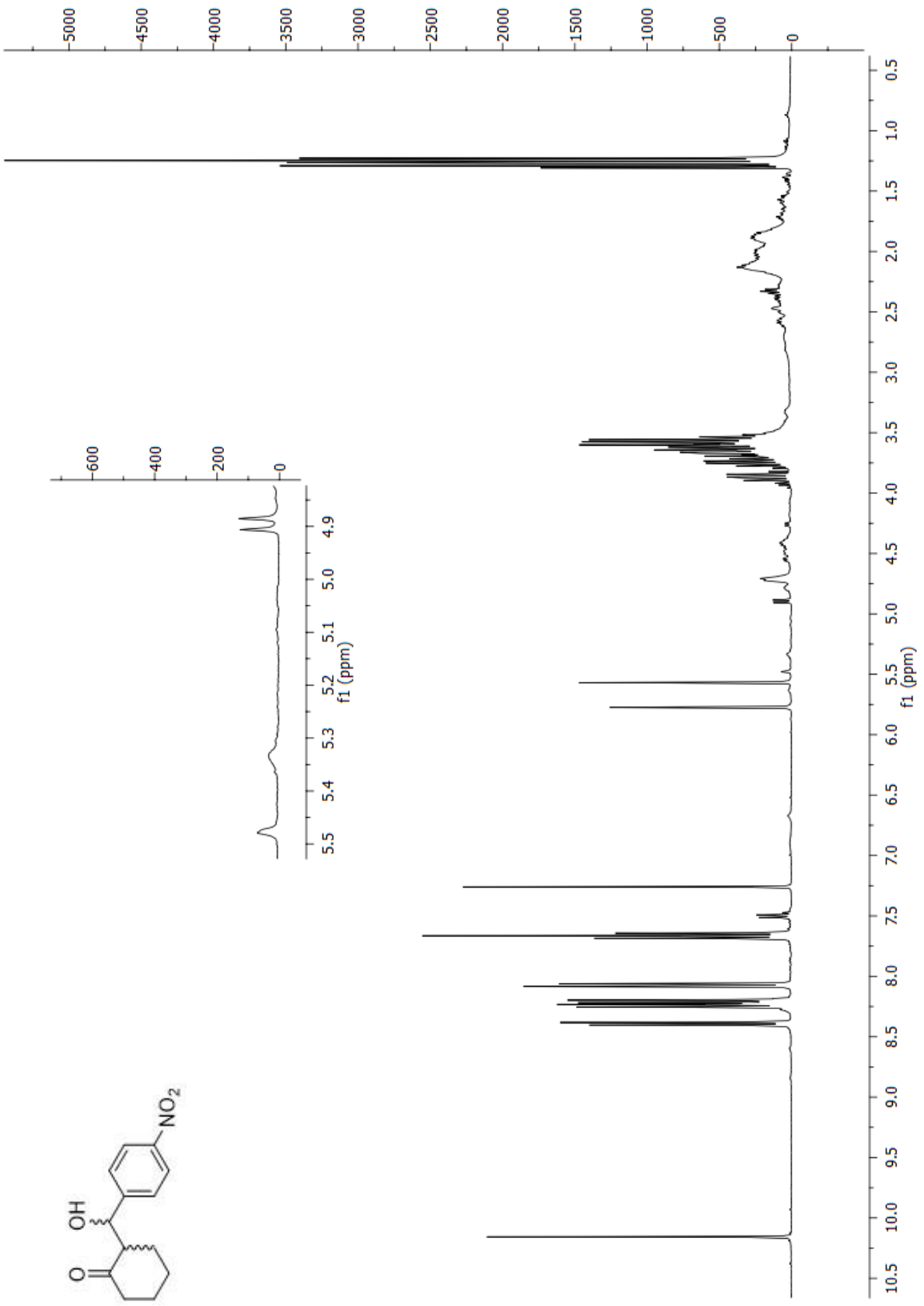

Figure 135: ^{1}H-NMR Spectrum ($CDCl_3$, 400 MHz) of 2-(hydroxyl-(p-nitrophenyl)methyl)cyclohexan-1-one Using **PP 1** (Table 5, Entry 8).

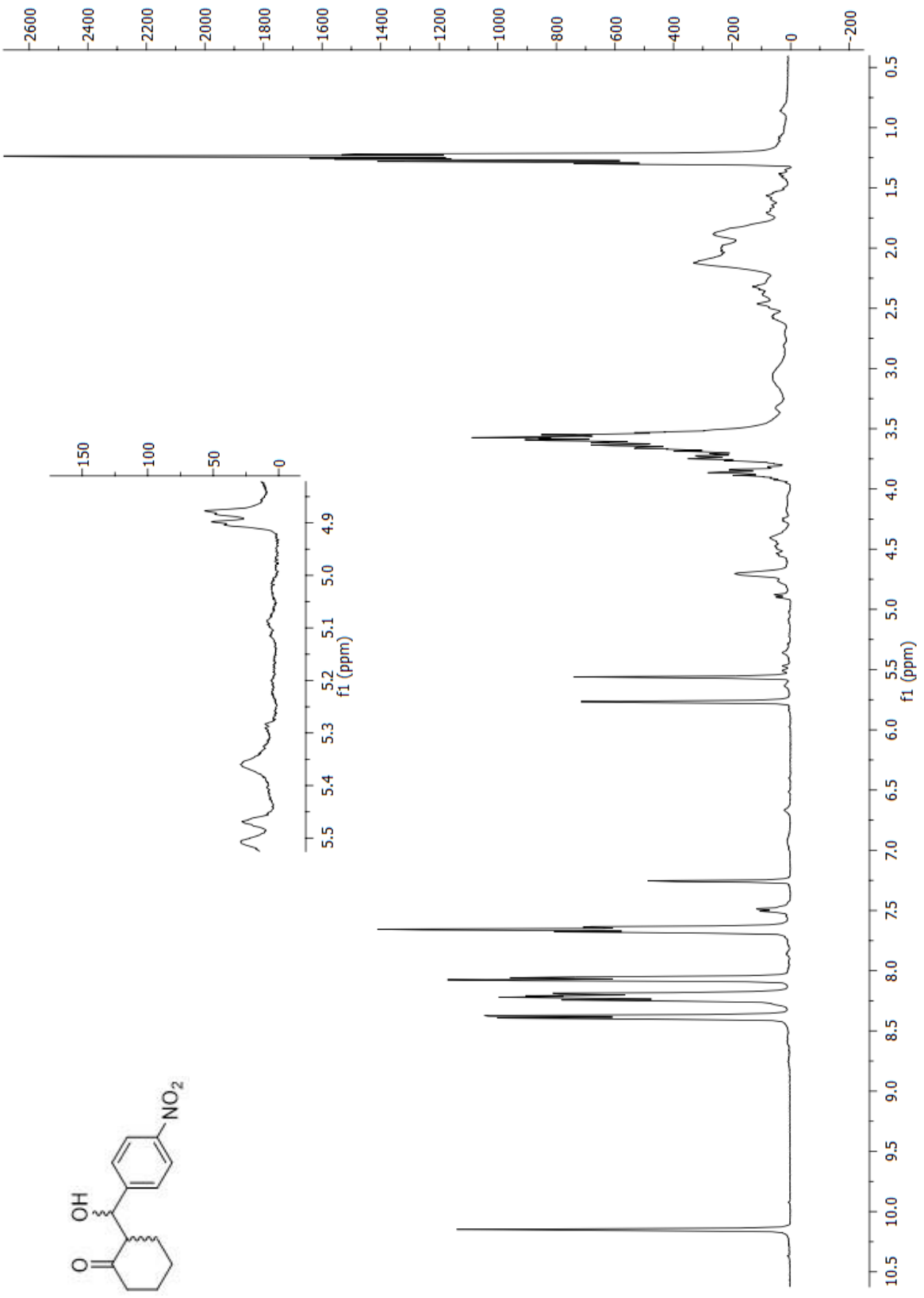

Figure 136: ^{1}H-NMR Spectrum ($CDCl_3$, 400 MHz) of 2-(hydroxyl-(p-nitrophenyl)methyl)cyclohexan-1-one Using **PP 1** (Table 5, Entry 9).

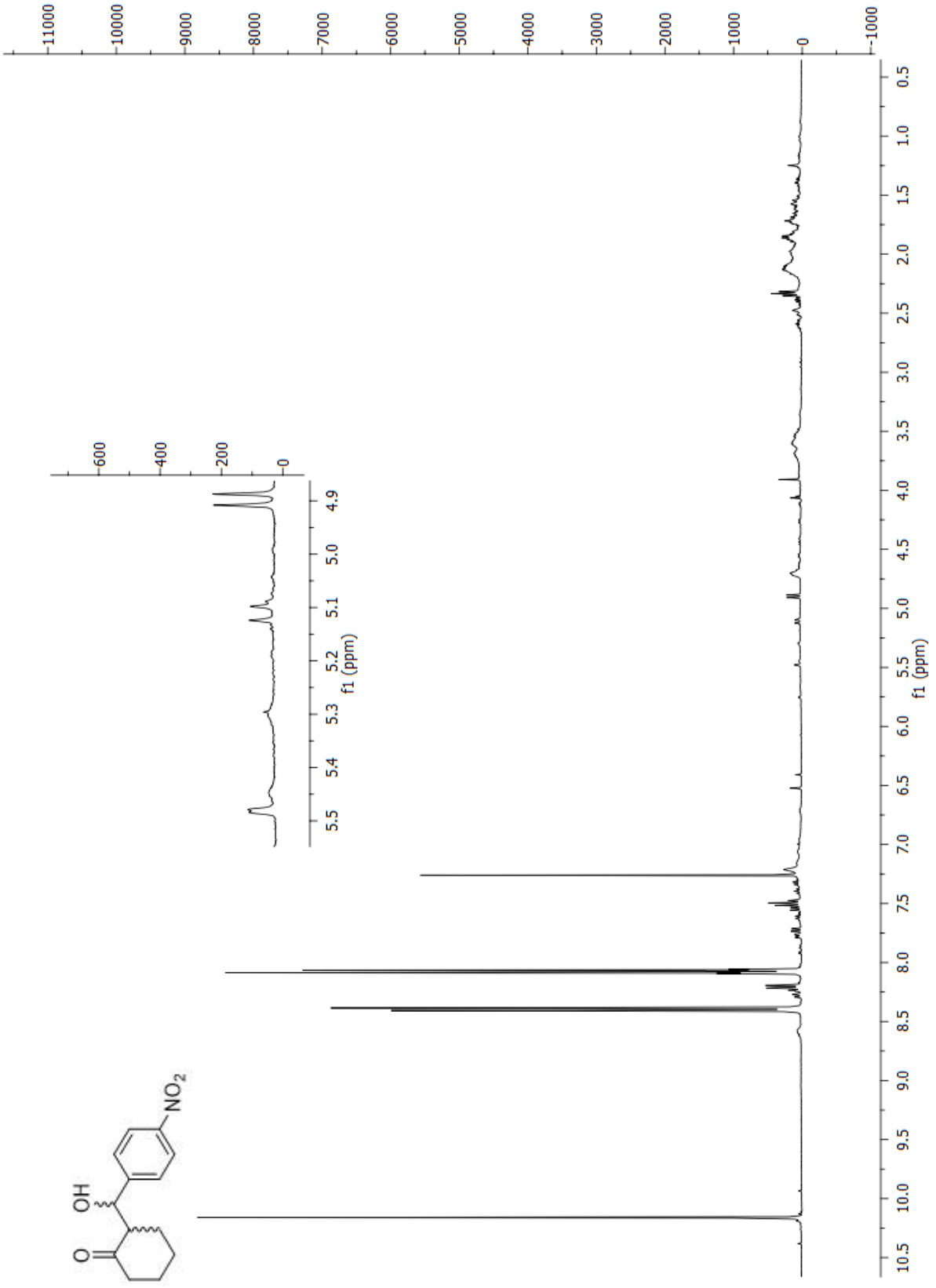

Figure 137: ^{1}H-NMR Spectrum ($CDCl_3$, 400 MHz) of 2-(hydroxyl-(p-nitrophenyl)methyl)cyclohexan-1-one Using **PP 1** (Table 5, Entry 10).

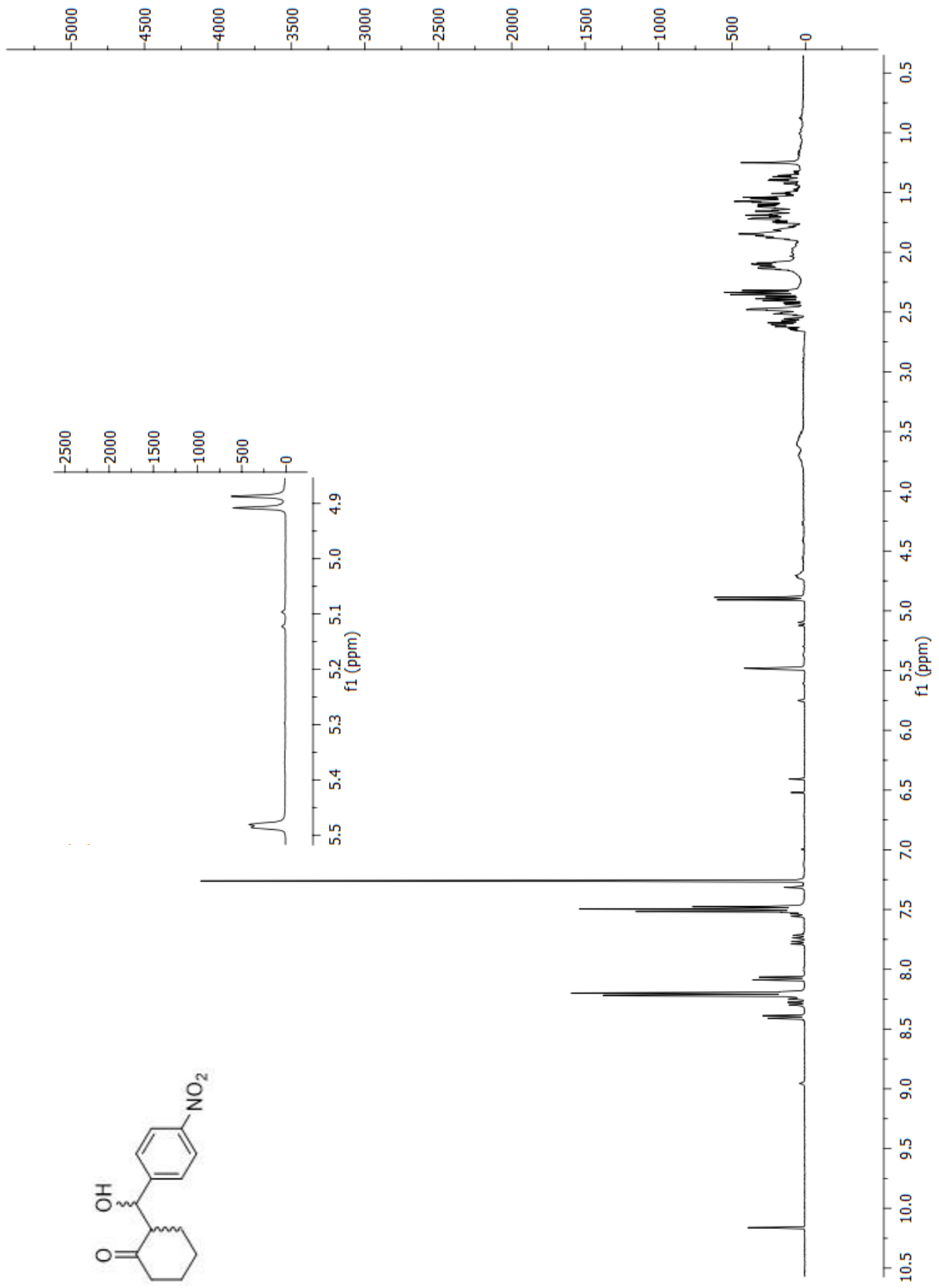

Figure 138: ^{1}H-NMR Spectrum ($CDCl_3$, 400 MHz) of 2-(hydroxyl-(p-nitrophenyl)methyl)cyclohexan-1-one Using **PP 1** (Table 5, Entry 11).

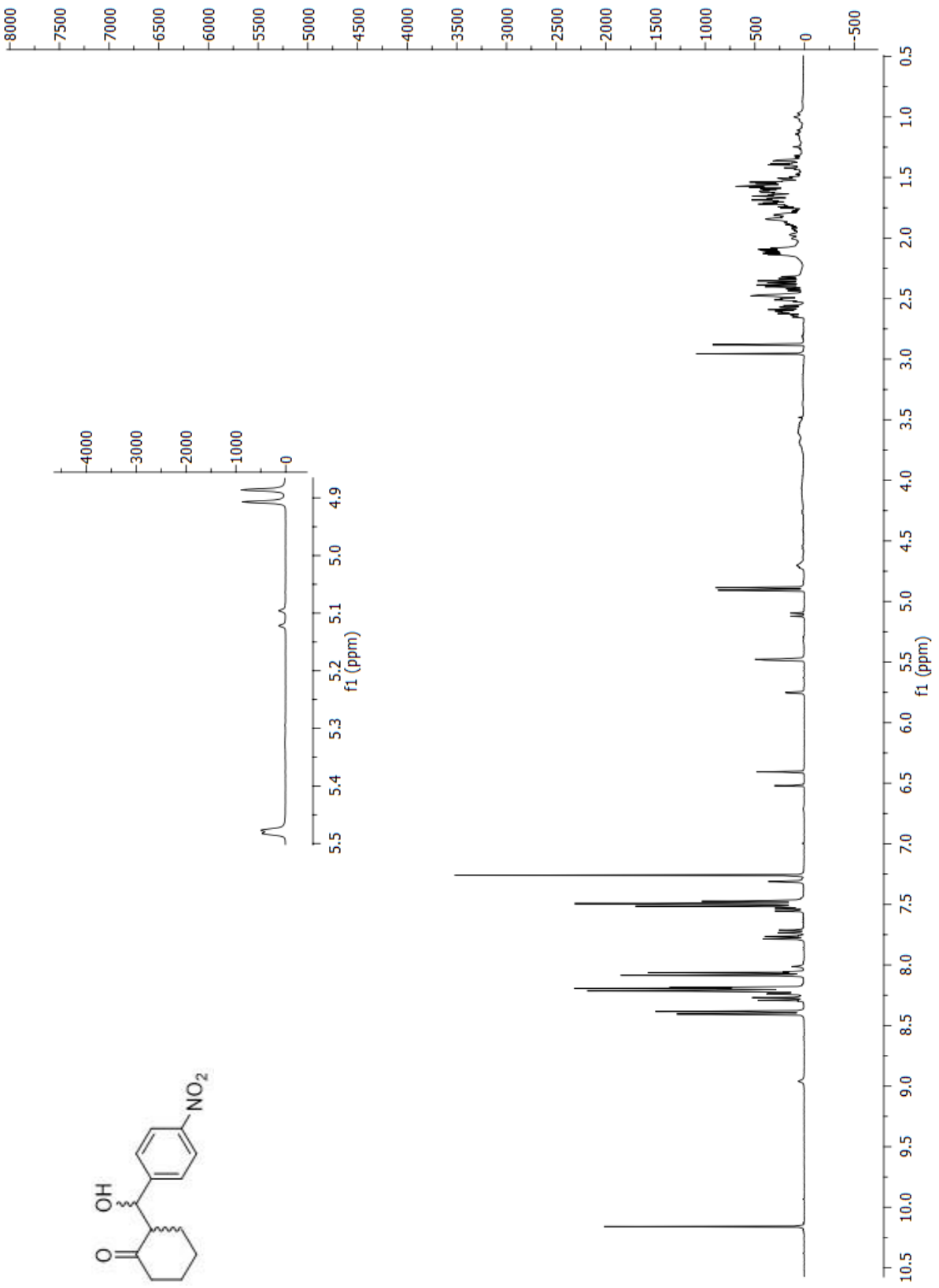

Figure 139: ^{1}H-NMR Spectrum ($CDCl_3$, 400 MHz) of 2-(hydroxyl-(p-nitrophenyl)methyl)cyclohexan-1-one Using **PP 1** (Table 5, Entry 12).

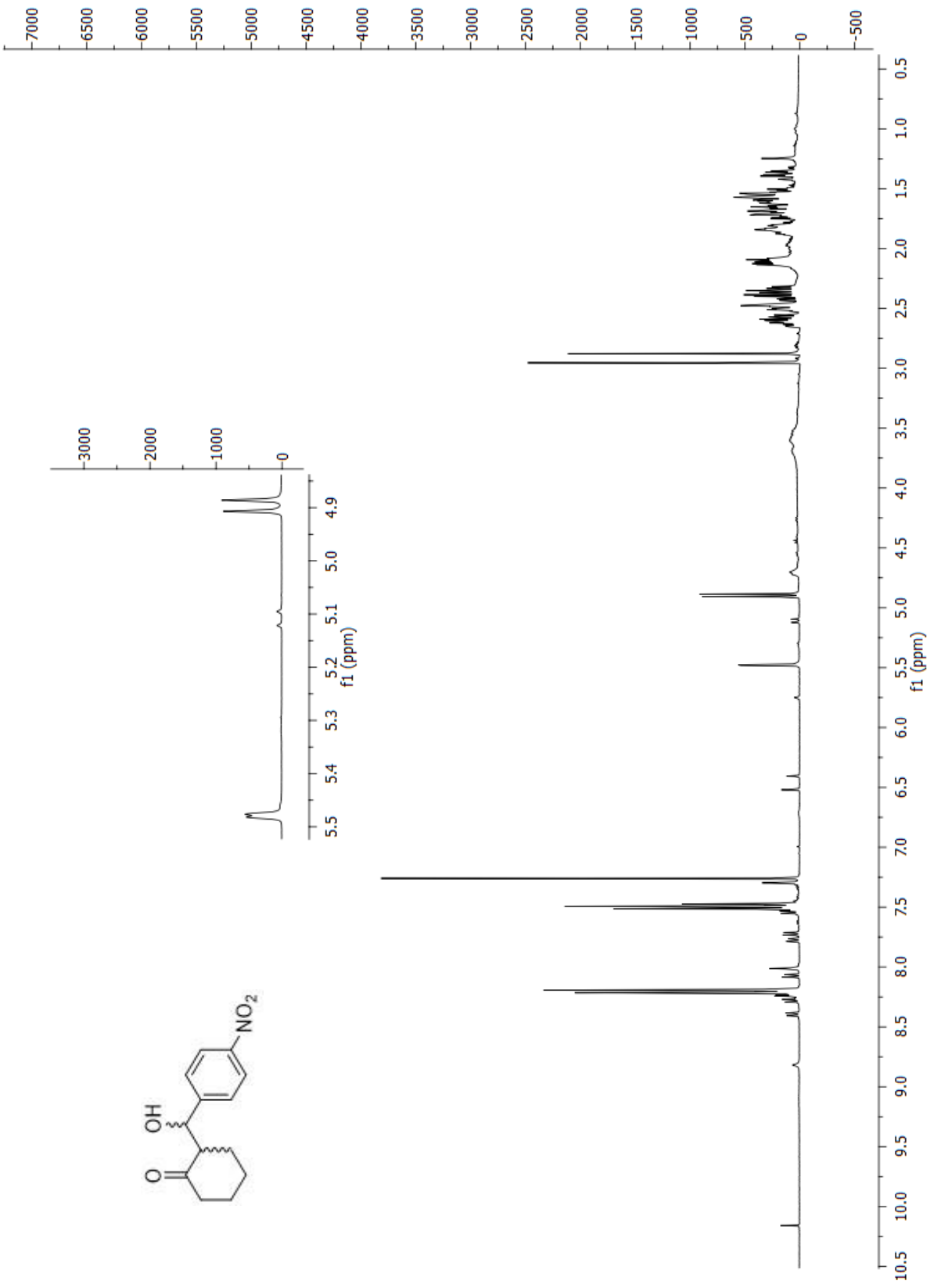

Figure 140: ^{1}H-NMR Spectrum ($CDCl_3$, 400 MHz) of 2-(hydroxyl-(p-nitrophenyl)methyl)cyclohexan-1-one Using **PP 1** (Table 5, Entry 13).

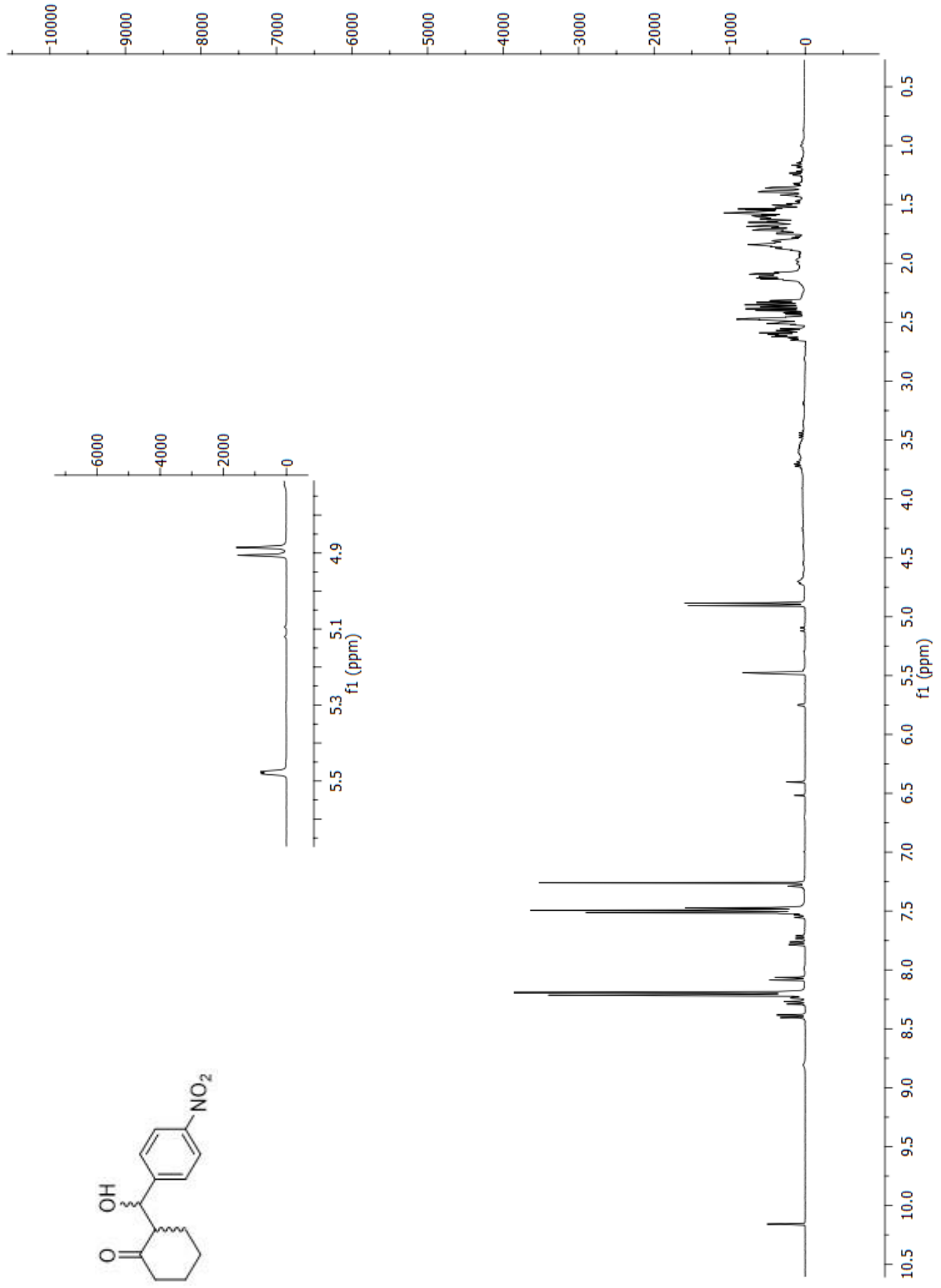

Figure 141: ^{1}H-NMR Spectrum ($CDCl_3$, 400 MHz) of 2-(hydroxyl-(p-nitrophenyl)methyl)cyclohexan-1-one Using **PP 1** (Table 5, Entry 14).

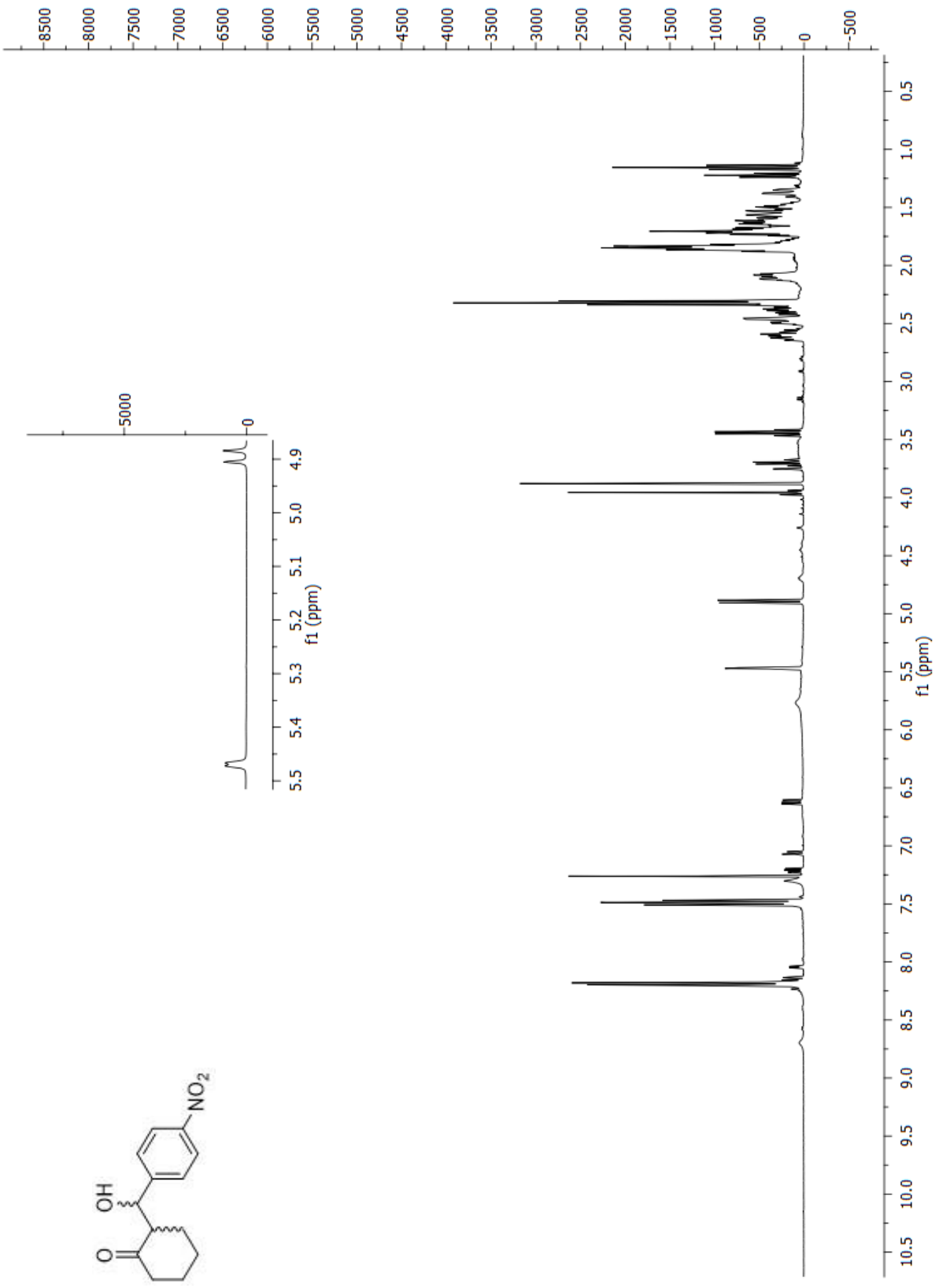

Figure 142: ^{1}H-NMR Spectrum ($CDCl_3$, 400 MHz) of 2-(hydroxyl-(p-nitrophenyl)methyl)cyclohexan-1-one Using **PP 1** (Table 5, Entry 15).

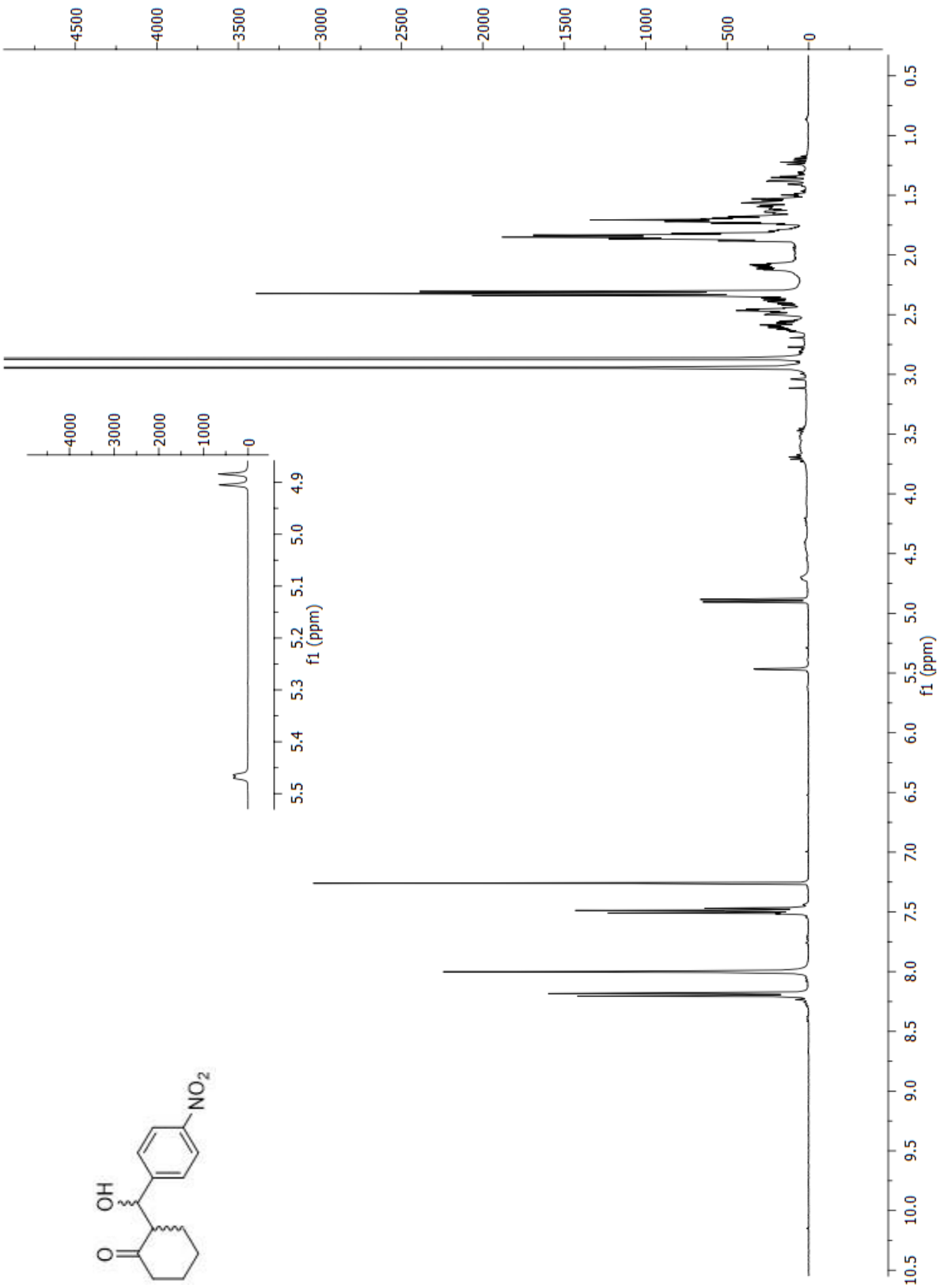

Figure 143: ^{1}H-NMR Spectrum ($CDCl_3$, 400 MHz) of 2-(hydroxyl-(p-nitrophenyl)methyl)cyclohexan-1-one Using **PP 1** (Table 5, Entry 16).

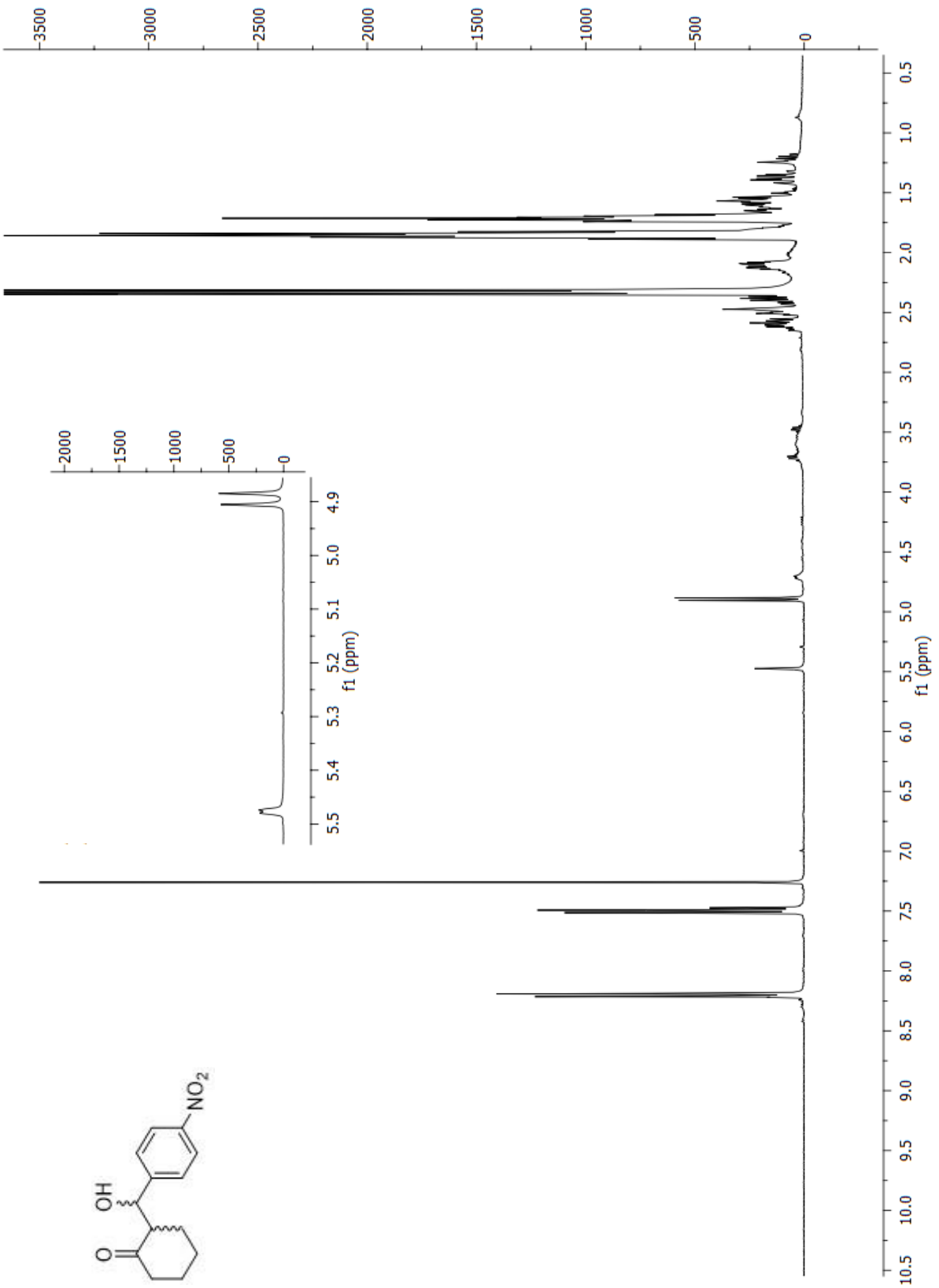

Figure 144: ^{1}H-NMR Spectrum ($CDCl_3$, 400 MHz) of 2-(hydroxyl-(p-nitrophenyl)methyl)cyclohexan-1-one Using **PP 1** (Table 5, Entry 17).

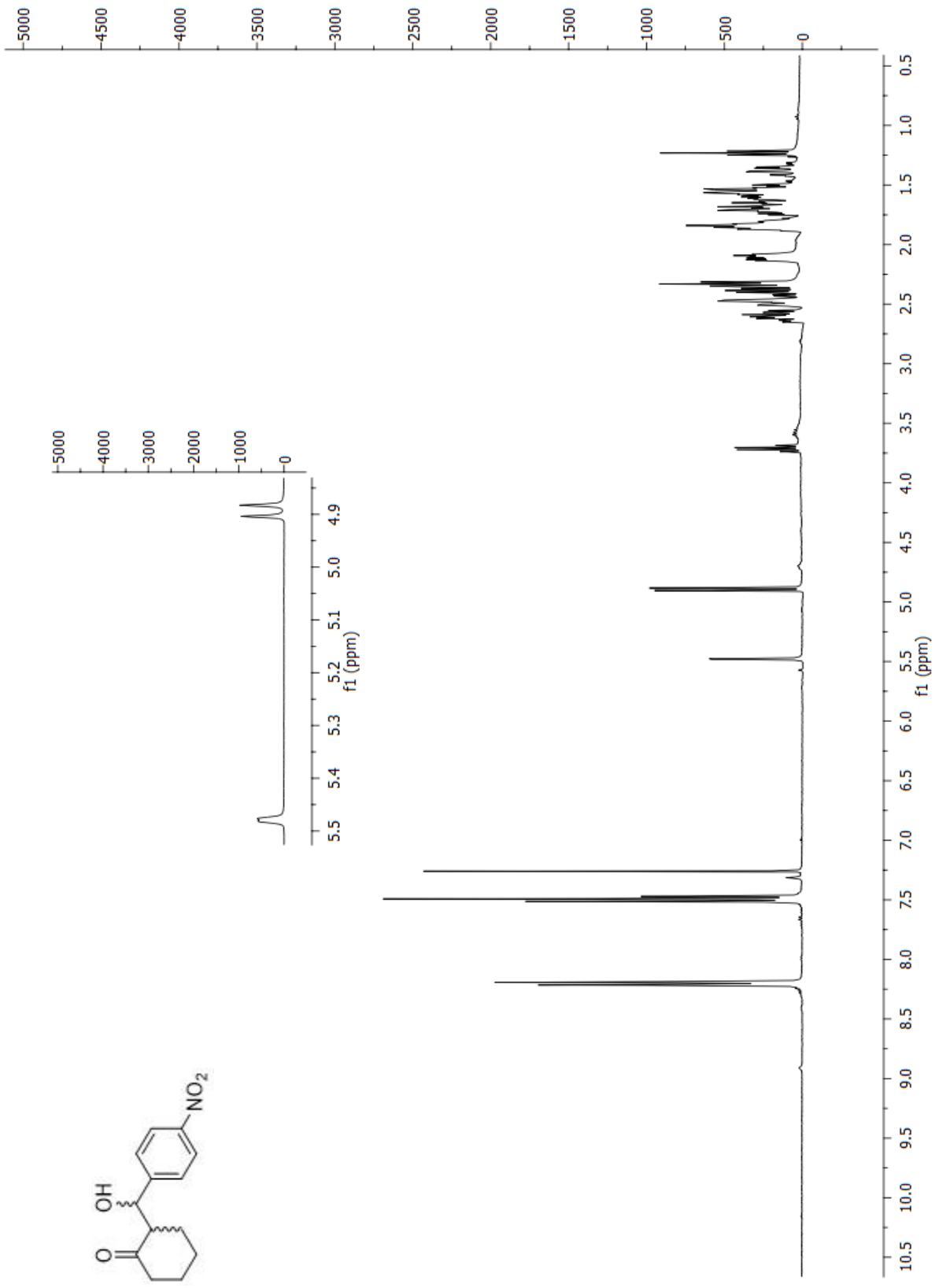

Figure 145: ^{1}H-NMR Spectrum ($CDCl_3$, 400 MHz) of 2-(hydroxyl-(p-nitrophenyl)methyl)cyclohexan-1-one Using **PP 1** (Table 5, Entry 18).

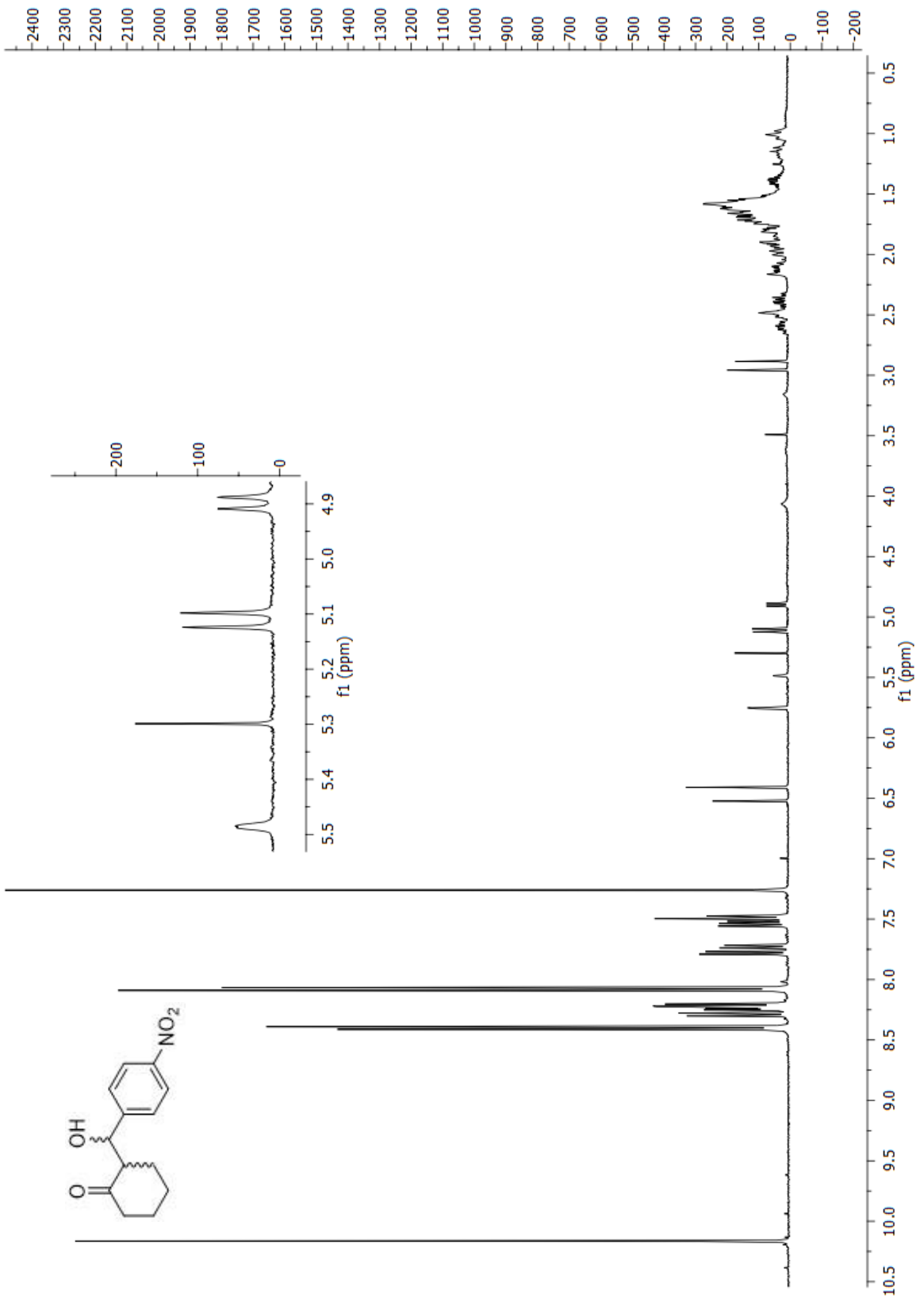

Figure 146: ^{1}H-NMR Spectrum ($CDCl_3$, 400 MHz) of 2-(hydroxyl-(p-nitrophenyl)methyl)cyclohexan-1-one Using **PP 2** (Table 6, Entry 19).

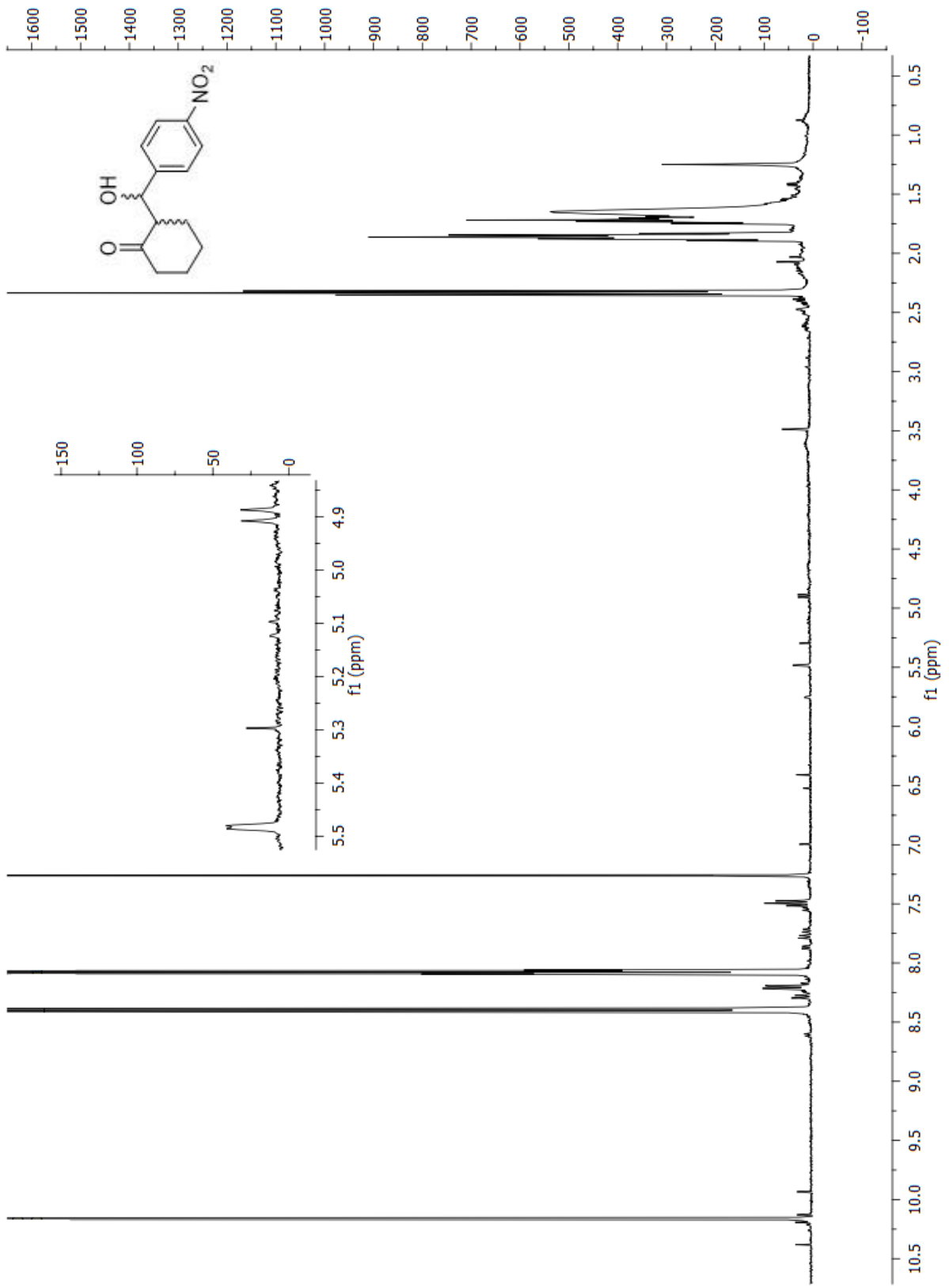

Figure 147: ^{1}H-NMR Spectrum ($CDCl_3$, 400 MHz) of 2-(hydroxyl-(p-nitrophenyl)methyl)cyclohexan-1-one Using **PP 2** (Table 6, Entry 21).

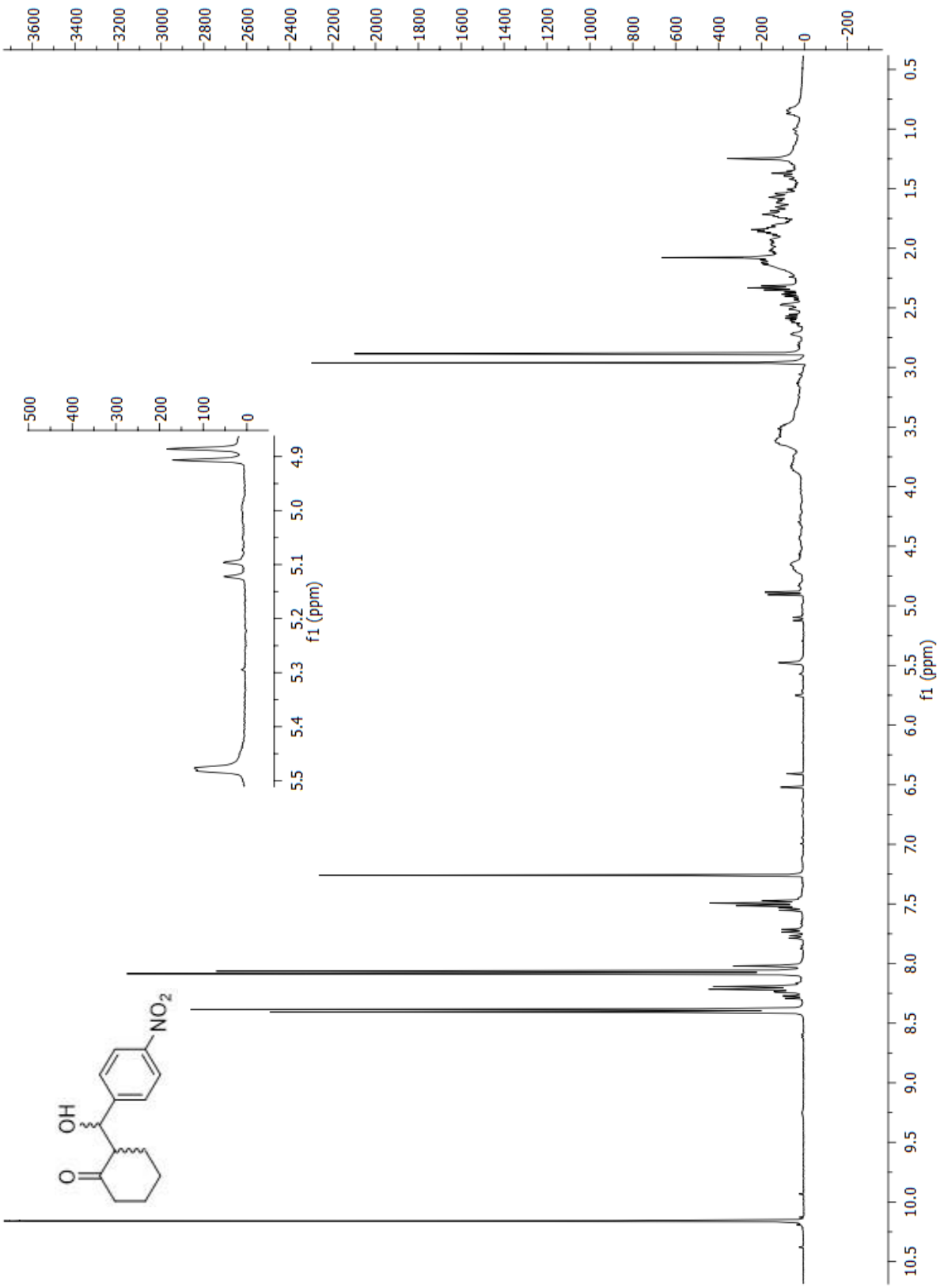

Figure 148: ^{1}H-NMR Spectrum ($CDCl_3$, 400 MHz) of 2-(hydroxyl-(p-nitrophenyl)methyl)cyclohexan-1-one Using **PP 2** (Table 6, Entry 22).

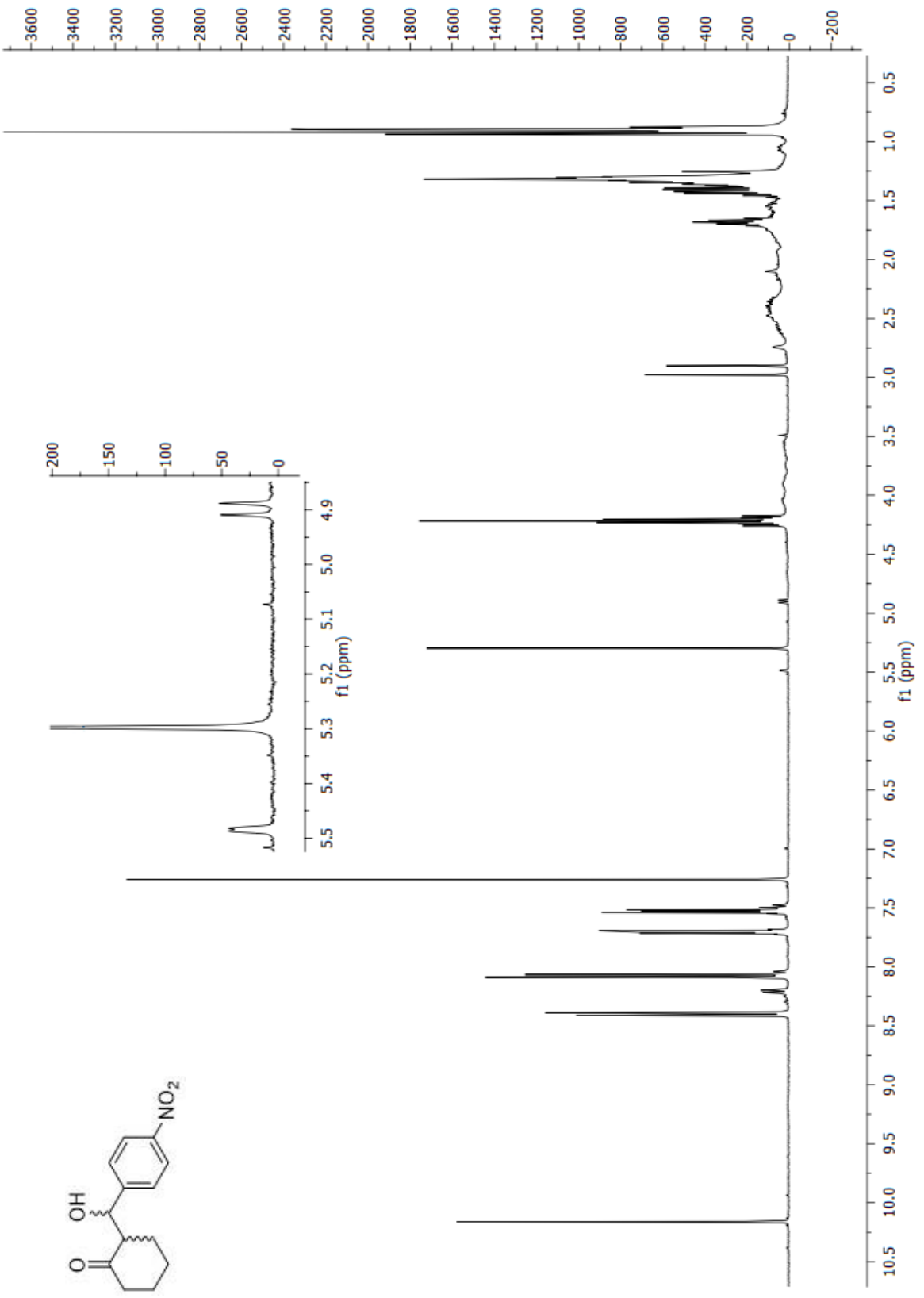

Figure 149: ^{1}H-NMR Spectrum ($CDCl_3$, 400 MHz) of 2-(hydroxyl-(p-nitrophenyl)methyl)cyclohexan-1-one Using **PP 2** (Table 6, Entry 23).

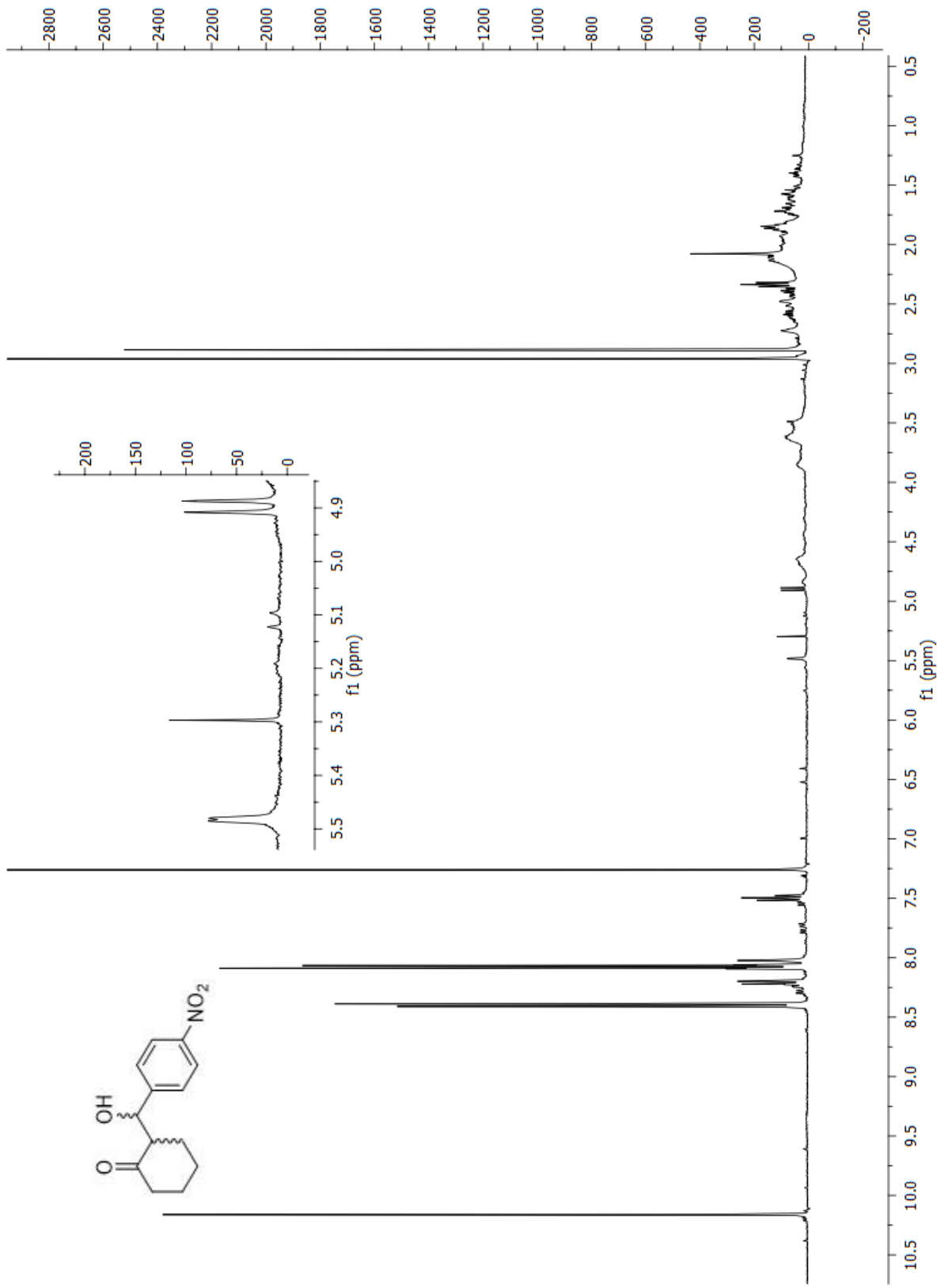

Figure 150: ^{1}H-NMR Spectrum ($CDCl_3$, 400 MHz) of 2-(hydroxyl-(p-nitrophenyl)methyl)cyclohexan-1-one Using **PP 2** (Table 6, Entry 24).

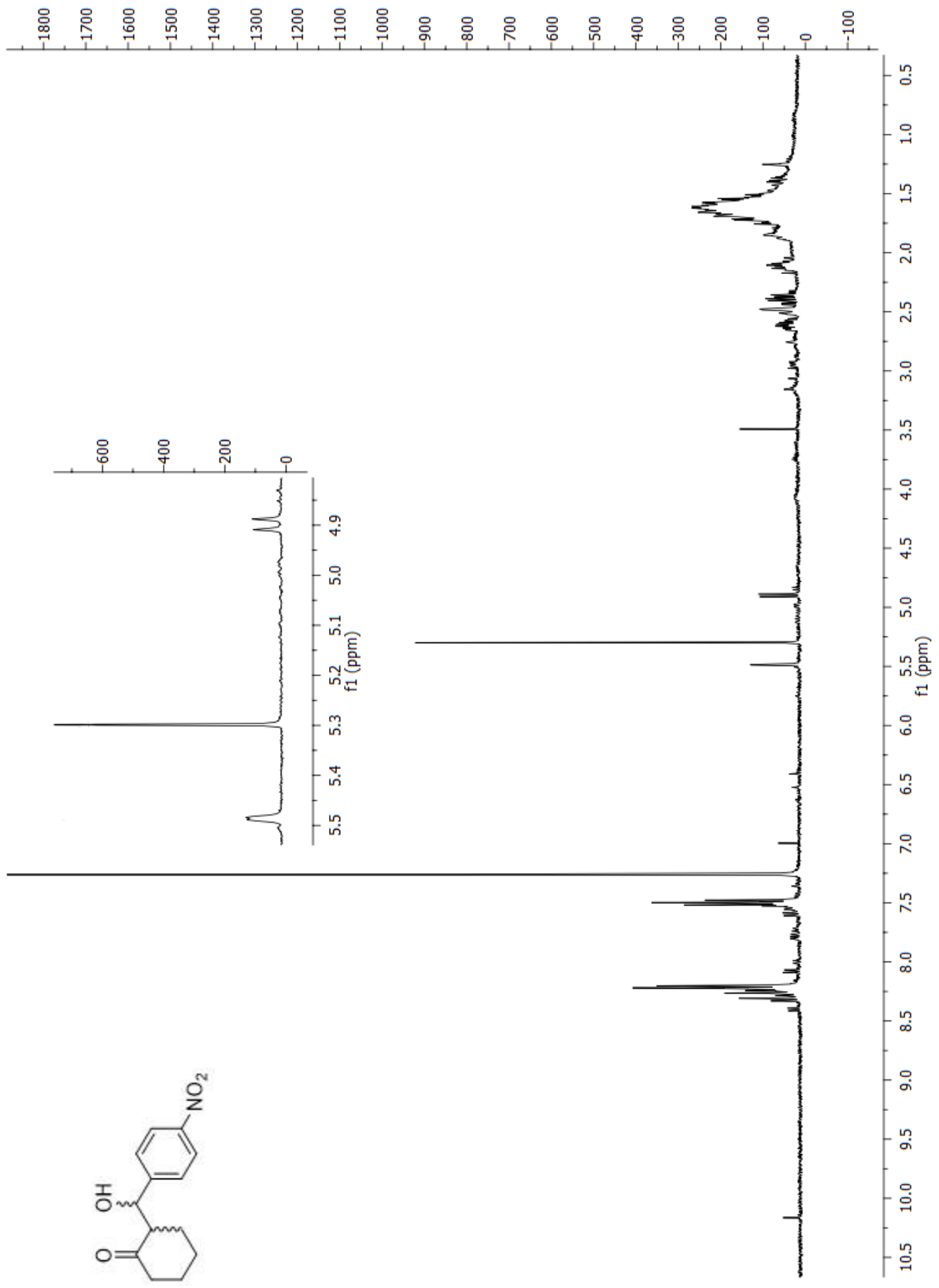

Figure 151: ^{1}H-NMR Spectrum ($CDCl_3$, 400 MHz) of 2-(hydroxyl-(p-nitrophenyl)methyl)cyclohexan-1-one Using **PP 2** (Table 6, Entry 25).

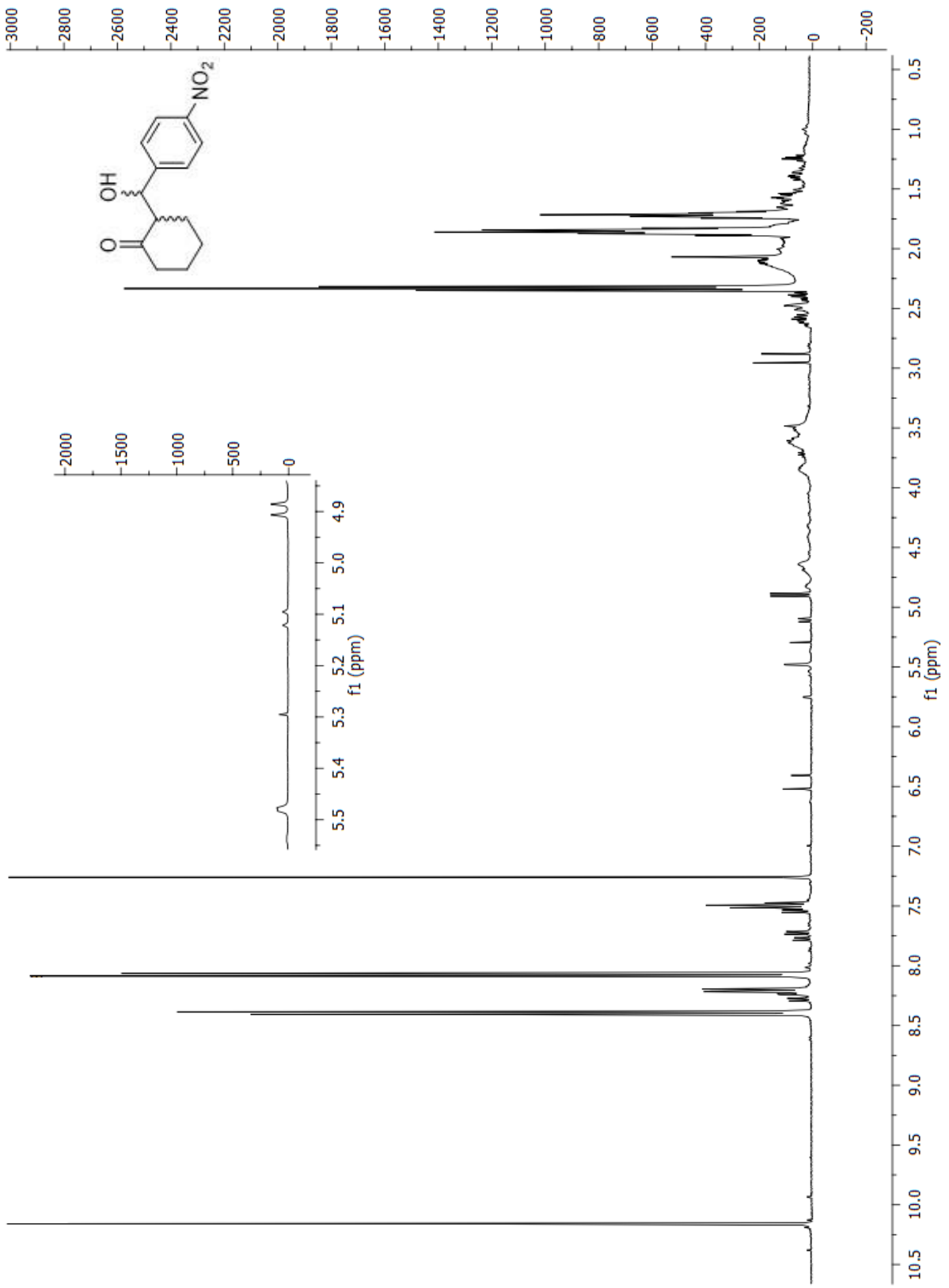

Figure 152: ^{1}H-NMR Spectrum ($CDCl_3$, 400 MHz) of 2-(hydroxyl-(p-nitrophenyl)methyl)cyclohexan-1-one Using **PP 2** (Table 6, Entry 26).

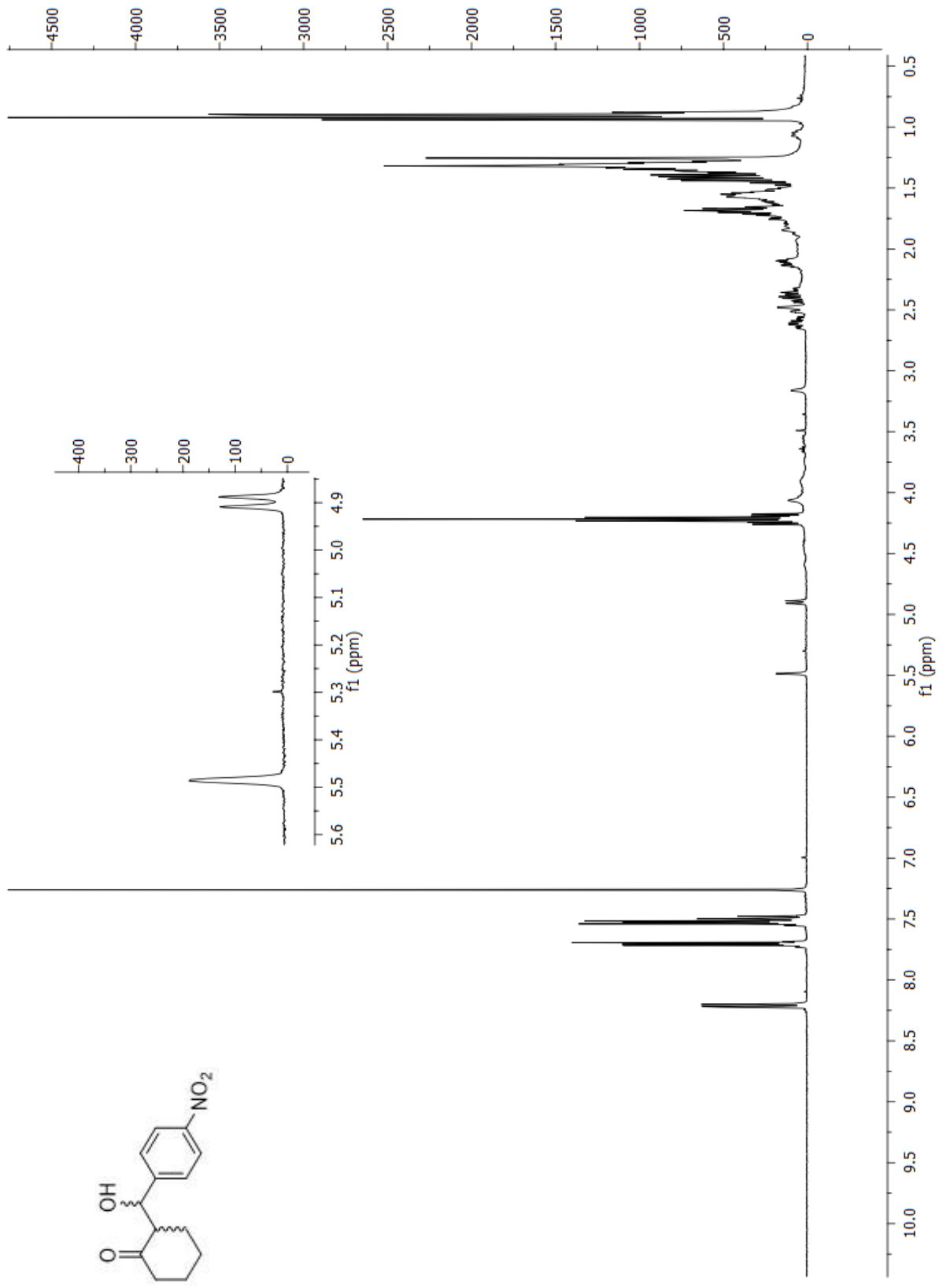

Figure 153: ^{1}H-NMR Spectrum ($CDCl_3$, 400 MHz) of 2-(hydroxyl-(p-nitrophenyl)methyl)cyclohexan-1-one Using **PP 2** (Table 6, Entry 27).

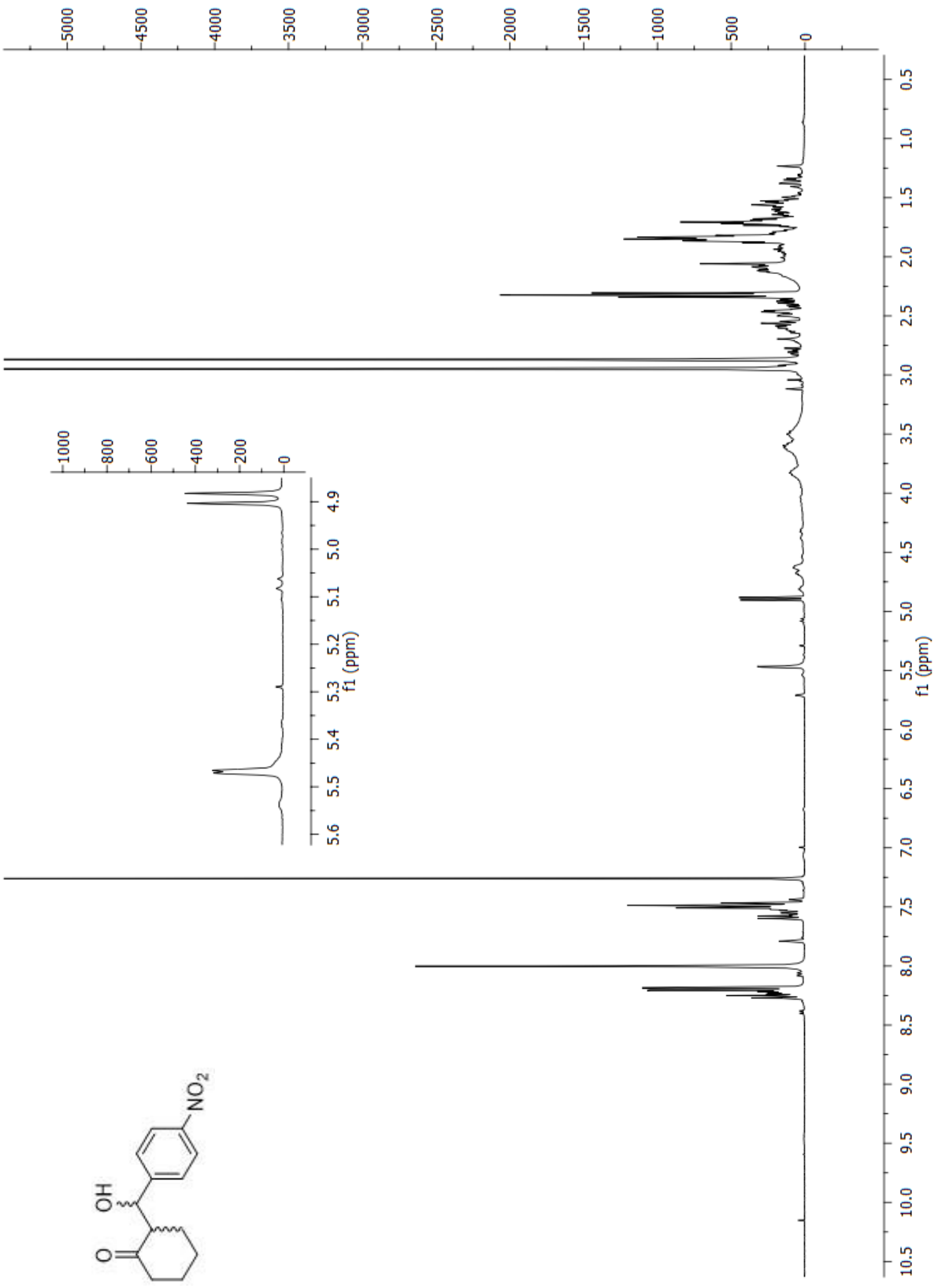

Figure 154: ^{1}H-NMR Spectrum ($CDCl_3$, 400 MHz) of 2-(hydroxyl-(p-nitrophenyl)methyl)cyclohexan-1-one Using **PP 2** (Table 6, Entry 28).

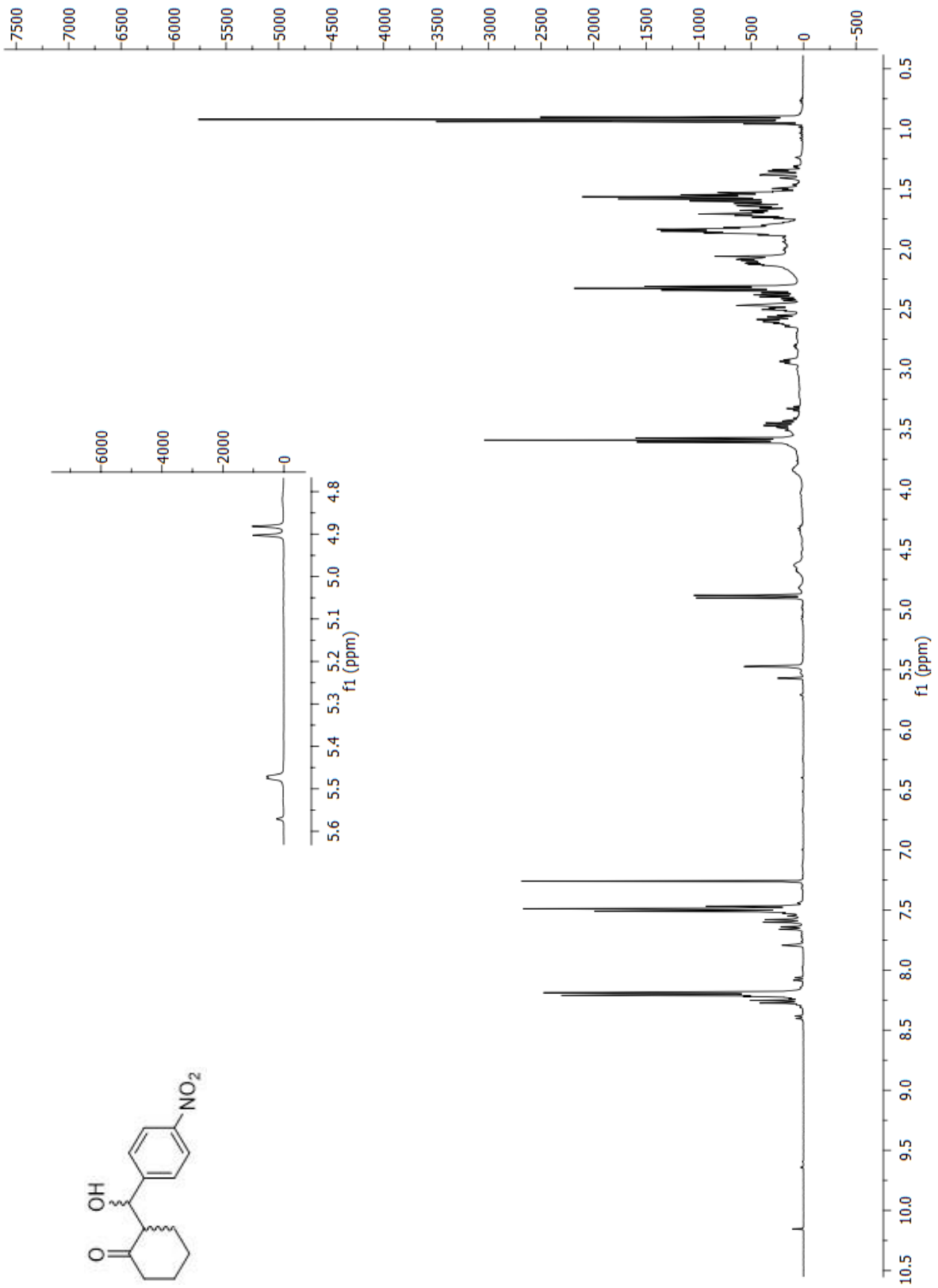

Figure 155: ^{1}H-NMR Spectrum ($CDCl_3$, 400 MHz) of 2-(hydroxyl-(p-nitrophenyl)methyl)cyclohexan-1-one Using **PP 2** (Table 6, Entry 29).

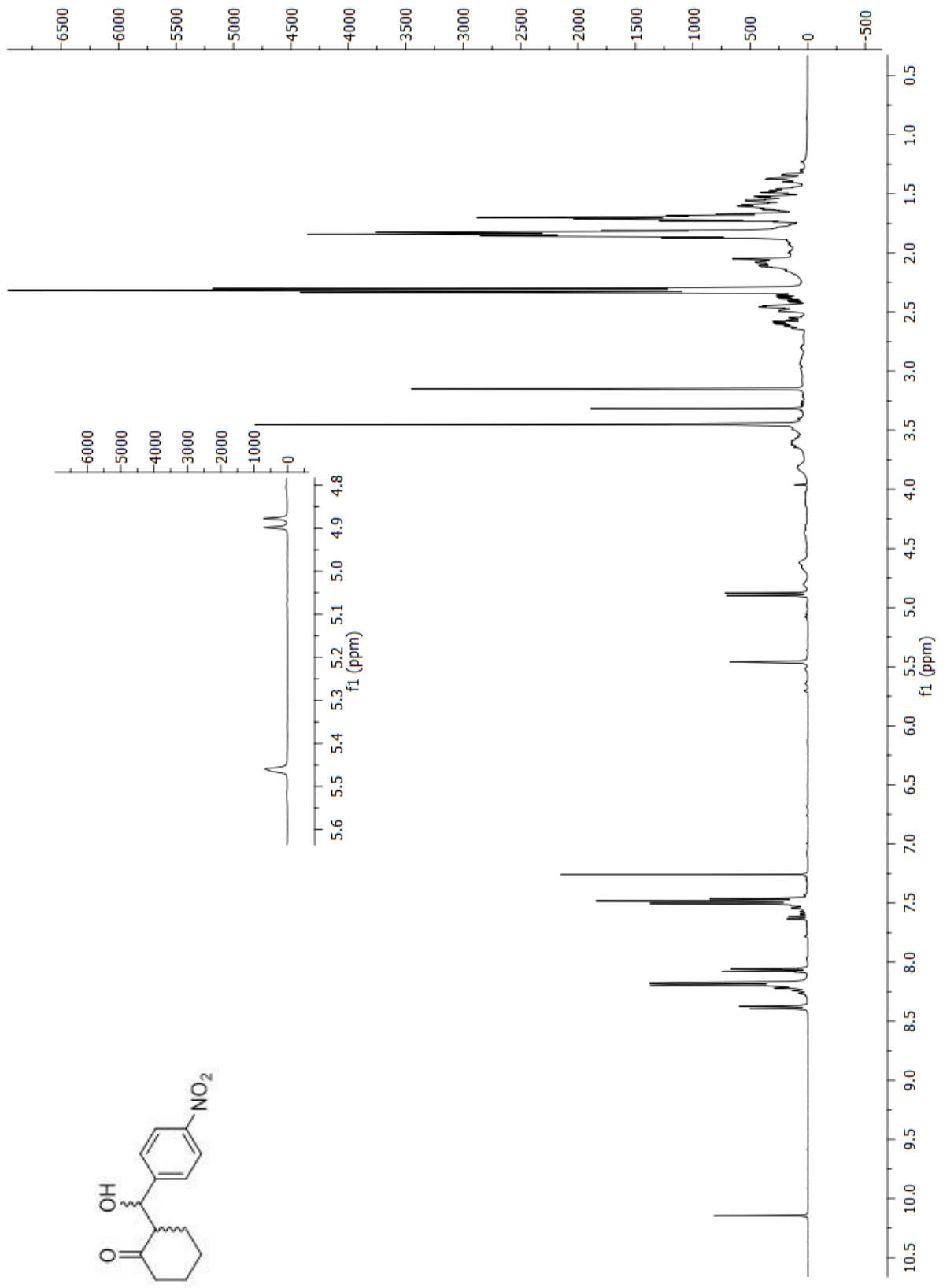

Figure 156: ^{1}H-NMR Spectrum ($CDCl_3$, 400 MHz) of 2-(hydroxyl-(p-nitrophenyl)methyl)cyclohexan-1-one Using **PP 2** (Table 6, Entry 30).

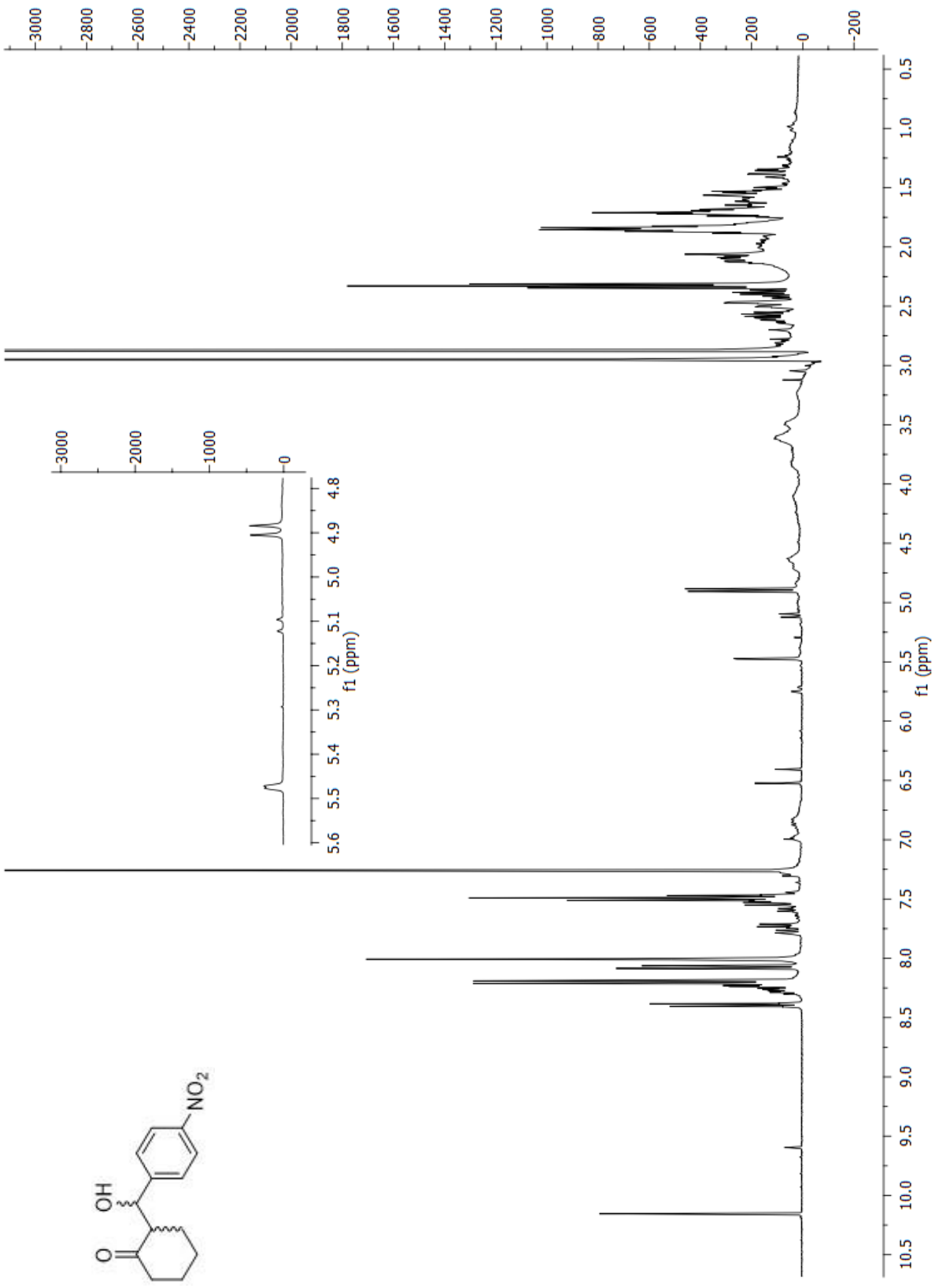

Figure 157: ^{1}H-NMR Spectrum ($CDCl_3$, 400 MHz) of 2-(hydroxyl-(p-nitrophenyl)methyl)cyclohexan-1-one Using **PP 3** (Table 7, Entry 31).

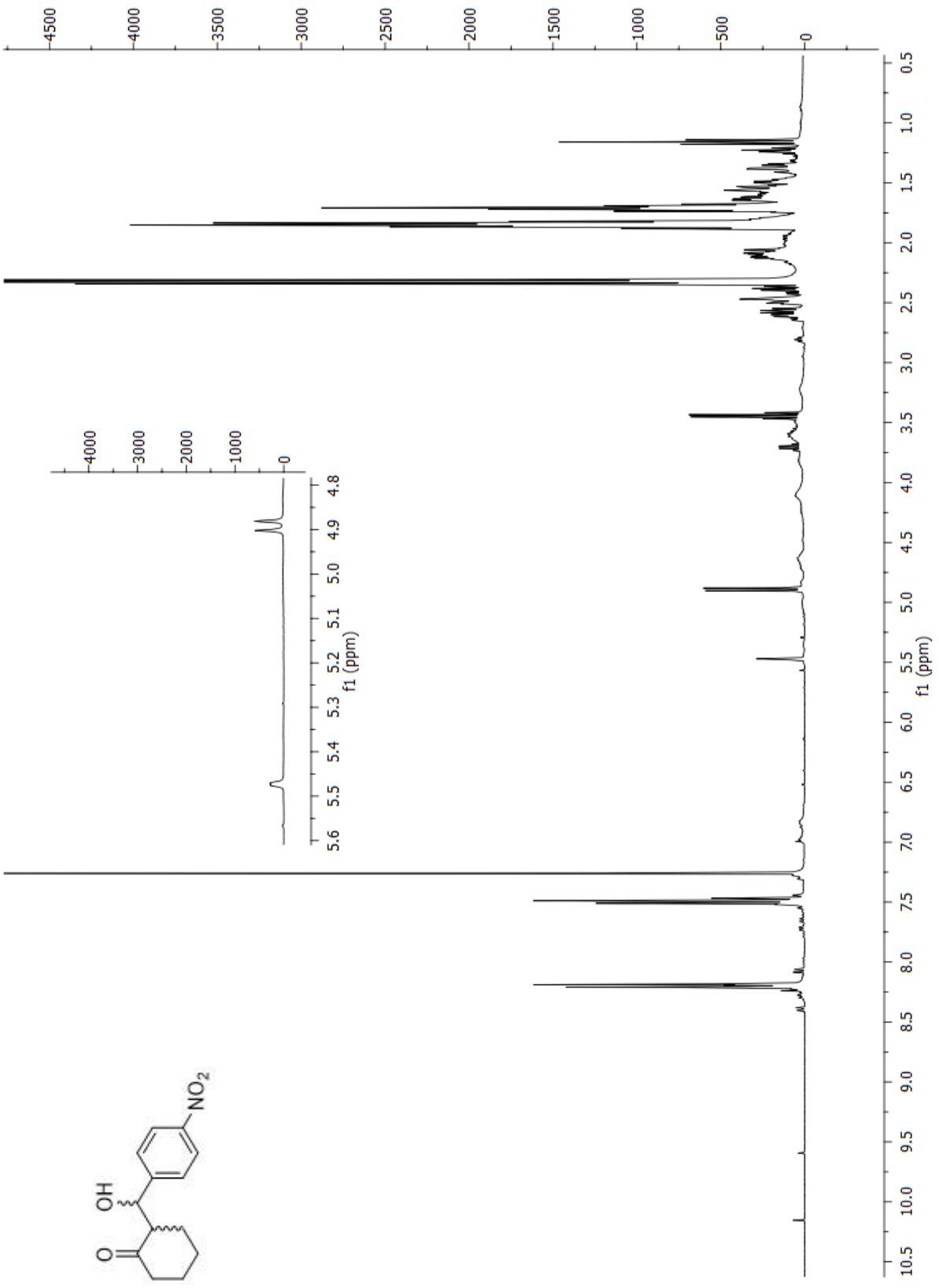

Figure 158: ^{1}H-NMR Spectrum ($CDCl_3$, 400 MHz) of 2-(hydroxyl-(p-nitrophenyl)methyl)cyclohexan-1-one Using **PP 3** (Table 7, Entry 32).

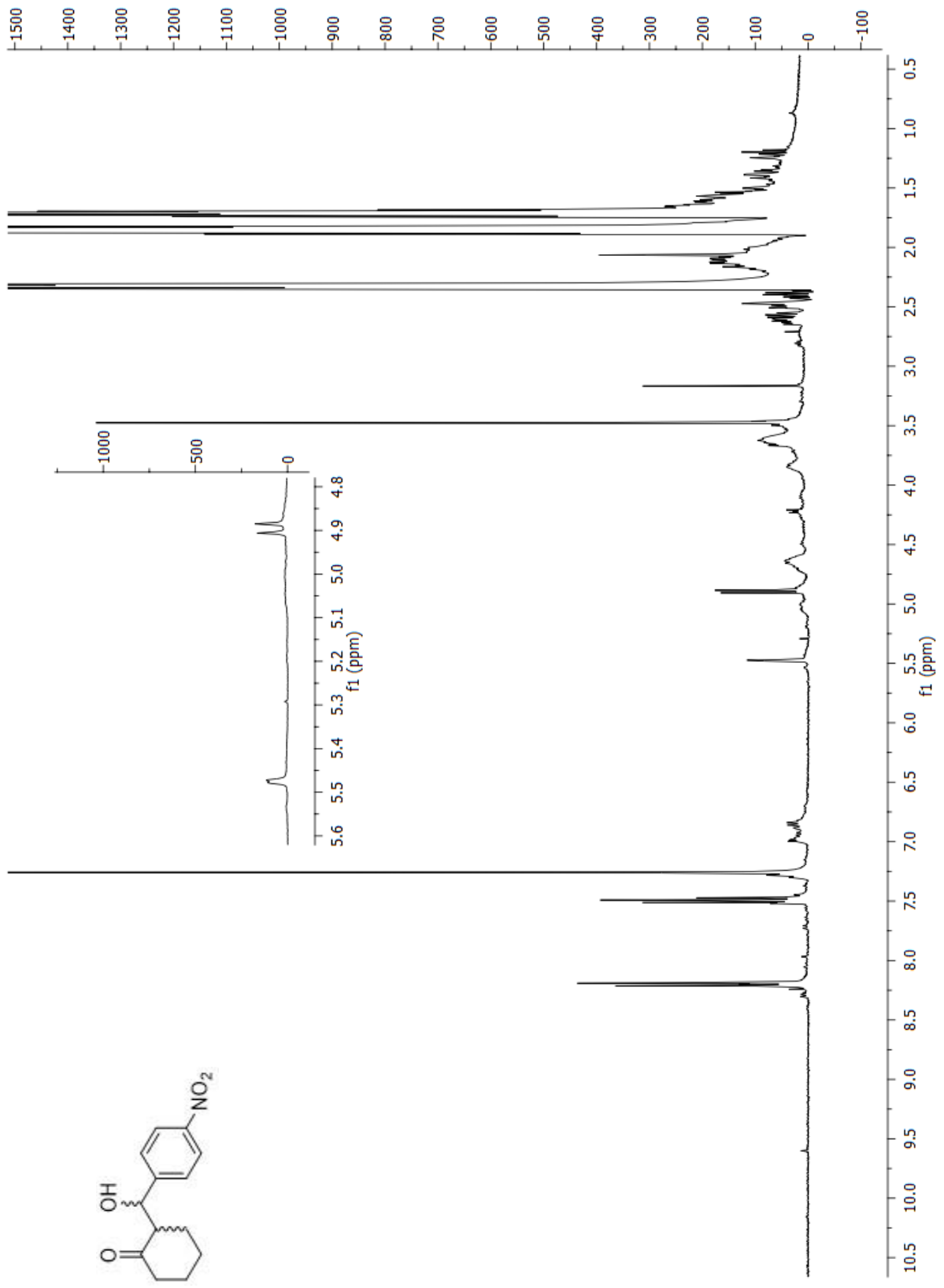

Figure 159: ^{1}H-NMR Spectrum ($CDCl_3$, 400 MHz) of 2-(hydroxyl-(p-nitrophenyl)methyl)cyclohexan-1-one Using **PP 3** (Table 7, Entry 33).

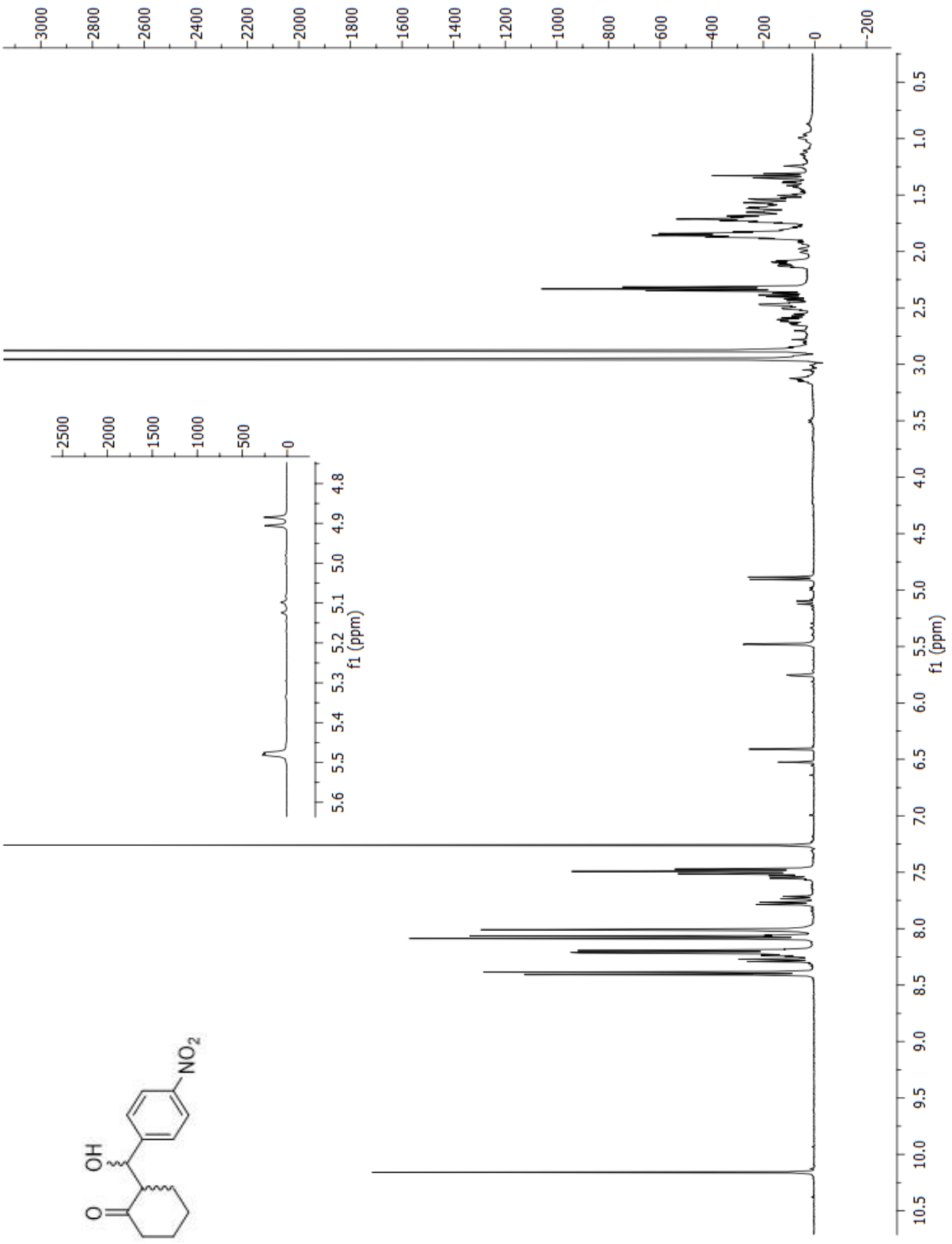

Figure 160: ^{1}H-NMR Spectrum ($CDCl_3$, 400 MHz) of 2-(hydroxyl-(p-nitrophenyl)methyl)cyclohexan-1-one Using **E3** (Table 8, Entry 34).

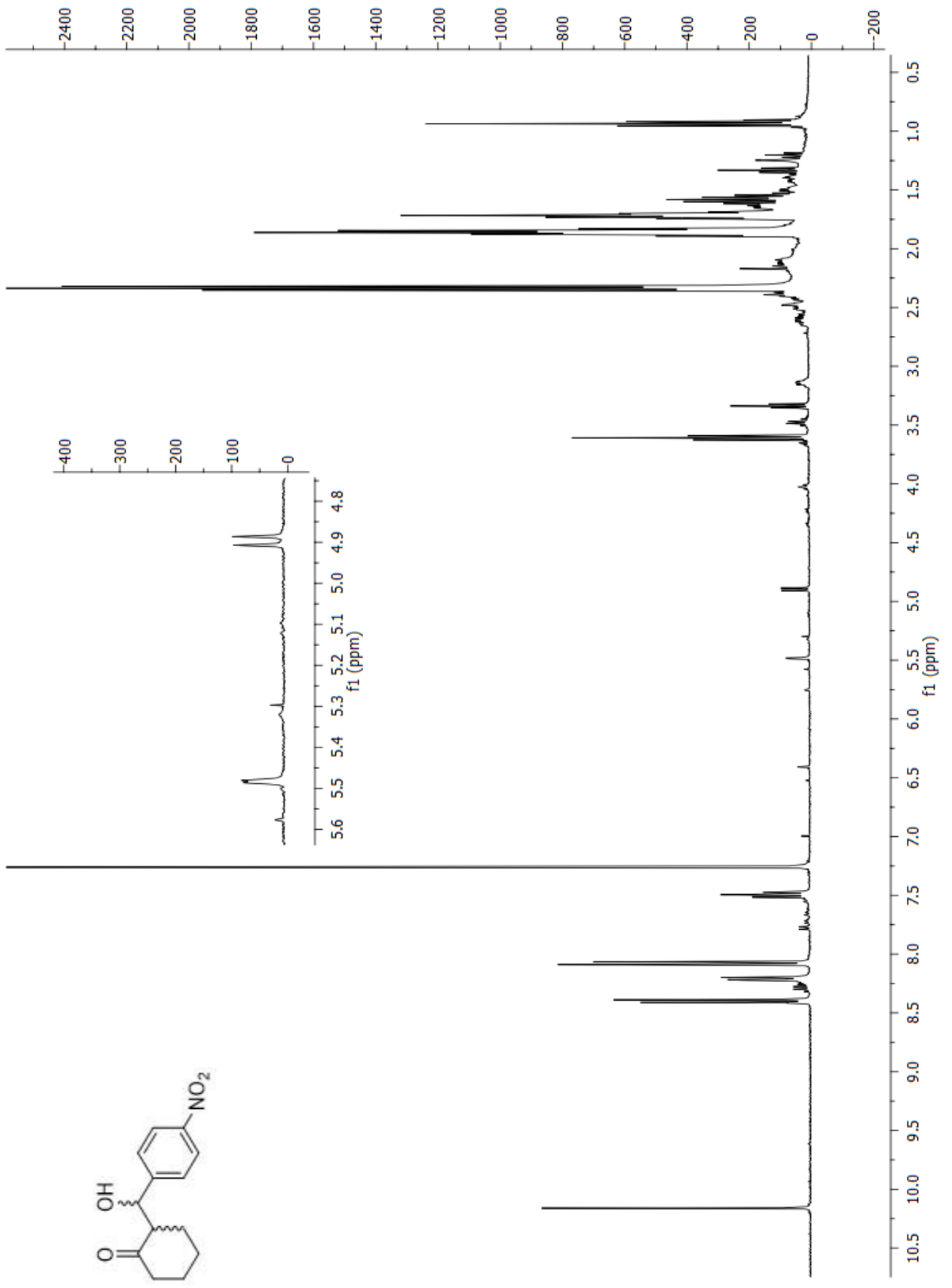

Figure 161: ^{1}H-NMR Spectrum ($CDCl_3$, 400 MHz) of 2-(hydroxyl-(p-nitrophenyl)methyl)cyclohexan-1-one Using **E3** (Table 8, Entry 35).

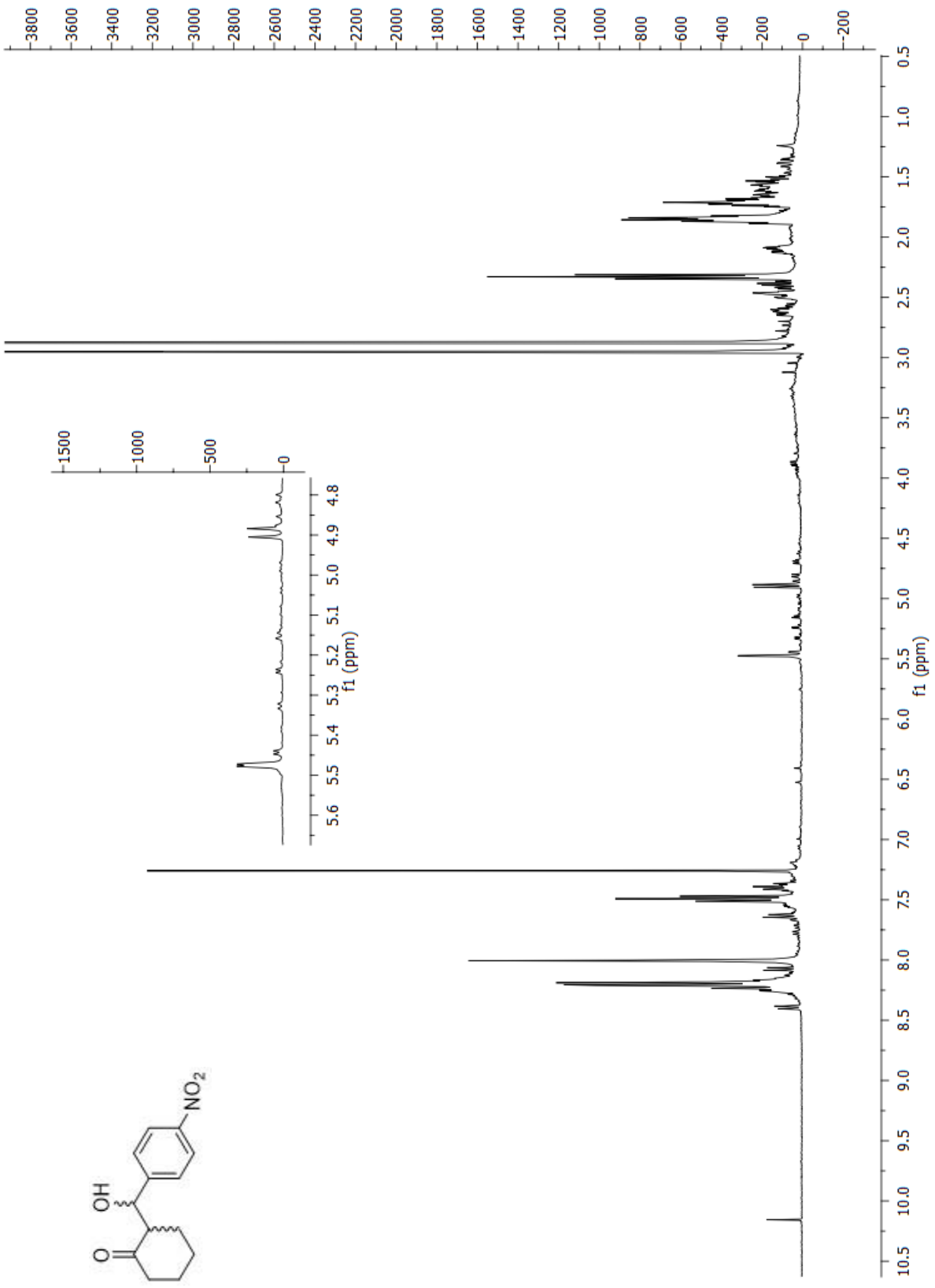

Figure 162: ^{1}H-NMR Spectrum ($CDCl_3$, 400 MHz) of 2-(hydroxyl-(p-nitrophenyl)methyl)cyclohexan-1-one Using L-Proline (Table 9, Entry 36).

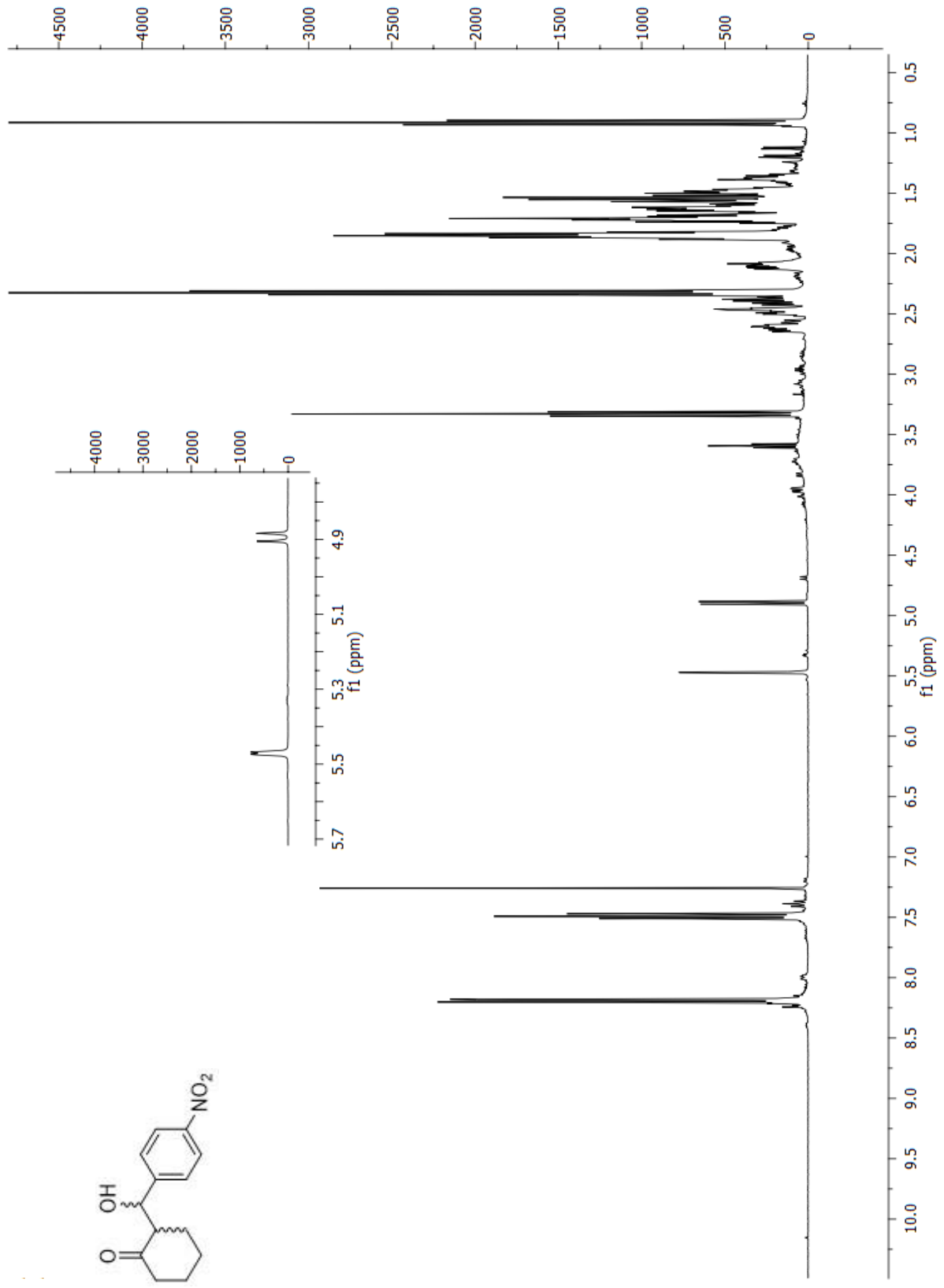

Figure 163: ^{1}H-NMR Spectrum ($CDCl_3$, 400 MHz) of 2-(hydroxyl-(p-nitrophenyl)methyl)cyclohexan-1-one Using L-Proline (Table 9, Entry 37).

AP1.3.2 ^{13}C-NMR Spectrum

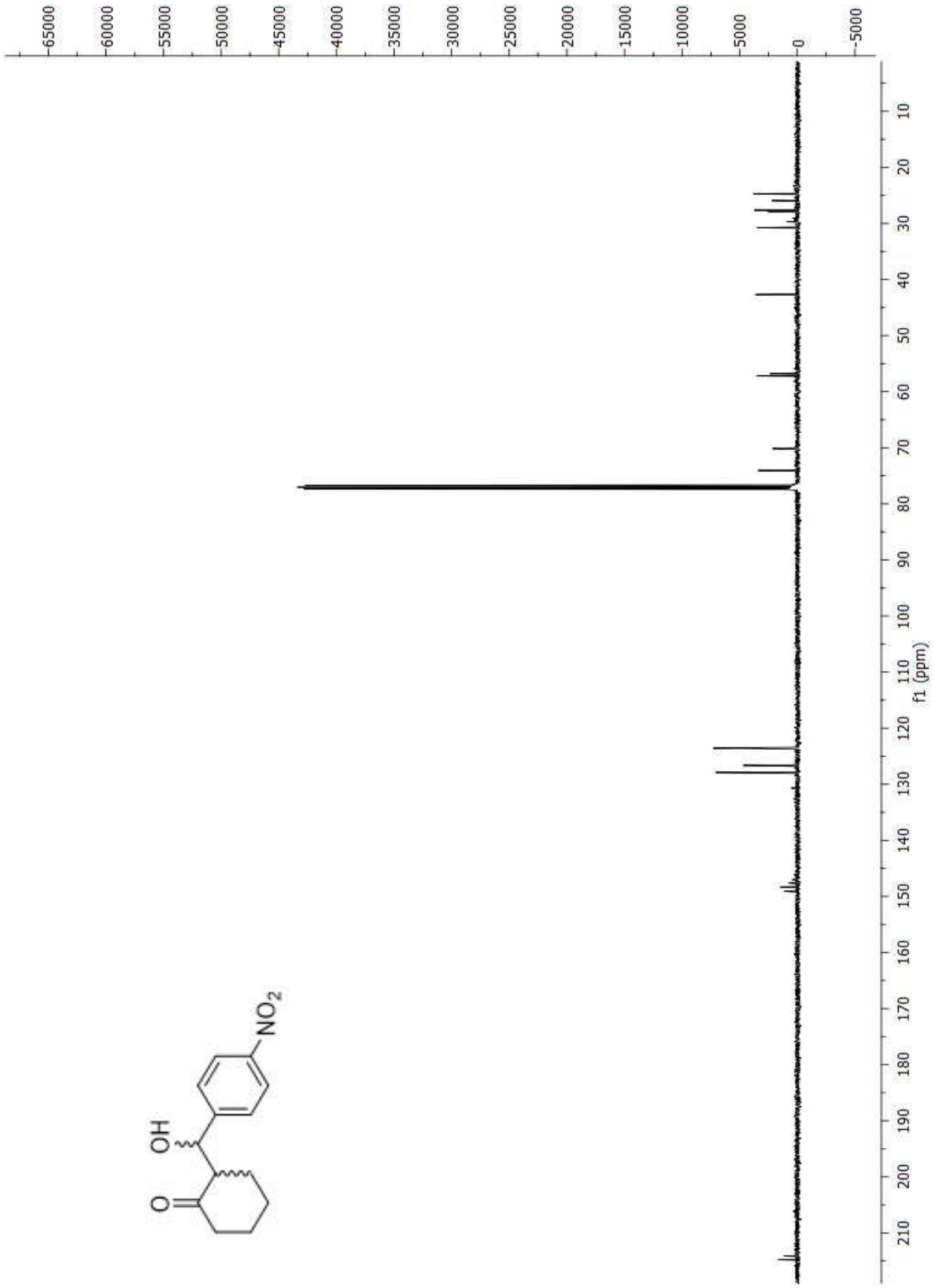

Figure 164: ^{13}C-NMR Spectrum ($CDCl_3$, 100 MHz) of 2-(hydroxyl-(p-nitrophenyl)methyl)cyclohexan-1-one.

AP1.3.3 Chiral HPLC

Aldol Reaction Using **PP 1** in DMF (Table 5, Entry 16)

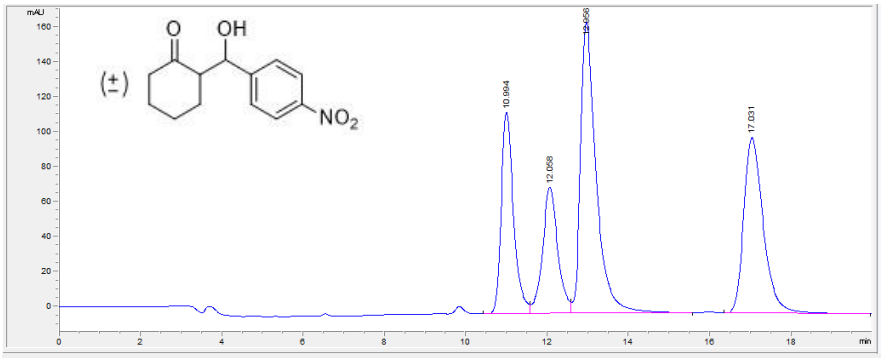

#	Time	Area	Height	Width	Area%	Symmetry
1	10.994	2429.9	115.1	0.3206	20.005	0.697
2	12.058	1885.6	72.2	0.3877	15.524	0.866
3	12.956	4451.2	166.3	0.3982	36.646	0.524
4	17.031	3379.8	100.7	0.5155	27.825	0.675

Figure 165: Chiral HPLC Analysis of Racemic 2-(hydroxyl-(p-nitrophenyl)methyl) cyclohexan-1- one (Chiralpak AD-H and a Mobile Phase n-hexane/i-PrPOH= 80/20 (v/v); 1 mL min-1; 254 nm; 25 ^{0}C).

Aldol Reaction Using **PP 1** Without Adding Any Solvent (Table 5, Entry 17)

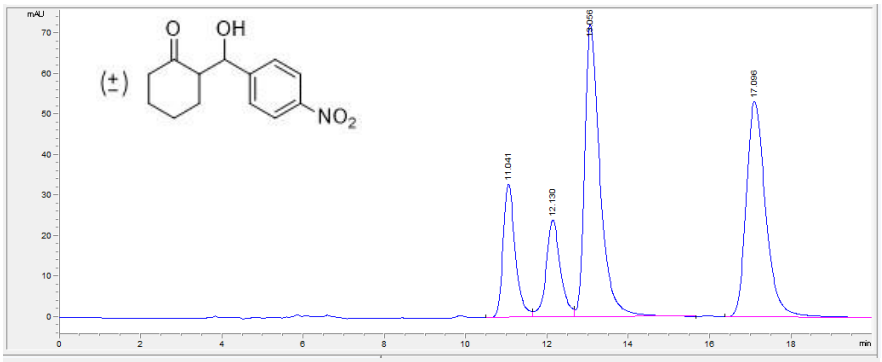

#	Time	Area	Height	Width	Area%	Symmetry
1	11.041	685.6	32.8	0.3163	13.876	0.73
2	12.13	584.8	24	0.3677	11.836	0.827
3	13.056	1901.6	72.3	0.3943	38.484	0.55
4	17.096	1769.2	53.2	0.5087	35.805	0.703

Figure 166: Chiral HPLC Analysis of Racemic 2-(hydroxyl-(p-nitrophenyl)methyl) cyclohexan-1- one (Chiralpak AD-H and a Mobile Phase n-hexane/i-PrPOH= 80/20 (v/v); 1 mL min-1; 254 nm; 25 °C).

Aldol Reaction Using **PP 1** in EtOH (Table 5, Entry 18)

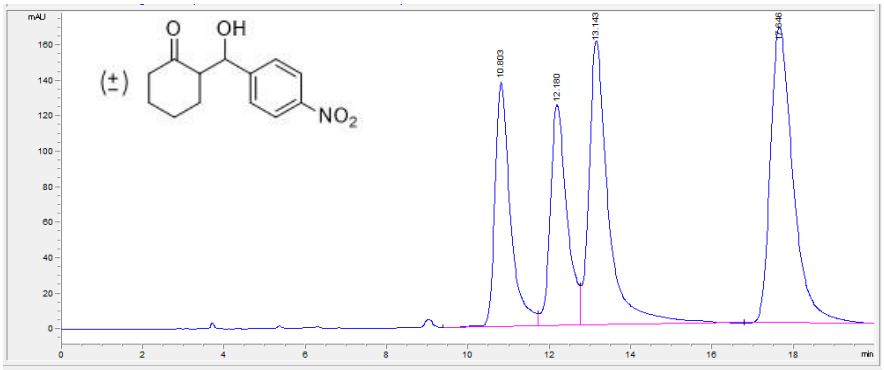

#	Time	Area	Height	Width	Area%	Symmetry
1	10.803	3658.1	138.1	0.3934	19.177	0.596
2	12.18	3557.4	124.4	0.4267	18.649	0.644
3	13.143	5376.4	160.2	0.4875	28.185	0.517
4	17.646	6483.6	166.7	0.5891	33.989	0.606

Figure 167: Chiral HPLC analysis of racemic 2-(hydroxyl-(p-nitrophenyl)methyl) cyclohexan-1- one (Chiralpak AD-H and a mobile phase n-hexane/i-PrPOH= 80/20 (v/v); 1 mL min-1; 254 nm; 25 ^{0}C).

Aldol Reaction Using **PP 2** in MeOH (Table 5, Entry 27)

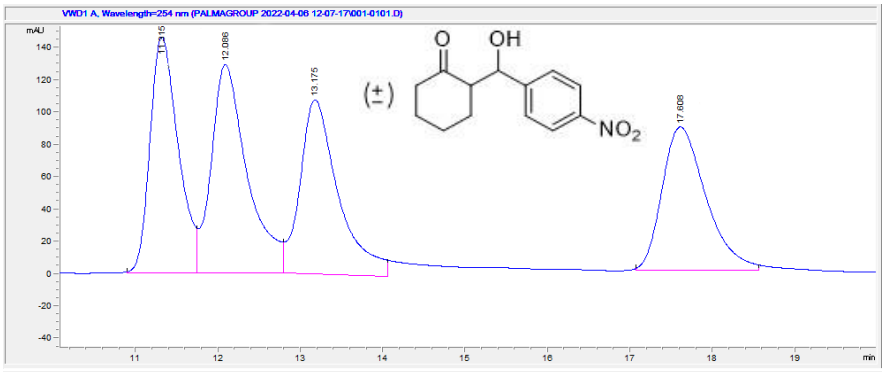

#	Time	Area	Height	Width	Area%	Symmetry
1	11.315	3486.1	146.2	0.3975	24.679	0.687
2	12.086	3903.4	129	0.5043	27.633	0.611
3	13.175	3460.7	107.8	0.535	24.499	0.61
4	17.608	3275.5	88.7	0.6155	23.188	0.681

Figure 168: Chiral HPLC Analysis of Racemic 2-(hydroxyl-(p-nitrophenyl)methyl) cyclohexan-1- one (Chiralpak AD-H and a Mobile Phase n-hexane/i-PrPOH= 80/20 (v/v); 1 mL min-1; 254 nm; 25 °C).

Aldol Reaction Using **PP 2** in DMF (Table 5, Entry 28)

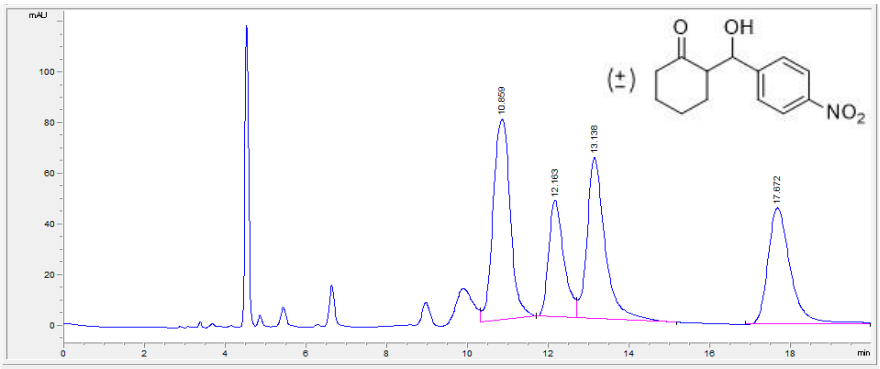

#	Time	Area	Height	Width	Area%	Symmetry
1	10.859	2327.7	79.2	0.4665	31.831	1.06
2	12.163	1211	45.9	0.3982	16.560	0.655
3	13.138	1964.1	63.6	0.4577	26.858	0.623
4	17.672	1809.9	46.1	0.5937	24.751	0.642

Figure 169: Chiral HPLC Analysis of Racemic 2-(hydroxyl-(p-nitrophenyl)methyl) cyclohexan-1- one (Chiralpak AD-H and a Mobile Phase n-hexane/i-PrPOH= 80/20 (v/v); 1 mL min-1; 254 nm; 25 °C).

Aldol Reaction Using **PP 2** in propanol (Table 5, Entry 29)

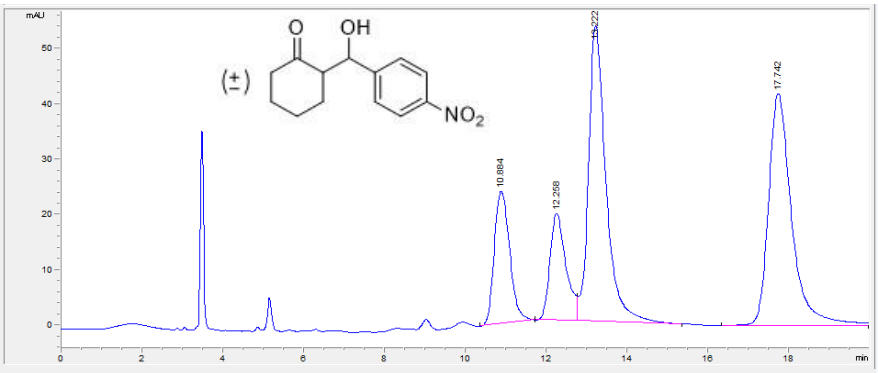

#	Time	Area	Height	Width	Area%	Symmetry
1	10.884	636.2	24	0.4215	14.323	0.751
2	12.258	540.8	19.3	0.4194	12.173	0.649
3	13.222	1597.7	53.4	0.4464	35.967	0.622
4	17.742	1667.4	41.9	0.5996	37.537	0.661

Figure 170: Chiral HPLC Analysis of Racemic 2-(hydroxyl-(p-nitrophenyl)methyl) cyclohexan-1- one (Chiralpak AD-H and a Mobile Phase n-hexane/i-PrPOH= 80/20 (v/v); 1 mL min-1; 254 nm; 25 °C).

Aldol Reaction Using **PP 2** in MeOH (Table 5, Entry 30)

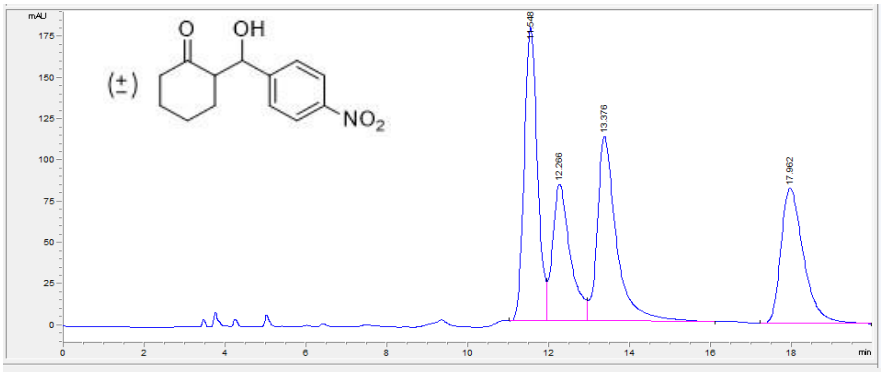

#	Time	Area	Height	Width	Area%	Symmetry
1	11.548	4048.7	178.6	0.3778	31.454	0.873
2	12.266	2479.1	80.9	0.5107	19.260	0.6
3	13.376	3334.7	110.6	0.5027	25.907	0.574
4	17.962	3009.5	81.1	0.6186	23.380	0.695

Figure 171: Chiral HPLC Analysis of Racemic 2-(hydroxyl-(p-nitrophenyl)methyl) cyclohexan-1- one (Chiralpak AD-H and a Mobile Phase n-hexane/i-PrPOH= 80/20 (v/v); 1 mL min-1; 254 nm; 25 °C).

Aldol Reaction Using **PP 3** in DMF (Table 7, Entry 31)

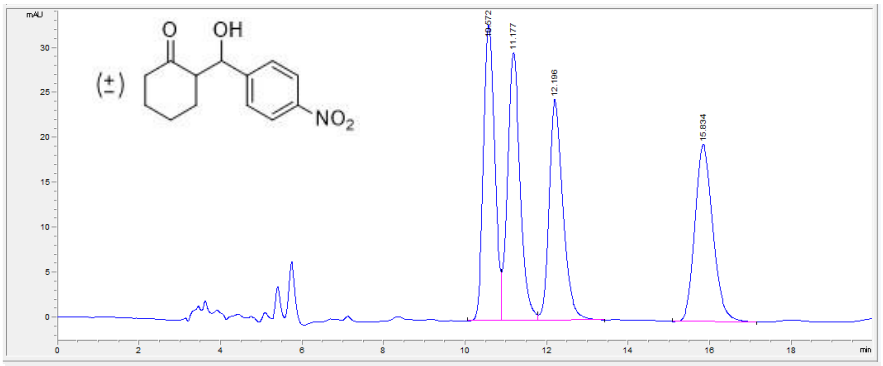

#	Time	Area	Height	Width	Area%	Symmetry
1	10.572	628.2	32.9	0.2957	25.554	0.838
2	11.177	641.4	29.8	0.3271	26.092	0.803
3	12.196	582.9	24.6	0.3614	23.714	0.682
4	15.834	605.7	19.7	0.4723	24.640	0.807

Figure 172: Chiral HPLC Analysis of Racemic 2-(hydroxyl-(p-nitrophenyl)methyl) cyclohexan-1- one (Chiralpak AD-H and a Mobile Phase n-hexane/i-PrPOH= 80/20 (v/v); 1 mL min-1; 254 nm; 25 °C).

Aldol Reaction Using **PP 3** in propanol (Table 7, Entry 32)

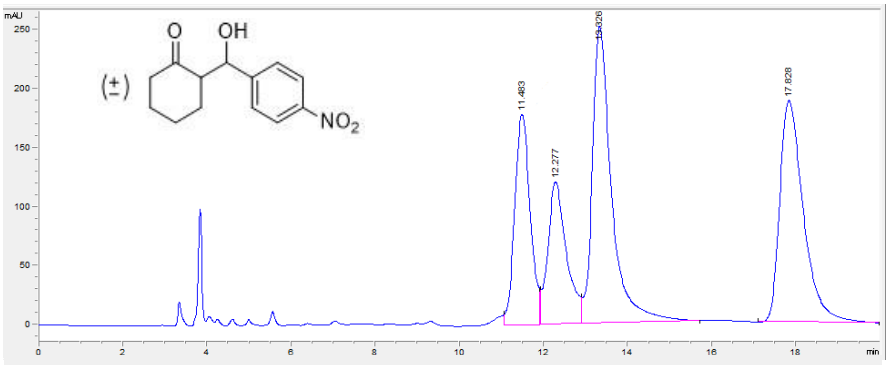

#	Time	Area	Height	Width	Area%	Symmetry
1	11.483	4557.1	178.5	0.4255	19.362	0.882
2	12.277	3708.4	120.5	0.4494	15.756	0.637
3	13.326	7924.8	251.9	0.4645	33.670	0.553
4	17.828	7346.3	188.4	0.5917	31.212	0.582

Figure 173: Chiral HPLC Analysis of Racemic 2-(hydroxyl-(p-nitrophenyl)methyl) cyclohexan-1- one (Chiralpak AD-H and a Mobile Phase n-hexane/i-PrPOH= 80/20 (v/v); 1 mL min-1; 254 nm; 25 °C).

Aldol Reaction Using **PP 3** in MeOH (Table 7, Entry 33)

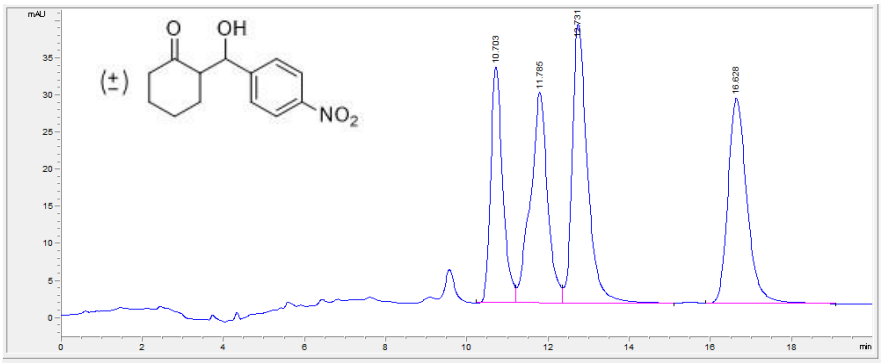

#	Time	Area	Height	Width	Area%	Symmetry
1	10.703	657.4	31.8	0.3152	19.535	0.717
2	11.785	830.9	28.4	0.4157	24.691	1.172
3	12.731	976.8	37.5	0.3909	29.026	0.595
4	16.628	900.1	27.7	0.5005	26.748	0.734

Figure 174: Chiral HPLC Analysis of Racemic 2-(hydroxyl-(p-nitrophenyl)methyl) cyclohexan-1- one (Chiralpak AD-H and a Mobile Phase n-hexane/i-PrPOH= 80/20 (v/v); 1 mL min-1; 254 nm; 25 °C).

Aldol Reaction Using **E3** in DMF (Table 8, Entry 34)

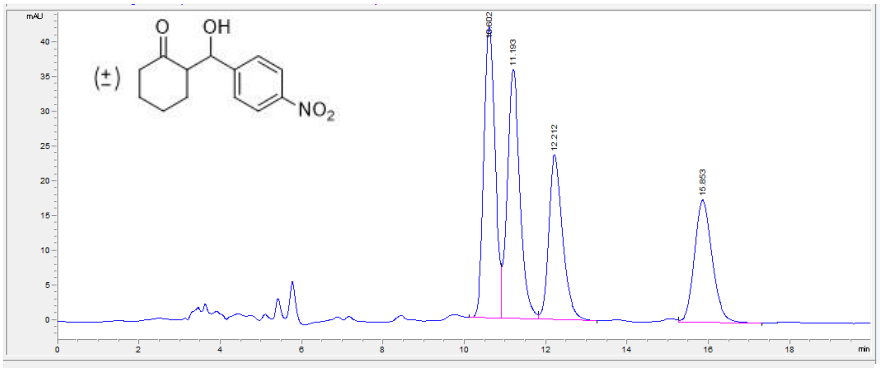

#	Time	Area	Height	Width	Area%	Symmetry
1	10.602	805.5	42	0.2967	30.007	0.836
2	11.193	774.1	35.9	0.3272	28.838	0.797
3	12.212	564	23.8	0.3641	21.013	0.687
4	15.853	540.7	17.7	0.4724	20.142	0.814

Figure 175: Chiral HPLC Analysis of Racemic 2-(hydroxyl-(p-nitrophenyl)methyl) cyclohexan-1- one (Chiralpak AD-H and a Mobile Phase n-hexane/i-PrPOH= 80/20 (v/v); 1 mL min-1; 254 nm; 25 °C).

Aldol Reaction Using **E3** in propanol (Table 8, Entry 35)

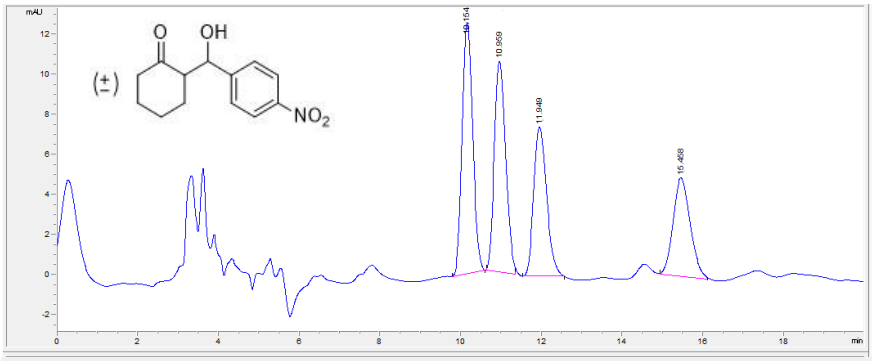

#	Time	Area	Height	Width	Area%	Symmetry
1	10.154	225.6	12.5	0.2997	30.560	0.862
2	10.959	204.4	10.5	0.3241	27.688	0.832
3	11.949	163.9	7.4	0.368	22.207	0.783
4	15.458	144.3	4.9	0.4889	19.544	0.843

Figure 176: Chiral HPLC Analysis of Racemic 2-(hydroxyl-(p-nitrophenyl)methyl) cyclohexan-1- one (Chiralpak AD-H and a Mobile Phase n-hexane/i-PrPOH= 80/20 (v/v); 1 mL min-1; 254 nm; 25 °C).

Aldol Reaction Using L-Proline in DMF (Table 9, Entry 36)

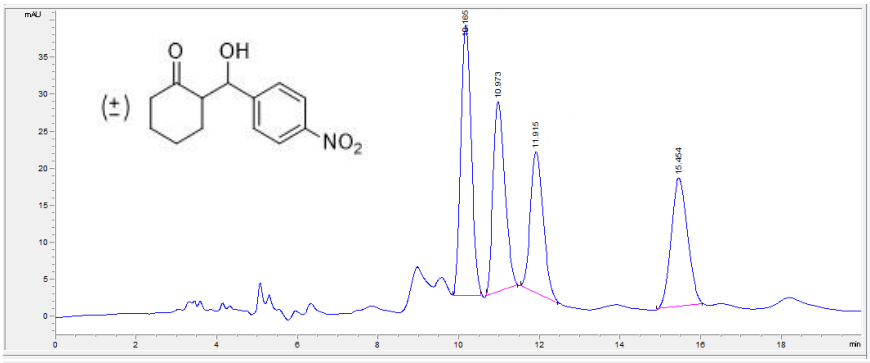

#	Time	Area	Height	Width	Area%	Symmetry
1	10.165	650.7	36.6	0.2964	31.369	0.835
2	10.973	516.4	25.6	0.3358	24.894	0.758
3	11.915	419.6	19.1	0.3668	20.230	0.767
4	15.454	487.6	17.3	0.469	23.507	0.882

Figure 177: Chiral HPLC Analysis of Racemic 2-(hydroxyl-(p-nitrophenyl)methyl) cyclohexan-1- one (Chiralpak AD-H and a Mobile Phase n-hexane/i-PrPOH= 80/20 (v/v); 1 mL min-1; 254 nm; 25 °C).

Aldol Reaction Using L-Proline in propanol (Table 9, Entry 37)

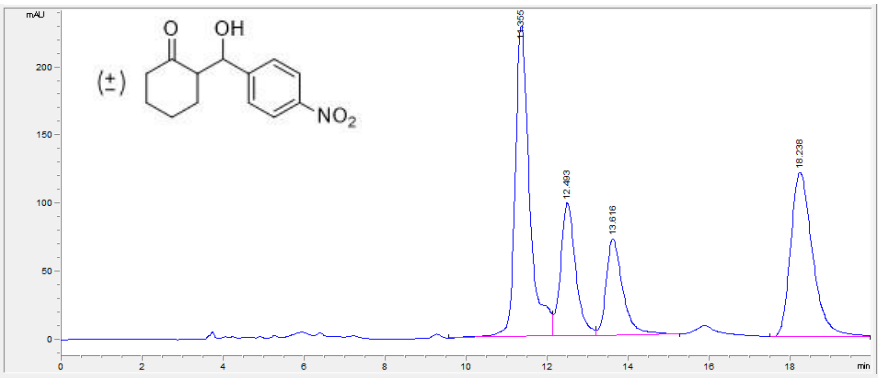

#	Time	Area	Height	Width	Area%	Symmetry
1	11.355	5728.6	228.9	0.3735	38.547	0.68
2	12.493	2538.2	98	0.3911	17.079	0.741
3	13.616	2033.6	70.8	0.4328	13.684	0.612
4	18.238	4561	120.9	0.5768	30.690	0.681

Figure 178: Chiral HPLC Analysis of Racemic 2-(hydroxyl-(p-nitrophenyl)methyl) cyclohexan-1- one (Chiralpak AD-H and a Mobile Phase n-hexane/i-PrPOH= 80/20 (v/v); 1 mL min-1; 254 nm; 25 ^{0}C).

Appendix 2

Further Analysis: Chapter 3

AP2.1 Monomers

AP2.1.1 ^{1}H-NMR Spectra

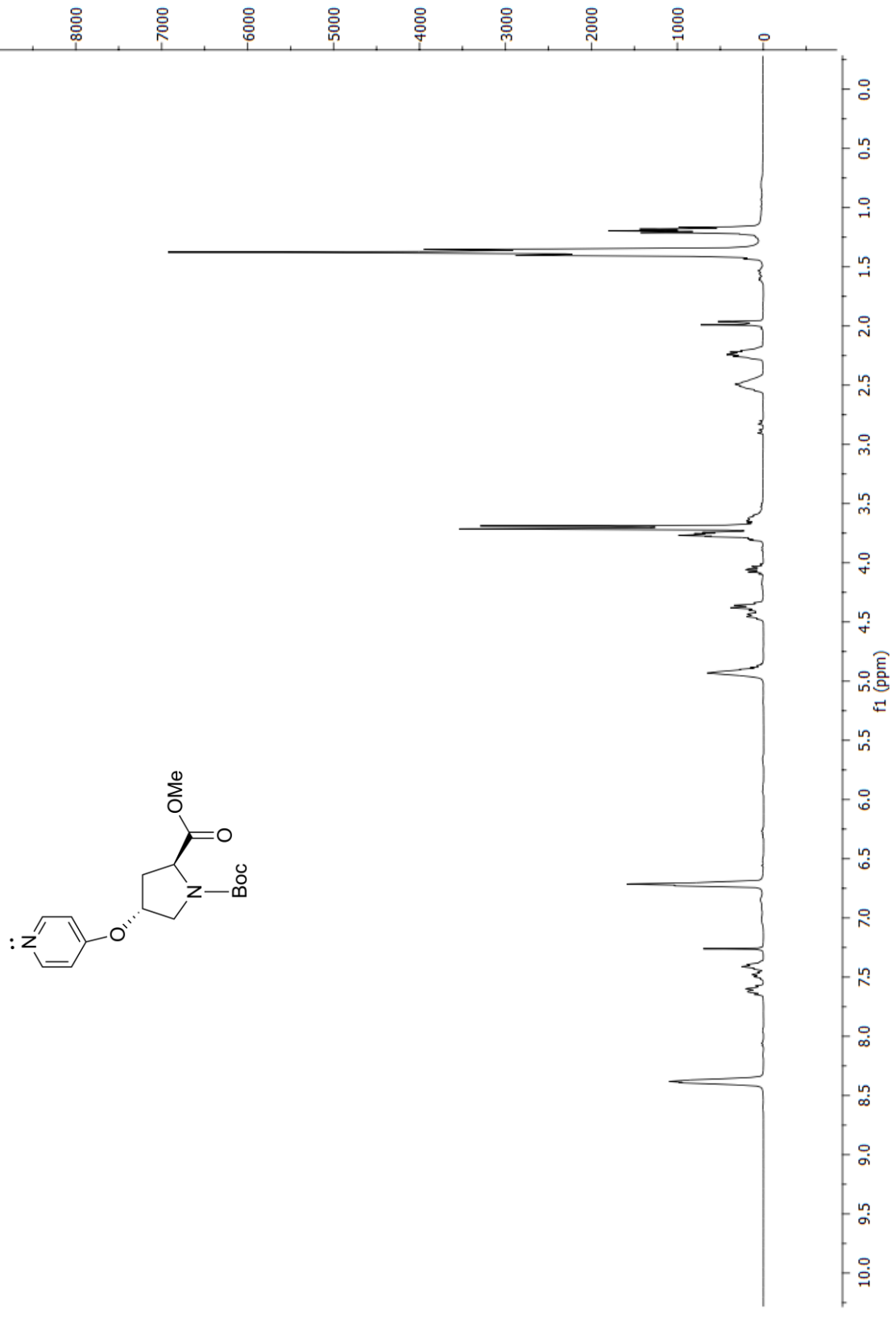

Figure 179: ^{1}H-NMR spectrum ($CDCl_3$, 400 MHz) of **F2**.

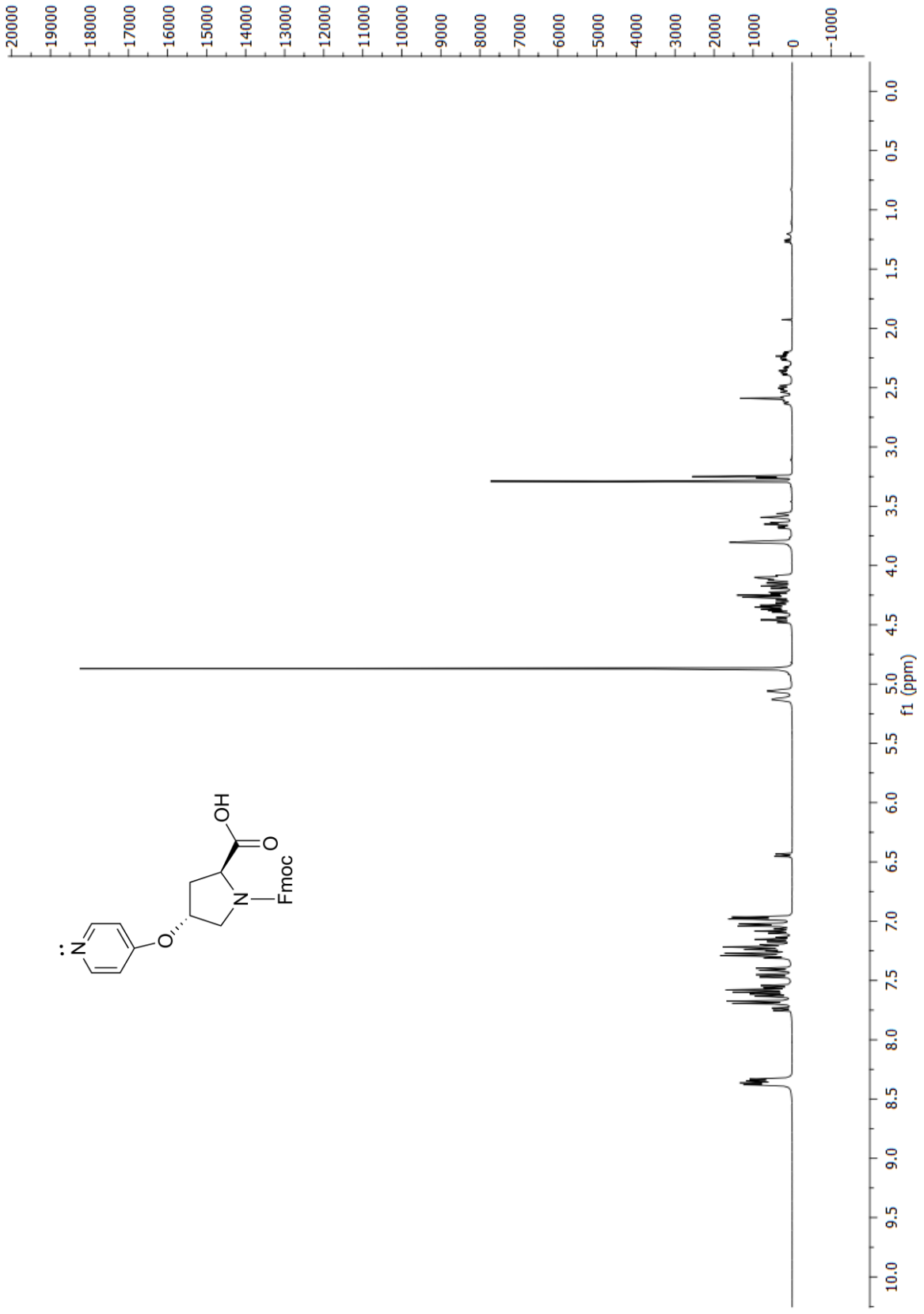

Figure 180: ^{1}H-NMR Spectrum (MeOD, 400 MHz) of **F3**.

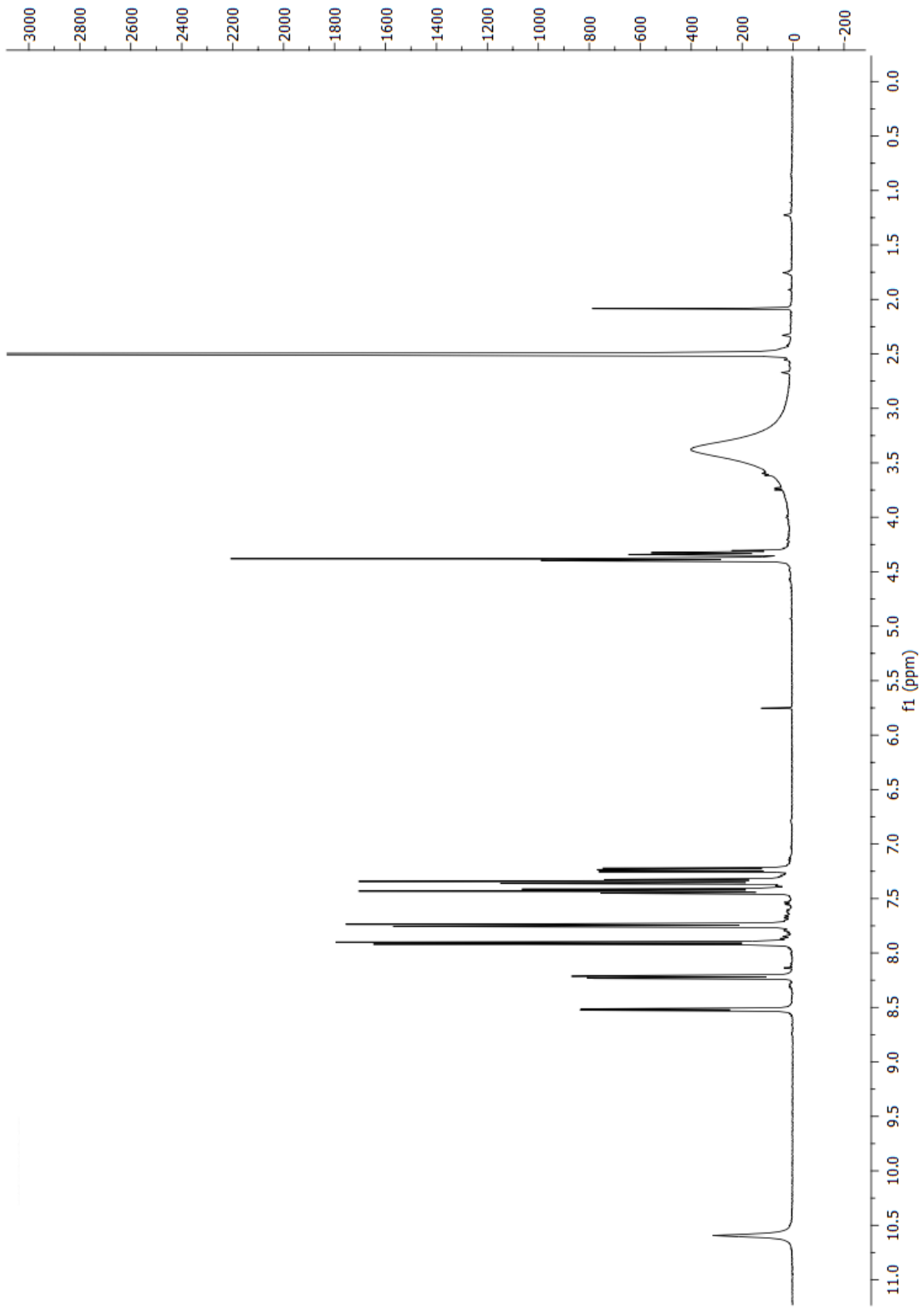

Figure 181: ^{1}H-NMR Spectrum (DMSO, 40 MHz) of **G4**.

AP2.1.2 ^{13}C-NMR Spectra

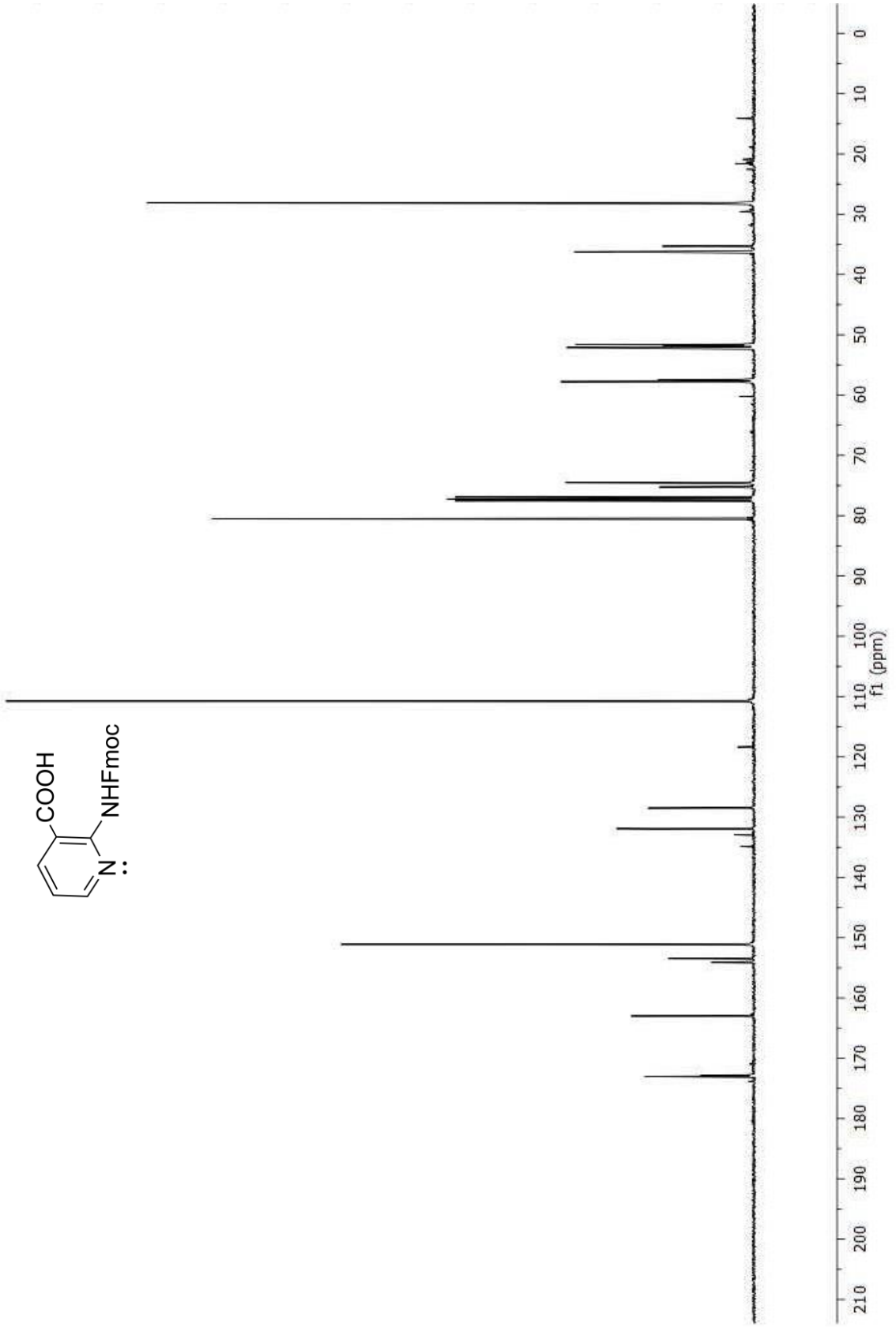

Figure 182: ^{13}C-NMR Spectrum ($CDCl_3$, 100 MHz) of **F2**.

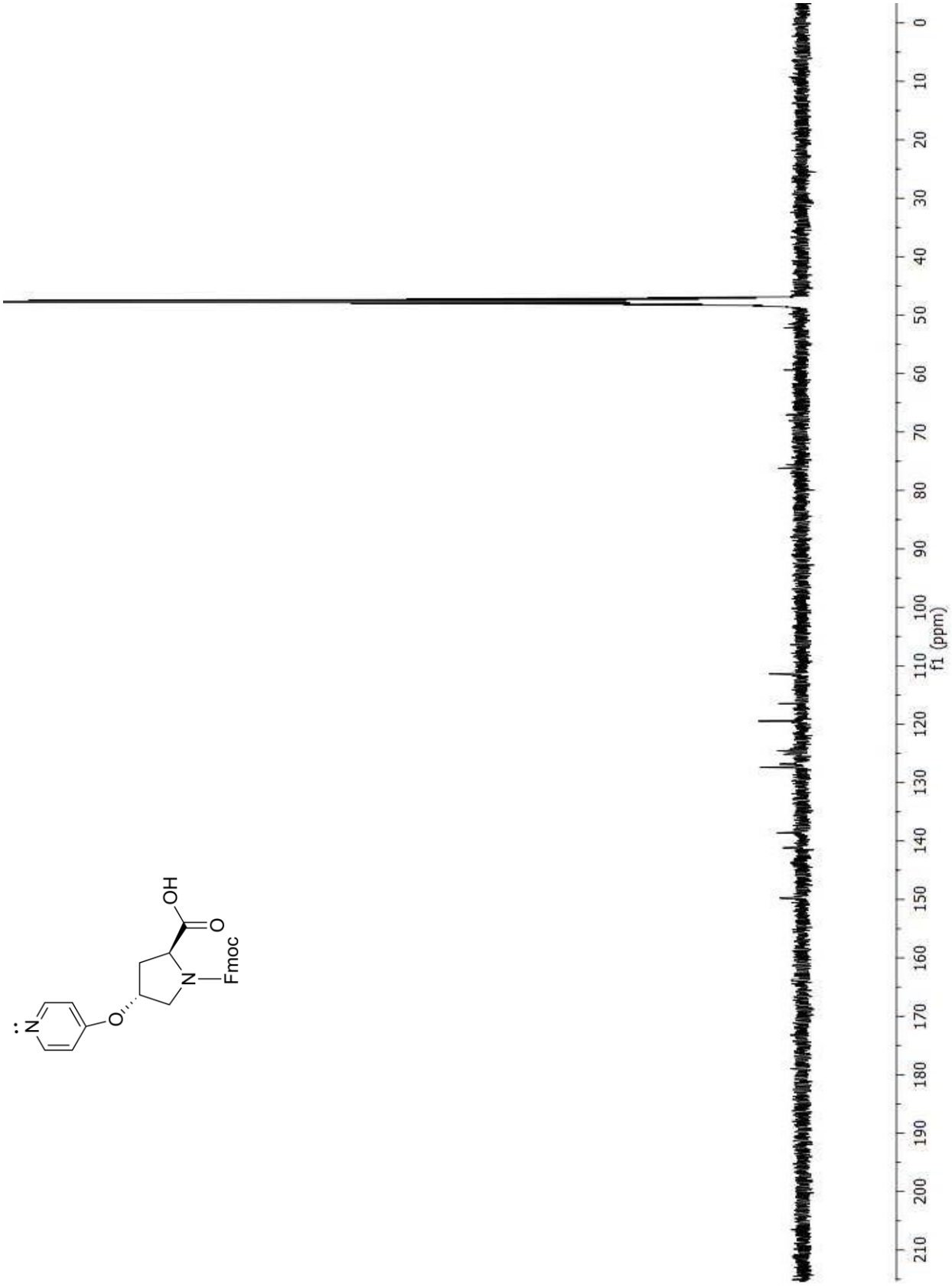

Figure 183: ^{13}C-NMR Spectrum (MeOD, 100 MHz) of **F3**.

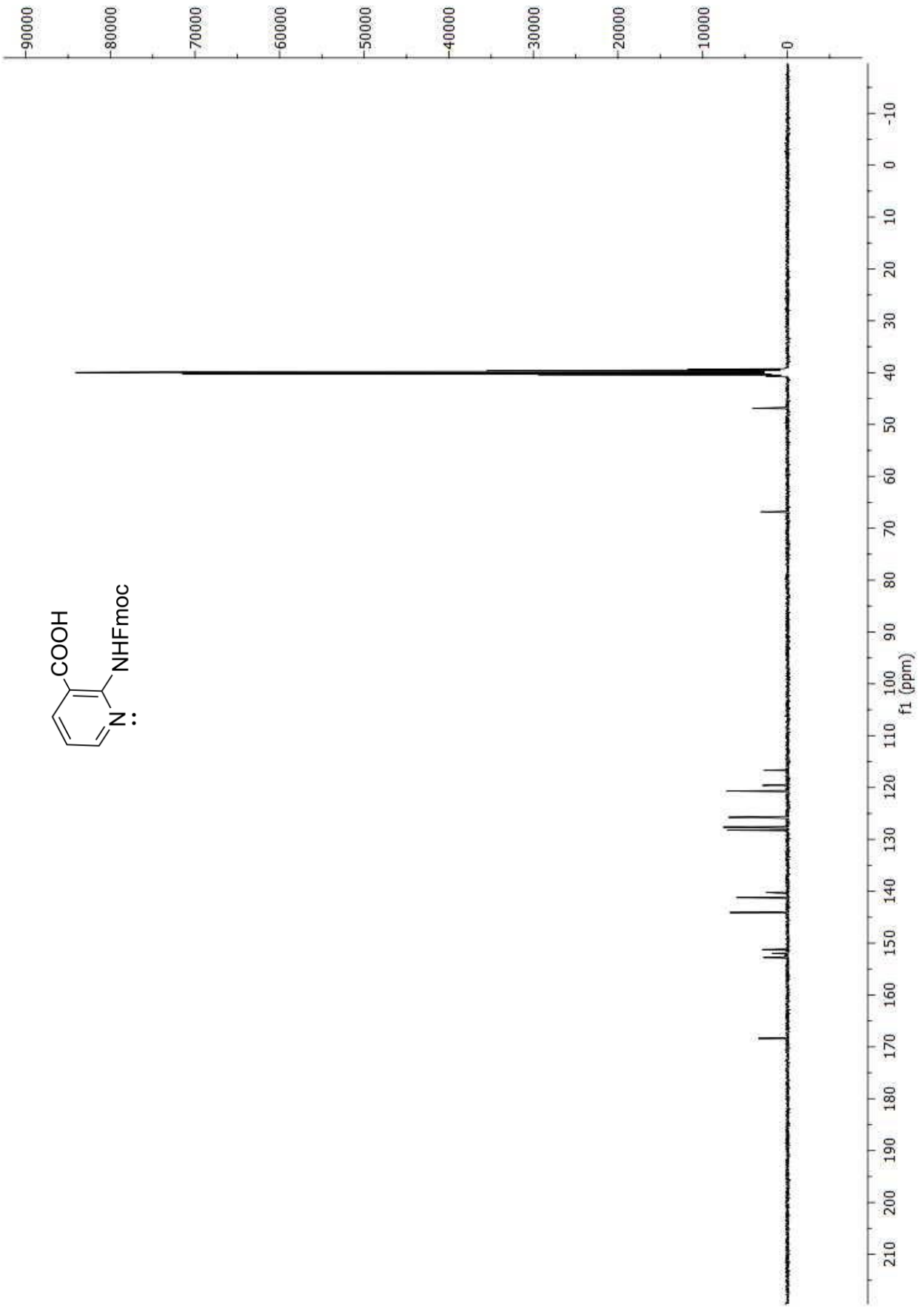

Figure 184: ^{13}C-NMR Spectrum ($CDCl_3$, 100 MHz) of **G4**.

AP2.2 Peptides
AP2.2.1 ^{1}H-NMR Spectra

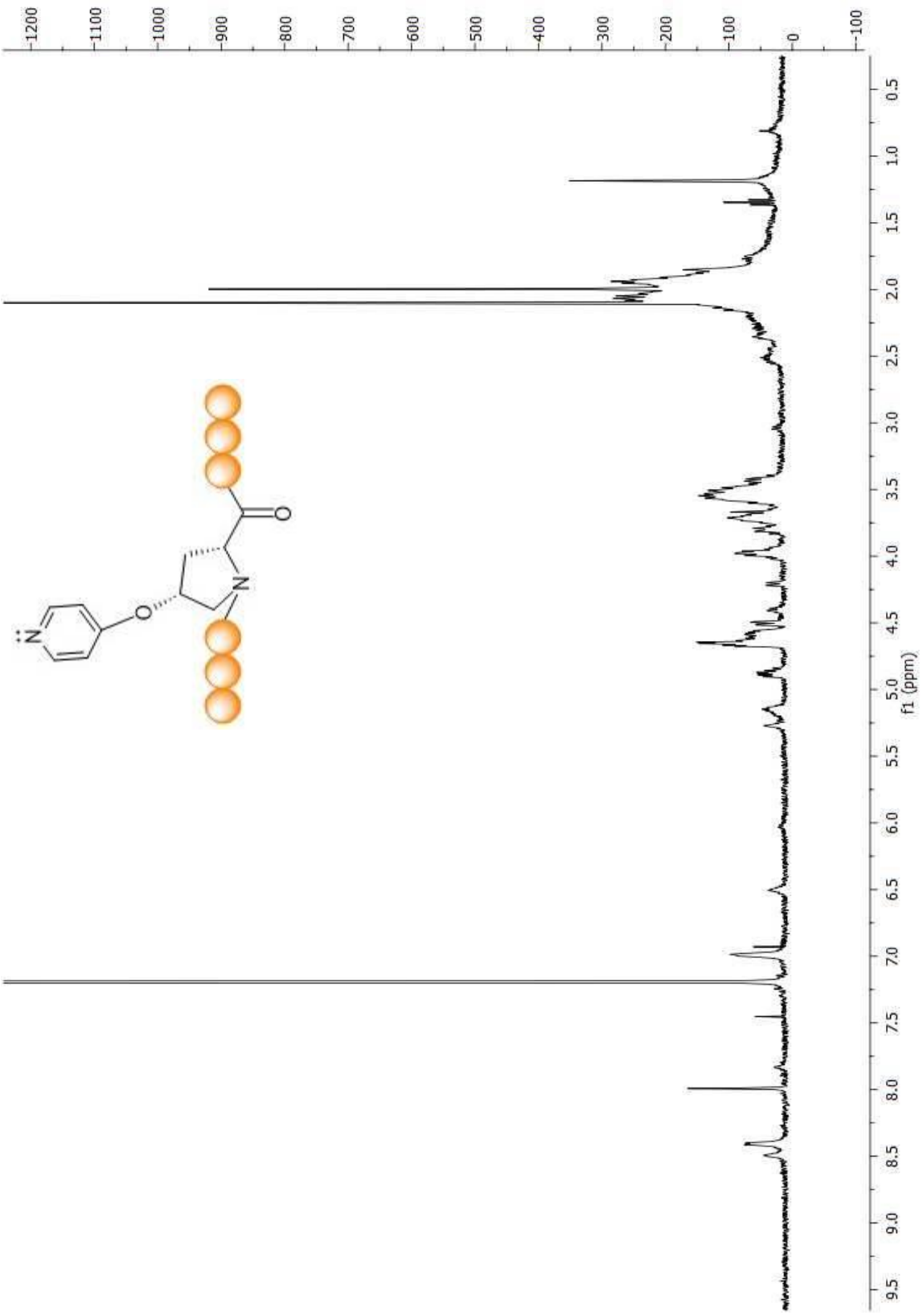

Figure 185: ^{1}H-NMR spectrum ($CDCl_3$, 400 MHz) of **PP 4**.

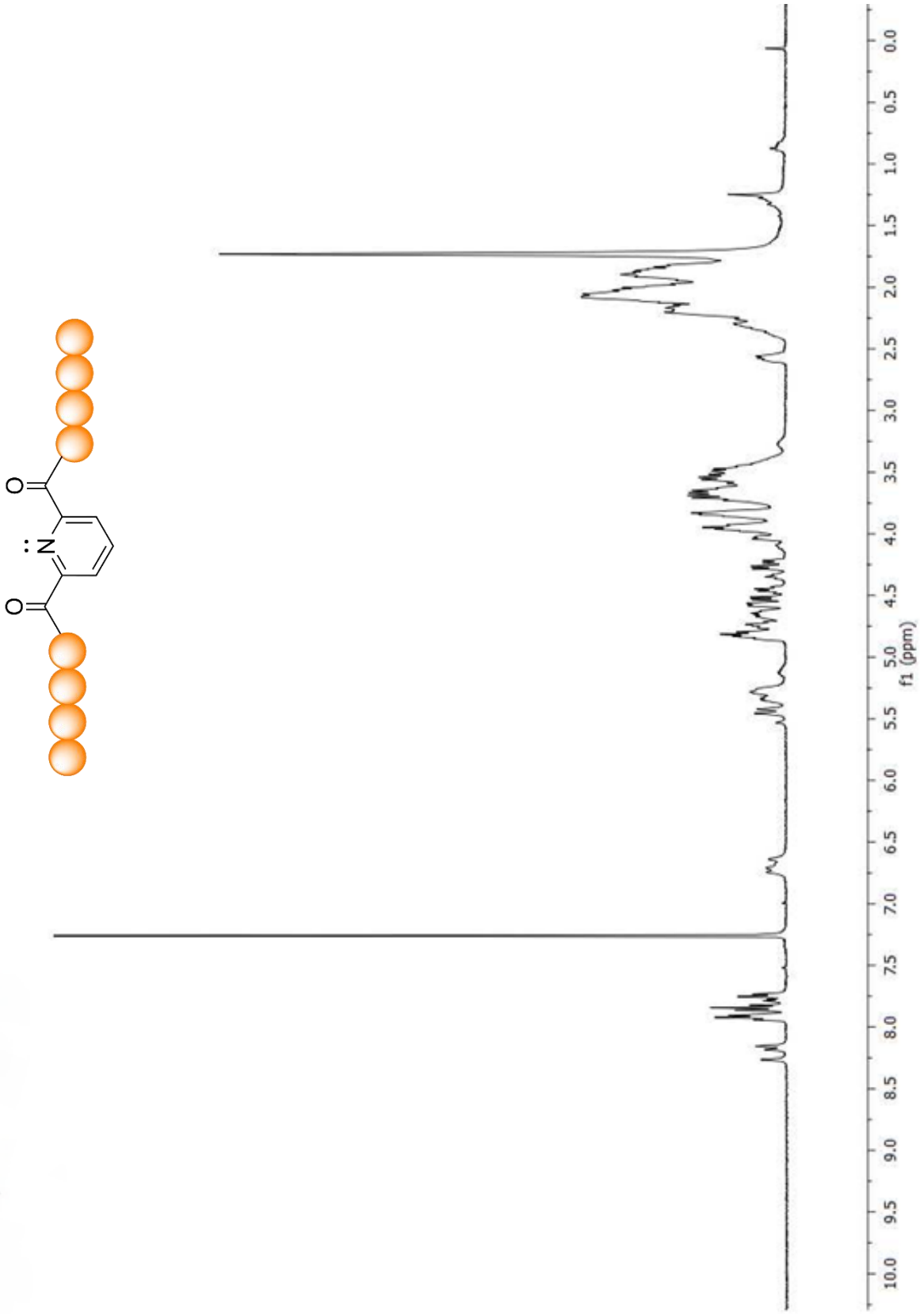

Figure 186: ^{1}H-NMR Spectrum ($CDCl_3$, 400 MHz) of **PP 7**.

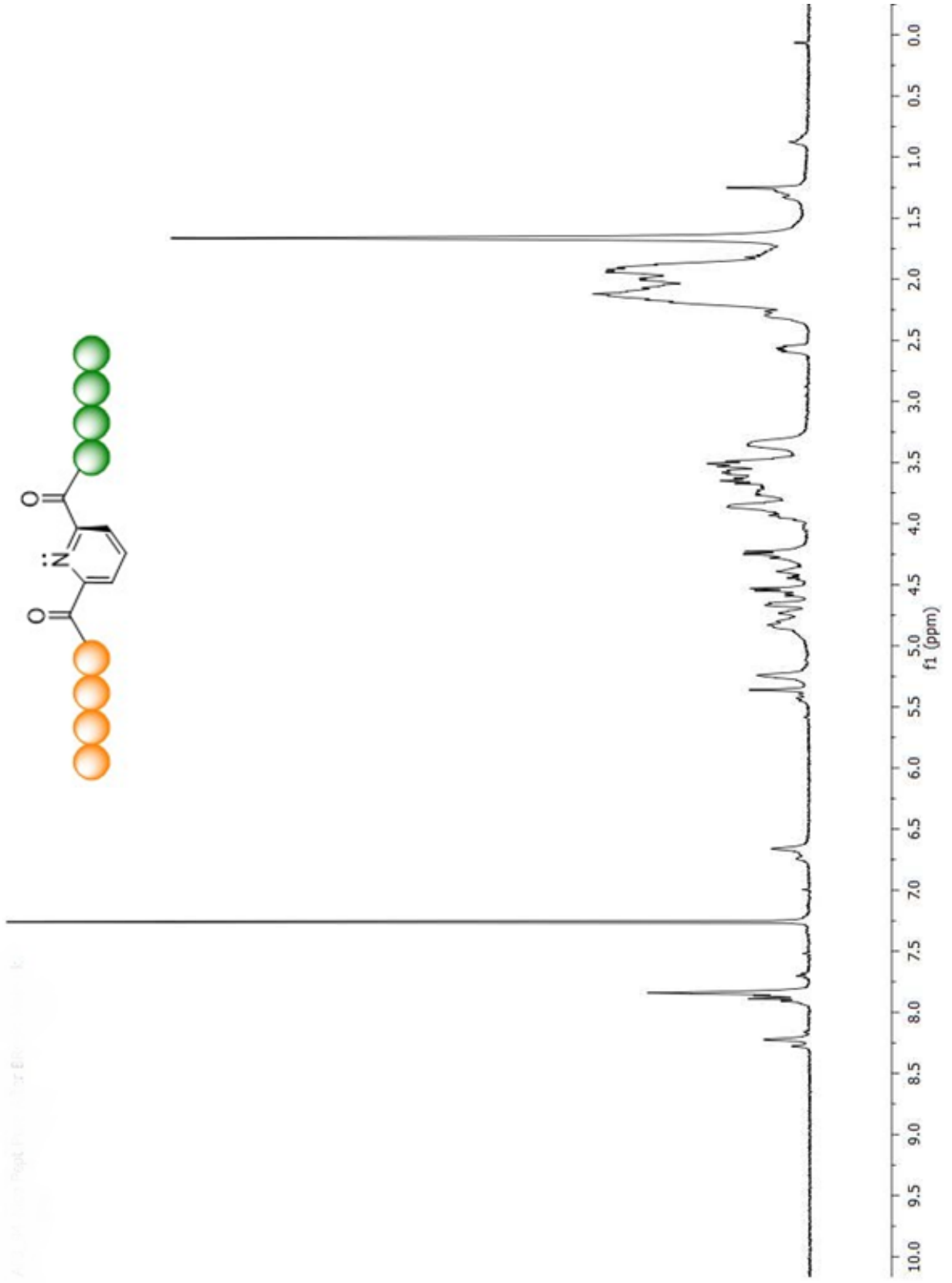

Figure 187: ^{1}H-NMR Spectrum ($CDCl_3$, 400 MHz) of **PP 8**.

AP2.3 Kinetic resolution of a Racemic Alcohol

AP2.3.1 ^{1}H-NMR Spectra

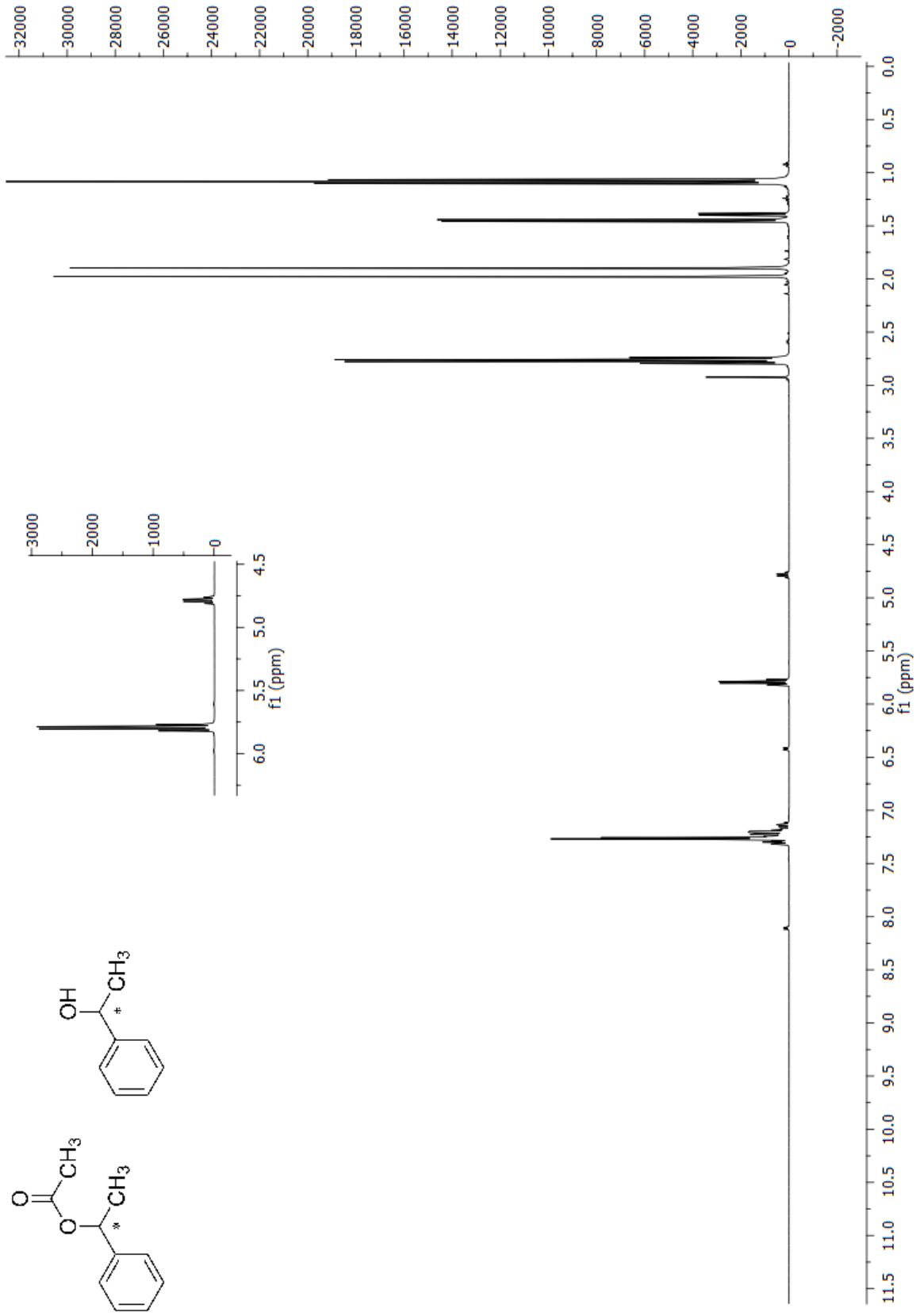

Figure 188: ^{1}H-NMR Spectrum ($CDCl_3$, 400 MHz) of 1-phenyl alcohol with Ac_2O Using DMAP (Table 11, Entry 1).

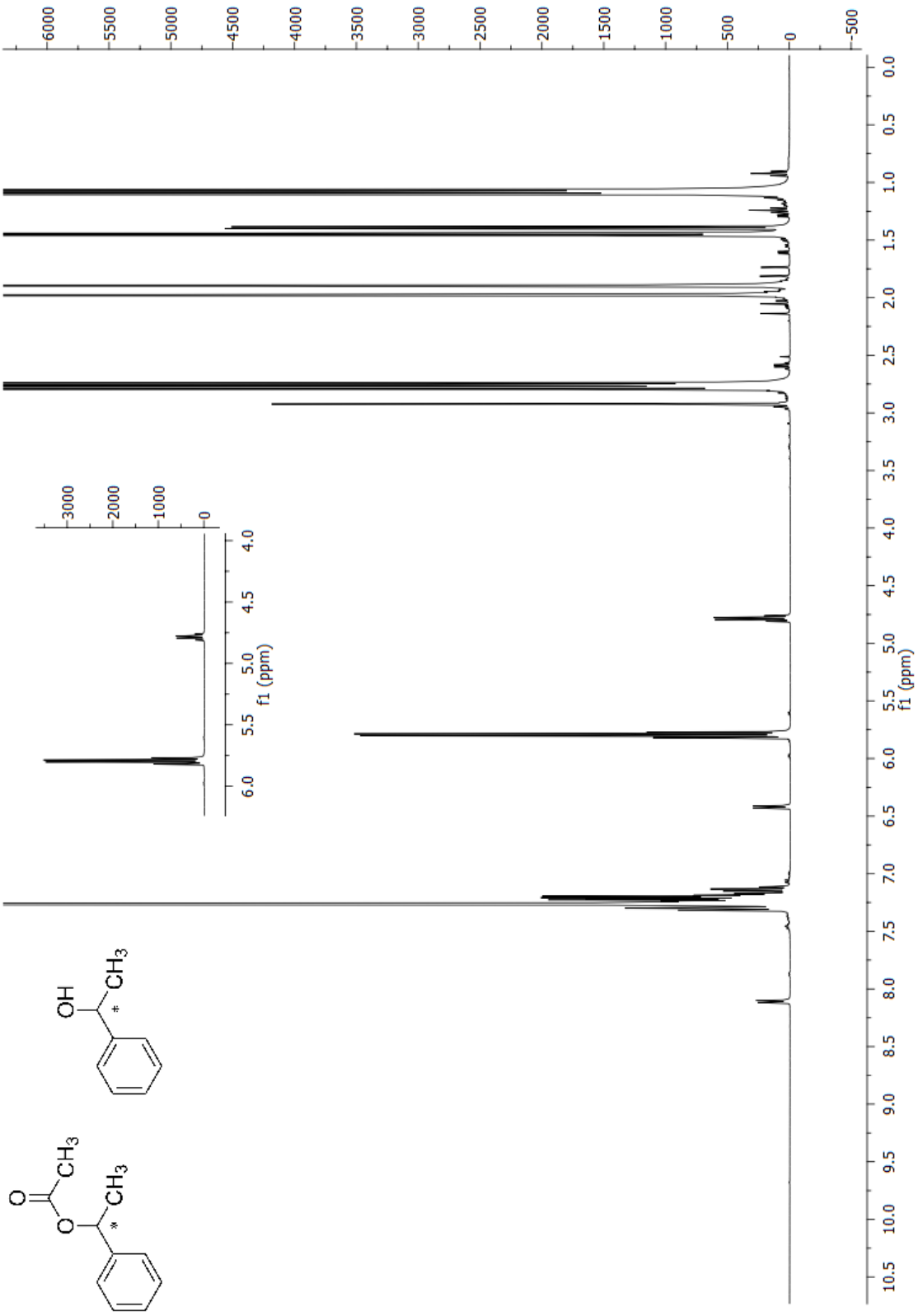

Figure 189: ^{1}H-NMR Spectrum ($CDCl_3$, 400 MHz) from the Reaction of 1-phenyl alcohol with Ac_2O Using DMAP (Table 11, Entry 2).

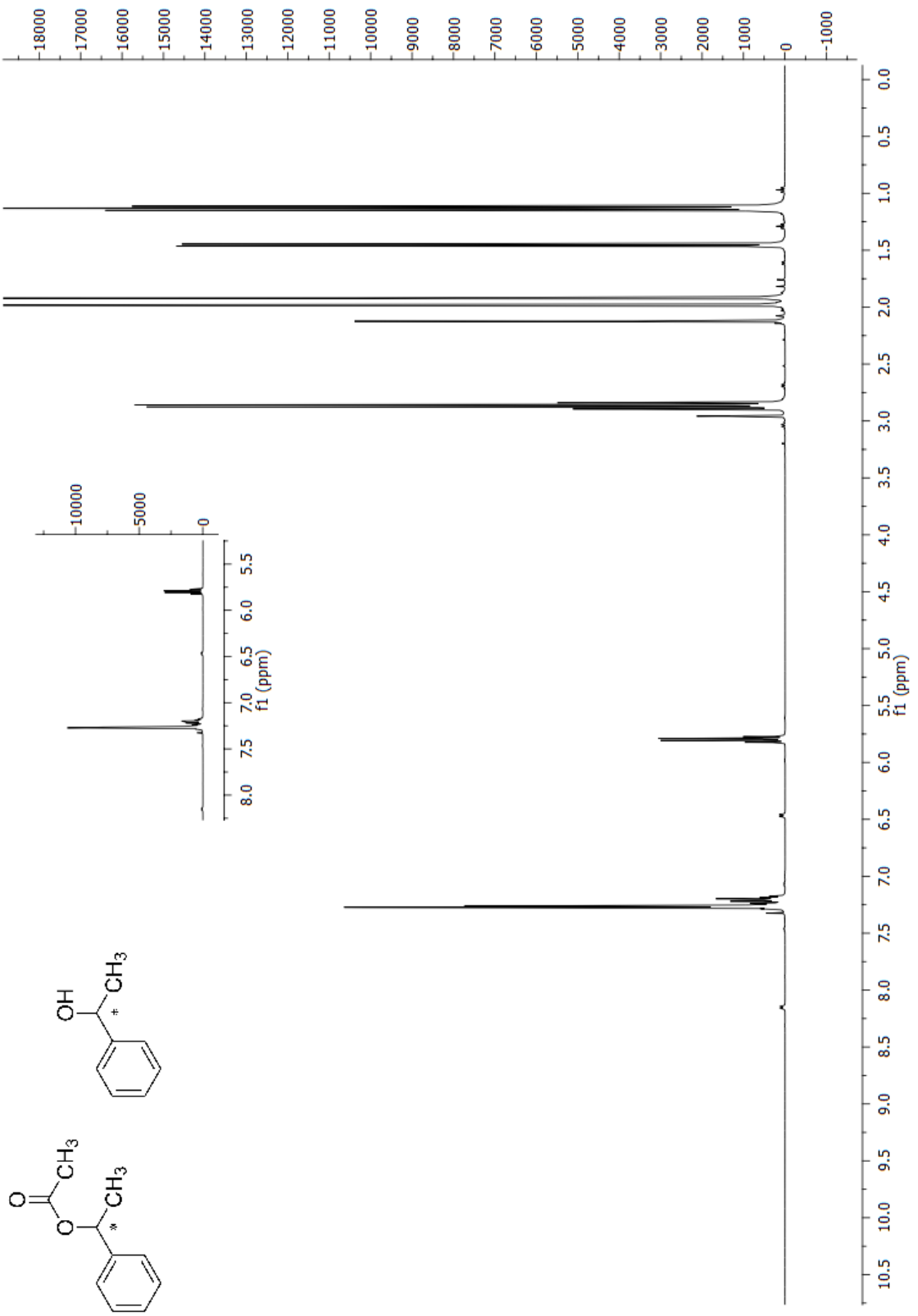

Figure 190: ^{1}H-NMR Spectrum ($CDCl_3$, 400 MHz) from the Reaction of 1-phenyl alcohol with Ac_2O Using DMAP (Table 11, Entry 3).

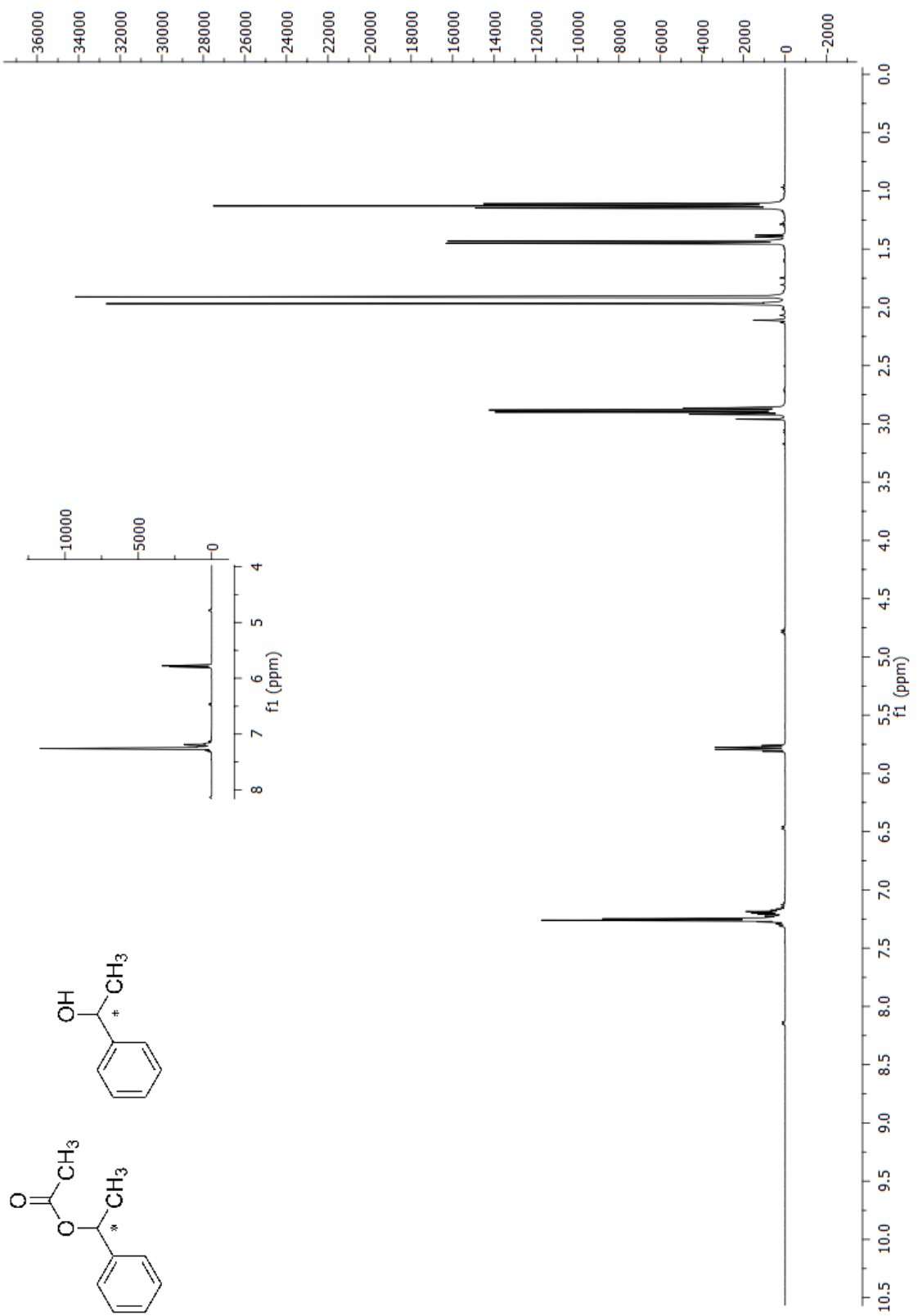

Figure 191: ^{1}H-NMR Spectrum ($CDCl_3$, 400 MHz) from the Reaction of 1-phenyl alcohol with Ac_2O Using DMAP (Table 11, Entry 4).

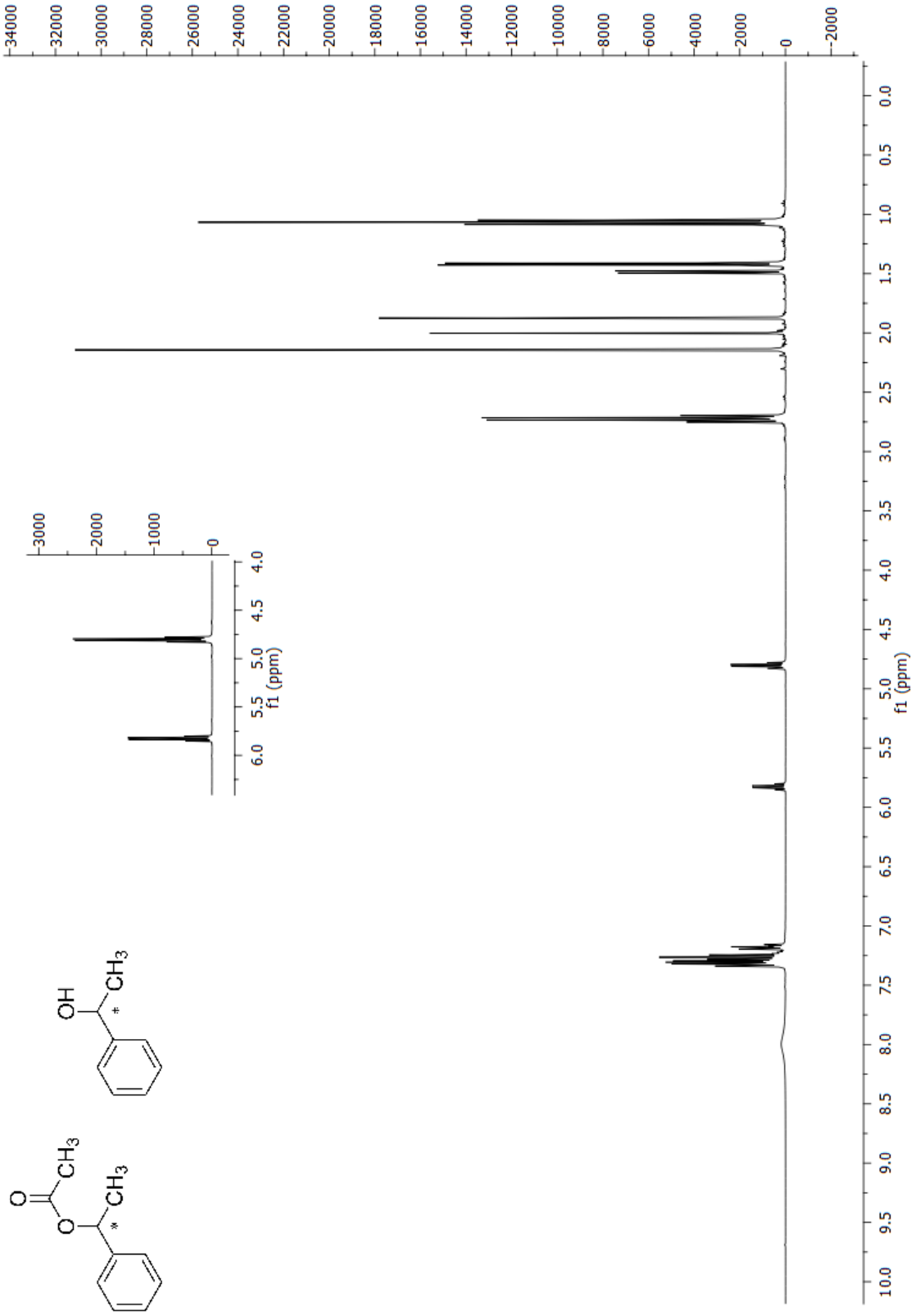

Figure 192: ^{1}H-NMR Spectrum ($CDCl_3$, 400 MHz) from the Reaction of 1-phenyl alcohol with Ac_2O Using No Catalyst (Table 12, Entry 5).

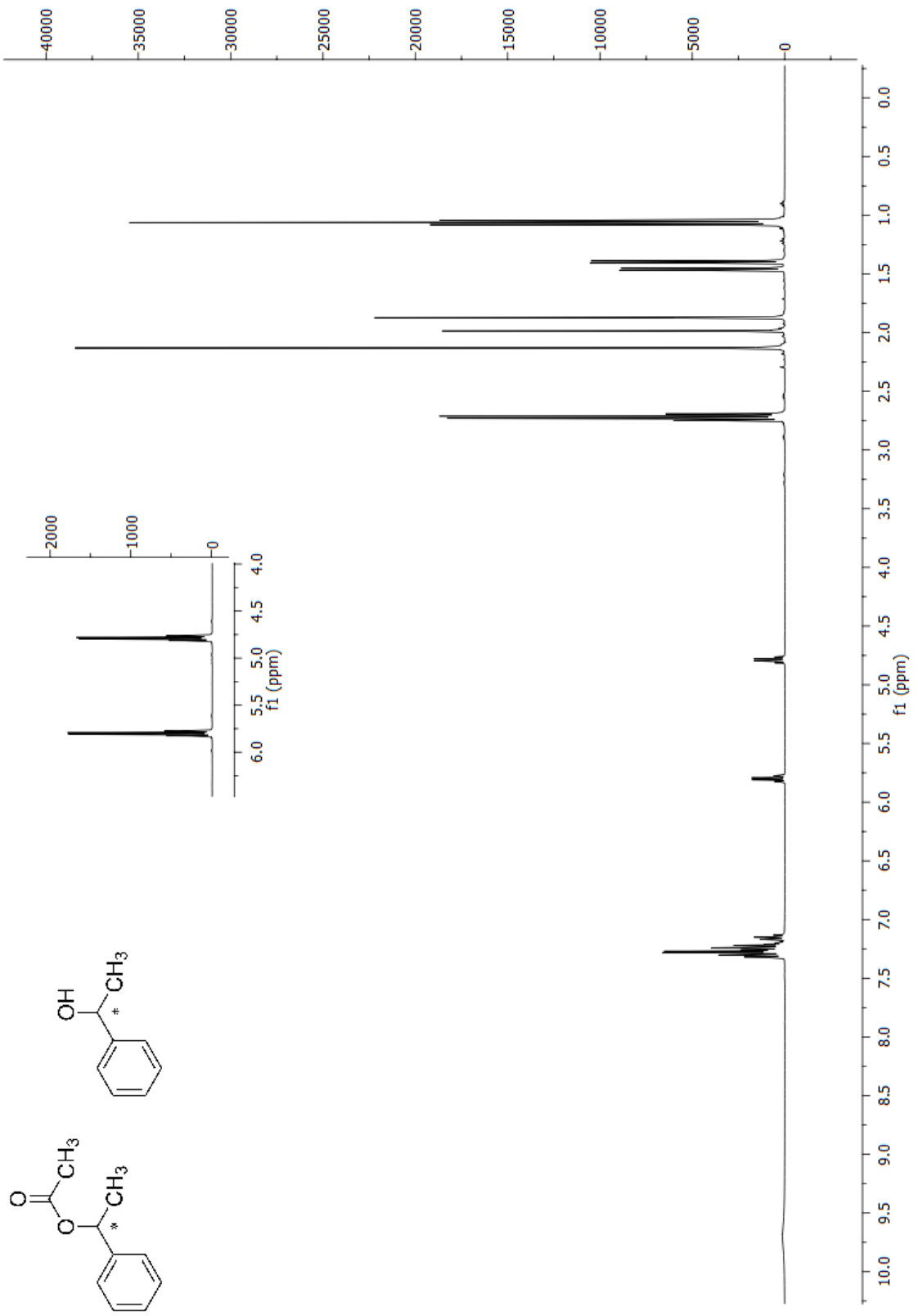

Figure 193: ^{1}H-NMR Spectrum ($CDCl_3$, 400 MHz) from the Reaction of 1-phenyl alcohol with Ac_2O Using No Catalyst (Table 12, Entry 6).

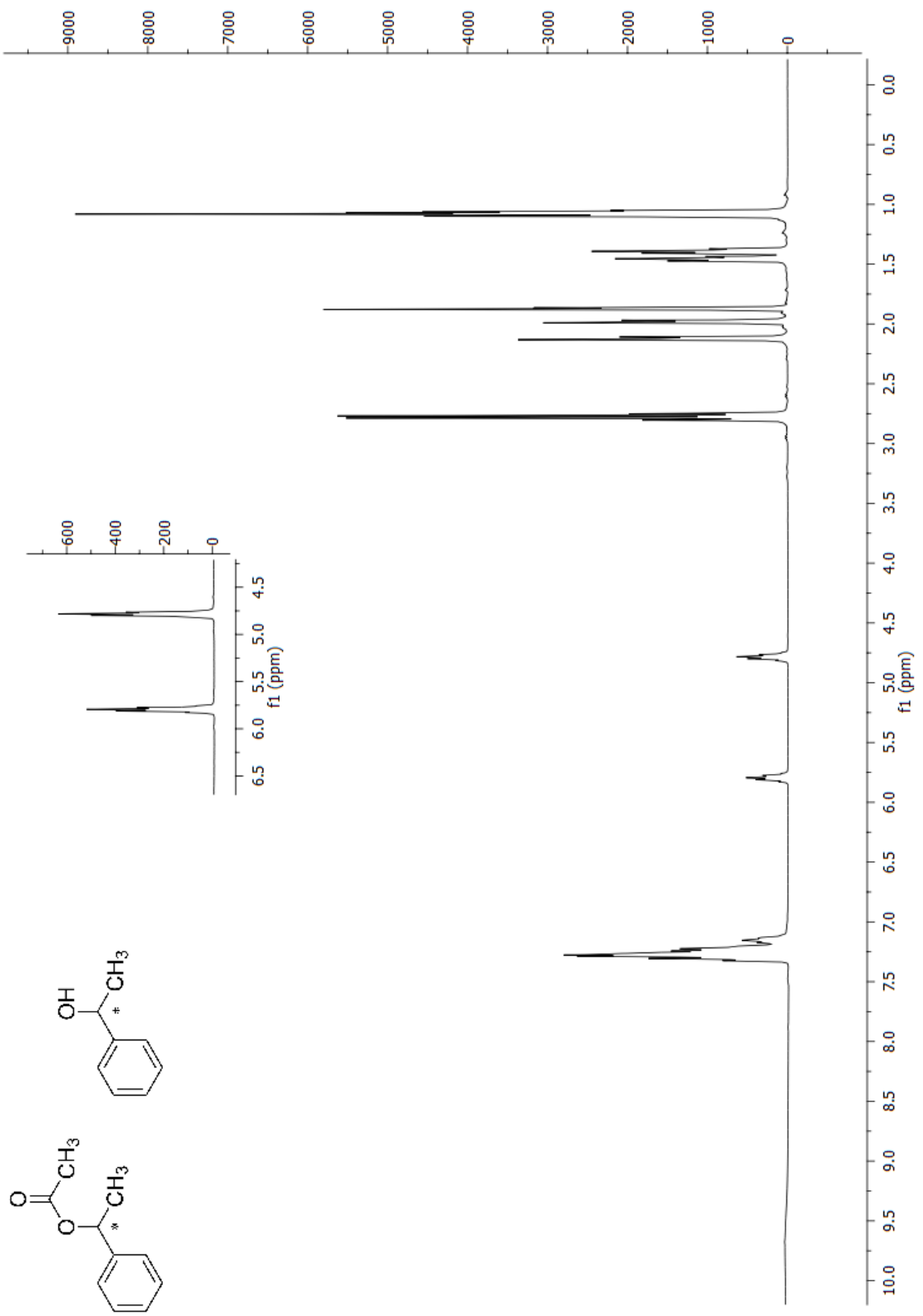

Figure 194: ^{1}H-NMR Spectrum ($CDCl_3$, 400 MHz) from the Reaction of 1-phenyl alcohol with Ac_2O Using No Catalyst (Table 12, Entry 7).

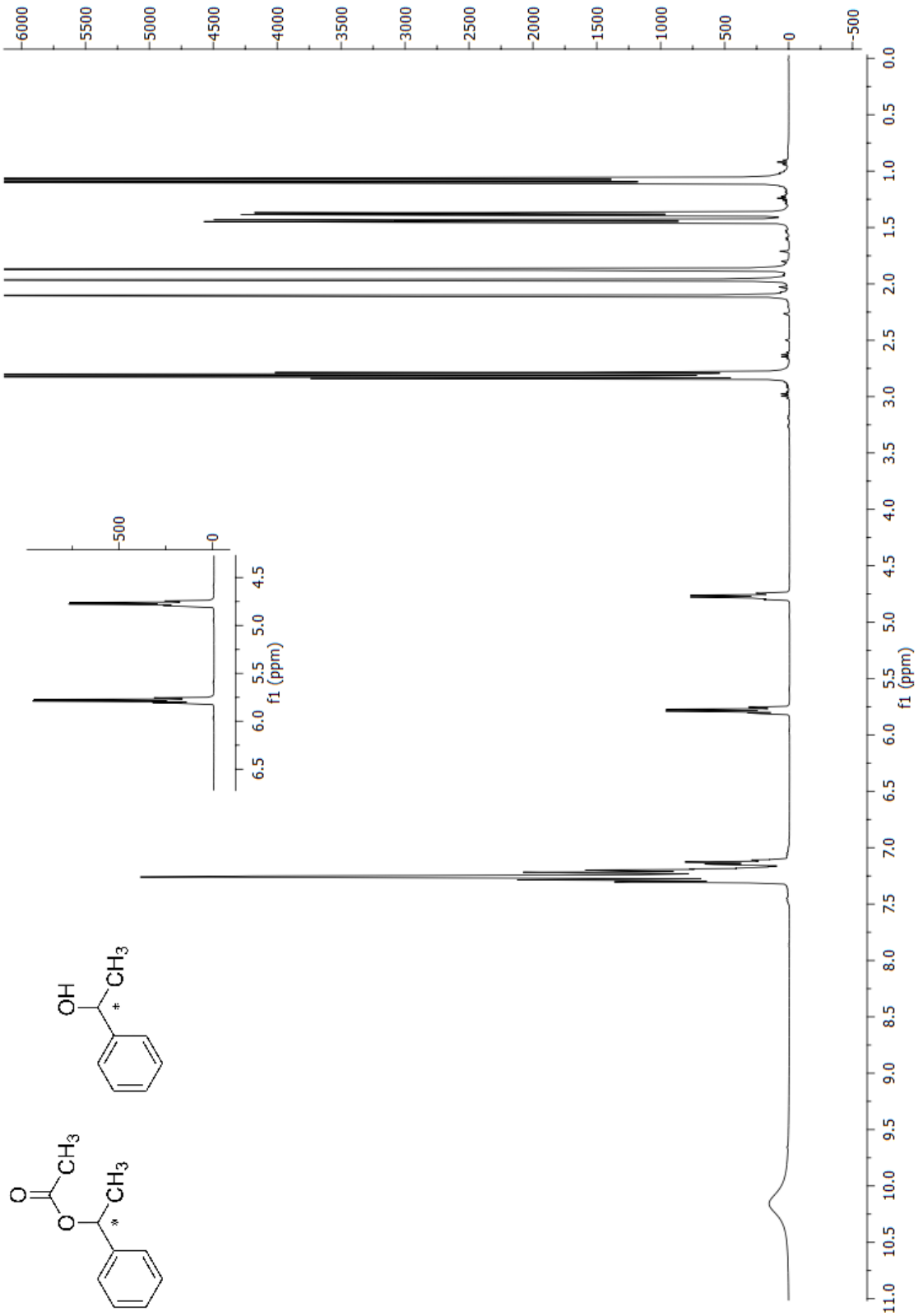

Figure 195: ^{1}H-NMR Spectrum ($CDCl_3$, 400 MHz) from the Reaction of 1-phenyl alcohol with Ac_2O Using No Catalyst (Table 12, Entry 9).

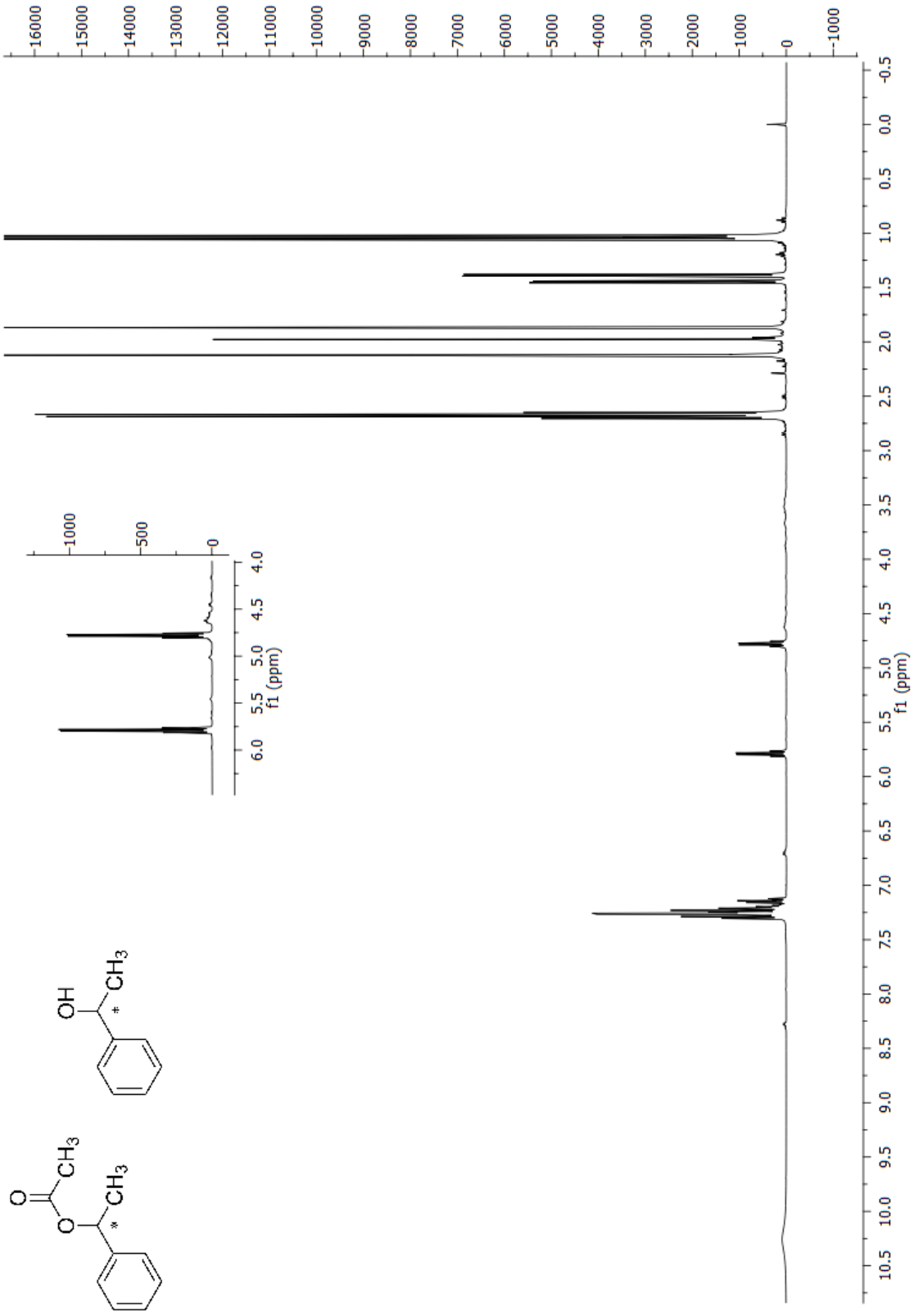

Figure 196: ^{1}H-NMR Spectrum ($CDCl_3$, 400 MHz) from the Reaction of 1-phenyl alcohol with Ac_2O Using **PP 4** (Table 13, Entry 10).

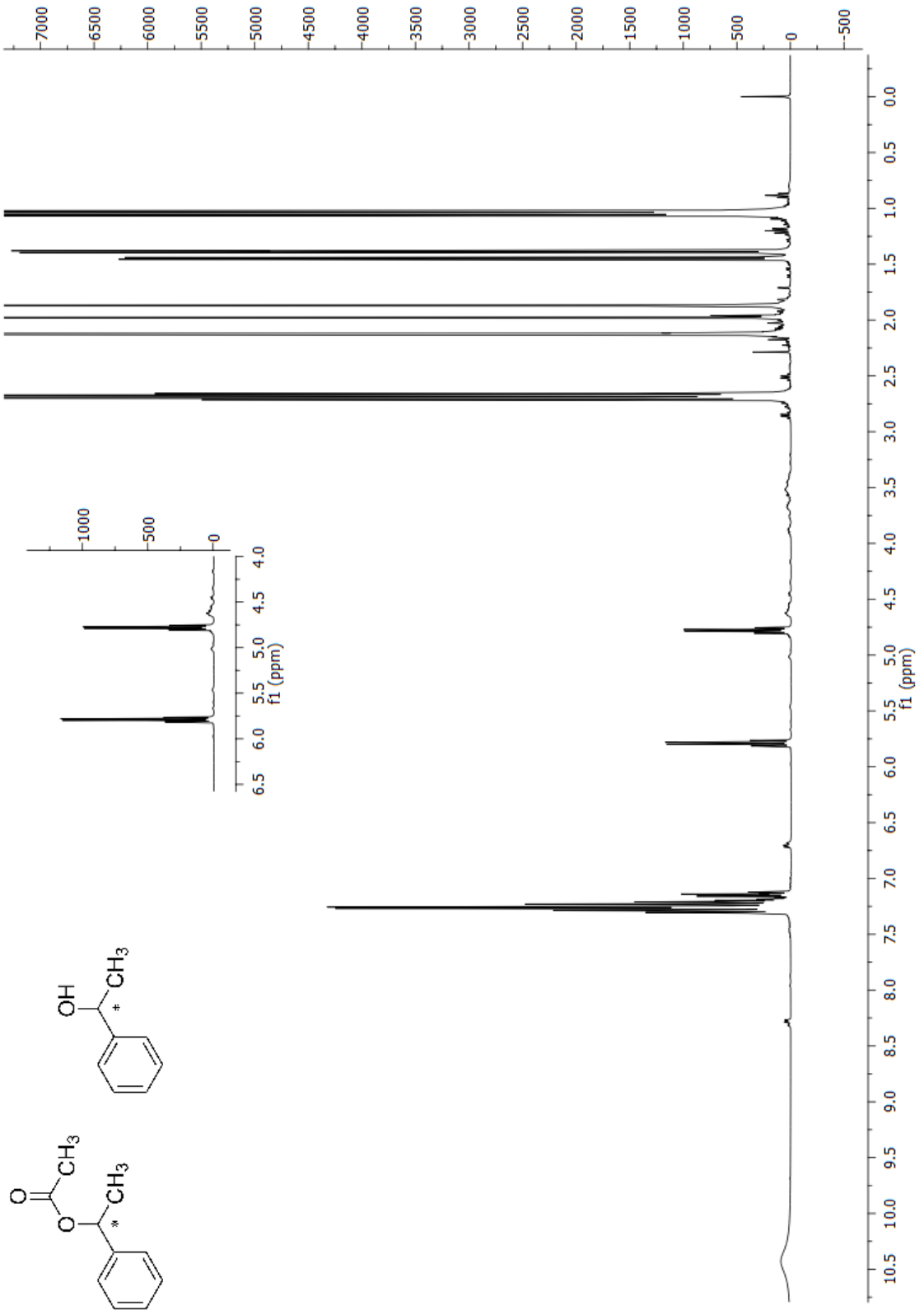

Figure 197: ^{1}H-NMR Spectrum ($CDCl_3$, 400 MHz) from the Reaction of 1-phenyl alcohol with Ac_2O Using **PP 4** (Table 13, Entry 11).

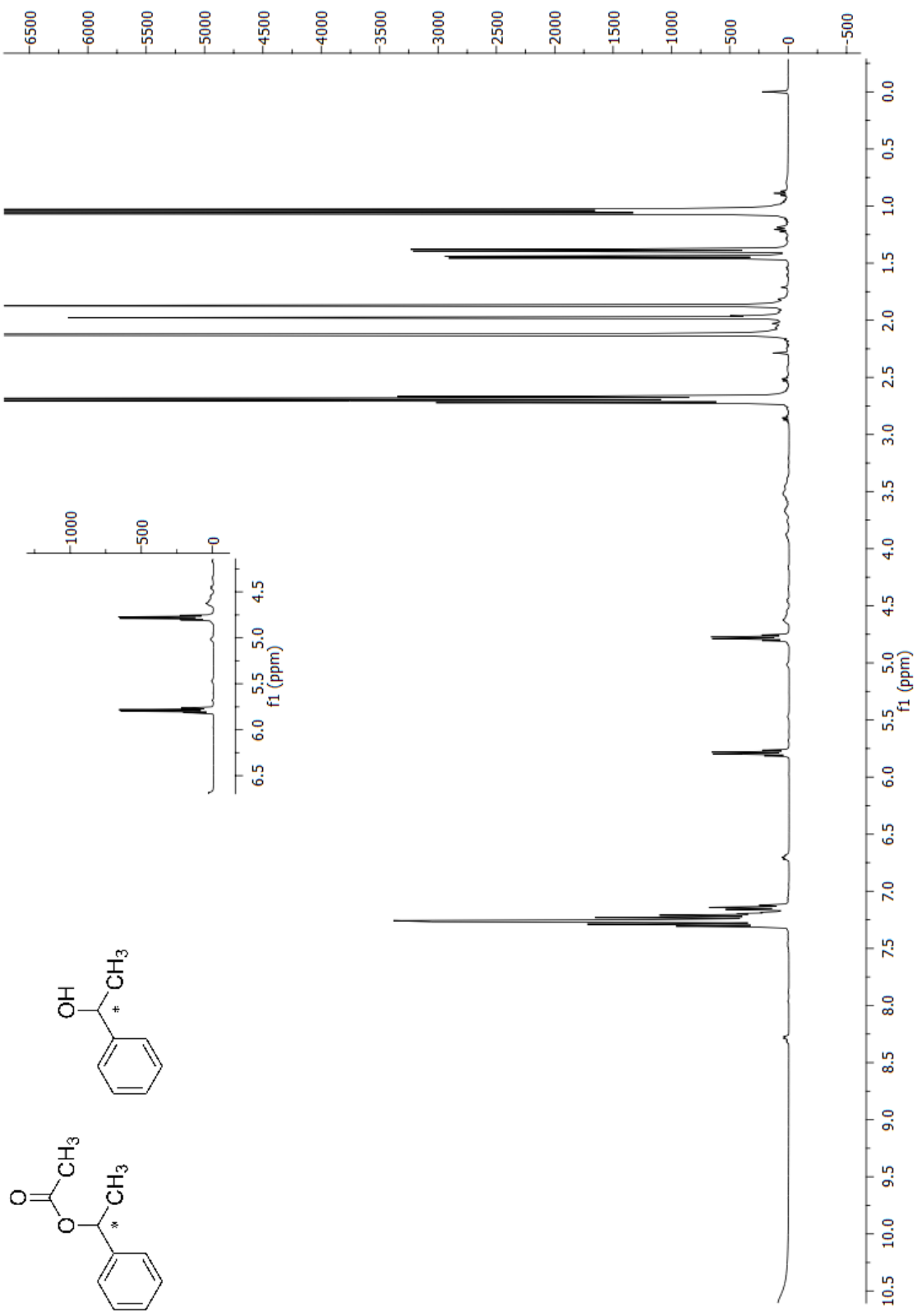

Figure 198: ^{1}H-NMR Spectrum ($CDCl_3$, 400 MHz) from the Reaction of 1-phenyl alcohol with Ac_2O Using **PP 4** (Table 13, Entry 12).

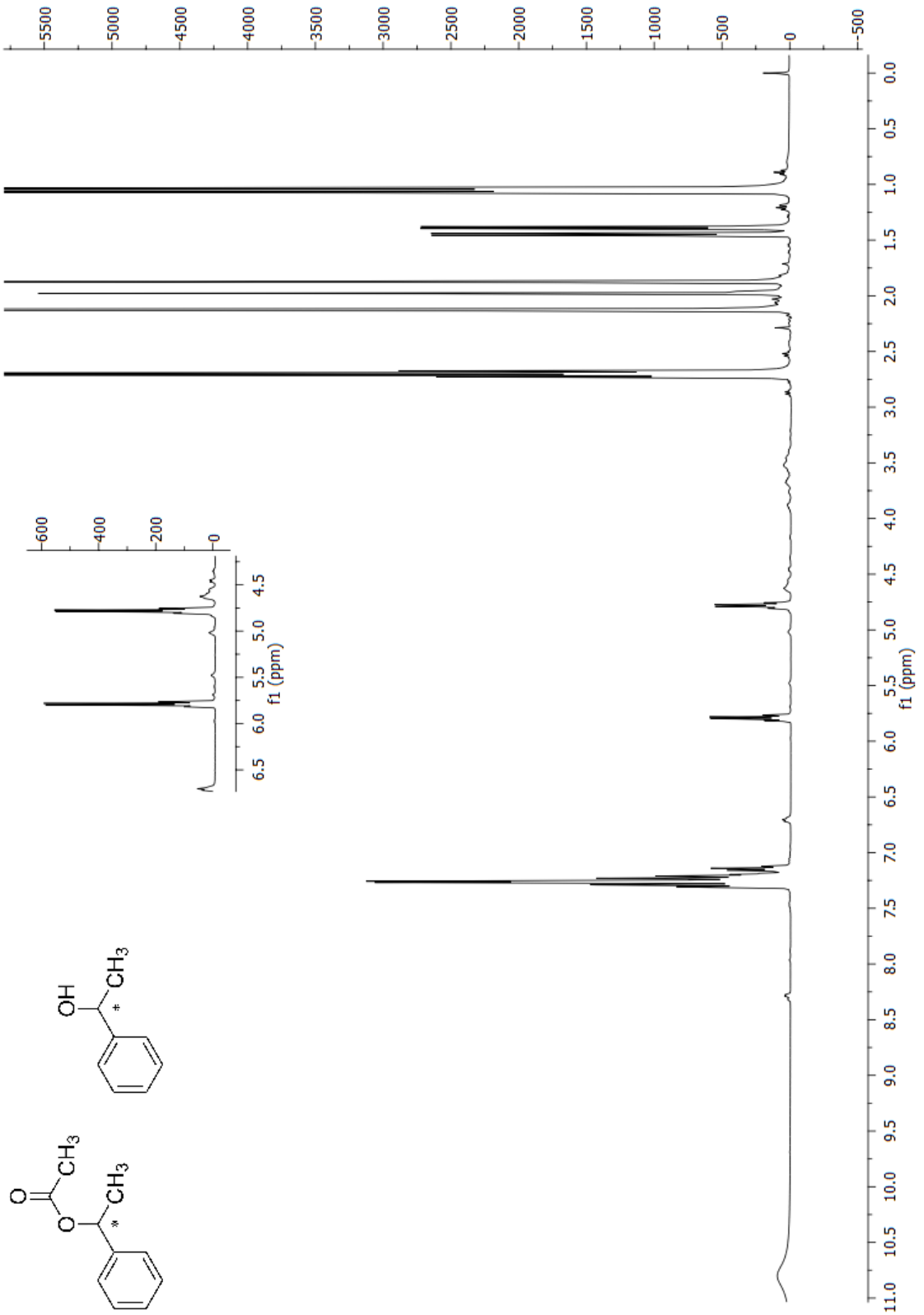

Figure 199: ^{1}H-NMR Spectrum ($CDCl_3$, 400 MHz) from the Reaction of 1-phenyl alcohol with Ac_2O Using **PP 4** (Table 13, Entry 13).

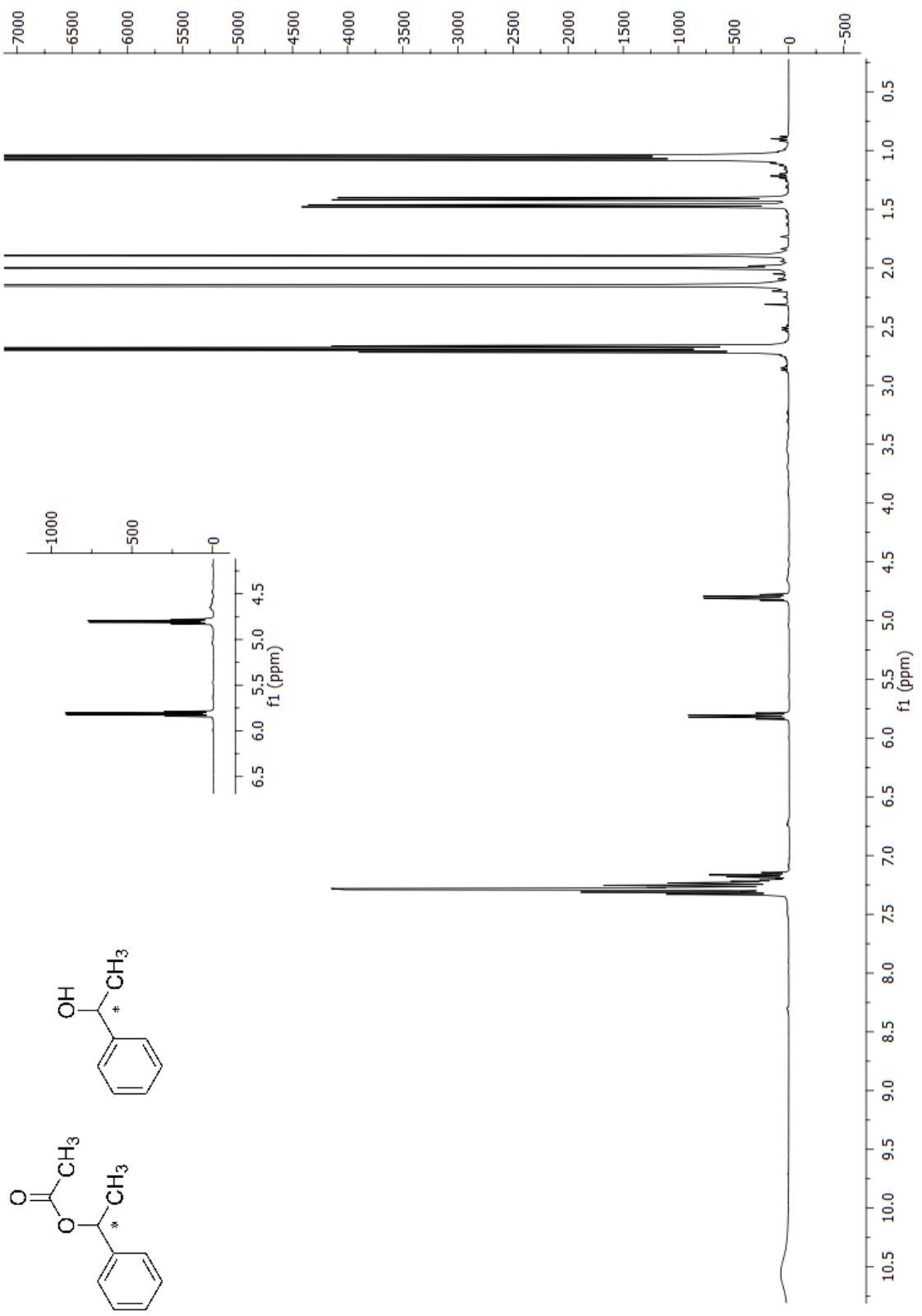

Figure 200: ^{1}H-NMR Spectrum ($CDCl_3$, 400 MHz) from the Reaction of 1-phenyl alcohol with Ac_2O Using **PP 4** (Table 13, Entry 14).

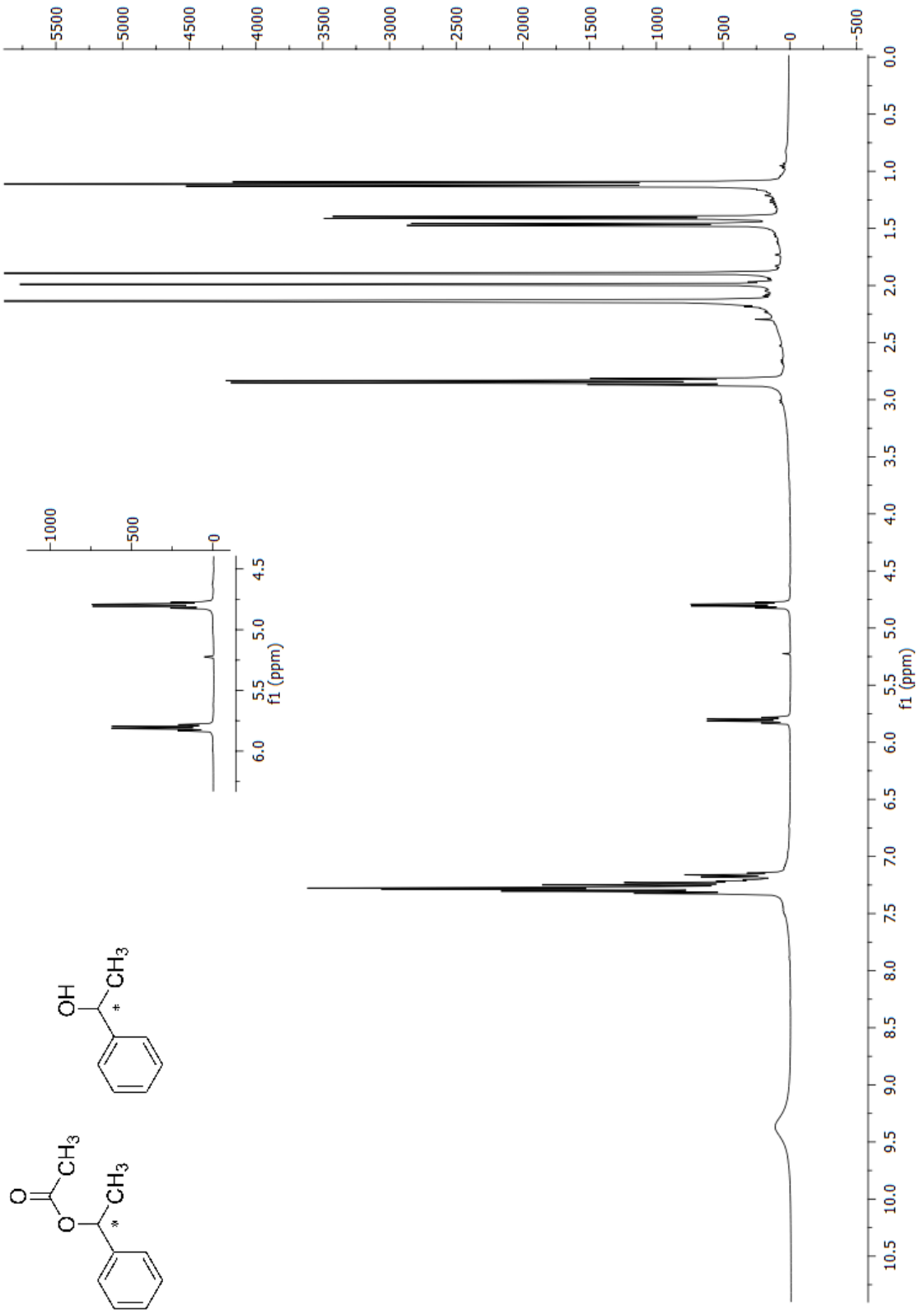

Figure 201: ^{1}H-NMR Spectrum ($CDCl_3$, 400 MHz) from the Reaction of 1-phenyl alcohol with Ac_2O Using **PP 4** (Table 13, Entry 15).

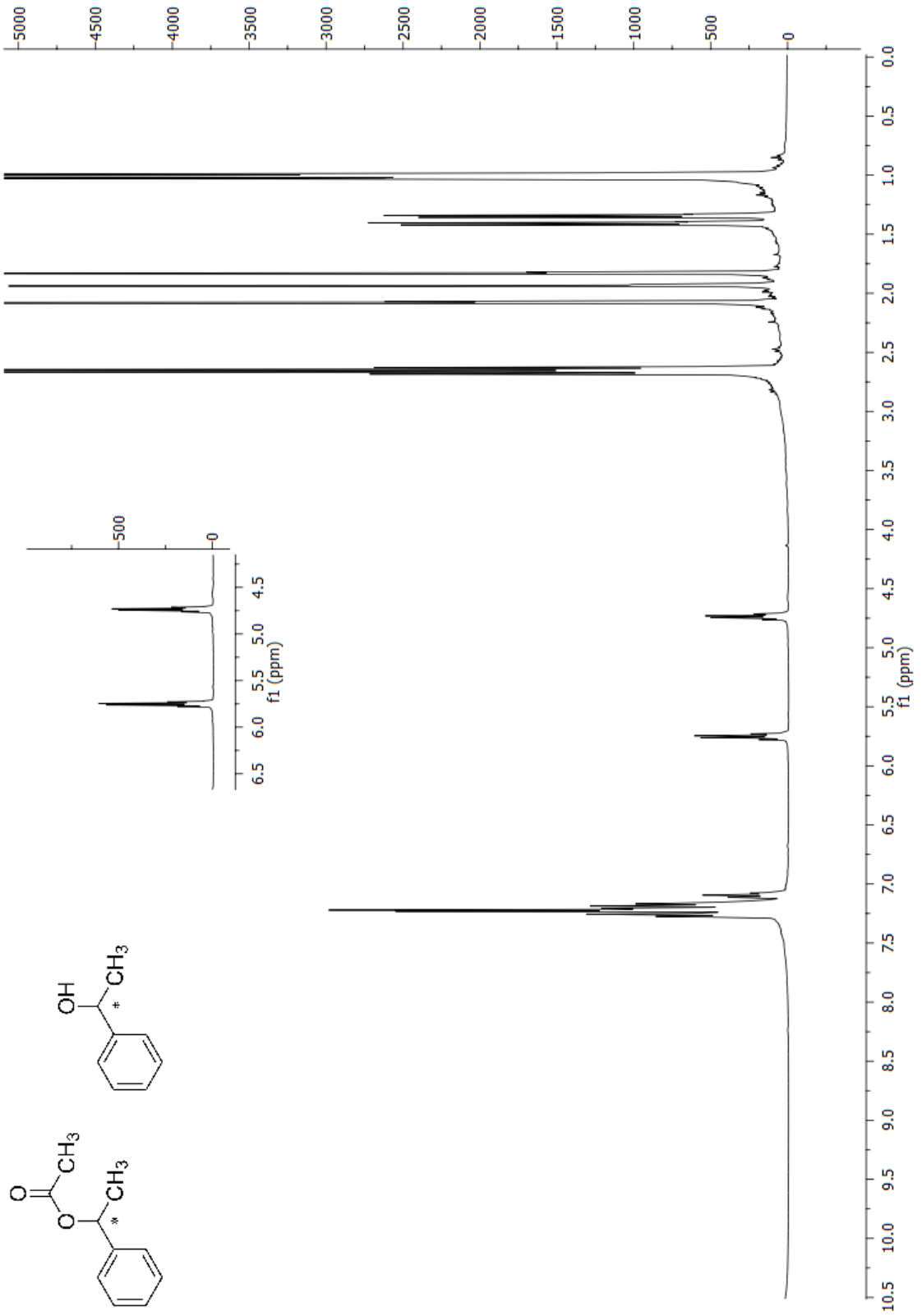

Figure 202: ^{1}H-NMR Spectrum ($CDCl_3$, 400 MHz) from the Reaction of 1-phenyl alcohol with Ac_2O Using **PP 4** (Table 13, Entry 16).

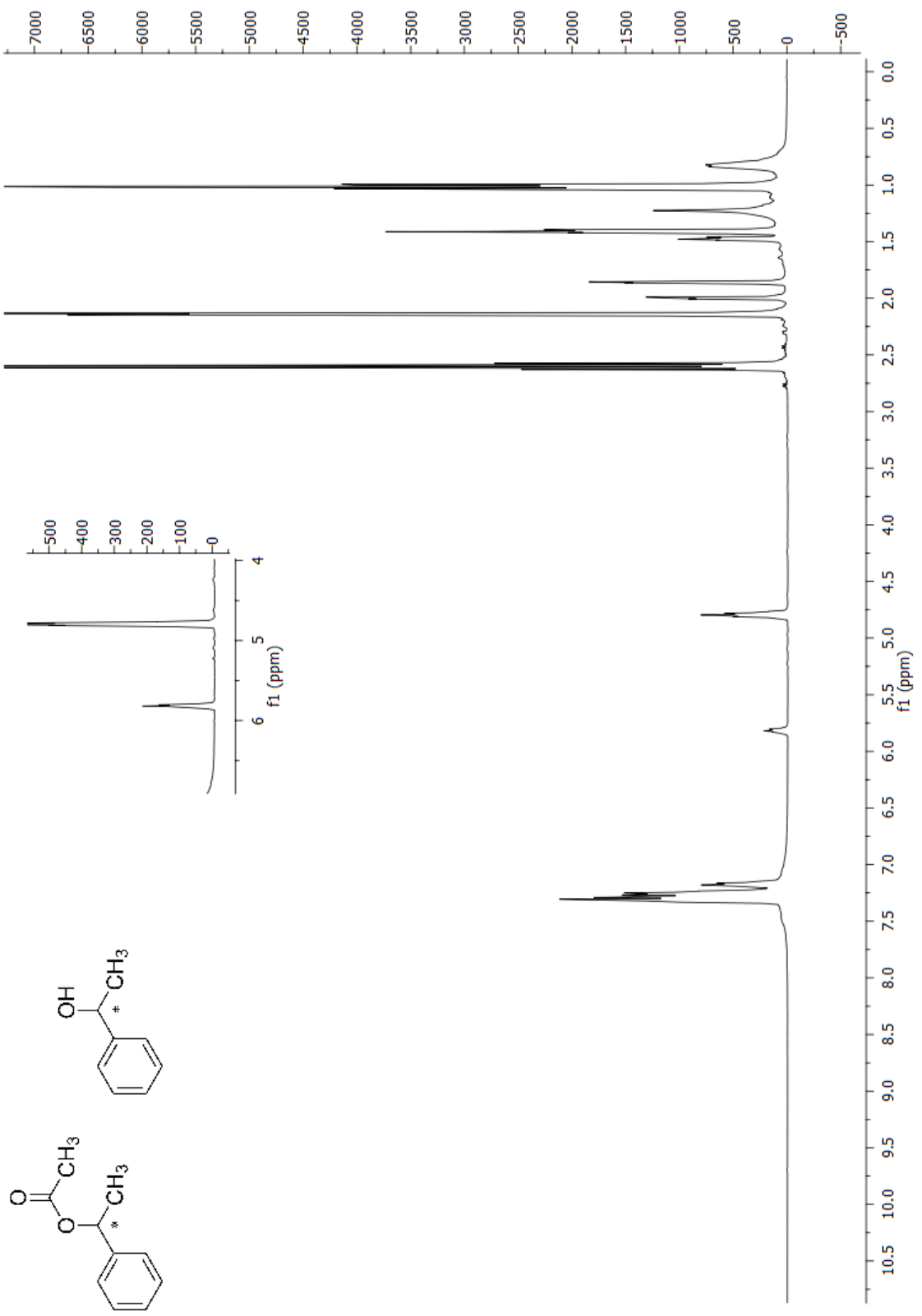

Figure 203*:* ^{1}H-NMR Spectrum ($CDCl_3$, 400 MHz) from the Reaction of 1-phenyl alcohol with Ac_2O Using **PP 4** (Table 14, Entry 17).

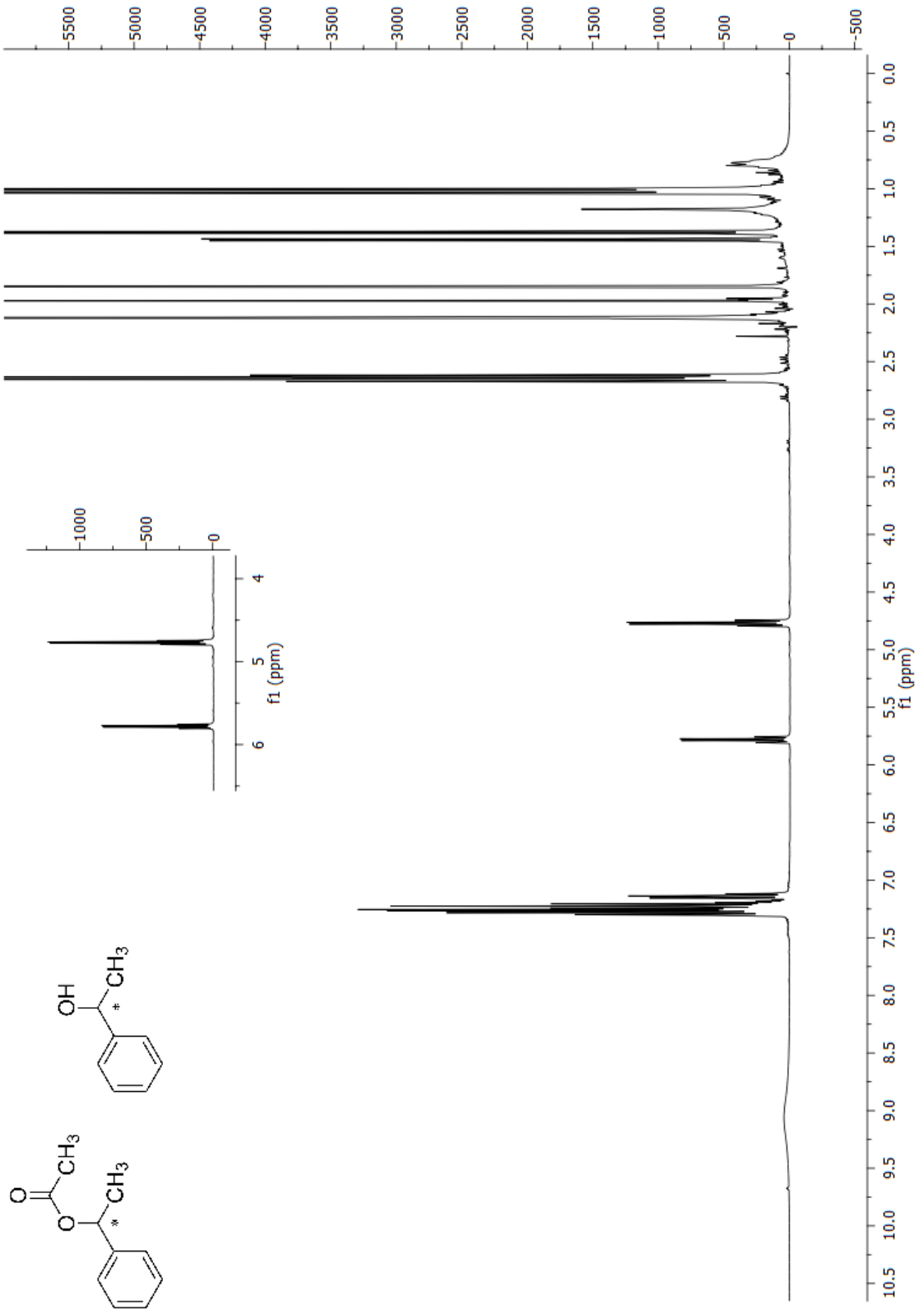

Figure 204: ^{1}H-NMR Spectrum ($CDCl_3$, 400 MHz) from the Reaction of 1-phenyl alcohol with Ac_2O Using **PP 4** (Table 14, Entry 18).

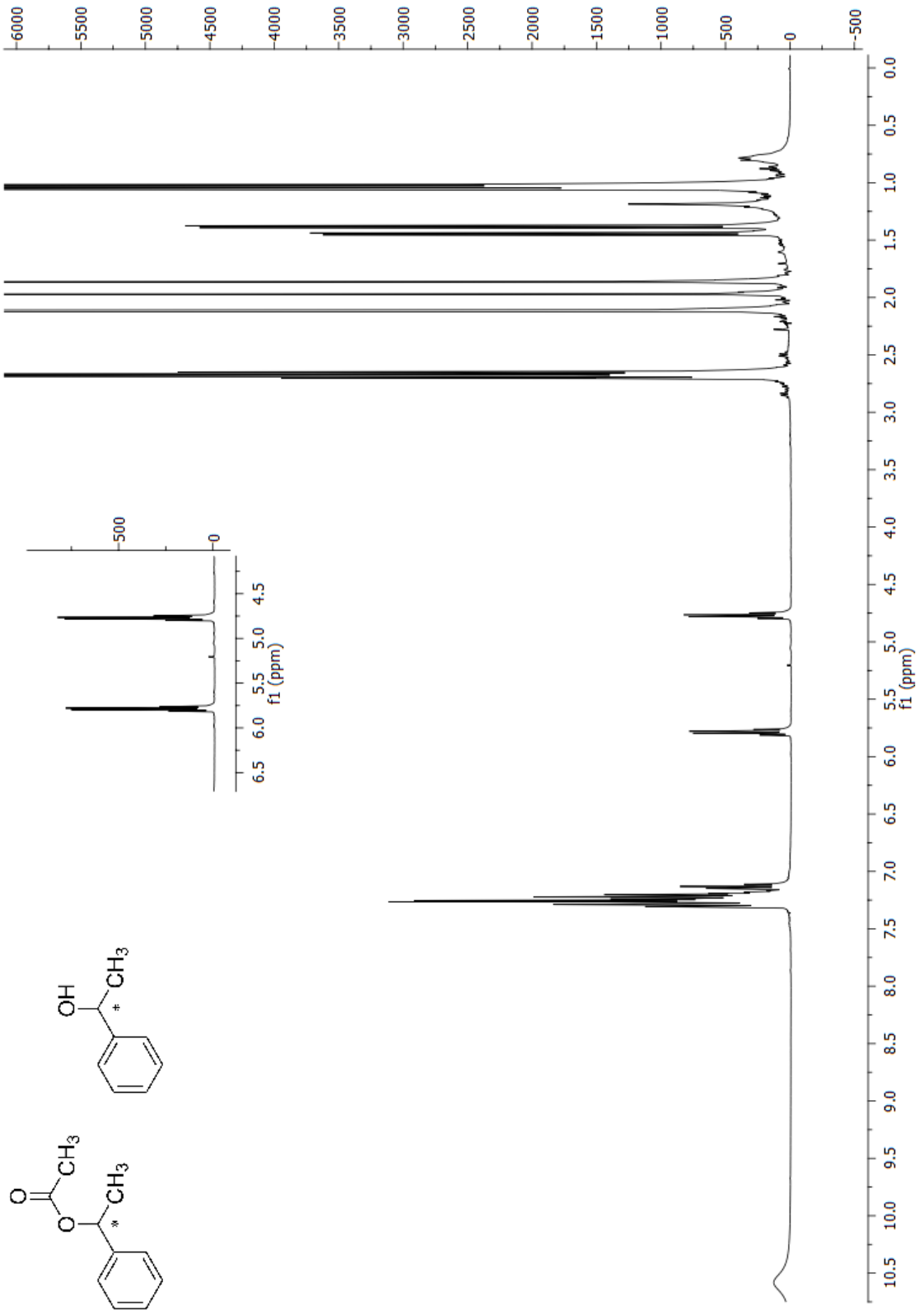

Figure 205: ^{1}H-NMR Spectrum ($CDCl_3$, 400 MHz) from the Reaction of 1-phenyl alcohol with Ac_2O Using **PP 4** (Table 14, Entry 19).

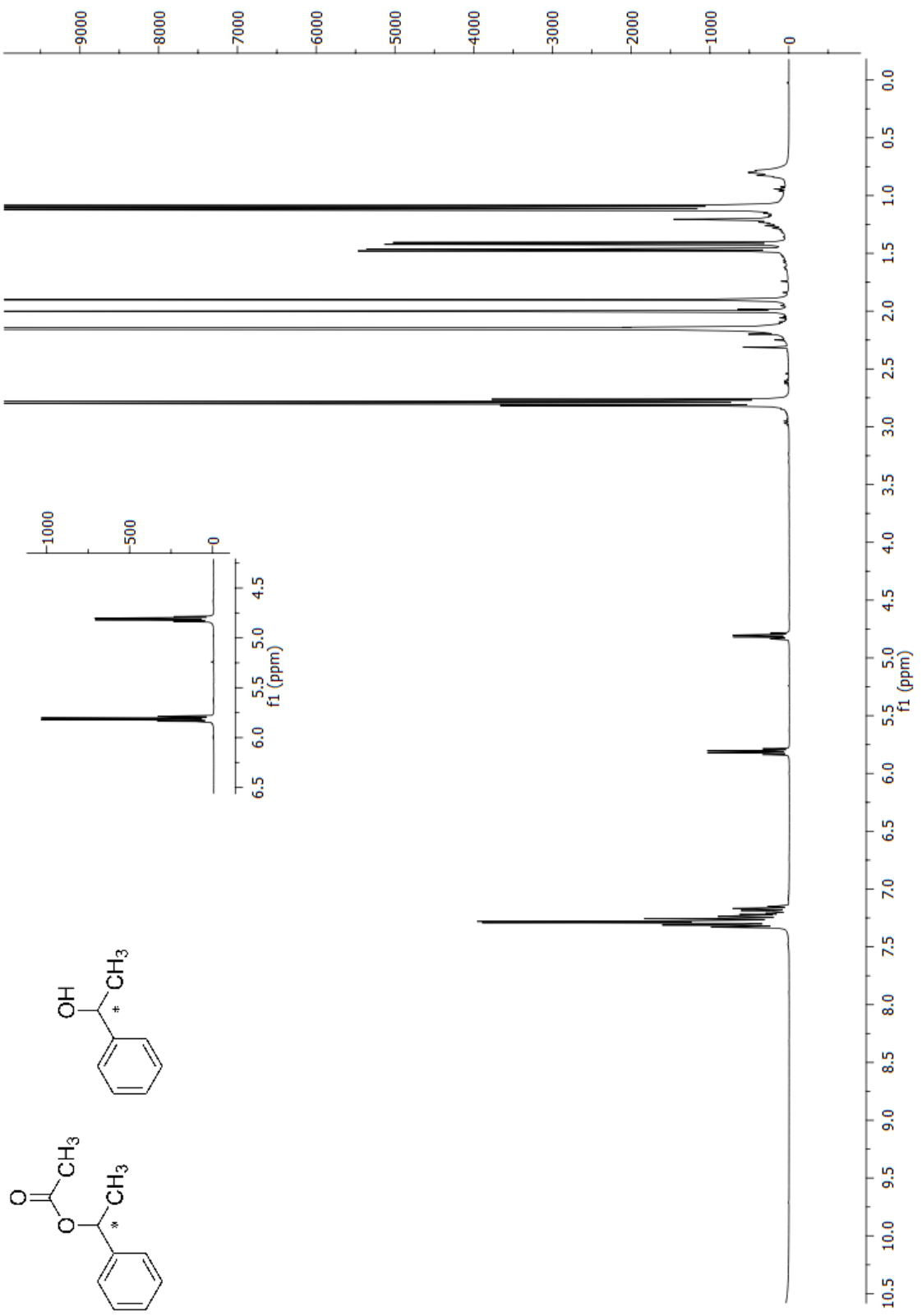

Figure 206: ^{1}H-NMR Spectrum ($CDCl_3$, 400 MHz) from the Reaction of 1-phenyl alcohol with Ac_2O Using **PP 4** (Table 14, Entry 20).

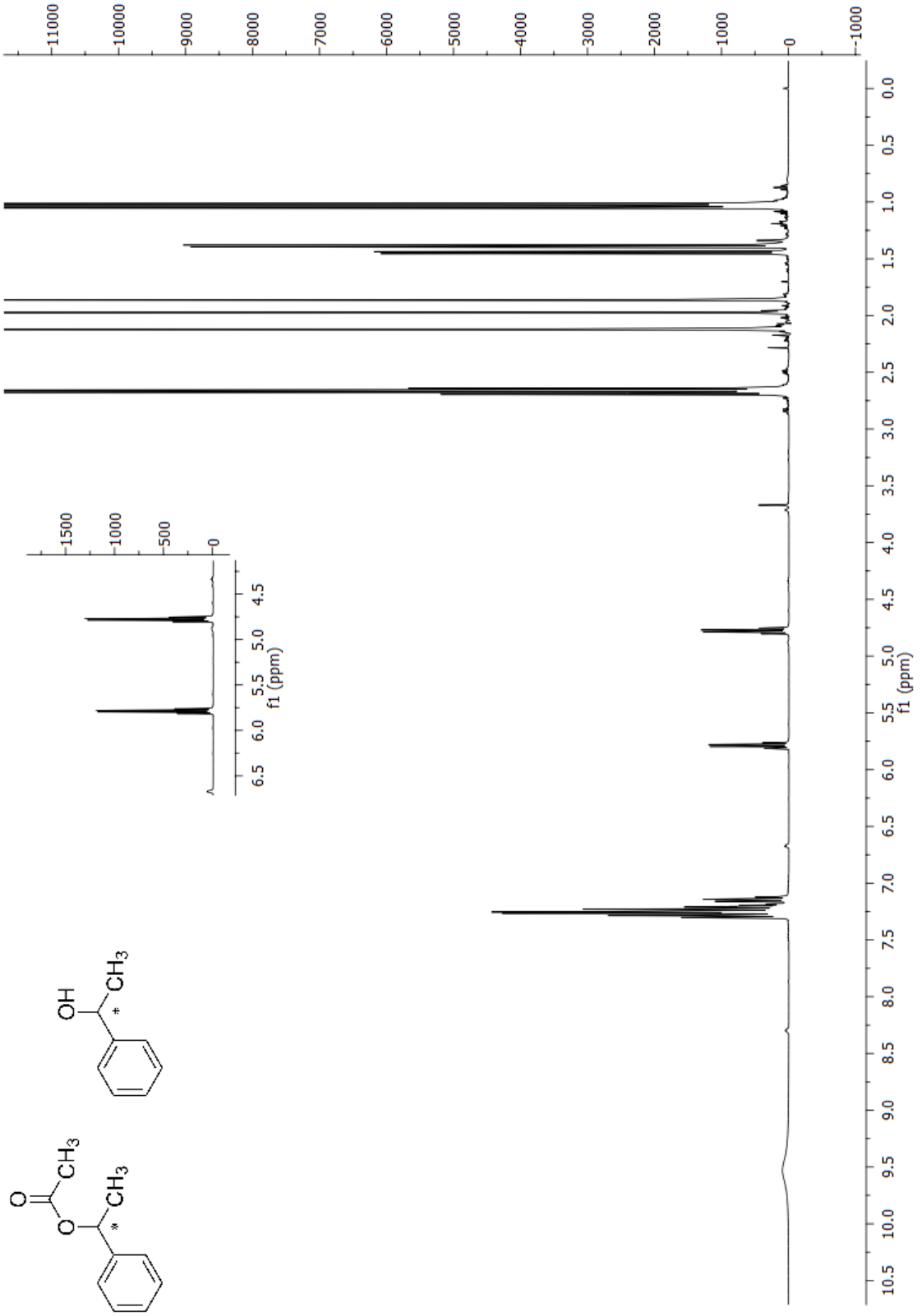

Figure 207: ^{1}H-NMR Spectrum ($CDCl_3$, 400 MHz) from the Reaction of 1-phenyl alcohol with Ac_2O Using **F2** (Table 15, Entry 21).

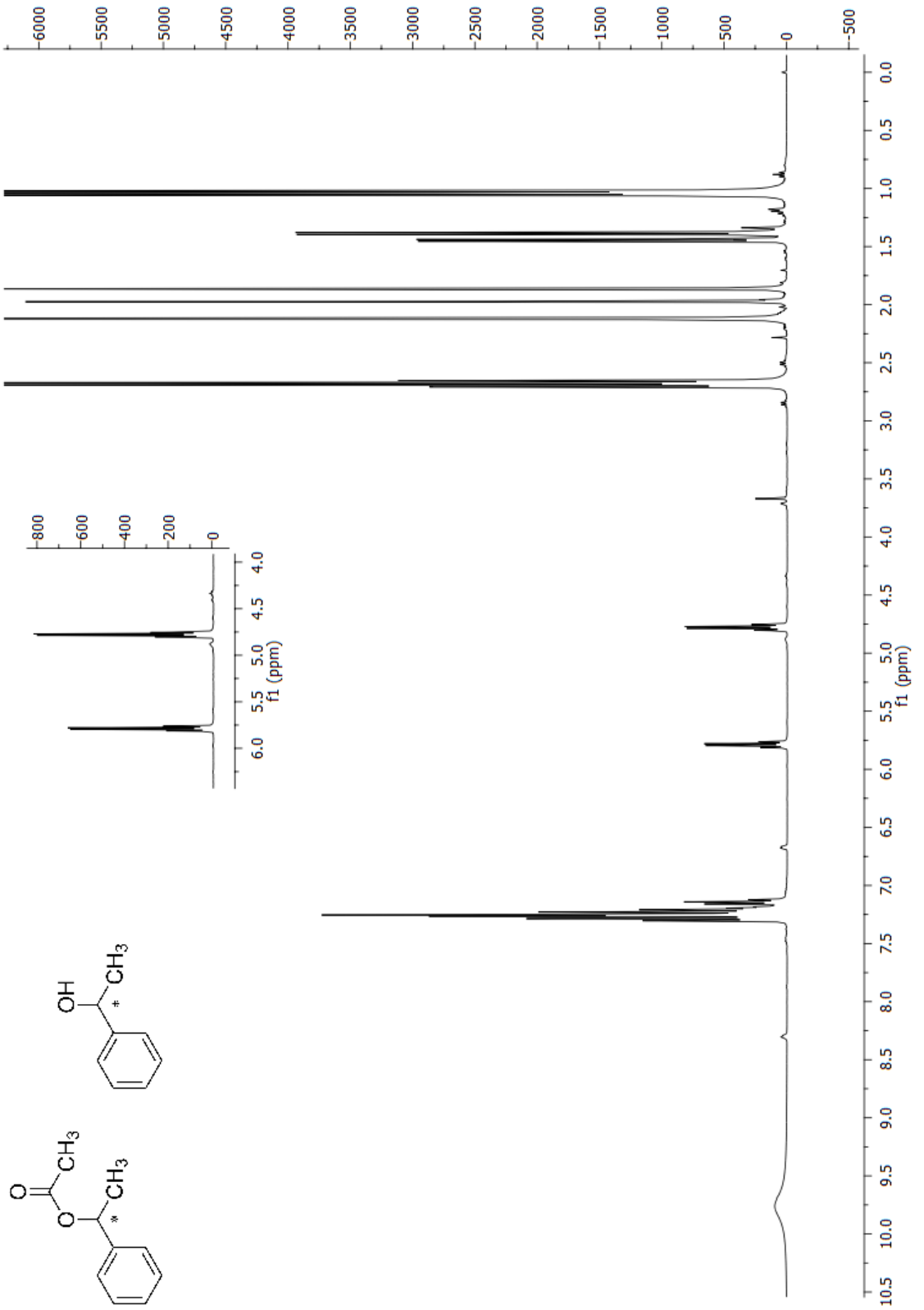

Figure 208: ^{1}H-NMR Spectrum ($CDCl_3$, 400 MHz) from the Reaction of 1-phenyl alcohol with Ac_2O Using **F2** (Table 15, Entry 22).

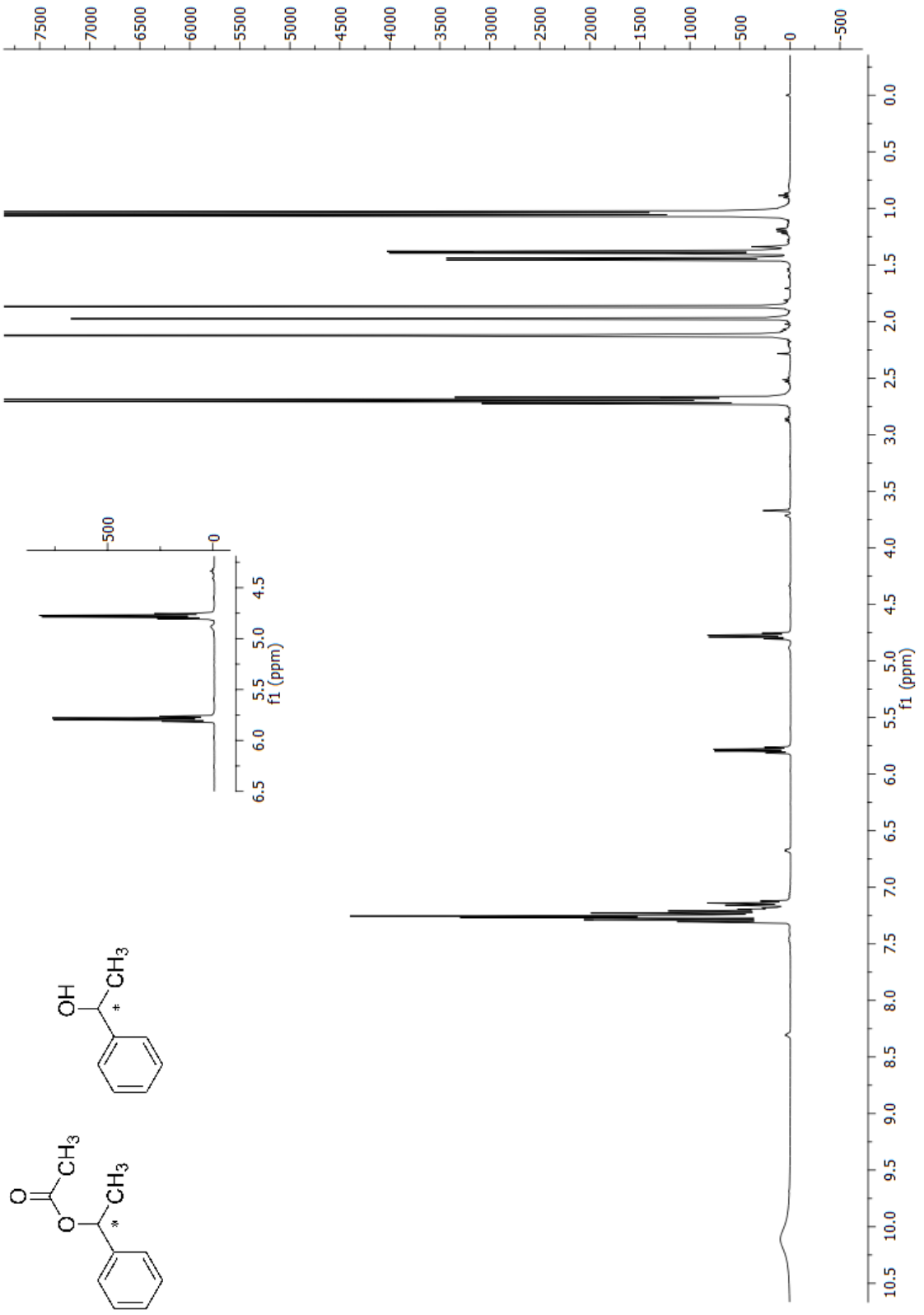

Figure 209: ^{1}H-NMR Spectrum ($CDCl_3$, 400 MHz) from the Reaction of 1-phenyl alcohol with Ac_2O Using **F2** (Table 15, Entry 23).

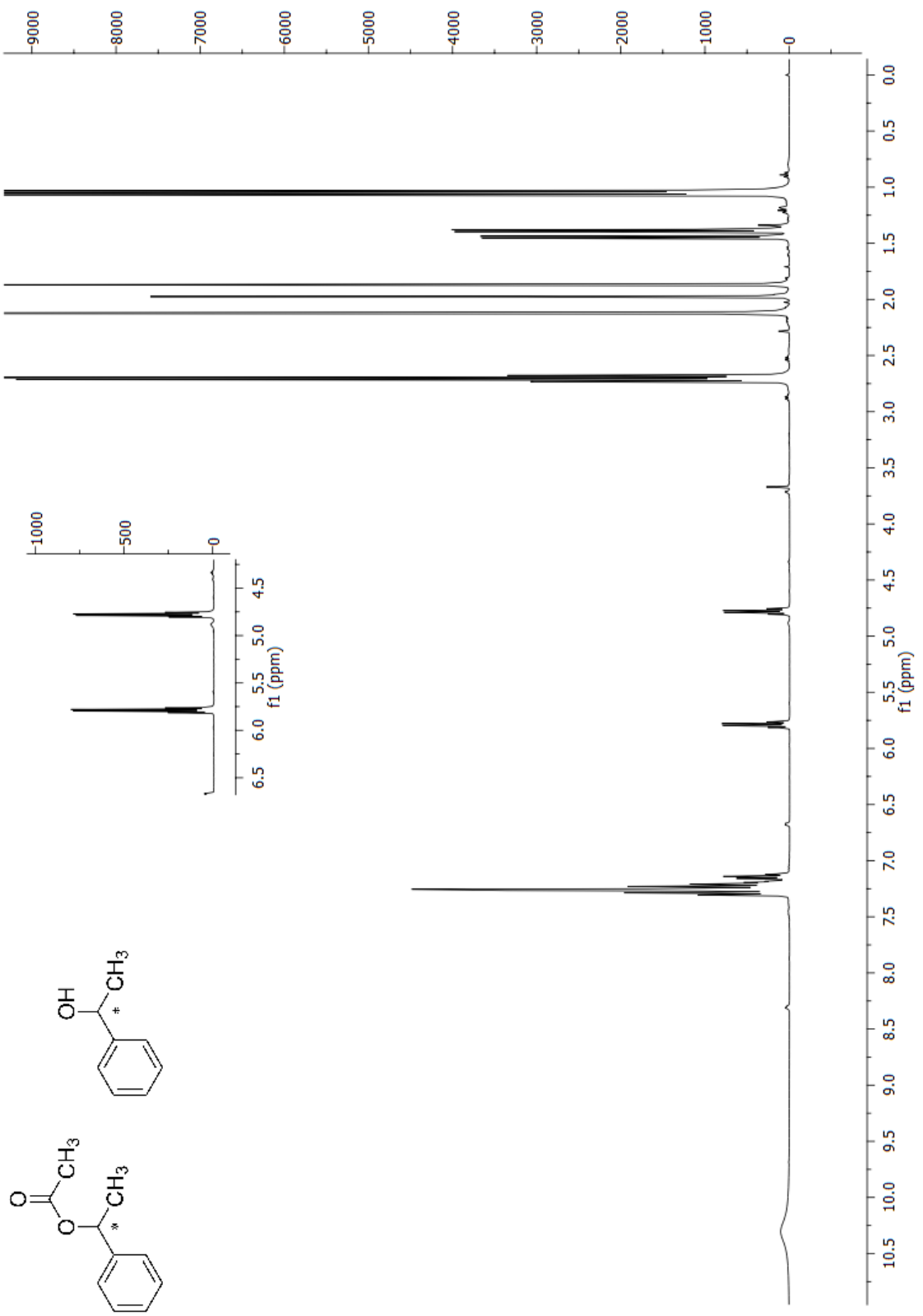

Figure 210: ^{1}H-NMR Spectrum ($CDCl_3$, 400 MHz) from the Reaction of 1-phenyl alcohol with Ac_2O Using **F2** (Table 15, Entry 24).

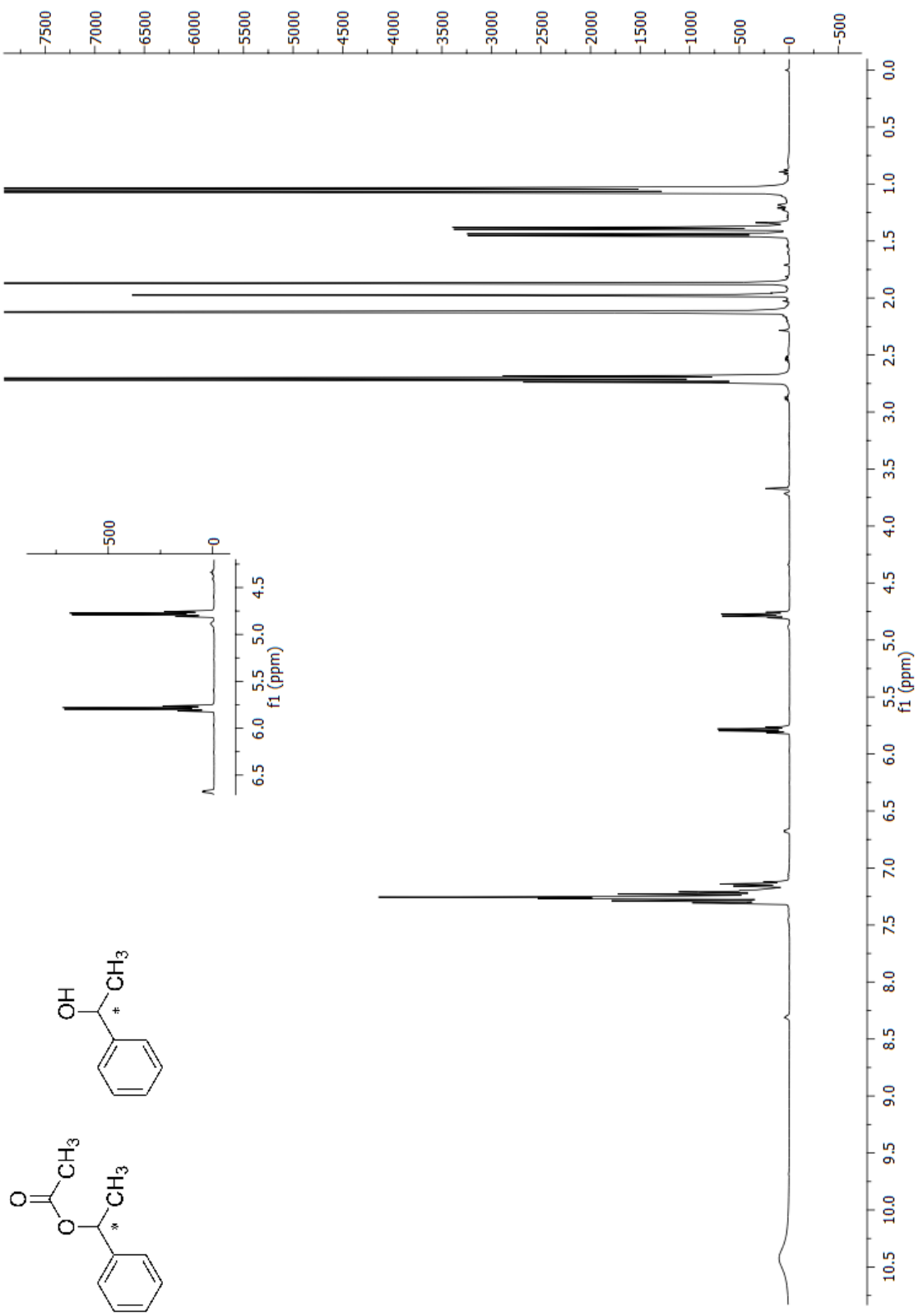

Figure 211: ^{1}H-NMR Spectrum ($CDCl_3$, 400 MHz) from the Reaction of 1-phenyl alcohol with Ac_2O Using **F2** (Table 15, Entry 25).

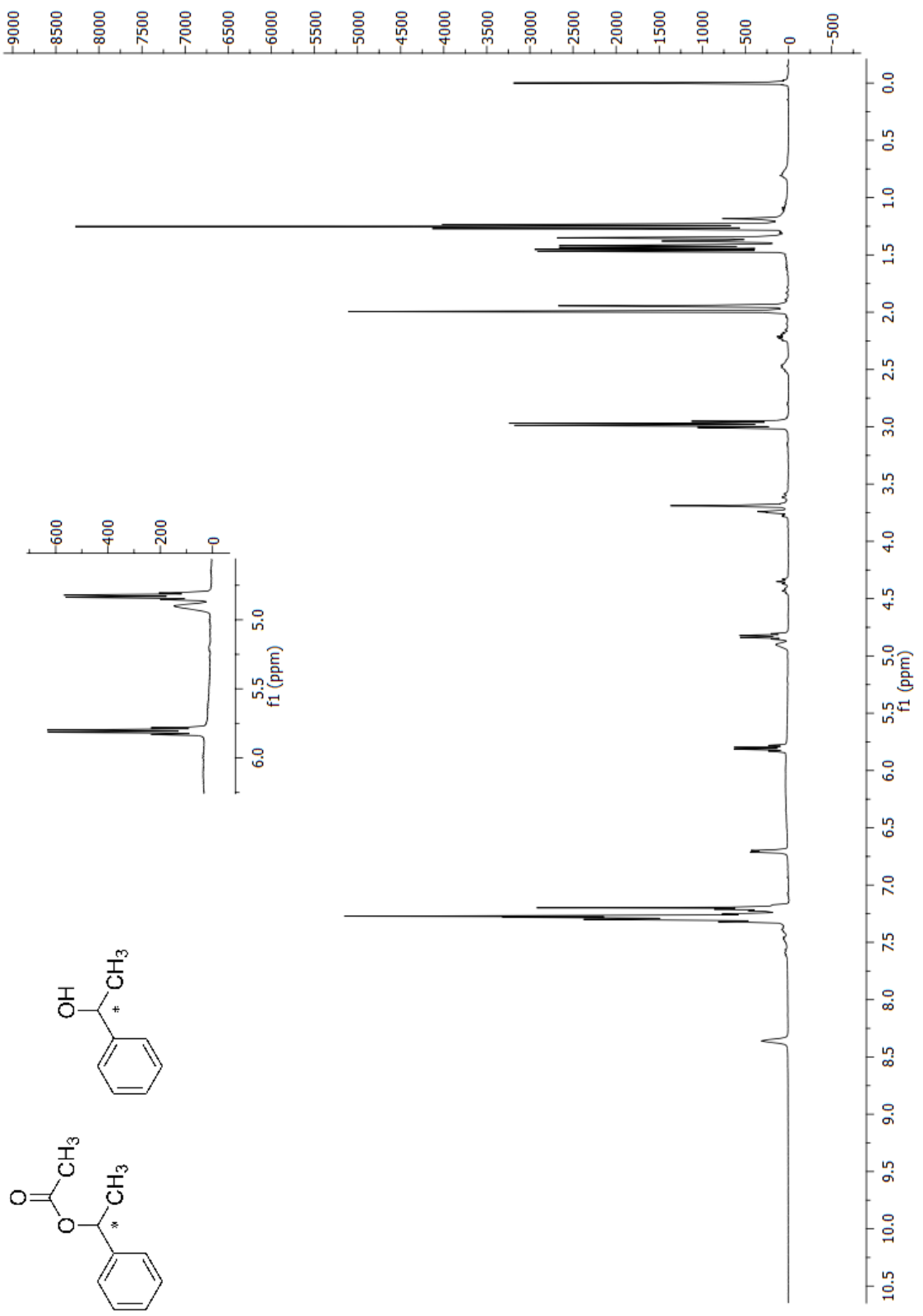

Figure 212: ^{1}H-NMR Spectrum ($CDCl_3$, 400 MHz) from the Reaction of 1-phenyl alcohol with Ac_2O Using **F2** (Table 15, Entry 26).

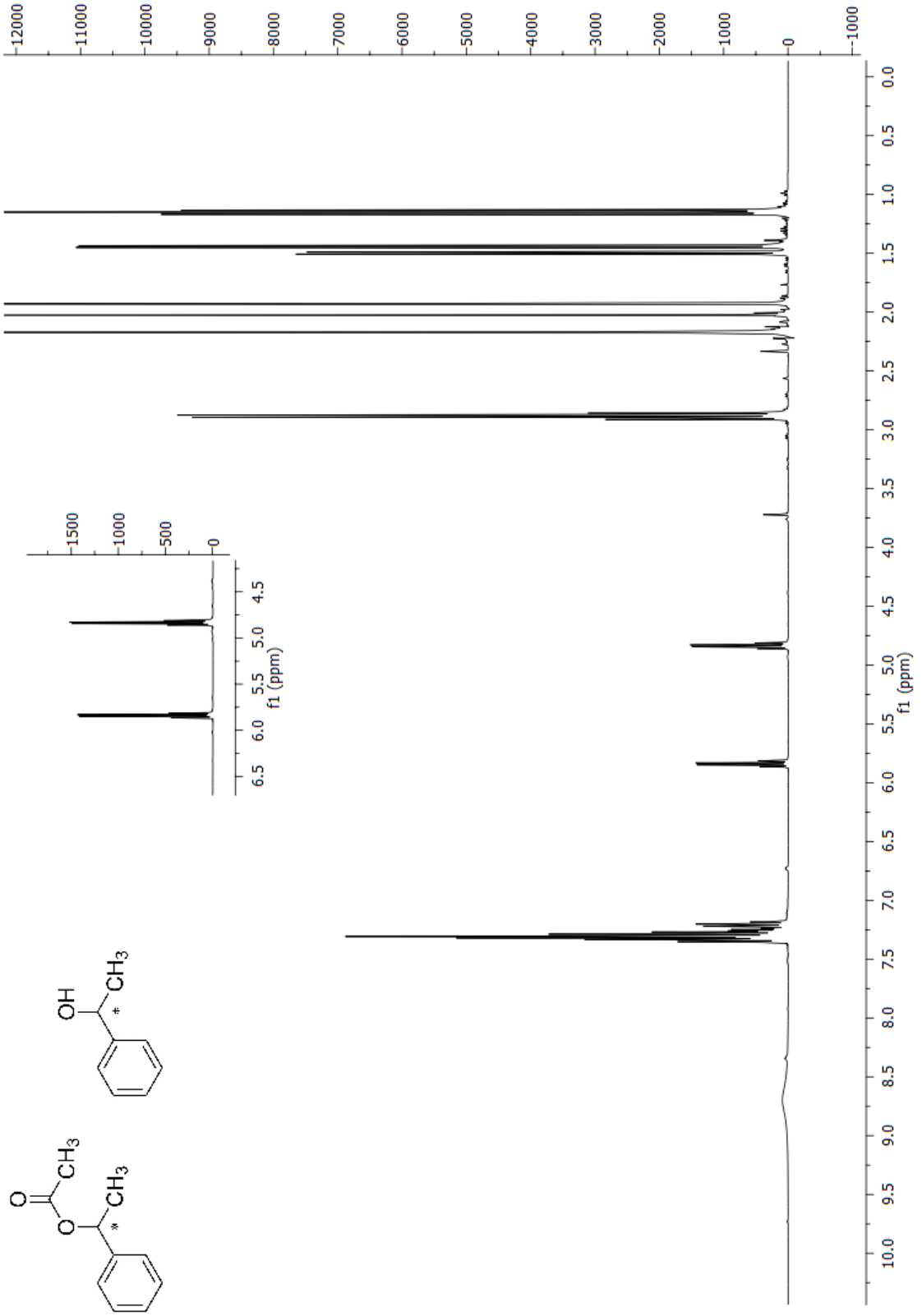

Figure 213: ^{1}H-NMR Spectrum ($CDCl_3$, 400 MHz) from the Reaction of 1-phenyl alcohol with Ac_2O Using **F2** (Table 15, Entry 27).

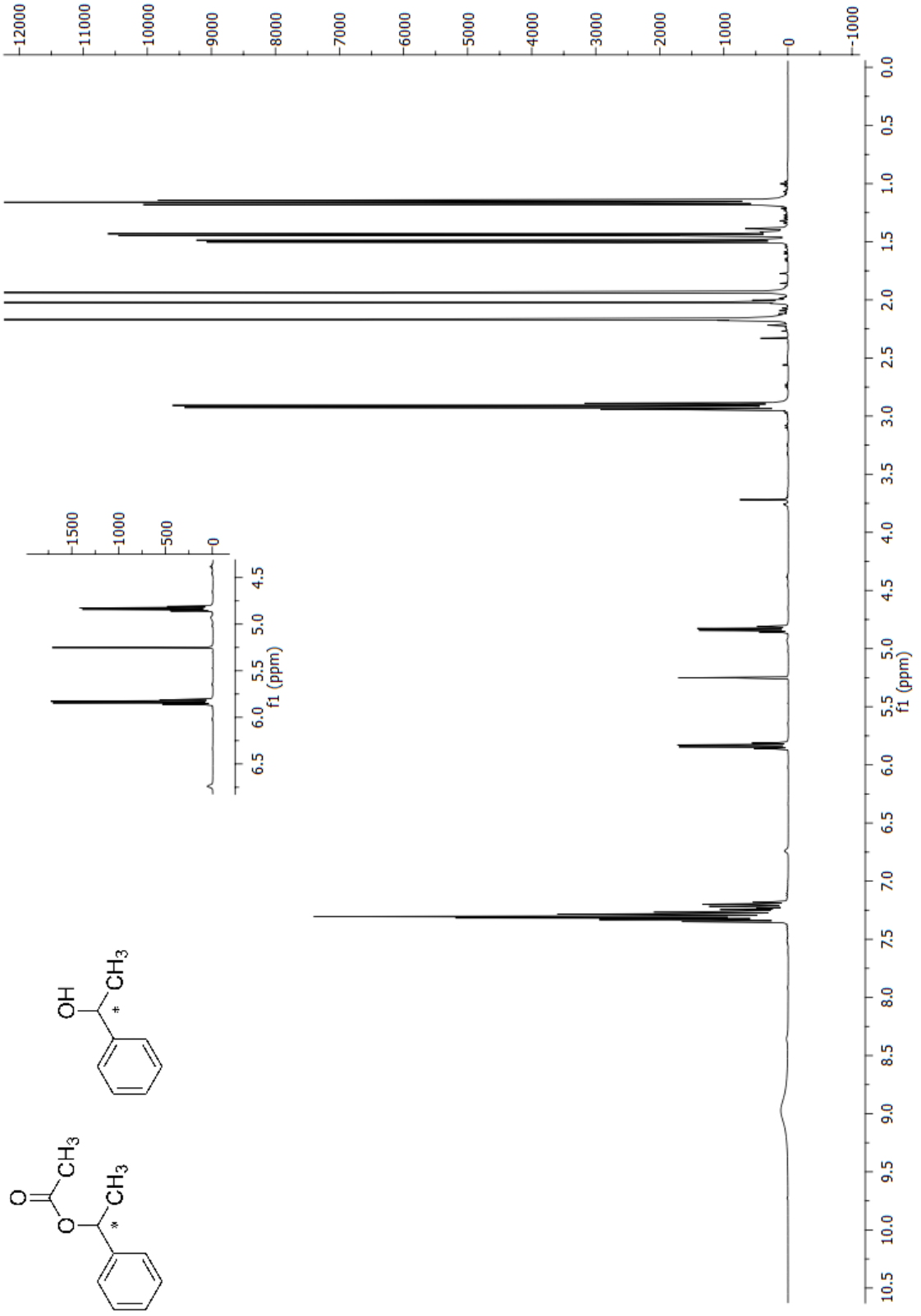

Figure 214: ^{1}H-NMR Spectrum ($CDCl_3$, 400 MHz) from the Reaction of 1-phenyl alcohol with Ac_2O Using **F2** (Table 15, Entry 28).

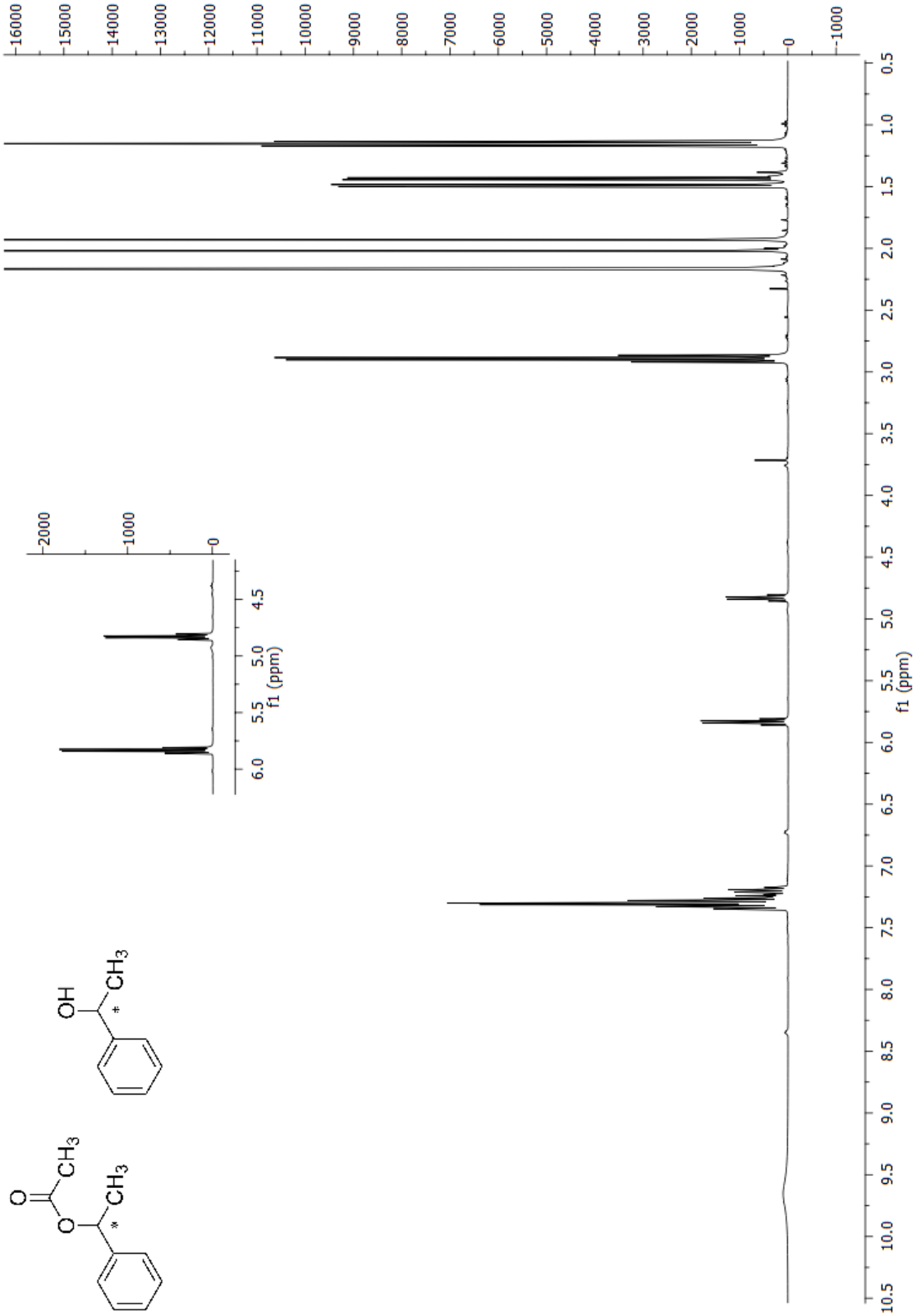

Figure 215: ^{1}H-NMR Spectrum ($CDCl_3$, 400 MHz) from the Reaction of 1-phenyl alcohol with Ac_2O Using **F2** (Table 15, Entry 29).

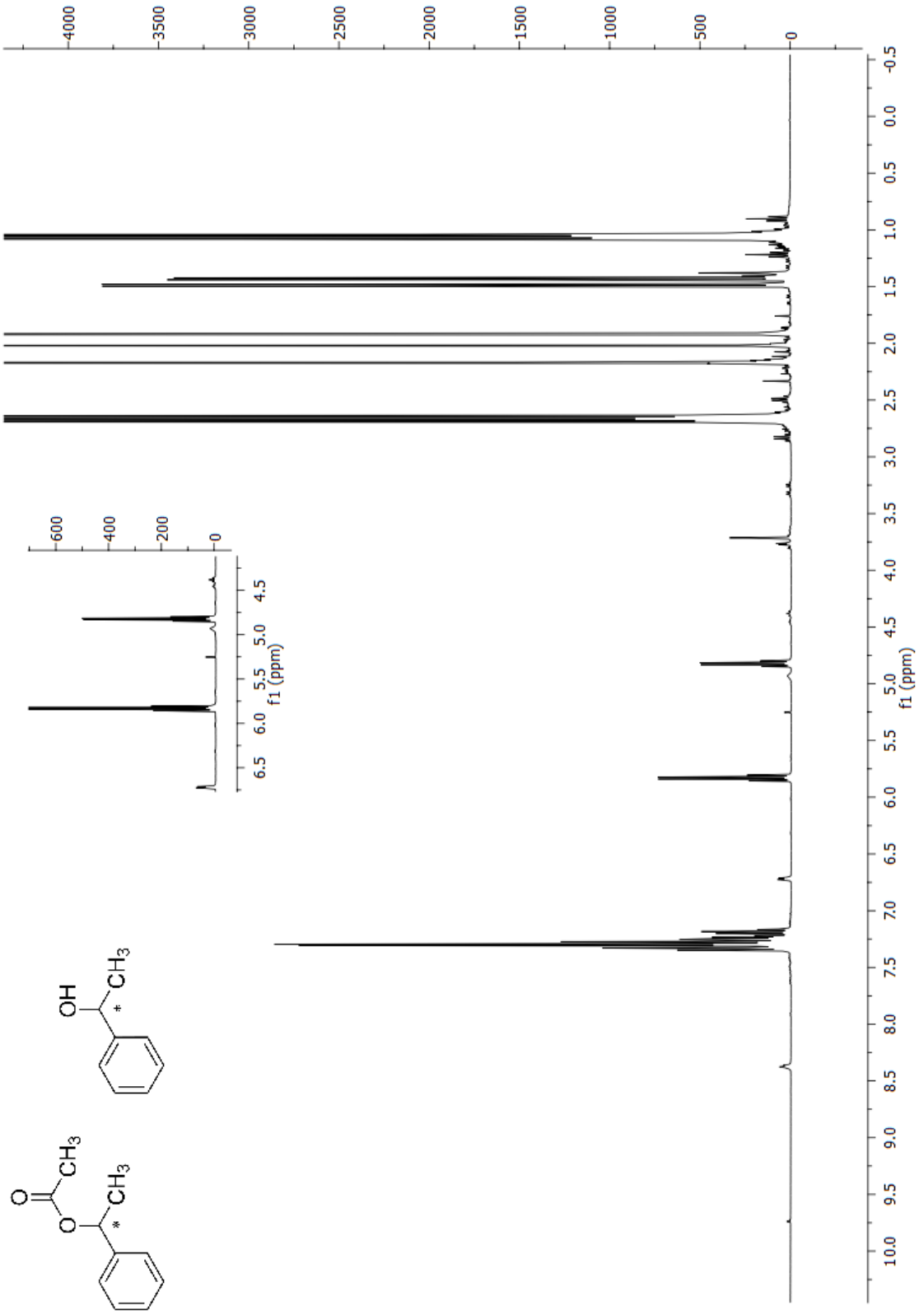

Figure 216: ^{1}H-NMR Spectrum ($CDCl_3$, 400 MHz) from the Reaction of 1-phenyl alcohol with Ac_2O Using **F2** (Table 16, Entry 30).

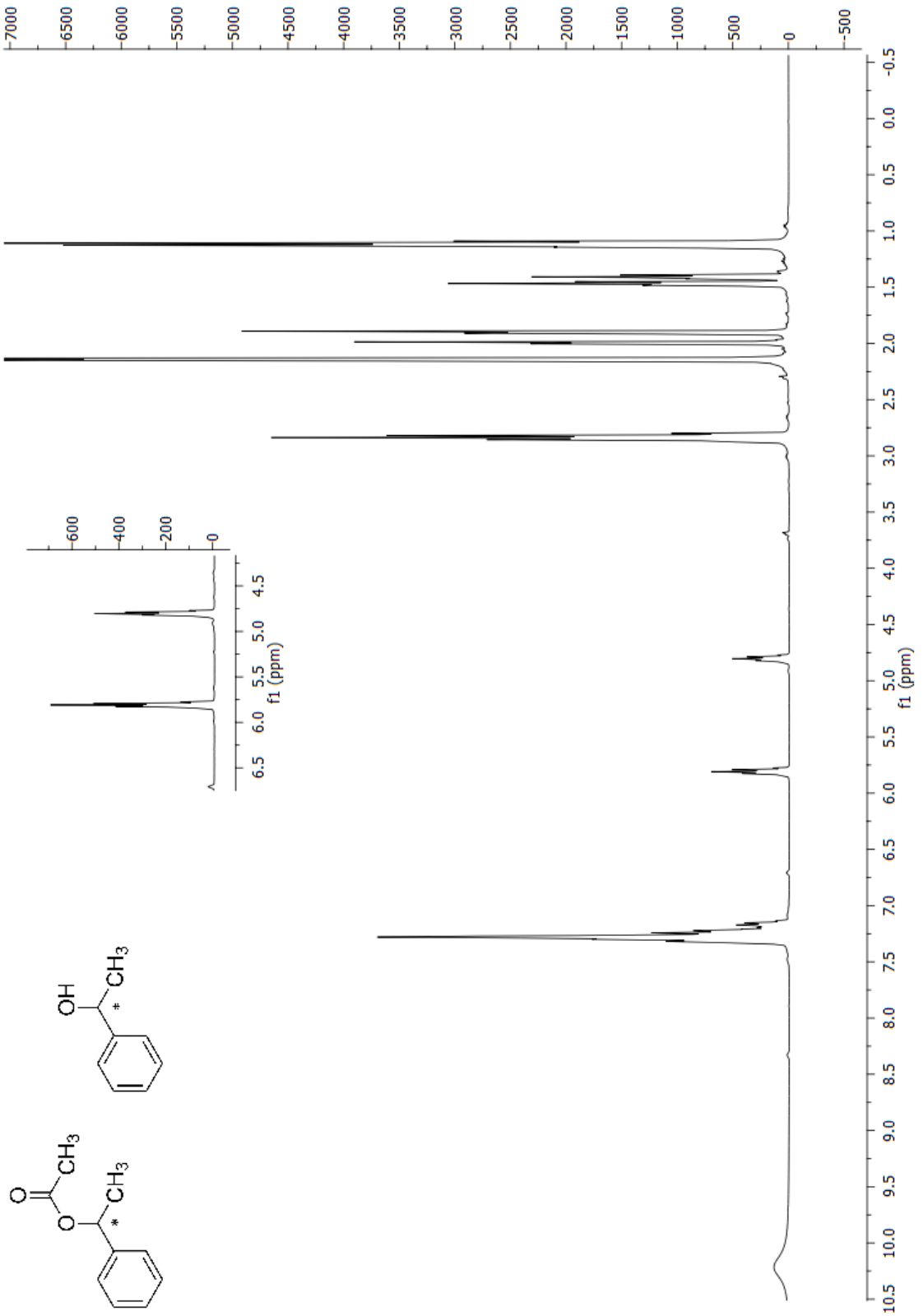

Figure 217: ^{1}H-NMR Spectrum ($CDCl_3$, 400 MHz) from the Reaction of 1-phenyl alcohol with Ac_2O Using **F2** (Table 16, Entry 31).

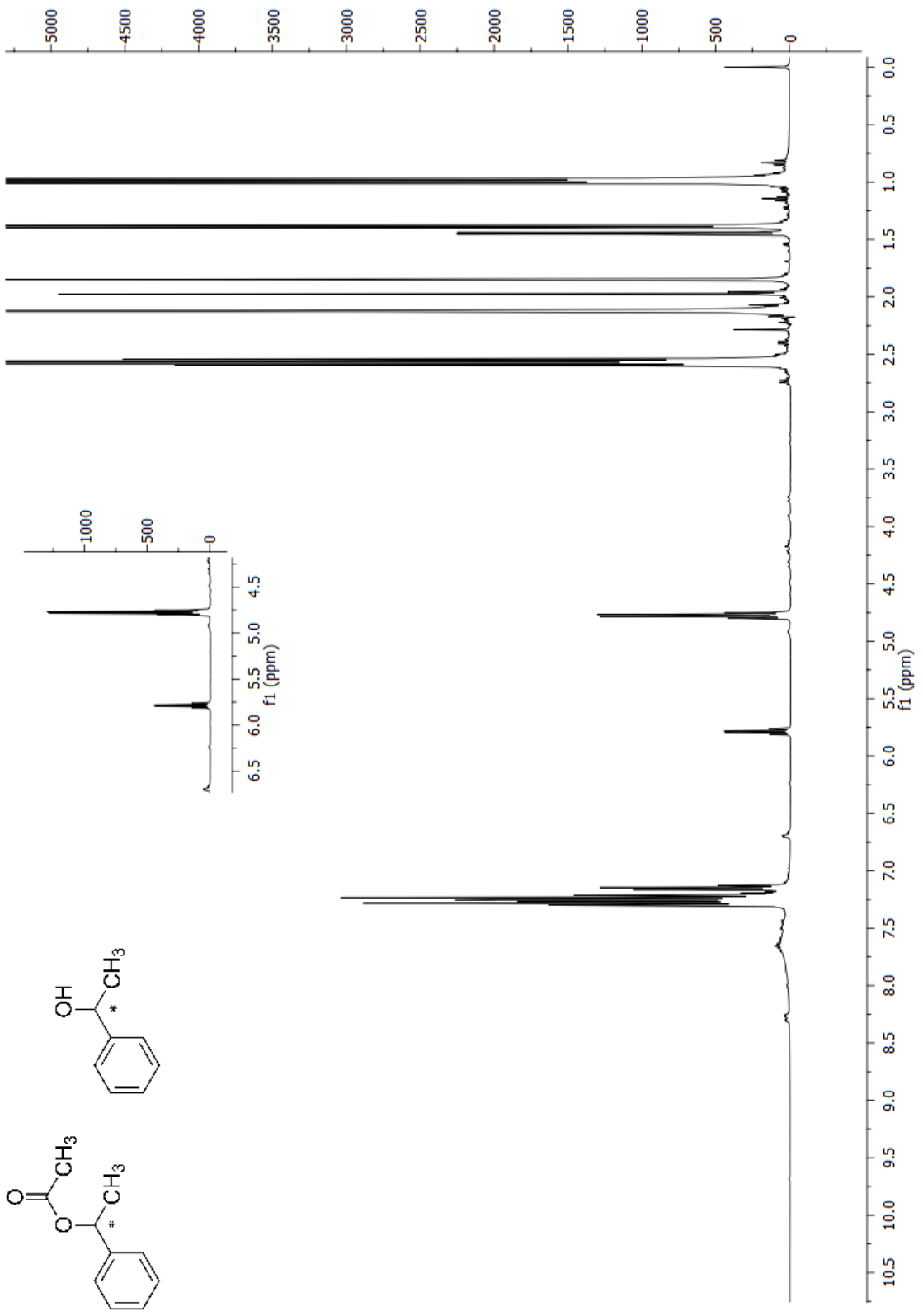

Figure 218: ^{1}H-NMR Spectrum ($CDCl_3$, 400 MHz) from the Reaction of 1-phenyl alcohol with Ac_2O Using **F3** (Table 17, Entry 32).

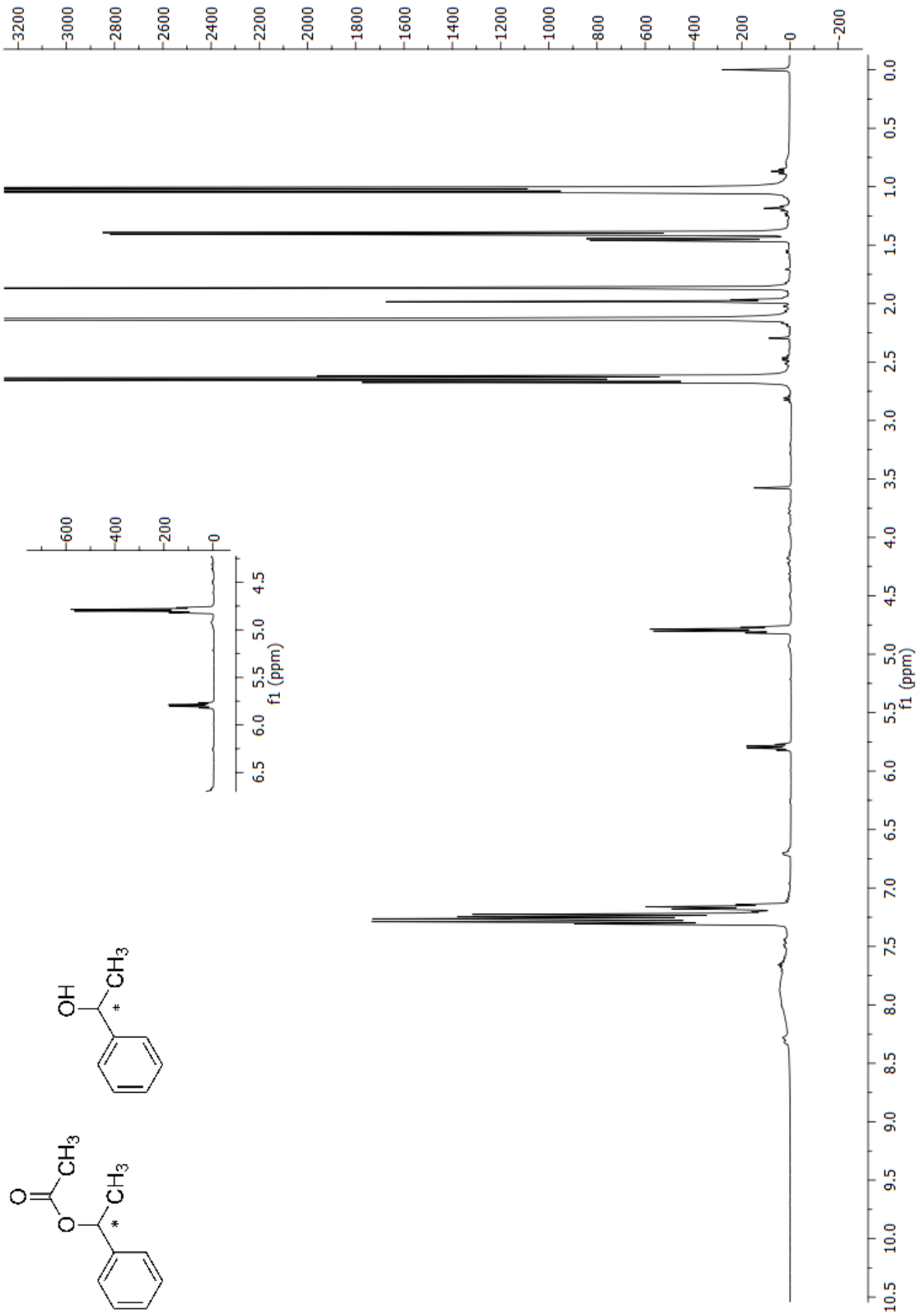

Figure 219: ^{1}H-NMR Spectrum ($CDCl_3$, 400 MHz) from the Reaction of 1-phenyl alcohol with Ac_2O Using **F3** (Table 17, Entry 33).

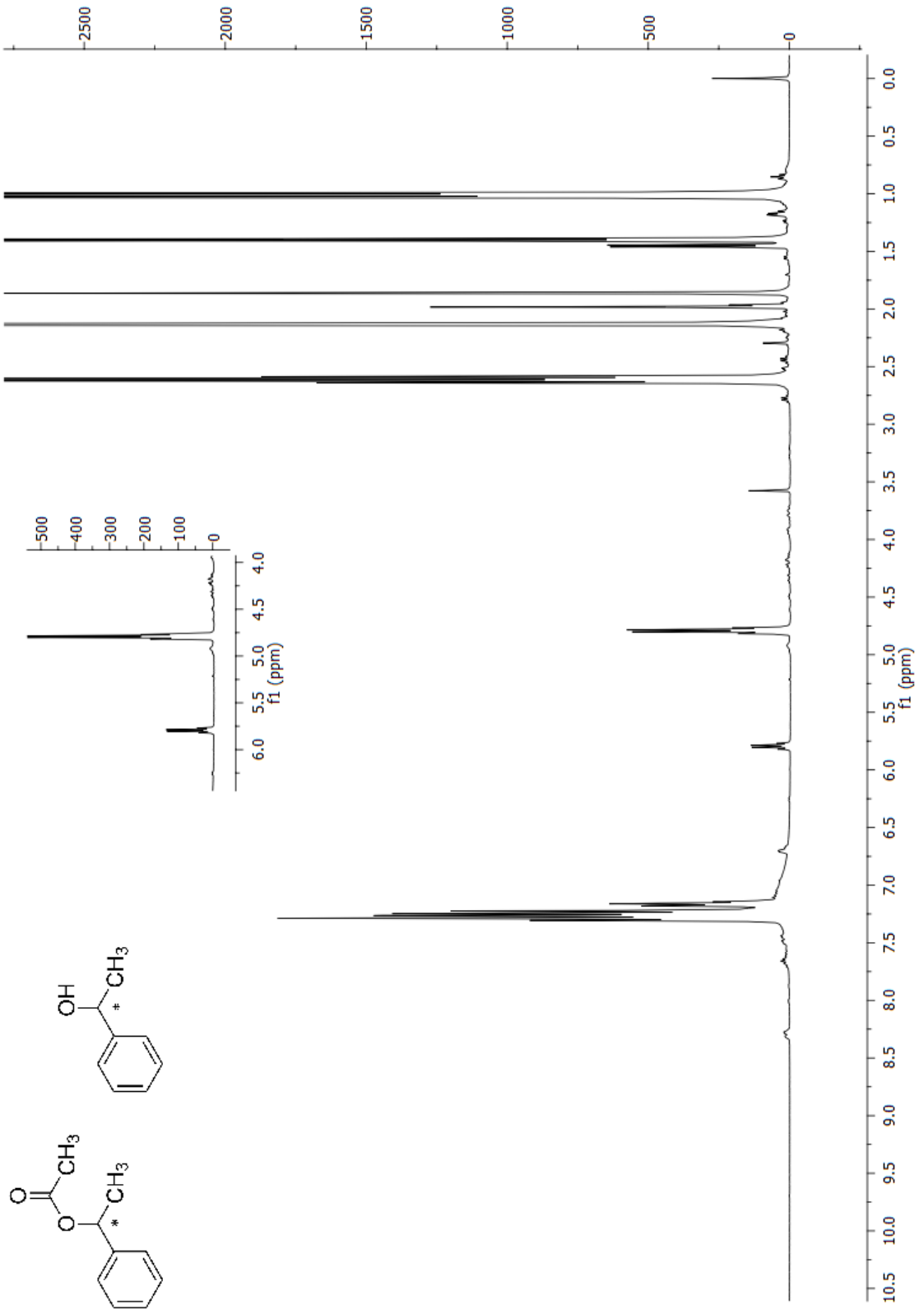

Figure 220: ^{1}H-NMR Spectrum ($CDCl_3$, 400 MHz) from the Reaction of 1-phenyl alcohol with Ac_2O Using **F3** (Table 17, Entry 34).

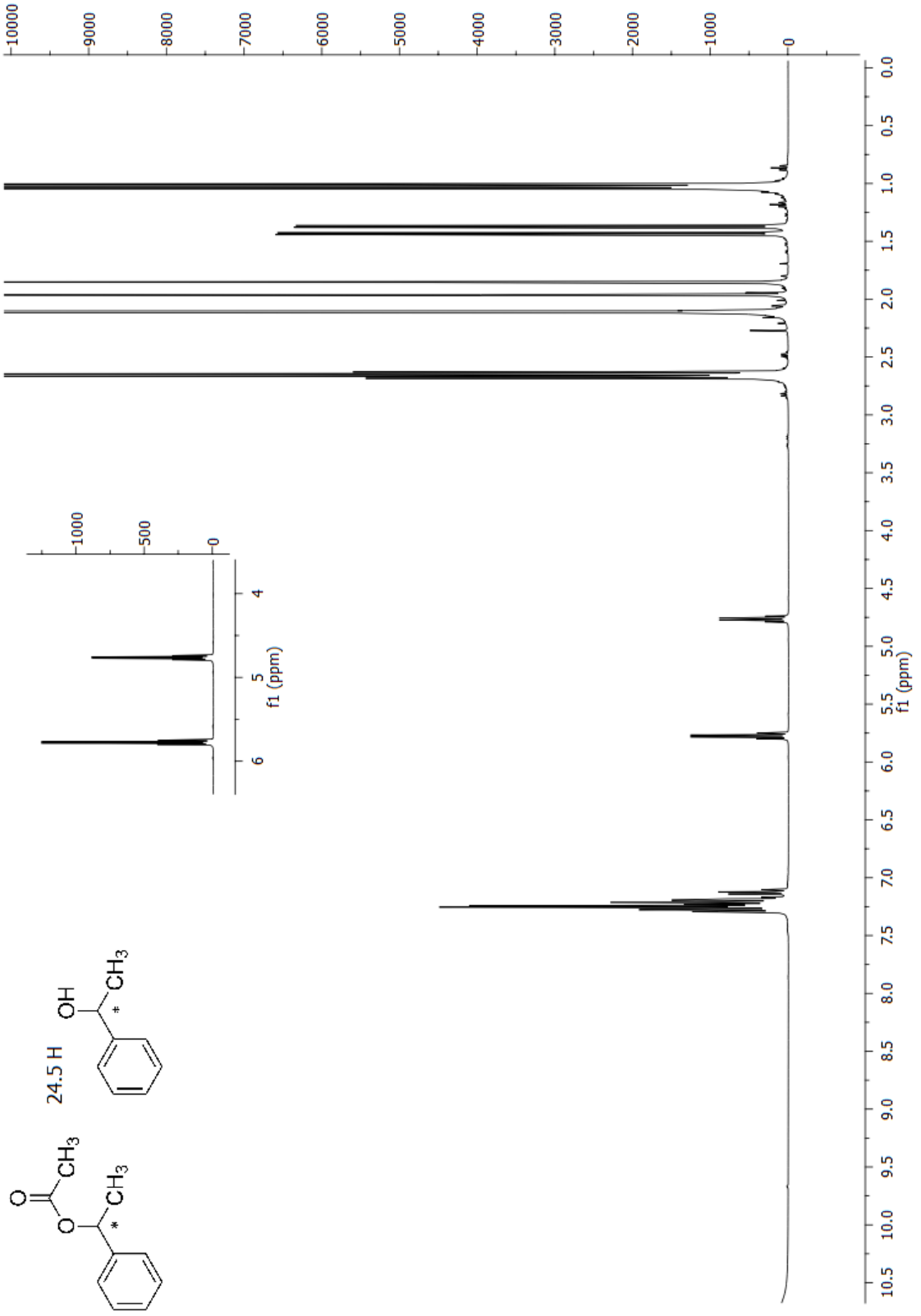

Figure 221: ^{1}H-NMR Spectrum ($CDCl_3$, 400 MHz) from the Reaction of 1-phenyl alcohol with Ac_2O Using **F3** (Table 17, Entry 35).

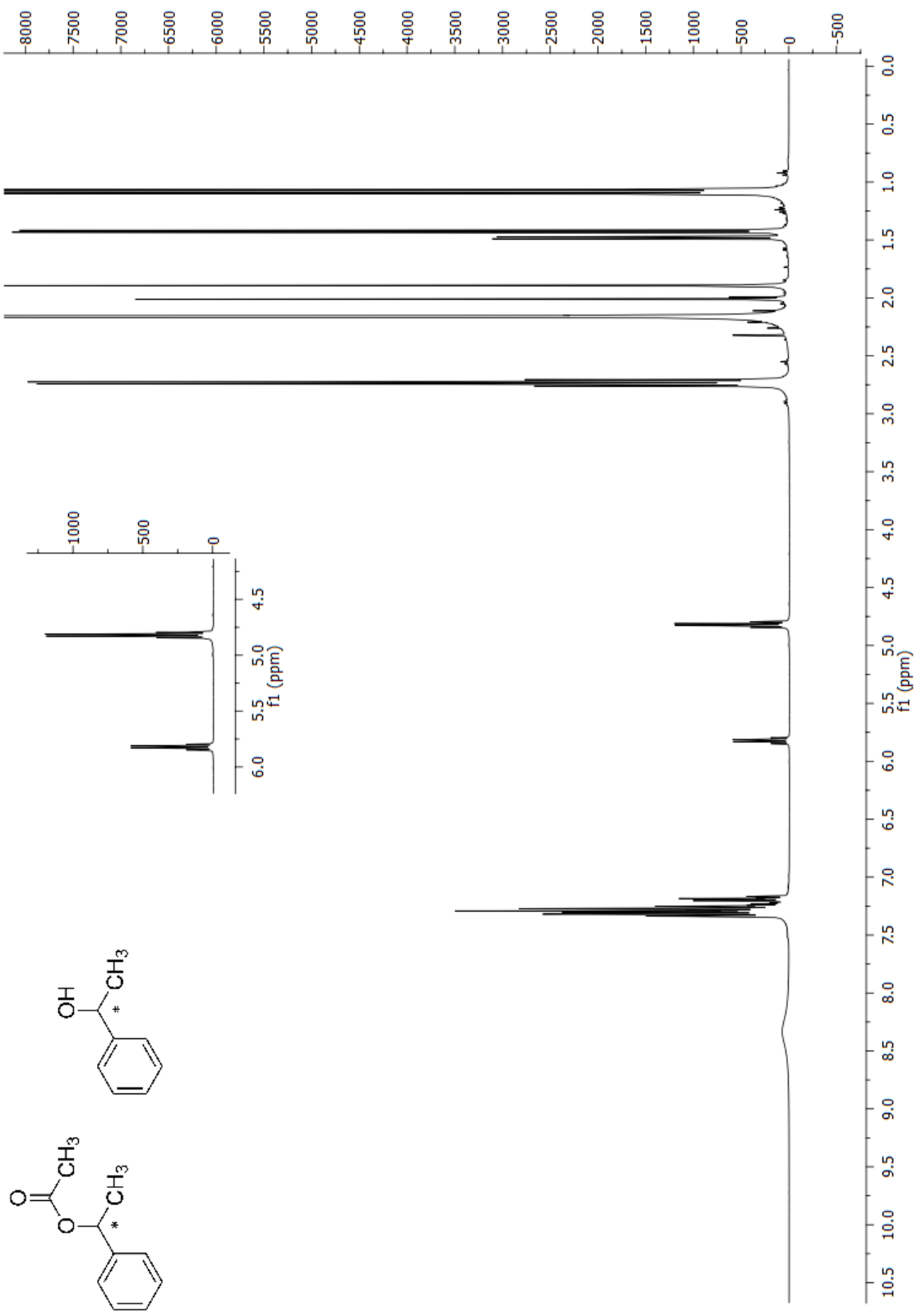

Figure 222: ^{1}H-NMR Spectrum ($CDCl_3$, 400 MHz) from the Reaction of 1-phenyl alcohol with Ac_2O Using **F3** (Table 17, Entry 36).

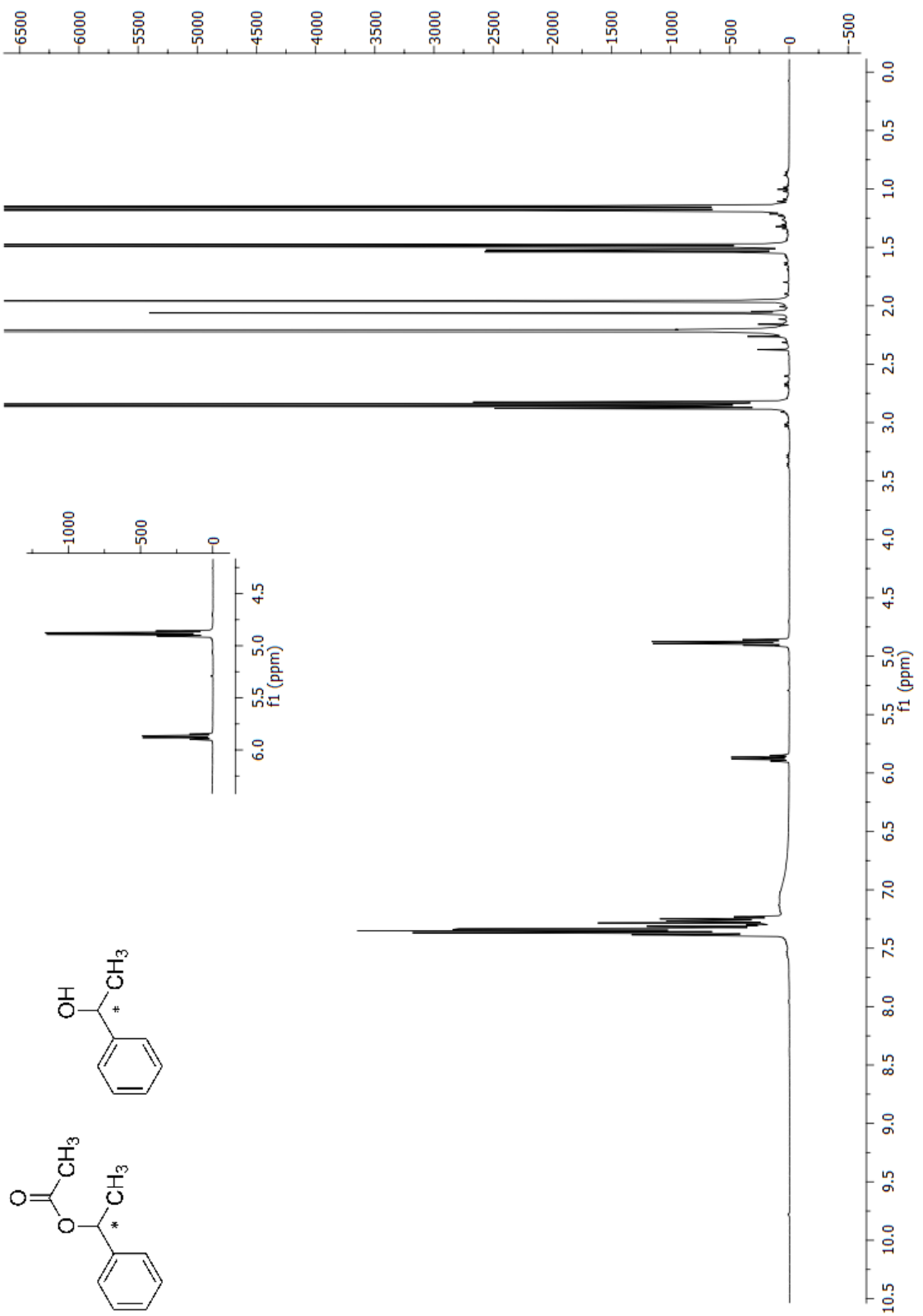

Figure 223: ^{1}H-NMR Spectrum ($CDCl_3$, 400 MHz) from the Reaction of 1-phenyl alcohol with Ac_2O Using **F3** (Table 17, Entry 37).

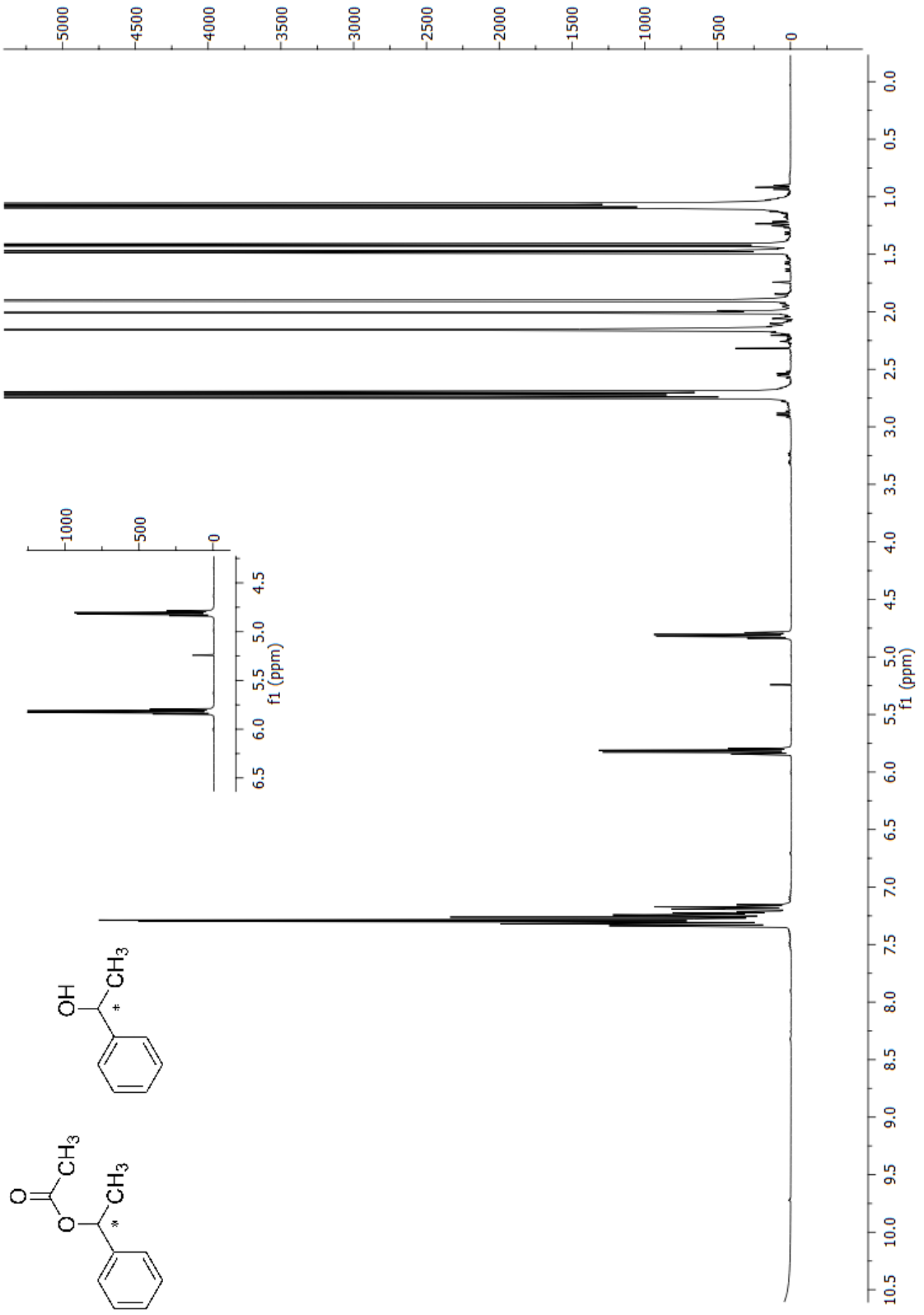

Figure 224: ^{1}H-NMR Spectrum ($CDCl_3$, 400 MHz) from the Reaction of 1-phenyl alcohol with Ac_2O Using **F3** (Table 18, Entry 39).

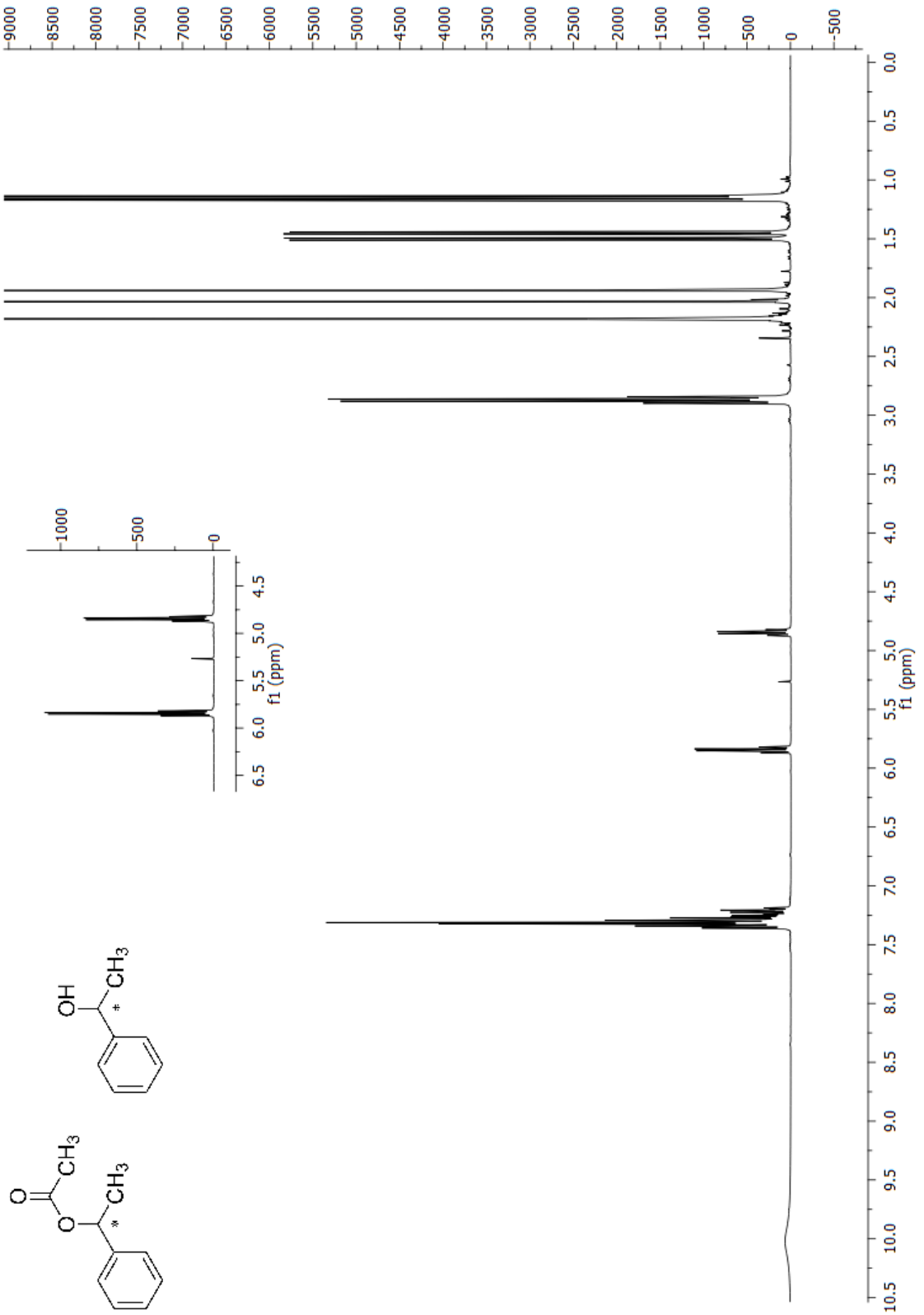

Figure 225: ^{1}H-NMR Spectrum ($CDCl_3$, 400 MHz) from the Reaction of 1-phenyl alcohol with Ac_2O Using **F3** (Table 18, Entry 40).

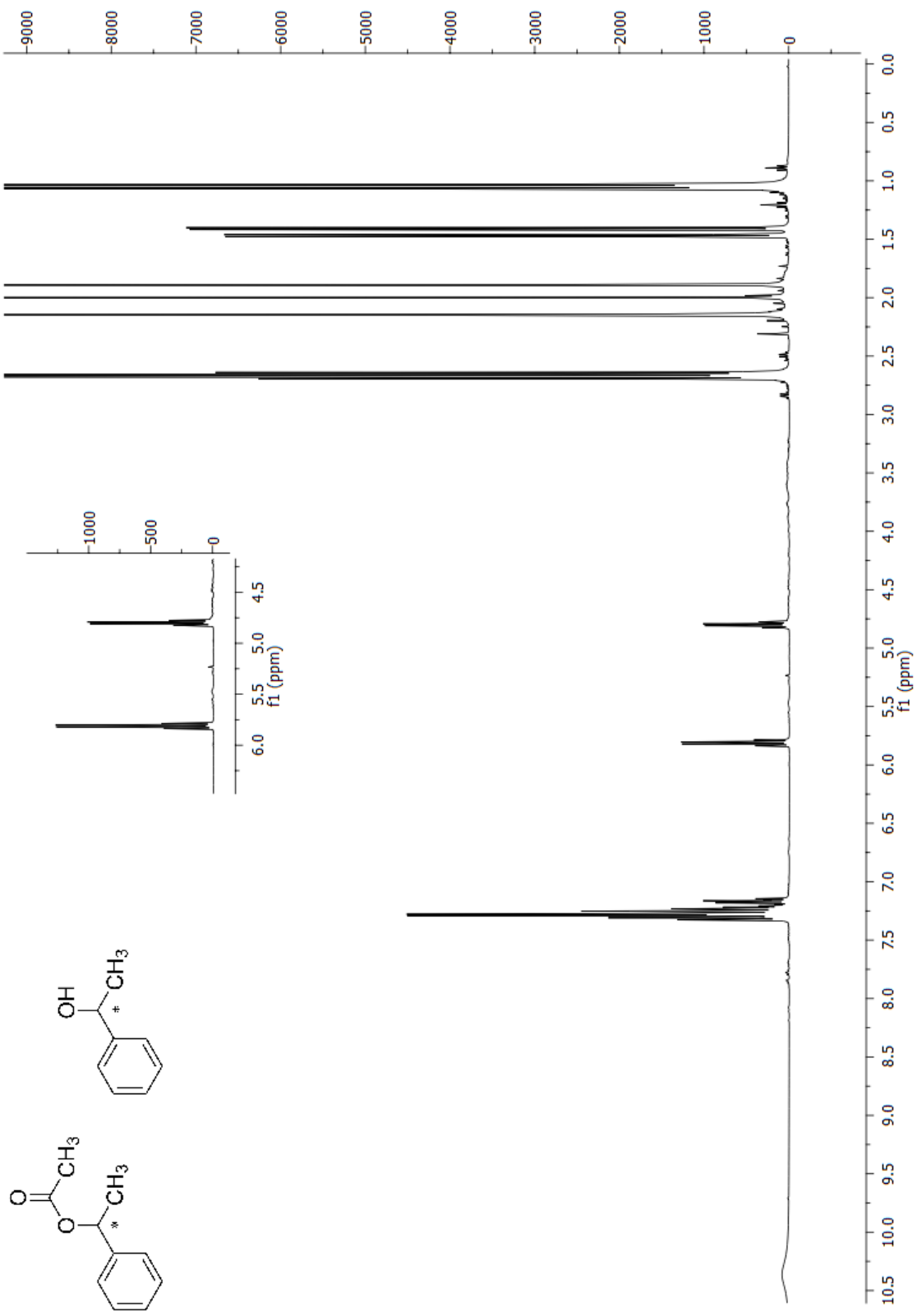

Figure 226: ^{1}H-NMR Spectrum ($CDCl_3$, 400 MHz) from the Reaction of 1-phenyl alcohol with Ac_2O Using **PP 7** (Table 19, Entry 41).

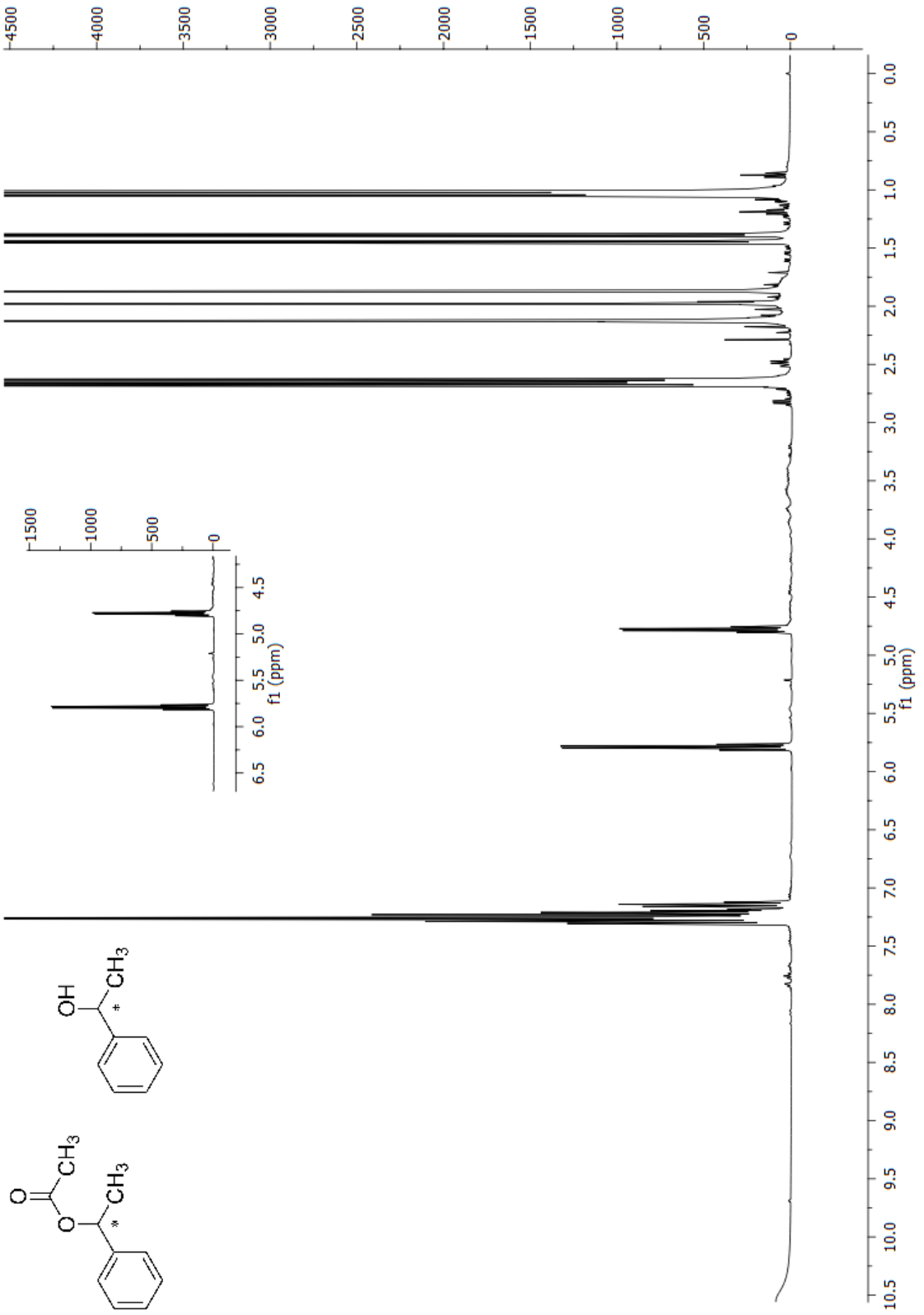

Figure 227: ^{1}H-NMR Spectrum ($CDCl_3$, 400 MHz) from the Reaction of 1-phenyl alcohol with Ac_2O Using **PP 7** (Table 19, Entry 42).

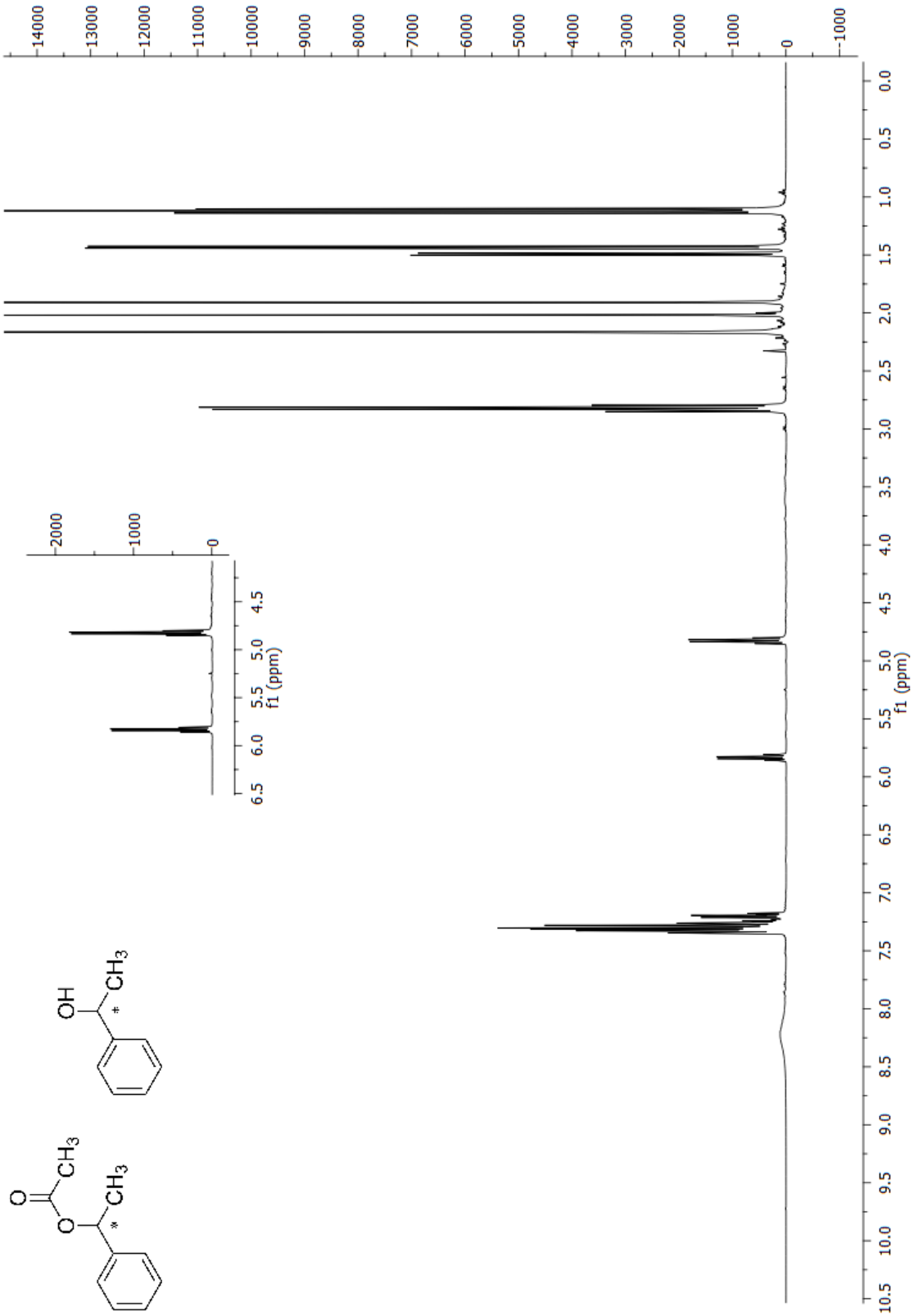

Figure 228: ^{1}H-NMR Spectrum ($CDCl_3$, 400 MHz) from the Reaction of 1-phenyl alcohol with Ac_2O Using **PP 7** (Table 19, Entry 43).

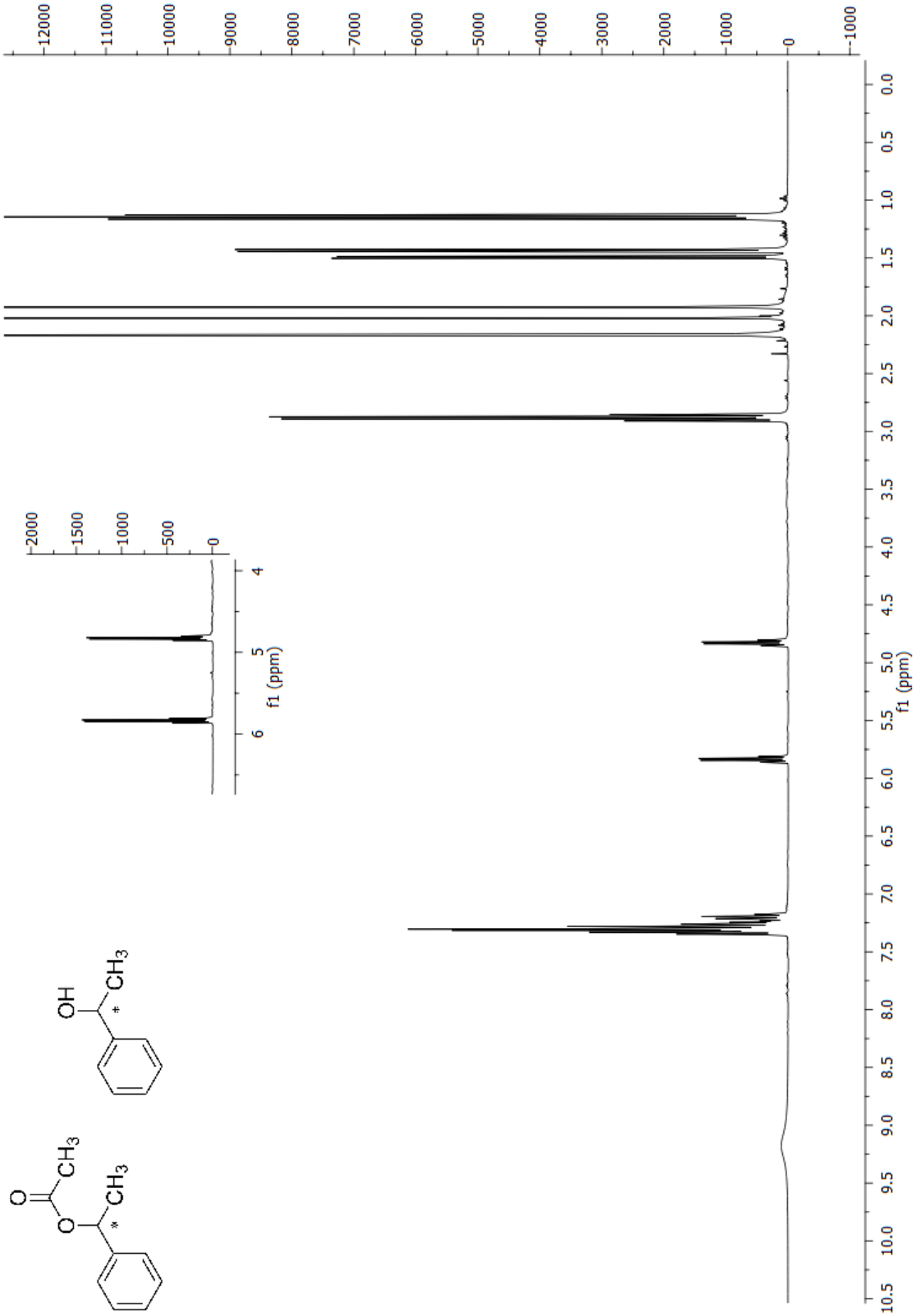

Figure 229: ^{1}H-NMR Spectrum ($CDCl_3$, 400 MHz) from the Reaction of 1-phenyl alcohol with Ac_2O Using **PP 7** (Table 19, Entry 44).

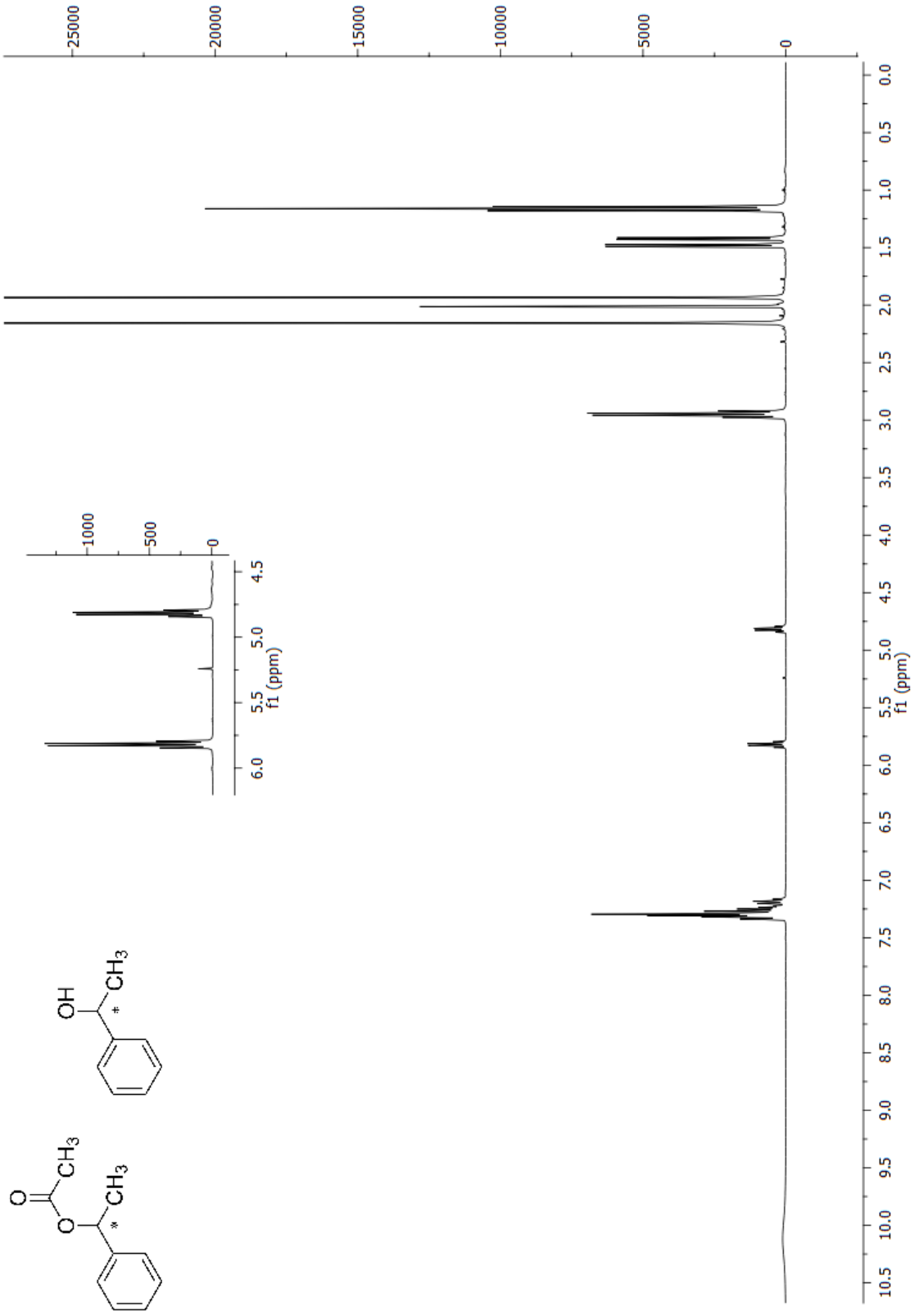

Figure 230: ^{1}H-NMR Spectrum ($CDCl_3$, 400 MHz) from the Reaction of 1-phenyl alcohol with Ac_2O Using **PP 7** (Table 20, Entry 45).

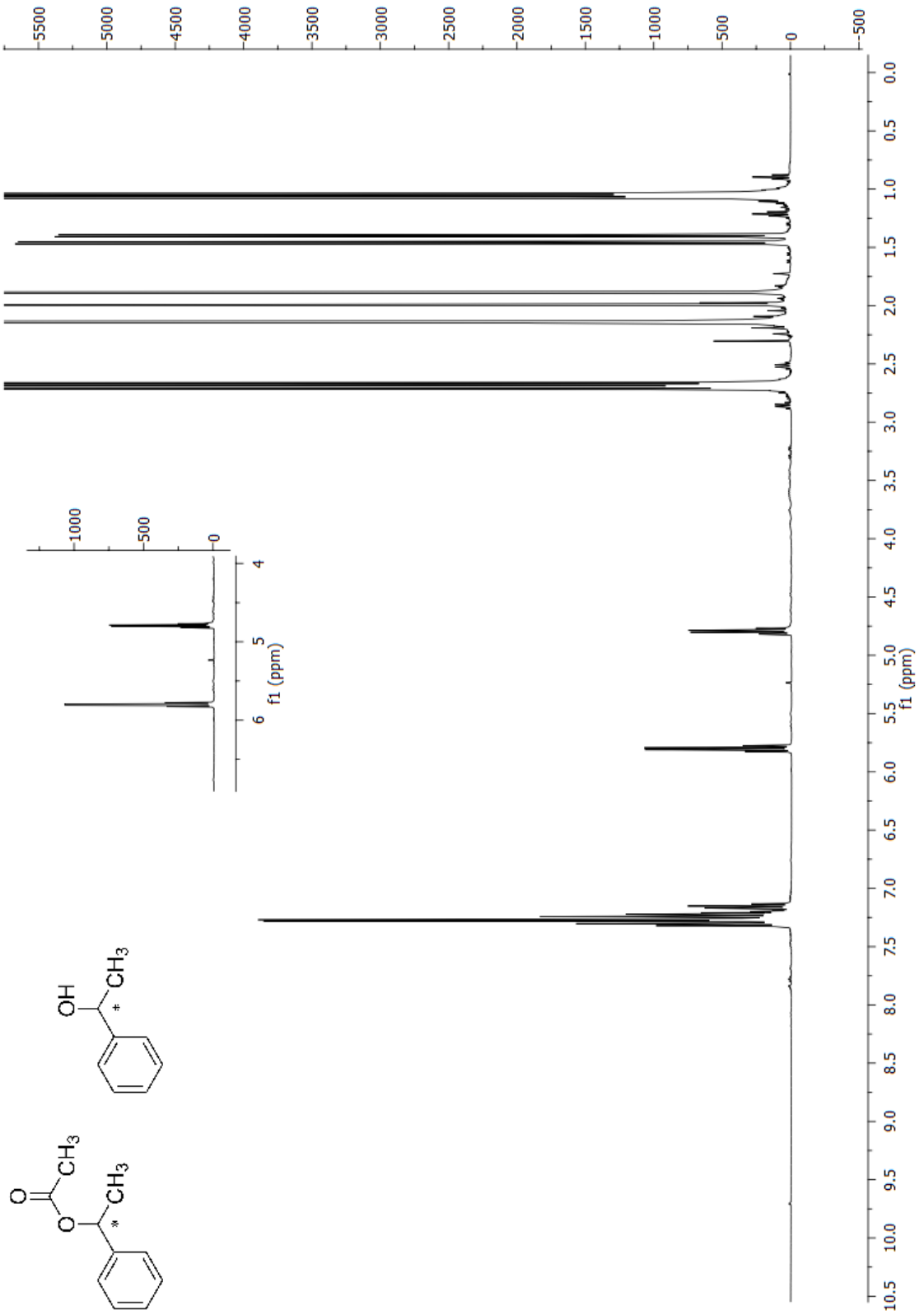

Figure 231: ^{1}H-NMR Spectrum ($CDCl_3$, 400 MHz) from the Reaction of 1-phenyl alcohol with Ac_2O Using **PP 7** (Table 20, Entry 47).

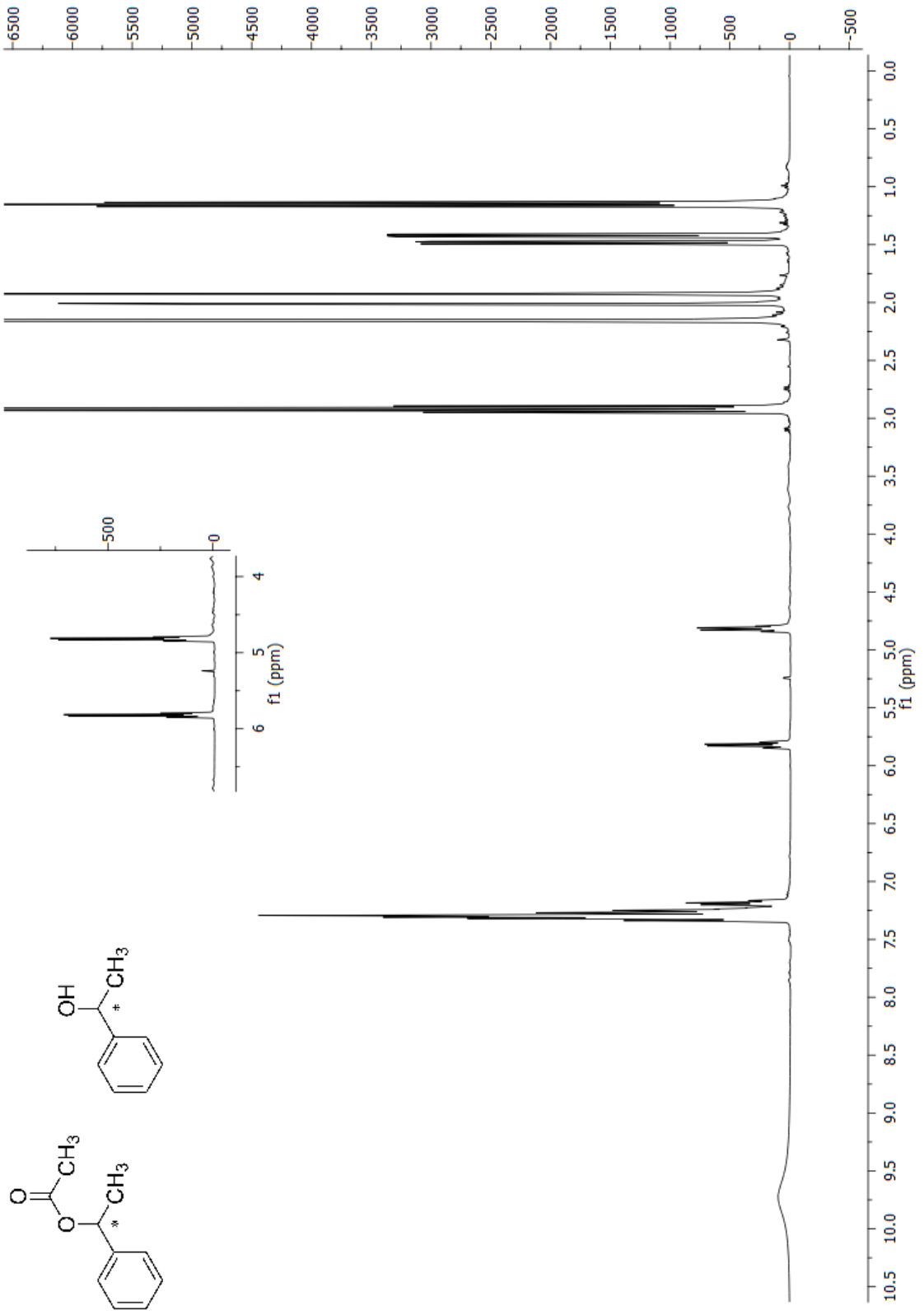

Figure 232: ^{1}H-NMR Spectrum ($CDCl_3$, 400 MHz) from the Reaction of 1-phenyl alcohol with Ac_2O Using **PP 7** (Table 20, Entry 48).

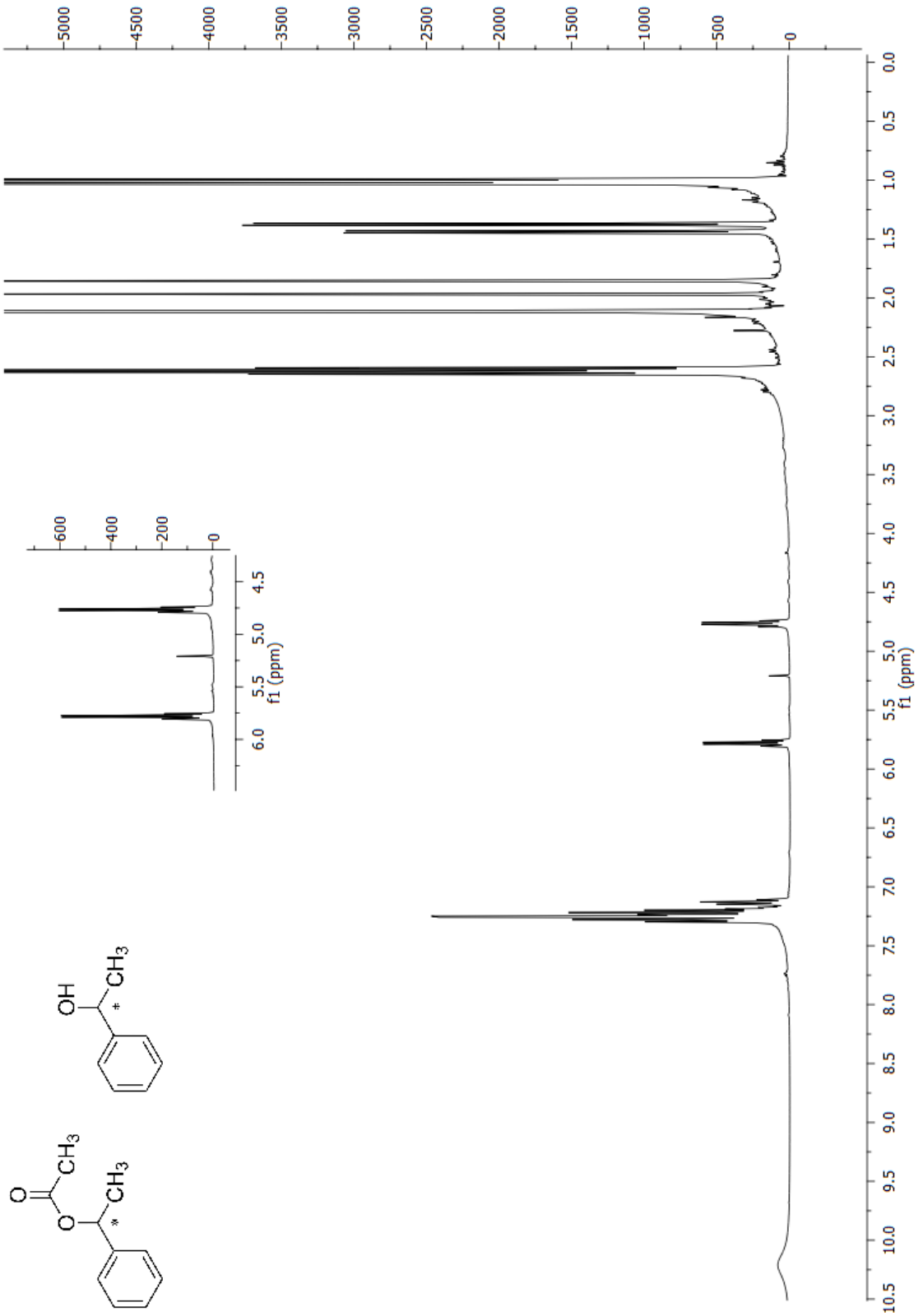

Figure 233: ^{1}H-NMR Spectrum ($CDCl_3$, 400 MHz) from the Reaction of 1-phenyl alcohol with Ac_2O Using **PP 8** (Table 21, Entry 49).

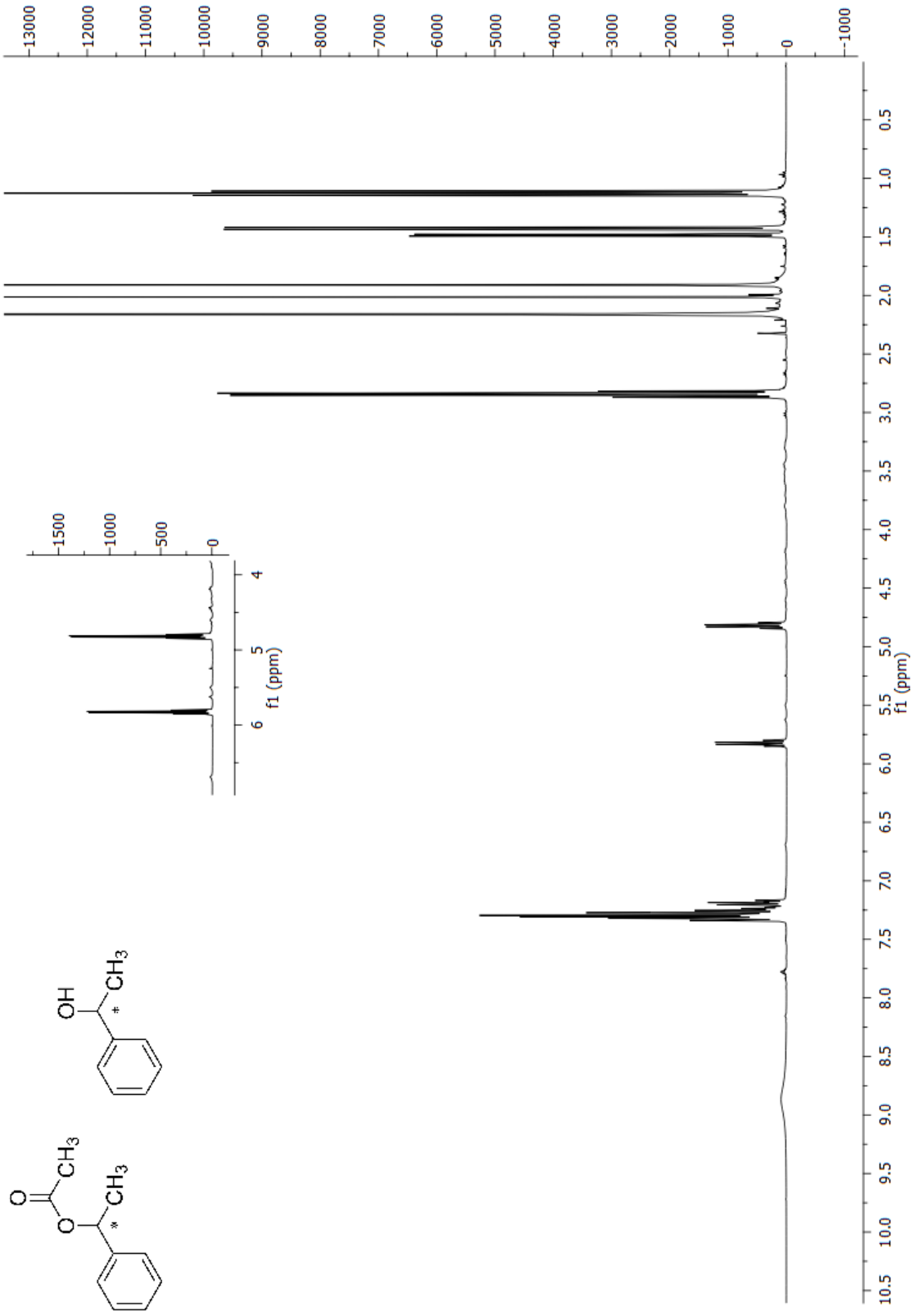

Figure 234: ^{1}H-NMR Spectrum ($CDCl_3$, 400 MHz) from the Reaction of 1-phenyl alcohol with Ac_2O Using **PP 8** (Table 21, Entry 50).

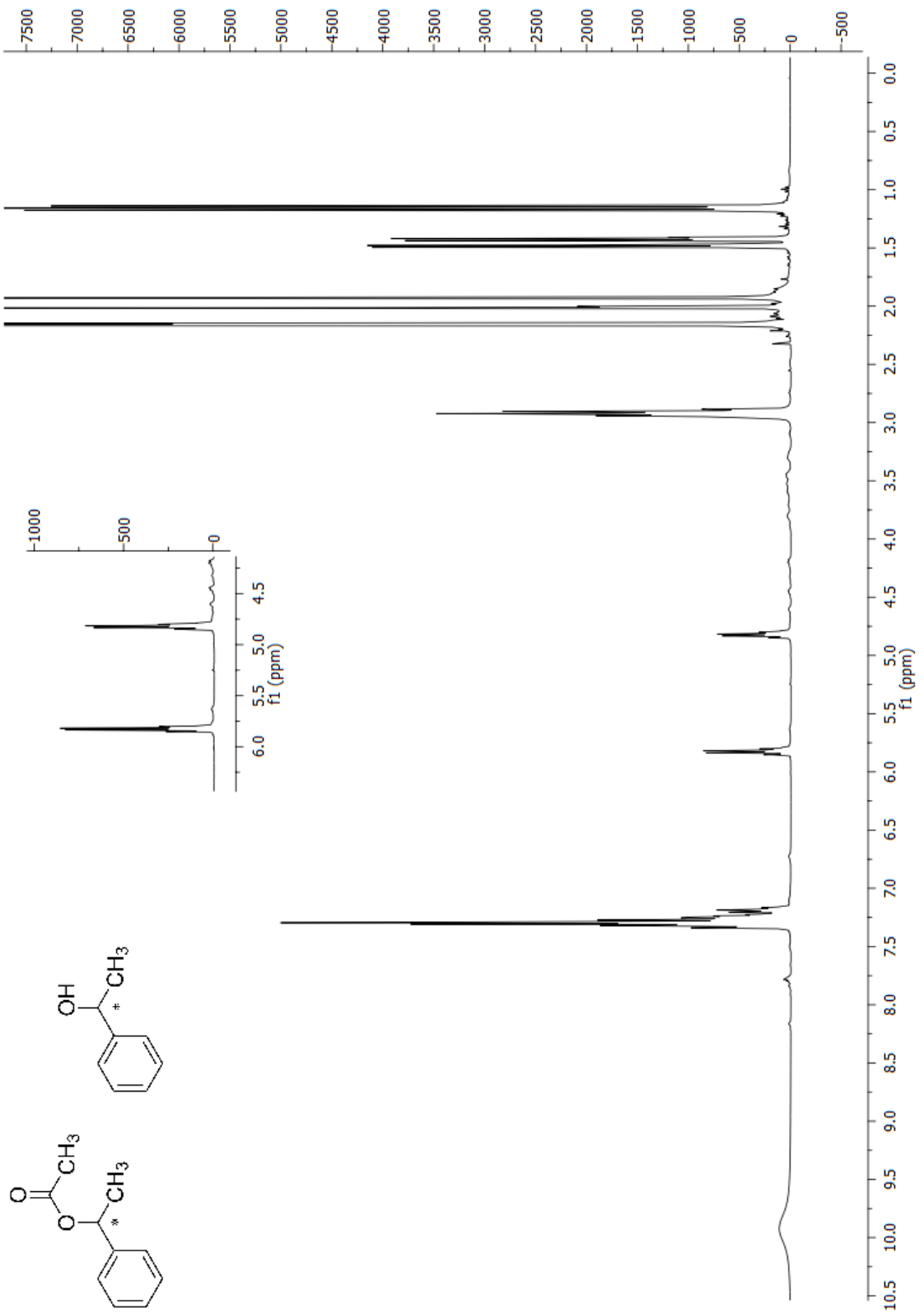

Figure 235: ^{1}H-NMR Spectrum ($CDCl_3$, 400 MHz) from the Reaction of 1-phenyl alcohol with Ac_2O Using **PP 8** (Table 21, Entry 51).

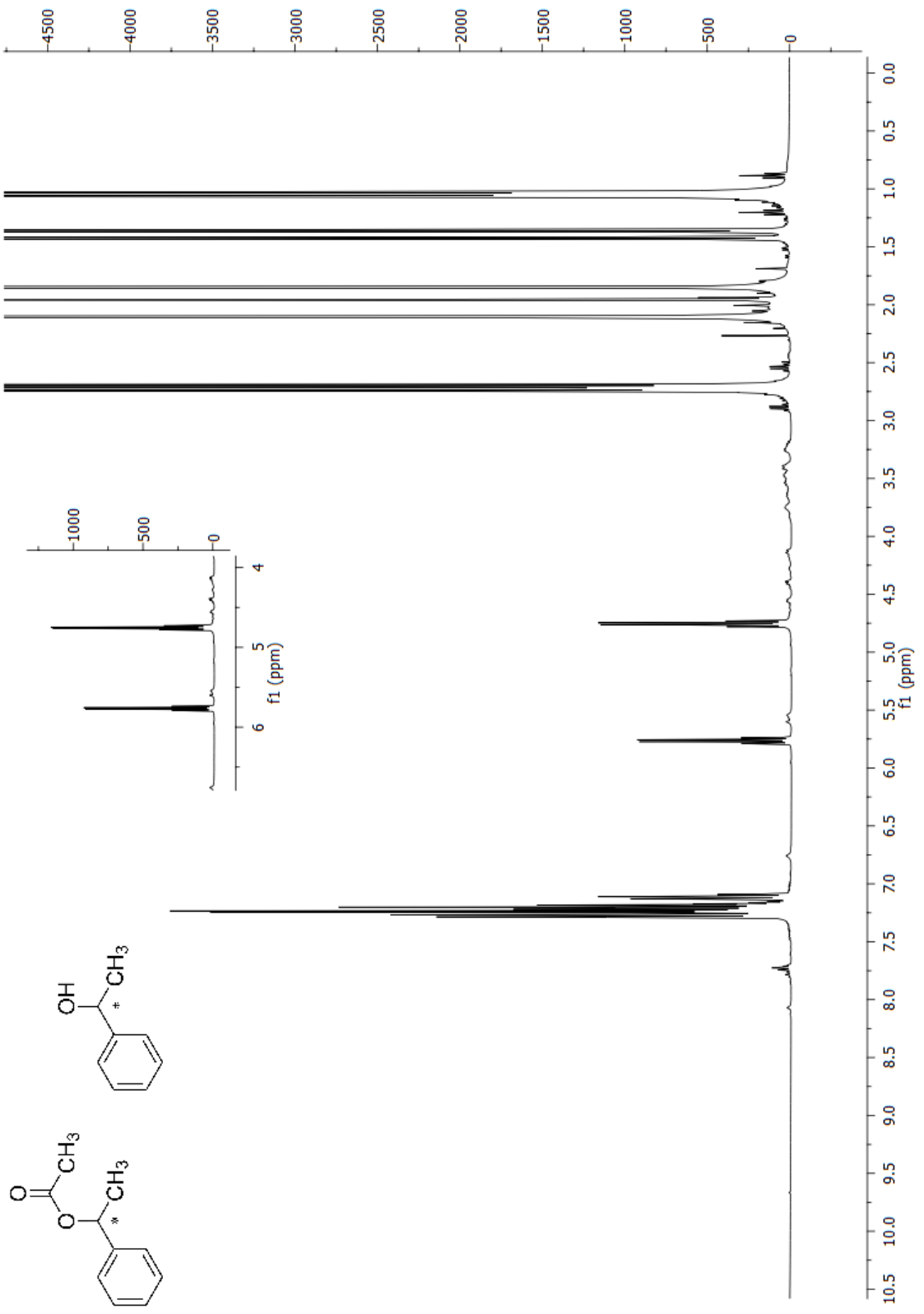

Figure 236: ^{1}H-NMR Spectrum ($CDCl_3$, 400 MHz) from the Reaction of 1-phenyl alcohol with Ac_2O Using **PP 8** (Table 22, Entry 52).

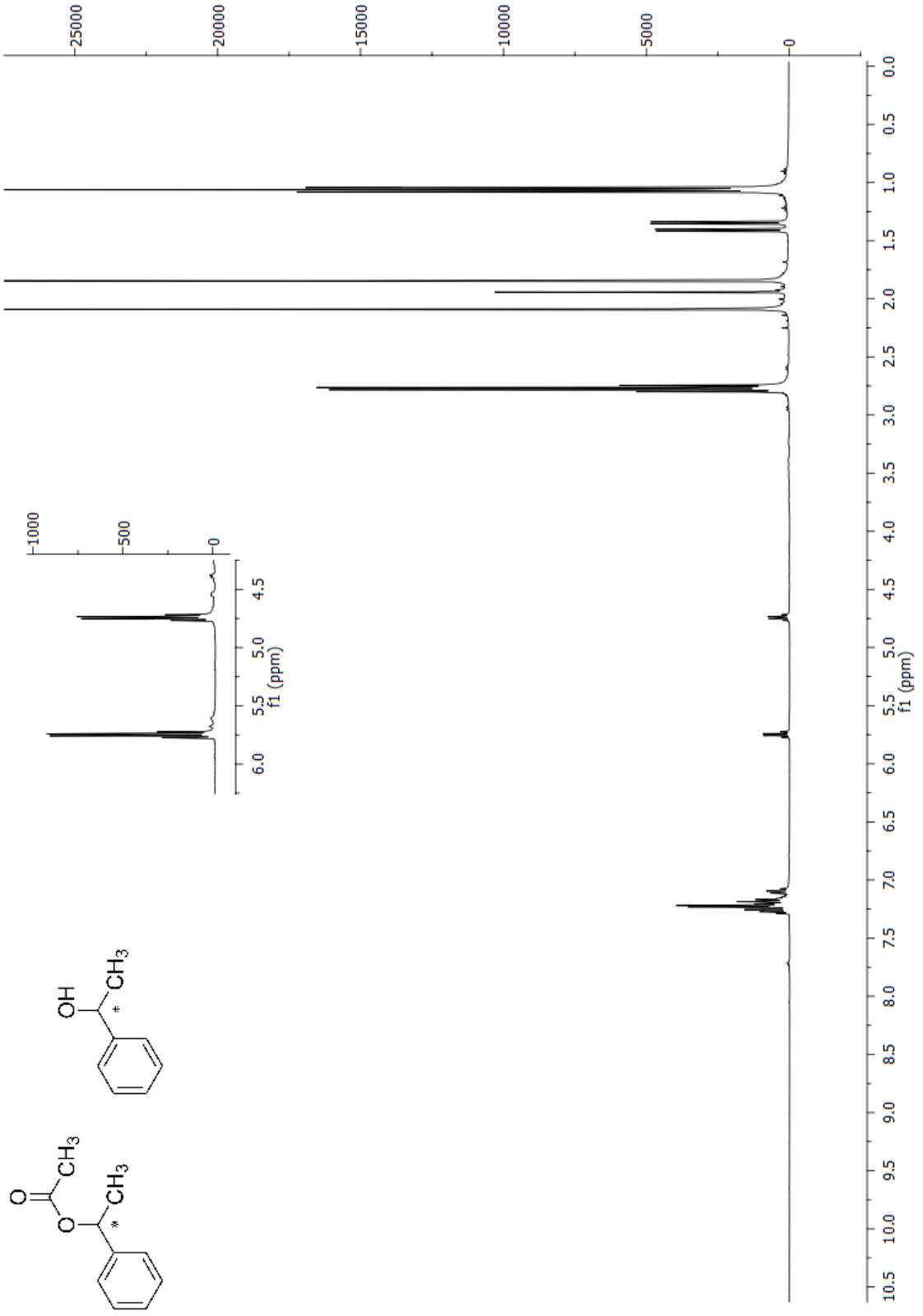

Figure 237: ^{1}H-NMR Spectrum ($CDCl_3$, 400 MHz) from the Reaction of 1-phenyl alcohol with Ac_2O Using **PP 8** (Table 22, Entry 53).

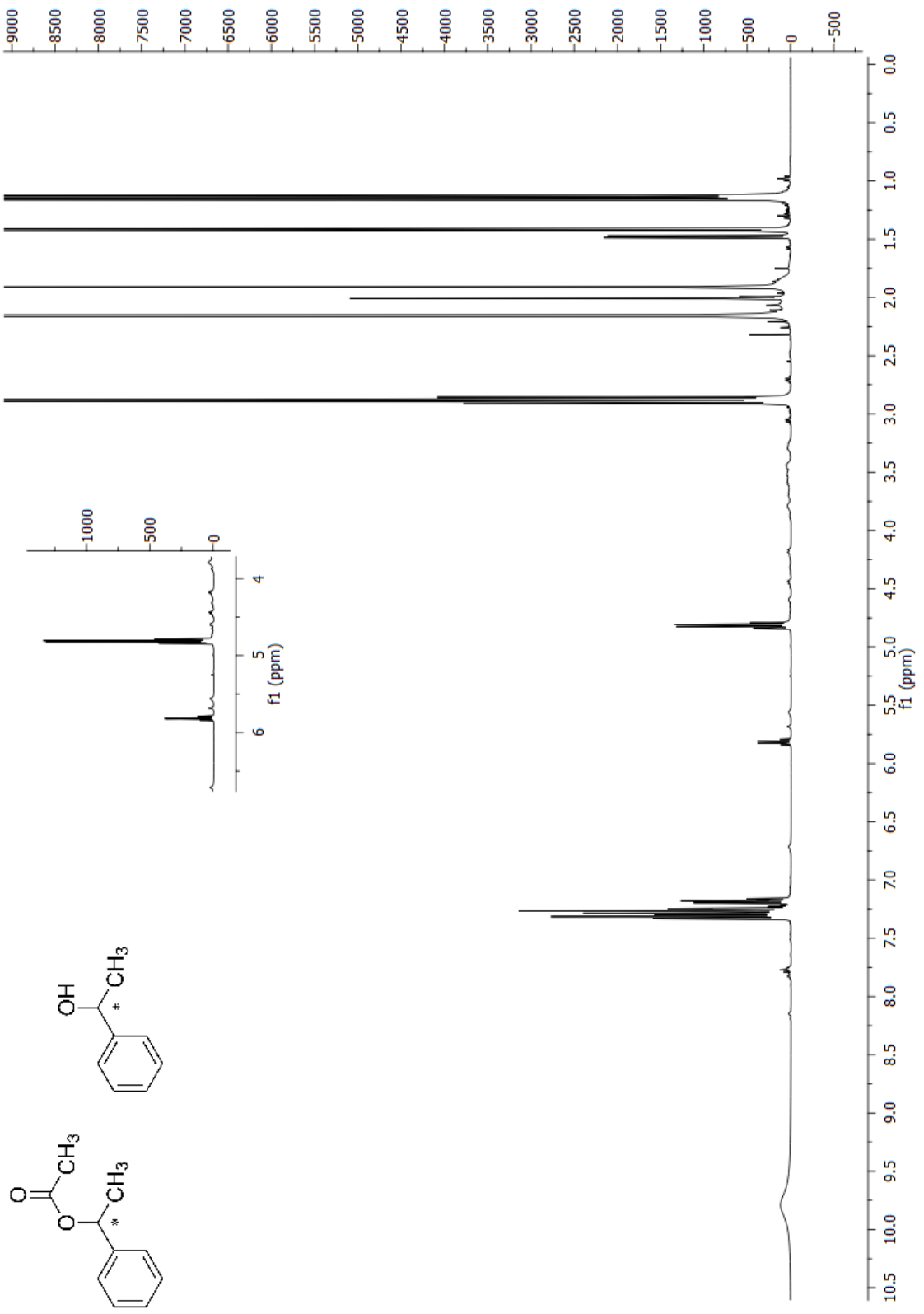

Figure 238: ^{1}H-NMR Spectrum ($CDCl_3$, 400 MHz) from the Reaction of 1-phenyl alcohol with Ac_2O Using **PP 8** (Table 22, Entry 54).

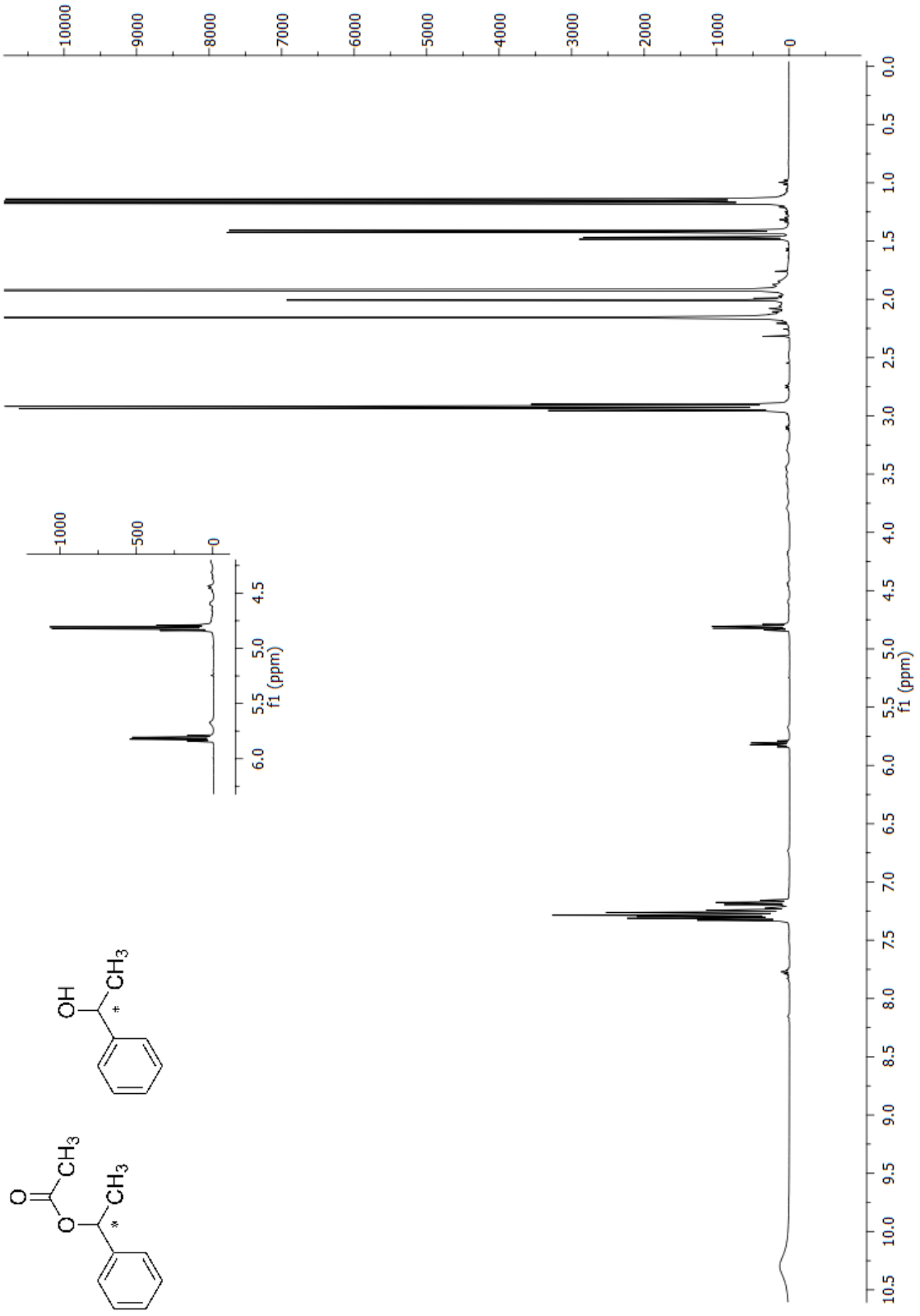

Figure 239: ^{1}H-NMR Spectrum ($CDCl_3$, 400 MHz) from the Reaction of 1-phenyl alcohol with Ac_2O Using **PP 8** (Table 22, Entry 55).

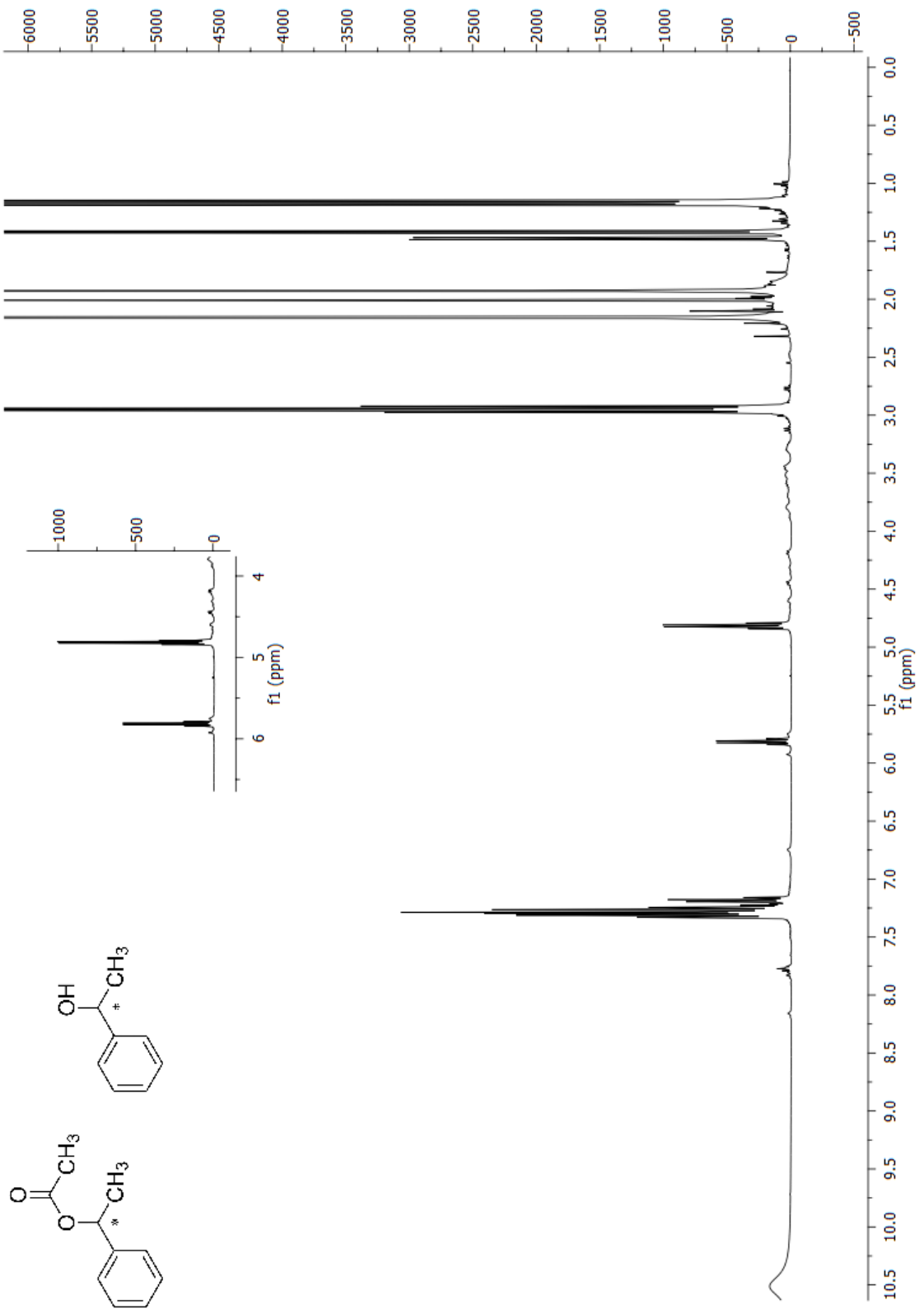

Figure 240: ^{1}H-NMR Spectrum ($CDCl_3$, 400 MHz) from the Reaction of 1-phenyl alcohol with Ac_2O Using **PP 8** (Table 22, Entry 56).

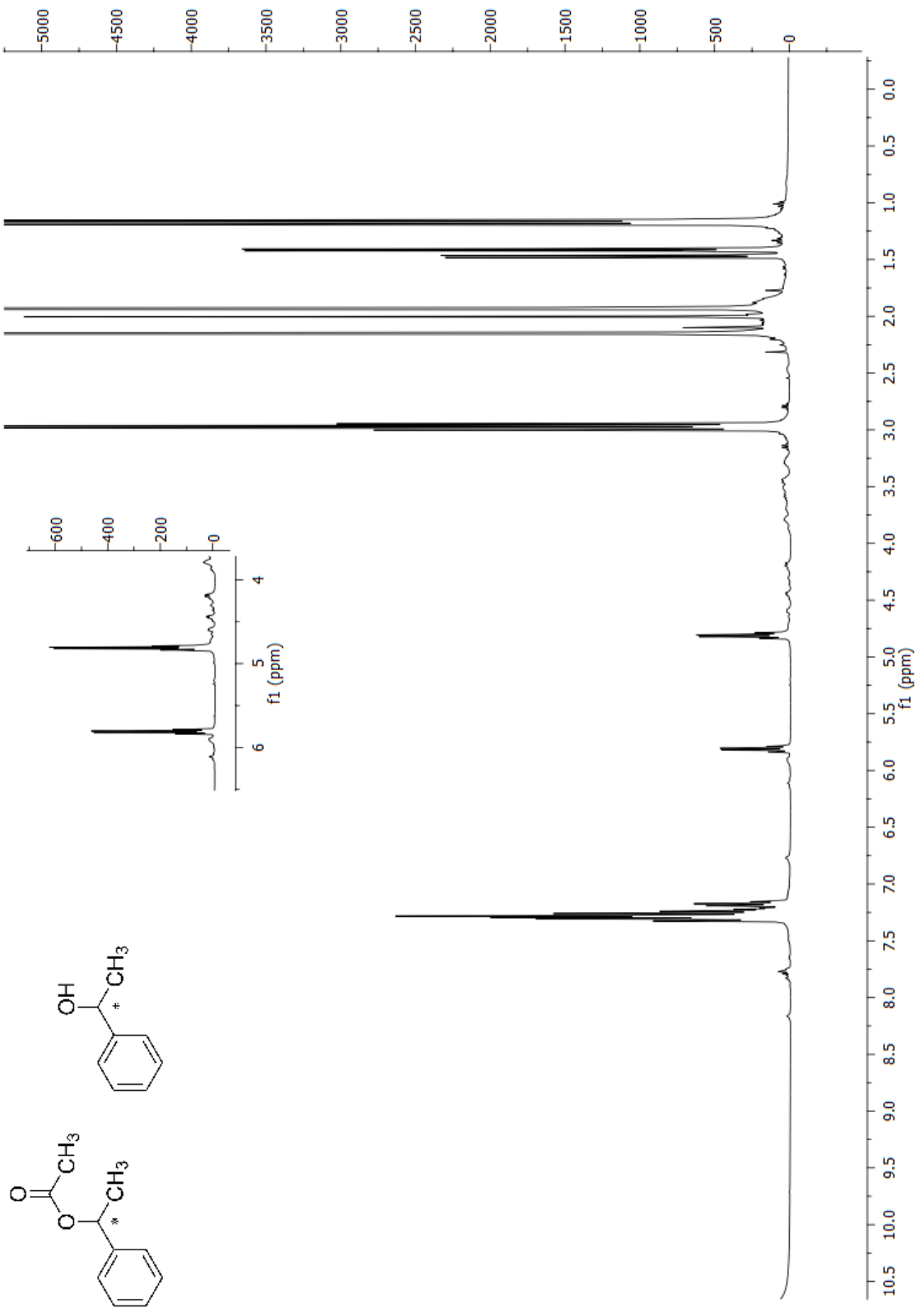

Figure 241: ^{1}H-NMR Spectrum ($CDCl_3$, 400 MHz) from the Reaction of 1-phenyl alcohol with Ac_2O Using **PP 8** (Table 22, Entry 57).

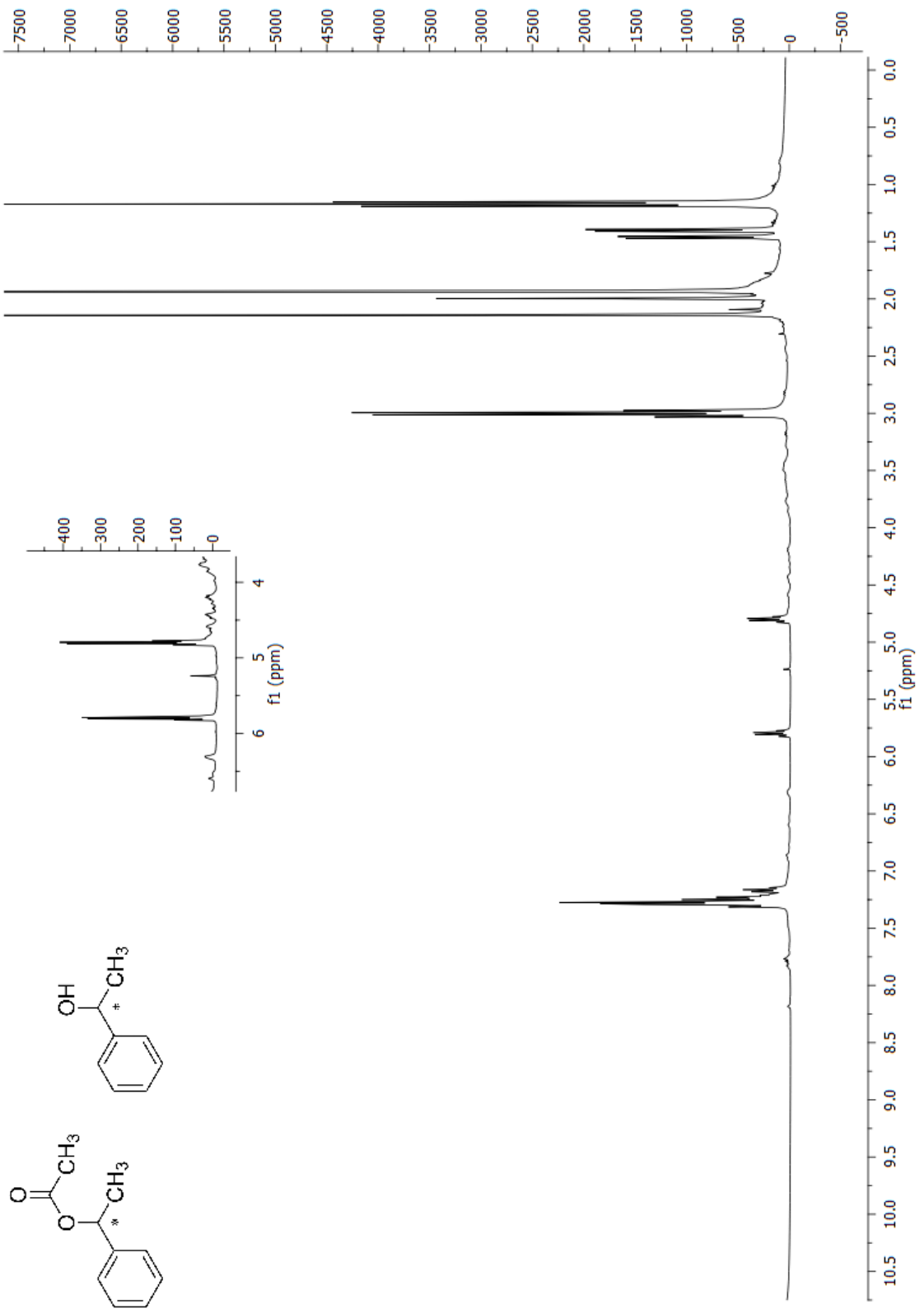

Figure 242: ^{1}H-NMR Spectrum ($CDCl_3$, 400 MHz) from the Reaction of 1-phenyl alcohol with Ac_2O Using **PP 8** (Table 22, Entry 58).

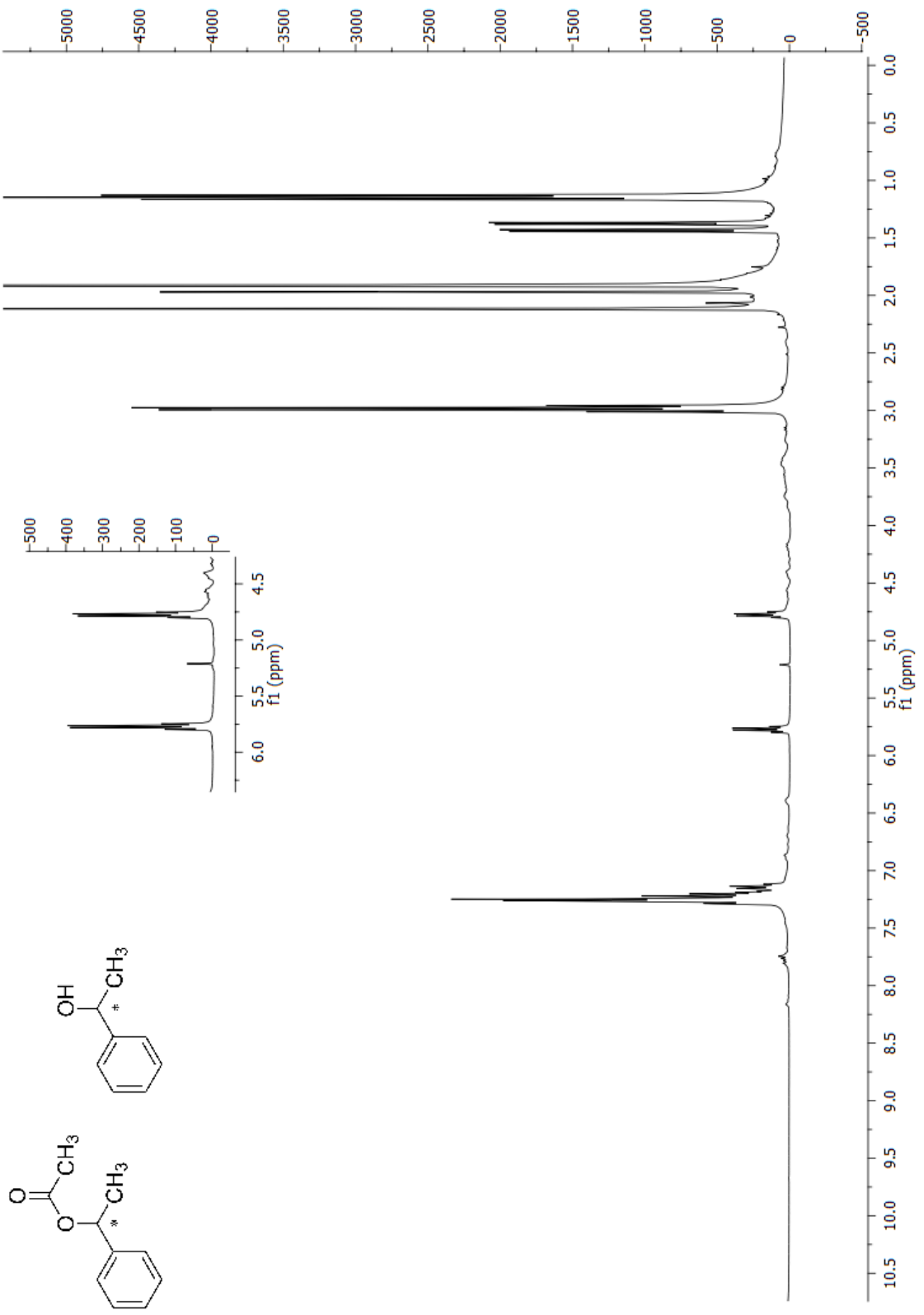

Figure 243: ^{1}H-NMR Spectrum ($CDCl_3$, 400 MHz) from the Reaction of 1-phenyl alcohol with Ac_2O Using **PP 8** (Table 22, Entry 59).

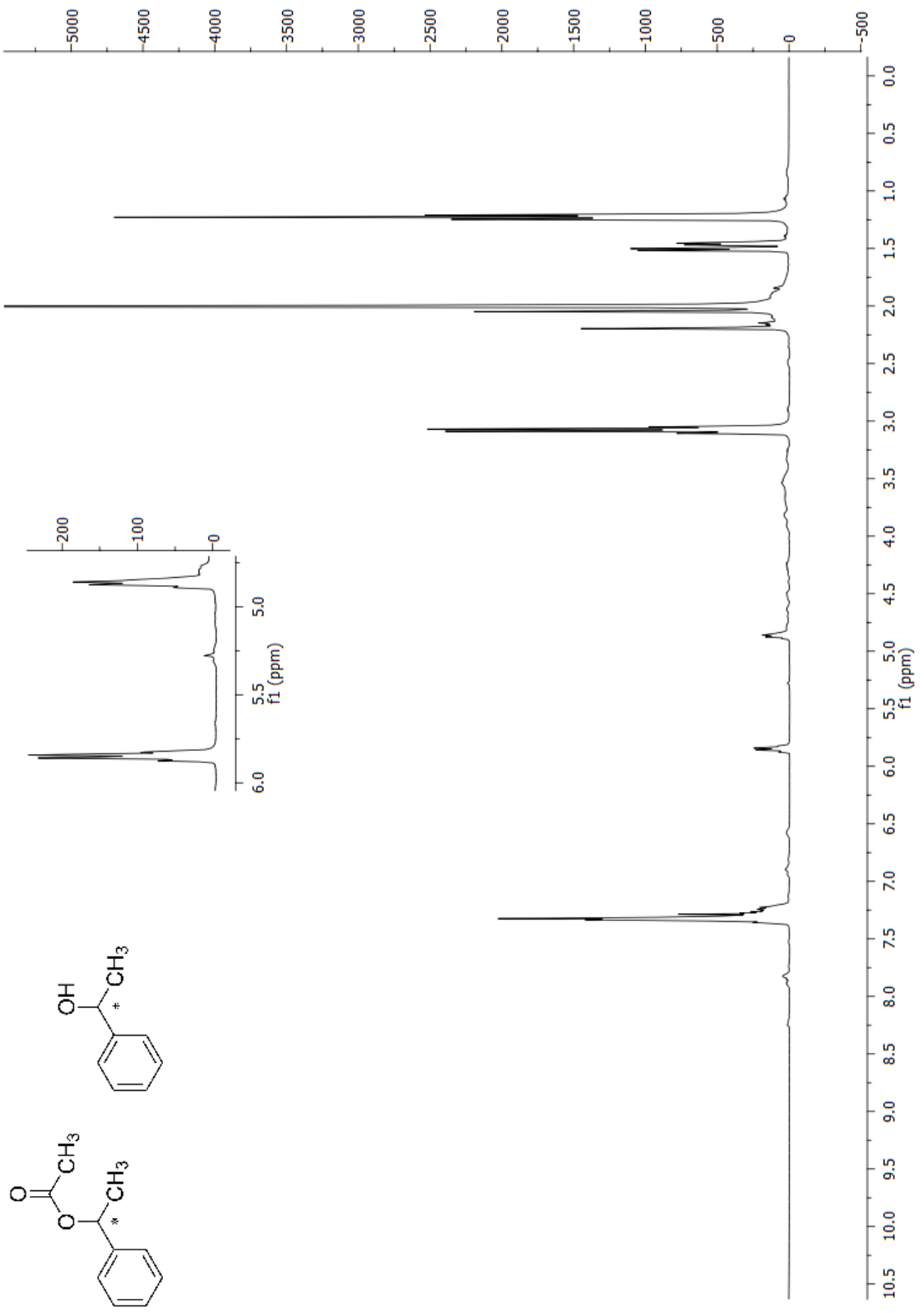

Figure 244: ^{1}H-NMR Spectrum ($CDCl_3$, 400 MHz) from the Reaction of 1-phenyl alcohol with Ac_2O Using **PP 8** (Table 22, Entry 60).

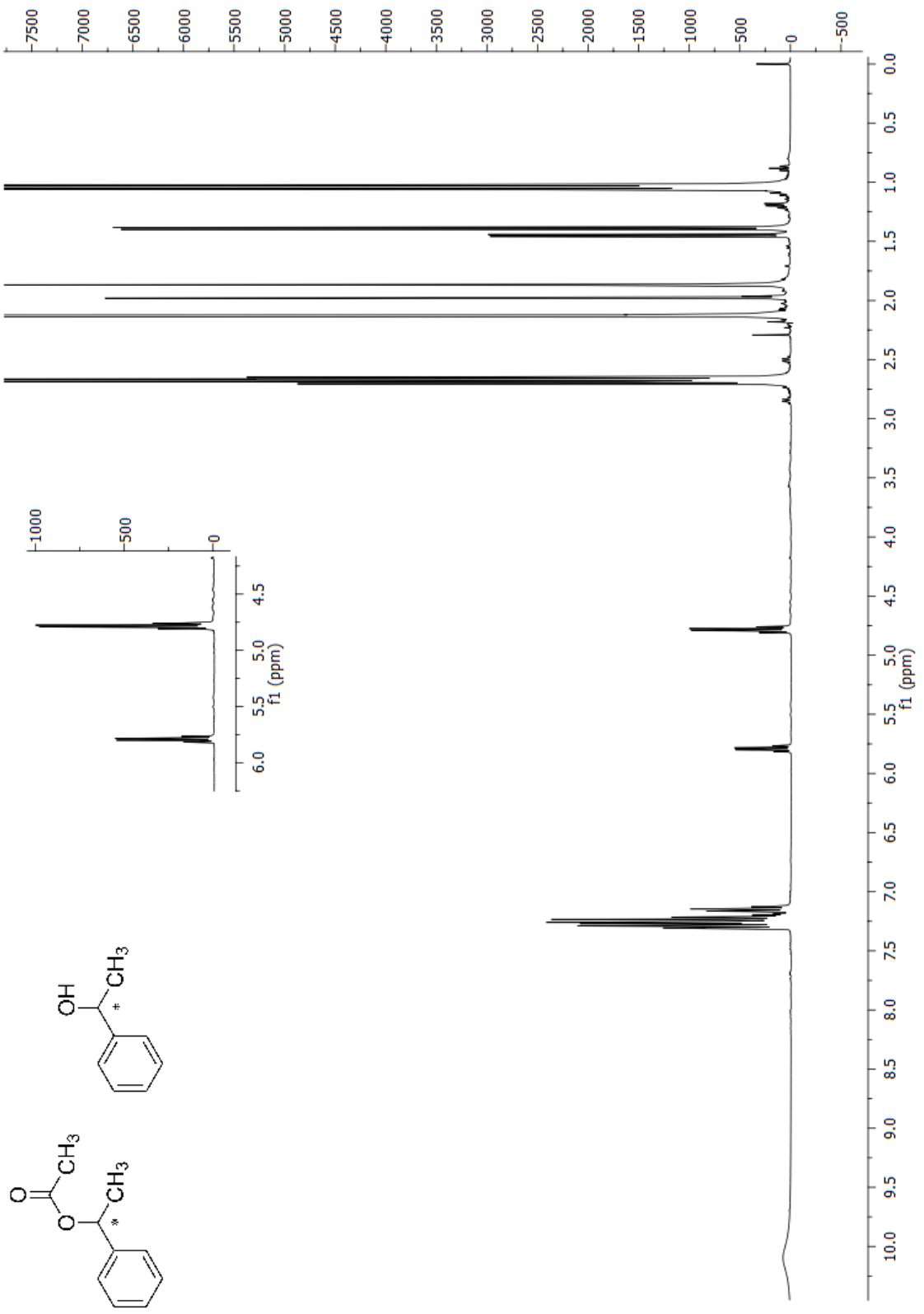

Figure 245: ^{1}H-NMR Spectrum ($CDCl_3$, 400 MHz) from the Reaction of 1-phenyl alcohol with Ac_2O Using **PP 9** (Table 23, Entry 61).

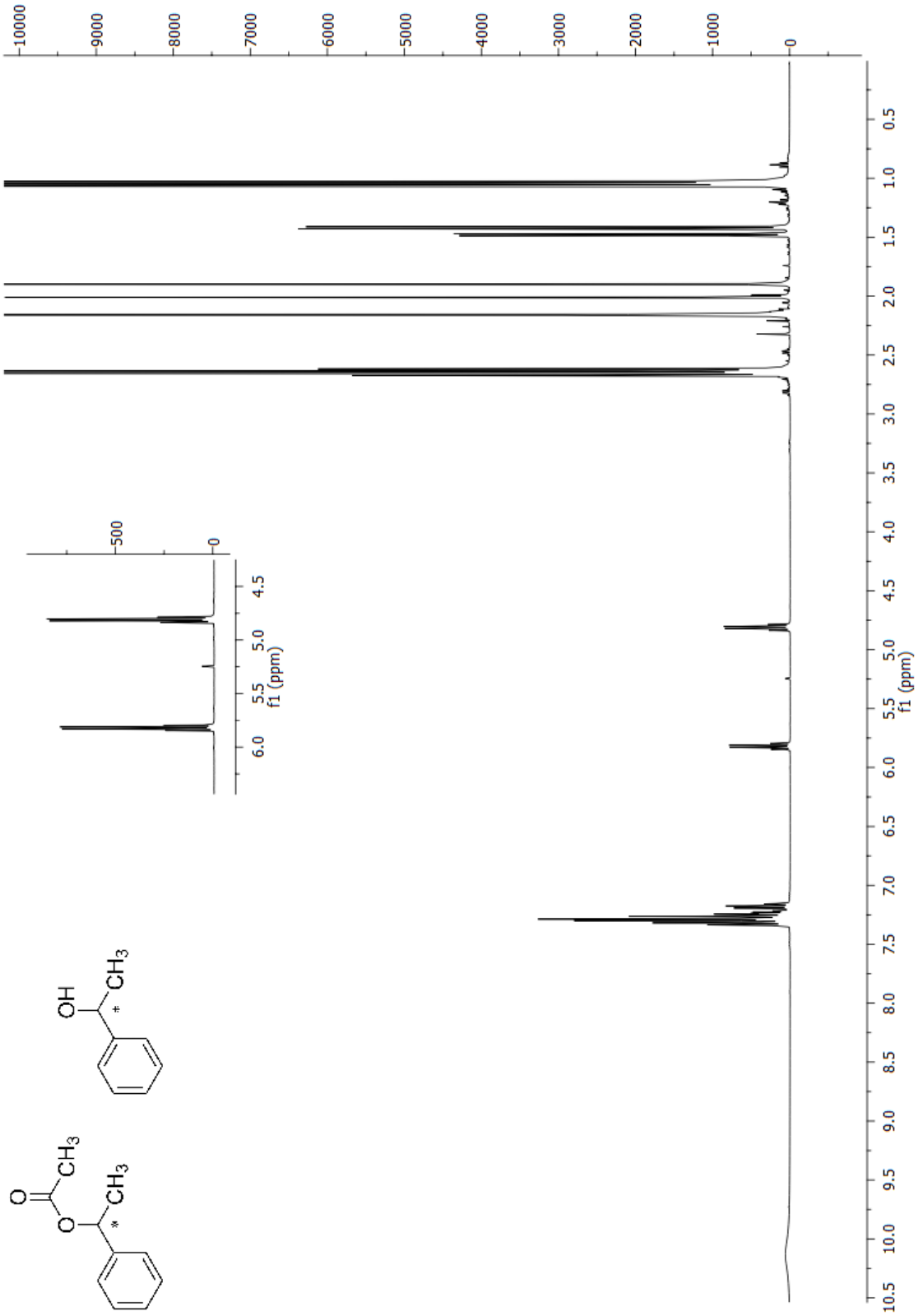

Figure 246: ^{1}H-NMR Spectrum ($CDCl_3$, 400 MHz) from the Reaction of 1-phenyl alcohol with Ac_2O Using **PP 9** (Table 23, Entry 62).

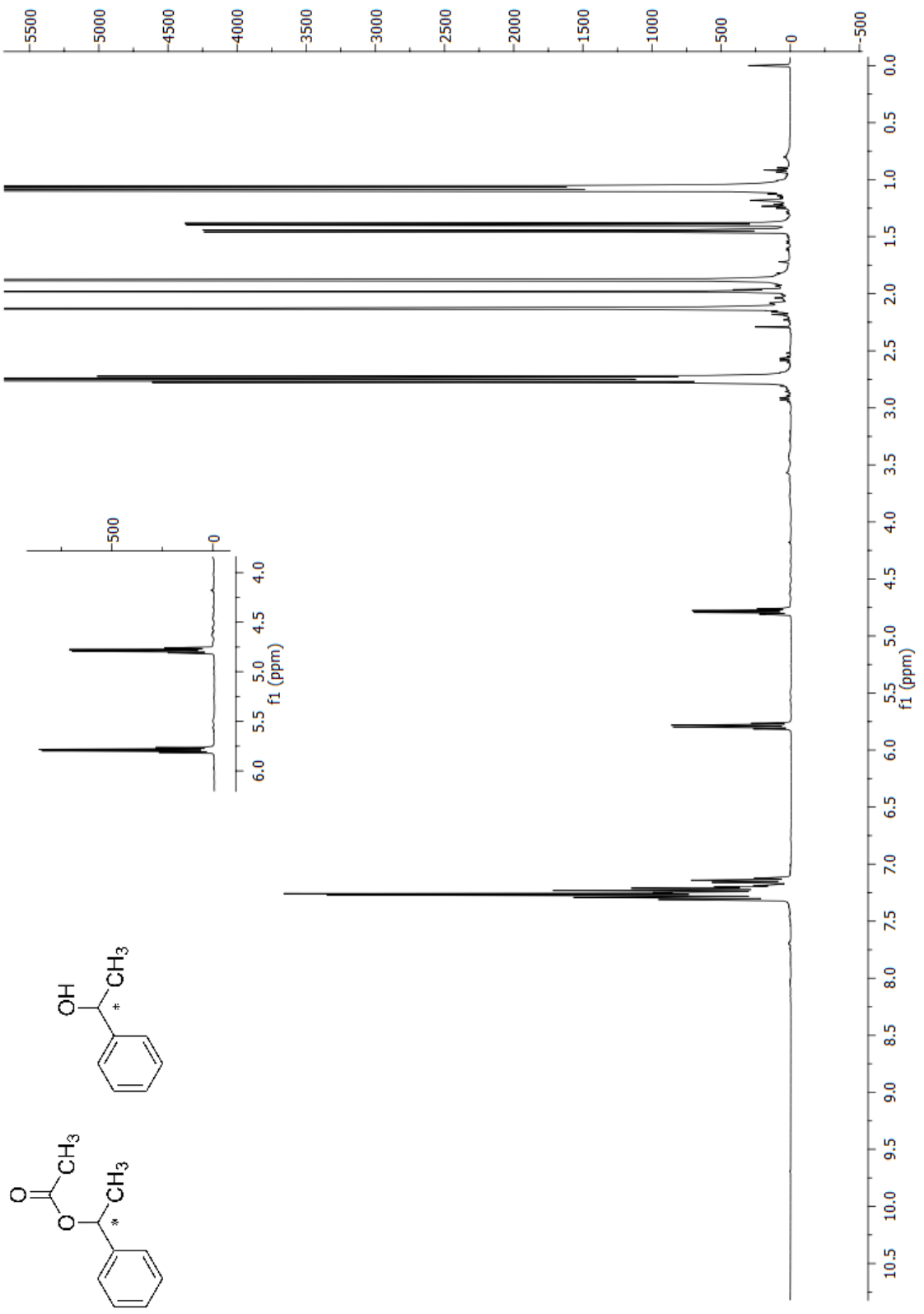

Figure 247: ^{1}H-NMR Spectrum ($CDCl_3$, 400 MHz) from the Reaction of 1-phenyl alcohol with Ac_2O Using **PP 9** (Table 23, Entry 63).

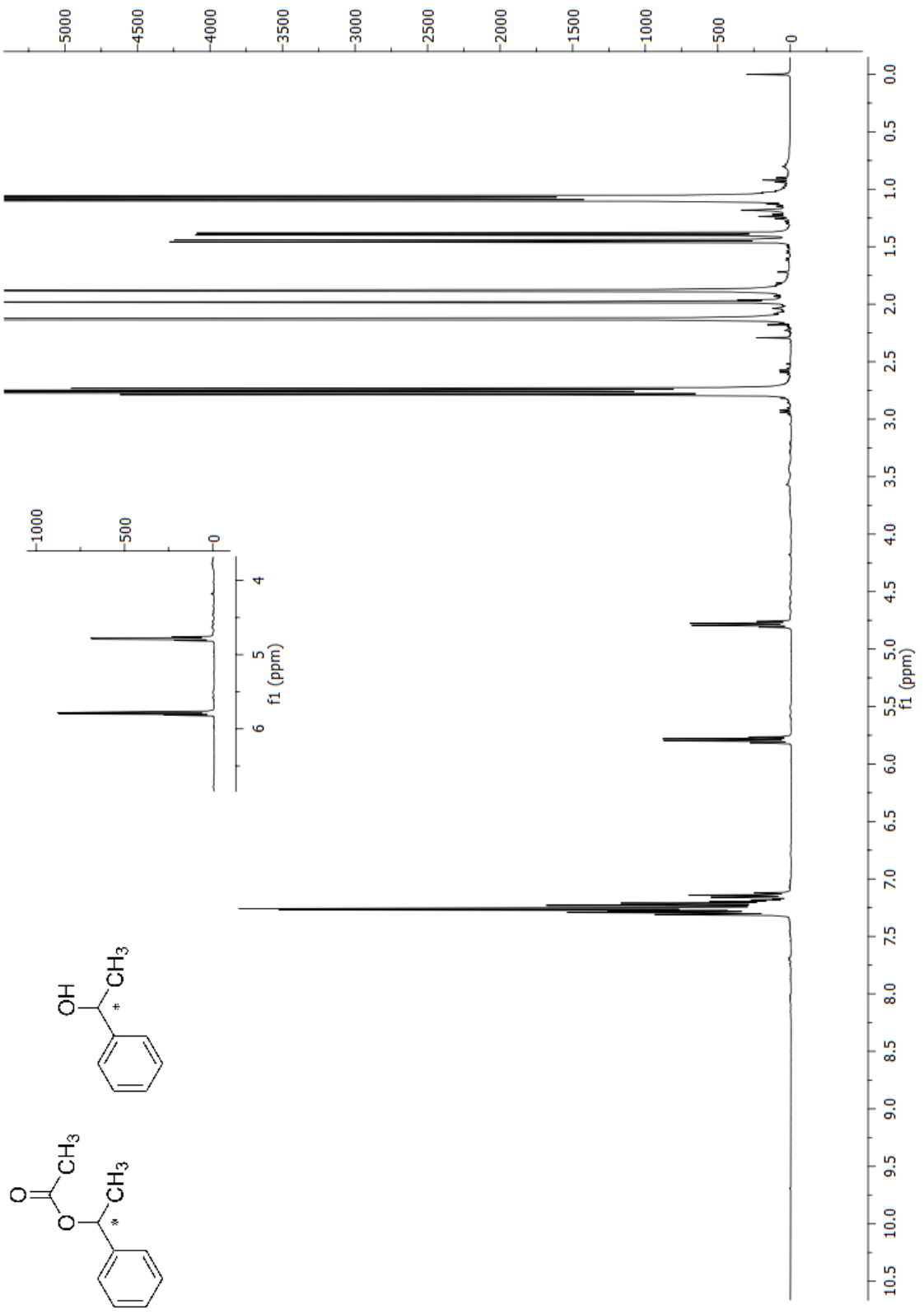

Figure 248: ^{1}H-NMR Spectrum ($CDCl_3$, 400 MHz) from the Reaction of 1-phenyl alcohol with Ac_2O Using **PP 9** (Table 23, Entry 64).

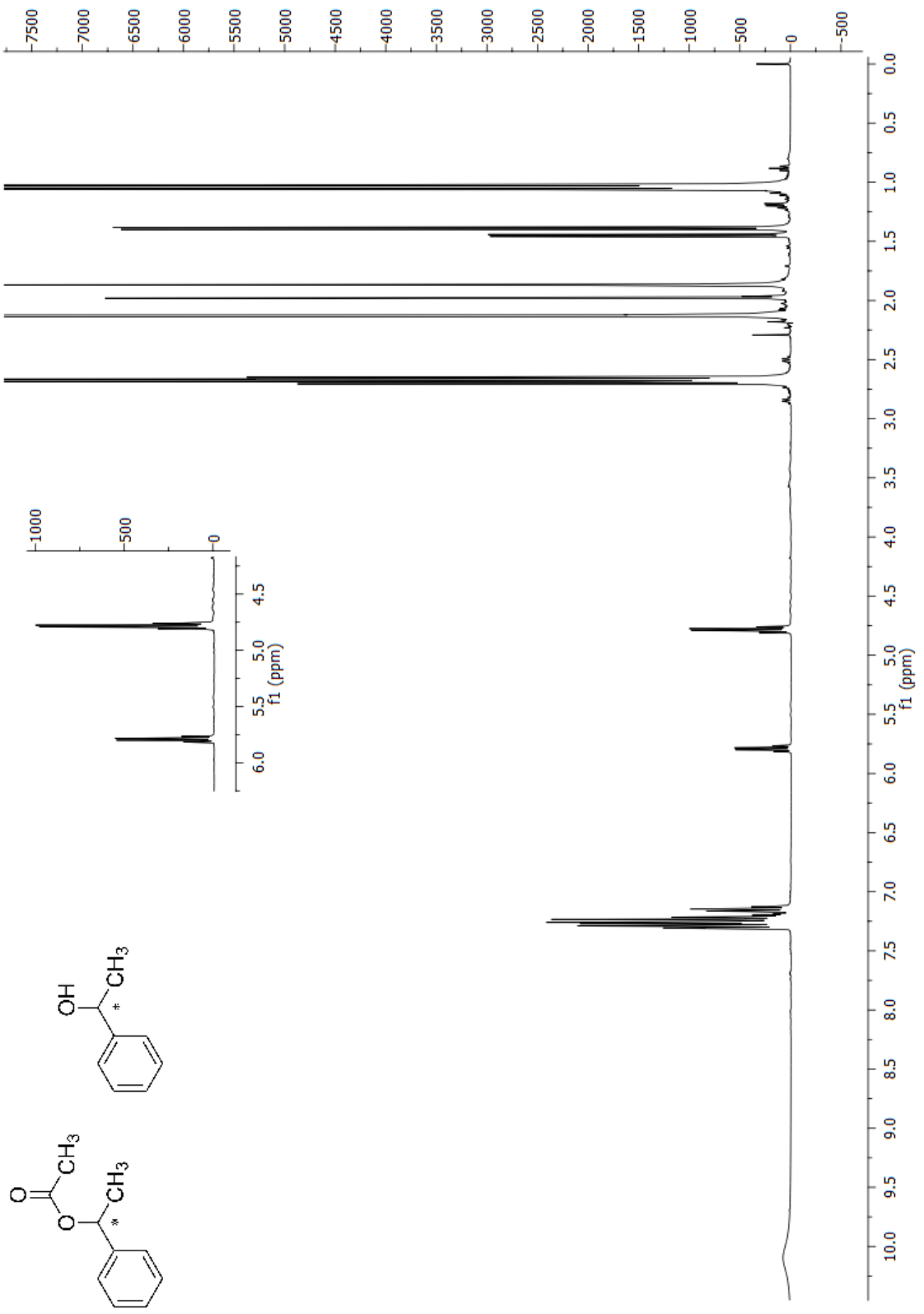

Figure 249: ^{1}H-NMR Spectrum ($CDCl_3$, 400 MHz) from the Reaction of 1-phenyl alcohol with Ac_2O Using **PP 9** (Table 23, Entry 65).

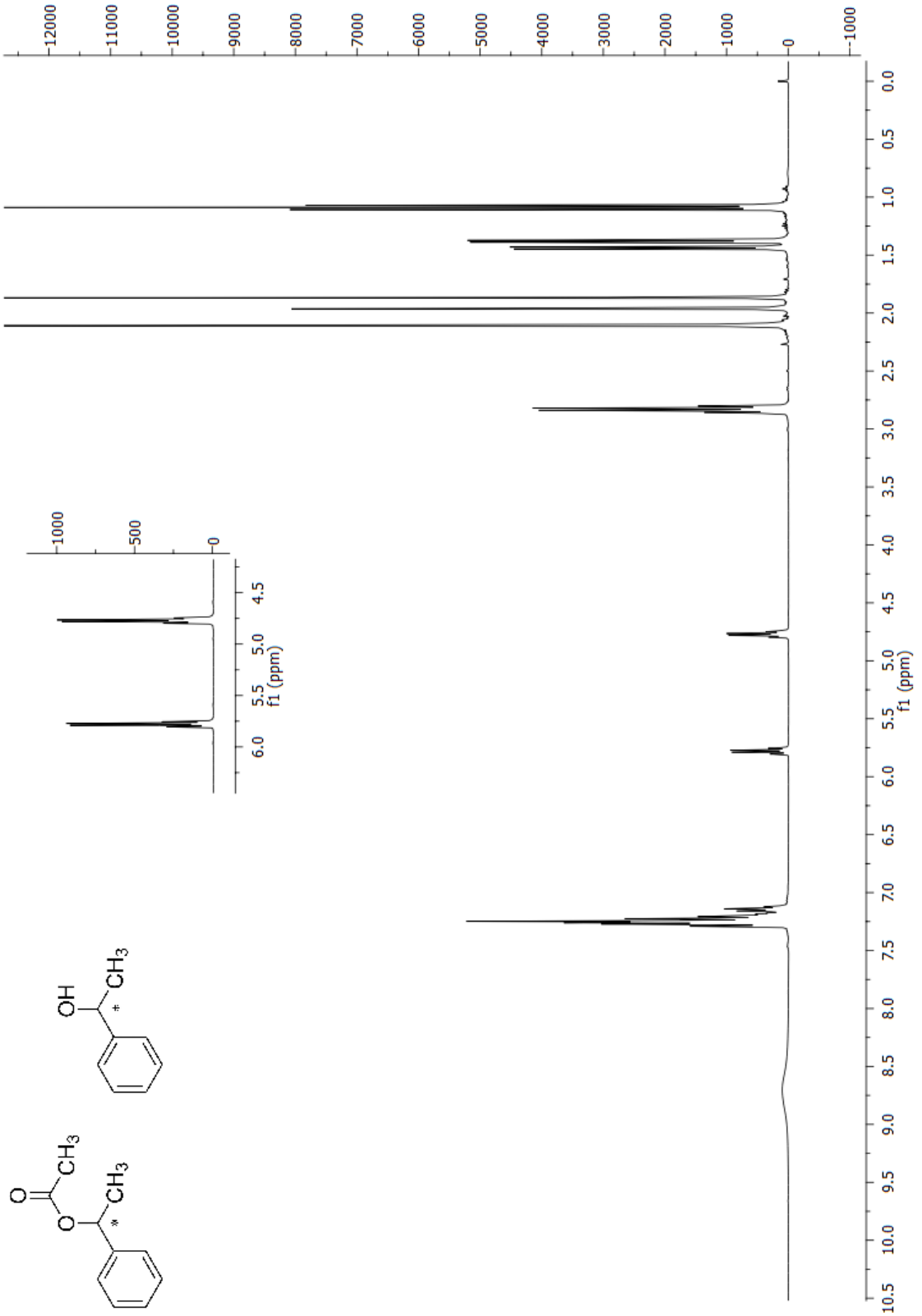

Figure 250: ^{1}H-NMR Spectrum ($CDCl_3$, 400 MHz) from the Reaction of 1-phenyl alcohol with Ac_2O Using **PP 9** (Table 23, Entry 66).

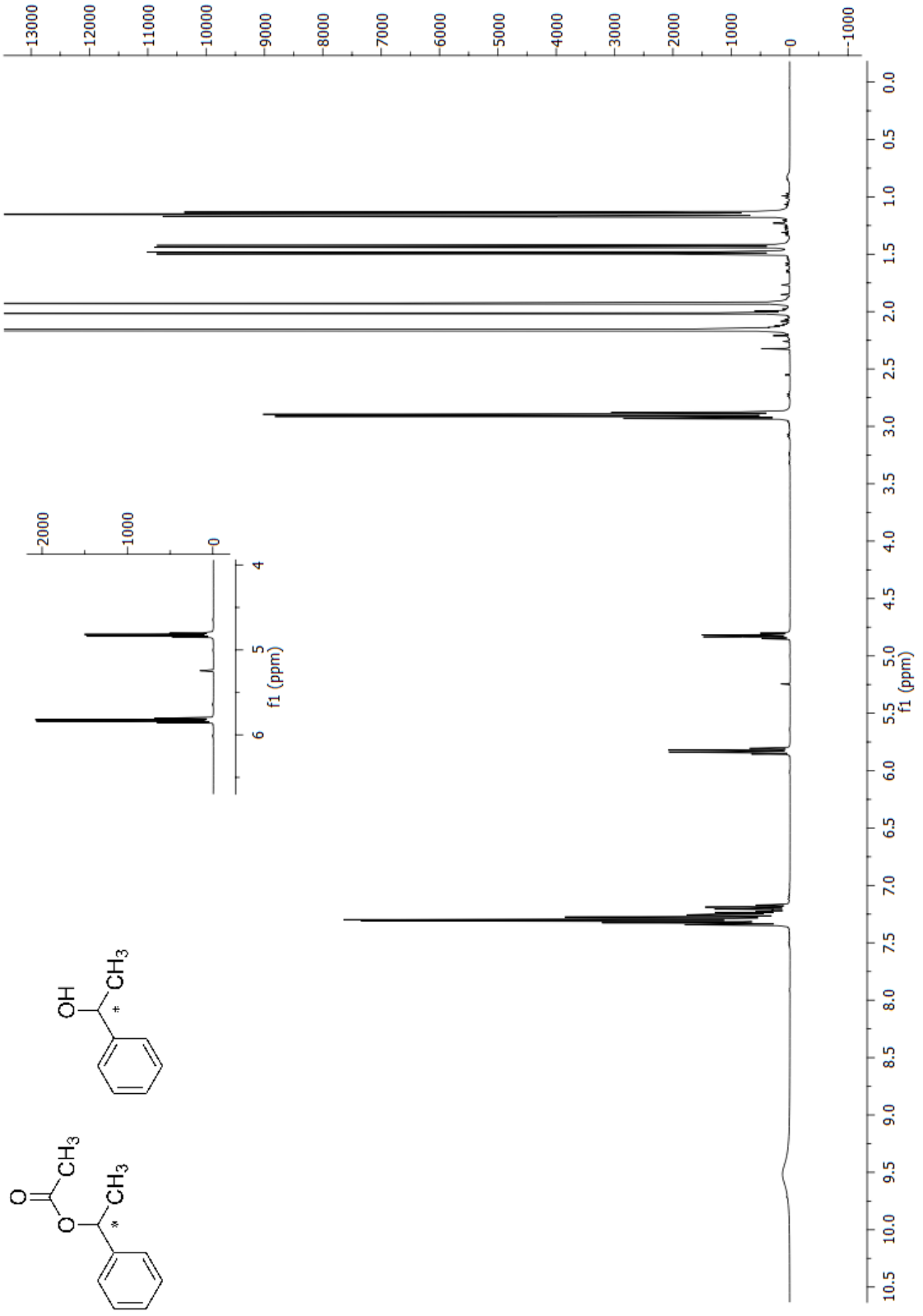

Figure 251: ^{1}H-NMR Spectrum ($CDCl_3$, 400 MHz) from the Reaction of 1-phenyl alcohol with Ac_2O Using **PP 9** (Table 23, Entry 67).

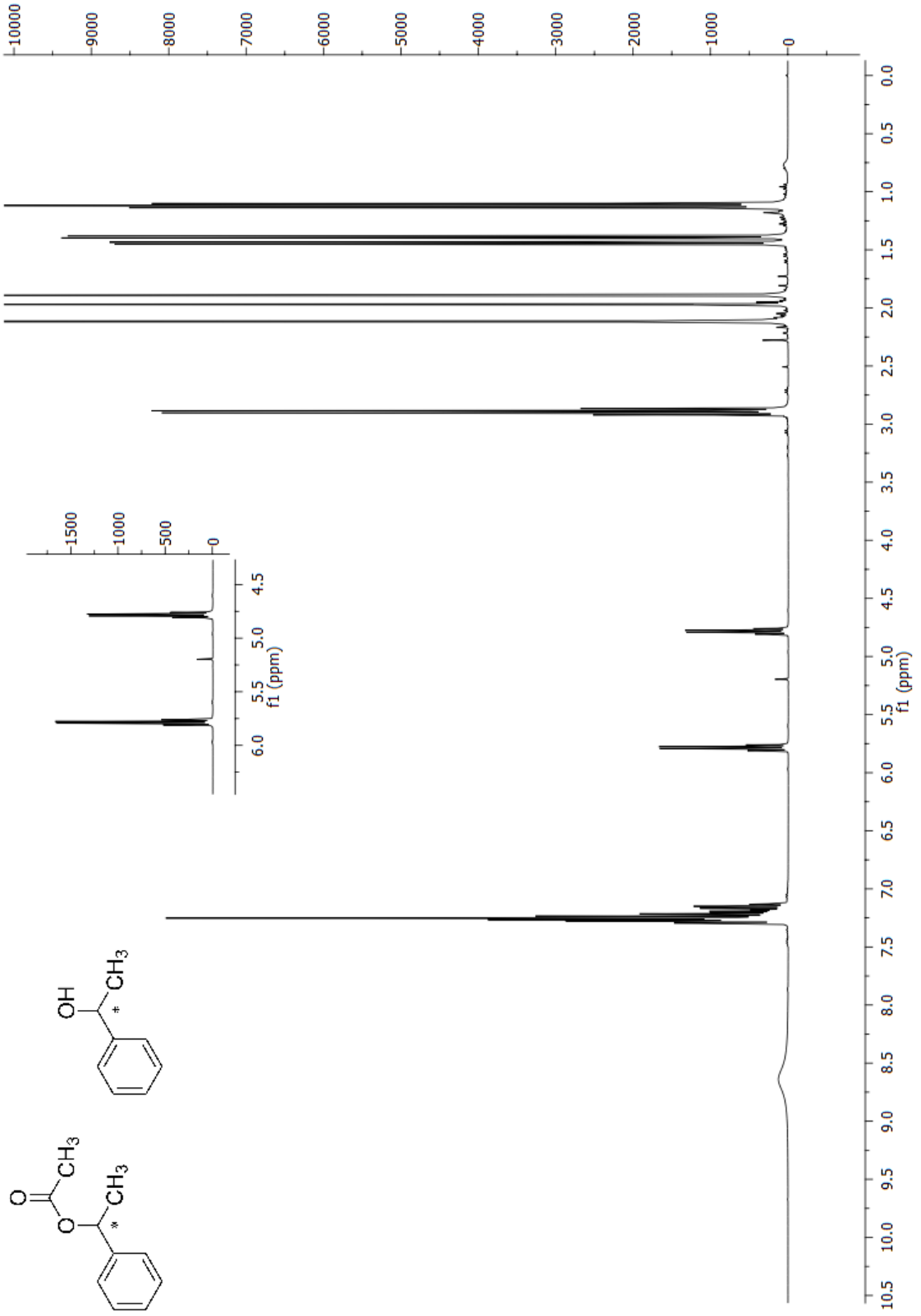

Figure 252: ^{1}H-NMR Spectrum ($CDCl_3$, 400 MHz) from the Reaction of 1-phenyl alcohol with Ac_2O Using **PP 9** (Table 24, Entry 68).

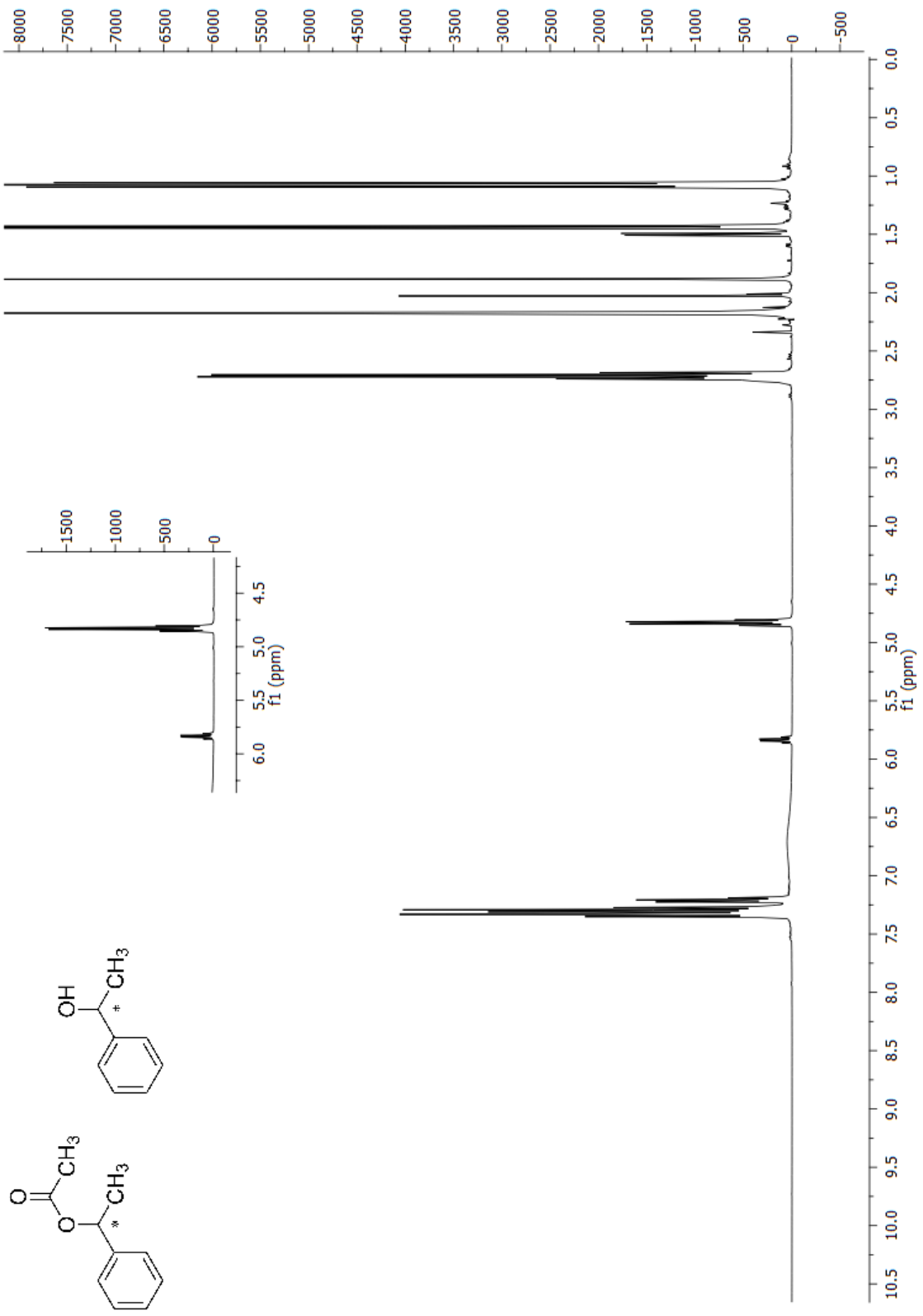

Figure 253: ^{1}H-NMR Spectrum ($CDCl_3$, 400 MHz) from the Reaction of 1-phenyl alcohol with Ac_2O Using **PP 9** (Table 24, Entry 69).

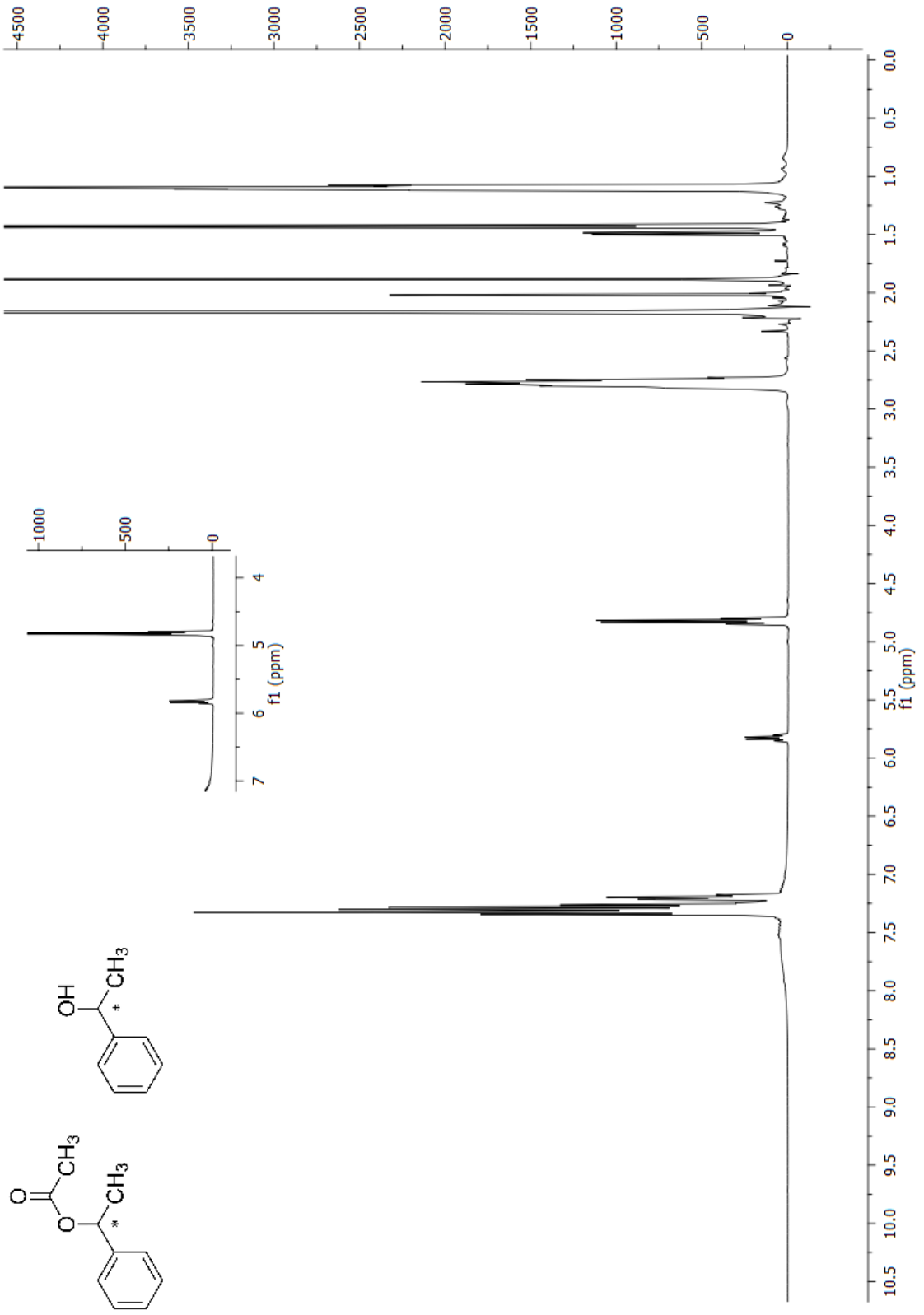

Figure 254: ^{1}H-NMR Spectrum ($CDCl_3$, 400 MHz) from the Reaction of 1-phenyl alcohol with Ac_2O Using **PP 9** (Table 24, Entry 70).

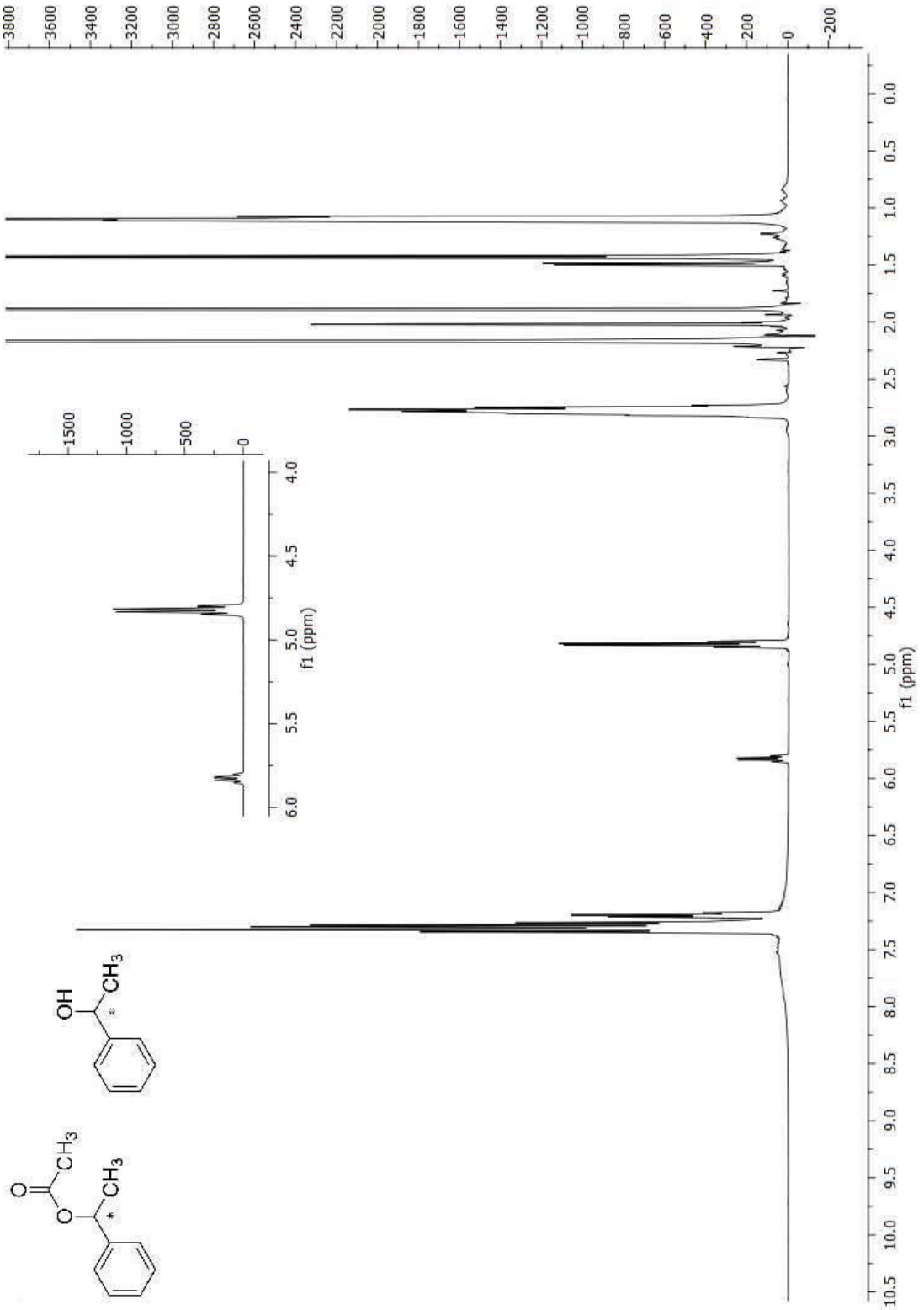

Figure 255: ^{1}H-NMR Spectrum ($CDCl_3$, 400 MHz) from the Reaction of 1-phenyl alcohol with Ac_2O Using **PP 9** (Table 24, Entry 71).

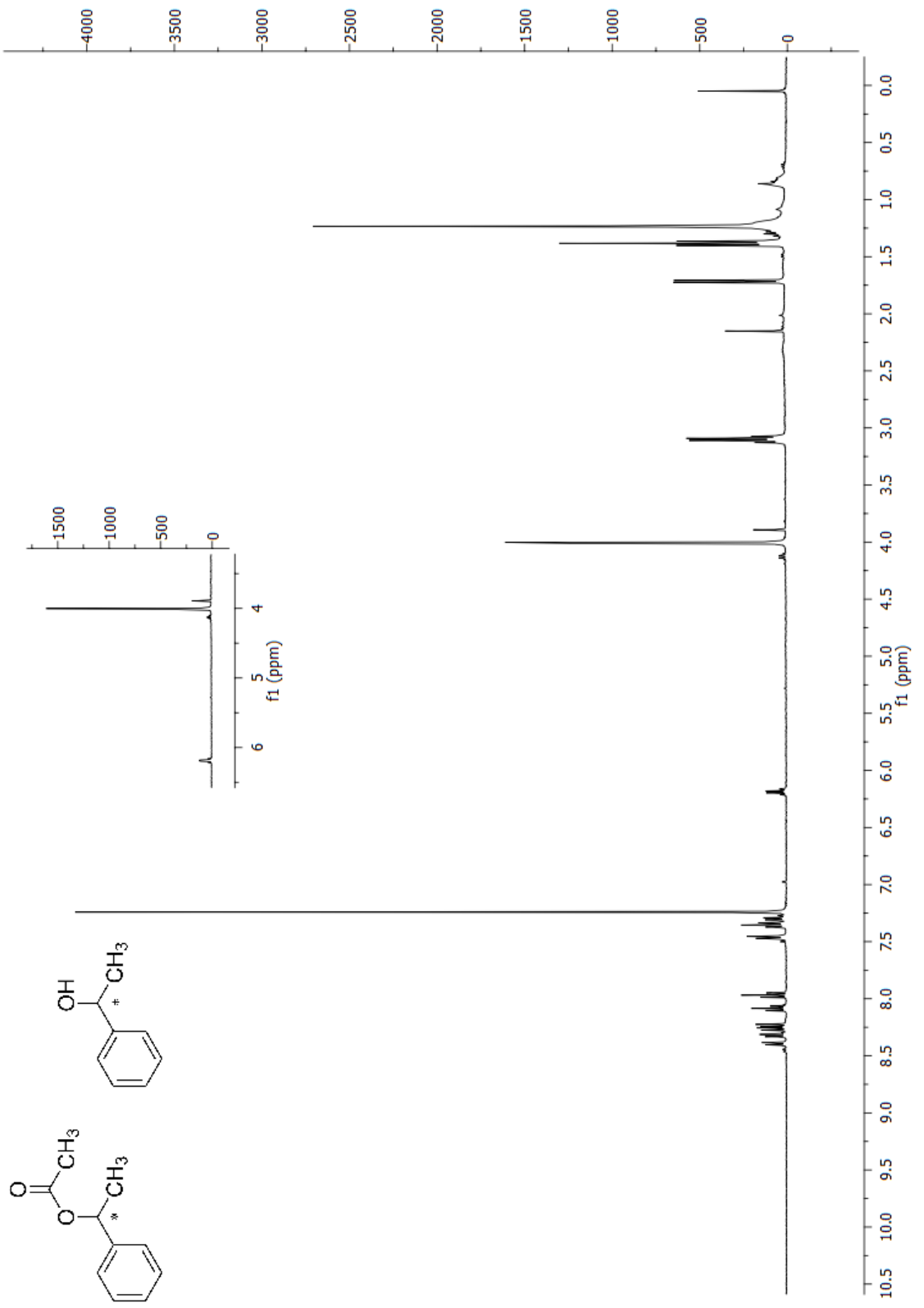

Figure 256: ^{1}H-NMR Spectrum ($CDCl_3$, 400 MHz) from the Reaction of 1-phenyl alcohol with Ac_2O Using **J1** (Table 25, Entry 72).

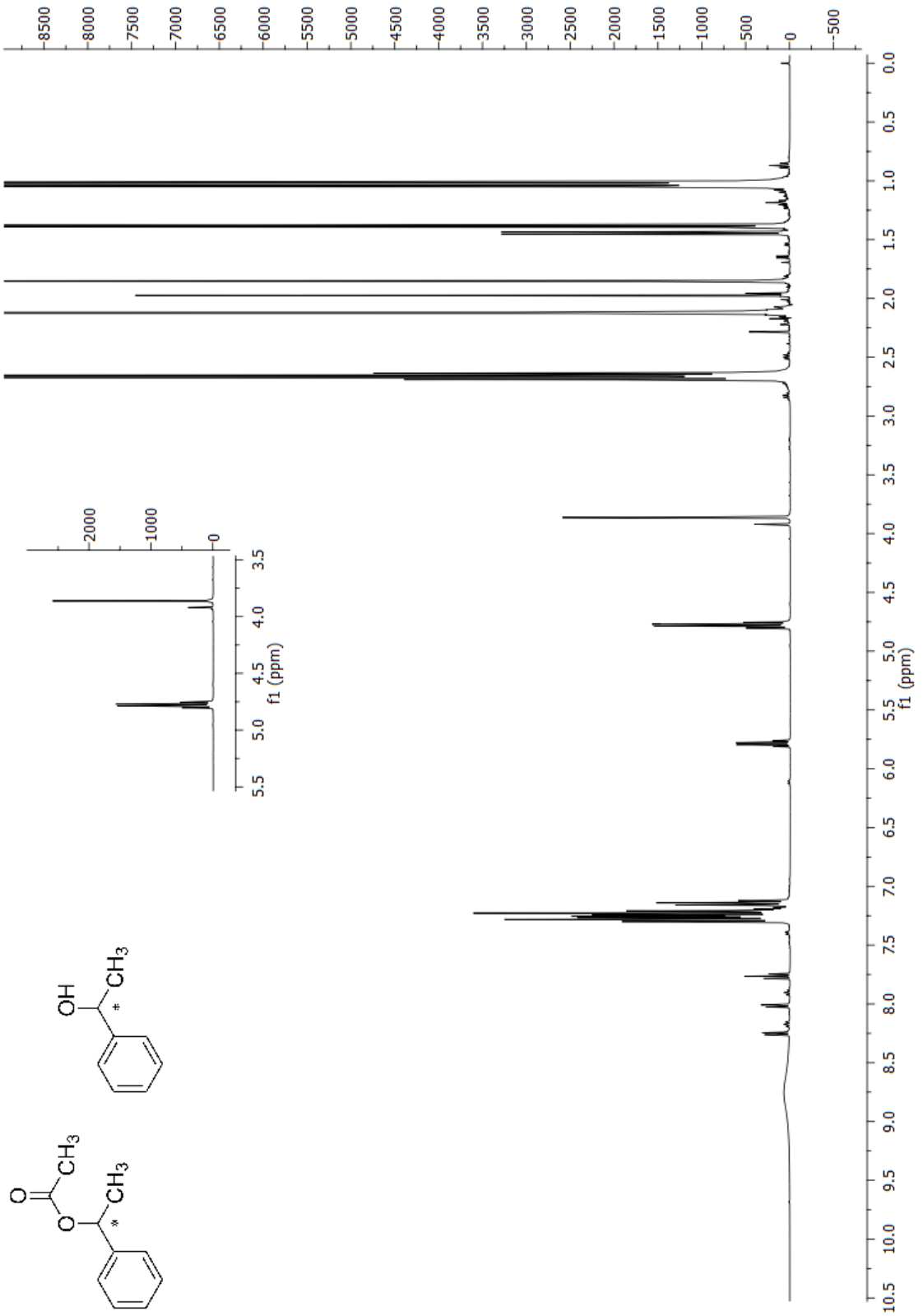

Figure 257: ^{1}H-NMR Spectrum ($CDCl_3$, 400 MHz) from the Reaction of 1-phenyl alcohol with Ac_2O Using **J1** (Table 25, Entry 73).

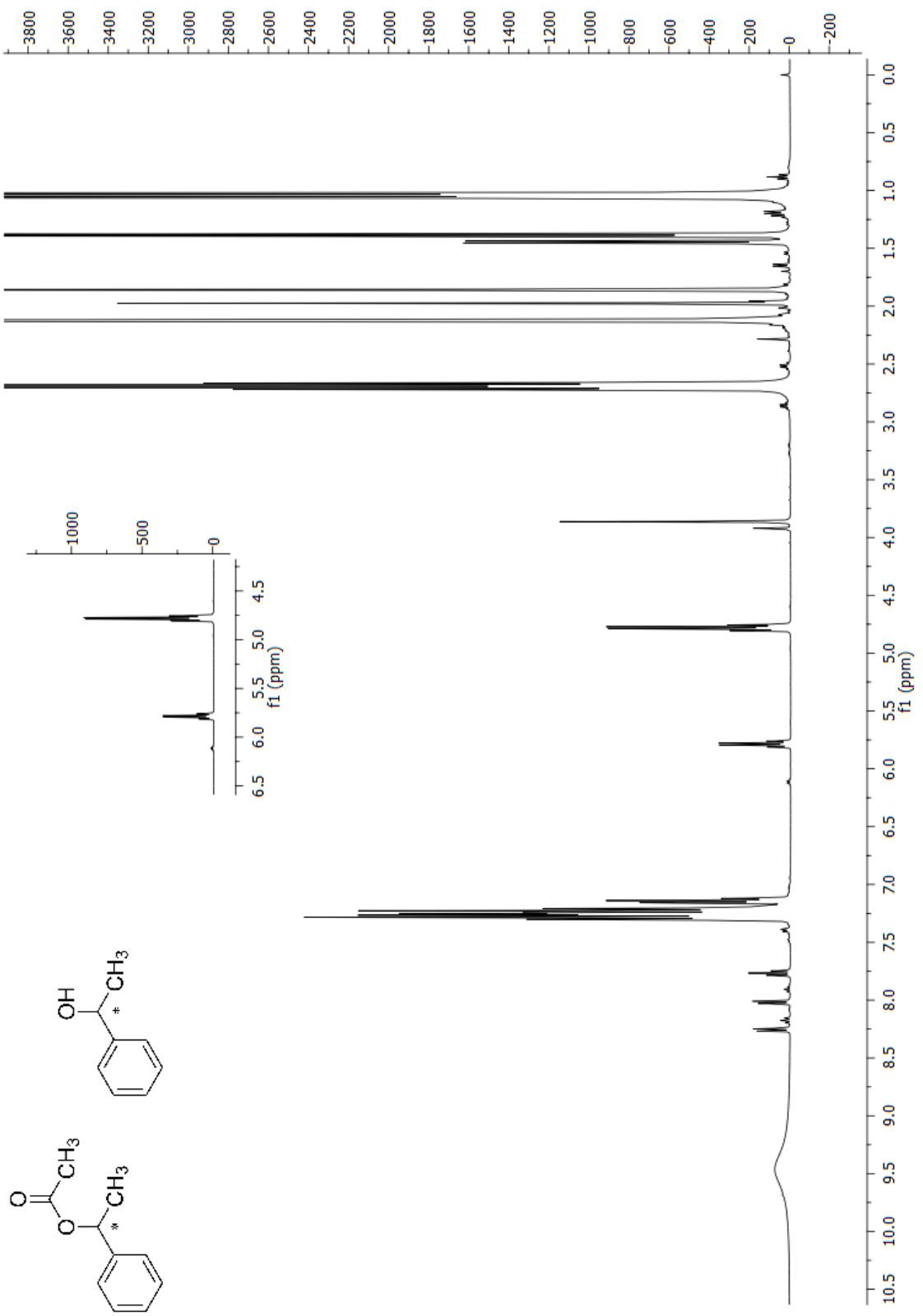

Figure 258: ^{1}H-NMR Spectrum ($CDCl_3$, 400 MHz) from the Reaction of 1-phenyl alcohol with Ac_2O Using **J1** (Table 25, Entry 74).

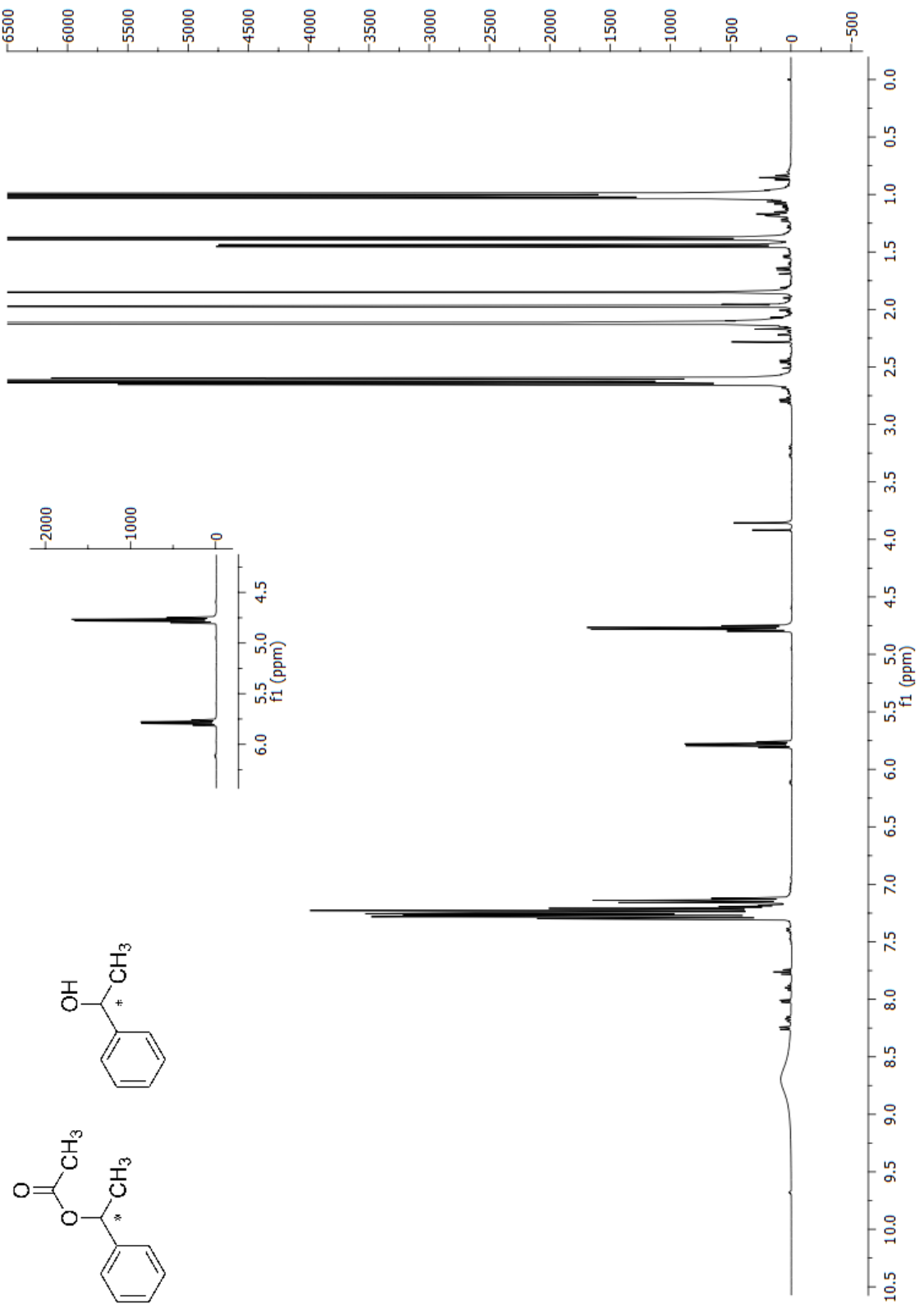

Figure 259: ^{1}H-NMR Spectrum ($CDCl_3$, 400 MHz) from the Reaction of 1-phenyl alcohol with Ac_2O Using **J1** (Table 25, Entry 75).

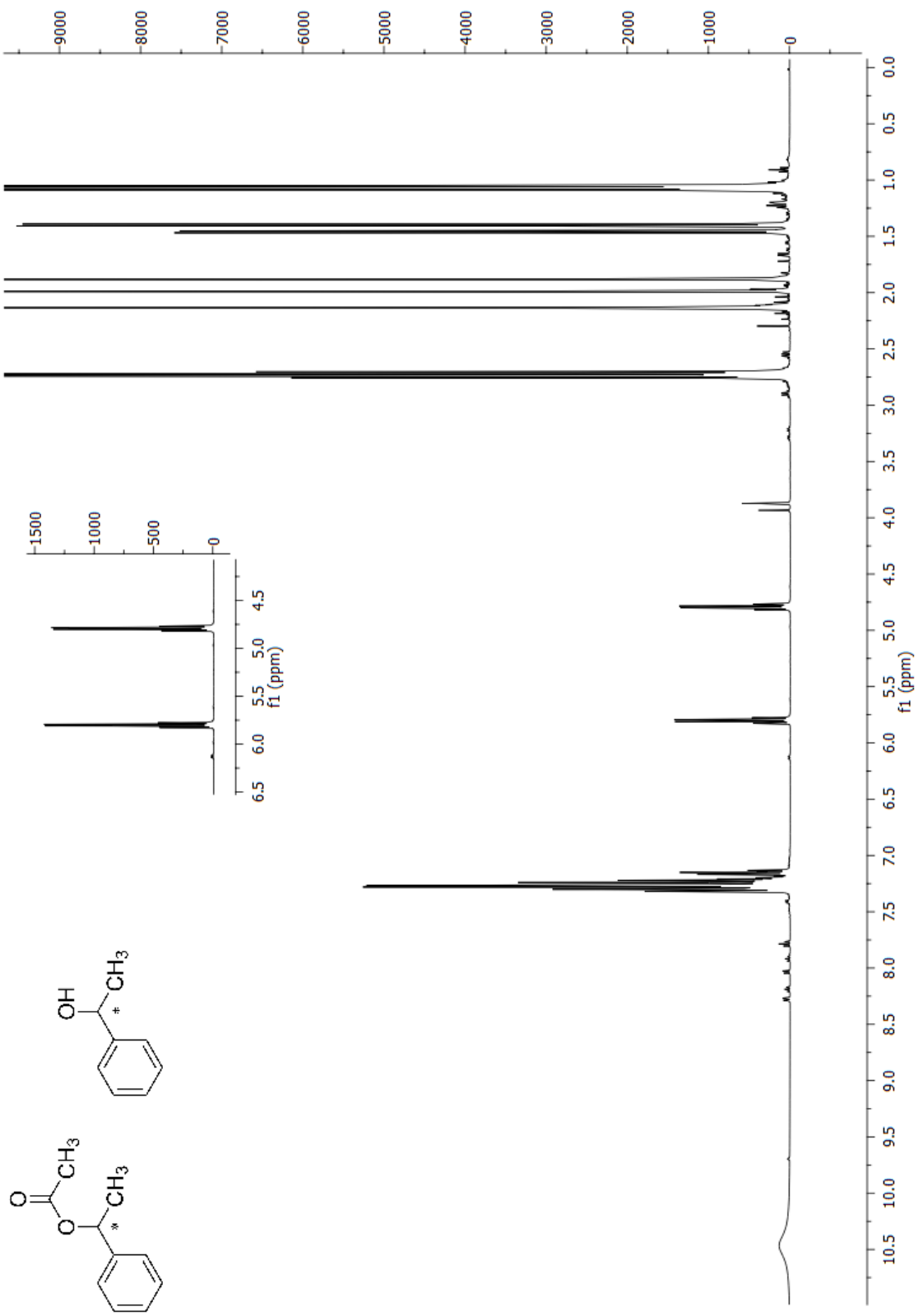

Figure 260: ^{1}H-NMR Spectrum ($CDCl_3$, 400 MHz) from the Reaction of 1-phenyl alcohol with Ac_2O Using **J1** (Table 25, Entry 76).

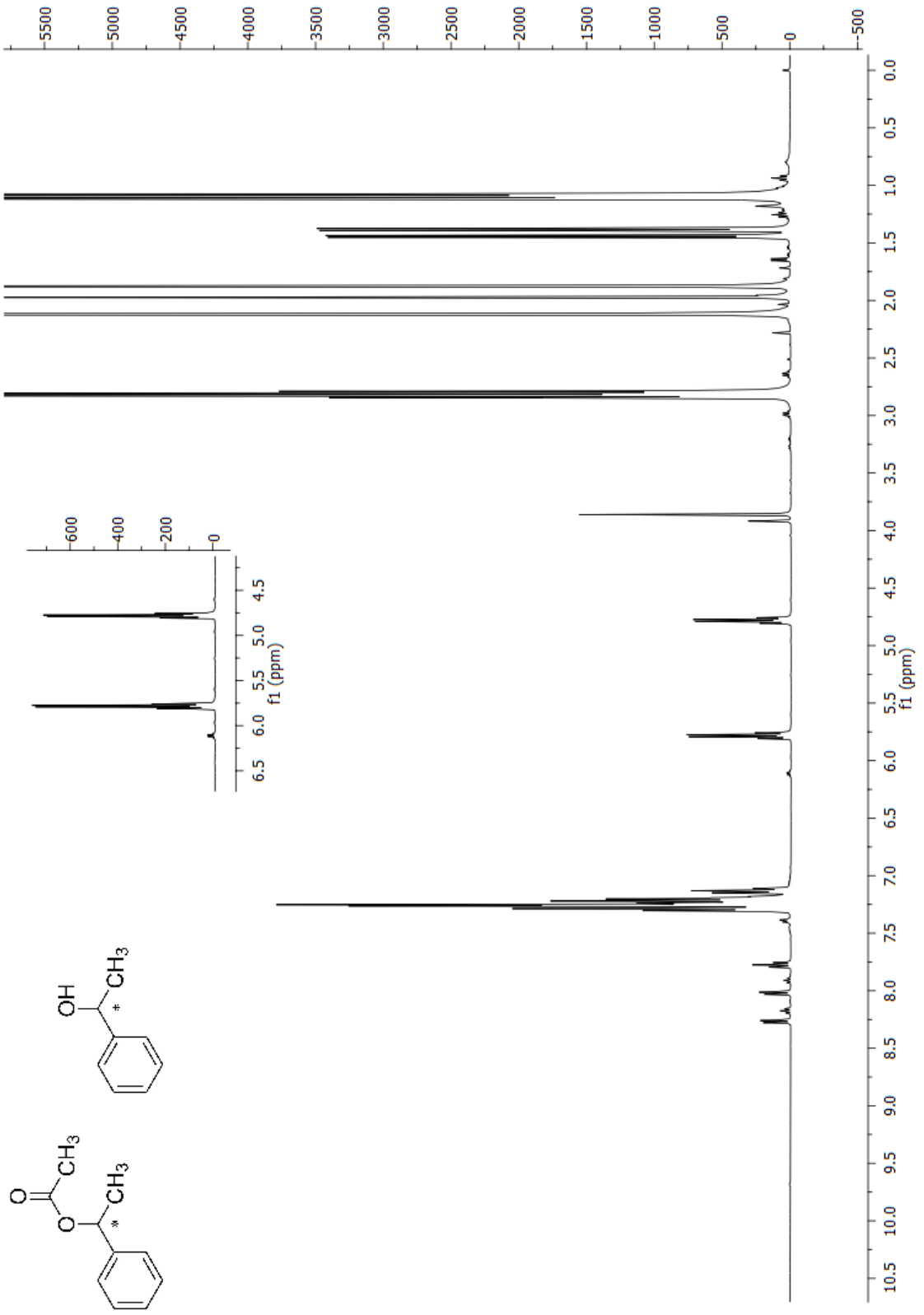

Figure 261: ^{1}H-NMR Spectrum ($CDCl_3$, 400 MHz) from the Reaction of 1-phenyl alcohol with Ac_2O Using **J1** (Table 25, Entry 77).

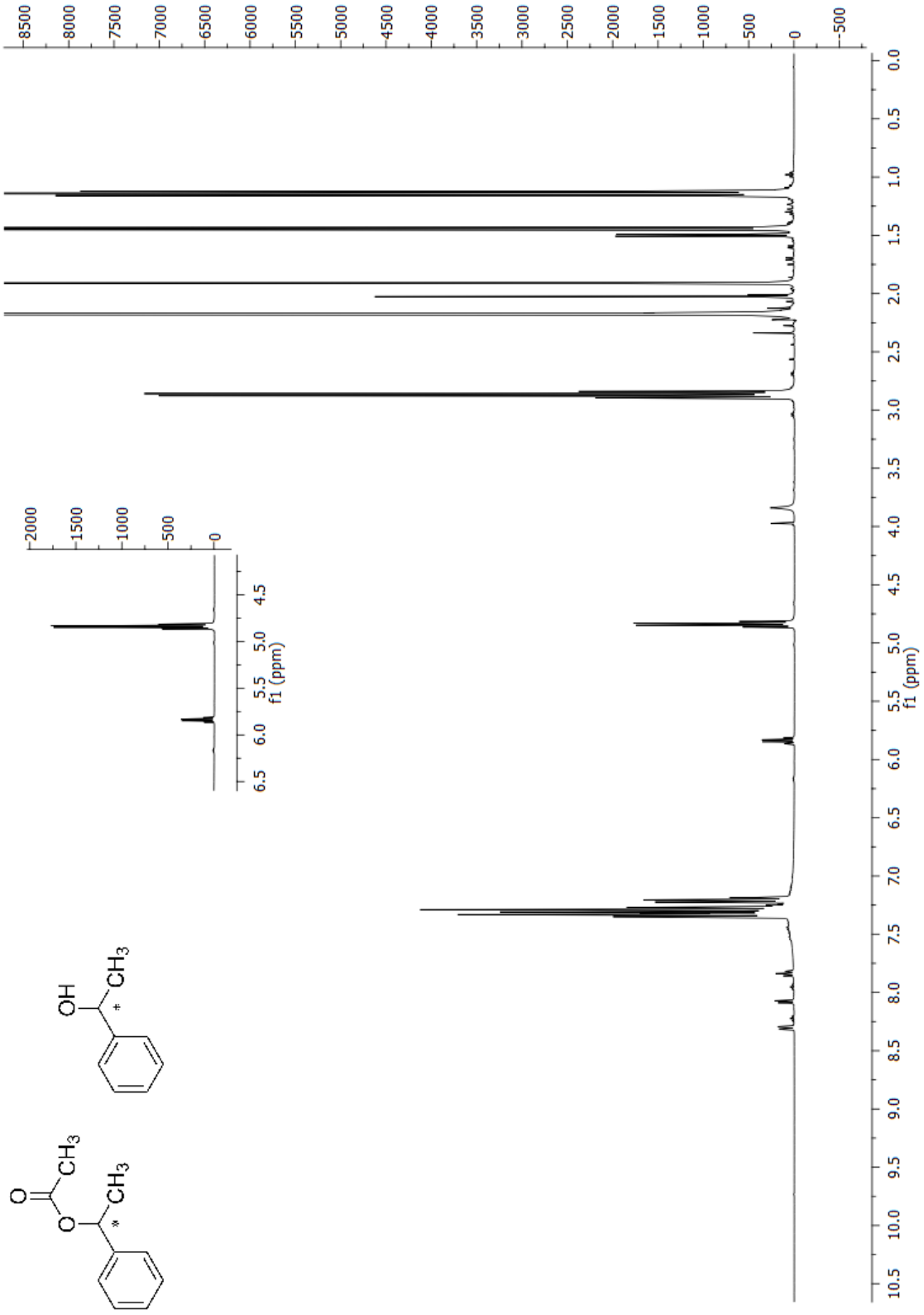

Figure 262: ^{1}H-NMR Spectrum ($CDCl_3$, 400 MHz) from the Reaction of 1-phenyl alcohol with Ac_2O Using **J1** (Table 25, Entry 78).

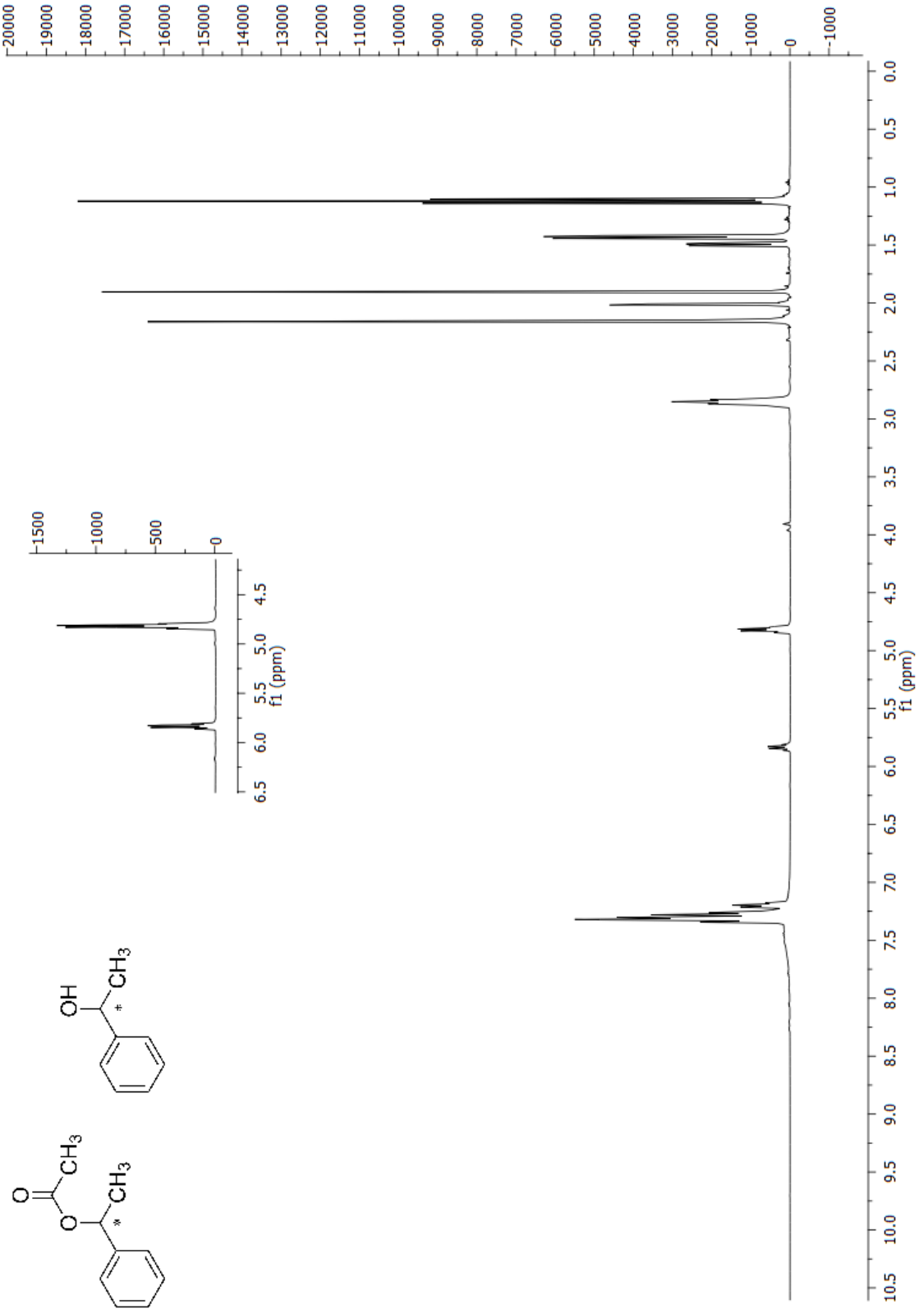

Figure 263: ^{1}H-NMR Spectrum ($CDCl_3$, 400 MHz) from the Reaction of 1-phenyl alcohol with Ac_2O Using **J1** (Table 25, Entry 79).

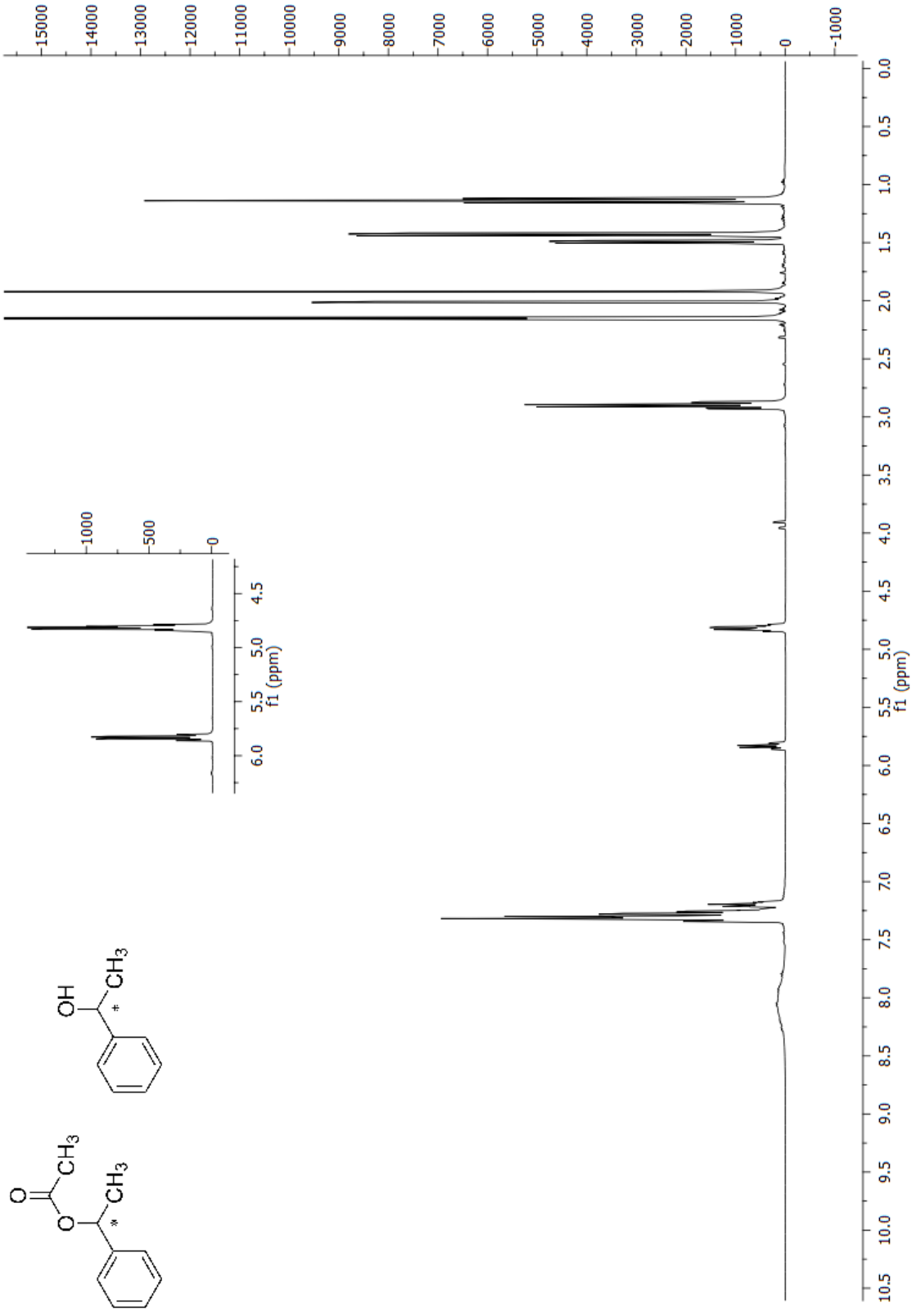

Figure 264: ^{1}H-NMR Spectrum ($CDCl_3$, 400 MHz) from the Reaction of 1-phenyl alcohol with Ac_2O Using **J1** (Table 25, Entry 80).

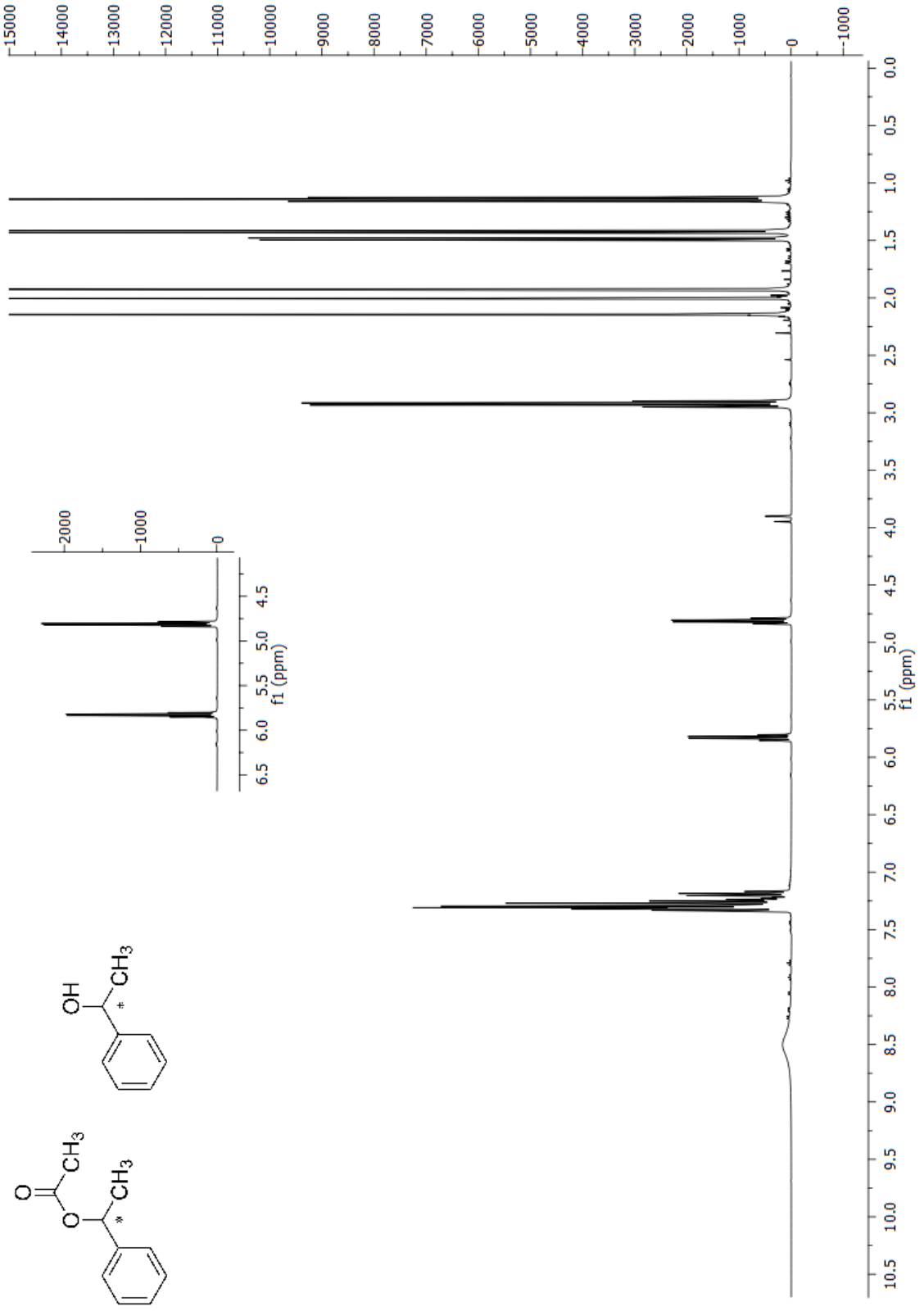

Figure 265: ^{1}H-NMR Spectrum ($CDCl_3$, 400 MHz) from the Reaction of 1-phenyl alcohol with Ac_2O Using **J1** (Table 25, Entry 81).

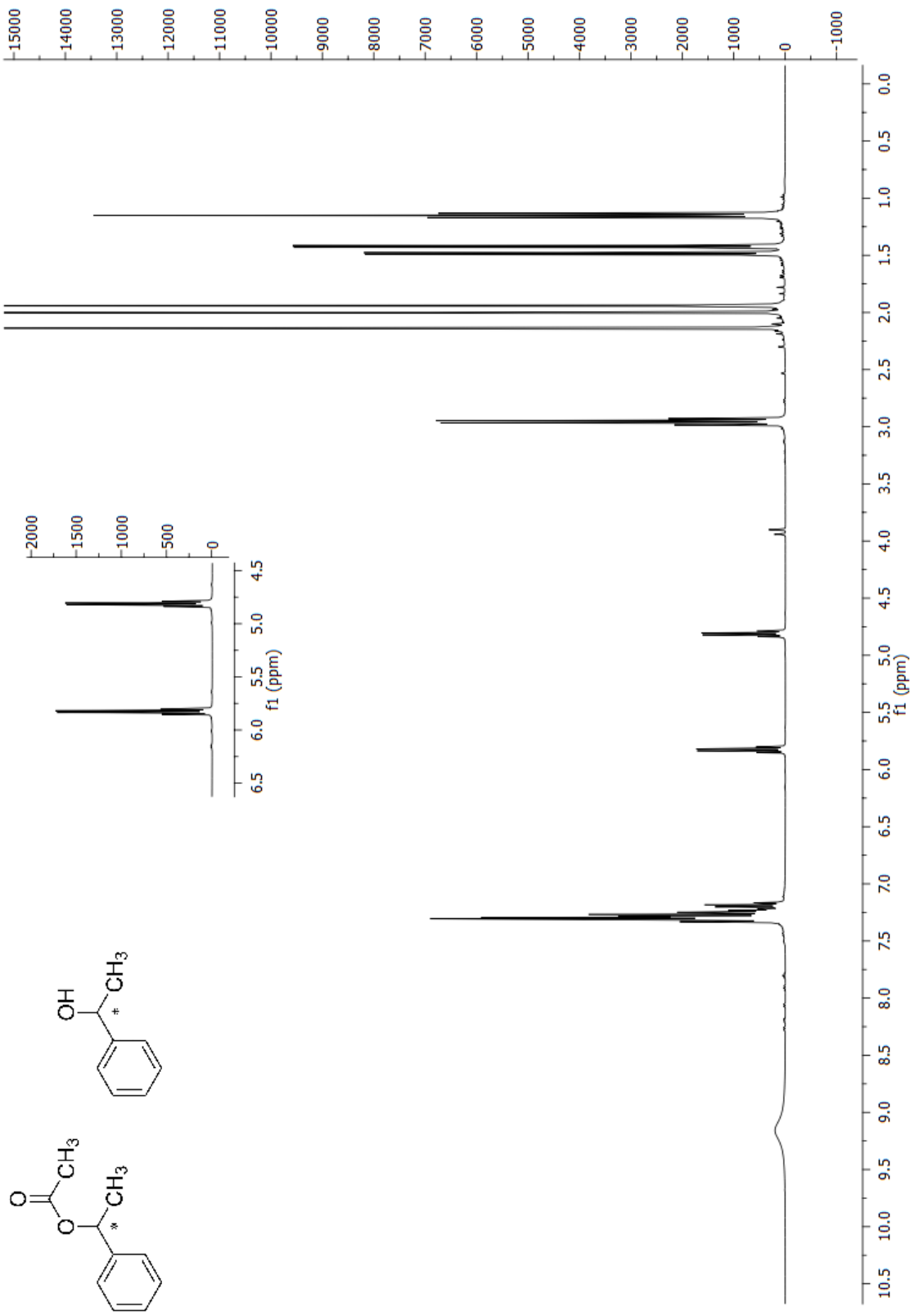

Figure 266: ^{1}H-NMR Spectrum ($CDCl_3$, 400 MHz) from the Reaction of 1-phenyl alcohol with Ac_2O Using **J1** (Table 25, Entry 82).

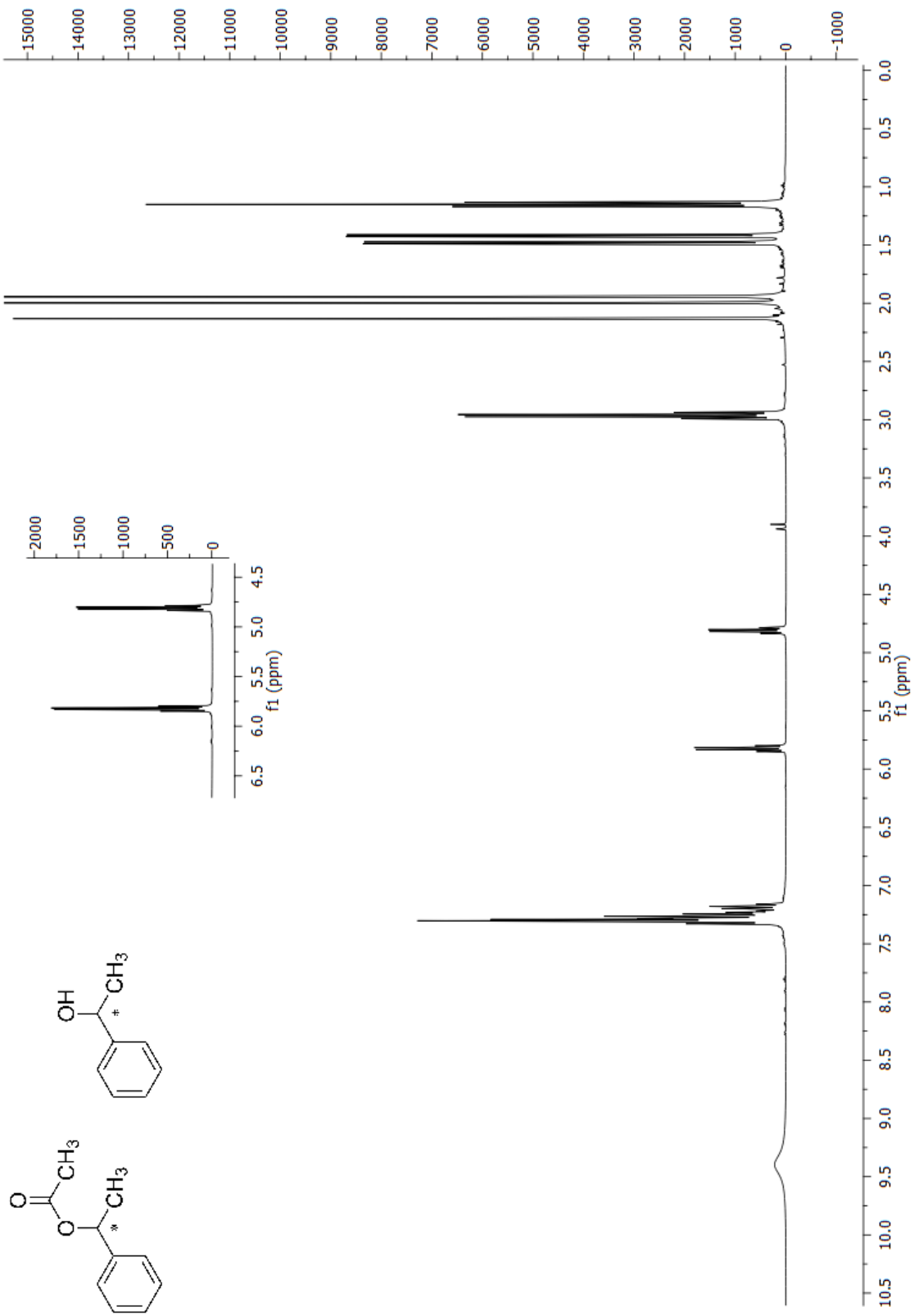

Figure 267: ^{1}H-NMR Spectrum ($CDCl_3$, 400 MHz) from the Reaction of 1-phenyl alcohol with Ac_2O Using **J1** (Table 25, Entry 83).

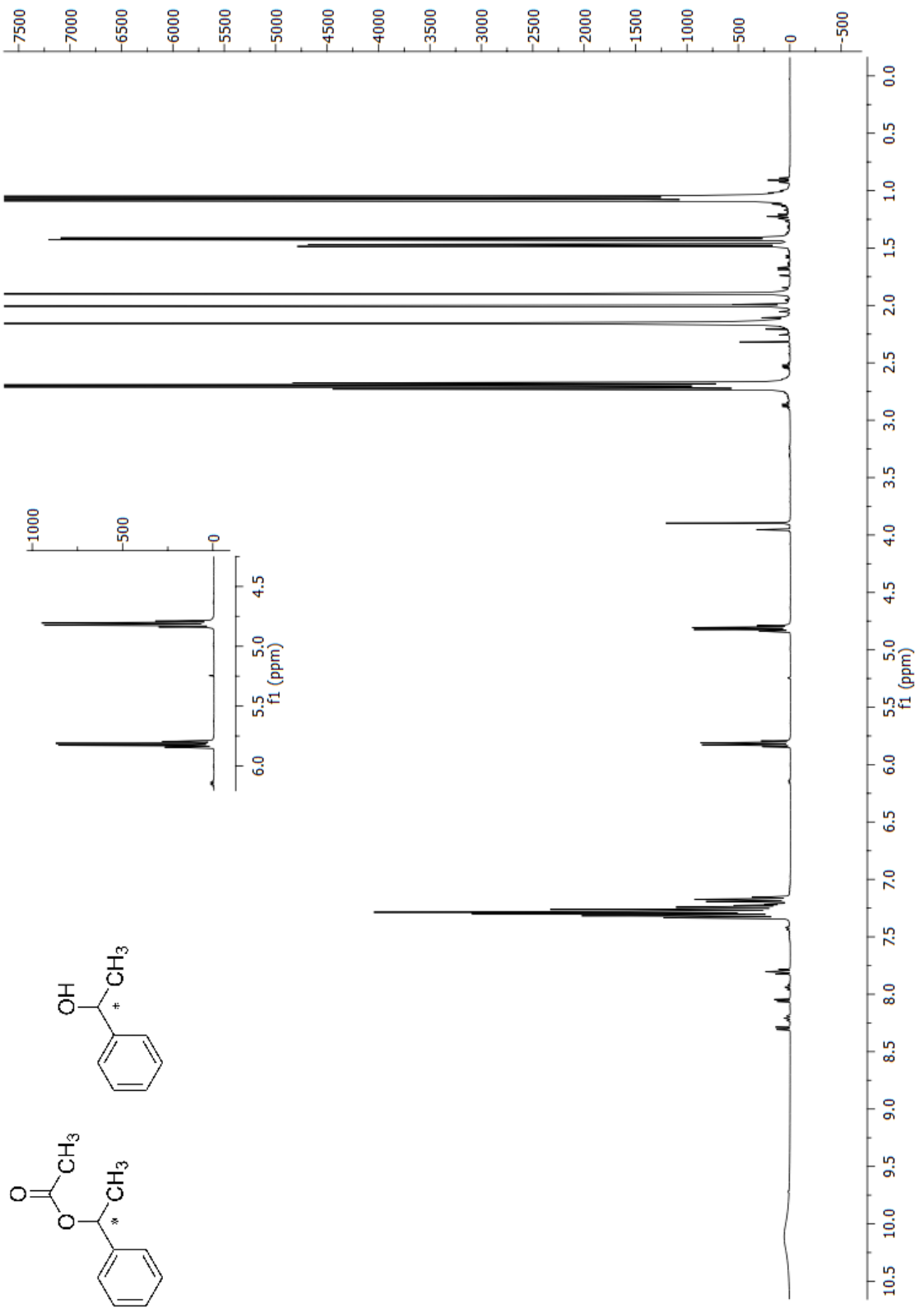

Figure 268: ^{1}H-NMR Spectrum ($CDCl_3$, 400 MHz) from the Reaction of 1-phenyl alcohol with Ac_2O Using **J1** (Table 26, Entry 84).

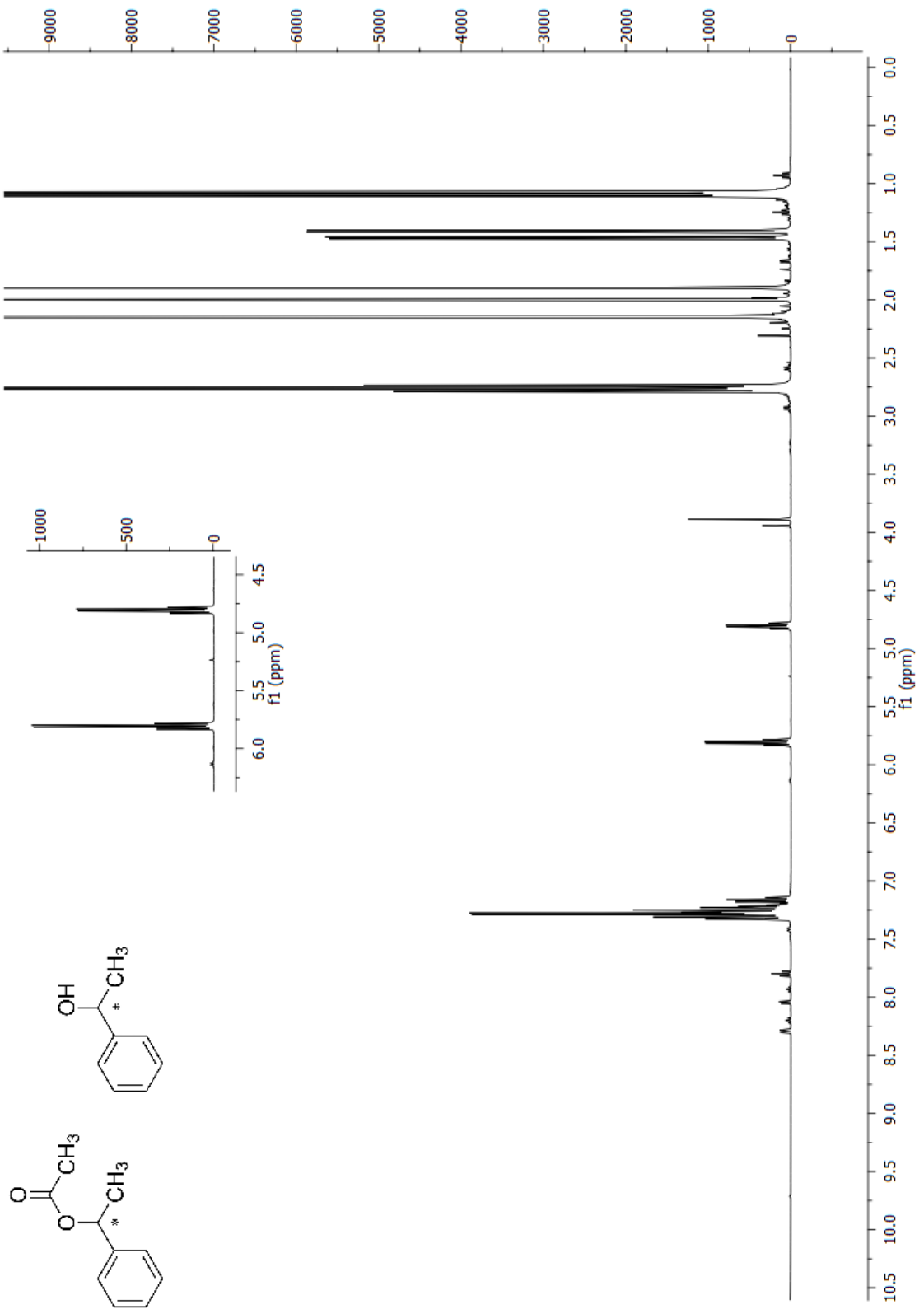

Figure 269: ^{1}H-NMR Spectrum ($CDCl_3$, 400 MHz) from the Reaction of 1-phenyl alcohol with Ac_2O Using **J1** (Table 26, Entry 85).

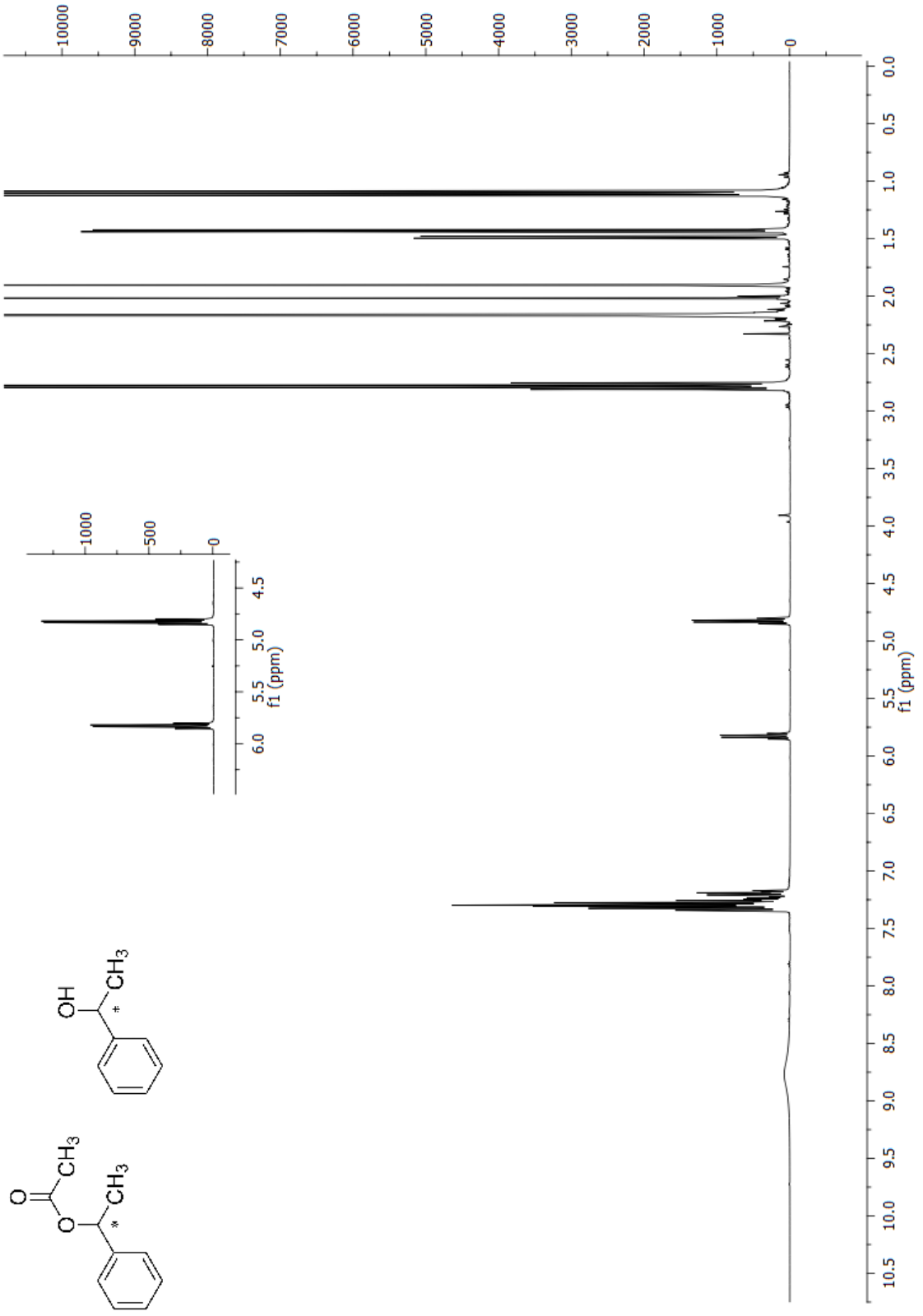

Figure 270: ^{1}H-NMR Spectrum ($CDCl_3$, 400 MHz) from the Reaction of 1-phenyl alcohol with Ac_2O Using **J1** (Table 26, Entry 86).

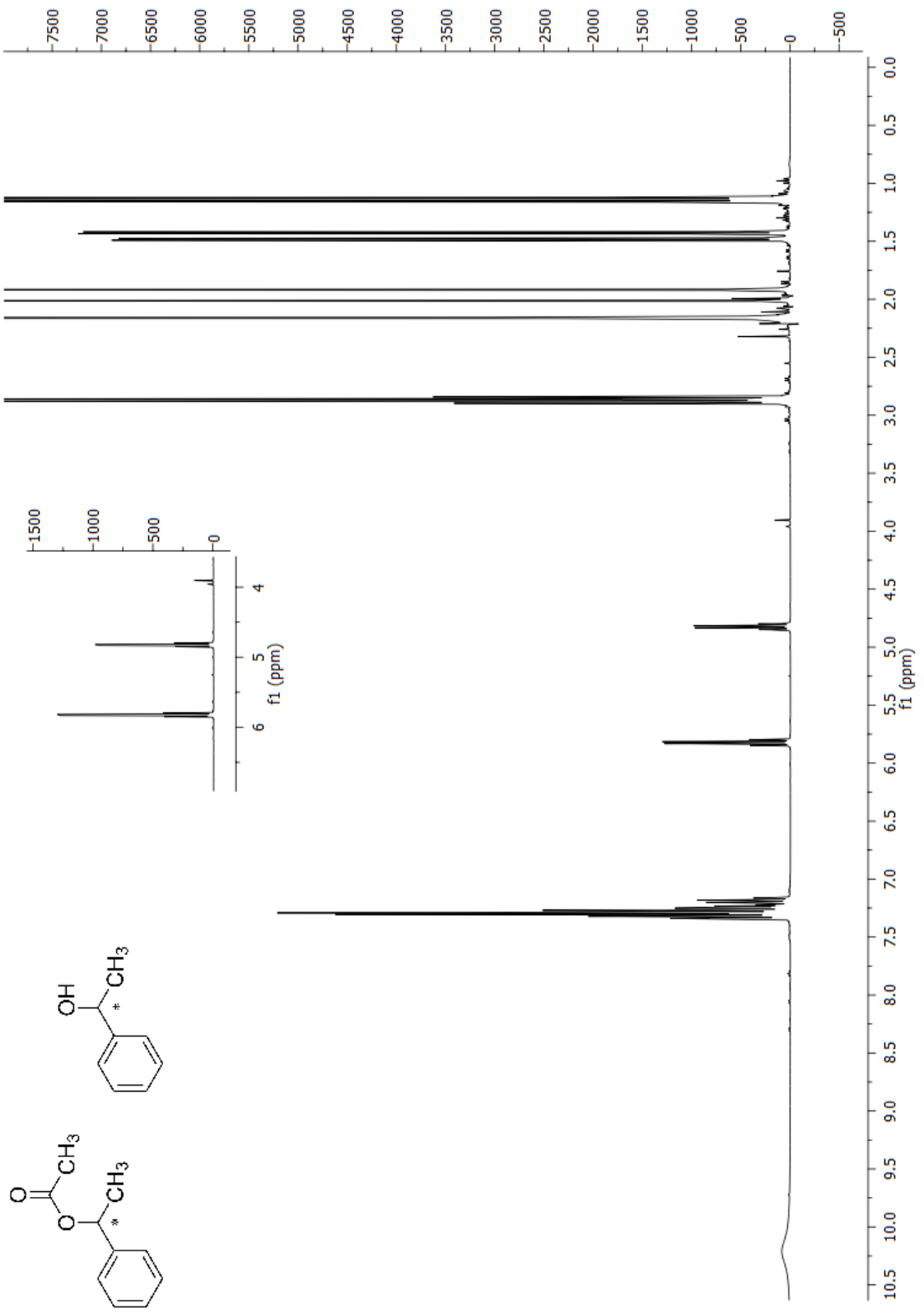

Figure 271: ^{1}H-NMR Spectrum ($CDCl_3$, 400 MHz) from the Reaction of 1-phenyl alcohol with Ac_2O Using **J1** (Table 26, Entry 87).

AP2.3.2 ^{13}C-Spectra

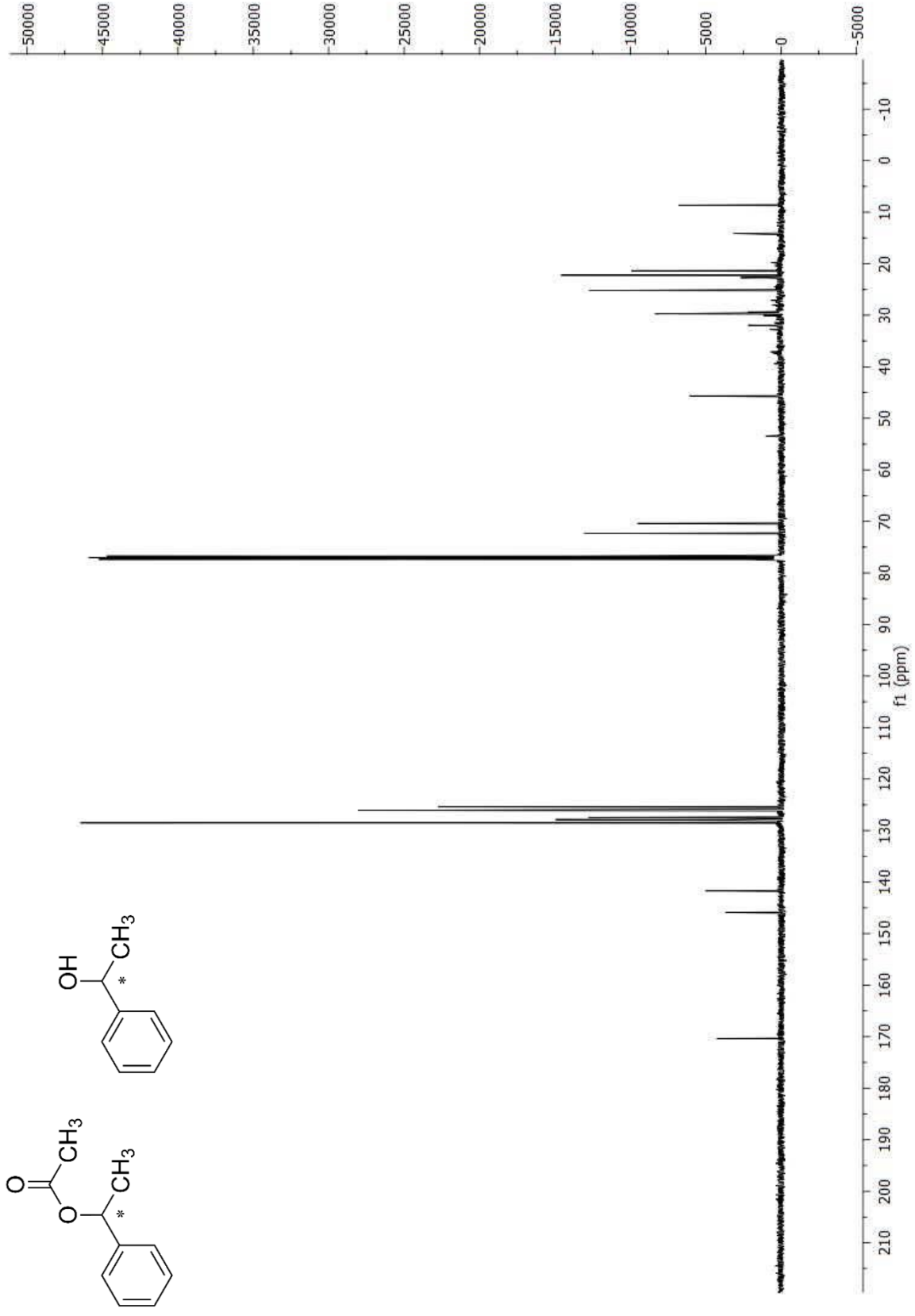

Figure 272: ^{13}C-NMR Spectrum ($CDCl_3$, 100 MHz) of Reaction of 1-phenyl alcohol with Ac_2O.